Synapse-Associated Protein 102 and Postsynaptic Density 95 Regulate Dopamine D1-Class Receptors in Subtype-Specific Manner

Bassam Albraidy

This thesis is submitted to the University of Ottawa in partial fulfillment of the requirements for the Ph.D. degree in Neuroscience.

Department of Cellular and Molecular Medicine
Faculty of Medicine
University of Ottawa

ABSTRACT

Neuromodulation by dopamine D1-class receptor subtypes (D1R and D5R) act via G-protein coupled receptors (GPCRs) and controls essential cognitive and motor functions. The dysfunction of D1R and D5R have been implicated in multiple neurological and psychiatric disorders. D1R and D5R are localized in the postsynaptic density (PSD) of dendritic spines within neurons, where they modulate intracellular signaling pathways and interact with scaffolding partners. Included among the many proteins highly enriched in the PSD are the scaffolding proteins; synapse-associated protein 102 (SAP102) and postsynaptic density 95 protein (PSD95). SAP102 and PSD95 belong to the membrane-associated guanylate kinase (MAGUK) family and regulate glutamate receptors, channel protein localization, and organize numerous signaling protein complexes required for synaptic development and plasticity. Despite the important role of dopaminergic and glutamatergic crosstalk, little is known about how PSD proteins regulate signaling and trafficking properties of dopaminergic receptors. Here, we specifically investigate the binary interaction of SAP102 and PSD95 with D1R and D5R, and the role these MAGUKs have in the regulation of signaling and trafficking of these D1-class receptor subtypes. Our results showed D1R•SAP102 and D1R•PSD95 complexes *in vivo* and *in vitro*, and these interactions differentially regulate agonist-mediated signaling, phosphorylation, and trafficking of D1R. In addition, we showed PSD95, but not SAP102, interacts with D5R *in vivo* and *in vitro*, and the D5R•PSD95 complex modulates agonist-mediated signaling and trafficking of D5R. Together, these results demonstrate an important role for SAP102 and PSD95 in regulating D1-class receptor in subtype-specific manner. Interestingly, we found that β-arrestin1 (βArr1) and β-arrestin2 (βArr2), versatile adaptor proteins that regulate desensitization and trafficking of GPCRs, including D1R, interact with SAP102 and PSD95 *in vivo* and *in vitro*. Additionally, we found that SAP102 and PSD95 positively mediate βArr2 recruitment to D1R, but not with βArr1, suggesting a potential ternary complex of D1R•MAGUK•βArr2. Future studies might exploit the pharmacological potential of D1R•SAP102, D1R•PSD95, and D5R•PSD95 complexes in the design of novel therapeutic approaches to mitigate abnormal dopaminergic D1-class function as seen in Parkinson's Disease.

AUTHORIZATION

Permission to include published figures as part of dissertation/thesis was obtained:

- "From [Xu et al. Structural genomics of the human dopamine receptor system. Cell Res. 2023]. Reprinted with permission from Springer Nature", to include figure 1. *(p. 286-287)*
- "From [Cizeron et al. A brainwide atlas of synapses across the mouse life span. Science. 2020]. Reprinted with permission from AAAS," to include figure 1. *(p. 288-289)*

LIST OF CONTENTS

LIST OF TABLES

LIST OF FIGURES

Chapter One: Introduction

Chapter Two: Methods and Materials

Manuscript II

Appendix II: Supplementary Figures for Manuscript II

Manuscript III

Appendix III: Supplementary Figures for Manuscript III

LIST OF ABBREVIATIONS

3-MT:	3-methoxytyramine
5-HT:	Serotonin (5-hydroxytryptamine)
5-HT_{2A}R:	5-HT_{2A} receptor
5-HT_{2C}R:	5-HT_{2C} receptor
6-OHDA:	6-hydroxydopamine
7-OH-DPAT:	7-hydroxydipropylaminotetralin
7TMRs:	Seven-transmembrane receptors
A_1R:	Adenosine A_1 receptor
A_{2A}R:	Adenosine A_{2A} receptor
AA:	Ascorbic acid
AADC:	Aromatic L-amino acid decarboxylase
AC:	Adenylyl cyclase
ACh:	Acetylcholine
AD:	Alzheimer's disease
ADHD:	Attention deficit hyperactivity disorder
AIM:	Abnormal involuntary movement
AKAP79/150:	A-kinase anchoring protein 79/150
Akt:	Protein Kinase B
Ala:	Alanine
AMPAR:	α-amino-3-hydroxy-5-methyl-4-isoxazole propionic acid receptor
AP:	Action potential
AP-2:	Adaptor protein -2
ARC:	Arcuate nucleus of the hypothalamus
ATP:	Adenosine triphosphate
BBB:	Blood brain barrier
BCS:	Bovine calf serum
BG:	Basal ganglia
B_{max}:	Maximal binding capacity
bp:	base pair
BRET:	Bioluminescence resonance energy transfer
BSA:	Bovine serum albumin
Ca^{2+}:	Calcium ions
CaMKII:	Calcium/calmodulin-dependent protein kinase II
cAMP:	Adenosine 3′,5′- cyclic monophosphate
CDK5:	Cyclin-dependent kinase 5
CK1:	Casein kinase 1
CK2:	Casein kinase 2
CNS:	Central nervous system

CoIP:	Coimmunoprecipitation
COMT:	Catechol-O-methyltransferase
COVID-19:	Coronavirus disease 2019
CREB:	cAMP response element-binding protein
CRFR1:	Corticotropin-releasing factor receptor 1
Cryo-EM:	Cryo-electron microscopy
CT:	Intracellular carboxy-terminus of the receptor
Cys:	Cysteine
D1R:	Dopamine D1 receptor
D1R-MSN:	D1R-expressing MSN
D2L:	Dopamine D2 receptor-long isoform
D2R:	Dopamine D2 receptor
D2R-MSN:	D2R-expressing MSN
D2S:	Dopamine D2 receptor-short isoform
D3Gly9:	Dopamine D3 receptor Gly9 polymorphic variant
D3R:	Dopamine D3 receptor
D3Ser9:	Dopamine D3 receptor Ser9 polymorphic variant
D4R:	Dopamine D4 receptor
D5R:	Dopamine D5 receptor
DA:	Dopamine
DAG:	Diacylglycerol
DARPP-32:	DA- and cAMP regulated phosphoprotein M.W. 32 kDa
DAT:	Dopamine transporter
DC Protein assay:	Detergent compatible protein assay
DHX:	Dihydrexidine
DIV:	Days *in vitro*
DLG:	Discs large homologue
DMEM:	Dulbecco's modified eagle medium
dMSN:	direct pathway of striatonigral MSN
DOPAC:	3,4-dihydroxyphenylacetic acid
DRD1:	Gene encoding D1R
DRD2:	Gene encoding D2R
DRD3:	Gene encoding D3R
DRD4:	Gene encoding D4R
DRD5:	Gene encoding D5R
DRIP:	Dopamine receptor-interacting protein
DRN:	Dorsal raphe nucleus
DRY:	Aspartate-arginine-tyrosine motif
DβH:	DA β-hydroxylase
E13-14:	Embryos aged E13-14

EC_{50}:	Half maximal effective concentration
EDTA:	Ethylenediaminetetraacetic acid
EL:	Extracellular loop of the receptor
ELISA:	Enzyme linked immunosorbent assay
E_{max}:	Maximal efficacy
EMEM:	Eagle's minimal essential medium
EPAC:	Exchange protein directly activated by cAMP
EPSC:	Excitatory postsynaptic current
ER:	Endoplasmic reticulum
ERK1/2:	Extracellular signal-regulated kinase 1 and 2
FBS:	Fetal bovine serum
fMRI:	Functional magnetic resonance imaging
FRET:	Fluorescence resonance energy transfer
FSK:	Forskolin
GABA:	γ-amino butyric acid
$GABA_AR$:	Ionotropic $GABA_A$ receptor
$GABA_BR$:	Metabotropic $GABA_B$ receptor
$GABA_BR$-GbR2:	Metabotropic $GABA_B$R subunit 2
GAP:	GTPase-activating protein
GDP:	Guanosine diphosphate
GEF:	Guanine nucleotide exchange factor
GK:	Guanylate kinase
GKAP:	Guanylate kinase-associated protein
GluA1:	AMPAR subunit 1
GluA2:	AMPAR subunit 2
GluA3:	AMPAR subunit 3
GluN1:	NMDAR subunit 1
GluN2A:	NMDAR subunit 2A
GluN2B:	NMDAR subunit 2B
GPCR:	G-protein coupled receptor
GPe:	External segment of globus pallidus
GPi:	Internal segment of globus pallidus
G-protein:	Guanine nucleotide-binding protein
GRIP:	Glutamate-receptor-interacting protein/AMPAR-binding protein
GRK:	G-protein coupled receptor kinase
GSK3:	Glycogen synthase kinase 3
GTP:	Guanosine triphosphate
$G\alpha_{i/o}$:	G-protein $\alpha_{i/o}$ inhibitory subunit
$G\alpha_q$:	G-protein α_q subunit
$G\alpha_{s/olf}$:	G-protein $\alpha_{s/olf}$ stimulatory subunit

Gβγ:	G-protein βγ subunit complex
H^+:	Hydrogen ion
HBSS:	Hanks' Balanced Salt Solution
HEK293:	Human embryonic kidney 293
HEPES:	4-(2-hydroxyethyl)-1-piperazineethanesulfonic acid
HPA:	Hypothalamic-pituitary-adrenal axis
HRP:	Horseradish peroxidase
HVA:	Homovanillic acid
I1:	Isoform insert 1 of SAP102
I2:	Isoform insert 2 of SAP102
IB:	Immunoblot
IBD:	Irritable bowel disease
IL:	Intracellular loop of the receptor
iMSN:	Indirect pathway of striatopallidal MSN
IP:	Immunoprecipitation
IP_3:	Inositol trisphosphate
ISO:	Isoproterenol
JNK:	c-Jun N-terminal kinase
K^+:	Potassium Ion
K_d:	Equilibrium dissociation constant
KD:	Knockdown approach
kDa:	Kilodalton
K_i:	Inhibitory dissociation constant
KO:	Knockout approach
LC:	locus coeruleus
L-DOPA:	L-3,4-dihydroxyphenylalanine
LID:	L-DOPA-induced dyskinesia
LTP:	Long-term potentiation
M1:	Primary motor cortex
MAGI:	Membrane-associated guanylate kinase inverted
MAGUK:	Membrane-associated guanylate kinase
MAO:	Monoamine oxidase
MAPK:	Mitogen-activated protein kinase
MDD:	Major depressive disorder
MEK1/2:	MAPK/ERK kinase 1 and 2
mGluR5:	Metabotropic glutamate receptor 5
mPins:	Mammalian homolog of Drosophila melanogaster partner of inscuteable
MPTP:	1-methyl-4-phenyl-1,2,3,6-tetrahydropyridine
MS:	Multiple sclerosis
MSN:	Medium spiny neuron

Na^+:	Sodium ion
NAc:	Nucleus accumbens
NE:	Norepinephrine
NET:	Norepinephrine transporter
NMDAR:	N-methyl-D-aspartate receptor
NT:	Upstream extracellular N-terminus of the receptor
OB:	Olfactory Bulb
OD:	Optical density
OPD:	O-phenylenediamine dihydrochloride
P21:	Postnatal day 21
P3:	Postnatal day 3
P60:	Postnatal day 60
P8:	Postnatal day 8
PBS:	Phosphate buffer saline
PCR:	Polymerase chain reaction
PD:	Parkinson's disease
PDE:	cAMP phosphodiesterase
PDZ:	PSD95/DLG/Zonula occludens-1
PET:	Positron emission tomography
PFC:	Prefrontal cortex
PI3K:	Phosphoinositide 3-kinase
PIP2:	Phosphatidylinositol-4,5-biphosphate
PKA:	Protein kinase A
PKC:	Protein kinase C
PLA:	Proximity ligation assay
PLC:	Phospholipase C
PLL:	Poly-L-lysine
PMA:	Phorbol-12-myristate-13-acetate
PMSF:	Phenylmethylsulfonyl fluoride
PNMT:	Phenylethanolamine N-methyltransferase
PP1:	Protein phosphatase 1
PP2A:	Protein phosphatase 2A
PP2B:	Protein phosphatase 2B
PSD:	Postsynaptic density
PSD93:	Postsynaptic density protein 93
PSD95:	Postsynaptic density protein 95
PSD-MAGUK:	PSD95 subfamily of MAGUK
PVDF:	Polyvinylidene difluoride
RapGEF2:	Rap guanine nucleotide exchange factor 2
RGS:	Regulators of G-protein signaling

RIPA: Radioimmunoprecipitation assay buffer
RLU: Relative luminescence unit
SAP102: Synapse-associated protein 102
SAP97: Synapse-associated protein 97
SCN: Suprachiasmatic nucleus
SDS-PAGE: Sodium dodecyl sulphate–polyacrylamide gel electrophoresis
Ser: Serine
SH3: Src homology 3
SNc: Substantia nigra pars compacta
SNP: Single nucleotide polymorphism
SNr: Substantia nigra pars reticulata
SNRI: 5-HT and NE reuptake inhibitors
Src: Src family of protein tyrosine kinases
STN: Subthalamic nucleus
SynGAP: Synaptic Ras GTPase-activating protein
TBS: Tris-buffered saline
TBS-T: Tris-buffered saline containing Tween 20
T-Cell: Peripheral T-lymphocytes
TH: Tyrosine hydroxylase
Thr: Threonine
THX: Thiothixene
TM: Transmembrane domain of the receptor
V_1R: Vasopressin 1 receptor
Val: Valine
VGAT: Vesicular GABA transporter
VGLUT: Vesicular glutamate transporter
VMAT2: Vesicular monoamine transporter type 2
VTA: Ventral tegmental area
WT: Wild-type
αMPT: α-methyl-p-tyrosine
β_1AR: β_1-adrenergic receptor
β_2AR: β_2-adrenergic receptor
βArr: β-arrestin
βArr1: β-arrestin1
βArr2: β-arrestin2
βArrs: β-arresting

ACKNOWLEDGMENTS

My graduate study was an enriching scientific experience about neuroscience and GPCRs, but more importantly about dopamine. This journey was filled with joyful moments as well intense emotions, thanks to the dopamine reward system! As a researcher, it was an opportunity to pursue my passion and trust my intuition in which I discovered myself through the lens of my work. This doctoral dissertation would not have been possible without the support and the encouragement of the kind people around me and my family, which I am extremely grateful.

First and foremost, I offer my profound appreciation and gratitude to my supervisor, **Dr. Mario Tiberi**, for unequivocal support and constant guidance during my Ph.D. studies. Thank you for your mentorship over the past six years; the training experience to expand my skills and knowledge, along with your constructive criticism that has greatly improved my critical reasoning and scientific thinking. The door to your office was always opened to new hypothesis and discussions, and the welcomed environment in the lab provided me the resources I needed to succeed. Most importantly, thank you for trusting me and giving me the opportunity to mentor and advise graduate and undergraduate students during their studies. Your continuous encouragement and counselling have been invaluable academically and personally. No doubt, this journey enriched my research curiosity, rewarded me academically and scientifically to be a "*future scientist*", which I am immensely grateful to you.

I would also like to thank my thesis advisory committee members: **Dr. Jean-Claude Béïque, Dr. Patrick Giguère, and Dr. Baptiste Lacoste**, for all their indispensable suggestions, thoughtful discussions, and critical assessments throughout my studies. I would also like to thank my thesis examiners: **Dr. Bruno Giros, Dr. Stephen Ferguson, Dr. Jean-Claude Béïque, and Dr. Paul Albert,** for reading my thesis and their valuable comments and recommendations.

I would like to acknowledge and thank our collaborators: Dr. Béïque, Dr. Ferguson, and Dr. Giguère, for their generosity in providing materials and resources utilized in my study. A special thanks to Dr. Béïque, in which I had training in his lab during my first year; thank you for insightful and exciting discussions, you inspired me to think outside the box! Thanks to the former members of the Béïque lab: Dr. Cary Soares, Dr. Kirk Multaz, and David Lemelin, as well past and current members of the Ferguson lab: Dr. Khaled Abd-Elrahman, Dr. Awatif Albaker, Dr. Karim Ibrahim,

Dr. Shaunik Sharma, and Jingwei Chen, for their insightful discussion, shared knowledge, technical assistance, encouragement, and supportive chats. To the members of the Cell Biology and Image Acquisition facility: thank you for the training and technical assistance. To the staff of neuroscience secretary and graduate office: thank you for the administrative support and assistance, and for organizing the seminars and annual events.

A huge thank you goes out to former and present members of the Tiberi lab that I had the fortune of knowing, for making the working environment creative and enjoyable. I wish you all the best in your future careers. Sincere thanks to Binhui Liang for her technical support; Aida Said, Chastity Kirkey, Hedieh Habibi Khorasani, and Duncan Baird for their friendship and for creating lighthearted lab atmosphere; Dr. Chantal Binda for her friendship, which extended to my family, I really appreciate all your kindness, encouragement, and stimulating conversations; Patricia Bilodeau for her friendship during this year, I was fortunate to meet her family for my birthday, thank you for your kindness, hospitality, and for the effort with the image quantification analysis and the time reading my thesis.

Special thanks must go to my lab mate and collaborator, **Bradley Mischuk** for his continuous encouragement, insightful feedback, and thoughtful discussion in reading my thesis, but most importantly, for your friendship over the past six years. Thank you for your technical assistance, your partnership in the SAP102 research, and your contribution in many other projects; I truly enjoyed working with you, and you're always there to help!

I would like to thank current and former graduate and undergraduate students in Tiberi's lab, whom I worked closely with during their studies, including Hedieh Habibi Khorasani, Josephine Zein, Duncan Baird, Deserae Ball, Raina Barara, Victoria Puzej, Meriam Zeghal, Étienne Sirois, Misha Kaniyath, Rita Murali, Oana Mirel, and Sador Bereketab. Thank you all for the valuable scientific discussion and providing the enjoyable working environment in the lab. Regardless, we overcame the obstacles, and seeing you now as a graduate, or soon to be, make me, nonetheless, proud!

To my wife, and soon to be a doctor, **Dalal Alsowiada**: completion of this degree would not have been possible without you, thank you for your unconditional love, enormous support, and patience; I truly could not have done this without you. Although this journey was not an easy ride for us, with us both pursuing Ph.D. studies, I'm proud of who we became, equipped with the knowledge and skills we acquired here, at the University of Ottawa. Regardless of the difficulties we

encountered, we made it strongly together. Thank you for hearing me complaining about failed experiments, as well celebrating new results, no matter how small, it was indeed rewarding ♥

To my kids: **Fahad** and **Lubna**, your presence made this journey loveable, memorable, and enjoyable! You are the source of my happiness and strength, and you were the best distraction I needed during my studies! Thank you for your loving, laughing, and patience; and for allowing me to go to the lab during the weekends; your understanding was truly appreciated! Certainly, you are the significant part of this journey; I admired your curiosity about science and enjoyed explaining to you, among many things, how the brain works. As I watched you growing over my Ph.D. years, and as a father, I hope I have a set a great example for you to never give up in the pursuit of all your life's dreams! The collective memories we made in Ottawa, will never be forgotten ♥

I would like to extend my deepest gratitude to our beloved neighbor, George and Louise McLaughlin, and our dear friend, Safia Haji Mohamud; we were blessed and fortunate knowing you. Since we met more than six years ago, my son and shortly thereafter my daughter, always enjoyed your presence, caring, and the motivational chats. Your generous gifts to my children, on their birthdays and many other uncountable occasions, always put big smiles on their faces and create genuine memories. You were our kids' Canadian grandparents; your tremendous kindness is beyond imagination, truly I appreciate your friendship; thank you, George, Louise, and Safia!

My sincere thanks must go to my best friend, **Dr. Hamood AlSudais,** for his friendship, encouragement, and pushing me forward. I was fortunate knowing him since we did undergraduate study at King Saud University, late 2000s, but Ottawa was a turning point into this fruitful friendship and collective moments. The little scientific chats with Tim Hortons coffee at the RGN will be remembered! Thank you for all the motivating discussions, as well listening to me when I needed! Your kindness towards my kids makes them always look forward to your visits. Thank you, Hamood, for being a brother and a true friend!

I could not have completed my studies without the prayers, love, encouragement, and wholehearted support from my family, my siblings, and my relatives. To **my mother**, thank you for the unwavering love and continuous prayers throughout my life. You have been with me in every step of this journey, and no words can thank you enough for all the sacrifices you did for me, as well for my siblings, but I hope I make you proud, and I am forever indebted ♥

*This thesis is dedicated to **my father**, may you rest in peace, I know you would have been proud. I truly miss you, but you have never left my heart! I also dedicate this thesis to the loved ones, who passed away, peacefully, while I was away from home. You are all dearly missed and forever remembered* ♥

Finally, as I'm approaching the end of this long-rewarding journey that started at Georgetown University, and ended here at University of Ottawa, I am grateful to the Ministry of Education in the Kingdom of Saudi Arabia, for their financial support and generous scholarship during my M.Sc. and Ph.D. studies. This scholarship program is of utmost importance and significant impact as it allowed me, as well as many others, to transform knowledge and efficiently contribute to the scientific community.

After many years of enjoyable bench work that was concluded with my Ph.D. defence (Dec 11th, 2023), this milestone will always be remembered ♥ Nonetheless, gaining a Ph.D. is a start of new journey, to which I'm excited to start!

This work was carried out on the unceded and unsurrendered land of the Algonquin Anishinaabe people, and supported by grant from the Canadian Institutes of Health Research (CIHR).

{وَآخِرُ دَعْوَاهُمْ أَنِ الْحَمْدُ لِلَّهِ رَبِّ الْعَالَمِينَ}

THESIS FORMAT

This thesis is written in a monograph format. ***Chapter One*** is a general introduction describing the theoretical background of the work presented herein. ***Chapter Two*** is a detailed methodological explanation of experimental approaches utilized in this thesis. ***Chapter Three*** is descriptive of the thesis results, consisting of three distinct manuscripts, titled as following: **manuscript I:** *Synapse Associated Protein 102 (SAP102) and Postsynaptic Density 95 (PSD95) Differentially Modulate Dopamine D1 Receptor,* **manuscript II:** *Postsynaptic Density 95 (PSD95) Modulates Dopamine D5 Receptor, and* **manuscript III:** *Synapse-Associated Protein 102 (SAP102) and Postsynaptic Density 95 (PSD95) Facilitate β-arrestin2 (βArr2) Signaling of Dopamine D1 Receptor.* ***Chapter Four*** is a discussion of the overall findings of this Ph.D. thesis.

CHAPTER ONE: INTRODUCTION

1. The Dopaminergic System

Dopamine (DA) is a catecholaminergic neurotransmitter expressed in a variety of organisms, from simple invertebrates to the more complex networks of the mammalian central nervous system (CNS). DA modulates fundamental physiological functions from motor control to mood regulation through the binding and activation of its DA receptors. Dysfunction in DA activity or its receptors underly various pathological disorders, such as Parkinson's disease (PD) and schizophrenia. Research on the dopaminergic system remains highly dynamic and extremely important in the shaping of our understanding of the complexity of DA in health and disease, which bridges basic with clinical neuroscience.

1.1. History of Synapses

The brain is the most complex organ, and a hallmark of this complexity lies within its vast number of synapses. Synapses are fundamental structures linking neurons together and are highly complex at the molecular level, with more than 1,000 genes encoding postsynaptic proteins that reside within them (Bayés et al, 2011). In the late 1800's, Camillo Golgi described the mechanistic function of intracellular organelles (the Golgi apparatus) and developed a staining method utilizing silver nitrate to visualize cellular compartments (de Castro, 2019). This method, adopted by Santiago Ramón Cajal, led to groundbreaking studies on nervous system structure and function. Cajal provided the basis for our current knowledge that the nervous system is composed of independent entities called neurons, which are connected to each other over gaps termed synapses (de Castro, 2019). Cajal's classic drawing of the nervous system highlights the cytoarchitecture and connectivity of neurons. Cajal noted that the dendrites of Purkinje neurons were covered with small protrusions, called *espinas* "spines" that are essential for synaptic transmission (Yuste, 2015). Cajal hypothesized that synaptic transmission is fundamental in the processing and transfer of information throughout the nervous system (de Castro, 2019). In 1906, the Nobel Prize in Physiology or Medicine was awarded jointly to Camillo Golgi and Santiago Ramón y Cajal in recognition of their work on the structure of the nervous system.

1.1.1. Retrospective View of Synaptic Transmission

Information processing within neurons depends on the connectivity pattern of synapses. Henry Dale and Otto Loewi demonstrated chemical synaptic transmission in the peripheral nervous

system (Todman, 2008a). During the 1930's-40's, the theory that both chemical and electrical synapses exist, also known as *soups and sparks debate,* was heavily questioned. John Eccles, an electrophysiologist, believed that the transmission at synapses was too fast to be a chemical process, instead considering it to be strictly electrical, resisting many aspects of chemical transmission proposed by Henry Dale and others (Todman, 2008b). In retrospect, it can be appreciated that this scientific philosophy defined the problems of synaptic transmission and produced landmark discoveries. Eccles ultimately identified that excitatory and inhibitory postsynaptic potentials are initiated by the release of chemical neurotransmitters in the synaptic cleft (Brock et al, 1952). The crucial experiment conducted by Eccles in 1951 supporting this notion concluded that the level of inhibition (hyperpolarization) recorded within intracellular microelectrodes could not be induced electrically, but chemically (Todman, 2008b). The Nobel Prize in Physiology or Medicine was awarded jointly to Henry Dale and Otto Loewi in 1936 for their discoveries relating to chemical transmission of nerve impulses. John Eccles, along with Allen Hodgkin and Andrew Huxley, were awarded the 1963 Nobel Prize for Physiology or Medicine for their discoveries concerning the ionic mechanisms involved in excitation and inhibition within the peripheral and central portions of the nerve cell membrane.

1.2. Dopamine History

In the 1950s, the emergence of research on biogenic amines, including catecholamines (DA, norepinephrine (NE) "*noradrenaline*", and epinephrine "*adrenaline*"), histamine, and serotonin revealed the biological significance of these amines and the enzymatic activity of their synthesis. DA was first identified by George Barger and James Ewens in 1910, but it was Henry Dale who described its biological activity and coined its name (Barger and Ewine, 1910; Barger and Dale, 1910). Dale suggested the name "**dopamine**" (3,4-**d**ihydr**o**xy**p**henylethyl**amine**; 3-hydroxytyramine) and described it as a weak sympathomimetic epinephrine-like substance (Barger and Dale, 1910; Hornykiewicz 2002). The next major DA observation did not occur until three decades later when Peter Holtz discovered the aromatic L-amino acid decarboxylase (AADC) enzyme in 1938 which represents the turning point in catecholamine biosynthesis research (Holtz et al, 1938; Hornykiewicz, 2002). Then in 1939, Hermann Blaschko assigned DA as an intermediary in the synthesis of NE and epinephrine. Since then, many reports observed the occurrence of DA to be comparable to epinephrine in many peripheral tissues, but without having

regulatory effects (Blaschko, 1957; Björklund and Dunnett, 2006a). *"What is the physiological significance of DA?"* a hypothesis proposed by Blaschko in 1957, to which he concluded *"This suggests the possibility that DA has some regulating functions of its own which are not yet known"* (Blaschko, 1957). Shortly thereafter, Kathleen Montagu reported the sensational observation of DA occurrence in the brain by itself, and at levels significantly higher than NE and epinephrine (Montagu 1957). This followed by series of seminal discoveries that uncovered the complexity of DA neurochemical system. In the following subsections, I briefly highlight the significant observations contributed by some of the prominent DA scientists.

1.2.1. Arvid Carlsson (1923-2018)

In 1950s, Arvid Carlsson defined the dopaminergic neurotransmission and its physiological function. Carlsson elegantly discovered that DA is a *bona fide* neurotransmitter, independent of its role as a mere precursor in the synthesis of NE and epinephrine (Carlsson et al, 1958). In a landmark experiment, Carlsson demonstrated treatment of animals with the antipsychotic drug, reserpine, caused monoamine depletion, which rendered them in an akinetic state (Carlsson et al, 1957; Carlsson et al, 1958). Intriguingly, when Carlsson injected the DA precursor, L-3,4-dihydroxyphenylalanine (L-DOPA) to reserpine-treated animals, it was efficient to recover the DA levels in the brain, but not epinephrine, and furthermore, normalized the akinetic behavior (Carlsson et al, 1957; Carlsson et al, 1958; Carlsson, 1959; Carlsson, 2002). The following year, observations by Carlsson's students Åke Bertler and Evald Rosengren and others documented that DA is highly concentrated in the putamen and caudate of dorsal striatum, a structure containing non-NE neurons, thus providing further support that DA is a putative, independent neurotransmitter that might have central role in the control of motor function (Bertler and Rosengren, 1959; Sano et al, 1959). Carlsson was also instrumental in developing the "dopamine theory of schizophrenia" based on his observation of the antipsychotic effects of haloperidol and chlorpromazine to reduce dopaminergic activity (Carlsson and Lindqvist, 1963). Carlsson's pioneering research prevails the importance of dopaminergic system to modulate multiple physiological and pathophysiological conditions.

1.2.2. Oleh Hornykiewicz (1926-2020)

In 1960s, Oleh Hornykiewicz discovered the pivotal role of dopamine in motor behavior. Hornykiewicz examined the distribution of DA in human postmortem brains, which surprisingly

showed that the DA concentration was markedly and consistently reduced in the caudate and putamen of striatum in patients with PD (Ehringer and Hornykiewicz, 1960; Hornykiewicz 2002). Soon afterwards, Hornykiewicz initiated the first trials of L-DOPA therapy in PD patients and concluded that L-DOPA was highly effective in alleviating motor symptoms, a treatment nowadays still clinically efficacious (Birkmayer and Hornykiewicz, 1961; Hornykiewicz 2002). The excitement and enthusiasm of the outcome of this first trial of L-DOPA by Hornykiewicz can be inferred by his written description: *"The effect of a single i.v. administration of L-dopa was, in short, a complete abolition or substantial relief of akinesia. Bed-ridden patients who were unable to sit up; patients who could not stand up when seated; and patients who when standing could not start walking, performed after L-dopa all these activities with ease. They walked around with normal associated movements and they even could run and jump. The voiceless, aphonic speech, blurred by pallilalia and unclear articulation, became forceful and clear as in a normal person. For short periods of time, the patients were able to perform motor activities which could not be prompted to any comparable degree by any other known drug."* (Birkmayer and Hornykiewicz, 1961; Hornykiewicz, 2002). Hornykiewicz's fundamental discoveries of striatal DA deficiency in PD patients and the amelioration of patients' symptoms by L-DOPA therapy represent milestone events not only in the DA research, but also in the history of medicine.

1.2.3. Paul Greengard (1925-2019)

In 1970s-80s, Paul Greengard elucidated the molecular basis of signaling mechanisms involved in slow synaptic transmission. Greengard found that DA, among other neurotransmitters, stimulates membrane-bound adenylyl cyclase (AC), then transduces cellular responses to elevate the second messenger adenosine 3',5'-cyclic monophosphate (cAMP), which in turn activates protein kinase A (PKA) (Miyamoto et al, 1968; Kebabian and Greengard, 1971; Kebabian et al, 1972; Greengard 2001a, b). Greengard also showed that PKA activation causes phosphorylation of substrate proteins, which serve as downstream effectors for physiological functions such as neuronal excitability, synaptic transmission, plasticity, and gene expression (Greengard 2001a, b). Greengard explained the underlying mechanisms of synaptic transmission by which slow-acting neurotransmitter, such as DA, modulates the efficacy of fast synaptic transmission, presynaptically and postsynaptically (Greengard 2001a, b). Greengard also discovered the central regulatory protein DA and cAMP regulated phosphoprotein M.W. 32KDa (DARPP-32), which was initially

identified as a major integrator for DA-activated AC in striatum (Walaas et al, 1983; Greengard 2001a, b). Greengard demonstrated that, among various regulatory functions, DARPP-32 phosphorylation/dephosphorylation is regulated by dopaminergic and glutamatergic signaling in an opposite fashion, thereby dictating the action of downstream physiological effectors (Walaas et al, 1983; Halpain et al, 1990; Greengard 2001a, b). Greengard's research on neuronal communication and postsynaptic signaling were central in our current understating on the DA basis of physiological and pathophysiological functions.

1.2.4. Marc Caron (1946-2022)

Between 1980s and 2010s, Marc Caron identified the regulatory mechanisms of DA receptors from structure to function. Caron demonstrated the pharmacological affinity and selectivity of numerous ligands that bound to DA receptors. He purified and genetically cloned several DA receptors: D1 receptor (D1R) and D5 receptor (D5R) (De Lean et al, 1982; Amlaiky and Caron, 1986; Amlaiky et al, 1987; Senogles et al, 1988; Dearry et al, 1990; Tiberi et al, 1991; Tiberi and Caron, 1994). Caron also characterized and cloned DA transporter (DAT) and clarified its physiological function in normal and abnormal DA homeostasis relevant to neuropsychiatric diseases (Giros et al, 1991a; Giros et al, 1992; Giros et al, 1996). Caron contributed greatly to the field of G-protein coupled receptor (GPCR), with his long-term collaborator, Robert Lefkowitz, by discovering the mechanistic function of G-proteins, G-protein coupled receptor kinases (GRKs), β-arrestins (βArrs), and dynamin, as major mediators in the phosphorylation, desensitization, and trafficking of GPCRs, including DA receptors (Fergusson, et al, 1996a; Tiberi, et al, 1996; Zhang et al,1996; Zhang et al, 1999; Oakley et al, 2000; Kim et al, 2001). Caron illustrated the important role of β-arrestin2 (βArr2) in mediating DA responsiveness. The Caron's lab showed that βArr2 acts as the biochemical connection between D2R, protein kinase B (Akt), and protein phosphatase 2A (PP2A). This lithium-sensitive biochemical connection mediates some of DA related behaviors (e.g. locomotor activity) and may be of relevance in the treatment of neuropsychiatric disorders such as schizophrenia and mood disorders (Beaulieu et al, 2004; Beaulieu et al, 2005; Beaulieu et al., 2008). Caron also demonstrated that βArr2 has clinical analgesic implication, and the biased signalling for D2R/βArr2 complex reduces the adverse effects of antipsychotic drugs (Bohn et al, 1999; Bohn et al, 2000; Masri et al, 2008; Urs et al, 2011; Peterson et al, 2014). Caron's contributions have shaped in particular our understanding of the neuropsychopharmacology of DA

receptors, neurobiology of DA transporter, and in the biology of other GPCRs, by revealing their implications in normal physiology and diseases.

1.2.5. 2000 Nobel Prize in Physiology or Medicine

The landmark discoveries led by Arvid Carlsson and Paul Greengard awarded them the 2000 Nobel Prize in Physiology or Medicine. They clarified the role of DA and its receptor in the brain and developed comprehensive understanding into the regulation of dopaminergic signaling system. Research by other respected scientists as well such as Hyman Niznik, Philip Seeman, Oliver Civelli, Jean-Charles Schwartz, and others had a significant impact on the understanding of physiological and pathophysiological function of dopaminergic systems, which advanced the DA research and transformed the treatments of dopaminergic related diseases.

1.3. Dopamine Neuronal Homeostasis

Since the catecholamines cannot cross blood brain barrier (BBB), DA derivative amino acid tyrosine and L-DOPA trigger their biosynthesis in the presynaptic dopaminergic terminal, via different sequential enzymatic modulations (Carlsson, 1959; Hornykiewicz, 1966; Kopin, 1968; Axelrod and Weinshilboum, 1972; Elsworth and Roth, 1997). Pharmacological intervention of the DA processes in particular (synthesis, storage, release, reuptake, and degradation) and its receptors have been extensively examined to characterize the physiological functions of dopaminergic neurotransmission. *Fig. 1.1. summarizes the metabolic pathways of DA biosynthesis and biodegradation.*

1.3.1. Dopamine Synthesis

DA synthesis starts with tyrosine, a derivative of phenylalanine. Tyrosine hydroxylase (TH) catalyzes the conversion of tyrosine to L-DOPA, which is then decarboxylated to DA by the action of AADC (Blaschko, 1957; Hess et al, 1961; Nagatsu, et al, 1965a, b; Hornykiewicz 1966; Kopin, 1968; Elsworth and Roth, 1997; Verhiej and Cools, 2008). Cytosolic DA is transported into synaptic vesicles by vesicular monoamine transporter 2 (VMAT2) (Blaschko, 1957; Lovenberg, et al, 1962; Kopin, 1968; Christenson et al, 1972; Kelly 1993; Elsworth and Roth, 1997; Verhiej and Cools, 2008). In non-dopaminergic neurons, DA can be modified into NE and epinephrine by DA β-hydroxylase (DβH) and phenylethanolamine N-methyltransferase (PNMT), respectively

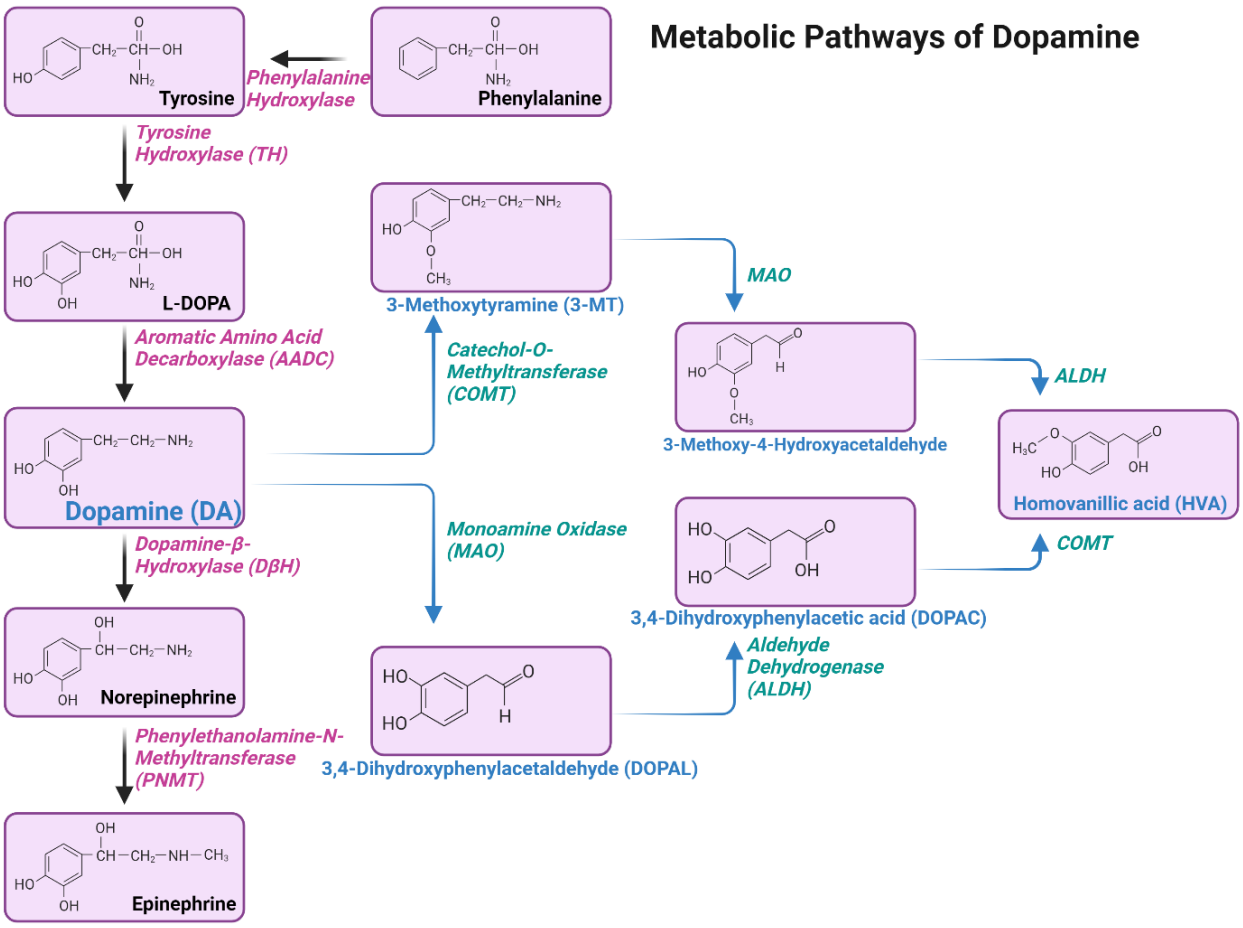

Fig. 1.1. Schematic Summary of DA Biosynthesis and Degradation.
Tyrosine produced from phenylalanine through the action of phenylalanine hydroxylase, followed by the hydroxylation of tyrosine by TH to generate L-DOPA. L-DOPA is converted to DA by AADC. DβH hydroxylates DA to form NE, which is converted to epinephrine by PNMT. DA is primarily metabolized by COMT and MAO. COMT converts DA to 3-MT, which is subsequently converted to 3-methoxy-4-hydroxyacetaldehyde by MAO, then HVA by the action of ALDH. In the other pathway, MAO converts DA to DOPAL, which is then converted by ALDH to DOPAC. DOPAC is then degraded to HVA by the COMT. TH: tyrosine hydroxylase; AADC: aromatic amino acid decarboxylase; L-DOPA: L-3,4-dihydroxyphenylalanine; DA: dopamine; DβH: dopamine beta hydroxylase; NE: norepinephrine; PNMT: phenylethanolamine-N-methyltransferase; COMT: catechol-O-methyltransferase; 3-MT: 3-methoxytyramine; MAO: monoamine oxidase; DOPAL: 3,4-dihydroxyphenylacetaldehyde; ALDH: aldehyde dehydrogenase: DOPAC: 3,4-dihydroxyphenylacetic acid; HVA: homovanillic acid. Created with BioRender.com.

(Blaschko, 1957; Levin et al, 1960; Kirshner, 1962; Hornykiewicz, 1966; Kopin, 1968). During catecholamine synthesis, α-methyl-p-tyrosine (αMPT) and carbidopa can block the rate-limiting enzyme TH and L-DOPA decarboxylase, respectively (Nagatsu et al, 1965b; Sjoerdsma et al, 1965; Ewing et al, 1983; Butcher et al, 1988; Leviel et al, 1989; Verhiej and Cools, 2008). The vesicular storage of bioamines, including DA, are blocked by antipsychotic compounds; reserpine (long-lasting, irreversible) and tetrabenazine (transient and reversible) (Carlsson et al, 1957; Carlsson et al, 1958; Krishner 1962; Kirshner et al, 1963; Butcher et al, 1988; Leviel et al, 1989; Verhiej and Cools, 2008).

1.3.2. Dopamine Release

DA is released mainly by exocytosis, and upon an action potential (AP), a change in membrane protein conformation allows influx of calcium ions (Ca^{2+}) into the neuronal terminal, which is responsible for the fusion of DA vesicles onto the presynaptic membrane and then release of vesicle's contents to synaptic cleft (McLennan, 1965; Katz and Miledi, 1967; Besson et al, 1969; Katz and Miledi, 1970; Javoy and Glowinski, 1971; Moore and Von Voigtlander 1971; Bunny et al, 1973; Raiteri et al, 1979; Ewing et al, 1983; McMillen 1983; Butcher et al, 1988; Leviel et al, 1989; Wolf and Roth, 1990; Kelly, 1993; Verhiej and Cools, 2008). DA release via exocytosis is dependent on the neuronal firing of presynaptic terminals, and is also released independently of Ca^{2+} by reverse transport; a process by which amphetamine inhibits the storage of DA in vesicles, thus enhancing the cytoplasmic release of DA via DAT (Moore and Von Voigtlander 1971; Raiteri et al, 1979; McMillen, 1983; Butcher et al, 1988; Leviel et al, 1989; Shimada et al, 1991; Kilty et al, 1991; Usdin et al, 1991; Giros et al, 1991a; Giros et al, 1992; Giros and Caron, 1993; Elsworth and Roth, 1997). The diffused DA across the synaptic cleft activates DA receptors localized either at postsynaptic membrane to propagate signaling pathways, or presynaptic autoreceptors via negative feedback to inhibit neurotransmitter release (Kehr et al, 1972; Wolf and Roth, 1990; Giros and Caron, 1993; Elsworth and Roth, 1997; Verhiej and Cools, 2008).

1.3.3. Dopamine Reuptake and Degradation

The postsynaptic effects of DA on DA receptors are regulated presynaptically by DAT and postsynaptically by catechol-O-methyltransferase (COMT). Extracellular DA in the synaptic cleft is cleared and transported back (reuptake) into presynaptic neurons by DAT, where it undergoes the same regulatory process of recycling DA into vesicles or metabolizing DA into 3,4-

dihydroxyphenylacetic acid (DOPAC) by intraneuronal monoamine oxidase (MAO) (McMillen, 1983; Leviel et al, 1989; Shimada et al, 1991; Kilty et al, 1991; Usdin et al, 1991; Giros et al, 1991a; Giros et al, 1992; Giros and Caron, 1993; Elsworth and Roth, 1997). NE transporter (NET) also regulates the reuptake of extracellular DA, but with much lower affinities than DAT, and/or in regions where DAT densities are restricted such as prefrontal cortex (PFC) (Morón et al, 2002; Costa and Schoenbaum 2022). Excess of DA on postsynaptic neurons is initially metabolized to 3-methoxytyramine (3-MT) by COMT, and further degraded to homovanillic acid (HVA) by extracellular MAO (McMillen, 1983; Elsworth and Roth, 1997). Both amphetamine and cocaine, which are psychostimulant drugs that promote DA activity, and nomifensine inhibit the synaptic reuptake of DA by DAT (McMillen, 1983; Butcher et al, 1988; Shimada et al, 1991; Kilty et al, 1991; Usdin et al, 1991; Giros et al, 1991a; Sulzer et al, 1993; Giros and Caron, 1993; Verhiej and Cools, 2008). The activity of MAO can be inhibited by rasagiline and deprenyl (selegiline), while COMT function is blocked by tolcapone and entacapone (Butcher et al, 1988). *Fig. 1.2. depicts the sequential enzymatic steps in DA biosynthesis, and pharmacological intervention at the dopaminergic synapse.*

1.4. Presynaptic Regulation of Dopamine Neurotransmission

The presynaptic control of DA neurotransmission is mediated by many components, including DA autoreceptors, DAT, VMAT2, and TH on dopaminergic neurons (Glowinski et al, 1988; Schmitz et al, 2003; Zhang and Sulzer, 2012; Costa and Schoenbaum, 2022). As described above, extracellular DA level results from a dynamic equilibrium between release and reuptake of dopaminergic terminals to modulate numerous physiological functions. Dysfunctions of presynaptic neurotransmission are implicated in a broad range of behaviors and disorders, such as PD, and schizophrenia (Glowinski et al, 1988; Schmitz et al, 2003; Zhang and Sulzer, 2012; Costa and Schoenbaum, 2022). The following subsections highlight the importance of DA autoreceptors, DAT, VMAT2, and TH in regulating presynaptic transmission.

1.4.1. Presynaptic Regulation of Dopamine Autoreceptors

DA neurons exhibit self-inhibitory activity that is controlled by presynaptic DA autoreceptors of D2-class receptors, localized at the axon terminals and somatodendritic compartments (Roth, 1984; Glowinski et al, 1988; Wolf and Roth, 1990; Feuerstein, 2008; Zhang and Sulzer, 2012;

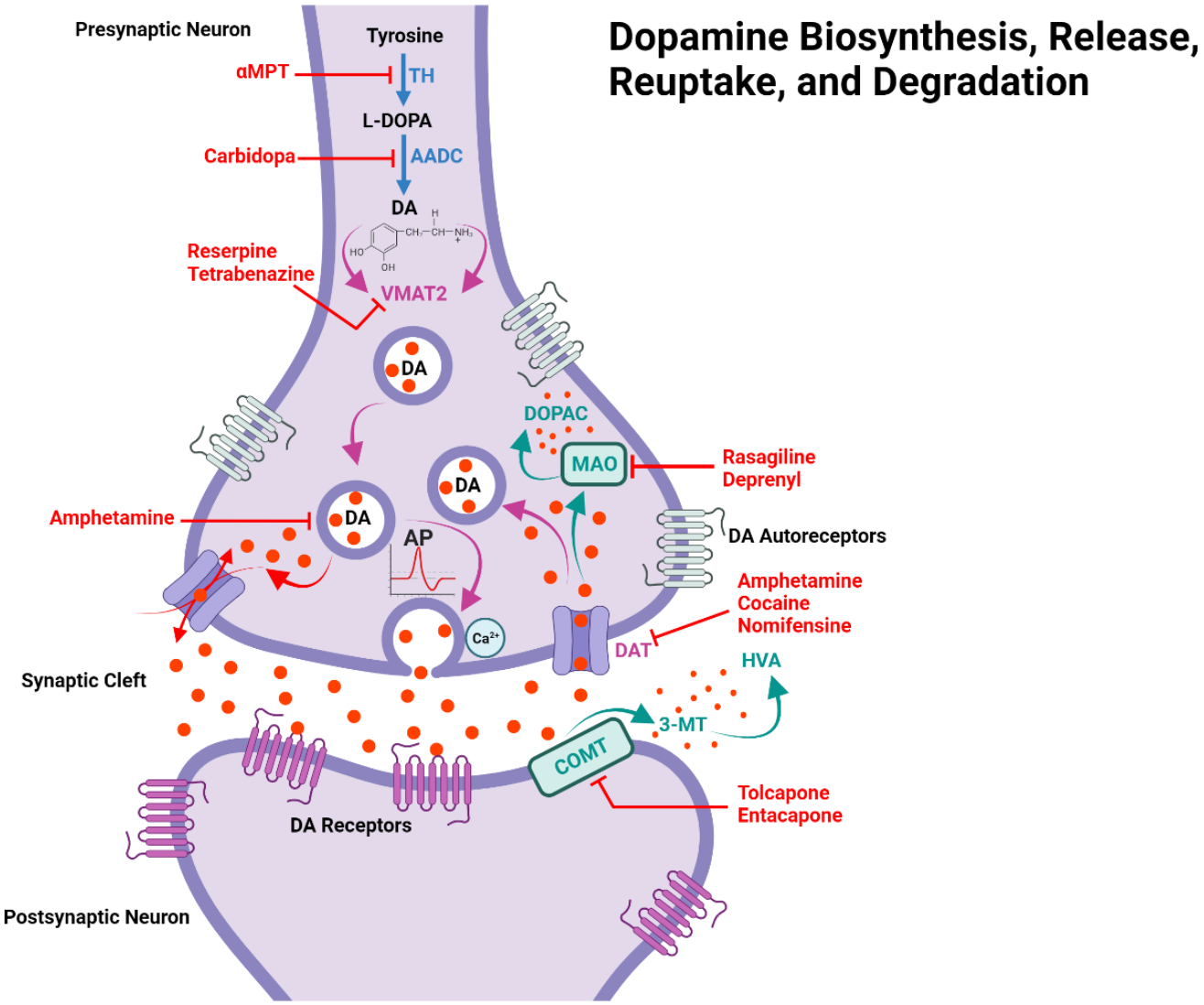

Fig. 1.2. Dopamine Biosynthesis in the Presynaptic Neuron.
DA synthesis in the presynaptic neurons starts with tyrosine. Tyrosine is converted to L-DOPA by TH and then AADC converts L-DOPA to DA. The key steps in the synthesis and degradation of DA. Once DA is produced, it is stored into vesicles by VMAT2. Upon an action potential (AP), DA is released into the synaptic cleft where it can bind to postsynaptic DA receptor or presynaptic autoreceptors. Excess DA can be reuptaken by DAT or metabolized by MAO and COMT. Drugs inhibiting associated activities of DA synthesis, release, reuptake, and degradation are in red. TH: tyrosine hydroxylase; AADC: aromatic amino acid decarboxylase; L-DOPA: L-3,4-dihydroxyphenylalanine; DA: dopamine; VMAT2: vesicular monoamine transporter 2; DAT: dopamine transporter; COMT: catechol-O-methyltransferase; 3-MT: 3-methoxytyramine; MAO: monoamine oxidase; DOPAC: 3,4-dihydroxyphenylacetic acid; HVA: homovanillic acid. Created with BioRender.com.

Costa and Schoenbaum, 2022). DA, in the synapse, binds and activates the presynaptic autoreceptors at axonal terminals to negatively regulate the feedback inhibition that result in a reduction of further DA synthesis and release (Roth, 1984; Glowinski et al, 1988; Wolf and Roth, 1990; Giros and Caron, 1993; Feuerstein, 2008). The main mechanism of DA autoreceptors is to maintain the optimal level of DA in the synapse, and prevent excessive DA release (Roth, 1984; Glowinski et al, 1988; Giros and Caron, 1993). Carlsson and others provided the first evidence for the existence of presynaptic autoreceptors, at which released DA can act to exert feedback inhibition of DA synthesis (Farnebo and Hamberger, 1971; Kehr et al, 1972; Glowinski et al, 1988; Wolf and Roth, 1990; Giros and Caron, 1993). DA can also be released from somatodendritic sites to exert its inhibitory effect through autoreceptors, which regulate dopaminergic and non-dopaminergic neurons (Björklund and Lindvall, 1975; Geffen et al, 1976; Cheramy et al, 1981). The dendrites have the capacity to synthesize, store, and release DA, but differ from the axon terminals as they contain very few vesicles and no transporter (Cheramy et al, 1981). In addition, activation of DA autoreceptors modulate the activity of DAT, VMAT2, and TH, which will be discussed in the following subsections (Glowinski et al, 1988; Giros and Caron, 1993; Schmitz et al, 2003; Zhang and Sulzer, 2012).

DA autoreceptors belong to D2-class receptors (D2 receptor “D2R”, D3 receptor “D3R”, D4 receptor “D4R”), and their activity is predominantly carried out by D2R, with a putative contribution of D3R (Meller et al, 1993; Lejeune and Millan, 1995; Kreiss et al, 1995; Gainetdinov et al, 1996; Tepper et al, 1997; Joseph et al, 2002; Schmitz et al, 2003; Zhang and Sulzer, 2012). D2R are expressed at the axon terminals and along the somatodendritic part of midbrain dopaminergic neurons (Schmitz et al, 2003; Zhang and Sulzer, 2012). Of two isoforms generated by alternative splicing of D2R; D2R-short (D2S) dominating the presynaptic expression, and D2R-long (D2L) primarily present postsynaptically (Khan et al, 1998; Usiello et al, 2000; Centonze et al, 2002; Schmitz et al, 2003; Lindgren et al, 2003; Zhang and Sulzer, 2012). DA autoreceptors can be anatomically and pharmacologically distinguished from postsynaptic receptors on the modulation of DA neurotransmission (Wolf and Roth, 1990; Goldstein et al, 1990; Khan et al, 1998; Usiello et al, 2000; Centonze et al, 2002; Schmitz et al, 2003; Zhang and Sulzer, 2012). Moreover, D2R-deficent mice exhibited no detectable autoreceptors response to D2R agonist in firing rate, DA release, or DA synthesis (L'hirondel et al, 1998; Dickinson et al, 1999; Schmitz et al, 2002; Schmitz et al, 2003; Bello et al, 2011; Zhang and Sulzer, 2012). However, presynaptic

response to D2R agonist was preserved in D2L-deficient mice, indicating that D2S mediates presynaptic autoreceptor activity (Usiello et al, 2000; Centonze et al, 2002). These findings support that DA autoreceptors provide the midbrain DA neuron with a complex feedback system at the soma and axon ending that is important for physiological behavioral functions (Feuerstein, 2008; Zhang and Sulzer, 2012).

1.4.2. Presynaptic Regulation of Dopamine Transporter

The DAT activity plays a major role in the regulation of DA neurotransmission by the reuptake of DA to presynaptic dopaminergic neurons (Giros and Caron, 1993; Miller et al, 1999; Gainetdinov et al, 2002; Schmitz et al, 2003). DAT is a biogenic amine transporter of SLC6A3 of solute carriers, with twelve putative transmembrane domains at the presynaptic plasma membrane (Shimada et al, 1991; Kilty et al, 1991; Usdin et al, 1991; Giros et al, 1991a; Giros and Caron, 1993; Pramod et al, 2013). DA autoreceptors and DAT collectively regulate the level of DA in the synapse and contribute to the termination of dopamine signaling (Giros and Caron, 1993; Cass and Gerhardt, 1994; Rothblat and Schneider, 1997; Dickinson et al, 1999; Schmitz et al, 2003; Zhang and Sulzer, 2012). Activation of DA autoreceptors reduces DAT function, leading to decrease in DA reuptake and increase DA contents in the synapse (Cass and Gerhardt, 1994; Rothblat and Schneider, 1997; Schmitz et al, 2003; Zhang and Sulzer, 2012). D2R-mutant mice were found to have decreased striatal DAT function, but not its binding expression, suggesting that D2R modulates clearance activity of the striatal DAT (Dickinson et al, 1999). DAT is also sensitive to psychostimulant drugs, which significantly induce extracellular DA concentration in the synapse (Shimada et al, 1991; Kilty et al, 1991; Usdin et al, 1991; Giros et al, 1991a; Giros and Caron, 1993; Giros et al, 1996; Jones et al, 1998; Rocha et al, 1998; Benoit-Marand et al, 2000). Genetic alteration of DAT in mice results in disrupted clearance of DA, elevation of extracellular DA concentration, spontaneous hyperlocomotion, and decrease in neurotransmitter and receptor level (Giros et al, 1996; Jones et al, 1998; Rocha et al, 1998; Benoit-Marand et al, 2000). Psychostimulants, however, have no effect on locomotor activity or DA release and reuptake in these deficient mice (Giros et al, 1996; Jones et al, 1998; Rocha et al, 1998; Benoit-Marand et al, 2000). These observations demonstrate the significant role of DAT in regulating DA neurotransmission, and its dysregulation is implicated in several dopaminergic diseases (Giros et al, 1996; Benoit-Marand et al, 2000; Gainetdinov et al, 2002).

1.4.3. Presynaptic Regulation of Vesicular Monoamine Transporter 2

The activity of VMAT2 on presynaptic neurons is an essential function to maintain physiological monoaminergic neurotransmission, by packaging respective monoamines from cytoplasm into secretory vesicles (Schmitz et al, 2003). In dopaminergic neurons, VMAT2 provides intracellular protection from neurotoxins by maintaining low cytosolic level of DA required for normal function (Miller et al, 1999; Schmitz et al, 2003). VMAT2 is a reserpine-sensitive transporter with twelve domains, known as SLC18A2 (Erickson et al, 1992; Pramod et al, 2013). Activation of DA autoreceptors decreases the activity of VMAT2, thereby decreasing the packaging of DA into vesicles (Miller et al, 1999; Brown et al, 2001; Brown et al, 2002; Schmitz et al, 2003). This feedback mechanism prevents excessive DA release by retaining optimal DA level in the synapse (Miller et al, 1999; Schmitz et al, 2003). D2-autoreceptors labeling is expressed in most dendrites that contain VMAT2 storage vesicles, thus D2R regulate the dendritic VMAT2 expression and allow DA release from somatodendritic sites (Pickel et al, 2002; Schmitz et al, 2003). VMAT2 is sensitive to amphetamine, thus it inhibits the storage of DA in vesicles, and enhances the cytoplasmic release of DA via DAT (Miller et al, 1999). The genetic deletion of VMAT2 reveals its obligatory role in maintaining monoaminergic neurotransmission (Fon et al, 1997; Wang et al, 1997). The homozygous mice of VMAT2 deficient were lethal, manifesting severely impaired monoamine storage and vesicular release, whereas the heterozygous mice exhibit reduced vesicular filling and release (Fon et al, 1997; Wang et al, 1997; Patel et al, 2003). $VMAT2^{+/-}$ mice show diminished extracellular DA levels but enhanced sensitivity to DA receptors (Wang et al, 1997). Overall, VMAT2 is crucial in monoaminergic neurotransmission, and involved in various physiological and pathological processes.

1.4.4. Presynaptic Regulation of Tyrosine Hydroxylase

The TH is a rate-limited enzyme involved in the biosynthesis of catecholamine neurotransmitters, and it regulates the presynaptic catecholaminergic neurotransmission (Blaschko, 1957; Masserano and Weiner, 1983; Wolf and Roth, 1990; Schmitz et al, 2003). TH is responsible for the initial step in DA synthesis, which converts tyrosine into L-DOPA, a precursor for DA (Blaschko, 1957; Masserano and Weiner, 1983; Wolf and Roth, 1990; Schmitz et al, 2003). Feedback inhibition of presynaptic neuron mediated by activation of DA autoreceptors inhibit TH, thereby decrease the DA synthesis (el Mestikawy et al, 1986; el Mestikawy and Hamon, 1986; Onali and Olianas, 1989;

Wolf and Roth, 1990; Goldstein et al, 1990; Schmitz et al, 2003). TH is also regulated by transcriptional factors and posttranslational modifications, which thus influence TH activity and the synthesis of catecholamine neurotransmitters (Masserano and Weiner, 1983; el Mestikawy and Hamon, 1986; Onali and Olianas, 1989; Goldstein et al, 1990; Schmitz et al, 2003). Moreover, DA-deficient mice (DD mice; selective deletion of TH gene in DA neurons) are severely hypoactive, adipsic, and aphagic, and required systemic administration of L-DOPA for survival, implying that DA is essential for movement and feeding (Zhou and Palmiter, 1995; Szczypka et al, 1999; Paladini et al, 2003). In addition, the behavioral phenotype of acute administration of TH inhibitor, αMPT, to DAT-KO mice/rats caused severe depletion of DA (DA-deficient DAT-KO: DDD models) and demonstrate severe akinesia, rigidity, and tremor (Sotnikova et al, 2006; Sukhanov et al, 2022). Due to loss of inward transport in DDD mice, the concentration of DA in striatal terminals becomes extremely sensitive to pharmacologic inhibition of DA synthesis by TH inhibitor (Sotnikova et al, 2006). Administration of high concentration of L-DOPA or in combination with carbidopa restored the motor functions of DDD models (Sotnikova et al, 2006; Sukhanov et al, 2022). The presynaptic regulation of TH is important for comprehending the control of monoamines, and dysregulation of TH activity and expression can have significant implications for various neurological and psychiatric disorders (Schmitz et al, 2003).

Moreover, TH expression is a hallmark for catecholaminergic neurons and involved in various function, including neural plasticity, motor control, reward, and cognition (Björklund and Dunnett, 2007b). TH-positive catecholaminergic neurons co-localized with AADC and VMAT2 (Björklund and Dunnett, 2007b). However, a subpopulation of TH-positive neurons express AADC, but not VMAT2 in striatum and cerebral cortex (Ikemoto et al, 1999; Ershov et al, 2002; Ershov et al, 2005; Weihe et al, 2006). Another subset of TH-positive neurons expressing neither AADC nor VMAT2 were identified in hypothalamus, cerebral cortex, and spinal cord (Weihe et al, 2006). A smaller population of dopaminergic neurons does not express TH but utilizes AADC to convert L-DOPA in arcuate nucleus of hypothalamus (Ershov et al, 2002; Ershov et al, 2005). The diversity of dopaminergic neuron subtypes highlights the complexity of the dopaminergic system and its functional roles in various regions of the brain (Björklund and Dunnett, 2007b).

1.4.5. Presynaptic Regulation of Heteroreceptors on Dopaminergic Neurons

The dynamic interaction between DA and other neurotransmitters in the synapse are widely investigated and have several important physiological and pathological processes (Björklund and Lindvall, 1975; Cheramy et al, 1981; Roth, 1984; Glowinski et al, 1988; Feuerstein, 2008; Zhang and Sulzer, 2012; Trudeau et al, 2014; Trudeau and El Mestikawy, 2018; Costa and Schoenbaum 2022). DA autoreceptors modulate the exocytotic release of other neurotransmitters, e.g., NE, glutamate, γ-amino butyric acid (GABA), serotonin (5-HT), and acetylcholine (ACh) (Björklund and Lindvall, 1975; Cheramy et al, 1981; Roth, 1984; Glowinski et al, 1988; Feuerstein, 2008; Zhang and Sulzer, 2012; Trudeau et al, 2014; Mamaligas and Ford, 2016; Trudeau and El Mestikawy, 2018; Cai and Ford, 2018; Costa and Schoenbaum 2022). Presynaptic receptors also occur as heteroreceptors on non-dopaminergic axon terminals (Feuerstein, 2008; Zhang and Sulzer, 2012). The crosstalk between DA•glutamate and DA•GABA are most abundant among other neurotransmitters, and have significant behavioral functions, including synaptic plasticity, neural circuits, neurodegenerative disease, and psychiatric disorders (Feuerstein, 2008; Zhang and Sulzer, 2012; Trudeau et al, 2014; Trudeau and El Mestikawy, 2018). DA presynaptically inhibits the release of glutamate and GABA in striatum through D2-auroreceptors and postsynaptic D2R (Delgado et al, 2000; Pisani et al, 2000; Momiyama and Koga, 2001; Gainetdinov et al, 2001; Guzmán et al, 2003; Bamford et al, 2004; Ibañez-Sandoval et al, 2006; Hernández et al, 2006; Feuerstein, 2008). The significant of these DA release and DA autoreceptors into multiple presynaptic regulatory mechanisms maintain normal physiological functions to control DA neurotransmission and signaling (Feuerstein, 2008; Zhang and Sulzer, 2012; Trudeau et al, 2014; Trudeau and El Mestikawy, 2018).

A subpopulation of midbrain dopaminergic neurons are highly heterogenous at axonal ending (Feuerstein, 2008; Zhang and Sulzer, 2012; Trudeau et al, 2014; Trudeau and El Mestikawy, 2018). These neurons express vesicular glutamate transporter 2 (VGLUT2) or vesicular GABA transporter (VGAT), in addition to VMAT2, which allow them to co-release DA and other transmitters; glutamate and GABA, respectively (Giorguieff et al, 1977; Sulzer et al, 1998; Chéramy et al, 1998; Chuhma et al, 2004; Dal Bo et al, 2004; Mendez et al, 2008; Hnasko et al, 2010; Tritsch et al, 2012; Fortin et al, 2012; Trudeau et al, 2014; Thibault et al, 2016; Trudeau and El Mestikawy, 2018; Kouwenhoven et al, 2020; Liu et al, 2022). The release of glutamate and

GABA indirectly play a prominent role in dopaminergic neurons to regulate postsynaptic DA signaling and to modulate presynaptic regulation of DA release (Giorguieff et al, 1977; Chéramy et al, 1998; Trudeau et al, 2014; Trudeau and El Mestikawy, 2018; Costa and Schoenbaum 2022). Moreover, in DAT-deficient mice, the expression of vesicular glutamate transporter 1 (VGLUT1) is enhanced, and the activation of N-methyl-D-aspartate receptor (NMDAR) regulates the glutamatergic transmission and inhibits psychostimulant-mediated hyperactivity (Gainetdinov et al, 2001; Targa et al, 2023). This supports the concept of a reciprocal DA•glutamate functional interaction in modulating glutamatergic transmission (Gainetdinov et al, 2001). Furthermore, DA released from somatodendritic compartments regulate the presynaptic release of GABA from GABAergic neurons. GABA is also released directly from dopaminergic and GABAergic neurons independently from VGAT, which requires activity of VMAT2 (Tritsch et al, 2012). Interestingly, expression of VGLUT2 and vesicular glutamate transporter 3 (VGLUT3) modulates presynaptic and postsynaptic dopaminergic neurons, which suggests DA neurotransmission is influenced by glutamatergic neurons (Hnasko et al, 2010; Trudeau and El Mestikawy, 2018; Ibrahim et al, 2022). Moreover, genetic deletion of NET displayed behavioral alterations in response to antidepressants and psychostimulants (Xu et al, 2000). NET deficient mice also exhibited a reduction in striatal presynaptic DA and its metabolites, but enhanced sensitivity to postsynaptic D2R and D3R agonists (Xu et al, 2000). Collectively, these findings expand the repertoire of synaptic mechanisms that is crucial for unraveling the complexities of the intricate interplay between these neurotransmitter systems and suggest the existence of numerous microcircuits involved in the regulation of DA transmission (Trudeau and El Mestikawy, 2018).

1.5. Dopamine Receptors

Once DA is synthesized and released in the synapse, it exerts its actions on a neuronal cell through one of five cognate genetically distinct subtype receptors, of which have been classified to either D1-class receptors (D1R and D5R, also previously known as D1A and D1B, respectively), or D2-class receptors (D2R, D3R, D4R). This classification originally proposed by Kebabian and Calne, in 1979, is based on biochemical observation that distinguishes D1R from D2R modulation on G-proteins coupling AC (Kebabian and Calne, 1979). Earlier discoveries recognized that DA activates two distinct physiological populations at the postsynaptic neuron, stimulatory and inhibitory, and thus were named as excitatory DA receptors (DAe “stimulatory”) and inhibitory

DA receptors (DAi) (Cools and Van Rossum, 1976; Cools and Van Rossum, 1980). Shortly thereafter, DAe and DAi receptors were renamed as D1R and D2R, respectively (Garau et al, 1978; Titeler, et al, 1978; Kebabian and Calne, 1979; Giros and Caron, 1993; Neve et al, 2004; Beaulieu and Gainetdinov, 2011).

Biochemical characterization of DA receptors began with the discovery of DA-stimulated AC (Kebabian and Greengard, 1971). In a series of experiments in the 1970s, Kebabian and Greengard noted that incubation of caudate nucleus homogenates of striatum with DA activates AC and increases the level of cAMP formation (Kebabian et al, 1972). This was the first evidence of stimulatory DA receptor-mediated cAMP increase in the brain, which was followed by reports showing DA-sensitive AC in different brain regions (Clement-Cormier et al, 1974; Clement-Cormier et al, 1975; Mishra et al, 1975; Phillipson and Horn, 1976). However, many reports also suggested the existence of a second population, perhaps a non-stimulatory DA receptor present in brain (Iversen, 1975; Seeman et al, 1975; Seeman and Lee, 1975; Cools and Van Rossum, 1976; Caron et al, 1978; Kebabian and Clan, 1979; Cools and Van Rossum 1980). De Camilli and colleagues showed DA-inhibited AC activity and decreased prolactin secretion from pituitary gland (De Camilli et al, 1979). Stoof and Kebabian observed a biphasic regulation of cAMP efflux in neostriatum: a stimulation and an inhibition of AC mediated by D1R and D2R, respectively (Stoof and Kebabian, 1981). This opposing effect suggested that D1R and D2R exist as two distinct DA receptor populations expressed within the same medium spiny neurons ("MSNs", also known as spiny projection neuron "SPN") in neostriatum, where they positively or negatively control AC activity, respectively, to modulate physiological processes. Although this was the original thinking, the colocalization of D1R and D2R in the same neuron is attributed to a small group of striatal neurons, while the vast majority of MSNs express either D1R or D2R (Gerfen et al, 1990), which will be further discussed in section 1.6.1.2.

Further studies have characterized the role of D1R and D2R by molecular cloning and purification methods. D2R was the first dopaminergic receptor to be cloned and characterized (Bunzow et al, 1988; Grandy et al, 1989a; Giros et al, 1989; Monsma et al, 1989), followed by molecular cloning of D1R (Monsma et al, 1990; Sunahara et al, 1990; Dearry et al, 1990; Zhou et al, 1990). Subsequent research have identified different genes, encoding for additional dopamine subtype receptors; D3R (Sokoloff et al, 1990), D4R (Van Tol et al, 1991), D5R (Sunahara et al, 1991;

Tiberi et al, 1991). Nowadays, D1- and D2-class receptors are further classified beyond G-protein coupling and AC activity, by their gene expression, biochemical, structural, and pharmacological properties, and their anatomical localization. *Fig.1.3A, B. shows the signaling differences between D1- and D2-class receptors and pharmacological ligands bound-DA receptors.*

These DA receptors can modulate different physiological functions, e.g. motor activity, learning, reward, and memory (Missale et al, 1998; Beaulieu and Gainetdinov, 2011). Therefore, pharmacologically targeting these receptors has provided further insight on significantly influencing dopaminergic transmission and DA-dependent functions in the treatment of various disorders (Missale et al, 1998; Beaulieu and Gainetdinov, 2011).

1.5.1. Genes Encoding for Dopamine Receptors

The D1- and D2-class receptors are derived from the divergence of two gene families, and primarily differ in the presence of introns at the level of genetic structure, which accounts for the presence of splice variants among this receptor/protein population (Civelli et al, 1993; Schwartz et al, 1993). Genetic analysis has identified polymorphisms of these DA receptor genes that may have potential implications for susceptibility to disease, pharmacogenetic outcome, or undesirable effects to therapeutic agents (Wong et al, 2000).

DRD1 and *DRD5* genes encode for D1-class receptor subtypes and are intron-less genes, thus D1R and D5R exist as a single isoform (Sunahara et al, 1990; Civelli et al, 1993; Schwartz et al, 1993). *DRD1* gene is located at chromosome 5q35.1; five polymorphisms have been identified, but none are associated with functional changes (Sunahara et al, 1990; Grandy et al, 1990; Liu et al, 1995; Wong et al, 2000; Al-Fulaij et al, 2008). *DRD5* gene is located at chromosome 4p15.1-p15.3, and two of nine polymorphisms reported for D5R altered the ligand properties (Sherrington et al, 1993; Sobell et al, 1995; Wong et al, 2000). Two pseudogenes for D5R have been identified, D5ψ1 and D5ψ2, which encode for a truncated nonfunctional receptor (Grandy et al, 1991; Wong et al, 2000). A recent genetic study conducted in a large human cohort from United Kingdom reveals the presence of a wide range of polymorphisms in the coding sequence of *DRD1* and *DRD5* genes (Hauser et al, 2018). While individuals screened for D1R and D5R polymorphisms did not have any overt pathological conditions, the study argued that these polymorphisms may impact the pharmacogenomic responsiveness of DA drugs (Hauser et al, 2018).

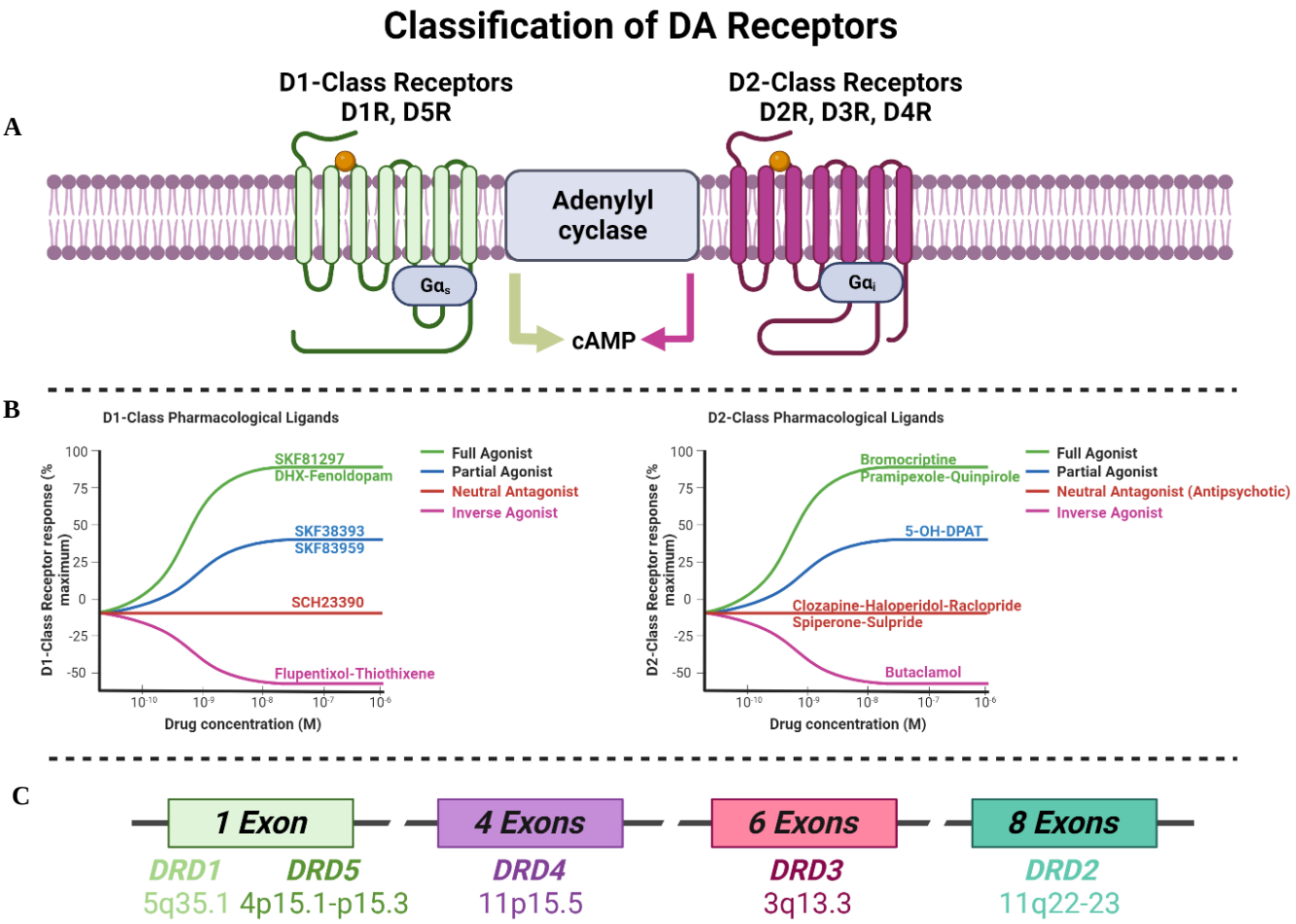

Fig. 1.3. Classification of DA Receptors.

(A) Activation of AC by D1- and D2-class receptors increase and decrease the level of cAMP, respectively. (B) DA receptors exist in a dynamic equilibrium between in active and active state in response to pharmacological ligands. The classical ligands bound-DA receptors are listed. Some ligands, however, may exhibit different affinity towards the receptor than the norm paradigm. (C) Illustrative summary of genetic differences of DA receptors, including number of exon(s) and chromosomal location. AC: adenylyl cyclase; cAMP, adenosine 3′,5′- cyclic monophosphate. Created with BioRender.com.

In contrast, *DRD2*, *DRD3*, and *DRD4* genes, which encode for D2-class receptor subtypes, have several introns (Civelli et al, 1993; Schwartz et al, 1993). The genetic organization of these receptor genes provide the basis for generating receptor splice variants in their coding sequences (Civelli et al, 1993; Schwartz et al, 1993). *DRD2* gene is located on chromosome 11q22-23 and consists of eight exons separated by seven introns (Grandy et al, 1989b; Wong et al, 2000). Alternative splicing in exon 5 of the *DRD2* gene leads to the generation of two functional isoforms: D2S and D2L, which harbours an additional 29 amino acids (87 base pair "bp") in intracellular loop 3 (IL3) of D2R (Giros et al, 1989; Monsma et al, 1989). Although these two functional variants of D2R mediate the control of basal behaviors, both isoforms mediate specific physiological functions, exhibit distinct anatomical localization, pre- and post-synaptic function, and pharmacological properties (Radi et al, 2018). Several polymorphisms were reported to change the function for *DRD2* gene that may be associated with variation in the levels of D2R expression, but the phenotypic differences linking susceptibility to alcoholism, abuse of other substances, and schizophrenia are inconsistent (Gejman et al, 1994; Wong et al, 2000).

DRD3 gene is located on chromosome 3q13.3, and its coding sequence consists of six exons, interrupted by five introns (Le Coniat et al, 1991). In humans, the Ser9Gly variant of D3R was reported to have functional and pharmacological importance. Several other nonfunctional splice variants and polymorphisms were identified (Giros et al, 1991b). There are no significant genetic and phenotypic linkages of schizophrenia and psychosis to either the D3Ser9 variant (allele 1) or the D3Gly9 variant (allele 2) (Crocq et al, 1992; Rietschel et al, 1993; Wong et al, 2000). *DRD4* gene is located on chromosome 11p15.5, and contains a remarkable number of polymorphic regions (Gelernter et al, 1992; Wong et al, 2000). The *DRD4* gene consist of four exons separated by three introns. Within the DRD4 coding sequence, there is a hypervariable region in IL3 of 2-10 imperfect 48 bp repeats, and is written as D4.x receptor, where x represents number of repeats (Van Tol et al, 1992; Asghari et al, 1994; Wong et al, 2000). Variations in the D4R sequence have been studied in relation to a variety of neuropsychiatric diseases and phenotypes, but no strong association has been linked to *DRD4* gene (Wong et al, 2000). *Fig.1.3C. summarizes the genetic differences between D1- and D2-class receptors.*

1.5.2. Expression of Dopamine Receptors in the Brain

The particular expression pattern and localization of DA receptors play a critical role in mediating dopaminergic physiological functions. Although there are similarities among subtypes of D1- and D2-class receptors, differences in the physiological properties, anatomical localization, and level of expression have been observed to modulate a variety of central behaviors (Civelli et al, 1993; Sokoloff and Schwartz, 1995; Jaber et al, 1996a; Beaulieu and Gainetdinov, 2011). Various methods have been used to determine the mRNA level and protein expression of DA receptors in different brain structures. Interestingly, mRNA and protein abundance do not always overlap, perhaps due to sensitivity of the methodological techniques or functionality of the receptors, e.g., cellular differentiation, and post-transcriptional processes.

D1R and D2R are the most abundant receptors in the brain and are highly expressed in substantia nigra pars compacta (SNc), putamen and caudate of dorsal striatum, cortex, hippocampus, and olfactory tubercle, with lower expression levels in the cerebellum (Bunzow et al, 1988; Giros et al, 1989; Monsma et al, 1989; Monsma et al, 1990; Sunahara et al, 1990; Dearry et al, 1990; Zhou et al, 1990; Fremeau et al, 1991; Huntley et al, 1992; Levey et al, 1993; Smiley et al, 1994; Schambra et al, 1994; Hersch et al, 1995; Araki et al, 2007; Beaulieu and Gainetdinov, 2011; Gangarossa et al, 2012; Rothmond et al, 2012). D2R is expressed more than D1R in other brain structures including ventral tegmental area (VTA), hypothalamus, nucleus accumbens (NAc) of ventral striatum, and amygdala (Albert et al, 1990; Yu et al, 2019). D3R, D4R and D5R have a considerable level of expression, but less than D1R and D2R, in the cortex, amygdala, hippocampus, striatum, NAc and hypothalamus (Sokoloff et al, 1990; Van Tol et al, 1991; Sunahara et al, 1991; Tiberi et al, 1991; Bouthenet et al, 1991; Huntley et al, 1992; Sokoloff et al, 1992a, b; Bergson et al, 1995a; Ciliax et al, 2000; Khan et al, 2000).

1.6. Dopamine Pathways, Neurophysiology, and Behaviour

DA neurotransmission contributes to a multitude of behaviors, *inter alia*, motor control, reward learning, cognitive control, decision making, and motivation (Jaber et al, 1996a; Missale et al, 1998; Wise, 2004; Beaulieu and Gainetdinov, 2011). Anatomical studies have greatly aided our understanding of the breadth of the dopaminergic neuronal innervations, which are mainly localized on neural circuitries of SNc and VTA of the midbrain (Bertler and Rosengren, 1959; Sano et al, 1959; Carlsson et al, 1962; Björklund and Dunnett, 2007b; Iversen and Iversen, 2007;

Gantz et al, 2018; Costa and Schoenbaum, 2022). These midbrain neurons project to the dorsal and ventral striatum and cortex, forming three anatomically and functionally distinct components: nigrostriatal (mesostriatal), mesolimbic, and meseocortical pathways, respectively (Anden et al, 1964; Dahlstroem and Fuxe, 1964; Battista et al, 1972; Fuxe et al, 2006; Björklund and Dunnett, 2007b; Iversen and Iversen, 2007; Costa and Schoenbaum, 2022). While these dopaminergic pathways are often characterized as distinct pathways, certain functions can be modulated by multiple pathways (Björklund and Dunnett, 2007b; Gantz et al, 2018; Costa and Schoenbaum, 2022). These three main pathways are the most well-studied, however, several dopaminergic projections stream from other brain regions such as hypothalamus, hippocampus, amygdala, olfactory tubercle, and have been functionally characterized to facilitate multiple behaviors (Björklund and Dunnett, 2007b; Costa and Schoenbaum, 2022). *Fig.1.4. shows the anatomical connectivity of major midbrain dopaminergic pathways.*

Although dopaminergic neurons represent a small fraction of the total neuronal population in the CNS, they influence large densities of the brain through their highly divergent branching network of fibers (Iversen and Iversen, 2007; Gantz et al, 2018; Costa and Schoenbaum, 2022). The presence of dense DA innervations to different brain regions have essential roles in mediating neuronal functions, mainly: movement and motor control, spatial memory, motivation, reward and reinforcement, learning, among others (Gantz et al, 2018; Costa and Schoenbaum, 2022). Furthermore, DA neurons project and innervate to several brain regions that have different biophysical, synaptic, structural, and molecular properties (Costa and Schoenbaum 2022). Subpopulations of these neurons also have striking physiological and anatomical properties, as they receive inputs from different regions, and reflect different functional specialization in behavior and disease vulnerability (Costa and Schoenbaum, 2022). In addition to excitatory glutamatergic and inhibitory GABAergic inputs, DA neuronal activity is also regulated by neuromodulatory inputs, including NE, 5-HT, ACh, neuropeptides, and peripheral hormones (Gantz et al, 2018; Costa and Schoenbaum, 2022).

Multiple human disorders have been linked to dysregulation of dopaminergic transmissions; prominently PD and schizophrenia (Iversen and Iversen, 2007; Beaulieu and Gainetdinov, 2011). DA dysfunction also has been associated with etiology of several pathological and psychological conditions, such as depression, drug abuse and addiction, and hyperprolactinemia (Missale et al,

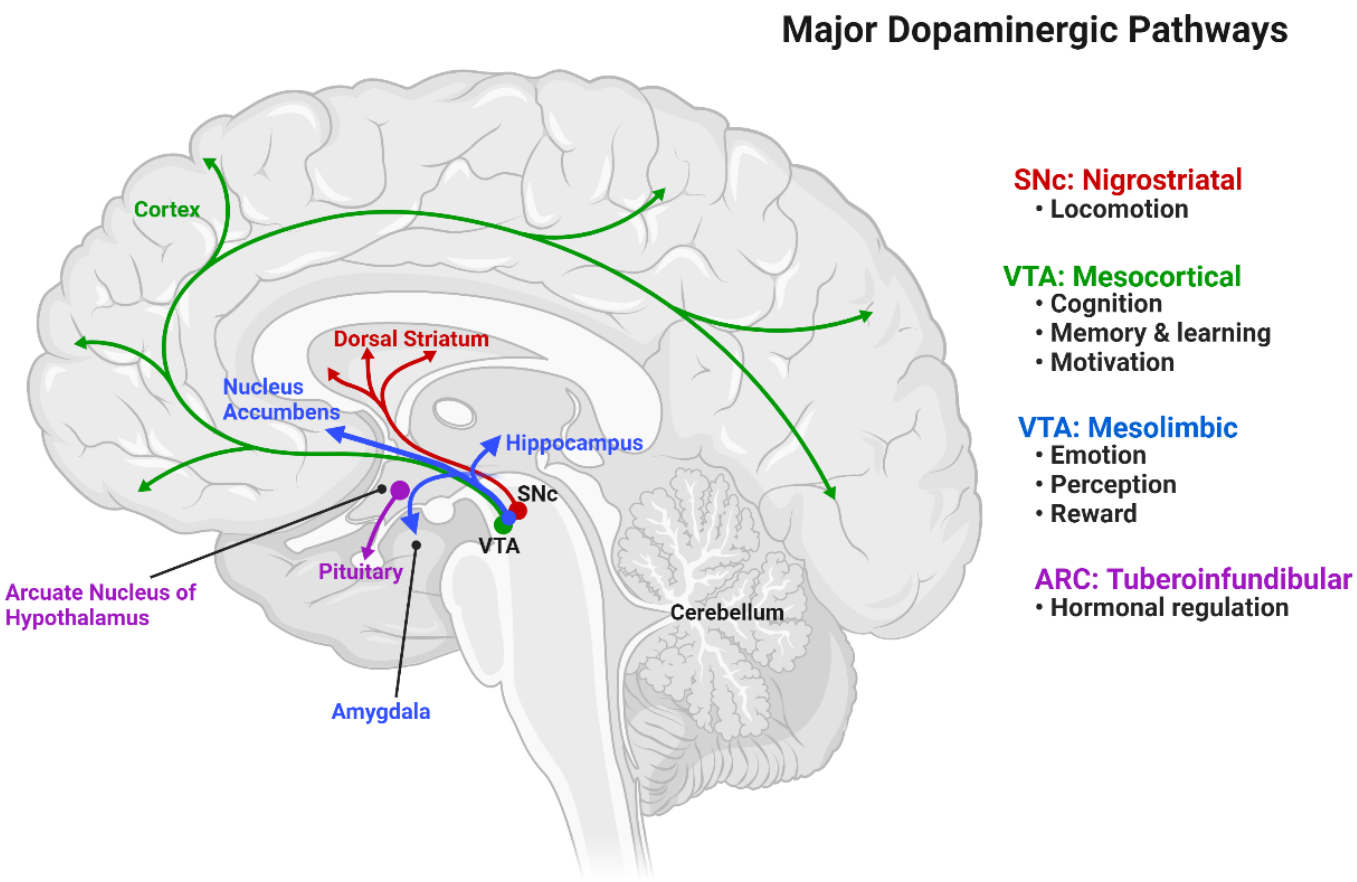

Fig. 1.4. Major Dopaminergic Pathways in the Brain.
Four major dopaminergic neuronal pathways are illustrated, including their projections and associated functions. The nigrostriatal pathway connects the substantia nigra (SNc) with the dorsal striatum; the mesocortical pathway connects the ventral tegmental area (VTA) to the cerebral cortex; the mesolimbic pathway connects the VTA to the ventral striatum/nucleus accumbens (NAc); and the tuberoinfundibular pathway connects the arcuate nucleus (ARC) of the hypothalamus to the pituitary gland. Created with BioRender.com.

1998; Björklund and Dunnett, 2007b; Iversen and Iversen, 2007; Beaulieu and Gainetdinov, 2011). The following section will briefly highlight the physiological and pathophysiological importance of these dopaminergic pathways, including certain behavioral functions.

1.6.1. The Nigrostriatal Pathway

The nigrostriatal pathway originates in the SNc and projects to the caudate nucleus and putamen of dorsal striatum, which are the main input nuclei of basal ganglia (BG) (Cheramy et al, 1981; Cheramy et al, 1998). The BG are a major brain system that modulate initiation, integration and regulation of motor function, and lesions herein cause devastating motor disorders, like PD (Ehringer and Hornykiewicz, 1960; Cheramy et al, 1981; Cheramy et al, 1998; Graybiel, 2000; Hornykiewicz, 2002; Cenci, 2007).

1.6.1.1. The Basal Ganglia

The BG are a group of interconnected subcortical nuclei that are prominent in maintaining the balance between direct and indirect pathways, which differentially contribute to the BG output nuclei, e.g. globus pallidus (consisting of internal segment, GPi, and external segment, GPe), substantia nigra pars reticulata (SNr) and subthalamic nucleus (STN) to form thalamo-cortico-striatal loops (Albin et al, 1989; Gerfen, 1992; Graybiel, 2000; Cenci, 2007). MSNs of dorsal striatum receive excitatory glutamatergic input from cortex and then send output to globus pallidus through direct and indirect pathway in parallel, and the output of these pathways ultimately facilitate or inhibit the motor thalamus, respectively (Albin et al, 1989; Gerfen, 1992; Graybiel, 2000; Cenci, 2007). *Fig. 1.5A, B. summarizes the basal-ganglia-thalamocortical circuits*.

In the direct pathway, the striatal output provides inhibitory input directly to GPi/SNr, which in turn modulates the activity of brainstem and thalamic nuclei involved in motor control and makes inhibitory connection in the thalamus, thus acting to promote motor activity (Albin et al, 1989; Graybiel, 2000; Surmeier et al, 2007; Cenci, 2007). However, striatal neurons of indirect pathways inhibit neurons of the GPe, which then inhibit GPi/SNr and STN (Albin et al, 1989; Gerfen, 1992; Graybiel, 2000; Surmeier et al, 2007; Cenci, 2007). The STN neurons are also excited by cortical axons, and its projection excites the GPi neurons, subsequently inhibiting the thalamus (Albin et al, 1989; Gerfen, 1992; Graybiel, 2000; Surmeier et al, 2007; Cenci, 2007). Ultimately, this pathway simultaneously suppresses motor behavior (Albin et al, 1989; Gerfen, 1992; Graybiel,

2000; Surmeier et al, 2007; Cenci, 2007). DA shapes the striatal activity and exerts opposite effects on these two neuronal pathways, which express either D1R or D2R. The D1R predominates in the "direct pathway" of striatonigral MSNs (dMSNs) and mediates facilitatory responses to enhance glutamatergic signaling. In contrast, the "indirect pathway" primarily contains D2R in striatopallidal MSNs (iMSNs) and decreases the neuronal excitability and glutamatergic signaling (Albin et al, 1989; Gerfen et al, 1990; Gerfen, 1992; Surmeier et al, 1996; Graybiel, 2000; Surmeier et al, 2007; Cenci, 2007). Both dMSNs and iMSNs are GABAergic, but they contain different peptide co-transmitters; substance P and enkephalin, respectively (Albin et al, 1989; Gerfen et al, 1990; Gerfen, 1992; Surmeier et al, 1996; Graybiel, 2000; Surmeier et al, 2007; Cenci, 2007). Interestingly, a small population of MSNs co-express D1R•D2R to establish an additional efferent striatal pathway that projects exclusively to GPe of the indirect pathway of thalamo-cortico-striatal motor circuit (Bonnavion et al, bioRxiv 2022). The D1R•D2R-MSNs have unique morphological and electrophysiological characteristics compared to D1R-expressing MSNs and D2R-expressing MSNs, and orchestrate the fine-tuning of motor balance control (Bonnavion et al, bioRxiv 2022).

In both neuronal populations, the activation of cAMP-dependent intracellular signaling to the nucleus is under opposing influences of DA receptors and adenosine receptors coupled to G-proteins. In striatonigral neurons, cAMP is modulated by D1R and adenosine A_1 receptor (A_1R) coupled to stimulatory G-protein ($G\alpha_{s/olf}$) and inhibitory G-protein ($G\alpha_i$), respectively, whereas cAMP production is controlled by D2R and adenosine A_{2A} receptor ($A_{2A}R$) coupled to $G\alpha_i$ and $G\alpha_{s/olf}$, respectively, in striatopallidal neurons (Ferré et al, 1997; Cenci, 2007; Nagai et al, 2016). dMSN neurons also expressing D3R and muscarinic M4 receptor (M4R) that are coupled to $G\alpha_i$ (Nagai et al, 2016). As D1R activates PKA and PKA phosphorylates substrate proteins, it increases the responsiveness of striatonigral neurons to modulate synaptic transmission of glutamate and ionotropic glutamate receptors, however, D2R activation in striatopallidal neurons diminishes presynaptic release of glutamate (Day et al, 2006; Surmeier et al, 2007). D1R and D2R regulate L-type Ca^{2+} by opposing mechanisms, whereby D1R enhances the channel opening through PKA, and D2R reduces the opening through the activation of a Ca^{2+}-dependent protein phosphatase (Surmeier et al, 1995; Hernandez-Lopez et al, 2000). *Fig. 1.6. illustrates the functional signaling pathway of the direct and indirect pathways.*

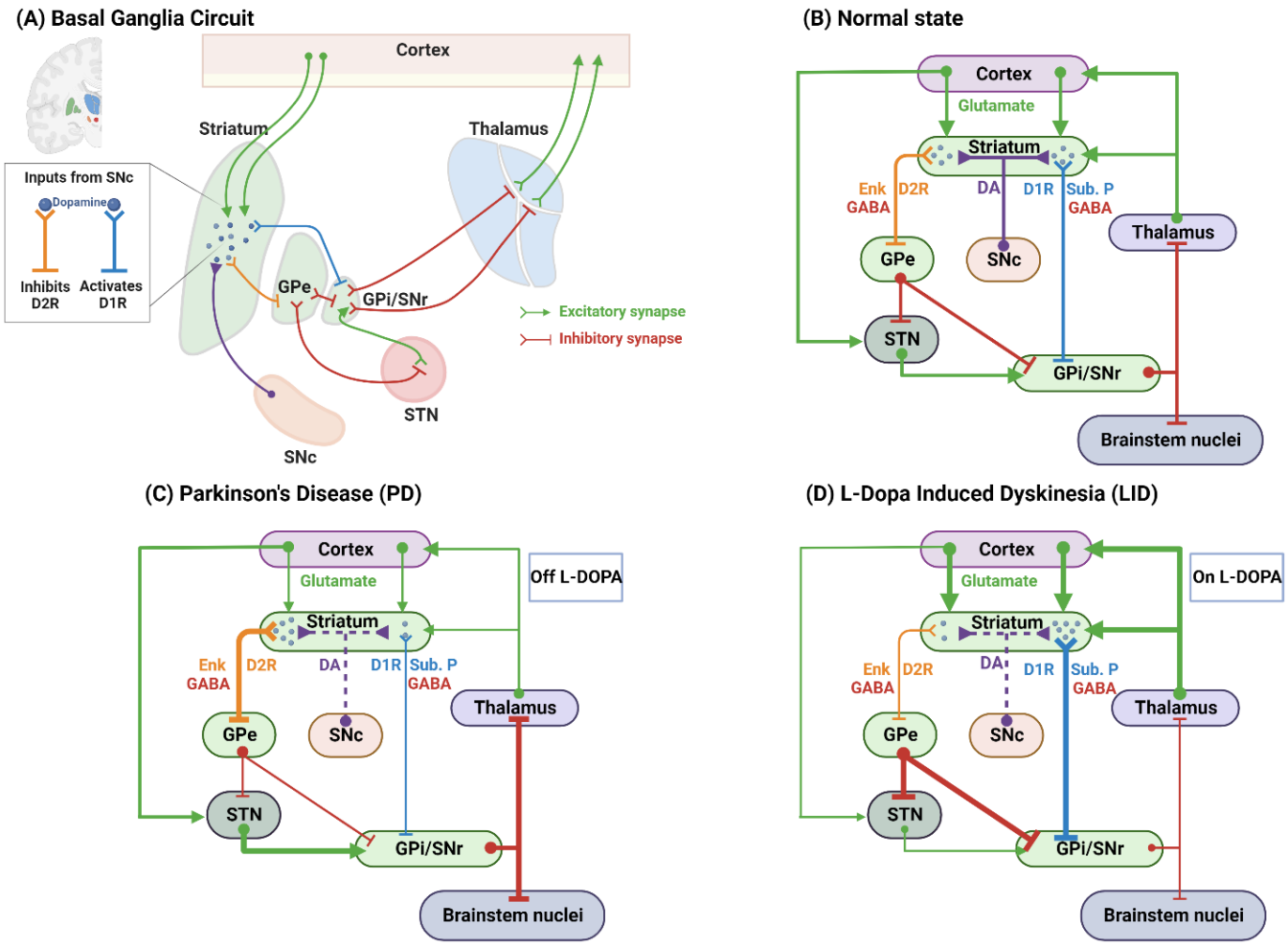

Fig. 1.5. The Basal-Ganglia-Thalamocortical Circuits.

(A-D) Schematic diagram of the classical basal ganglia (BG) circuits in normal state (A, B), Parkinson disease (C), and L-DOPA induced dyskinesia (D). The basal ganglia consist of the striatum, GPe, GPi, SNc, SNr, STN. These structures are linked to form a complex network of excitatory and inhibitory connections, depicted in green and red lines, respectively. The basic circuit model of BG function involving the inhibitory connections of "direct" and "indirect" pathways (depicted in blue and orange clines, respectively). Striatum receives excitatory glutamatergic connection from cortex, and then sends inhibitory GABAergic information through the direct and indirect pathways projecting to GPi/Snr and GPe, respectively. GPe then sends inhibitory output to GPi/SNr and STN. The glutamatergic neurons of the STN can excite the GPi/SNr. The inhibitory output of GPi/SNr neurons modulate the activity of the brainstem and thalamic nuclei to promote or suppress locomotor activity. GPe: external segments of the globus pallidus; GPi: internal segments of the globus pallidus; SNc: the pars compacta of substantia nigra; SNr: pars reticulata of the substantia nigra; STN: subthalamic nucleus. Created with BioRender.com.

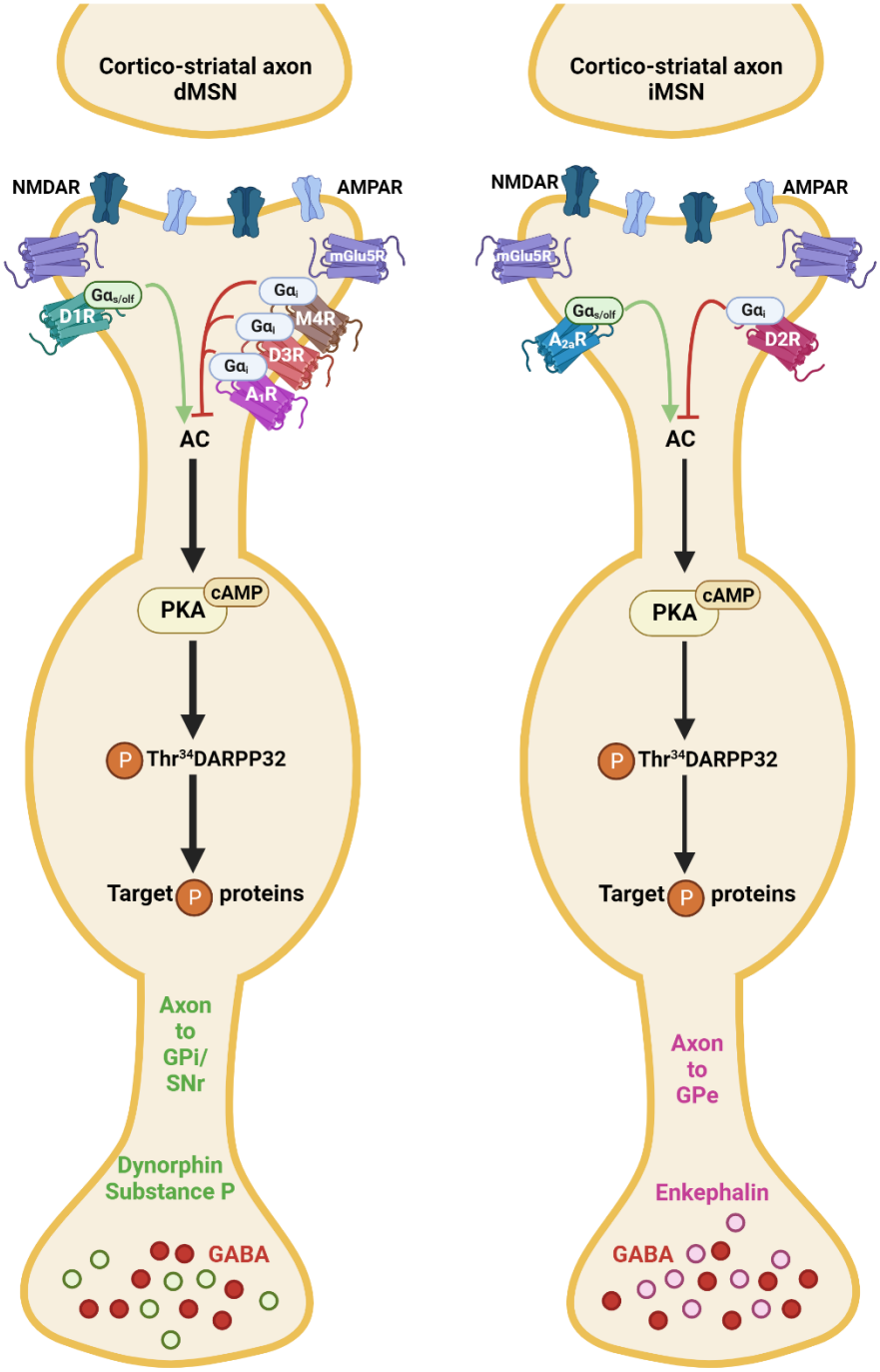

Fig. 1.6. The Signaling Pathway of D1R-MSN and D2R-MSN.
D1R and adenosine $A_{2A}R$ are primarily coupled to $G\alpha_{s/olf}$ and stimulate the activity of AC, followed by activation of PKA through cAMP accumulation. By contrast, D2R, D3R, A1R, and M4R are associated with $G\alpha_i$ and inhibit cAMP production. D1R- and D2R-mediated PKA activation phosphorylates numerous proteins, e.g., DARPP-32, to modulate transcriptional and cellular responses. Created with BioRender.com.

1.6.1.2. The Mosaic of D1R and D2R in Neostriatum

Striatum is the major structure of the BG and is mostly composed of GABAergic MSNs of two segregated neuronal populations, which are distinguished based on the efferent projections of direct pathway MSNs expressing substance P and indirect pathway MSNs expressing enkephalin (Albin et al, 1989; Valjent et al, 2009; Bertran-Gonzalez et al, 2010; Gerfen and Surmeier, 2011; Gerfen, 2023). Roger Albin and colleagues proposed that these two pathways differentially promote or supress the locomotor activity in BG disorders (Albin et al, 1989). Furthermore, Charles Gerfen discovered that the vast majority of D1R and D2R are expressed distinctly in the direct and indirect pathway, respectively, to exert opposing locomotor modulations (Gerfen et al, 1990). However, the degree of segregation between these circuits was much debated in the 1990s and 2000s, stemming primarily from discrepancies in the results obtained from anatomical and functional studies (Surmeier et al, 1992; Surmeier et al, 1993; Aizman et al, 2000). At present, compelling evidence exists to support the notion that the population of D1R localized in MSNs are typically segregated from those of D2R, with only a small subset of MSNs found to co-express D1R and D2R (Le Moine and Bloch, 1995; Surmeier et al, 1996; Shuen et al, 2008; Bertran-Gonzalez et al, 2008; Thibault et al, 2013; Frederick et al, 2015; Escande et al, 2016; Gagnon et al, 2017). *In situ* hybridization studies have suggested that D1R mRNA is found in substance P-expressing MSNs projecting to the GPi/SNr, and was segregated from the neuronal population of D2R mRNA localized with enkephalin-expressing MSNs projecting to GPe, with small subset of co-expressed D1R and D2R in the MSNs (Gerfen et al, 1990; Le Moine and Bloch, 1995; Surmeier et al, 1996). The advancement of transgenic reporter mice further validated the segregation of striatal neurons between D1R and D2R (Shuen et al, 2008; Bertran-Gonzalez et al, 2008; Thibault et al, 2013; Escande et al, 2016; Gagnon et al, 2017; Yu et al, 2019).

1.6.1.3. Striatal TH-Interneurons

As the MSNs receive abundant excitatory glutamatergic input and regulate DA activity, they account for 95% of the neuronal population of striatum. The remaining neurons composing the striatum are cholinergic interneurons and GABAergic interneurons (Kawaguchi, 1993; Tepper and Bolam, 2004). Studies have investigated the possibility of DA contribution to the transmission of interneurons (Ibáñez-Sandoval et al, 2010; Xenias et al, 2015). Striatal TH-positive interneurons receive cortical and striatal input, and exert GABAergic inhibition onto MSN, hence these

interneurons are not dopaminergic, but rather are a type of GABAergic interneurons that express TH, and exert GABAergic inhibition onto direct and indirect MSN pathways (Ibáñez-Sandoval et al, 2010; Xenias et al, 2015).

1.6.1.4. Parkinson's Disease

As mentioned earlier, degeneration of dopaminergic neurons in the SNc leads to severe motor deficits, a hallmark of PD (Greenfield and Bosanquet, 1953; Ehringer and Hornykiewicz, 1960). PD was first described by James Parkinson more than 200 years ago as a shaking palsy (or paralysis agitans) (Parkinson, 1817). PD is the second most common age-related neurodegenerative disease, affecting more than one million people in North America (Beitz, 2014; Balestrino and Schapira, 2020). There are two forms of PD: familial and sporadic. In the familial form of PD (10-15%), the genetic aberrations (e.g., *LRRK2* and *PRKN*) are reported in patients with family history of PD symptoms (Tran et al, 2020). While most patients suffer from sporadic PD (85-90%), the exact cause is not completely known, and involve a combination of genetic (e.g., *SNCA*, the gene encoding αSynuclein) and environmental factors (e.g., toxins) (Rietdijk et al, 2017; Tran et al, 2020). Braak's hypothesis states that sporadic PD is progressed in stages in which the olfactory system is initially compromised by pathological Lewy bodies (α-synuclein aggregates) (Braak et al, 2003). According to the hypothesis, a pathogen that enter the body via nasal cavity subsequently reaches the gut and initiates the pathogenesis of Lewy bodies in the nose and digestive tract (Braak et al, 2003). As the olfactory dysfunction is one of the earliest symptoms displayed by PD patients, the motor symptoms are an expression of advanced Lewy body pathology (Braak et al, 2003; Tran et al, 2020).

The neuropathogenesis of PD makes it challenging to target effective therapies due to the variable clinical, genetic, and pathological nature of the disease, thus current treatments consist of symptomatic relief (Iversen and Iversen, 2007; Beitz, 2014; Balestrino and Schapira, 2020; Blesa et al, 2022). While DA neurons are known to degenerate in normal aging subjects, in parkinsonian patients this neurodegeneration is accelerated and is accompanied by the presence of intracytoplasmic inclusions of Lewy bodies in surviving neurons (Greenfield and Bosanquet, 1953; Beitz, 2014; Balestrino and Schapira, 2020; Blesa et al, 2022). The ensuing depletion of DA in the SNc causes motor deficits such as akinesia, rigidity, tremor, and postural dysfunction (Cenci,

2007; Beitz, 2014; Balestrino and Schapira, 2020; Blesa et al, 2022). *Fig. 1.7. summarizes the pathophysiology and clinical symptoms observed in PD patients.*

DA replacement therapy is one of the strategies used to alleviate the symptoms of PD, in addition to surgical treatments and stem cell therapies (Beitz, 2014; Balestrino and Schapira, 2020). As mentioned earlier, Hornykiewicz started the first clinical trials to treat PD with DA precursor L-DOPA in 1961 (Birkmayer and Hornykiewicz, 1961). A few years after, George Cotzias developed the clinically efficacious, high dose oral L-DOPA treatment that is still used today (Cotzias et al, 1968). L-DOPA administration ultimately increases the level of DA in surviving dopaminergic neurons of the SNc, but this supply of DA does not stop disease progression (Hornykiewicz, 1974; Beitz, 2014; Balestrino and Schapira, 2020). Further still, cumulative exposure and/or prolonged repetitive administration of L-DOPA in PD patients might have the adverse effect of abnormal involuntary movement (AIM), a phenomenon known as L-DOPA induced dyskinesia (LID), which is positively associated with the severity of parkinsonism (Espay et al, 2018; Zheng and Zhang, 2021). L-DOPA therapy has been further improved by its combination with carbidopa, a decarboxylase inhibitor that prevents peripheral metabolism of L-DOPA in the liver and increases its bioavailability in the brain (Beitz, 2014; Balestrino and Schapira, 2020). Other compounds have also been co-administered for the treatment of PD, e.g. dopaminergic agonists (pramipexole and ropinirole), COMT inhibitors (entacapone), or MAO-B inhibitors (selegiline and rasagiline) (Beitz, 2014; Balestrino and Schapira, 2020).

DA deficiency in PD causes an imbalance in the DA activity of striatofugal pathways and triggers a cascade of functional changes that affect the basal ganglia network (Cenci, 2007). As described in section 1.6.1.1., for the normal BG circuit, lesions in striatum for PD lead to changes in the efferent MSNs projecting to the direct pathway are reduced, while they are increased in the indirect pathway (Mallet et al, 2006; Cenci, 2007; Galvan et al, 2015). In the indirect pathway, the firing activity in GPe neurons is reduced, which leads to disinhibition of STN neurons (Mallet et al, 2006; Cenci, 2007; Galvan et al, 2015). Moreover, there is a selective loss in dendritic spines and excitatory glutamatergic synapses following DA depletion in PD observed only in the indirect pathway, which implicates a D2R-mediated activation of a L-type- Ca^{2+}; Cav1.3 channel (Day et al, 2006; Gerfen, 2006). Subsequently, this leads to excessive excitation of GPi/SNr due to the

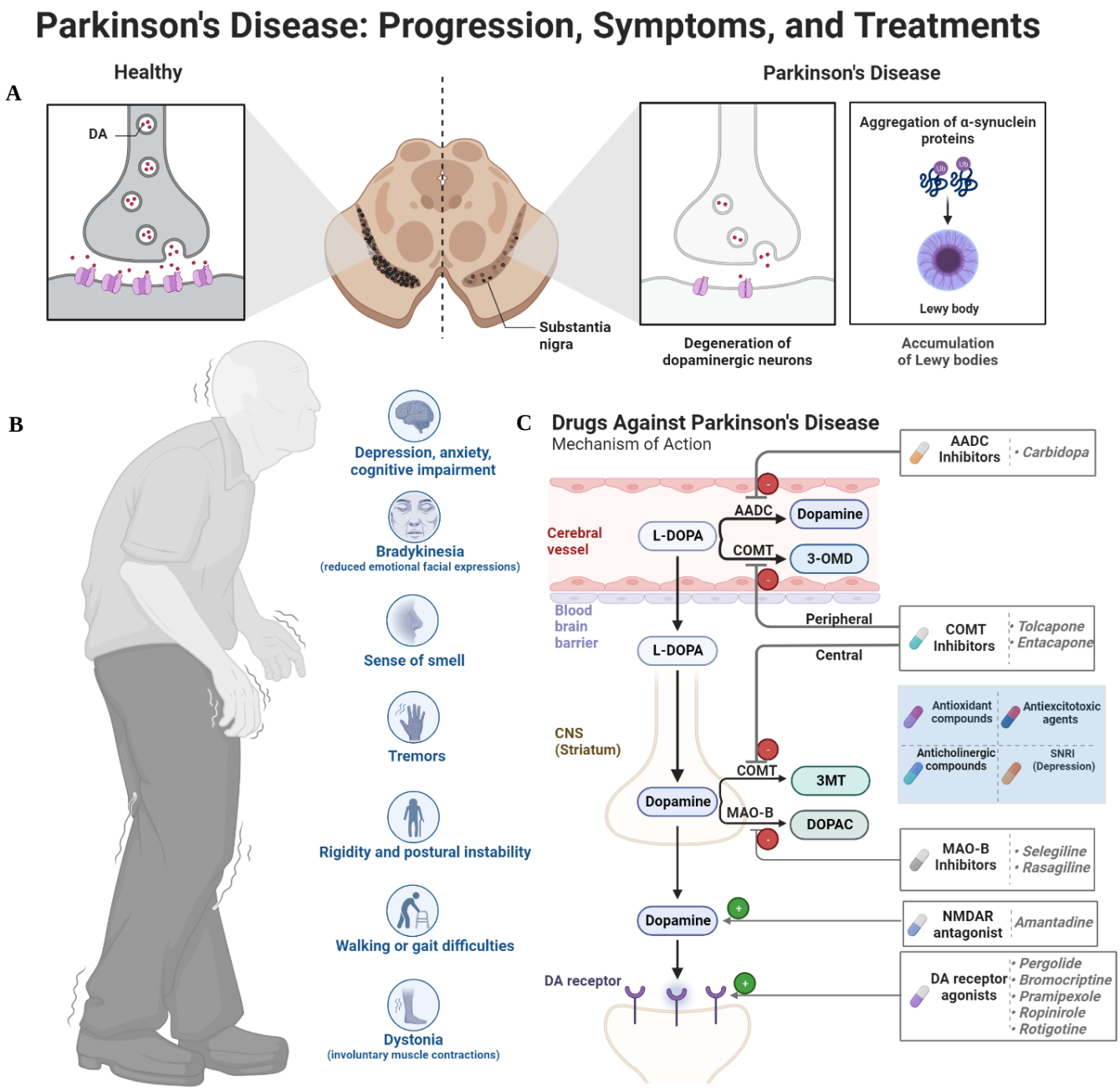

Fig. 1.7. Parkinson's Disease.
A schematic illustration summarizes the pathophysiology of Parkinson's disease (A), motor and non-motor symptoms (B), and the mechanism of action of drugs linked to the treatment of the disease (C). Created with BioRender.com.

lack of inhibition from direct pathway neurons, which exert a greater than normal inhibition on their thalamic and brainstem targets of BG (Mallet et al, 2006; Galvan et al, 2015). Chronic L-DOPA treatment enhanced the D1R activity, without altering abnormal D2R activity, consequently, leads to increased cortical activation and facilitates movement (Cenci, 2007).

The thalamo-cortico-striatal loop of LID is altered by the striatal efferent projecting to the direct pathway than indirect pathway, and is causally linked to an abnormal activation of the D1R (Aubert et al, 2005; Cenci, 2007; Iversen and Iversen, 2007). The striatal efferents provide an enhanced direct inhibitory input to GPi/SNr, which in turn disinhibit the activity of brainstem and thalamic nuclei (Cenci, 2007; Iversen and Iversen, 2007). In PD patients, D1R, but not D2R, agonists induced dyskinesias in a similar manner to monotherapy L-DOPA treatment, hence the pharmacological blockage of D1R in LID diminish the therapeutic efficacy of L-DOPA (Aubert et al, 2005; Cenci, 2007). The use of NMDAR antagonists has a promising therapeutic approach in the treatment of LID and in preventing undesirable side-effect caused by D1R agonists (Cenci, 2007). Moreover, D1R and D3R are co-expressed in the MSNs of direct pathway, and L-DOPA-induced changes in D3R expression that is corelated with the severity of LID (Schwartz et al, 1998; Bézard et al, 2001; Cenci, 2007). *Fig. 1.5C, D. shows the basal-ganglia-thalamocortical circuits in PD and LID.*

1.6.1.5. Parkinson's Disease: Pre-Clinical Models and Clinical Trials

As DA replacement therapy only improves the symptoms for parkinsonian patients, rather than slowing or halting the progression of the disease, there have been concerted efforts aimed at both understanding the causative and pathogenic factors responsible for neuronal death and designing neuroprotective treatments that protect, rescue, or restore dopaminergic neurons in PD (Dauer and Przedborski, 2003; Fox and Brotchie, 2010; Jackson-Lewis et al, 2012; Konnova and Swanberg, 2018). Preclinical models of PD and clinical trials have been used to further investigate the effectiveness of different compounds on the prognosis of PD. Two main experimental approaches have been used: neurotoxin- and genetics-based approaches (Dauer and Przedborski, 2003; Fox and Brotchie, 2010; Jackson-Lewis et al, 2012; Konnova and Swanberg, 2018). Exposure of rodents or non-human primates to the neurotoxin 6-hydroxydopamine (6-OHDA) and 1-methyl-4-phenyl-1,2,3,6-tetrahydropyridine (MPTP) induces strong nigrostriatal dopaminergic cell death, motor deficits and behavioral changes, but does not induce the formation of Lewy bodies

(Ungerstedt, 1968; Ungerstedt, 1976; Langston et al, 1983; Carli et al, 1985; Dauer and Przedborski, 2003; Schober, 2004; Fox and Brotchie, 2010; Jackson-Lewis et al, 2012; Konnova and Swanberg, 2018). By contrast, genetic based approaches such as the mutagenesis of genes involved in monogenic Parkinson's disease (e.g. *LRRK2*, *PRKN* and *PINK1*) demonstrate variable cell loss, reduced motor symptoms, and α-synuclein pathology (Dauer and Przedborski, 2003; Fox and Brotchie, 2010; Jackson-Lewis et al, 2012; Konnova and Swanberg, 2018). Despite the limitations of these parkinsonian-like animal models, such as: rapid but not progressive loss of dopaminergic neurons, mild or uninterrupted motor deficit, and lack of Lewy body formation in remaining neurons, there is no doubt of the importance of these models in helping us understand the pathogenesis of the disease and in testing new potential neuroprotective agents and strategies (Dauer and Przedborski, 2003; Fox and Brotchie, 2010; Jackson-Lewis et al, 2012; Konnova and Swanberg, 2018).

Clinical trials have also advanced in our understanding of the cause and pathogenesis of PD. Many compounds presently in trials, derived from pre-clinical research, show promising findings. However, how these compounds interact in the human body remains to be investigated. Randomized, double-blinded, placebo-controlled clinical trial studies have shown the potential efficacy for certain compounds, such as antioxidants compounds, MAO-B inhibitors, antiexcitotoxic agents, and dopamine agonists, that may have neuroprotective functions (Stocchi and Olanow, 2003; Rascol et al, 2006; Beitz, 2014; Balestrino and Schapira, 2020). Despite the evidence that a number of these compounds may possess neuroprotective activity, the interpretation is often confused by the symptomatic effects of the tested compound, and thus the positive results for a compound cannot be interpreted as neuroprotective or as disease modifying drug (Stocchi and Olanow, 2003).

1.6.1.6. The Spatiotemporal Organization of the Striatum

The neuronal activity within the MSNs relies on a dynamic spatiotemporal organization (Barbera et al, 2016; Klaus et al, 2017). Interestingly, the direct and indirect pathways of BG can bidirectionally control movement velocity, a form of learning behavior. Yttri and Dudman examined experience-dependent plasticity associated with goal-directed movements in mice, combined with closed-loop, time-locked optical stimulation of MSNs. The stimulation increased and decreased, respectively, dMSN and iMSN movement velocities during the fastest movements

(Yttri and Dudman, 2016). During the slowest movements, however, stimulation of dMSN inhibited movement velocity, but increased the activity of iMSN (Yttri and Dudman, 2016). Blockade of D1R and D2R abolished these effects observed of dMSN and iMSN (Yttri and Dudman, 2016). These findings demonstrated unprecedented specificity and flexibility in the control of volition by the basal ganglia (Yttri and Dudman, 2016).

Moreover, Parker and colleagues showed that dMSNs and iMSNs are simultaneously activated and have indistinguishable kinetics during motion onset and offset, in freely moving mice (Parker et al, 2018). These data challenge the current simplified model of dMSN and iMSN to initiate and supress movement (Parker et al, 2018). As predicted by the conventional model, movement-associated spiking activity, was decreased in dMSN and increased in iMSN, in parkinsonian model (Parker et al, 2018). L-DOPA treatment increase and decrease the activity of dMSN and iMSN, respectively. As the D2R agonism, quinpirole inhibits iMSN activity, the author unexpectedly found quinpirole enhances the dMSN motion activity (Parker et al, 2018). The recording from dyskinetic mice treated with L-DOPA were hyperactive in dMSNs and hypoactive in iMSNs (Parker et al, 2018). iMSNs, however, were more responsive to motion onset rather than dMSN (Parker et al, 2018). These results show that the loss of dopaminergic neurotransmission causes subtle changes in the specificity and spatial aspects of neuronal firing in parkinsonians model (Parker et al, 2018).

1.6.2. The Mesocorticolimbic Pathway

In the mesocorticolimbic pathway, neuronal cell bodies of the VTA extend their axons that terminate and release DA at mesocortical and mesolimbic structures: the PFC and NAc of the ventral striatum, respectively (Björklund and Dunnett, 2007b; Iversen and Iversen, 2007; Gantz et al, 2018; Costa and Schoenbaum, 2022). Cortical and limbic pathways have been shown to differ in their molecular markers, anatomical organization, and in their response to stimuli. VTA-dopaminergic neurons projects to cingulate the PFC that composes the mesocortical pathway and modulates a variety of functions including working memory, emotion, and cognitive functions. Whereas VTA terminals to the limbic structures, including the NAc, the amygdala, and the hippocampus, constitute the mesolimbic pathway and are involved in motivation and reward (Björklund and Dunnett, 2007; Iversen and Iversen, 2007; Grace, 2016; Gantz et al, 2018; Costa and Schoenbaum, 2022). In addition, VTA-dopaminergic neurons strongly innervate the locus

coeruleus (LC), and to a lesser extent, the dorsal raphe nucleus (DRN) (Swanson, 1982; Kalén et al, 1988). As these pathways control a variety of functions, their impairment underlies the etiology of conditions, such as schizophrenia, depression, and drug addiction (Björklund and Dunnett, 2007b; Iversen and Iversen, 2007; Grace, 2016; Gantz et al, 2018; Costa and Schoenbaum, 2022).

1.6.2.1. Schizophrenia

Schizophrenia is a chronic, highly debilitating psychiatric disease characterized by psychosis, apathy, social withdraw, and cognitive impairment that impairs daily functioning of those affected (Carpenter and Buchanan, 1994; Mueser and McGurk, 2004; Marder and Cannon, 2019). About 1% of the population is affected by schizophrenia, with illness onset typically observed early in life (16-30 years). Most patients also have indirect adverse effects that include staggeringly high unemployment rate and a reduced life expectancy (by 10-20 years) due to the increased susceptibility to suicide (Carpenter and Buchanan, 1994; Mueser and McGurk, 2004; Marder and Cannon, 2019; Costa and Schoenbaum, 2022). Prior to the onset of schizophrenia, patients are often characterized as having subtle changes in behavior and declining daily function, known as psychosis prodrome (Marder and Cannon, 2019). Complex interplays, rather than a single factor, contribute to schizophrenia. While the exact etiology of the disease is unknown, neurotransmitter and circuitry dysfunctions in the brain, neurodevelopmental abnormalities, genetic inheritance, and even social and environmental influences have been implicated as contributing factors (Carpenter and Buchanan, 1994; Mueser and McGurk, 2004; Marder and Cannon, 2019). No biological alterations are pathognomonic of schizophrenia; thus the research is highly versatile in schizophrenia, and the search for antipsychotic drugs (Carpenter and Buchanan, 1994; Mueser and McGurk, 2004; Marder and Cannon, 2019).

Dopaminergic transmission plays a key role in the clinical manifestation of schizophrenia (Klerman, 1974; Langer et al, 1981; Brisch et al, 2014; Grace, 2016; Costa and Schoenbaum, 2022). In 1967, the “dopamine hypothesis of schizophrenia” proposed by Van Rossum, states that the hyperactivity of dopamine transmission contributes to the etiology of schizophrenia (Carlsson and Lindqvist, 1963; Meltzer and Stahl, 1974; Seeman and Kabur, 2000; Brisch et al, 2014; Grace, 2016; Costa and Schoenbaum, 2022). This hypothesis was introduced based on the study from Carlsson and Lindqvist that showed the antipsychotic effects of haloperidol and chlorpromazine. The finding that these two antipsychotics were in fact D2R antagonists provided early support of

the involvement of DA in schizophrenia by blocking the activity of DA receptors, (Carlsson and Lindqvist, 1963; Meltzer and Stahl, 1974; Seeman and Kabur, 2000; Brisch et al, 2014; Costa and Schoenbaum, 2022). Unlike other neuroleptic drugs such as reserpine, haloperidol and chlorpromazine have no effect on the level of monoamines in the brain (Brisch et al, 2014; Kesby et al, 2018; Marder and Cannon, 2019). The alteration in DA function underpins the clinical symptoms of schizophrenia, and subcortical D2R blockade underlie the clinical efficacy of antipsychotic medications (Brisch et al, 2014; Kesby et al, 2018; Marder and Cannon, 2019).

Schizophrenia is characterized by positive and negative symptoms, and cognitive impairments (Carpenter and Buchanan, 1994; Mueser and McGurk, 2004; Kesby et al, 2018; Marder and Cannon, 2019). Positron emission tomography (PET) imaging of schizophrenic patients has shown an increase in subcortical synaptic DA synthesis and release, which is associated with positive symptoms: hallucination, delusion, thought disorganization, and paranoia (Brisch et al, 2014; Kesby et al, 2018; Marder and Cannon, 2019). These symptoms are most recognizable during the period of acute psychosis, as a result of augmentation of D2R activity (Abi-Dargham et al, 2000; Seeman and Kabur, 2000; Brisch et al, 2014; Kesby et al, 2018; Marder and Cannon, 2019). Moreover, drugs that enhance DA release or increase DA transmission, such as L-DOPA or amphetamine, will exacerbate psychosis in schizophrenia patients and induce schizophrenia-like symptoms in healthy individuals (repeated or high dosage) (Kesby et al, 2018; Costa and Schoenbaum, 2022). The negative symptoms of schizophrenia, including anhedonia (lack of desire and motivation), alogia (communication deficits), and social withdrawal, are thought to arise from reduced DA/D1R activation in cortex, which also impair the cognitive functions, e.g. learning, memory, and attention (Brisch et al, 2014; Kesby et al, 2018; Marder and Cannon, 2019). After decades of research, the revised "dopamine hypothesis of schizophrenia" posits that hyperactive dopamine in the mesolimbic areas and hypoactive dopamine transmission in the PFC underlies schizophrenia (Abi-Dargham, 2004; Brisch et al, 2014). *Fig. 1.8. summarizes the positive and negative symptoms associated with schizophrenia.*

Despite the importance of dopaminergic neurotransmission in schizophrenia, the "dopamine hypothesis of schizophrenia" is seen as a simplified model that doesn't comprehend the complexity of this mental disorder, and has been challenged by preclinical and clinical findings (Abi-Dargham, 2004; Kesby et al, 2018). For instance, all antipsychotic drugs are antagonists at the D2R with

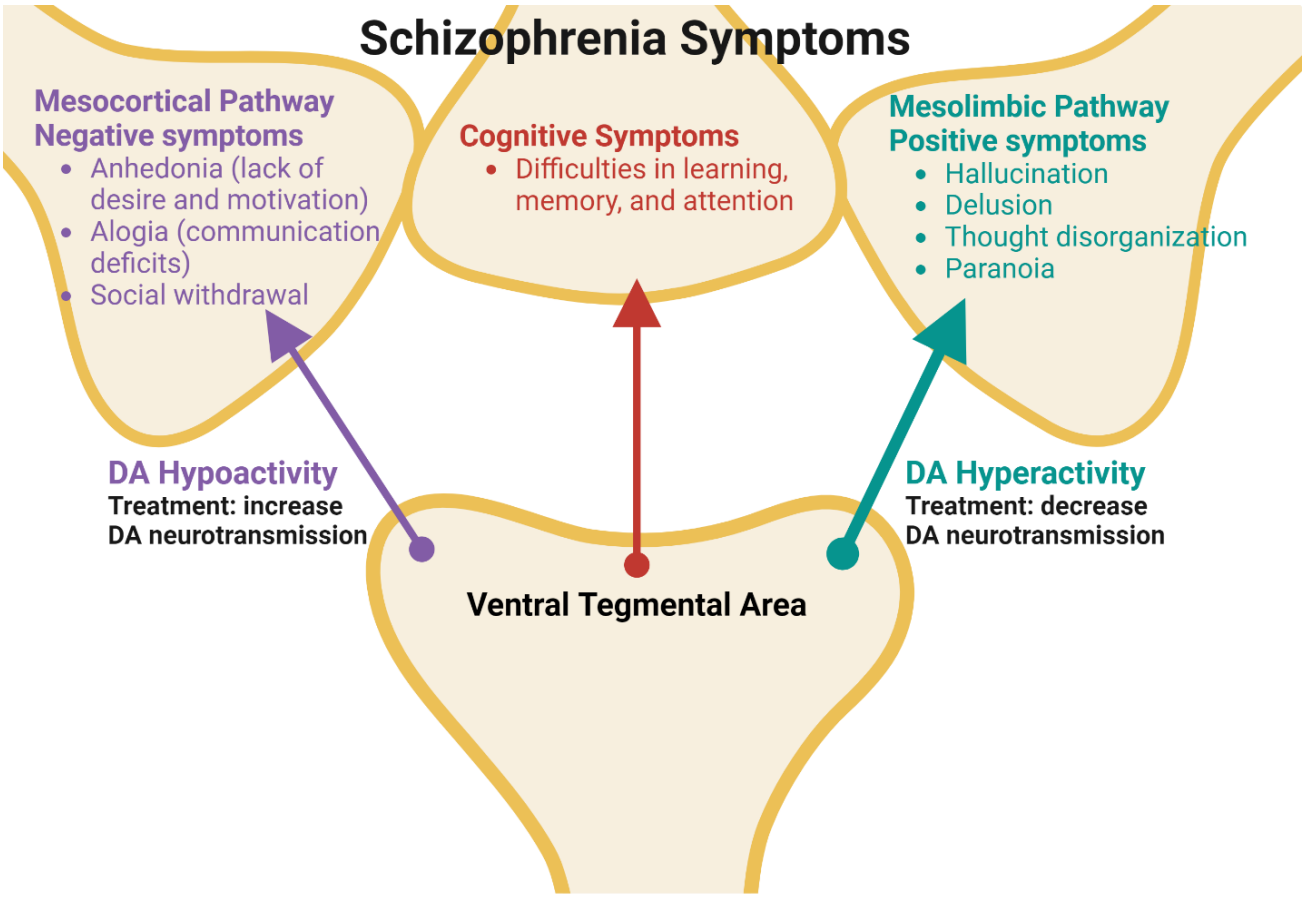

Fig. 1.8. Schizophrenia Symptoms.
Summary of the positive, negative, and cognitive symptoms associated with schizophrenia. Created with BioRender.com.

different potencies, however, their therapeutic doses vary in occupying D2R in schizophrenic patients (Kesby et al, 2018; Marder and Cannon, 2019). Postmortem studies support that this variation is dependent on either the localization of D2R (presynaptic or postsynaptic), or the interaction with other neurochemicals, such as glutamate, GABA, or 5-HT, in modulating the function of cortical circuits (Kesby et al, 2018).

Because schizophrenic symptoms cannot be accurately reproduced in animal models, it is difficult to use such models to explore the role of neurotransmitters and circuitries in schizophrenia and other psychiatric diseases (Jones et al, 2011; Kesby et al, 2018). Most schizophrenia phenotypic models resemble positive-like symptoms of schizophrenia, which reflect altered mesolimbic dopamine function (Jones et al, 2011). Among these pharmacological-based models is amphetamine-induced locomotion, which is largely driven by limbic dopamine release following amphetamine administration that ultimately increases locomotor activity and mimics the positive-like symptoms of schizophrenia (Kesby et al, 2018). Fewer models have shown negative and cognitive symptoms of schizophrenia, including social interaction, and learning and memory impairments (Jones et al, 2011). Nonetheless, the use of animal models to elucidate the neurochemical and neurobiological changes of schizophrenia has evolved and provided insight into mesolimbic dopaminergic function, and the complex heterogeneity of schizophrenia (Jones et al, 2011; Kesby et al, 2018). Therefore, incorporating new clinical findings in these behavioral models will enable more effective therapeutic strategies to comprehend and treat schizophrenia (Jones et al, 2011; Kesby et al, 2018).

1.6.2.2. Depression and Monoamine Hypothesis

Major depressive disorder (MDD) is a psychiatric disorder characterized by extreme emotional distress, which carries the risk of suicidal tendency (Hamon and Blier, 2013). The neurological basis of clinical depression is characterized by the level of monoamines such as 5-HT, NE, and DA, which also reflect a strong link in the pathophysiology of depression (Hamon and Blier, 2013). The reciprocal involvement of these monoamines particularly when regarding brain functional connectivity, has profound effects in mediating mood, emotion, and cognitive functions (Hamon and Blier, 2013). Various studies have demonstrated the anatomical similarities and functional interactions between 5-HT neurons of the DRN, NE neurons of the LC, and the DA neurons of VTA. Lesions in these neurons, or receptor activation/inhibition of these monoamines, mediates

the neuronal firing activity of these monoamines (Arborelius et al, 1993; Lejeune et al, 1996; Lejeune and Millan, 1998; Martín-Ruiz et al, 2001; Aman et al, 2007; Guiard et al, 2008). For instance, the effect of a dopaminergic lesion with 6-OHDA on the electrophysiologic activity of 5-HT neurons in the DRN was decreased, whereas increased in LC-NE neurons (Guiard et al, 2008). However, the dopaminergic neuronal activities were enhanced following the lesion of 5-HT-DRN and NE-LC neurons (Guiard et al, 2008). These findings suggest an excitatory and inhibitory effect of DA on 5-HT and NE neurons, respectively, plus an inhibitory effect of 5-HT and NE on DA neurons (Guiard et al, 2008). In addition, neuroimaging studies showed that the expression of D2R and DAT were enhanced and decreased, respectively, in depressed patients (D'haenen and Bossuyt, 1994; Shah et al, 1997; Martinot et al, 2001; Meyer et al, 2001). Depression is also highly prevalent in patients with PD, yet treating the non-motor symptoms often interferes with dopaminergic replacement therapy (Tandberg et al, 1996; Barone et al, 2020; Prange et al, 2022). Treatment with 5-HT and NE reuptake inhibitors (SNRI) or DA agonists have shown to improve the severity of depression in patients with PD (Barone et al, 2020; Prange et al, 2022). Taken together, these findings emphasize functional complex regulations of these monoamines in regulating neuronal activity, and in the contribution of DA neurotransmission in depression.

1.6.2.3. Long-Term Memory

Memory is an essential behavior that enables organisms to guide future choices based on past experiences (Goldman-Rakic, 1995; Shohamy and Adcock, 2010). The hippocampus plays a crucial role in the formation, consolidation, and retrieval of various types of memory (Goldman-Rakic, 1995; Shohamy and Adcock, 2010). Damage or dysfunction of the hippocampus can lead to profound memory impairments (Shohamy and Adcock, 2010). Brenda Milner, a pioneer in the field of clinical neuropsychology and cognitive neuroscience, contributed to the scientific understanding of long-term memory through studies on patients who had undergone brain excisions. In 1955, Milner met the famous patient Henry Molaison (H.M.), a 29-year-old man who underwent the experimental removal of parts of his medial temporal lobe, including the hippocampus to relieve severe epileptic seizures (Scoville and Milner, 1957; Squire, 2009). Milner observed that H.M. experienced a profound amnesia characterized by an inability to form new

long-term memories (Scoville and Milner, 1957; Squire, 2009). This provided valuable insights into the roles of specific brain structures in memory processes.

Eric Kandel revealed the molecular mechanisms that underlie the formation of memories (Kandel and Schwartz, 1982). Kandel utilized *Aplysia* and mice to elucidate the basis of memory and learning and found that specific strength and plasticity cause memory formation (Kupfermann et al, 1971; Carew et al, 1972; Pinsker et al, 1973; Dale et al, 1988). Kandel also demonstrated that learning can lead to long-lasting changes in synaptic connection via phosphorylating key proteins, including PKA and transcription factor cAMP response element-binding protein (CREB) (Shuster et al, 1985; Goelet et al, 1986). Kandel's contribution in the field of memory and learning has awarded him a 2000 Nobel Prize in Medicine or Physiology, shared with Carlsson and Greengard.

Midbrain dopaminergic neurons project directly to hippocampus, and emerging findings indicate DA modulates hippocampal functions and memory processes (Montague, 1995; Lisman and Grace, 2005; Shohamy and Adcock, 2010). Studies by Kandel and others suggested that DA affects long-term potentiation (LTP), a form of synaptic plasticity that encodes for long-term memory, which is mediated by D1-class receptors in hippocampal neurons (Frey et al, 1990; Frey et al, 1991; Huang and Kandel, 1995; Otmakhova and Lisman, 1998; Rossato et al, 2009; Kempadoo et al, 2016). Additionally, D1R-PKA activation phosphorylates substrates, including transcriptional factors and translational regulators, that are required for long-term synaptic changes. In the heterozygous D1R-deficient mice, the facilitating effect of D1R on LTP was dramatically dysregulated (Huang et al, 2004). Activation of DA in hippocampus facilitates the activity of dopaminergic neurons in midbrain, which indirectly enhances hippocampal plasticity to behaviorally mediate novelty (Lisman and Grace, 2005; Shohamy and Adcock, 2010). These findings support the assertion that DA signaling is involved in the memory process of the hippocampus, and that the imbalance of DA levels may have significant pathophysiological consequences such as in Alzheimer's disease (AD).

AD is the most common neurodegenerative disease characterized by progressive deterioration of memory and cognition that are associated with brain atrophy (Martorana and Koch, 2014; D'Amelio et al, 2018). The histological features of AD are accompanied with the presence of extracellular amyloid beta plaques, intracellular neurofibrillary (tau) tangles, neuronal loss, oxidative stress and neuroinflammation (Martorana and Koch, 2014; D'Amelio et al, 2018). The

role of DA in AD is complex and involves interactions with multiple neurotransmitter systems and pathological processes (Martorana and Koch, 2014; D'Amelio et al, 2018). It was postulated that the mesolimbic pathway is potentially impacted in AD pathophysiology, thus contributing to the memory deficits (Martorana and Koch, 2014; D'Amelio et al, 2018). Degeneration of VTA-dopaminergic neurons projecting to the hippocampus potentially contributed to the memory impairments in AD experimental models, and DA treatments improved the memory tasks in these models (Ambrée et al, 2008; Guzmán-Ramos et al, 2012; Nobili et al, 2017; D'Amelio et al, 2018). Further research is needed to better understand the specific mechanisms by which DA dysfunction contributes to AD manifestation.

1.6.2.4. Dopaminergic Reward System

The reward system is a set of structures in a brain that are activated by rewarding or reinforcing stimuli (Wise and Rompre, 1989; Schultz, 1998; Schultz, 2002; Wise, 2004; Schultz, 2007a, b; Di Chiara and Bassareo, 2007). The term reward describes the unconditional motivational effect of stimuli that act as positive reinforcers, and have the ability to enhance associative learning, affect decision making, induce approach behavior, and elicit positive emotion. In 1954, James Olds and Peter Milner discovered the reward behavioral mechanisms in the brain. After they implanted electrodes in the brains of rats, the animals were placed in a Skinner box, arranged in such a manner that they would receive a burst of electrical stimulation by pressing a lever (Olds and Milner, 1954). They found that numerous parts of the brain were specialized in mediating a reward experience (Olds and Milner, 1954). Wolfram Schultz discovered that midbrain dopaminergic neurons mediate this reward activity, and DA is the substrate of prediction and reward (Schultz et al, 1997). The axons of midbrain dopaminergic neurons project to the striatum, NAc, and frontal cortex, which are brain structures that are strongly associated with reward, learning, motivation, and goal-directed behaviors (Wise and Rompre, 1989; Schultz, 1998; Spanagel and Weiss, 1999; Wise, 2004; Schultz, 2007a, b). Midbrain dopaminergic neurons exhibit burst activity (phasic activation) following reward-driven learning, and code an error in the prediction of the occurrence of reward (Schultz et al, 1997; Schultz, 1998; Schultz, 2007a, b). Schultz's work in primates revolutionized the behavioral function of DA to include learning, conditioned and unpredictability of reward, and neuronal decision making (Schultz, 1986; Romo and Schultz, 1990; Ljungberg et al, 1992; Schultz et al, 1993; Mirenowicz and Schultz, 1994; Mirenowicz and Schultz, 1996;

Hollerman and Schultz, 1998; Hollerman et al, 1998; Waelti et al, 2001; Hassani et al, 2001; Schultz, 2007a. b).

Reward-prediction error is among numerous learning paradigms proposed for assessing reward-mediated events (Wise, 2004; Schultz, 2007a, b). The response to a reward occurs after reward-predicting stimulus positively reinforces feedback and produces reward predictions through associative conditioning by the modulation of neural activity. This modulation acts in a way that unpredicted reward enhances activation (positive-prediction error), a fully predicted reward elicits no response, and an omitted reward induced depression (negative-prediction error) (Schultz et al, 1997; Schultz, 2007a, b). To further illustrate, when a subject experiences an unanticipated reward in response to a cue's presence, a prediction error is enhanced and elicited (Schultz et al, 1997). Therefore, it drives learning for upcoming events by the anticipation of associated cues to direct motivated behavior toward the outcome. After the subject is trained that a conditioned stimulus predicts a reward, the dopaminergic neurons elicit a burst firing responding to the appearance of the predicted cue, but not the reward (Schultz et al, 1997; Schultz, 1998; Schultz, 2007a, b). The quantitative discrepancy between the predicted and delivered outcome is defined as a reward-prediction error, and it varies among different objects to produce large or smaller prediction error depending on the significance of the motivational event. Interestingly, there is a reduction in the number of DA neurons firing in response to a repetitive or successive reward associated with the expected reward, which elicits minimum phasic excitation after the presentation of the cue. However, when a predicted reward fails to deliver, there is a firing reduction of dopaminergic neurons at the same time rewards failed to occur (Schultz et al, 1997; Schultz, 1998; Schultz, 2007a, b). *Fig. 1.9. illustrates the activity of DA in reward-predicted errors model.*

Moreover, reward uncertainty is one of the reward models to assess neuronal decision-making behavior and is defined as the degree of uncertainty within a given distribution of all-or-none probable outcome (Schultz, 2007a, b). During the stimulus reward interval, slow, sustained, and moderate neuronal activation of dopaminergic neurons co-varies with uncertainty or uncertain events, whereas short latency, but strong-phasic neuronal response co-varies with expected or predicted outcome (Fiorillo et al, 2003; Preuschoff et al, 2006; Tobler et al, 2007; Schultz, 2007a, b). The postsynaptic neuronal coding of reward and uncertainty is distinct and in both, evokes high and low DA concentrations appropriate for stimulating D1R and D2R, respectively (Schultz,

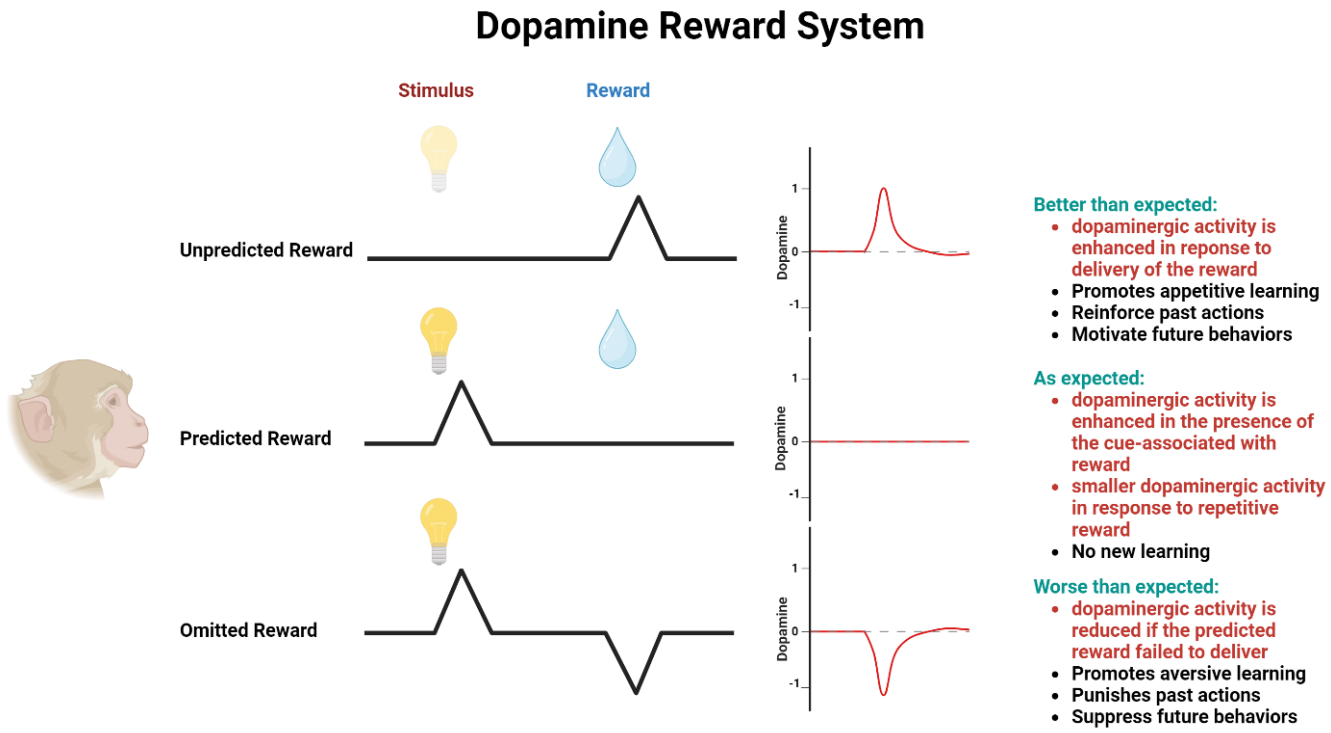

Fig. 1.9. Dopamine Reward System.
Schematic diagram for the classical model of the reward prediction error, which depicts the dopaminergic activity in response to unpredicted reward, predicted reward, and omitted reward. Created with BioRender.com.

2007a, b). Overall, midbrain dopaminergic neurons have a centric role in mediating learning and essential behavioral responses including attention-based learning and risk-taking behaviors (Phillips et al, 2003; Stuber et al, 2005; Saunders et al, 2018).

1.6.2.5. Pavlovian Fear Learning

Beyond the NAc, the mesolimbic dopamine system projects to the amygdala, a structure that is crucial for associative learning (Pavlovian) (Pezze and Feldon, 2004; Lee et al, 2017; Salinas-Hernández and Duvarci, 2021; Frick et al, 2022). Pavlovian fear conditioning is a form of associative memory formation where a conditioned stimulus, such as an order or an auditory tone, is paired with a fear arousing unconditioned stimulus, such as a foot shock (Rogan et al, 1997). The affective response of animals to such salient events can induce neuronal plasticity in lateral nucleus of the amygdala, LTP and memory formation (Rogan et al, 1997). Neurons expressing DA receptors in amygdala are selectively activated by stress, in which DA neurotransmission contributes to the process of Pavlovian fear conditioning (Coco et al, 1992; Hamati et al, 2023). D1R agonist and D1R/D2R antagonists, respectively, facilitate and attenuate the conditioned freezing, suggesting that DA is crucial in the process of emotional memory formation (Guarraci et al, 1999; Guarraci et al, 2000; Greba et al, 2001; Rosenkranz and Grace, 2002; Takahashi et al, 2010; Hamati et al, 2023). In summation, understanding the dopaminergic mechanisms underlying fear-related memories provide insight on the neurobiology of anxiety disorders, and could lead to improved therapeutic approaches of their treatment.

1.6.2.6. Addiction and Drug of Abuse

Drug addiction is a chronic disease characterized by drug seeking and use that has harmful consequences on human health and quality of life. Examples of addictive habits include the consumption of amphetamine, cocaine, opioids (heroine and fentanyl), nicotine, and ethanol (Everitt and Robbins, 2005; Costa and Schoenbaum, 2022). The transition from recreational drug usage to compulsive addictive drug use underlies the seriousness of substance use, including the potential for overdose that can cause serious injury or death (Everitt and Robbins, 2005; Costa and Schoenbaum, 2022). As described in previous subsections, midbrain dopaminergic neurons regulate reward activities and reinforce behaviors, including the use of addictive drugs following reward cues (Everitt and Robbins, 2005; Costa and Schoenbaum, 2022). Cocaine mediates a substantial release of DA in dorsal striatum upon presentation of a drug-associated cue and

enforces drug-seeking behavior (Ito et al, 2000; Ito et al, 2002; Phillips et al, 2003; Di Ciano and Everitt, 2004; Vanderschuren et al, 2005; Stuber et al, 2005). Psychostimulants block the activity of DAT, thereby increasing the level of DA in the synapses and inducing hyperlocomotion activity (Giros et al, 1991a; Giros et al, 1996; Rocha et al, 1998; Carboni et al, 2001; Salahpour et al, 2008). The neuronal and behavioral responses of dopaminergic receptor activation also mediate psychostimulant induced locomotor activity and contribute to addictive behavior (Chausmer et al, 2002; Elliot et al, 2003; Katz et al, 2003; Anderson et al, 2003; Anderson et al, 2006; Schmidt et al, 2006; Schmidt and Pierce, 2006; Karlsson et al, 2008; Thompson et al, 2010; Urs et al, 2011; Sutton and Caron, 2015; Porter-Stransky et al, 2020). Together, these finding support the involvement of DA in psychostimulant-mediated activity and highlight the neural basis and mechanism of addictive behavior.

1.6.2.7. Reward Behavior of Feeding

Feeding is a motivated survival behavior that is guided by internal states such as energy needs driven by hunger and satiety (Palmiter, 2007; Abizaid, 2009; Godfrey and Borgland, 2019; Geisler and Hayes, 2023). The hypothalamus integrates various hormonal and neuronal circuits to regulate homeostatic and reward control, including appetite, metabolism, and motivation (Palmiter, 2007; Abizaid, 2009; Godfrey and Borgland, 2019; Geisler and Hayes, 2023). Metabolic regulation is a process to maintain the balance of energy production, storage, and expenditure that supports various physiological functions, in which both central and peripheral DA modulate associated behaviors (Palmiter, 2007; Geisler and Hayes, 2023). Midbrain dopaminergic neurons projecting to the NAc are essential in mediating reward behaviors of feeding (Palmiter, 2007; Geisler and Hayes, 2023). DA is released in the NAc in response to food-related cues, such as sight, smell, and taste (Palmiter, 2007; Godfrey and Borgland, 2019; Geisler and Hayes, 2023). The hormonal input of pancreatic insulin, white adipose produced leptin, and stomach synthesized ghrelin, directly affect DA reward pathways and activate DA receptors on VTA-dopaminergic neurons (Palmiter, 2007; Abizaid, 2009; Godfrey and Borgland, 2019; Geisler and Hayes, 2023). DA signaling in the NAc is dynamically regulated through stimulation by ghrelin and inhibition by insulin and leptin. These opposing dynamics directly influence the metabolic feeding behavior mediated by hunger or satiety, respectively (Palmiter, 2007; Abizaid, 2009; Godfrey and Borgland, 2019; Geisler and Hayes, 2023). Other molecules contribute indirectly to feeding behavior modulations such as those

derived from the lateral hypothalamus, arcuate and paraventricular nucleus of hypothalamus: glutamate, GABA, and neuropeptides (orexin, neuropeptide Y, agouti-related protein) (Palmiter, 2007; Abizaid, 2009; Godfrey and Borgland, 2019; Geisler and Hayes, 2023). It is important to note that the role of DA in feeding behavior is also influenced by different genetic and environmental factors. Medically, the dysregulation of DA feeding behaviors can contribute to eating disorders, obesity, and other feeding-related disorders (Palmiter, 2007; Abizaid, 2009; Godfrey and Borgland, 2019; Geisler and Hayes, 2023). *Fig. 1.10. shows the excitatory and inhibitory inputs to VTA DA neurons to mediate feeding behaviors.*

Obesity is a complex disease involving excessive body weight and health concerns (Palmiter, 2007; Abizaid, 2009; Godfrey and Borgland, 2019; Geisler and Hayes, 2023). Obesity is influenced by genetic, behavioral, metabolic, and hormonal factors, neurotransmitter release, as well as by dysregulation of the hypothalamic-pituitary-adrenal (HPA) axis (Palmiter, 2007; Geisler and Hayes, 2023). DA plays a major role in reward-mediated obesity which is characterised by a dysfunctional central and peripheral dopaminergic system (Palmiter, 2007; Geisler and Hayes, 2023). The increase in striatal DA neurotransmission and reduced availability of DA receptors may represent a risk factor for the onset of obesity (Palmiter, 2007; Geisler and Hayes, 2023). Johnson and Kenny showed that DA reward systems are modified to drive the development of compulsive food seeking in mice subjected to obesity-inducing diets of high-fat and high-sugar foods. This behaviour is similar to the adaptive behaviour exhibited by persons who self-administer addictive drugs (Johnson and Kenny, 2010). The D2R agonist, bromocriptine, reduces hyperphagia and adiposity in rodents, whereas knockdown of striatal D2R induces the onset of compulsive food seeking (Johnson and Kenny, 2010; Epstein and Shaham, 2010; DiFeliceantonio and Small, 2019). Findings linking obesity to a reduced D2R signaling in the striatum were also reported in humans, implying that more DA release induces activated mesolimbic food-reward system (Wang et al, 2001; Stice et al, 2008; Epstein and Shaham, 2010; DiFeliceantonio and Small, 2019). This established a causal link between diet-induced obesity, downregulation of D2R, and the emergence of addictive behavior (DiFeliceantonio and Small, 2019). Moreover, VTA-dopaminergic neurons respond to a motivational state induced by food deprivation (Branch et al, 2013; Godfrey and Borgland, 2020). Both chronic food restriction and acute fasting induce strong metabolic and behavioral changes, increase food-seeking behavior, and influence synaptic transmission onto VTA-dopaminergic neurons (Branch et al, 2013; Godfrey and Borgland, 2020).

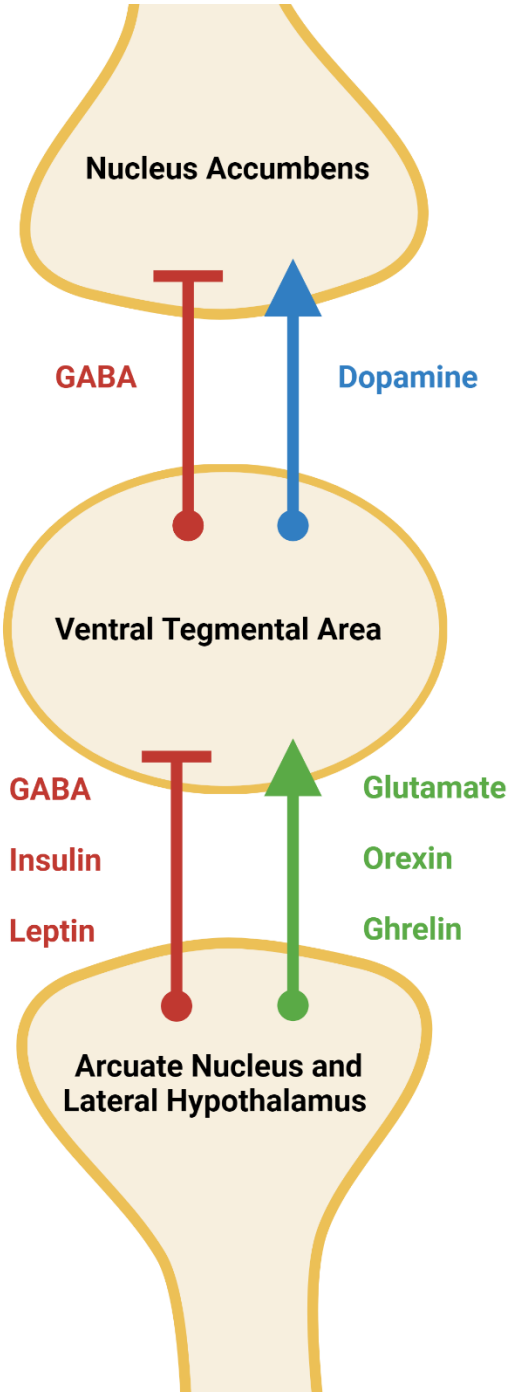

Fig. 1.10. Dopamine Reward Circuitry of Feeding Behavior.
Schematic illustration of hypothalamic nuclei sending excitatory glutamatergic and inhibitory GABAergic inputs toward midbrain dopaminergic neuron, ventral tegmental area (VTA). Leptin and insulin inhibit VTA dopamine neurons, while ghrelin and orexin activate them. VTA project to the nucleus accumbens (NAc), a structure associated with reward system to mediate homeostatic and motivational associated-behaviors. Created with BioRender.com.

Overall, understanding the mechanisms of behavioral mediated metabolic regulation is crucial for maintaining overall health and preventing metabolic imbalances.

1.6.3. Dopaminergic Modulation of Primary Motor Cortex

The primary motor cortex (M1) is crucial region in the cortical brain essential not only for planning and execution of motor commands, but also for motor performance and learning (Luft and Schwarz, 2009; Cousineau et al, 2022). M1 microcircuits are organized in six layers of interconnected glutamatergic excitatory pyramidal neurons and inhibitory GABAergic neurons (Luft and Schwarz, 2009; Cousineau et al, 2022). M1 directly controls the execution of voluntary movements by sending signals to the spinal cord and lower motor neurons, which in turn activate specific muscles contractions for the precise and purposeful control of body movements (Cousineau et al, 2022).

DA system is highly express in cortical areas, and retrograde tracing in rodents suggested that DA projection in M1 originated mainly from VTA, but also from SNc (Hosp et al, 2011; Vitrac et al, 2014; Cousineau et al, 2022). Both D1- and D2-class receptors are expressed in M1 layers and modulate neuronal excitability and plasticity, and pharmacological blockade of D1R or D2R in M1 induces impaired motor skill learning (Molina-Luna et al, 2009; Cousineau et al, 2022). Clinically, M1 activity is altered in PD patients, and they experience significant disability in executing fine motor task (Underwood and Parr-Brownlie, 2021; Cousineau et al, 2022). The severity of depleted DA neurons in SNc dysfunctionally altered M1 circuits and impacted movement-related behaviors (Underwood and Parr-Brownlie, 2021; Cousineau et al, 2022). Understanding the functions of M1 is crucial for comprehending how the brain controls voluntary motor actions and how motor deficits can result from neurological conditions or injuries.

1.6.3.1. Stroke Recovery

Stroke is a medical condition that occurs when blood supply in some regions of brain region is interrupted or severely reduced (Oczkowski, 2013; Gower and Tiberi, 2018). Consequently, this result in depriving the neurons from oxygen and essential nutrients and leading to neuronal damage or death (Gower and Tiberi, 2018). Stroke is a major cause of disability in adults, and survivors suffer motor deficit and behavioral dysfunction (Oczkowski, 2013; Gower and Tiberi, 2018). DA transmission is among the widespread impacted systems by stroke that involves various processes

related to neuroplasticity, motor function, and cognitive function (Cramer, 2015; Gower and Tiberi, 2018). Following the onset of ischemic stroke, the DA metabolites DOPAC and HVA are decreased, but a massive transient release of DA into the ipsilateral striatum is observed in animal models (Slivka et al, 1988). It is important to note that the association between stroke recovery and dopamine is complex and influenced by various factors, including the location and extent of the stroke, individual characteristics, and the interplay of other neurotransmitters and neurochemical systems (Cramer, 2015; Gower and Tiberi, 2018; Stinear, 2019). Tiberi's lab examined the DA contribution in axonal remodeling and motor activity of in mice with cortical photothrombosis stroke. Following 7-days administration of dihydrexidine (DHX), a selective D1-class receptor agonist, we observed accelerated motor recovery and a specific dopaminergic, but not noradrenergic, TH-positive axon remodelling in the ipsilateral cortical regions, an effect was not present in sham mice (Said et al, manuscript in preparation). These findings provide a proof of principle of potential pharmacological approach by activating D1-class receptor in the post-recovery of stroke (Said et al, manuscript in preparation). Further research is needed to fully understand the specific mechanisms by which DA influences stroke recovery and to develop targeted interventions to optimize functional outcomes after a stroke (Stinear, 2019).

1.6.4. The Tuberoinfundibular Pathway and Prolactin Secretion

DA also regulates neuroendocrine secretion of prolactin, a hormone that is predominantly synthesized and secreted from lactotroph cells of the anterior pituitary gland (MacLeod et al, 1970; Kamberi etal, 1970; Ben-Jonathan, Hnasko, 2001; Fitzgerald and Dinan, 2008; Grattan 2015). This secretion is mediated via the tuberoinfundibular pathway, in which the action of dopaminergic neurons in the arcuate and paraventricular nuclei of hypothalamus tonically inhibit prolactin secretion in the median eminence of pituitary gland (Ben-Jonathan, Hnasko, 2001; Fitzgerald and Dinan, 2008; Grattan 2015). The physiological action of DA via D2R stimulation on pituitary lactotrophs is to inhibit basal and hormone stimulated secretion of prolactin (Albert et al, 1990). Some antipsychotic drugs block DA receptors in this pathway causing hyperprolactinemia, which is often treated with a D2R agonist, e.g. bromocriptine, to normalize prolactin level (Ben-Jonathan, Hnasko, 2001; Fitzgerald and Dinan, 2008; Grattan 2015). Interestingly, D2R-deficent mice display increased prolactin levels, enlarged lactotrophs, and ultimately develop pituitary tumors (Kelly et al, 1997; Saiardi et al, 1997). In contrast, DAT-mutant mice exhibit reduced lactotroph

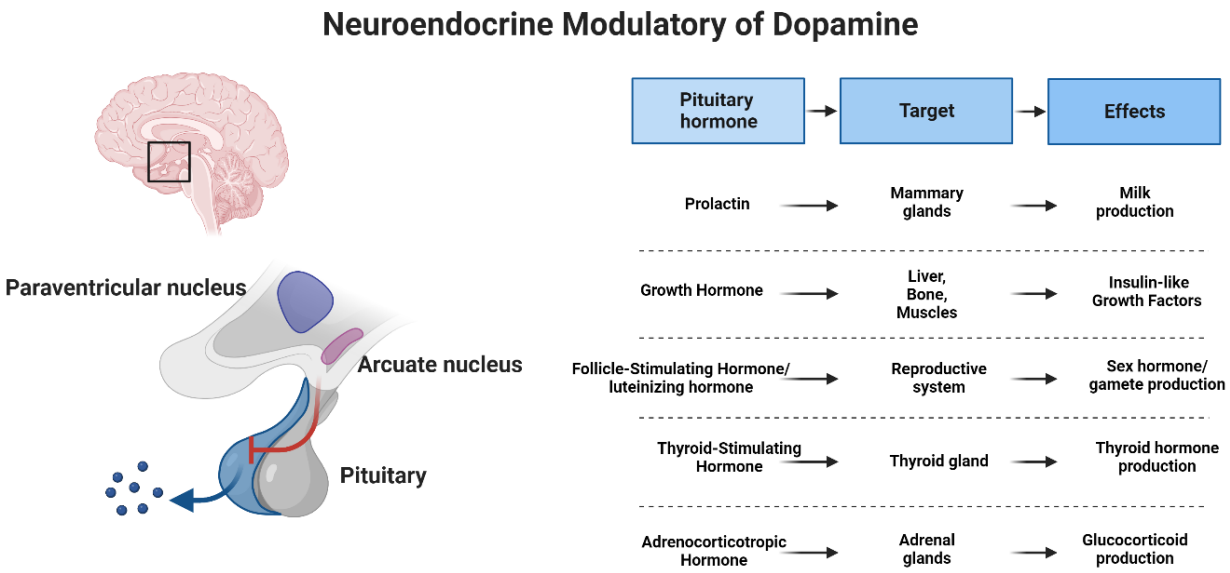

Fig. 1.11. Dopamine Neuromodulation of Different Hormones in the Pituitary Gland.
Dopamine regulates the secretion of prolactin via the tuberoinfundibular pathway. The action of dopaminergic neurons in the arcuate and paraventricular nuclei of hypothalamus inhibit prolactin secretion. Dopamine is also involved in the modulation of numerous hormones secreted from the anterior pituitary gland. Created with BioRender.com.

size, inability to lactate, and dwarfism (Bossé et al, 1997). Interestingly, DA has also been shown to modulate, either directly or indirectly, secretion of other anterior pituitary hormones; growth hormone, follicle-stimulating hormone, luteinizing hormone, thyroid-stimulated hormone, and adrenocorticotropic hormone (Beaulieu and Gainetdinov, 2011). These findings demonstrate the significance of DA in the control and development of the pituitary gland. *Fig. 1.11. summarizes the DA neuromodulation of different hormones secreted from pituitary.*

1.6.1. D1-Class Receptors: Knockout Models and Physiological Functions

Genetic deletion approaches have been employed to decipher the subtype-specific physiological roles of DA receptors and have uncovered functional and behavioural phenotypes (Holmes et al, 2004). The ability to target a specific DA receptor gene allows for elucidation of the physiological functions mediated by these receptors and enables pharmacological discrimination of DA receptor subtypes (Holmes et al, 2004). Midbrain levels of DA are elevated in D1R-knockout (KO) mice suggesting that there may be a compensatory increase in DA biosynthesis following inactivation of the D1R (Holmes et al, 2004). Striatal levels of substance P and dynorphin, both of which are synthesized in MSNs of D1R-expressing neurons, are reduced in D1R-KO mice, however, the level of enkephalin, found selectively in D2R-expressing neurons, remains unchanged (Xu et al, 1994a, b; Drago et al, 1994). The null D1R mice display an increase in spontaneous locomotor activity, and D1R-class agonists psychostimulant cocaine fail to induce locomotor activity (Xu et al, 1994a, b; Centonze et al, 2003; Karlsson et al, 2008). Interestingly, the D1-class antagonist either had no effect or decreased locomotion, implying an important role for both D1R and D5R in locomotion, perhaps by exerting distinct behavioral actions on spontaneous motor activity (Xu et al, 1994a; Centonze et al, 2003). Locomotor activity appeared to be normal in D5R mutant mice, however, a hyperactivity-inducing effect of D1-class agonists, cocaine, and methamphetamine were mildly attenuated (Holmes et al, 2001; Elliot et al, 2004; Karlsson et al, 2008; Hayashizaki et al, 2013; Sasamori et al, 2022). In contrast to the genetic deletion of D1R and D5R, deletion of D2R in mice, however, significantly reduced spontaneous movement and mimicked parkinsonian-like behavior (Baik et al, 1995).

Studies found that single or double gene deletion of D1R and D5R in forebrain impairs spatial learning and memory, suggesting an important role for both D1R and D5R in these processes (Matthies et al, 1997; El-Ghundi et al, 1998; Sariñana and Tonegawa, 2016). Electrophysiological

recording showed impairment of LTP in mice lacking D1R and D5R, suggesting their importance in neuronal plasticity (Levine et al, 1996; Matthies et al, 1997; Centonze et al, 2003; Moraga-Amaro et al, 2016). Psychostimulants or morphine administration in D1R-deficient mice lead to attenuated reinforcing and behavioral-sensitizing effects relative to wild-type mice (Xu et al, 1994b; Xu et al, 2000; Becker et al, 2001; Urs et al, 2011). D5R-KO animals experience attenuated hippocampal acetylcholine release and NMDAR-GluN2B expression, which suggests the importance of D5R in the modulation of hippocampal cholinergic and glutamatergic neurotransmissions (Laplante et al, 2004; Berlanga et al, 2005; Moraga-Amaro et al, 2016). DAT phosphorylation activity is enhanced in D5R-KO mice, whereas the binding expression for D1- and D2-class are unaltered (Hollon et al, 2002; Hayashizaki et al, 2013). Moreover, single gene knockout mice for each DA receptor subtype exhibit peripheral abnormalities not discussed in further detail here. These mutant mice could potentially be used as a model for investigating novel therapies to correct dysfunctions of the dopaminergic system (Holmes et al, 2004).

1.6.2. Other Behaviors and Disorders Modulated by Dopaminergic Neurotransmission

As described in previous subsections, dopaminergic projections are widespread throughout the brain and are involved in many different central behavioral processes. Moreover, DA also targets other circuits not discussed herein that have linked to several other behavioral functions and diseases, further underscoring its general role as neuromodulator (Iversen and Iversen, 2007; Beaulieu and Gainetdinov, 2011; Costa and Schoenbaum, 2022). Dysfunctional DA transmission has been linked to other neurodegenerative and mental diseases, e.g., Huntington's disease, Tourette's disorder, attention deficit hyperactivity disorder (ADHD), and bipolar disease, yet the precise mechanism of DA involvement in these conditions is presumably complex, and not yet fully understood (Iversen and Iversen, 2007; Beaulieu and Gainetdinov, 2011; D'Amelio et al, 2018; Costa and Schoenbaum, 2022). Thus, future research is warranted to elucidate the molecular and cellular interplay between DA and these diseases. Indeed, improving our understanding of the dopaminergic system in this regard could lead to the development of better therapeutic strategies for various brain diseases and alleviate some of the economic burden they present to our health care system.

1.6.3. Electrophysiological Recording of Dopaminergic Neurons

Midbrain DA neurons display three characteristic features during electrophysiological recordings: tonic single spike firing interspersed with spontaneous bursts (2-10 action potentials) and pauses (>2.5 msec) (Grace and Bunney, 1980; Grace and Bunney, 1983; Grace and Bunney, 1984a. b; Zhang and Sulzer, 2012). Midbrain dopaminergic neurons are autonomous pacemakers that exhibit continuous regular firing (0.5 to 8 Hz) and release of DA in the absence of synaptic input, which is required for proper behavioral function (Grace and Bunney, 1995; Zhang and Sulzer, 2012). Changes in the firing patterns of midbrain dopaminergic neurons are thought to encode for information of certain type of behaviors (Costa and Schoenbaum, 2022). In the striatum, the orchestration of DA firing, release, and activation of D1R-MSN and D2R-MSN are controlled by multiple factors (e.g., neuronal excitability, presynaptic and postsynaptic activity) (Beckstead et al, 2007; Ford, 2014; Marcott et al, 2014; Marcott et al, 2018; Costa and Schoenbaum, 2022). The constitutive activation of D2R, but not D1R, maintain the single spike firing of tonic DA release into target neurons (Costa and Schoenbaum, 2022). Burst firing transiently increase the DA release to bind D1R and activate the direct pathway (Costa and Schoenbaum, 2022). Following intense burst, transient decrease of DA release that bind D2R and activate indirect pathway cause pause in DA firing (Costa and Schoenbaum, 2022). These increase and decrease in the phasic release of DA at the target loci can influence numerous behavioral functions such as synaptic plasticity, reward/punishment-based learning, and locomotor initiation and suppression (Costa and Schoenbaum, 2022).

In addition to electrophysiological recording, several experimental approaches have been used to measure *in vivo* release of DA in the brain, including optogenetics imaging, voltammetry, radiolabeling-based approach for DA or its metabolites, or intracerebral microdialysis (Iversen and Iversen, 2007; Patriarchi et al, 2019). These methods can be done at single-cell level or at larger scale through simultaneous recording from hundreds or thousands of neurons (Iversen and Iversen, 2007). Because these methods cannot be used to study the brain of living human subjects, other non-invasive procedures such as PET, and functional magnetic resonance imaging (fMRI) have been introduced for this purpose. These methods have provided a completely new way of assessing bioradiotracer binding selectivity in the functional dopamine system (transporter, receptors,

biosynthetic enzymes) of human brain (Sulzer et al, 2018; Cassidy et al, 2019; Ceccarini et al, 2020; Hamati et al, 2023).

1.6.4. Evolution and Dopamine

A remarkable feature of DA is its ability to mediate similar behavioral functions, including learning, and movement, across a wide range of invertebrate and vertebrate species, from nematodes to humans (Costa and Schoenbaum 2022). In the invertebrate and non-mammalian vertebrate, DA organization is phylogenetically conserved, as DA excites striatal neurons that express D1R and inhibits neurons that express D2R (Chu et al, 2001; Ding and Perkel, 2002; Boehmler et al, 2004; Li et al, 2007; Schweitzer et al, 2009; Barral et al, 2010; Ericsson et al, 2013; Grillner and Robertson, 2016). In the invertebrate *Aplysia*, which contains a simpler nervous system, DA has been shown to be a key mediator with both inhibitory and excitatory effect to modulate certain behaviors, e.g. memory, associative learning, and reinforcement signals (Sweeney, 1963; Ascher, 1972). In nematodes, *Caenorhabditis elegans* contain eight dopaminergic neurons that are involved in various behaviors, such as locomotion, and learning (Sulston et al, 1975; Wintle et al, 2001; Suo et al, 2004; McDonald et al, 2006). In the insect model of *Drosophila*, DA containing neurons are widespread in the fly brain and the organization of dopaminergic neurotransmission has striking similarities to vertebrates in orchestrating behavioral functions, including movement, learning, and motivation (Tunnicliff et al, 1969; Livingstone et al, 1983; Feany et al, 2000; Keene et al, 2005). The simplicity and well-characterized nervous system of the three invertebrate organisms mentioned above, make them important models widely used in neuroscience to understand fundamental principles of neural circuitry and the behavior of DA.

1.7. Dopaminergic Sensory Systems

In addition to the central nervous system, neuromodulatory actions of DA are involved in the neural sensory systems: vision and olfaction, which are processed by retina and olfactory bulb (OB), respectively. DA also acts as neuromodulator for the circadian system that maintains diurnal activity. The activity of DA in spinal and cerebellar neurons modulate pain perception and sensory-motor information, respectively. Below, I briefly describe the involvement of DA system in mediating these behaviors.

1.7.1. Dopaminergic Visual system

Retina, which is the light sensitive tissue located at the back of the eye, is a crucial component of the visual system, as it receives and processes light and visual information to the optic nerve that carries visual messages to the rest of brain (Popova, 2014; Korshunov et al, 2020). Retina consists of rod and cone photoreceptor cells, bipolar cells, horizontal cells, amacrine cells, and ganglion cells (Nguyen-Legros et al, 1999; Popova, 2014; Korshunov et al, 2020). DA is a major catecholamine in the retina, and it is involved in various visual processes including light adaptation and regulation of melatonin biosynthesis, a hormone that is produced in darkness to induce sleep (Dowling, 1991; Korshunov et al, 2020). The DA containing cells are endogenously activated by light exposure to synthesized and released DA from the retina that activates DA receptors (Brown and Makman, 1972; Schorderet and Nowak, 1990; Dowling, 1991; Popova, 2014; Korshunov et al, 2020). D1R are found on horizontal, amacrine, and bipolar cells, while D5R are found in retinal pigment layer (Nguyen-Legros et al, 1999; Witkovsky, 2004; Korshunov et al, 2020). D2R function as autoreceptors for DA neurons, while D4R localizes on rod and cone of photoreceptors (Dubocovich, 1990; Zawilska and Nowak, 1997; Witkovsky, 2004; Korshunov et al, 2020). Activation of D1R uncouple gap junctions between horizontal cells, regulate the activity of responsiveness of ganglion cells to light stimuli, and evoke Ca^{2+} dependent release of ACh (Korshunov et al, 2020). D2-class receptors are activated via D4R localized on photoreceptors, rapidly suppressing the nocturnal cyclic AMP-dependent activity of serotonin N-acetyltransferase, a key regulatory enzyme in melatonin biosynthesis (Nowak et al, 1989; Nir et al, 2002; Korshunov et al, 2020). The melatonin-dopamine feedback mechanism to light:dark conditions is essential for circadian rhythm, in which light increases the activity of DA of the retinal dopaminergic cells and melatonin inhibits DA synthesis and its release from the retinal dopaminergic cells in dark cycle (Nowak et al, 1989; Korshunov et al, 2020). Disruption in the retinal DA signaling contributes to visual impairments and retinal disorders. Thus, understanding the mechanisms of DA action is essential for comprehending normal retinal functions and pathophysiology of retinal diseases.

1.7.2. Dopaminergic Olfaction system

The OB is a brain structure that is crucial for the sense of smell, as it deciphers a volatile milieu of chemical odorants coming from olfactory nerve (Cave and Baker, 2009; Korshunov et al, 2020). The OB consists of juxtaglomerular cells, mitral cells, tufted cells, and granule cells (Cave and

Baker, 2009; Korshunov et al, 2020). DA is the only catecholamine in the OB and plays a significant role in modulating the function of the OB, which is involved in the processing, discriminating, and perception of odors (Korshunov et al, 2020). In the OB, the number of DA neurons are estimated to outnumber other DA populations in the brain and when co-expressed with GABA, are mostly inhibitory (Korshunov et al, 2020). The inhibitory action upon activation and co-release of DA and GABA increases the odor detection and discrimination through the activity of D1R and D2R, respectively (Korshunov et al, 2020). Interestingly, olfactory impairment is one of the earliest non-motor traits of PD. Whether DA neurons in OB contribute to the loss remains to be investigated.

1.7.3. Dopaminergic Circadian System

Circadian rhythms are biological processes that follow a 24-hours oscillation and optimize various physiological and behavioral function in living organisms, e.g. sensory perception, sleep, body temperature, hunger, and hormonal regulation (Korshunov et al, 2017). These rhythms are synchronized with the daily light:dark cycles and help organisms to adapt to environmental changes; its disruption has health risks (Korshunov et al, 2017). The suprachiasmatic nucleus (SCN), which is a bilateral structure located in the anterior part of the hypothalamus, is the essential pacemaker of the circadian system and regulates most circadian rhythms in the body (Korshunov et al, 2017).

DA, among several other neuromodulators, is critical for maintaining proper rhythmicity through its actions within hypothalamus, striatum, retina, and OB, where DA is regulated by SCN and clock genes, such as period genes *Per1* and *Per2* (Mendoza and Challet, 2014; Korshunov et al, 2017; Korshunov et al, 2020). DA receptors are expressed in SCN and other hypothalamic regions, the supraoptic nucleus and paraventricular nucleus, and modulate hormonal and homeostatic functions via tuberoinfundibular dopaminergic neurons, tuberohypophyseal dopaminergic neurons, and periventricular hypophyseal dopaminergic neurons (Rivkees and Lachowicz, 1997; Bender et al, 1997; Korshunov et al, 2017). In the striatum, DA receptor activation either enhances or diminishes clock gene expression and is mediated by D1R or D2R, respectively, to modulate certain cortical or limbic behaviors (Imbesi et al, 2009; Hood et al, 2010; Mendoza and Challet, 2014; Korshunov et al, 2017). Indeed, psychostimulant-induced regulation in clock gene expression in striatum may cause disruption in sleep and circadian rhythmicity of addictive

behavior (Lynch et al, 2008; Korshunov et al, 2017). The neurons of retina and OB maintain the synchrony of their circadian rhythms independently from the SCN (Korshunov et al, 2017; Korshunov et al, 2020). DA in the retina and OB demonstrate diurnal activity, with the highest activity during daytime and the lowest activity during nighttime (Corthell et al, 2013; Korshunov et al, 2017; Korshunov et al, 2020). Dysregulation of dopamine signaling or alterations in DA levels can disrupt circadian rhythms and contribute to circadian-related disorders (Doi et al, 2006; Korshunov et al, 2017; Korshunov et al, 2020).

1.7.4. Dopaminergic Spinal System

The spinal cord plays a crucial role in transmitting sensory and motor signals between the brain and the rest of the body (Millan, 2002; Bannister and Dickenson, 2016; Puopolo, 2019). Pain perception is the process by which the brain interprets and responds to sensory signals that involves various stages of sensory processing and emotional response (Millan, 2002; Bannister and Dickenson, 2016; Puopolo, 2019). Noxious stimuli result from the activation of sensory receptors (nociceptors) specialized in perceiving pain (Millan, 2002; Bannister and Dickenson, 2016; Puopolo, 2019). The ascending transmission of stimuli from peripheral neuronal damage are onward passed to the spinal cord and then to the sensory component of the brain (Millan, 2002; Bannister and Dickenson, 2016; Puopolo, 2019). The inhibitory or facilitatory pain message is generated in the midbrain and brainstem, which is then sent down to the dorsal horn of spinal cord through a mechanism known as top-down pathway (Millan, 2002; Bannister and Dickenson, 2016; Puopolo, 2019). DA system, among other neurotransmitter systems, represents a potential target for top-down pain transmission via hypothalamic-spinal projection (Millan, 2002; Bannister and Dickenson, 2016; Puopolo, 2019). The descending circuit of facilitatory or inhibitory innervation is mediated by spinal D1R or spinal D2R, respectively, in response to pain or nerve injury (Zhu et al, 2007; Liu et al, 2019; Sharples et al, 2020). The dopaminergic system, DA fibers and varicosities are present in all laminae of the spinal grey matter throughout the spinal cord, and DA can act on all spinal DA receptors that are expressed in the spinal cord and dorsal root ganglia to influence sensory, motor, and autonomic systems (Holstege et al, 1996; Millan, 2002; Bannister and Dickenson, 2016; Puopolo, 2019). Following nerve injury, agonist stimulation of spinal NMDAR in dorsal horn neurons induces hyperexcitability that is dependent on subtype activation of D1-class receptors (Aira et al, 2016). This implies that spinal D1-class receptors mediated input

descending to the spinal dorsal horn where it can modulate central sensitization and pathogenic pain (Aira et al, 2016). Additionally, heterodimerization of D1R and D2R in the spinal cord promotes chronic neuropathic pain by activating the $G\alpha_q$-mediated protein kinase C (PKC) cascade to increase the excitability of spinal neurons (Bao et al, 2021). The integration of spinal D3R regulates the spinal cord reflex excitability, and its dysfunction contributes to abnormal limb sensation involved in restless leg syndrome (Clemens et al, 2004; Clemens et al, 2022). Mice lacking D5R are hypersensitive and have increased sympathetic tone (Hollon et al, 2002). Moreover, DA is also involved in the emotional aspects of pain perception as well as analgesic activity mediated by the opioid system (Brewer et al, 2014; Rodgers et al, 2019; Rodgers et al, 2020). Understanding the contributions of spinal DA receptors to sensory processing, pain modulation, and motor control may lead to new insights into the development of novel therapeutic approaches for pain.

1.7.5. Dopaminergic Cerebellar System

Cerebellum is an important brain region for different motor functions: learning and movement adaptation. The neural circuitry of cerebellar cortex integrates sensory and motor information to ensure smooth, precise, and efficient movements (Schweighofer et al, 2004; Flace et al, 2021). Dopaminergic system, among other neurotransmitters, modulates cerebellar activity to regulate goal-oriented cerebellar learning and fine-tuning-coordinated movement (Schweighofer et al, 2004; Flace et al, 2021). In addition to midbrain dopaminergic innervation to cerebellum, a wide distribution of cerebellar DA neurons observed in molecular layer, Purkinje neuron layer, and granular layer (Ikai et al, 1992; Barili et al, 2000; Schweighofer et al, 2004; Giompres et al, 2005; Flace et al, 2021). These cerebellar neurons synthesized and released DA to interact with uneven distributed cerebellar DA receptors (Heskje et al, 2020; Flace et al, 2021; Cutando et al, 2022; Mahoney-Rafferty et al, 2023). DA receptors are also found on axonal inputs to the cerebellum, such as mossy fibers and climbing fibers, implying a possible role of DA on the transmission of sensory and motor information to the cerebellum (Flace et al, 2021). DA receptors are predominantly expressed in the principal output neurons of cerebellar cortex, Purkinje cells, in which their activity influence their role in motor control and learning (Flace et al, 2021). Moreover, cerebellar DA receptors modulate cerebellum-linked cognitive function, cerebellar neuronal plasticity, and cerebellar-midbrain pathways (Heskje et al, 2020; Flace et al, 2021; Cutando et al,

2022; Mahoney-Rafferty et al, 2023). Alterations in the cerebellar dopaminergic system may contribute to the regulation of motor behaviors including the control of posture, balance, and coordination of voluntary movements, and possibly in the pathophysiology of movement disorders and cognitive deficits observed in PD (Mirdamadi et al, 2016; Mahoney-Rafferty et al, 2023).

1.8. Dopaminergic Peripheral Systems

Prior to the discovery of DA as a neurotransmitter in the brain, DA had been found in peripheral tissues and presumed to be merely a precursor of NE and epinephrine (Goodall, 1951; Von Euler and Hellner, 1951; Blaschko, 1957). In the 1950s, the occurrence of DA in peripheral tissues was observed to be equivalent to the amount observed for NE and epinephrine (Blaschko, 1957). Since then, peripheral DA has been shown to influence many physiological and pathophysiological functions (Channer et al, 2023). The first regulatory function observed for DA was its effect on reducing the arterial blood pressure, independently from NE and epinephrine (Hornykiewicz, 1958; Goldberg, 1972). The peripheral biosynthesis of DA originates in non-neuronal tissues and peripheral organs such as the sympathetic nerves, adrenal medulla, kidney, and immune cells, in which DA can act as an autocrine/paracrine regulator of local organ function (Blaschko, 1957; Jose et al, 1998; Mezey et al, 1996; Thomas Broome et al, 2020; Channer et al, 2023).

Although peripheral and central DA systems have similar enzymes, metabolites, and receptors, DA does not cross BBB (Channer et al, 2023). Therefore, DA signaling in the brain is now known to be functionally distinct from peripheral pathways (Channer et al, 2023). Emerging evidence supports and clarifies the idea that the DA machinery modulates a variety of peripheral physiological functions, *inter alia*, renal and cardiovascular function, hormonal secretion, sympathetic regulation, immune activation, respiration, and gastrointestinal motility (Jose et al, 1998; Pinoli et al, 2017; Matt and Gaskill, 2020; Thomas Broome et al, 2020; Channer et al, 2023). Thus, disruption of these functions underlies the pathogenesis of numerous peripheral diseases, e.g. hypertension, inflammation and pain, autoimmune diseases, metabolic imbalance, stress, and cancer proliferation (Jose et al, 1998; Pinoli et al, 2017; Matt and Gaskill, 2020; Thomas Broome et al, 2020; Channer et al, 2023). The following subsections briefly describe the significant role of dopaminergic system in modulating peripheral regulations.

1.8.1. Dopaminergic Sympathoadrenal System

The sympathetic nerves and adrenal glands (medulla and cortex) are the main source of peripheral catecholamines that are secreted into systemic circulation (Amenta et al, 1994; Goldstein and Holmes, 2008). Peripheral DA synthesis is predominantly dependent on sympathetic nerves and is subsequently released into parenchyma of target organs (Amenta et al, 1994; Goldstein and Holmes, 2008). DA is also released directly into the circulation from chromaffin cells of the adrenal medulla, similar to NE and epinephrine, where it acts as a paracrine factor on local target organs (Amenta et al, 1994; Pivonello et al, 2004). Although DA receptors are expressed in the adrenal medulla, their function in the medulla is unclear. The administration of D2R antagonist, but not D2R agonist, increases plasma aldosterone levels, without intensifying aldosterone release (Missale et al, 1989). D2R is expressed in the adrenal cortex, and its activation inhibits angiotensin-stimulated aldosterone secretion (Missale et al, 1988; Missale et al, 1989). Moreover, most peripheral DA is conjugated as sulfates or glucuronides, which are biologically inactive prior to entering the bloodstream (Claustre et al, 1983; Strobel et al, 1990; Richard et al, 2001; Pellock et al, 2017). Sulfation mechanism is mainly mediated by adrenal gland, and conjugated DA sulfate is converted back to active DA by the enzyme arylsulfatase A on target tissues, e.g., liver, lung, and adipose tissue (Strobel et al, 1990; Richard et al, 2001). The level of DA glucuronidation varies with sympathetic input, and as human cells lack the ability to remove glucuronidation, gut microbiome express β-glucuronidase that reverse inactive DA to functional DA (Claustre et al, 1983; Pellock et al, 2017). Overall, the mechanisms by which DA influences the circulatory system involve interactions with different body systems and deregulation of DA signaling in these processes can contribute to a variety of diseases.

1.8.2. Dopaminergic Renal System

Peripheral DA regulation in the kidney has been extensively characterized and contributes to the control of electrolyte balance and blood pressure (Jose et al, 1992; Jose et al, 1998; Jose et al, 2000; Contreras et al, 2002; Cuevas et al, 2013; Yang et al, 2021). In the kidney, DA is synthesized independently from nerve activity, and is formed in proximal tubule cells. Renal proximal tubules do not express TH, the enzyme that converts tyrosine to L-DOPA. The renal glomeruli uptake the circulated or filtered L-DOPA into renal proximal tubule, and as these tubules highly express AADC enzyme, decarboxylation of L-DOPA to DA occurs (Jose et al, 1992; Jose et al, 1998; Jose

et al, 2000). Unlike neurons or other tissues, these renal tubules do not express DβH, and therefore, synthesized DA is not converted to NE (Jose et al, 1992; Jose et al, 1998; Jose et al, 2000). DA produced in the proximal tubule is not stored, but is instead transported both to basolateral membrane and into tubular lumen, where it can act on receptors locally and at more distal nephron segments (Jose et al, 1992; Jose et al, 1998; Jose et al, 2000; Contreras et al, 2002; Cuevas et al, 2013; Yang et al, 2021). DA produced by renal tubules plays an essential role as paracrine substance regulating tubular electrolytes, NA^+ homeostasis, and water transport, through modulating the function of membrane proteins such as Na^+/H^+-exchanger and Na^+/K^+-ATPase pump (Jose et al, 1992; Jose et al, 1998; Jose et al, 2000; Contreras et al, 2002; Cuevas et al, 2013; Yang et al, 2021). In the kidney, DA receptors maintain redox balance and have protective effects on oxidative stress, in which D1R and D5R inhibit nicotinamide-adenine dinucleotide phosphate (NADPH) oxidase activity and D2R decreases reactive oxygen species (ROS) production (Jose et al, 2010; Cuevas et al, 2013; Yang et al, 2021). The reciprocal regulation between renal DA receptors and oxidative activities play an important role in the physiological renal regulation, and its aberration is involved in the pathogenesis of hypertension (Jose et al, 1992; Jose et al, 1998; Jose et al, 2000; Contreras et al, 2002; Jose et al, 2010; Cuevas et al, 2013; Yang et al, 2021).

1.8.3. Dopaminergic Cardiovascular System

DA plays a role in the regulation of cardiovascular function through its interactions with various systems and organs involved in cardiovascular control of heart, arteries, and veins (Jose et al, 2003; Rubí and Maechler, 2010). D1R and D2R are differentially distributed within blood vessels, which consist of three layers (Kim et al, 1999). D1R is expressed in *tunica media* (middle layer) of arterial smooth cells and is known as a postjunctional receptor (Amenta et al, 1990; Kim et al, 1999). D1R activation leads to vasodilation that reduces blood pressure by both renal and nonrenal mechanisms (Amenta et al, 1990; Jose et al, 1992; Jose et al, 1998; Rubí and Maechler, 2010). Prejunctional D2R however, localizes on preganglionic sympathetic terminal and is expressed on *tunica intima* (inner layer) and *tunica adventitia* (outer layer) of arterial smooth muscle (Amenta et al, 1990; Kim et al, 1999). D2R activation inhibits NE release from sympathetic neuroeffector junctions (Amenta et al, 1990). No DA receptor is expressed in the veins, indicating that the effect of DA on the vasculature are primarily around arterial vessels (Okamura and Toda, 1995; Kim et al, 1999). All DA receptors participate in the modulation of renal sodium transport/balance to

maintain blood pressure, and mice lacking any of the DA receptors exhibit high blood pressure (Zeng et al, 2008; Rubí and Maechler, 2010). In addition, DA acting through D2-class receptors modulates angiogenesis-induced inhibition of procoagulant von Willebrand factor, vascular permeability factor/vascular endothelial growth factor, and vascular contractibility (Krimer et al, 1998; Basu et al, 2001; Rubí and Maechler, 2010). Overall, the mechanisms by which DA influences cardiovascular regulation involve interactions with blood vessels, the central and sympathetic nervous system, the kidney, and the heart (Rubí and Maechler, 2010). Dysregulation of DA signaling in these processes can contribute to cardiovascular disorders such as hypertension, heart disease, and impaired vascular function (Jose et al, 2003; Rubí and Maechler, 2010).

1.8.4. Dopaminergic Pancreatic System

DA contributes to the regulation of pancreatic function through direct interaction with the pancreatic islands. DA is released from sympathetic nerves that innervate the pancreas, and DA is also formed directly within pancreatic cells (Mezey et al, 1996; Rubí and Maechler, 2010). DA regulates glucose homeostasis through its receptors expressed in pancreatic β-cells (Rubí et al, 2005; García-Tornadú et al, 2010; Rubí and Maechler, 2010). D2R activation inhibits glucose-stimulated insulin secretion, and mice lacking D2R exhibit a reduced β-cell pancreatic mass that impairs insulin secretion and causes glucose intolerance (Rubí et al, 2005; García-Tornadú et al, 2010; Rubí and Maechler, 2010). Deregulation of DA signaling in these processes can contribute to pancreatic metabolic disorders, such as diabetes and insulin resistance.

1.8.5. Dopaminergic Immune System

The immune system is regulated by central and peripheral sympathetic nervous system, which is primarily achieved by several neurotransmitters, neuropeptides, hormones, and cytokines. These players interact with different immune effector cells to regulate the homeostatic response to infection, disease, and other environmental stresses (Basu and Dasgupta, 2000; Sarkar et al, 2010; Pinoli et al, 2017; Matt and Gaskill, 2020; Thomas Broome et al, 2020). The interaction between the nervous system and the immune system occurs through the HPA axis and also through sympathetic and parasympathetic innervations (Matt and Gaskill, 2020). Catecholamines are among many neural mediators of homeostasis and play a significant role in the immune system (Basu and Dasgupta, 2000; Sarkar et al, 2010; Matt and Gaskill, 2020). DA has a substantial impact on the immune cells in both CNS and periphery, and its immunomodulation affects both innate

and adaptive immunity (Channer et al, 2023). The immunomodulatory role of DA is supported by the presence of endogenously synthesized DA and the expression of its receptors in leukocytes, other immune cells, and lymphoid organs: thymus, spleen, and lymph nodes (Basu and Dasgupta, 2000; Mignini et al, 2009; Sarkar et al, 2010; Pinoli et al, 2017; Matt and Gaskill, 2020; Thomas Broome et al, 2020). The presence of DA receptors suggests that DA acts as an immunoregulator to mediate physiological immune functions, such as cell activation and adhesion, proliferation, chemotaxis, cytokine secretion, cytotoxicity, and apoptosis (Pinoli et al, 2017).

Dopaminergic modulation of the immune response is implicated in several immune-mediated diseases that arise in response to neuroinflammation, autoimmunity, and cancer (Pinoli et al, 2017; Matt and Gaskill, 2020; Thomas Broome et al, 2020). Activation of DA receptors on distinct immune cells might have different sensitivities to DA for modulating downstream signaling (Matt and Gaskill, 2020; Thomas Broome et al, 2020). Peripheral T-lymphocytes (T-cells), monocytes, and dendritic cells express functional DA and plasma membrane DA receptors, suggesting they have the capacity to synthesize, store, and release dopamine and activate DA receptors (Santambrogio et al, 1993; McKenna et al, 2002; Besser et al, 2005; Cosentino et al, 2007; Huang et al, 2010; Kustrimovic et al, 2014; Pinoli et al, 2017; Matt and Gaskill, 2020; Thomas Broome et al, 2020). Resident glial cells, microglia (predominant immune macrophages) and astrocytes (nonimmune glial cells), are non-neuronal cells essential in immune response, homeostasis, and synaptic support of CNS; interestingly, these cells express DA metabolites and DA receptors (Zanassi et al, 1999; Khan et al, 2001; Färber et al, 2005; Mastroeni et al, 2009; Huck et al, 2015; Pinoli et al, 2017; Kopec et al, 2018; Matt and Gaskill, 2020; Thomas Broome et al, 2020). DA receptors are strongly upregulated/downregulated in activated immune cells and shows specific patterns in different immune cell populations during pathologic stimuli. In PD and schizophrenia, an abnormal immune response to hypodopaminergic and hyperdopaminergic activities were respectively associated to decreased and increased CD4+ lymphocytes (helper T cells) (Basu and Dasgupta, 2000; Sarkar et al, 2010; Elgueta et al, 2019). These findings support the idea that targeting DA receptors and their inflammatory signaling pathways in these immune cells could have therapeutic value in the treatment of immune system diseases.

1.8.5.1. Dopamine and autoimmunity

Autoimmunity is a complex condition where the immune system is unable to distinguish between self and non-self antigens. This is due to the loss of immune tolerance that affects both innate and adaptive immunity. Inflammatory pathologies, such as multiple sclerosis (MS), irritable bowel disease (IBD), systemic lupus erythematosus, and rheumatoid arthritis are autoimmune diseases, in which DA is one among many contributors regulating the inflammatory response. DA is synthesized and stored in immune cells, including T cells and dendritic cells, which may act in an autocrine manner to stimulate/suppress DA receptors in normal and autoimmunity conditions. MS, as an example of autoimmune disease potentially impacted by DA, is a chronic demyelinating disease induced by autoimmune response of CD4+ T-cell-mediated progressive loss of neurological function due to destruction of axonal myelin sheath in brain and spinal cord (Pacheco et al, 2014; Pinoli et al, 2017; Vidal and Pacheco, 2020). Peripheral blood mononuclear cells of MS patients display altered expression of DA receptors and reduced TH; interestingly, when MS patients are treated with interferon-β (IFN-β), they experience a reversion in these dopaminergic alterations (Zaffaroni et al, 2008; Pacheco et al, 2014; Vidal and Pacheco, 2020). Moreover, the risk of developing MS has been associated with increased D3R and D5R mRNA expression in regulatory T-cells (Cosentino et al, 2016; Vidal and Pacheco, 2020). This may underly the relationship between DA and the pathogenesis of MS, however, further research is needed to fully elucidate the mechanisms involved (Pacheco et al, 2014; Vidal and Pacheco, 2020).

1.8.6. Dopaminergic Gastrointestinal System

Dopaminergic mechanisms are important for the regulation of gastrointestinal motility and gut homeostasis. The expression and activity of TH is high throughout the gastrointestinal system and plays significant roles in DA biosynthesis, involving enteric nerves, stomach epithelial cells, mesenteric tissue, and gut microbiome. Epithelial cells of intestinal mucosa contain a high abundance of AADC, which is necessary for the formation of DA, but lack TH expression (Pacheco et al, 2014; Vidal and Pacheco, 2020). DA receptors are expressed in stomach and intestines (Li et al, 2006). Genetic deletion of D2R alters the intestinal motility in experimental models (Li et al, 2006). DA contributes to the pathogenesis of IBD, which is a chronic inflammatory condition triggered by an excessive immune response against normal constituents in the gastrointestinal tract (Pacheco et al, 2014; Vidal and Pacheco, 2020). The level of

catecholamines is reduced in IBD patients and experimental models, which could be attributed to interferon-γ (IFN-γ)-mediated inhibition of L-DOPA uptake by epithelial cells, reduced TH and DAT expression, or altered DA-mediated T-cell signaling (Pacheco et al, 2014; Vidal and Pacheco, 2020). As the relationship between DA and IBD is not fully understood, future research is needed to explore the potential of DA receptors as therapeutic targets (Pacheco et al, 2014; Vidal and Pacheco, 2020).

1.8.7. Dopaminergic Respiratory System

DA is produced by a number of cells in the lung, including alveolar epithelial cells and pulmonary endocrine cells, and exert various effects on the respiratory system (Vicario et al, 2000; Ciarka et al, 2007). DA is also involved in modulating the respiratory functions of ventilation, the tone of the pulmonary blood vessels, the reabsorption of alveolar fluids, and bronchial exchange (Cabezas et al, 2003; Ciarka et al, 2007; Mizuta et al, 2013). DA mediates these functions by its actions on the carotid body, the primary synapses of the afferent neurons of carotid body's nerve, and on neurons on the nucleus tractus solitary (Vicario et al, 2000; Cabezas et al, 2003; Ciarka et al, 2007; Matsuyama et al, 2018). Genetic deletion of DAT, which is characterized by locomotor hyperactivity, leads to a significantly lower respiratory frequency, a reduced ventilatory response to hypoxia, and a decrease in resting circadian body temperature (Vincent et al, 2007). The altered DA neurotransmission from deletion of DAT deteriorates the respiratory function by prolonging inspiratory time and attenuating tidal volume response (Vincent et al, 2007). The administration of DA results in the vasodilation of bronchial blood vessels and the reduction of arterial pulmonary hypertension (Cabezas et al, 2003; Ciarka et al, 2007; Mizuta et al, 2013). Through these complex mechanisms, DA has beneficial effects on pulmonary function, however, it has a detrimental impact in patients with heart failure (Cabezas et al, 1999; Ciarka et al, 2007). Moreover, activated D4R induce differentiation of naïve CD4+ T-cells to T-helper 2 cells, major effector cells in allergic asthma of young mice (Wang et al, 2019). This observance is thought to be mediated by the sympathetic nerve in the postnatal lung, which undergoes a shift from dopaminergic innervation during development to adrenergic innervation in maturity (Wang et al, 2019). Unlike other peripheral systems, the role of DA in respiratory system physiology and disease remains poorly defined, thus, further research in this system is warranted.

1.8.7.1. Dopamine and COVID-19

Since 2020, the whole world has been affected by coronavirus disease 2019 (COVID-19) caused by SARS-CoV-2 virus, which has inflicted unprecedented consequences on health and on the global economic system (Attademo and Bernardini, 2021). As the world recovers from this pandemic, it has been observed that some people who have endured a COVID-19 infection may further suffer from short- and long-term mental health problems (Attademo and Bernardini, 2021). It has been postulated that an alteration in neurotransmitters, including DA, might be involved in this COVID-19 pathophysiology (Nataf, 2020). Angiotensin-converting enzyme 2 receptor (ACE2), which are the main receptor for SARS-CoV-2, are highly expressed in DA neurons, in addition to non-neuronal cell types. Furthermore, it is co-expressed and co-regulated with AADC, an enzyme that catalyzes the biosynthesis of DA (Nataf, 2020; Attademo and Bernardini, 2021). Mental illness observed in patients with COVID-19 could thus be partially explained by deregulation of DA neurotransmission. However, this requires further investigation. It is worthwhile to note that persons with vulnerability to PD may represent a population with potential for increased severity of disease from COVID-19 (Antonini et al, 2020; Sulzer et al, 2020).

1.8.8. Dopamine and Cancer

The relationship between DA and cancer is multifaceted and has been implicated in various aspects of cancer development, progression, and anti-inflammatory and treatment responses (Rubí and Maechler, 2010). Previous subsections briefly described DA system involvement in a variety of peripheral endocrine systems, in which DA is associated with abnormal growth and proliferation, e.g., pituitary, adrenal, and pancreas (Kelly et al, 1997; Saiardi et al, 1997; Bossé et al, 1997; Pivonello et al, 2004; García-Tornadú, et al, 2010; Rubí and Maechler, 2010). However, the specific mechanisms and effects can vary depending on the cancer type, stage, and individual characteristics (Rubí and Maechler, 2010). Further research is needed to fully understand the intricate interactions between DA and cancer and to explore potential therapeutic strategies targeting dopamine signaling in cancer treatment.

1.9. Conclusions: Dopaminergic Systems

New discoveries in recent years have further evolved our knowledge of DA systems. The breadth of DA system contribution, not only in brain, but also in the periphery, is very diverse and complex. The findings presented here demonstrate that the dopaminergic system is found in many tissues, regulates a variety of functions, and displays complex regulatory effects. Further delineation of how DA modulates all these processes should open new avenues in the prevention and treatment of many different neurological and peripheral diseases. *Fig. 1.12. depicts the DA systems found in human body.*

My objective of writing the previous sections is to appreciate the depth, outreach, and complexity of the dopaminergic system in modulating numerous physiological functions and behaviors, by highlighting the direct supporting evidence. The above-described functions of DA system, along with other proposed processes that were not discussed here, have been reviewed in great detail within these excellent comprehensive resources (Jose et al, 1998; Pinoli et al, 2017; Matt and Gaskill, 2020; Channer et al, 2023; Geisler and Hayes, 2023).

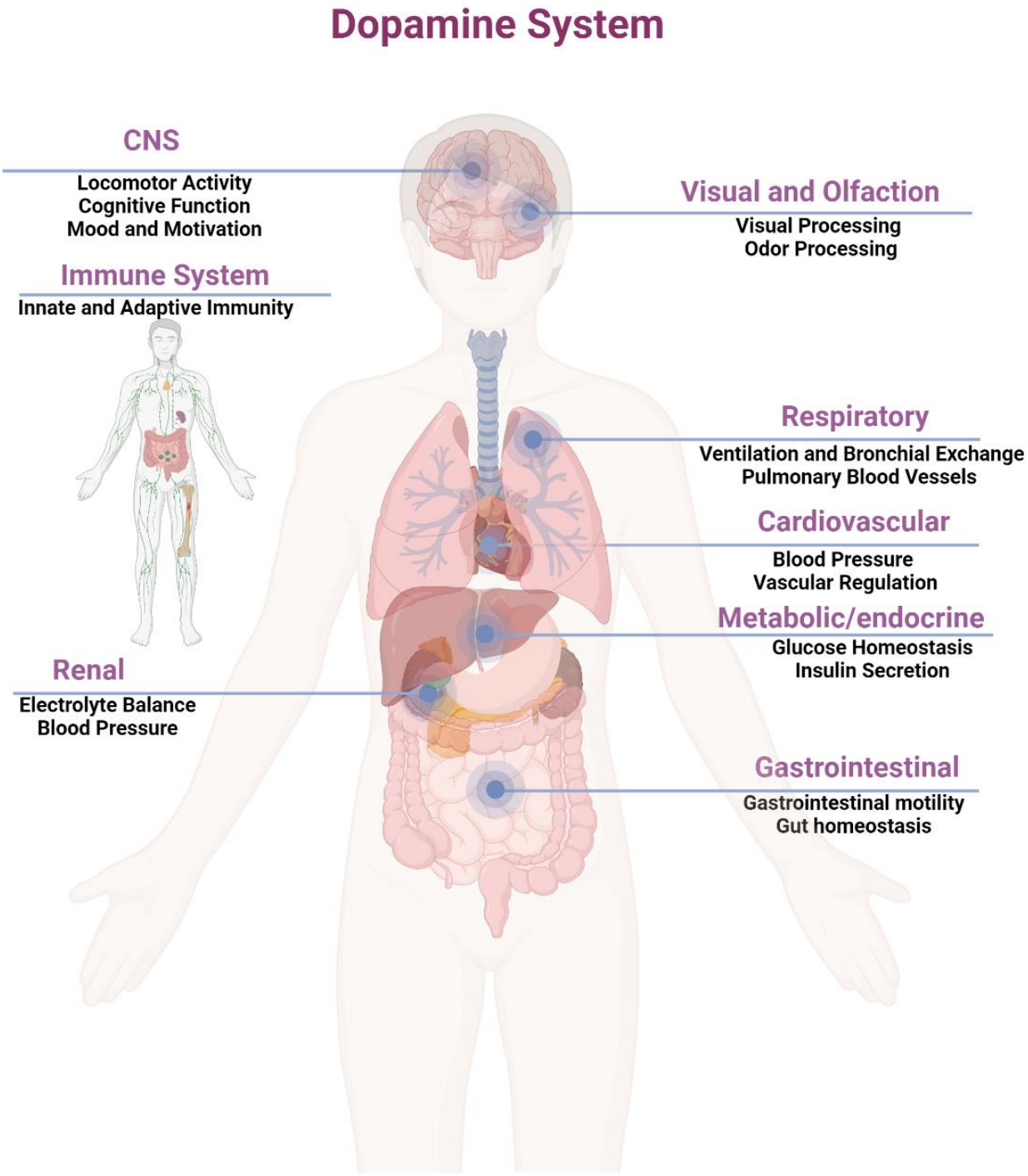

Fig. 1.12. Peripheral Dopamine Systems.
Schematic illustration of dopamine systems found throughout the periphery. Created with BioRender.com.

2. Dopaminergic G-Protein Coupled Receptors

DA regulates numerous central and peripheral functions through the binding and activation of cell surface receptors belonging to the superfamily of GPCRs (Beaulieu and Gainetdinov, 2011). In the adaptation of neurons/cells to the dynamic milieu, GPCRs serve as gatekeepers and primary sensors of external cues, either endogenously activated (neurotransmitters, hormones, lipids, and enzymes) or exogenously stimulated (agonists, light, odorants, and pheromones) to modulate neuronal/cellular responses (Pierce et al, 2002). The classical signaling transduction of GPCRs is best explained by the "receptor—G-protein—effector" (Pierce et al, 2002). To achieve this, cue-bound GPCRs use a sophisticated *modus operandi* entailing the recruitment of intracellular partners, e.g., heterotrimeric G-proteins, βArrs, to orchestrate specific signaling outcomes through the regulation of diverse second messenger-producing effectors such as the ACs (Gether, 2000; Pierce et al, 2002; Luttrell, 2006). GPCRs are very diverse in structure and function, and represent more than 4% of genes present in the human genome that encode for about 800 annotated receptor genes (Gloriam et al, 2007; Schöneberg and Liebscher, 2021). Most of these receptors have now been functionally characterized and have a ligand assigned to them. However, some are still without a proper ligand and are considered orphans (Tang et al, 2012).

GPCRs have a diverse spectrum of physiological actions in humans, including the modulation of synaptic transmission, sensory perception, and the peripheral regulation of renal, hormonal, and cardiovascular functions (Gether, 2000; Pierce et al, 2002; Luttrell, 2006). Signaling impairment of GPCRs has been linked to many disorders notably of the brain, heart, metabolism, and human genetic diseases (Schöneberg and Liebscher, 2021; Calebiro et al, 2021). GPCRs are immensely important in the physiology of diseases and are targets for approximately 30-40% of currently marketed drugs (Pierce et al, 2002; Overington et al, 2006). Notably, DA receptors are among the most frequently targeted GPCRs in term of the number of available drugs (Sriram and Insel, 2018).

2.1. GPCRs: Historical Perspective

The notion of cellular receptors was first introduced by John Langley, in 1905, and he wrote *"So we may suppose that in all cells two constituents at least are to be distinguished. The receptive substance affects or is capable of affecting the metabolism of the chief substance"* (Langley, 1901; Langley, 1905). Langley postulated that there are two inter-linked functions of these hypothetical

receptors that interact with stimuli and exert function upon effectors within the cell. Fifty years later, Langley's hypothetical receptor was studied by numerous laboratories to elucidate the cellular communications that are necessary for coordinating cellular functions mediated by hormones and other proteins, as briefly discussed in the following sections.

2.1.1. The Discovery of the cAMP

In the 1950s-60s, Earl Sutherland described the process of "*the second messenger*" system by uncovering a previously unknown compound called cAMP, which is present in different organs (Rall and Sutherland, 1958). cAMP is generated through cyclization of adenosine triphosphate (ATP), a chemical which had been characterized to play an intermediary role in many hormonal functions (Rall and Sutherland, 1958). How do hormones stimulate the formation of cAMP? According to Sutherland's scheme, epinephrine serves as "*the first messenger*", which binds to the cell surface receptor, then stimulates membrane bound AC, causing the formation of cAMP, which then exerts metabolic processes (Sutherland et al, 1962). Sutherland later suggested that the effect of many other hormones could be explained similarly, in which hormones bind the receptor and stimulate formation of cAMP via activating AC (Kresge et al, 2008). However, this hypothesis was met with strong criticisms as to how a single substance, cAMP, leads to numerous effects caused by different hormones (Kresge et al, 2008). Eventually it was proven that the large scale of hormones, peptides, and receptors exert their effect via cAMP (Kresge et al, 2008). Earl Sutherland was awarded the 1971 Nobel Prize in Physiology or Medicine for his discoveries concerning the mechanism of action of hormones.

2.1.2. The Discovery of Protein Kinases

Also, during the 1950s-60s, Edmond Fischer and Edwin Krebs discovered that certain enzymes, now known as protein kinases, can transfer phosphate groups from ATP to specific proteins, altering their activity and function (Krebs and Fischer, 1955; Fischer and Krebs, 1955). Fischer and Krebs delineated the regulatory reversible mechanisms of protein phosphorylation whereby proteins are covalently phosphorylated by kinases and dephosphorylated by phosphatases allowing fine control over elaborate networks, a fundamental mechanism of cellular processes (Krebs et al, 1958; Krebs et al, 1959; Kresge et al, 2011). Krebs contributed to the discovery and characterization of cAMP-dependent protein kinase and the importance of kinase-mediated phosphorylation in cellular regulation (DeLange et al, 1968; Walsh et al, 1968; Walsh et al, 1971;

Kresge et al, 2011). Edmond Fischer and Edwin Krebs were jointly awarded the 1992 Nobel Prize in Physiology or Medicine for their discovery of cAMP-dependent protein kinase and the regulatory mechanism of protein phosphorylation.

2.1.3. The Discovery of G-Proteins

In the 1960s-70s, Martin Rodbell demonstrated that the signaling mechanism of hormonal stimulation of AC requires guanosine triphosphate (GTP) (Pohl et al, 1969; Londos et al, 1974). Rodbell illustrated that signal transduction requires GTP to integrate the functional signal, which occurs in three essential steps: receptor "*discriminator*" that recognizes external stimuli; transducer "*transfer*" that requires GTP; and effector "*amplifier*" that generates intracellular activity of second messenger (Hammes and Rodbell, 1976; Rodbell, 1980). The transducer function is wholly dependent on the guanine nucleotide binding protein, known as G-protein (Northup et al, 1982). Indeed, Alfred Gilman showed that hormone-bound receptor triggers G-protein exchange of GTP for guanosine diphosphate (GDP), causing the dissociation of βγ subunit from α subunit-bound GTP to activate AC (Northup et al, 1983a, b). Rodbell's and Gilman's research emphasizes the importance of G-proteins as integrators of external signals, which act on cell surface receptors to transduce effector proteins by activating different cellular amplifier systems (Rodbell, 1980; Gilman, 1984). Additionally, Rodbell's and Gilman's work elucidate the mechanism of AC signaling mediated by G-protein activity (Rodbell, 1980; Gilman, 1984; Tang and Gilman, 1992; Taussig et al, 1993). Martin Rodbell and Alfred Gilman were jointly awarded the 1994 Nobel Prize in Physiology or Medicine for their discovery of G-proteins and the role of these proteins in cellular signal transduction.

2.1.4. The Breakthrough of GPCRs

Robert Lefkowitz is a key pioneer in GPCR research, who's work revolutionized the fields of molecular and cellular biology. Lefkowitz's research shaped our understanding of GPCRs and revealed their central role in mediating the effects of hormones, neurotransmitters, and many other signaling molecules. In the 1970s-90s, Lefkowitz and his long-term influential collaborator, Marc Caron, investigated the adrenergic receptor, and revealed multistate binding of that receptor (Lefkowitz et al, 1970; Mukherjee et al, 1975). Lefkowitz also examined the regulatory G-proteins, and their ability to form a ternary complex with agonist-bound receptors (Lefkowitz et al, 1976; De Lean et al, 1980). Lefkowitz and Brian Kobilka pioneered the modern study of GPCRs by

cloning and sequencing the gene for the first GPCRs, β_2-adrenergic receptor (β_2AR) and α_2-adrenergic receptor (α_2AR) (Dixon et al, 1986; Kobilka et al, 1987). Lefkowitz and Kobilka additionally created the first chimeric receptor, α2 and β2-adrenergic receptors, and these studies demonstrated the structural specificity of the receptors with their respective ligand binding and G-protein—mediated effector activation (Kobilka et al, 1988). Since then, the molecular cloning of GPCRs began to show that GPCRs have a unique, conserved seven transmembrane organization (Pierce et al, 2002). Lefkowitz also identified and characterized the novel kinase and arrestin proteins responsible for the β-adrenergic receptor phosphorylation and recruitment, respectively, known as GRKs and βArrs (Benovic et al, 1986a, b; Benovic et al, 1989; Lohse et al, 1990). Lefkowitz's research broadly contributed to the current knowledge of GPCRs, by revealing the functionality of these regulatory proteins with ligand-bound receptor, which represent the classical cellular signaling paradigm for GPCRs (Sibley and Lefkowitz, 1985; Benovic et al, 1986a, b; Bouvier et al, 1988; Pitcher et al, 1992; Dawson et al, 1993; van Biesen et al, 1995; Luttrell et al, 1999; McDonald et al, 2000; Pierce et al, 2002).

In the 2000s, Kobilka's research focused on the molecular and structural activity of GPCRs and developed direct methods to obtain high-resolution crystal structure and conformational changes for a ligand-bound β_2AR with G-protein (Rasmussen et al, 2007; Rosenbaum et al, 2007; Bokoch et al, 2010; Rosenbaum et al, 2011; Rasmussen et al, 2011). Kobilka's work provided novel insight into the structural basis of signal transduction by these key proteins at the molecular level, which is also crucial for drug discovery (Rosenbaum et al, 2009; Shoichet and Kobilka, 2012; Hilger et al, 2018).

Robert Lefkowitz and Brian Kobilka were awarded jointly the 2012 Nobel Prize in Chemistry for their breakthrough discoveries of GPCRs and their exceptional contributions to the field of molecular biology and drug discovery. Their research revolutionized our understanding of how cells communicate with their environment and paved the way for the development of new drugs targeting these receptors. Research by Lefkowitz's former trainees, Jeff Benovic, Michel Bouvier, David Sibley, and his long-term collaborator, Marc Caron, among others, has profoundly impacted our understanding of the broad spectrum of GPCR physiological processes. Research in this field continues to yield important insights into human health and disease, offering potential avenues for drug screening and therapeutic intervention.

2.2. Classification of GPCRs

Assiduous work to identify human genes encoding for GPCRs has led to the classification of GPCRs in five main subfamilies forming the *GRAFS* system: Glutamate (15 members, Class C), Rhodopsin (701 members, Class A), Adhesion (24 members, Class D), Frizzled/Smoothened/Taste2 (24 members, Class F), and Secretin (15members, Class B) (Schiöth and Fredriksson, 2005; Luttrell, 2006; Gloriam et al, 2007). DA receptors belong to the subfamily of the rhodopsin-class receptors (Class A) of GPCRs, the most studied subfamily of GPCRs that accounts for more than 80% of receptors in humans (Gether, 2000; Luttrell, 2006; Beaulieu and Gainetdinov, 2011). Members of the rhodopsin-class receptors possess great binding specificity towards their respective ligands, and include biogenic amine receptors (dopaminergic, adrenergic, serotonergic, histaminergic, and muscarinic), adenosine receptor, angiotensin receptor, prostaglandin receptor, cannabinoid receptor, opioid receptor, chemokine receptor, vasopressin receptor, and other receptors (Gether, 2000; Beaulieu and Gainetdinov, 2011).

2.2.1. Classification of DA Receptors

As noted earlier, DA activates five distinct but closely related cell surface proteins that belong to subgroups of GPCRs referred to as DA receptors (Civelli et al, 1993; Jaber et al, 1996a; Missale et al, 1998; Beaulieu and Gainetdinov, 2011). DA receptors are classified into D1-class receptors (D1R and D5R) and D2-class receptors (D2R, D3R, and D4R) based on their structure, pharmacology, and canonical signaling. DA receptors modulate several central and peripheral physiological functions such as locomotion, reward, learning, cognition, and hypertension (Civelli et al, 1993; Jaber et al, 1996a; Missale et al, 1998; Beaulieu and Gainetdinov, 2011). From ligand binding to signal transduction and receptor trafficking, regulation of DA receptors is complex and involves many effector proteins. ***For the purpose of my thesis, the following sections will provide an overview about GPCRs, but the major emphasis will be on detailing DA receptors in brain, specifically D1R and D5R, the principal elements of my project.***

2.3. Structure of GPCRs

Despite their multitude in numbers and their functional diversity, members of GPCR superfamily, including DA receptors, share a common structural topology, which consists of upstream extracellular amino-terminus (NT), seven hydrophobic transmembrane alpha helical

transmembrane domains (TM1-TM7), three extracellular loops (EL1-EL3), three intracellular loops (IL1-IL3), and intracellular carboxy-terminus (CT) (Gether, 2000; Luttrell, 2006). Although all GPCRs share a structural homology and certain conserved residues, distinct differences between them still exist (Gether, 2000; Luttrell, 2006). Site-directed mutagenesis, receptor chimeras/truncation, and crystal structures revealed the importance of different structural components of GPRCs in regulating their functionality and ligand binding (Kobilka et al, 1988; Bouvier et al, 1988; Gether, 2000; Luttrell, 2006).

The NT of receptors contain glycosylation sites that are important for stability of receptor and aid cell surface expression (Missale et al, 1998; Luttrell, 2006). Most GPCRs contain a disulfide bridge between EL1 and EL2 that is crucial for proper protein folding conformation (Luttrell, 2006). The extracellular loops (EL) and TM domains are important for ligand binding and structural integrity of the GPCRs (Luttrell, 2006). TM domains are highly conserved among rhodopsin-class receptors and share the common structural characteristic of having conserved DRY (aspartate-arginine-tyrosine) and NPxxY (asparagine-proline-xx-tyrosine) motifs located in TM3 and TM7, respectively, to stabilize the receptor in the inactive state (Luttrell, 2006). The intracellular domains have more functional role for GPCRs, as their mutation/truncation leads to the impairment of signaling properties. IL3 and CT are the most disordered, divergent regions and are principal determinants for G-protein coupling specificity, modulation of intracellular signaling and scaffolding of GRKs and βArrs (Luttrell, 2006). The CT contains palmitoylated cysteines, anchoring the CT to plasma membrane and forming what could be described as a fourth intracellular loop (IL4); however, based on GPCR crystallography studies this region is considered an α-helix region, referred to as helix 8 (Luttrell, 2006).

2.3.1. Structure of DA Receptors

DA receptors have a high level of sequence homology in their transmembrane domains; however, amino acid sequences of the extra- and intracellular domains are more divergent (Missale et al, 1998; Beaulieu and Gainetdinov, 2011). D1-class receptors share 80% homology in their TM domains and exhibit a relatively short IL3 and a long serine/threonine rich CT (Missale et al, 1998; Beaulieu and Gainetdinov, 2011). *Fig. 1.13. depicts the amino acid sequences for D1-class receptors*. However, D2-class receptors are characterized by having a long IL3 and a very short CT (Missale et al, 1998; Beaulieu and Gainetdinov, 2011). In their TM domains, D2R:D3R share

75% homology, while 53% identity is observed between D2R:D4R (Missale et al, 1998; Beaulieu and Gainetdinov, 2011). The length of the IL3 appears to be a characteristic feature for G-protein coupling, not for only DA receptors, but for all GPCRs (Beaulieu and Gainetdinov, 2011). Short IL3 receptors couple to stimulatory G-protein, and long IL3 receptors couple to inhibitory G-protein (Beaulieu and Gainetdinov, 2011). The NT of all DA receptors have a similar number of amino acids; however, the CT of D1-class is seven times longer than that of the D2-class receptor (Missale et al, 1998).

2.3.2. Structural Mapping of D1-Class Receptors

Studies from the Tiberi lab and others investigating the functionality of structural domains of D1-class receptors were performed by utilizing chimeric and truncation approaches to generate mutant forms of D1R and D5R. **As other labs made significant contributions to the structural mapping of D1-class receptors, in this section, I briefly review findings from the Tiberi lab, as some of these mutants have been used for my Ph.D. studies.**

Results showed that activation of chimeric NT or TM1 forms of D1R and D5R differentially modulated the binding properties and G-protein coupling efficacy (D'Aoust and Tiberi, 2010). TM1 is also essential in modulating intrinsic activity and efficacy of agonists of D1R and D5R (D'Aoust and Tiberi, 2010). Swapping either the CT or IL4 segment within the CT between D1R and D5R altered the binding affinity of ligands and switched the constitutive cAMP activity, implying the importance of these regions in the regulation of the thermodynamic equilibrium between active and inactive conformations of D1-class receptors (Iwasiow et al, 1999; Jackson et al, 2000; Tumova et al, 2002; Tumova et al, 2004). As IL3 and CT domains are critical for G-protein coupling, oligomerization, or protein interactions, the Tiberi lab used deletion approaches of IL3 and CT to generate mutant forms of D1R and D5R lacking the cytosolic extension of either TM5 or TM6 within IL3, referred to as ΔIL3N or ΔIL3C, or different segments of D1R CT. IL3 mutants of D1R and D5R had opposing effects on regulating $G\alpha_s$ activity in which ΔIL3N mutants reduced agonist independent-and dependent-mediated cAMP, whereas ΔIL3C mutant enhanced these activities (Charette, Albaker et al, manuscript in preparation). The CT region of D1R regulates G-protein coupling, and receptor responsiveness, and such a deletion alters these crucial functions (Chaar et al, 2001; Jackson et al, 2002).

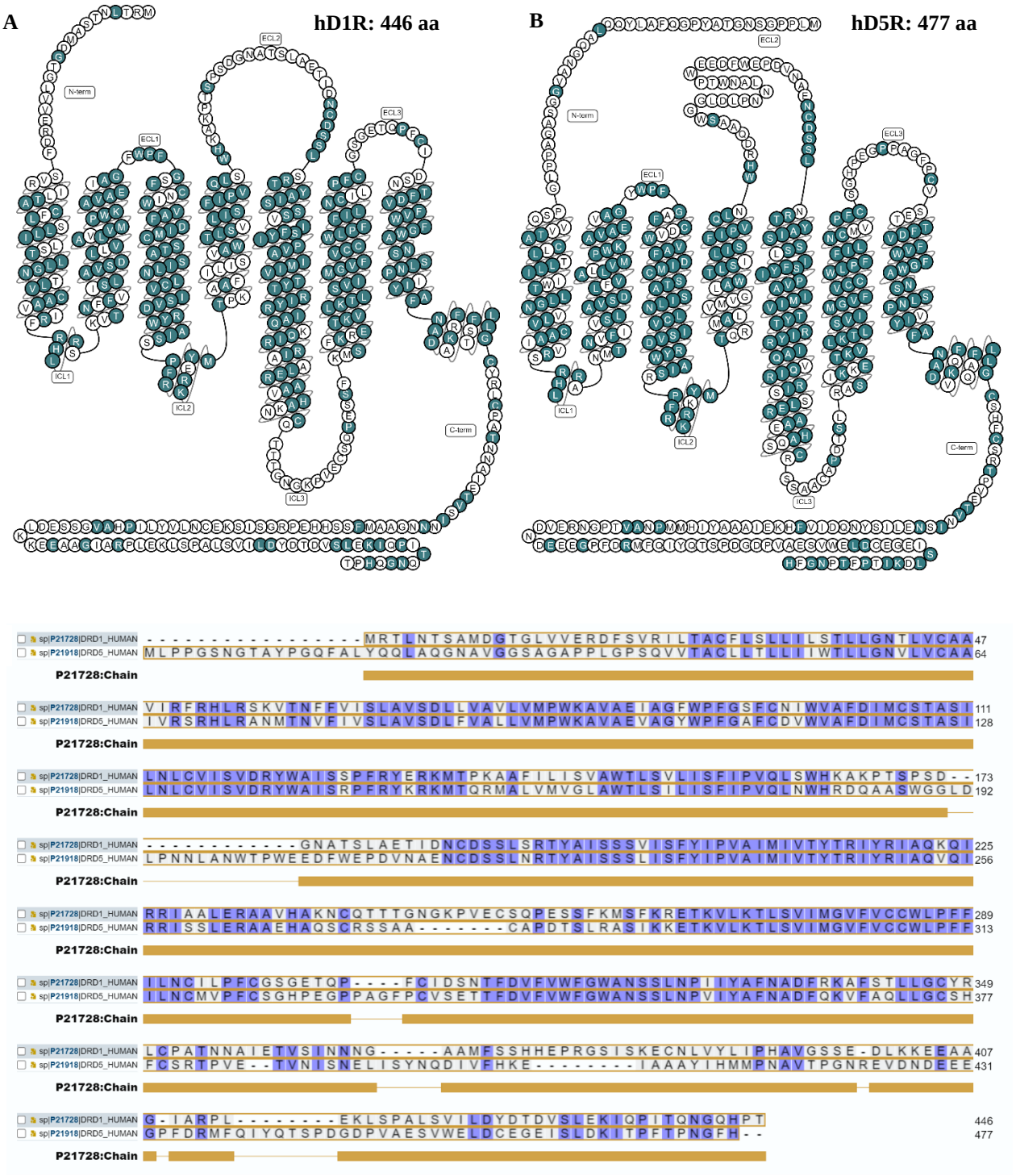

Fig. 1.13. Secondary Structure of human D1-Class Receptors.

Dark circles represent conserved identical amino acid residues conserved between D1R (A) and D5R (B), and white circles represent the divergent residues among them. Created with gpcrdb.org. (C) Amino acid alignment of human D1R and human D5R showed 58.08% of identity. Conserved amino acids are highlighted. Alignment analysis by uniprot.org.

Serine (Ser) and threonine (Thr) residues in GPCRs are important in regulating receptor phosphorylation, desensitization and signaling mechanisms. Our lab generated phosphodeficient mutant forms of intracellular domains IL1, IL2, IL3, and CT of D1R and D5R by substituting Ser/Thr residues with Alanine (Ala)/Valine (Val), respectively, by site direct mutagenesis. Results showed that IL1 phosphodeficient mutations of D1R and D5R exhibit reduced binding expression and constitutive cAMP production, but increased DA-mediated cAMP production (Zhang et al, 2015). IL2 phosphodeficient mutants exhibited contrasting properties of agonist affinity, constitutive activity, and dopamine potency, relative to D1R and D5R (Zhang et al, manuscript in preparation). Although IL2 phosphodeficient mutants underwent internalization, they displayed weakened desensitization compared to D1R and D5R (Zhang et al, manuscript in preparation). The agonist-independent cAMP was decreased in phosphodeficient IL3 and CT mutants of D1R and D5R, with the CT mutants also showing reduced expression and desensitization-mediated cAMP (Plouffe et al, manuscript in preparation; Laquerre et al, manuscript in preparation).

2.4. Crystallography for GPCRs

Crystallography studies have yielded a plethora of information on the structural biology of GPCRs to understand the receptor mechanisms of ligand binding that are important for drug discovery (Stenkamp et al, 2002; Kobilka and Schertler, 2008; Rosenbaum et al, 2008; Hilger et al, 2018). These sophisticated tools provide a foundation for drug discovery by revealing the conformational heterogeneity, which will need to be integrated in the development of more precise and effective therapeutics targeting GPCRs (Stenkamp et al, 2002; Kobilka and Schertler, 2008; Rosenbaum et al, 2009; Hilger et al, 2018). In 2000, Krzysztof Palczewski crystalized the first GPCR structure, a bovine rhodopsin receptor covalently bound in its basal state to its inverse agonist 11-*cis*-retinal (Palczewski et al, 2000). This highly resolved 2.8 Å crystal structure of rhodopsin revealed highly organized, anti-clockwise, compacted heptahelical transmembrane bundles and provided structural information for the molecular mechanism of GPCR activation (Palczewski et al, 2000; Stenkamp et al, 2002). These tightly connected TM domains are composed of α-helices and serve as the main site for ligand docking to mediate specific affinity for each receptor with its respective ligands (Palczewski et al, 2000; Stenkamp et al, 2002). The intracellular domains are not as packed as extracellular domains, in order to facilitate the activation of G-proteins (Palczewski et al, 2000; Stenkamp et al, 2002).

Crystallization of GPCRs has been challenging because many GPCRs display structural instability linked to agonist-independent activity and detergent removal of receptors from native plasma membrane (Kobilka and Schertler, 2008; Rosenbaum et al, 2009). Methods to increase receptor stability and enhance crystal efficiency of target receptor-bound ligands include truncation of disordered regions, complex formation with purified antibody fragment (e.g., Nb35, scFv16), and fusion of soluble, highly crystallizable protein (e.g., T4 lysozyme) at IL3 (Kobilka and Schertler, 2008; Rosenbaum et al, 2009). This field has extensively advanced in research and development following this prime discovery, and in 2007, Kobilka and colleagues resolved crystallography structure of β_2AR, the first GPCR with diffusible ligands (Cherezov et al, 2007; Rasmussen et al, 2007; Rosenbaum et al, 2007). With the technology breakthroughs in membrane protein engineering and crystallography, more than 450 structures have been published for more than 80 receptors in complex with ligands, G-proteins/arrestins, or both (Zhang et al, 2015; Yang et al, 2021). These structures shed unprecedented light on structural similarity and diversity of the GPCRs superfamily, molecular basis of ligand recognition and allosteric modulation (Zhang et al, 2015; Yang et al, 2021).

2.4.1. Crystallography for DA Receptors

In the last five years, tremendous efforts have been devoted to crystallizing DA receptors and determining their distinct conformational differences. To date, 27 crystal structures of different DA receptors bound to different ligands alone or in complex with Gα subunits have been resolved. These structures revealed that the ligand-binding pockets of all DA receptors contain conserved motifs and are highly negatively charged. Additionally, some of these structures gave additional insights on DA receptor allosteric regulation and Gα coupling mechanism. *Table 1.1. summarizes the active DA receptors with different ligands.*

Recent cryo-electron microscopy (cryo-EM) structures of all five subtypes of human DA receptors coupled with their respective G-protein ($G\alpha_s$ or $G\alpha_i$) in complex with rotigotine, an agonist for DA receptors used in PD treatment, revealed high resolutions of D1R-$G\alpha_s$ (3.2 Å), D2R-$G\alpha_i$ (3.0 Å), D3R-$G\alpha_i$ (2.7 Å), D4R-$G\alpha_i$ (3.2 Å), and D5R-$G\alpha_s$ (3.1 Å) (Xu et al, 2023). *Fig. 1.14. shows the Cryo-EM structure for DA receptor bound to rotigotine.* The solved crystal structure for rotigotine-bound DA receptors exhibit similar backbone conformations, and lead to the downward movement of the “toggle switch” residue W6.48, which further induces conformational changes in the DRY

and NPxxY motifs (Xu et al, 2023). The conformation of the TM5 domain represents the most notable difference, as the D1-class receptors are extended with three extra helical turns into the cytoplasmic side compared to the D2-class receptors (Xu et al, 2023). Interestingly, the ligand-binding pockets showed that D5R has more negative charges on the extracellular surface than D1R, and positively charged DA and rotigotine have higher potencies to enrich within the pocket of D5R over D1R (Xu et al, 2023).

Taken together, these new cryo-EM structures of active DA receptor—G-protein complexes mentioned above and summarized in Table 1.1., provide new insights into the structural bases of DA receptor's recognition and activation by agonists, allosteric regulation, and selective coupling. Future work directed toward solving DA receptors in inactive state structures and active state structures coupled with different ligands, as well as crystalizing mutant forms of DA receptors coupled with G-protein should provide useful information for therapeutic drug development for numerous dopaminergic diseases.

2.5. Pharmacology of DA Receptors

Progress in the pharmacological characterization of DA receptors began with the discovery of DA-stimulated AC and radiolabelled binding assay to study the action of ligands using *in vitro* studies, which provided better correlation between DA receptors and ligand's affinity (Kebabian and Greengard, 1971; Creese et al, 1975). Due to the high homology of DA receptors, most dopaminergic drugs are non-selective and highly polypharmacologic as they target multiple DA receptors as well as other aminergic GPCRs, with various affinity, from picomolar to micromolar (Civelli et al, 1993; Jaber et al, 1996; Missale et al, 1998; Beaulieu and Gainetdinov, 2011; Jones-Tabah et al, 2022). On the other hand, highly selective ligands are important pharmacological tools for functional and binding investigations to distinguish between D1- and D2-class receptors (Civelli et al, 1993; Jaber et al, 1996; Missale et al, 1998; Beaulieu and Gainetdinov, 2011). D5R has a higher agonist affinity, but lower inverse agonist and antagonist potency than D1R (Tiberi and Caron 1994; Charpentier et al. 1996). Compared to the D2R, D3R has higher agonist affinity, particularly for DA and quinpirole, and lower affinity for antagonists including spiperone and haloperidol (Sokoloff et al. 1990; Robinson et al., 1994). D4R have higher affinity for clozapine (agonist) than D2R and D3R (Van Tol et al, 1994).

Table 1.1. Summary of Crystal Structures of Ligand-Bound DA Receptors.

Active DA Receptor Complex	Structure Resolution	Reference
Rotigone-D1R-Gα_s	**3.2 Å**	(Xu et al, 2023)
SKF81297-D1R-Gα_s	**3.0 Å**	(Zhuang et al, 2021a)
SKF83959-D1R-Gα_s	**2.9 Å**	(Zhuang et al, 2021a)
apomorphine -D1R-Gα_s	**3.0 Å**	(Zhuang et al, 2021a)
Fenoldopam-D1R-Gα_s	**3.2 Å**	(Xiao et al, 2021)
A77636-D1R-Gα_s	**3.5 Å**	(Xiao et al, 2021)
SKF83959-D1R-Gα_s	**3.3 Å**	(Xiao et al, 2021)
Compound1-D1R-Gα_s (non-catechol agonist)	**3.8 Å**	(Sun et al, 2021)
PW0464-D1R-Gα_s	**3.1 Å**	(Xiao et al, 2021)
LY3154207-D1R-Gα_s	**3.1 Å**	(Xiao et al, 2021)
DA+LY3154207-D1R-Gα_s	**3.0 Å**	(Teng et al, 2022)
DA+LY3154207-D1R-Gα_s	**3.2 Å**	(Zhuang et al, 2021b)
SKF81297+ LY3154207-D1R-Gα_s	**3.0 Å**	(Zhuang et al, 2021b)
Fenoldopam+LY3154207-D1R-Gα_s	**3.2 Å**	(Teng et al, 2022)
Tavapadon+ LY3154207-D1R-Gα_s	**3.3 Å**	(Teng et al, 2022)
Rotigone-D2R-Gα_i	**3.0 Å**	(Xu et al, 2023)
Bromocriptin-D2R-Gα_i	**2.8 Å**	(Zhuang et al, 2021a)
Bromocriptine-D2R-Gα_i	**3.7 Å**	(Yin et al, 2020)
Haloperidol-D2R	**3.1 Å**	(Fan et al, 2020)
Risperidone-D2R	**2.9 Å**	(Wang et al, 2018)
Rotigone-D3R-Gα_i	**2.7 Å**	(Xu et al, 2023)
PD128907-D3R-Gα_i	**2.7 Å**	(Xu et al, 2021)
Pramipexole-D3R-Gα_i	**3.0 Å**	(Xu et al, 2021)
Eticlopride-D3R (antagonist)	**3.15 Å**	(Chien et al, 2010)
Rotigone-D4R-Gα_i	**3.2 Å**	(Xu et al, 2023)
Nemonapride-D4R	**1.95 Å**	(Wang et al, 2017)
Rotigone-D5R-Gα_s	**3.1 Å**	(Xu et al, 2023)

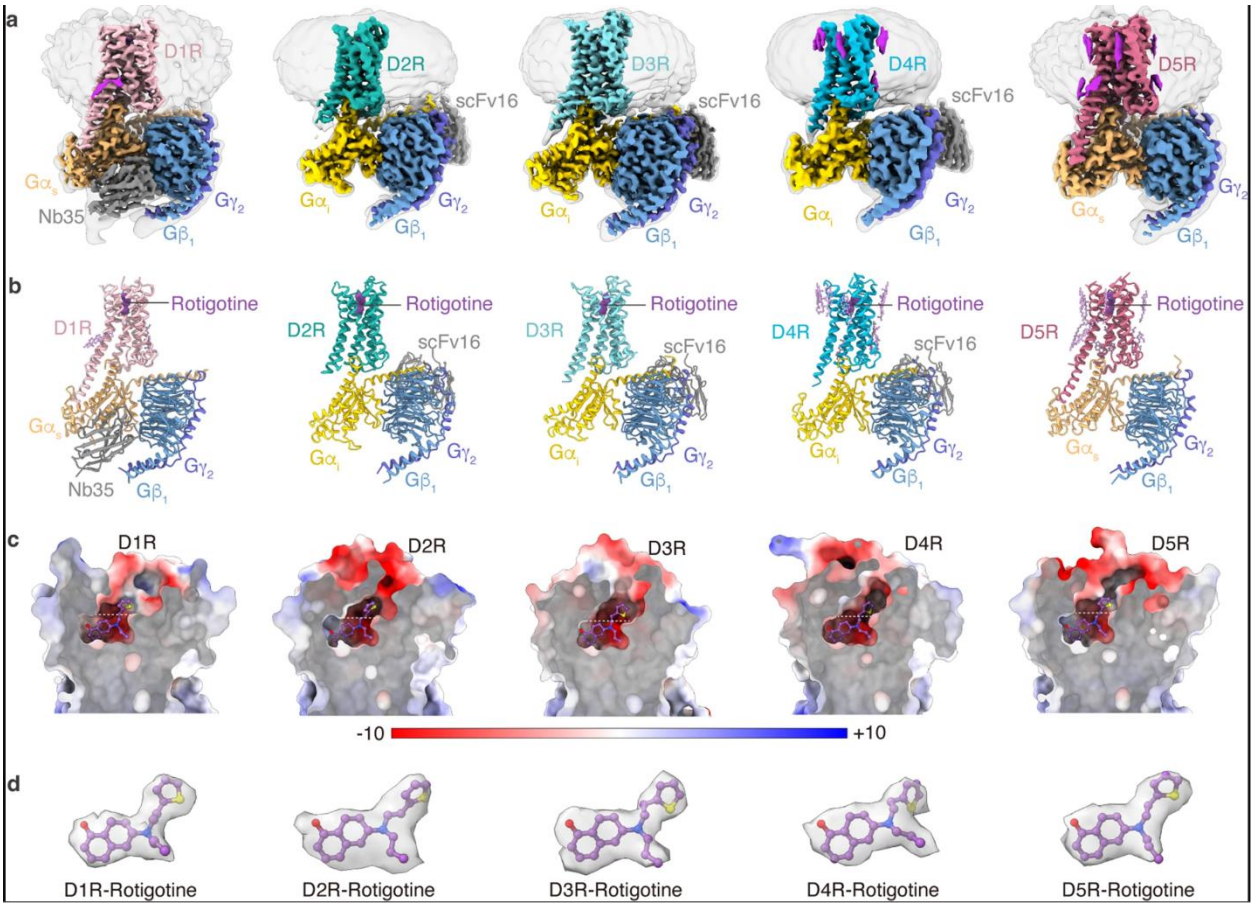

Fig. 1.14. Cryo-EM Structures of D1R, D2R, D3R, D4R and D5R Signaling Complexes.
a, b The cryo-EM density maps (a) and models (b) of the D1R–Gs, D2R–Gi, D3R–Gi, D4R–Gi, and D5R–Gs complexes. c The ligand-binding pockets of the D1R–Gs, D2R–Gi, D3R–Gi, D4R–Gi, and D5R–Gs complexes. Electrostatic surface potential is colored by red (−10 kT/e), blue (+10 kT/e), and white (neutral). d The rotigotine structure in the D1R–Gs, D2R–Gi, D3R–Gi, D4R–Gi, and D5R–Gs complexes. The EM densities of rotigotine in the five structures are shown. "From [Xu et al. Structural genomics of the human dopamine receptor system. Cell Res. 2023]. Reprinted with permission from Springer Nature."

A recent study suggested that in mice under hyperlocomotion activity driven by amphetamine, D1R-MSN and D2R-MSN activity levels were increased and decreased, respectively (Yun et al, 2023). As antipsychotic activity inhibited locomotion, it also suppressed amphetamine-induced hyperdopaminergic activity (Yun et al, 2023). Surprisingly, the selective D2R antipsychotic efficacy of haloperidol and clozapine increased D1R-MSN activity, and under hyperdopaminergic conditions, these drugs attenuated D1R-MSN hyperactivity (Yun et al, 2023). These findings suggested an important pharmacological activity of haloperidol and clozapine, in which it partially modulate the function for D1R-MSN (Yun et al, 2023).

The development of pharmacological ligand for specific D1-class receptor subtype has proven to be challenging. The highly dynamic conformation state of D1R and D5R, and the contribution of multiple sites in ligand binding, are hindering the development of receptor subtype specific ligand. As described previously, exchanging the CT domains between D1R and D5R led to a full switch of DA affinity and basal activity of G-protein (Jackson et al., 2000; Tumova et al, 2004). In addition, crystal structures for D1R and D5R have revealed similar docking motifs for ligand binding (Xu et al, 2023). Thus, the subtleties discriminating D1R and D5R ligand binding pockets remain elusive.

2.6. Heterotrimeric G-Proteins

Heterotrimeric G-proteins represent the main communication of GPCRs by linking the ligand-bound receptors with intracellular signaling proteins (Rodbell, 1980; Gilman, 1984; Simon et al, 1991; Tang and Gilman, 1992). G-protein activation by GPCRs leads to the activation of downstream effectors to mediate subsequent physiological effects (Rodbell, 1980; Gilman, 1984; Simon et al, 1991; Tang and Gilman, 1992; Gether, 2000; Pierce et al, 2002; Luttrell, 2006). These proteins are composed of: α, β, and γ subunits. α subunit defines the basic function of a heterotrimeric G-protein and is tightly bound with βγ subunits (Rodbell, 1980; Gilman, 1984; Tang and Gilman, 1992; Gether, 2000; Pierce et al, 2002; Luttrell, 2006; Hilger et al, 2018). Multiple isoforms of each G-protein subunit have been found in human: 16 α subunits, 5 β subunits, and 12 γ subunits, each of which have specific expression patterns and different effector proteins (Simon et al, 1991; Downes and Gautam, 1999; Masuho et al, 2021). Based on sequence homology and functional properties, members of Gα subunits are divided into four classes: $G\alpha_{s/olf}$, $G\alpha_{i/o}$, $G\alpha_{q/11}$, and $G\alpha_{12}$ (Simon et al, 1991; Clapham and Neer, 1997; Downes and Gautam, 1999). The Gα

subunits contain a guanine nucleotide binding domain, a GTPase domain (for GTP hydrolysis), and binding sites for GPCRs, Gβγ dimers, and downstream effectors (Gether, 2000; Pierce et al, 2002; Luttrell, 2006; Hilger et al, 2018). The Gβ subunit and Gγ subunit form a functional dimer, with 60 possible combinations of Gβγ dimers. The large array and complexity of these heterotrimeric G-protein subunits herein bestows receptors with great diversity in signaling capabilities, with almost 1000 possible heterotrimeric combinations for activated GPCRs (Simon et al, 1991; Clapham and Neer, 1997; Downes and Gautam, 1999; Masuho et al, 2021).

2.6.1. G-Protein Activation of GPCR Signaling

In their inactive state, heterotrimeric G-proteins are bound to GDP on their α subunits. Upon activation of GPCR by a ligand, either endogenous or exogenous, in the extracellular milieu, a change in GPCR conformation promotes exchange of GDP for GTP on the G-protein α subunit (Gether, 2000; Pierce et al, 2002; Luttrell, 2006; Hilger et al, 2018). This leads to dissociation of the Gα subunit and the Gβγ heterodimeric subunit from the ligand-bound GPCR. Subsequently, free Gα-bound GTP and Gβγ dimer can regulate the action of effector protein, such as ACs and ion channels, to produce small molecules that transmit signals intracellularly (Gether, 2000; Pierce et al, 2002; Luttrell, 2006; Hilger et al, 2018). The signaling outcome is thus dependent on the particular combination of ligand bound-GPCR, Gα and Gβγ subunits, and activated intracellular partners. This transduction process allows GPCRs to successfully transfer extracellular signaling "*first messenger*" into specific intracellular signaling "*second messenger*" (Gether, 2000; Pierce et al, 2002; Luttrell, 2006; Hilger et al, 2018).

Signaling continues until there is hydrolysis of GTP to GDP, which inactivates Gα and results in its subsequent reassociation with the Gβγ dimer, thereby reforming the inactive heterotrimeric G-protein once again (Hermans, 2003; Luttrell, 2006). The balance between active and inactive G-protein states is modulated by two families of proteins: the guanine nucleotide exchange factors (GEFs), which promote active state formation by stimulating GDP-GTP exchange on the α subunits, and the GTPase activating proteins (GAP), which facilitate GTP hydrolysis to supress G-protein activity (Hermans, 2003; Luttrell, 2006). Moreover, regulators of G-protein signaling (RGS) are responsible for enhancing Gα GTPase activity and feedback regulation of G-protein functions as well integration of G-protein signaling with other cellular systems (Dohlman and Thorner, 1996; Hermans, 2003; Luttrell, 2006).

2.6.2. Pharmacological Multistates for GPCR

GPCRs exist in a dynamic equilibrium between inactive (R) and active (R*) multi-state conformations (Lefkowitz et al, 1993; Pierce et al, 2002; Luttrell, 2006; Hilger et al, 2018). These conformations underlie the extended ternary complex model in response to pharmacological ligands (agonist, antagonist, and inverse agonist). Some GPCRs possess an inherent basal level of G-protein activation, referred to as constitutive activity. Indeed, agonist-independent activity of GPCRs modulate a variety of intracellular effector proteins secondary to G-protein activation. In the R* state, agonists promote conformational changes to activate and stabilize the receptor by maximizing G-protein binding. Constitutive activity, however, can be abrogated by inverse agonist binding which shifts the equilibrium toward R state and thus maintains receptors in the inactive conformation. Antagonists (neutral ligands) have an equal affinity for both R and R* states, and merely serve to block the ligand binding site for agonist and inverse agonist. Full and partial agonist/inverse agonist promote different degrees of receptor conformational change, which result in a maximal or partial G-protein activation, respectively (Lefkowitz et al, 1993; Pierce et al, 2002; Luttrell, 2006; Hilger et al, 2018). *Fig. 1.3B. shows the pharmacological ligands and differences between DA receptors.*

2.6.3. Constitutive Activity of D1-Class Receptors

Several GPCRs exhibit a tonic level of activation both *in vivo* and *in vitro*, known as constitutive activity (Lefkowitz et al, 1993; Zhang et al, 2014). Pharmacologically, receptor subtypes with constitutive activity generally have higher agonist potency (Lefkowitz et al, 1993). The high structural similarity of D1-class receptor subtypes makes it challenging to develop subtype-selective ligands to investigate specific roles for these receptors (Zhang et al, 2014). However, functional differences are observed between D1R and D5R that account for subtype-specific signaling, both dependent and independent of ligand activation (Zhang et al, 2014). D5R displays higher constitutive AC activity and higher agonist potency than D1R (Tiberi and Caron 1994; Charpentier et al. 1996; Plouffe et al, 2010; Zhang et al, 2014). Structural differences between D1R and D5R are central to their unique pharmacological characteristics (Plouffe et al, 2010). Exchanging the CT domain between D1R and D5R lead to a full switch of their DA affinity and basal activity (Tiberi and Caron 1994; Jackson et al, 2000; Tumova et al, 2004; Zhang et al, 2014).

In the striatum, the constitutive activation of D2R, but not D1R, maintain the single spike firing of tonic DA release into target neurons (Costa and Schoenbaum, 2022). D5R agonist-independent constitutive activity facilitate the burst-firing activity in the STN, and contribute to the pathological firing of PD to inhibit STN (Baufreton et al, 2003; Chetrit et al, 2013). Thus, the application of D5R inverse agonist was shown to normalize the pathological firing to normal tonic firing, which result in attenuation of observed Parkinson-like motor impairment (Chetrit et al, 2013). Due to the lack of a subtype-selective inverse agonist or antagonist, the role of constitutive activity in normal and pathological situations for D1-class receptors has yet to be fully appreciated (Zhang et al, 2014).

2.7. GPCR-mediated Signaling Pathways

GPCRs transmit signals mainly toward two transducer-coupled systems: the heterotrimeric G-protein activation and G-protein—independent βArr-dependent signaling (Pierce et al, 2002; Luttrell, 2006; Beaulieu and Gainetdinov, 2011). The various structural elements in each activated receptor, including DA receptors, determine their preferential protein coupling to mediate the signaling pathway. The D1-class primarily acts through $G\alpha_{s/olf}$-cAMP-PKA-DARPP-32-dependent pathways. On the other hand, the D2-class acts via $G\alpha_{i/o}$-cAMP-PKA-DARPP-32 and Gβγ-mediated signaling pathways (Beaulieu and Gainetdinov, 2011; Beaulieu et al, 2015). DA receptor-mediated signaling pathways regulate various physiological processes, e.g., cell survival, proliferation, and neuronal plasticity. Dysregulation in DA receptor signaling thus has important implications for various physiological and pathological processes (Beaulieu and Gainetdinov, 2011; Beaulieu et al, 2015). *Fig. 1.15. illustrates the canonical G-protein signaling events mediated by DA receptors.*

2.7.1. $G\alpha_{s/olf}$-mediated cAMP-PKA Pathway

The signaling of an active receptor is determined by the Gα subunit it is coupled to. Activation of Gα subunit that belongs to the $G\alpha_{s/olf}$ class or $G\alpha_i$ class leads to the activation or inhibition of AC, respectively (Tang and Gilman, 1992; Pierce et al, 2002; Luttrell, 2006; Beaulieu and Gainetdinov, 2011). There are nine different isoforms of transmembrane AC and one soluble form of AC. Each of transmembrane AC composed of twelve membrane-spanning regions that together catalyze the conversion of ATP into cAMP, a second messenger that amplifies receptor signaling primarily by activating PKA or Exchange Protein Activated by cAMP (EPAC) (Fischer and Krebs, 1955;

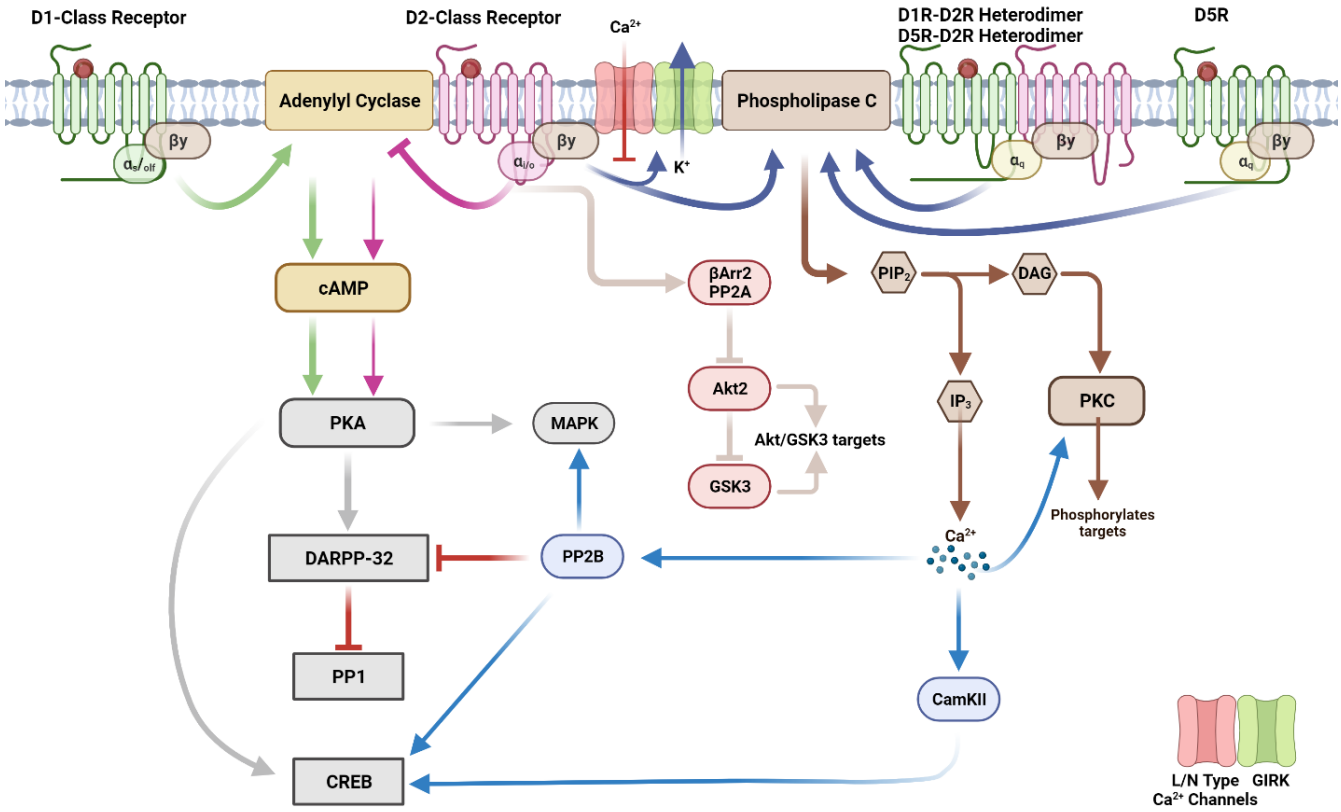

Fig. 1.15. Canonical Signaling Cascades of D1- and D2-Class Receptors.
Ligand-bound D1-class receptor coupled to $G_{\alpha s/olf}$ to activate AC-mediated cAMP-PKA pathway. D2-class receptors signaling pathways are mediated by $G_{\alpha i/o}$ and Gβγ subunits. $G_{\alpha i/o}$ exhibits an inhibitory effect on AC activity and decrease the level of cAMP, whereas Gβγ subunits stimulate PLC. In addition to D5R, D1R•D2R heterodimerization regulates the coupling of D1R to $G_{\alpha q}$ which stimulates PLC. PLC catalyzes the hydrolysis of PIP_2 into DAG and IP_3. IP_3 increases the release of Ca^{2+} and Ca^{2+} and DAG then activates the PKC. AC; adenylyl cyclase; cAMP: adenosine 3′,5′- cyclic monophosphate; CREB: cAMP response element-binding protein; DARPP-32: dopamine and cAMP-regulated phosphoprotein 32kDa; PIP_2, phosphatidylinositol-4,5-biphosphate; IP_3, inositol trisphosphate; DAG, diacylglycerol; PKA, protein kinase A; PKC, protein kinase C; PLC, phospholipase C; PP1, protein phosphatase 1; CaMKII, calcium/calmodulin-dependent PK II; PP2A: protein phosphatase 2A; PP2B: protein phosphatase 2B; Akt2: protein kinase B; GSK3: glycogen synthase kinase 3; GIRK: G protein-regulated inwardly rectifying K^+ channel; MAPK: mitogen-activated protein kinase. Created with BioRender.com.

Walsh et al, 1968; Tang and Gilman, 1992; Devasani and Yao, 2022; Ostrom et al, 2022).

PKA is a tetramer protein, consisting of two regulatory subunits and two catalytic subunits (Søberg and Skålhegg, 2018). cAMP binding to regulatory subunit of PKA induces conformational changes within these subunits that cause them to dissociate from PKA catalytic subunits (Søberg and Skålhegg, 2018). The catalytic subunits of PKA then bind ATP to phosphorylate a wide range of effector proteins, including receptors, ion channels, and transcription factors (Søberg and Skålhegg, 2018). cAMP can be enzymatically degraded by cAMP phosphodiesterase (PDE) through cleavage of its phosphodiester bond, which generates AMP, thus terminating cAMP-mediated signalling pathway (Luttrell, 2006; Søberg and Skålhegg, 2018).

2.7.1.1. DA Receptor-mediated cAMP-PKA Pathway

The D1-class receptors couple to $G\alpha_{s/olf}$ subunit to stimulate AC and enhance the production of cAMP (Miyamoto et al, 1968; Kebabian and Greengard, 1971; Kebabian et al, 1972; Beaulieu and Gainetdinov, 2011). In contrast, the D2-class receptors couple to $G\alpha_{i/o}$ subunit to inhibit AC, thus decreasing the intracellular cAMP level (Civelli et al, 1993; Jaber et al, 1996; Missale et al, 1998; Beaulieu and Gainetdinov, 2011; Beaulieu et al, 2015). Altered levels of cAMP induced by DA receptor activation thereby regulates PKA-mediated activation of several downstream targets, including DARPP-32, CREB, and ion channels, to modulate various biological processes such as neuronal excitability, synaptic transmission, plasticity, and gene expression (Missale et al. 1998; Greengard 2001a, b; Neve et al., 2004; Beaulieu and Gainetdinov, 2011). Interestingly, increased PKA activity could also be positively modulated by D2-class receptors. Indeed, activation of heterologously expressed D2R and D4R, but not D3R, leads to a Gβγ permissive stimulating effect of a select group of AC isoforms (AC2, AC4, and AC7), through the conditional activation of $G_{\alpha s}$; thus, the stimulatory effect of $G_{\alpha s}$ on AC and likely PKA, is enhanced in the presence of free Gβγ dimers (Watts and Neve, 1997; Robinson and Caron, 1998; Neve et al, 2004).

2.7.1.2. DA Receptor-mediated DARPP-32 Phosphorylation

Greengard and colleagues discovered DARPP-32 and elucidated its mechanistic phosphorylation activity (Walaas et al, 1983; Halpain et al, 1990; Greengard 2001a, b). DARPP-32 is primarily expressed in MSNs, where it acts as a robust integrator of DA and glutamate signals through its modulation by both PKA and Ca^{2+} signaling (Svenningsson et al, 2004; Beaulieu and Gainetdinov,

2011). Indeed, DARPP-32 regulation is complex due to the existence of several phosphorylatable residues capable of modulating its functions (Greengard, 2001a, b; Svenningsson et al, 2004). D1- and D2-class receptor induced modulation of PKA respectively promote and inhibit phosphorylation of DARPP-32 at Thr34 (Nishi et al, 2000; Svenningsson et al, 2004; Bateup et al, 2008). D2-class activation also increases intracellular Ca^{2+} to activate calmodulin-dependent protein phosphatase 2B (PP2B, also known as calcineurin), causing dephosphorylation of DARPP-32 at Thr34 (Svenningsson et al, 2004). Thr34-DARPP-32 is a potent inhibitor of protein phosphatase 1 (PP1), thereby, promoting phosphorylation of different neurotransmitter receptors, including α-amino-3-hydroxy-5-methyl-4-isoxazole propionic acid receptor (AMPAR) and NMDAR (Hemmings et al, 1984). The psychostimulant cocaine increases Thr34-DARPP-32 phosphorylation selectively in striatonigral neurons, whereas the antipsychotic haloperidol increases Thr34-DARPP-32 phosphorylation in striatopallidal neurons (Bateup et al, 2008; Bateup et al, 2010; Santini et al, 2012). The differential regulation of these two neuronal populations can explain the drug opposing behavioral effect, as they couple to opposing output pathways (Bateup et al, 2008). Although Thr34-DARPP-32 phosphorylation is not altered in 6-OHDA mice, Thr34 phosphorylation is enhanced in dyskinetic mice treated with L-DOPA (Picconi et al, 2003). Furthermore, DARPP-32 is phosphorylated by casein kinase 1 (CK1) and casein kinase 2 (CK2), which respectively decrease and increase PKA-mediated Thr34 phosphorylation (Desdouits et al, 1995). In contrast, cyclin-dependent kinase 5 (Cdk5) phosphorylates DARPP-32 at Thr-75, which increases PP2A activity, leading to reduced Thr34-DARPP-32 phosphorylation and PKA activity, along with enhanced PP1 function (Bibb et al, 1999). Ultimately, DA receptor-PKA-DARPP-32-mediated signaling pathway is capable of both positively and negatively regulating the function of voltage-gated ion channels depending on cellular and physiological context.

2.7.1.3. DA Receptor-mediated ERK1/2 Activation

D1- and D2-class receptors regulate the mitogen-activated protein kinases (MAPKs), including extracellular signal-regulated kinase-1 and -2 (ERK1/2) (Beaulieu and Gainetdinov, 2011). Convergent activation of ERK1/2 via distinct signaling pathways imparts ERK1/2 with coincidence detector function that integrates the actions of DA with other neurotransmitter systems to control CREB phosphorylation (Beaulieu and Gainetdinov, 2011). Activation of D1-class receptors predominantly stimulates ERK1/2 activity, leading to modulation of numerous

physiological responses (Beaulieu and Gainetdinov, 2011). D1R is capable of activating ERK1/2 through both a $G\alpha_{s/olf}$-cAMP-mediated PKA cascade and through a pathway independent of PKA activity that utilizes the GEFs: RapGEF2 and EPAC2 (Woolfrey et al, 2009; Beaulieu and Gainetdinov, 2011; Jiang et al, 2017; Jiang et al, 2021). However, D1R-mediated ERK1/2 activation involves both $G\alpha_s$-cAMP pathway and cAMP-independent βArr cascade (Kaya, et al 2020). Interestingly, a single-cell analytical approach examining the signaling crosstalk between cytosolic and nuclear PKA and ERK1/2 within striatal neurons demonstrated a novel role for D1R-mediated ERK1/2 in promoting nuclear activation of PKA (Jones-Tabah et al, 2021). *Fig. 1.16. illustrate the D1R-mediated ERK1/2 activation.*

Activation of D1R-PKA-mediated DARRP-32-Thr34 phosphorylation is found necessary for activation of ERK1/2 in striatum (Valjent et al, 2005; Gerfen et al, 2008). The psychostimulant cocaine and the antipsychotic haloperidol both increase ERK1/2 phosphorylation in the striatum, but within segregated populations of D1R- or D2R-expressing MSNs, respectively, thereby demonstrating that D2R normally functions to inhibit ERK1/2 activation within striatal neurons (Bertran-Gonzalez et al, 2008). Indeed, in 6-OHDA-lesioned mice, L-DOPA administration leads to ERK1/2 pathway activation through a D1R-dependent mechanism, thus underscoring the respective facilitatory and inhibitory roles of D1R and D2R on striatal ERK1/2 activation (Westin et al, 2007; Santini et al, 2009). Chronic L-DOPA administration in PD patients can trigger the onset of dyskinesia, which is associated with activation of ERK1/2 signaling in striatonigral MSNs. However, studies have also demonstrated that repeated L-DOPA treatment downregulates D1R-mediated PKA and ERK1/2 activation (Santini et al, 2009; Jones-Tabah et al, 2020).

2.7.1.4. DA Receptor-mediated CREB Phosphorylation

Another important PKA substrate is Ser133 of the transcription factor CREB; this leads to transcription of genes with cAMP response element (CRE), which ultimately have an important role in synaptic plasticity (Konradi et al, 1994; Cole et al, 1994; Cole et al, 1995; Liu FC, Graybiel, 1996; Shaywitz and Greenberg, 1999). Agonist activation of D1R, but not D2R, in striatal neurons selectively induces phosphorylation of CREB. Psychostimulants similarly increase CREB phosphorylation downstream of D1R activation (Cole et al, 1995; Das et al, 1997; Liu FC, Graybiel, 1998). Additionally, stimulation of D1R induces the PKA-CREB pathway through

phosphorylation of GluN1-containing NMDAR by PKA (Dudman et al, 2003). Gene transcription facilitated by CREB can also be promoted via activation of DARPP-32 and ERK1/2.

2.7.2. $G\alpha_q$-mediated Ca^{2+}-PKC Pathway

In addition to $G\alpha_s$ and $G\alpha_i$, activated GPCRs, including DA receptors, that are coupled to $G\alpha_q$ subunit enhance the activity of phospholipase C (PLC), an enzyme catalyzing the hydrolysis of phosphatidylinositol bisphosphate (PIP2) into diacylglycerol (DAG) and inositol trisphosphate (IP_3) (Pierce et al, 2002; Luttrell, 2006; Beaulieu et al, 2015). IP_3 increases intracellular Ca^{2+} release through the activation of IP_3 receptor on the endoplasmic reticulum (ER). DAG in cooperation with phosphatidylserine and Ca^{2+} activate PKC, which ultimately phosphorylates various receptors, kinases, and transcription factors (Pierce et al, 2002; Luttrell, 2006; Beaulieu et al, 2015). Both activation of PKC and increased intracellular Ca^{2+} have widespread regulatory effects on GPCRs and other cellular machinery. IP_3 and DAG can also be enzymatically metabolized by phosphatidylinositol phosphatases and diacylglycerol kinases, respectively, to mediate signaling events (Pierce et al, 2002; Luttrell, 2006; Beaulieu et al, 2015).

2.7.2.1. DA Receptor-mediated Ga_q Pathway

Activation of D5R, but not D1R, couples to $G\alpha_q$-PLC-Ca^{2+} signaling pathway that regulates PKC-mediated physiological responses (Felder et al, 1989; Undie and Friedman, 1990; Undie and Friedman, 1992; Undie et al, 1994; Friedman et al, 1997; Sahu et al, 2007; So et al, 2009; Lee et al, 2014a). Interestingly, while D1R alone cannot stimulate PLC signalling, George and colleagues show that co-activation of D1R and D2R within D1R•D2R heterodimers leads to $G\alpha_q$-mediated PKC and Ca^{2+} signaling. Although D1R•D2R can couple to $G\alpha_q$-mediated PLC, D1R-mediated $G\alpha_q$ coupling was observed in transfected HEK293 cells, whereas coupling to PLC was found in Ltk-fibroblast cells transfected with D1R alone, in which DA increased cytosolic Ca^{2+}; thus other mechanisms or chaperones may direct this coupling (Liu et al, 1992; Okashah et al, 2019; Inoue et al, 2019). Indeed, both D1R•D2R heterodimers and D5R•D2R heterodimers couple to $G\alpha_q$-mediated PKC activation in striatal culture (Lee et al, 2004; So et al, 2005; Rashid et al, 2007; So et al, 2009; Hasbi et al, 2010; Verma et al, 2010; Perreault et al, 2010; Perreault et al, 2012). Although heterodimerization of D1R•D2R imply that both colocalize in MSNs, Lee and colleagues reported that 50% of neurons from striatal cultures show a colocalization of D1R and D2R,

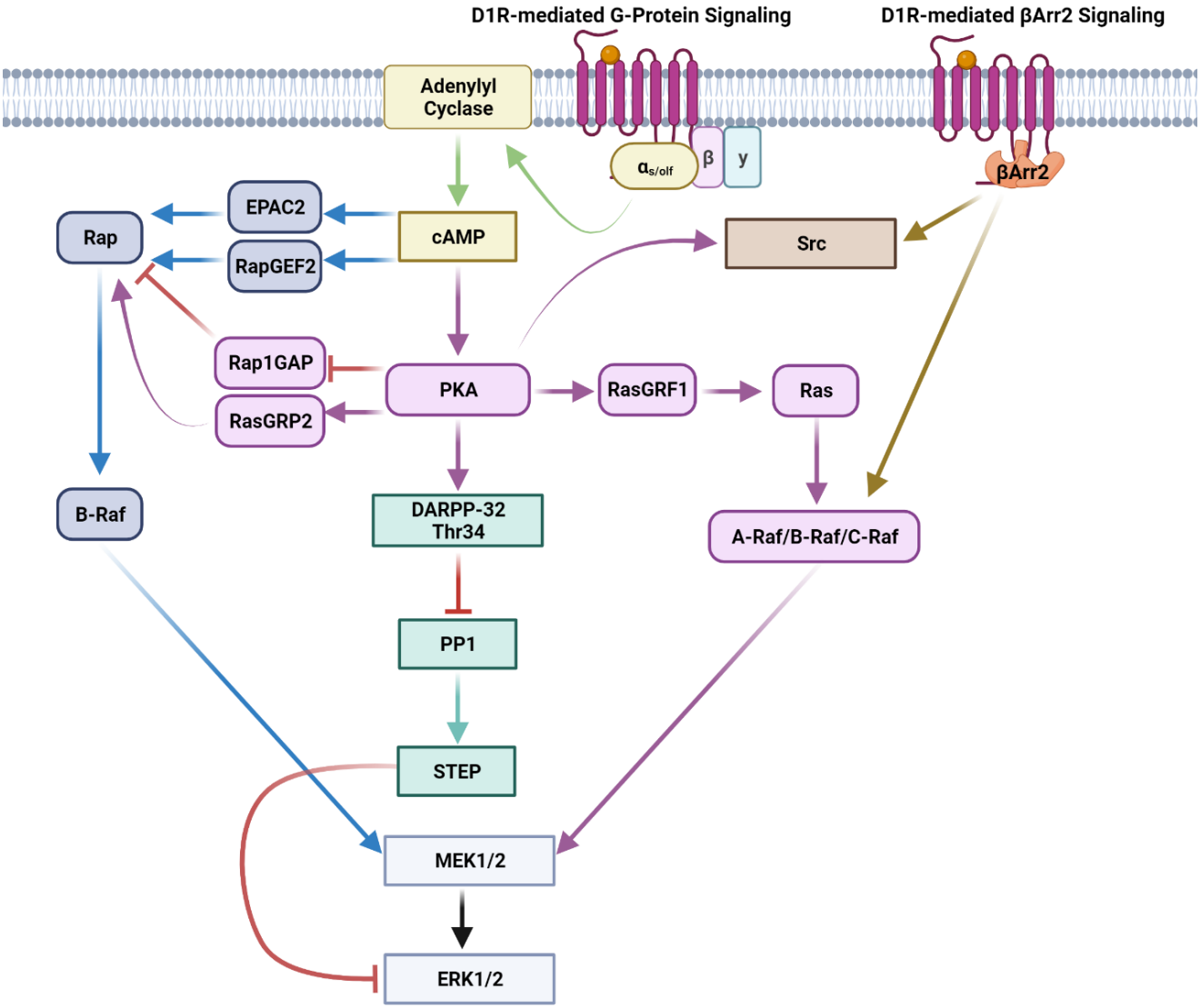

Fig. 1.16. Mechanisms of D1R-mediated ERK1/2 Activation.

D1R-mediated G-protein signaling and D1R-mediated βArr2 activation regulate the downstream signaling events. cAMP: adenosine 3′,5′- cyclic monophosphate; PKA, protein kinase A; DARPP-32: dopamine and cAMP-regulated phosphoprotein 32kDa; PP1, protein phosphatase 1; STEP: striatal-enriched tyrosine phosphatase; MEK1/2: mitogen-activated protein kinase 1 and 2; ERK1/2: Extracellular signal-regulated protein kinases 1 and 2. Src: Src kinase; EPAC2: exchange protein directly activated by cAMP 2; Rap: Rap proteins; RapGEF2: Rap guanine nucleotide exchange factor 2; Rap1GAP: Rap1 GTPase-activating protein; RasGRP2: Ras guanyl-releasing protein 2; RasGRF1: Ras-specific guanine nucleotide-releasing factor 1; A-Raf: Raf isoform A; B-Raf: Raf isoform B; C-Raf: Raf isoform C. Created with BioRender.com.

which suggests a potential role for the lack of afferent innervation in *ex vivo* culture in this high level of colocalization (Lee et al, 2004; Hasbi et al, 2010). In addition, the authors suggested that SKF83959, a D1R partial agonist, is highly biased to stimulate PLC, but not AC (Jin et al, 2003; Hasbi et al, 2010). However, other research groups showed that SKF83959 also mediates D1R and D5R coupling to and activation of AC (Ryman-Rasmussen et al, 2005; D'Aoust and Tiberi, 2010; Lee et al, 2014b). In contrast, D2R and D5R are expressed in cholinergic interneurons, suggesting that these interneurons might contain D5R•D2R heterodimers capable of activating $G\alpha_q$-mediated signaling (Hasbi et al, 2010). $G\alpha_q$ mediating signaling via D1R•D2R and D5R•D2R heterodimers differs not only in neuronal localization (MSNs versus cholinergic interneurons), but also in its dependence on extracellular Ca^{2+} and Calcium/calmodulin-dependent protein kinase type II (CaMKIIα) activation, which is required only for D1R•D2R heterodimers (Hasbi et al, 2010; Perreault et al, 2016; Rico et al, 2017). Furthermore, the native heterodimerization of D1R•D2R was demonstrated from striatum and other brain regions of different species: rodent, monkey, and human (Perreault et al, 2016; Rico et al, 2017; Hasbi et al, 2018; Hasbi et al, 2020a, b). Despite the findings above, the existence of D1R•D2R heterodimer-mediated $G\alpha_q$ signaling remains controversial. The Javitch's lab provided evidence against D1R•D2R heterodimer, and could not detect $G\alpha_q$ coupling to D1R, D2R, or D1R•D2R heterodimers, yet both D1R and D2R were found to be completely segregated in NAc shell and thus do not form a complex in this brain region (Frederick et al, 2015). To further complicate matters, postmortem striatal coimmunoprecipitation studies showed heterodimerization of D1R•D2R, and this complex is upregulated in subjects suffering major depression (Pei et al, 2010). The analysis also revealed that D1R-CT mediates the interaction with D2L-IL3 but not D2S-IL3 (Pei et al, 2010). This study also identified an interfering peptide of D2L-IL3 that disrupt D1R•D2R *in vivo* and exert antidepressant behavioral effect (Pei et al, 2010).

2.8. β-Arrestins

Arrestins act as important regulators of GPCRs by orchestrating a variety of physiological signaling and scaffolding mechanisms (Krupnick and Benovic, 1998; Pierce and Lefkowitz, 2001; Luttrell and Lefkowitz, 2002; Shenoy and Lefkowitz, 2011; Wess et al, 2023). Structurally, arrestins contains two major domains (N and C), which consist of large β-sheets and connecting loops (Krupnick and Benovic, 1998; Wess et al, 2023). Arrestins are divided into two different

classes, retinal arrestins and βArrs, based on their sequence homology, tissue distribution, and how they regulate GPCR functions (Krupnick and Benovic, 1998). Retinal arrestins, consisting of visual arrestin (*arrestin1*) and cone arrestin (*arrestin4*), exclusively bind to rhodopsin and opsin receptors, respectively (Krupnick and Benovic, 1998). βArrs, comprising βArrestin1 (βArr1 "*arrestin2*") and βArr2 (*arrestin3*), are ubiquitously expressed in all tissues and act on most GPCRs (Krupnick and Benovic, 1998). βArr1 and βArr2 have 78% sequence homology and exhibit similar localization and modulation of GPCR function; nonetheless, important differences among them are observed (Krupnick and Benovic, 1998). Rhodopsin-class receptors, including DA receptors, have higher binding affinity for βArr2 than for βArr1 (Oakley et al, 2000; Pierce and Lefkowitz, 2001). Given how many different non-visual GPCRs are seemingly regulated by the βArrs, various mechanisms for GPCR•βArr binding interactions are essential to ensure a specific modulation of GPCR activity. Studies from mutant mice showed that βArrs play critical roles in regulating numerous central and peripheral behaviors (Gainetdinov et al, 2004; Wess et al, 2023).

2.8.1. GPCR Binding to β-Arrestin

The binding of GPCR to βArr is influenced by various factors, and are classified into two major classes, depending on the translocation of βArrs to the activated GPCRs (Ferguson, 2001). Class-A GPCRs, including adrenergic receptor, opioid receptors, and DA receptors, have higher affinity towards βArr2, whereas class-B GPCRs (e.g., angiotensin receptors and vasopressin receptors), have similar affinity to both βArr isoforms (Ferguson, 2001). These characteristic differences derived mainly from Ser/Thr clusters of class-B GPCR-CT, but not class-A. Following the internalization of GPCR•βArr complex, βArr2 is easily dissociated from class-A GPCR, but not with class-B GPCRs. Differences in βArrs affinity eventually induces different patterns of signaling and trafficking of GPCR•βArr complex (Ferguson, 2001).

2.8.2. Interaction Modes of β-Arrestins

βArrs employ dynamic, biphasic mechanisms to engage with receptors (Kang et al, 2015; Kahsai et al, 2018). Two different modes of interaction contribute to phosphorylated GPCR•βArr complex formation: tail and core interactions (Shukla et al, 2014; Kahsai et al, 2018). βArr tail interactions involve phosphorylated residues on CT of GPCR, whereas βArr core interactions occur with

transmembrane regions of GPCR (Shukla et al, 2014). These tail and core interactions are mediated by two different sites on βArr, namely, phosphorylation and activation sensors, respectively (Shukla et al, 2014; Kahsai et al, 2018). The conformational arrangement of GPCR•βArr complex usually preclude engagement with G-protein heterotrimer but facilitate bimodal βArr-mediated signaling effects (Cahill et al, 2017; Eichel et al, 2018; Latorraca et al, 2018; Kahsai et al, 2018; Maharana et al, 2023; Maharana et al, 2024). Interestingly, recent findings suggest that phosphorylated CT of D1R drives βArr2 recruitment, whereas D1R-IL3 is responsible for βArr2 activation, thus implying distinct functions for βArr2 tail and core interactions with D1R (Kaya et al, 2020; Moritz et al, 2023). Ultimately, these two processes lead to receptor internalization and D1R-mediated ERK1/2 activation.

2.8.3. β-Arrestin-mediated Signaling

βArrs are multifunctional adapter proteins that regulate a variety of cellular functions independently from canonical G-protein signaling (Pierce and Lefkowitz, 2001; Luttrell and Lefkowitz, 2002; Shenoy and Lefkowitz, 2011; Shukla et al, 2011; Wess et al, 2023). While βArrs do not have intrinsic signaling function, as they lack kinase and phosphatase activity, their scaffolding properties enable the recruitment of different signaling proteins capable of initiating signaling pathways in conjunction with different GPCRs (Shenoy and Lefkowitz, 2011; Shukla et al, 2011). Indeed, βArrs have been demonstrated to facilitate the activation of multiple downstream signaling proteins including members of ERK1/2 and Jun N-terminal kinase 3 (JNK3) cascades, Src family kinases, and receptor tyrosine kinases (Shenoy and Lefkowitz, 2011; Shukla et al, 2011). Luttrell, Ferguson, and colleagues described the first signaling function of βArrs—βArr1, in which activated β_2AR bound to the tyrosine kinase c-Src and mediated its activation (Luttrell et al, 1999). Following this landmark finding, numerous GPCRs were shown to be regulated by βArr signalling, which was demonstrated to have important physiological functions (McDonald et al, 2000; Luttrell et al, 2001; Shenoy et al, 2001; Perry et al, 2002; Bhattacharya et al, 2002). One noteworthy example from Caron's lab involved a novel βArr2•Akt•PP2A signalling complex that forms in response to D2R activation and triggers the inhibition of lithium-sensitive phosphoinositide 3-kinases (PI3K)/Akt to modulate glycogen synthase kinase 3 (GSK3) signaling (Beaulieu et al, 2004; Beaulieu et al, 2005; Beaulieu et al, 2008).

2.8.3.1. D1R-mediated β-Arrestin Signaling

βArr2 also contributes to D1R-mediated activation of Src and ERK1/2 in a manner independent of cAMP (Kaya et al, 2020). Interestingly, phosphorylated D1R can simultaneously bind $G\alpha_s$ and βArr2 to activate ERK1/2 cascade in a synergistic manner (Kaya et al, 2020). It is hypothesized that ERK1/2 signaling could be a bridge for the crosstalk between D1R-mediated $G\alpha_s$-cAMP signaling, and D1R-mediated βArr2 signaling (Kaya et al, 2020). Notably, the initial ERK1/2 activation mediated by D1R•$G\alpha_s$ enhances the ERK1/2-dependent βArr2 signaling of D1R, suggesting that βArr2, but not $G\alpha_s$, is obligatory for ERK1/2 activation by D1R (Kaya et al, 2020). Urs and colleagues provided potential role for D1R-depndent βArr2•pERK1/2 signaling complex in mediating psychomotor activation, but not the rewarding properties, of morphine (Urs et al, 2011). βArr1-KO model exhibits a reduced locomotor activity in response to apomorphine, a non-selective DA agonist, suggesting that βArr1 positively modulates behavioral D1R response (Gainetdinov et al, 2004). However, the contribution of βArr2 to D5R signaling remains to be examined.

2.8.3.2. GPCR•$G\alpha_s$•β-Arrestin Signaling

Contrary to the classical paradigm, under some circumstances G-protein coupling to receptor can occur in the presence of βArr; these tripartite complexes are termed super-complexes or "megaplexes" (Marshall, 2016; Nguyen and Lefkowitz, 2021). Such super-complexes appear to exert a unique cellular function. In particular, the Bouvier and Lefkowitz groups showed that some GPCRs bound to βArrs activate $G\alpha_s$ from within internalized cellular compartments, resulting in sustained endosomal cAMP signaling (Thomsen et al, 2016). Interestingly, von Zastrow's group showed that D1R mediates endosomal cAMP signaling (Kotowski et al, 2011). Whether βArr2 contributes to this endosomal signaling remains to be determined.

2.8.3.3. GPCR•$G\alpha_i$•β-Arrestin Signaling

Noncanonical scaffolding of GPCR•$G\alpha_i$•βArr2 has been observed to occur in a manner independent of the canonical Gα protein subtype for a given GPCR (Smith et al, 2021). D1R, among other GPCRs coupling to $G\alpha_s$, formed D1R•$G\alpha_i$•βArr2 ternary complex in response to agonist treatment, but did not form complex with $G\alpha_s$•βArr2. This unexpected tripartite

D1R•Gα_i•βArr2 complex could conceivably have unique signaling signatures compared to both D1R•Gα_s and D1R•βArr2 (Smith et al, 2021).

2.8.4. Biased GPCR Signaling

In response to ligand binding, GPCRs can adopt multiple different conformational states that depend on the particular ligand, and facilitate downstream signaling through G-protein and/or βArr (Violin and Lefkowitz, 2007; Shenoy and Lefkowitz, 2011; Shukla et al, 2011; Smith et al, 2018; Wess et al, 2023). Indeed, ligands can induce distinct active receptor conformations that exhibit bias (also termed "functional selectivity") toward either G-protein- or βArr-mediated signaling pathways capable of producing distinct physiological effects (Violin and Lefkowitz, 2007; Shukla et al, 2011). Recent studies also suggested extended biased signaling for the GPCR among G-protein subunits and βArr isoforms, implying a complex picture of functional selectivity of GPCRs. Taking into account biased GPCR signaling, thus might aid the development of improved pharmacological treatment options for GPCR-related diseases (Shukla et al, 2011; Smith et al, 2018). *Fig. 1.17. depicts the signaling pathway of balanced and biased ligand-bound GPCR.*

2.8.4.1. Biased D1R Signaling

A study by Sibley's lab showed that D1R activated with benzazepine agonists (SKF83959, SKF38393, SKF82957, SKF77434, and SKF75670) induced cAMP accumulation but failed to recruit βArr2 or promote D1R internalization (Conroy et al, 2015). Interestingly, the biased signaling was unique for D1R, as the same compounds stimulated both D5R-mediated cAMP production and βArr2 recruitment (Conroy et al, 2015). A study from Biogen, Inc. led by Michael Ehlers reported a novel series of selective, potent, non-catechol D1R agonists (PF1119, PF2334, PF6142, and PF8294) that enhance cAMP levels but exhibit minimal D1R desensitization and recruitment of βArr2 (Gray et al, 2018). These findings suggest that the above-mentioned compounds are biased ligands for D1R-mediated Gα_s pathway. In contrast, a biased ligand for D1R-mediated βArr2 signaling has yet to be discovered. Identification of such a ligand is indeed desired for its potential therapeutic value in improving the treatments of various neuropsychiatric diseases, for which side effects of current treatment regimens might be attributed to excessive activation of G-protein mediated signaling.

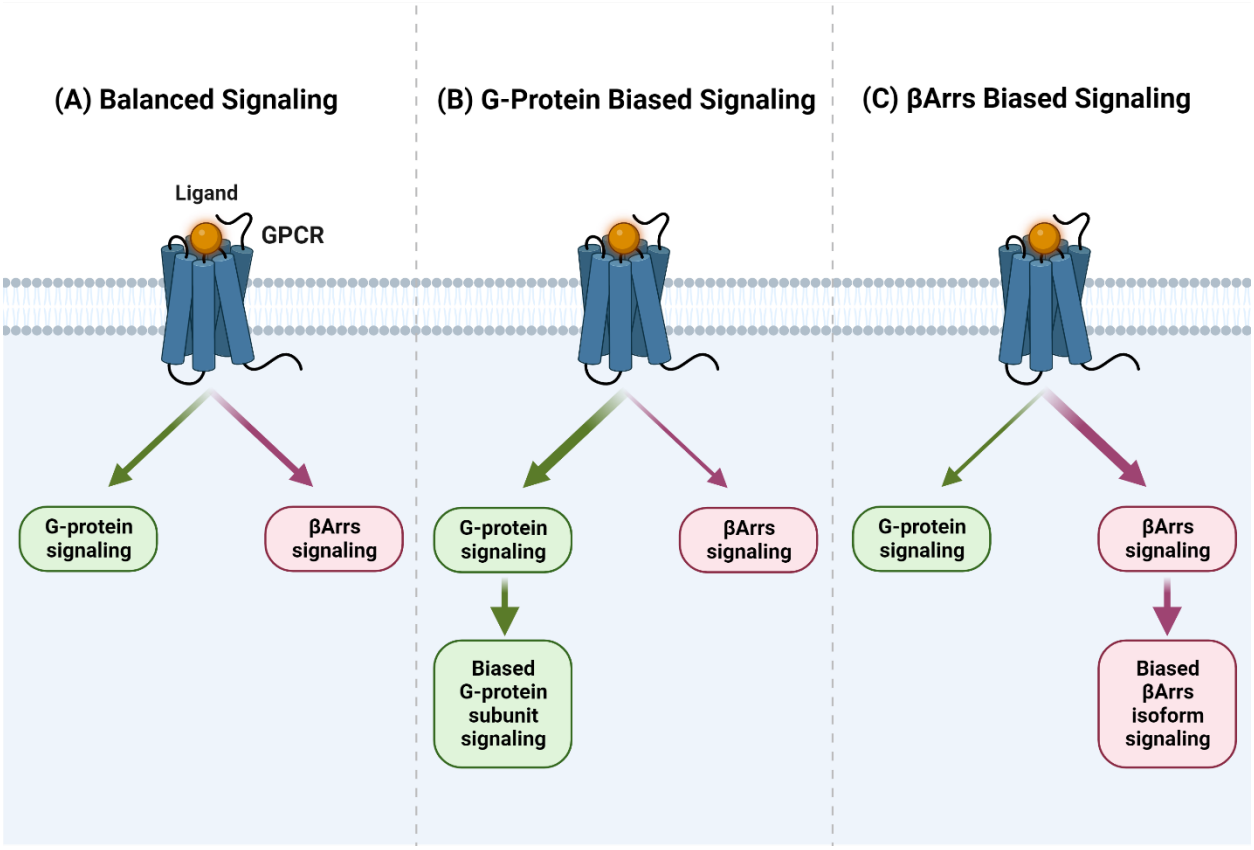

Fig. 1.17. Ligand-Bound GPCR Signaling Pathway.
(A) Balanced agonist binding to a balanced receptor in an unbiased system. (B, C) Biased agonism is encoded through a ligand that preferentially signal through GPCR•G-protein (B) or GPCR•βArrs (C). Created with BioRender.com.

2.8.4.2. Functional Selectivity of D1R-mediated Gα Subunits in the Brain

Intriguingly, D1R agonist, DHX, acts as a full agonist with $G\alpha_s$- and a partial agonist with $G\alpha_{olf}$-dependent signaling (Yano et al, 2018). $G\alpha_s$ and $G\alpha_{olf}$ differentially predominate stimulatory Gα subunits in the cortex and striatum, respectively (Hervé et al, 1993). Consequently, DHX behaves as a full D1R agonist in the cortex, but with low efficacy in striatum. This reciprocal effect of DHX on D1R-mediated $G\alpha_s$ and $G\alpha_{olf}$ signaling potentially provides therapeutic benefit of DHX targeting cortical, but not striatal, D1R in neuropsychiatric disorders (Yano et al, 2018).

2.9. G-Protein Coupled Receptor Kinases

The activated state of GPCRs acts not only as an activator of G-proteins, but also as a substrate for protein phosphorylation by GRKs (Gainetdinov et al, 2004; Ribas et al, 2006). GRK-mediated receptor phosphorylation is one of the well-characterized mechanisms for GPCR homologous desensitization to increase the receptor binding affinity for βArrs. GRKs are classified in three subfamilies based on sequence and functional similarity: the GRK1 subfamily consists of rhodopsin GRKs (GRK1 and GRK7); the GRK2 subfamily consists of β-adrenergic receptor kinases (GRK2 and GRK3); and the GRK4 subfamily consists of GRK4, GRK5, and GRK6. These seven highly ubiquitous kinases are all catalytically activated by stimulated GPCRs, but differ in their specificity for phosphorylating a particular subset of receptors (Gainetdinov et al, 2004; Ribas et al, 2006). Co-expression of GRK isoforms with different GPCRs generally promotes agonist-induced phosphorylation of the receptor, in which GRK KO-cells were utilized to validate such a phenotype. Moreover, Gβγ binds to and mediates translocation of GRK2 and GRK3 to the plasma membrane to modulate the agonist-stimulated phosphorylation of the receptor (Pitcher et al, 1992; Daaka et al, 1997).

2.9.1. Role of GRKs in Parkinsonian Models

Studies from mutant mice suggested essential roles of GRK isoforms in normal physiological functions, e.g., cardiac development (Jaber et al, 1996b; Peppel et al, 1997; Gainetdinov et al, 2004). Interestingly, Bezard' group showed that GRK6 plays an important role in D1R-mediated LID. They showed that dyskinesia is attenuated by lentivirus-mediated overexpression of GRK6 in the striatum in MPTP-lesioned monkey, in which reduction of GRK6 concentration exacerbated dyskinesia (Ahmed et al, 2010). These findings suggest that the increased availability of GRK6

ameliorates dyskinesia and increases duration of the antiparkinsonian action of L-DOPA (Ahmed et al, 2010).

2.10. Regulation of GPCR Trafficking: Desensitization and Resensitization

Activated GPCRs initiate different regulatory mechanisms mediated by βArr signaling pathway independently of G-protein activation. In the classical model of GPCR regulation, βArrs terminate receptor signalling by blocking further G-protein activation (Ferguson, 2001). This regulation occurs in different steps, in which the receptor undergoes the following temporally distinct regulatory processes: phosphorylation, desensitization, internalization, and resensitization (Premont et al, 1995; Ferguson et al, 1996a; Pierce and Lefkowitz, 2001; Ferguson, 2001; Sun and Kim, 2021; Wess et al, 2023). *Fig. 1.18. illustrates the GPCRs desensitization and trafficking mechanisms.*

2.10.1. GPCR Homologous Desensitization

Following ligand binding and subsequent G-protein activation, the intracellular regions of GPCRs get phosphorylated to begin the process of desensitization (Ferguson et al, 1996b; Pierce and Lefkowitz, 2001; Ferguson, 2001). Specifically, activated receptors bind GRKs that phosphorylate Ser/Thr residues present in the receptor IL3 and CT regions (Benovic et al, 1986b; Strasser et al, 1986; Sibley et al, 1986; Lohse et al, 1990; Pippig et al, 1993; Barak et al, 1994; Tsuga et al, 1994; Ferguson et al, 1995; Freedman et al, 1995; Barak et al, 1997; Zhang et al, 1999; Ferguson, 2001). This serves to recruit βArrs and induce the loss of responsiveness of receptors for their respective ligands. Indeed, GRK-phosphorylated receptors have higher affinity for βArrs, which, when bound to GPCR, blocks GPCR—G-protein interactions and serves as a docking site for endocytic machinery proteins to facilitate internalization (Lohse et al, 1990; Ferguson, 2001).

Internalization is the rapid removal of phosphorylated receptor from plasma membrane to intracellular compartments, in which the sequestered receptor can still mediate signaling, but is unable to interact with the extracellular environment (Pierce and Lefkowitz, 2001; Ferguson, 2001). The CT of βArr contains binding motifs for clathrin and adapter protein-2 (AP-2), which facilitate the internalization processes (Goodman et al, 1996; Laporte et al, 1999; Laporte et al, 2000; Ferguson, 2001; Laporte et al, 2002; Grimes et al, 2023). These endocytic proteins aggregate at the membrane to form a pit, which becomes further invaginated and ultimately cleaved by the

GTPase dynamin, in an overall process known as clathrin-mediated endocytosis (van der Bliek et al, 1993; Hinshaw and Schmid, 1995; Takei et al, 1995; Pucadyil and Schmid, 2008). The end result of this process is fully-internalized clathrin-coated vesicles containing GPCRs (Zhang et al, 1996; Ferguson, 2001; Kim and Benovic, 2002). The phosphorylated receptor complex then becomes part of an early endosome in the cytoplasm, at which point the stability of the receptor•βArr complex primarily determines the sorting fate of the sequestered receptor (von Zastrow et al, Kobilka, 1992; Ferguson et al, 1996b; Oakley et al, 1999; Ferguson, 2001; Seachrist and Ferguson, 2003).

Internalized receptors that experience a strong and long-lasting interaction with βArr are targeted to the late endosome, where receptors are either recycled back (resensitized) to the plasma membrane following receptor dephosphorylation, or degraded by lysosomal proteins (von Zastrow et al, Kobilka, 1992; Yu et al, 1993; Barak et al, 1994; Zhang et al, 1999; Oakley et al, 1999; Oakley et al, 2000; Ferguson, 2001). The endosomal trafficking of internalized receptors is orchestrated in large part by Rab family of small GTPase proteins which are involved in the budding, transport, docking and fusion of intracellular vesicles (Seachrist and Ferguson, 2003).

Internalization might not be mandatory for the resensitization of receptor responsiveness because under certain circumstances receptors are weakly bound to βArr and capable of being rapidly dephosphorylated at the cell surface without being subjected to endocytosis and recycling. GPCR responsiveness is also regulated by two other endocytic pathways that function independently of βArr and clathrin activity: dynamin-dependent caveolae-mediated endocytosis and dynamin-independent fast-endophilin-mediated endocytosis (Ferguson et al, 1996a; Pierce and Lefkowitz, 2001; Ferguson, 2001).

2.10.1.1. Regulation of D1-Class Receptors: Homologous Desensitization

D1-class receptors undergo agonist-induced desensitization and resensitization both *in vitro* and *in vivo*, which is important for modulating various physiological functions, e.g., neuronal excitability (Ariano et al, 1997; Dumartin et al, 1998; Martin-Negrier et al, 2006; Kotowski et al, 2011). D1R initially undergo DA-induced phosphorylation, and overexpression of GRK2, GRK3, GRK4, and GRK5, but not GRK6, promote further D1R phosphorylation in heterologous cells (Tiberi et al, 1996; Barak et al, 1997; Gardner et al, 2001; Mason et al, 2002; Rankin et al, 2005;

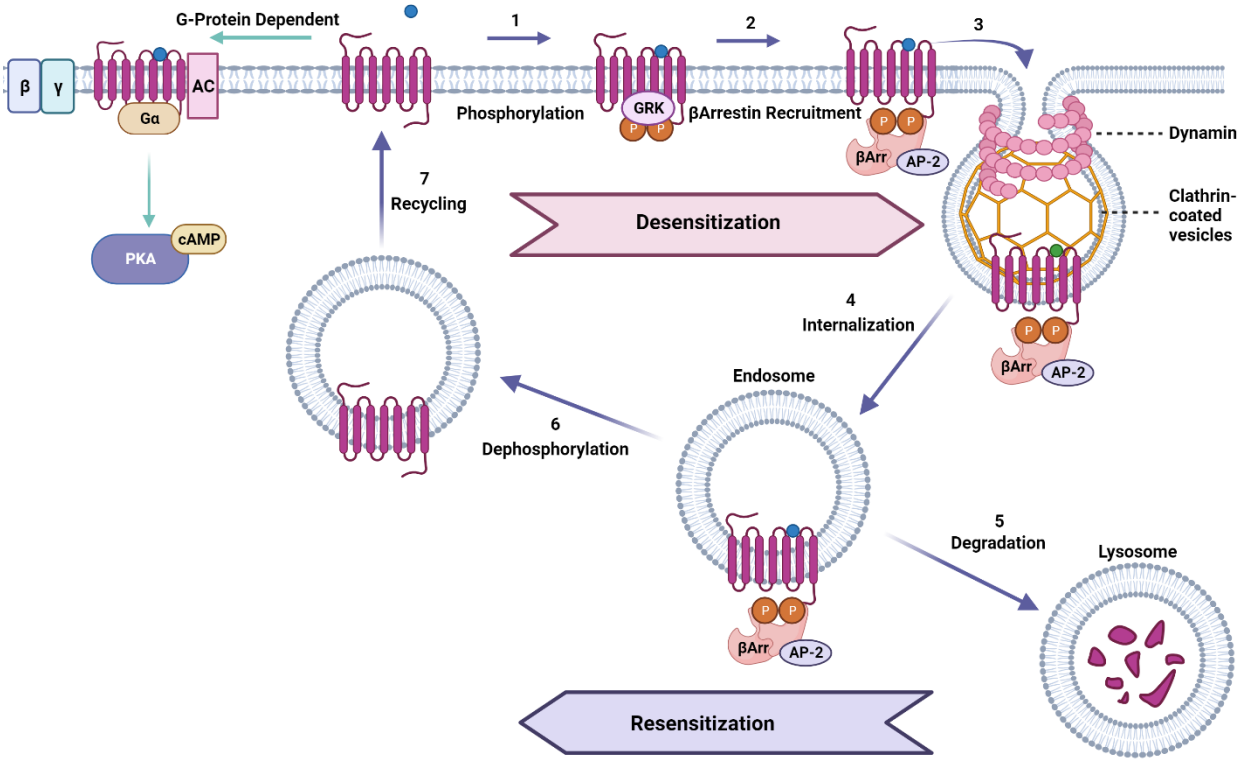

Fig. 1.18. Schematic Diagram of GPCR Desensitization and Resensitization.
Signaling cascades of GPCR signaling is regulated in many events; 1: exposure to ligand leads to rapid uncoupling of the GPCR from its G-protein due to receptor phosphorylation by GRKs on the CT and/or IL3; 2: phosphorylation of activated GPCR by GRKs promotes the binding of β-arrestins to phosphorylated receptors, which disrupts the GPCR/G protein interaction leading to desensitization; 3: following receptor phosphorylation, GPCR-βArr complex is targeted for endocytosis and dynamin-dependent internalization of GPCRs occurs through clathrin-coated vesicles; 4: internalized GPCRs are sorted into 5: lysosomes for degradation or 6: dephosphorylated and recycled back to the cell surface. Created with BioRender.com.

Sedaghat and Tiberi, 2011). Moreover, GRK4 constitutively phosphorylates D1R, inhibits D1R-mediated cAMP, and promotes internalization of D1R (Rankin et al, 2006). GRK2 and GRK3 associate with D1R *in vivo* and *in vitro,* and desensitization of D1R is significantly enhanced in cells expressing GRK3 relative to GRK2 (Tiberi et al, 1996; Sedaghat and Tiberi, 2011). In L-DOPA treated 6-OHDA rats, GRK6 viral expression normalizes the altered D1R signaling in dMSN by promoting D1R internalization, and the attenuated D2R signaling in iMSN by reducing the enkephalin expression (Ahmed et al, 2010).

GRK2 further enhances βArr2 translocation to the plasma membrane following agonist stimulation of D1R (Barak et al, 1997). Both βArrs do not contribute equally to regulation of D1R and D5R, with both receptors exhibiting greater affinity for βArr2 than βArr1 (Zhang et al, 1999; Oakley et al, 2000; Kim et al, 2004; Macey et al, 2005; Thompson and Whistler, 2011). Activated D1-class receptors transiently interact with βArr2 at the plasma membrane, and while they undergo internalization, they quickly dissociate from βArr2 as they are trafficked in endosomes (Zhang et al, 1999; Kim et al, 2004; Macey et al, 2005; Thompson and Whistler, 2011). The endocytosis of D1R and D5R are mediated mainly by a βArr2, clathrin, and dynamin-dependent pathway (Zhang et al, 1999; Kim et al, 2004; Macey et al, 2005; Thompson and Whistler, 2011). However, internalized D1R and D5R are inefficiently targeted for endosomal degradation; instead they quickly resensitize to the plasma membrane (Vickery and von Zastrow, 1999; Jackson et al, 2002; Kotowski et al, 2011; Thompson and Whistler, 2011). D1R also undergo caveolar endocytosis, independent of the clathrin-mediated pathway (Kong et al, 2007).

Importantly, IL3 and CT of D1R harbor the structural elements required to mediate agonist-induced desensitization and resensitization (Jackson et al, 2002; Lamey et al, 2002; Mason et al, 2002; Vargas and Von Zastrow, 2004; Macey et al, 2005; Sedaghat and Tiberi, 2011). David Sibley proposed that under basal conditions, the CT of D1R is in close association with the IL3, and that agonist binding induces conformational changes allowing G-protein coupling but also renders the receptor a substrate for GRK-mediated phosphorylation (Kim et al, 2004). GRK binds to and phosphorylates Ser/Thr residues of CT of D1R, which leads to IL3 phosphorylation and ultimately βArr2 recruitment and disrupts G-protein coupling (Kim et al, 2004). Thus, IL3 phosphorylation is dependent on CT phosphorylation (Jackson et al, 2002; Kim et al, 2004; Kaya et al, 2020; Moritz et al, 2023).

2.10.1.2. GPCR Heterologous Desensitization

Various signaling events within a cell can also lead to GPCR phosphorylation by second messenger-dependent protein kinases, such as PKA and PKC, though a process termed heterologous desensitization that causes a generalized loss of GPCR responsiveness (Pierce and Lefkowitz, 2001; Pierce et al, 2002; Sun and Kim, 2021). This process does not require a receptor to be bound to its respective agonist and can therefore occur following the activation of other nearby receptors. GPCR phosphorylation from heterologous desensitization processes is generally targeted to receptor regions that disrupt G-protein coupling (Pierce and Lefkowitz, 2001; Pierce et al, 2002; Sun and Kim, 2021).

2.10.1.3. Regulation of D1 Class Receptors: Heterologous Desensitization

D1-class receptors undergo subtype-specific heterologous desensitization. Studies from the Tiberi lab and other research groups have demonstrated that phorbol-12-myristate-13-acetate (PMA) induces PKC-mediated desensitization and resensitization of D1R and D5R, respectively, which is facilitated by the IL3 (Jackson et al., 2005; Rankin and Sibley, 2010; Thompson and Whistler, 2011; Plouffe et al, 2012). D5R, but not D1R, undergo endocytosis secondary to heterologous signaling events, in a clathrin- and dynamin-dependent process, independent of βArr2 activity (Thompson and Whistler, 2011).

2.11. Dopamine Receptor-Interacting Proteins

GPCRs physically interact with numerous proteins to form large signaling complexes that shape different properties of the receptor. Indeed, the particular complement of protein-protein interactions associated with a given GPCR influence its pharmacology, G-protein coupling, βArr2 recruitment, signaling pathway activation, localization, and trafficking. Dopamine Receptor-Interacting Proteins (DRIPs) interact primarily with IL3 and CT of DA receptors in a subtype-specific manner to ensure proper receptor folding, surface expression, and signaling function (Yao et al, 2008; Scott and Aperia, 2009; Wang et al, 2012). However, the mechanisms regulating DRIP targeting to DA receptors, and subsequent modulation of DA receptor trafficking and signaling are largely unexplored. DRIPs include receptor heterodimers, channels, scaffolds, adaptors, cytoskeletal and signaling proteins (Yao et al, 2008; Scott and Aperia, 2009; Wang et al, 2012;

Misganaw, 2021). *Table 1.2. summarizes the D1-class receptors interacting proteins with non-canonical GPCR signaling (G-proteins, GRKs, βArrs).*

2.11.1. DA Receptor Modulation of GABA and Glutamate Neurotransmission

Dopaminergic transmission is intricately linked with both inhibitory GABAergic transmission and excitatory glutamatergic transmission through respective DA receptor interactions with ionotropic GABA and glutamate receptors (Yao et al, 2008; Scott and Aperia, 2009; Wang et al, 2012). GABA is the primary inhibitory neurotransmitter in the brain, exerting its function through two postsynaptic receptors: ionotropic $GABA_A$ receptor ($GABA_AR$) and metabotropic $GABA_B$ receptor ($GABA_BR$) (Cherubini and Conti, 2001; Bowery and Smart, 2006). $GABA_AR$ mediate fast inhibitory synaptic transmission at the vast majority of inhibitory synapses (Cherubini and Conti, 2001; Bowery and Smart, 2006). $GABA_AR$ physically interacts with D5R, but not D1R, and the activation of this complex attenuates $GABA_AR$-mediated inhibitory postsynaptic currents and D5R-mediated cAMP production (Liu et al, 2000). These findings thus suggest that D5R•$GABA_AR$ complex functions as a brake on both GABAergic and dopaminergic transmission.

Glutamate is the most abundant excitatory neurotransmitter in the brain, and is capable of activating three ionotropic receptors: AMPAR, NMDAR and kainate receptor, and eight metabotropic glutamate receptors (mGluRs) (Carroll and Zukin, 2002; Cull-Candy and Leszkiewicz, 2004; Niciu et al, 2012). AMPAR and NMDAR are critically involved in fast excitatory synaptic transmission along with other important brain functions, such as synaptic plasticity and neurodevelopment (Carroll and Zukin, 2002; Cull-Candy and Leszkiewicz, 2004; Niciu et al, 2012). Indeed, NMDAR dysfunctions have been linked to various neurological disorders, including PD and schizophrenia, two conditions well-known to have concomitant impairments in dopaminergic function (Carroll and Zukin, 2002; Cull-Candy and Leszkiewicz, 2004; Gonzalez et al, 2015).

Excitatory synapses, rich in glutamate receptors, are most often localized on dendritic spines, a neuronal compartment where DA receptors are also commonly present (Carroll and Zukin, 2002; Kim and Sheng, 2004; Yao et al, 2008; Scott and Aperia, 2009; Wang et al, 2012). The postsynaptic density (PSD) is a specialized structure at the spine's head containing a multitude of proteins organized by dedicated scaffolding proteins, such as PDZ (**P**SD95, drosophila **D**isc large, and tight junction **Z**ona occludens-1)-containing proteins (Carroll and Zukin, 2002; Kim and

Sheng, 2004). These scaffolding proteins are especially critical for proper glutamate receptor localization, trafficking and signaling within the PSD, and could also conceivably anchor DA receptors to facilitate integration of dopaminergic and glutamatergic transmission (Carroll and Zukin, 2002; Kim and Sheng, 2004; Yao et al, 2008; Scott and Aperia, 2009; Wang et al, 2012; Dunn and Ferguson, 2015; Zhu et al, 2016; Won et al, 2017).

2.11.2. Modulation of D1R•NMDAR Complex

NMDAR is one of the most extensively studied DRIPs in the context of its interactions with both D1R and D2R, which play a crucial role in maintaining optimal balance of dopaminergic-glutamatergic transmission, independently of classical second messenger signaling (Liu et al, 2006; Yao et al, 2008; Wang et al, 2012). Through a series of studies from different research groups led by Fang Liu, Anita Aperia, and Christina Missale, several important findings were made concerning the relationship between D1R and NMDAR: i) D1R and NMDAR are colocalized in the PSD; ii) D1R, but not D5R, physically interact with NMDAR via their CT; iii) NMDAR regulates the cellular distribution of D1R at the plasma membrane; iv) NMDAR activation increases surface expression and cAMP production of D1R, while abolishing agonist-induced D1R endocytosis; v) NMDAR activation traps diffusible D1R in spines, as well increases the number of D1R-positive spines; vi) D1R activation suppresses NMDAR-mediated currents by decreasing NMDAR synaptic trafficking; vii) D1R activation exerts a neuroprotective effect by attenuating NMDAR-induced apoptosis through a PI3K-dependent mechanism (Scott et al, 2002; Lee et al, 2002; Fiorentini et al, 2003; Pei et al, 2004; Scott et al, 2006; Kruusmagi, et al. 2009; Wang et al, 2012). These findings clearly demonstrate a great importance for D1R•NMDAR complex in linking together dopaminergic and glutamatergic neurotransmission.

2.11.3. Modulation of D1R•mGluR5 Complex

Metabotropic glutamate type 5 (mGlu5) is highly expressed in brain, and particularly colocalized with D1R in striatonigral pathway (Sebastianutto and Cenci, 2018). Several lines of evidence indicate that antagonism of mGluR5 is of special interest for the treatment of LID (Mela et al, 2007; Sebastianutto and Cenci, 2018). A recent study from Cenci's and Perroy's group suggests that D1R and mGluR5 form a heterodimer *in vivo* and *in vitro*, and activation of D1R•mGluR5 complex coupled to $G\alpha_q$ promotes cAMP production and Ca^{2+} release by their respective agonist (Sebastianutto et al, 2020). This suggests that the allosteric interaction between D1R and mGluR5

allows biased signaling for D1R through $G\alpha_q$-PLC-Ca^{2+} pathway (Sebastianutto et al, 2020). Interestingly, endogenous D1R•mGluR5 interaction is significantly increased in DA-denervated striatum, and further recruitment is observed following L-DOPA treatment (Sebastianutto et al, 2020). D1R•mGluR5 synergistically activates PLC signaling, and the inhibition of PLC or mGluR5 reduces D1R-mediated dyskinesia (Sebastianutto et al, 2020). These findings demonstrated the importance of the physiological D1R•mGluR5 complex and disrupting this complex potentially provide promising therapeutic approach for LID treatment.

2.12. Subcellular Neuronal Localization of D1-Class Receptors

D1-class receptor subtypes expressed or co-expressed in different brain regions and have significant impact on neuronal plasticity (Bergson et al, 1995b). Both D1R and D5R are highly mobile, primarily transported via lateral diffusion in the dendritic tree, and are localized postsynaptically at the dendritic spines (Scott et al, 2002; Scott et al, 2006; Kruusmägi et al, 2009). Both receptor subtypes are abundant in the dendrites, but D1R is highly localized in spine's head, while D5R is more expressed in spines' neck (Bergson et al, 1995b; Scott et al, 2006; Kruusmägi et al, 2009). Differences in subcellular localization of D1R and D5R within the spines imply that both have different, not redundant, physiological functions within pyramidal neurons (Scott et al, 2006; Kruusmägi et al, 2009).

D1R and D5R differentially interact with glutamatergic and GABAergic receptors to modulate synaptic plasticity (Liu et al, 2000; Scott et al, 2002). Activation of NMDAR in striatal neuronal culture was shown to restrict the mobility of D1R and increase the formation of D1R-positive spines, while having no effect on D5R diffusion or spine localization (Scott et al, 2002; Scott et al, 2006; Kruusmägi et al, 2009). D1R functionally interacts and colocalizes with NMDAR in the PSD and demonstrates a direct modulation of fast excitatory synaptic transmission (Lee et al, 2002). In contrast, the $GABA_AR$ colocalizes with D5R in hippocampal neuronal culture, and the physical association between $GABA_AR$ and D5R, but not D1R, dynamically regulates the inhibitory synaptic transmission (Liu et al, 2000).

By using high resolution single-molecule imaging approach, Laurent Groc and colleagues showed that D1R and D5R are highly dynamic at the surface of hippocampal neurons and have different interactome signatures in the synapse (Ladepeche et al, 2013a, b; Maingret and Groc, 2021).

Table 1.2. Summary of D1-Class Receptor Interacting Proteins with non-Canonical GPCR Signaling (G-proteins, GRKs, βArrs). Other functions may have been reported by these DRIPs that were not discussed in this summary table. H3R: Histamine 3 receptor; σ1R: Sigma-1 receptor; PSD95: Post-synaptic density 95 protein; SynGAP: Synaptic Ras GTPase-activating protein; GSK-3β: Glycogen synthase kinase-3β; DRiP78: Dopamine receptor interacting protein-78; γ-COP: gamma subunit of the coatomer protein complex; NF-M: Neurofilament-M; NSF: N-ethylmaleimide-sensitive factor; NSC-1: Neuronal calcium sensor-; SNX-1: Sorting Nexin-1.

D1R-Interacting Protein	Interacting Domain	DRIP Functions	References
D1R•D2R		• **Interaction demonstrated *in vitro, in vivo* (brain), and postmortem tissues.** • **D1R and D2R coactivation of D1R•D2R heteromer leads to $G\alpha_q$-mediated PKC and Ca^{2+} signaling.** • **Desensitization of D1R•D2R heteromer is mediated by activation of D1R or D2R.** • **D1R•D2R heteromer exerts tonic inhibitory control of basal natural and cocaine reward.**	(Lee et al, 2004; So et al, 2007; Pei et al, 2010; Perreault et al, 2016; Rico et al, 2017; Hasbi et al, 2018; Hasbi et al, 2020a; Hasbi et al 2020b)
D1R•D3R		• **Interaction demonstrated *in vitro* and *in vivo* (brain).** • **D3R stimulation increases D1R agonist affinity.** • **Ligand-induced changes in $G\alpha_s$ and $G\alpha_i$ coupling to the D1R•D3R heteromer.** • **D3R activation decreases D1R-mediated cAMP production.** • **D1R and D3R coactivation inhibits the level of AC signaling.** • **D1R and D3R coactivation potentiates recruitment of βArr1.** • **D1R and D3R coactivation positively modulates PKA-ERK1/2 signaling.** • **βArr1/2 are required for activation of Erk1/2 induced with D1R and D3R stimulation.** • **D3R activation in the D1R•D3R heteromer switches D1R-mediated MAPK activation from a G-protein dependent to a G-protein independent mechanism *in vitro*.** • **Chronic l-DOPA increases D3R expression in the DA-depleted dorsal striatum.**	(Fiorentini et al, 2008; Marcellino et al, 2008; Guitart et al, 2014; Solís et al, 2017; Guitart et al, 2019; Bono 2023)
D1R•A_1R		• **Interaction demonstrated *in vitro* and *in vivo*.** • **Coactivation of D1R and A_1R decreases D1R-mediated cAMP.** • **A_1R activation of D1R•A_1R. potentiates D1R-mediated desensitization.**	(Ferré et al, 1998; Ginés et al, 2000; Torvinen et al, 2002; Cao et al, 2007)
D1R•NMDAR (GluN1, GluN2A, GluN2B)	**D1R-CT GluN1-CT** **D1R-CT GluN2A-CT**	• **Interaction demonstrated *in vitro* and *in vivo* (brain).** • **D1R activation of D1R•NMDAR complex potentiates D1R-mediated cAMP, and coactivation leads to further enhancement.** • **D1R activation of D1R•NMDAR complex decreases NMDAR-mediated EPSCs.** • **NMDAR activation of D1R•NMDAR complex facilitates D1R surface expression and abolish D1R-mediated endocytosis.** • **NMDAR activation of D1R•NMDAR complex increases the number of D1R-positive spines.** • **D1R activation of D1R•NMDAR complex facilitates NMDAR-mediated-LTP in hippocampus.**	(Lee et al, 2002; Fiorentini et al, 2003; Pei et al, 2004; Scott et al, 2006)
D1R•mGluR5		• **Interaction demonstrated *in vitro, ex vivo,* and *in vivo*.** • **Heterodimer of D1R•mGluR5 couples to $G\alpha_q$, and D1R activation increases D1R-mediated intracellular Ca^{2+} release.** • **Endogenous D1R•mGlu5 clusters are increased in the DA-denervated striatum, and further enhancement following L-DOPA treatment.**	(Sebastianutto et al, 2020)
D1R•H3R		• **Interaction demonstrated *in vitro* and *in vivo* (brain).** • **Activation of D1R or H3R in D1R•H3R complex signals toward MAPK pathway.** • **Activation of D1R in D1R•H3 complex couples to G*α*i pathway.**	(Ferrada et al, 2009; Moreno et al, 2011; Rodríguez-Ruiz et al, 2017)

D1R•H3R•NMDAR		• **Interaction demonstrated *in vitro* and *in vivo* (brain).** • **Antagonism activity of D1R and H3R reduced NMDA-mediated excitotoxicity.**	(Rodríguez-Ruiz et al, 2017)
D1R•μOR		• **Interaction demonstrated *in vitro* and *in vivo* (brain).** • **μOR surface expression is enhanced due to heterodimerization of D1R•μOR.** • **D1R antagonist inhibited μOR-mediated ERK1/2 phosphorylation and c-Fos induction levels.** • **D1R antagonist inhibited morphine-induced locomotor activity.**	(Juhasz et al, 2008; Tao et al, 2017)
D1R•σ1R		• **Interaction demonstrated *in vitro*.** • **Expression of D1R facilitates the translocation and colocalization of σ1R from ER to plasma membrane, and cocaine further increases the colocalized D1R•σ1R.** • **Cocaine potentiate D1R-mediated cAMP that is dependent on σ1R.** • **SKF81297 and cocaine induced MAPK activation of D1R, that is dependent on the function of σ1R.**	(Navarro et al, 2010)
D1R•PSD95	**D1R-CT** **PSD95-NT**	• **Interaction demonstrated *in vitro* and *in vivo* (brain).** • **PSD95 inhibits (or did not alter) D1R-mediated cAMP production.** • **PSD95 does not alter D1R desensitization but enhances D1R resensitization.** • **NT-PSD95 facilitates constitutive D1R internalization in dynamin-dependent fashion.** • **PSD95 accelerates membrane D1R recovery via enhancement of receptor recycling.** • **Enhanced behavioral responses to D1R agonists in PSD95-KO mice.**	(Zhang et al, 2007; Zhang et al, 2009; Sun et al, 2009)
D1R•PSD95•NMDAR	**D1R-CT**	• **Interaction demonstrated *in vitro* and *in vivo* (brain).** • **PSD95 and NMDAR-GluN1 subunit bind to an overlapping region on the D1R-CT.** • **PSD95 inhibits D1R•NMDAR-GluN1 interaction.** • **Removal of PSD95 enhances D1R•NMDAR-GluN1 association.** • **PSD95 removes NMDAR inhibition of D1R internalization.** • **PSD95 blocks NMDAR modulation of D1R signaling.**	(Zhang et al, 2009)
D1R•SynGAP	**D1R-IL3**	• **Interaction demonstrated *in vitro* and *in vivo* (brain).** • **SynGAP enhances D1R-mediated cAMP, PKA, p38 MAPK signaling.** • **SynGAP increases cell surface localization of D1R.** • **Disruption of D1R•SynGAP complex inhibits GABAergic interneuron migration, promotes actin depolymerization, and changes microtubule dynamics.**	(Su et al, 2019)
D1R•GSK-3β	**D1R-CT**	• **Interaction demonstrated *in vitro* and *in vivo* (brain).** • **inhibition of GSK-3β decreases the association between D1R and GSK-3β.** • **Inhibition of GSK-3β decreases the binding expression of D1R.** • **Inhibition of GSK-3*β* attenuates D1R-mediated Gα_s protein activation.** • **Inhibition of GSK-3β reduces D1R-mediated endocytosis, desensitization, and βArr2 translocation to D1R.**	(Wang et al, 2017)
D1R•DRiP78	**D1R-CT**	• **Interaction demonstrated *in vitro*.** • **DRiP78 exports D1R to ER.** • **DriP78 decreases ligand binding.**	(Bermak et al, 2001)
D1R•γ-COP	**D1R-CT**	• **Interaction demonstrated *in vitro*.** • **γ-COP transports D1R to ER.**	Bermak et al, 2002)
D1R•Calnexin		• **Interaction demonstrated *in vitro*.** • **Calnexin functions as ER retention protein and chaperone for D1R.** • **Calnexin decreases D1R binding expression.** • **Calnexin inhibits D1R-mediated cAMP production.**	(Free et al, 2007)

D1R•Calveolin-1		• **Interaction demonstrated *in vitro* and *in vivo* (brain).** • **Agonist-induced translocation of D1R into caveolin-1-enriched fractions.** • **D1R internalizes through a caveolar pathway.**	(Kong et al, 2007)
D1R•Calveolin-2		• **Interaction demonstrated *in vitro*.** • **Colocalization of D1R with Calveolin-2 observed in renal proximal tubule cells.** • **Activation of D1R enhances-AC in lipid rafts than in non-raft plasma membranes.** •	(Yu et al, 2004)
D1R•NF-M	**D1R-IL3**	• **Interaction demonstrated *in vitro*.** • **NF-M decreases D1R binding expression.** • **NF-M inhibits D1R-mediated cAMP signaling.** • **NF-M promotes constitutive endocytosis of D1R.**	(Kim et al, 2002)
D1R•NSF	**D1R-CT**	• **Interaction demonstrated *in vitro*.** • **Possibly modulates D1R recycling.**	(Heydorn et al, 2004)
D5R-Interacting Protein	**Interacting Domain**	**DRIP Functions**	**References**
D5R•D2R		• **Interaction demonstrated *in vitro* and *in vivo* (brain).** • **D1R and D2R coactivation of D1R•D2R complex leads to $G\alpha_q$-mediated PKC and Ca^{2+} signaling.** • **D2R activation of D5R•D2R attenuates D5R-mediates Ca^{2+} signaling.**	(So et al, 2009)
D5R•$GABA_AR$-γ2 subunit	**D5R-CT**	• **Interaction demonstrated *in vitro* and *in vivo* (brain).** • **D5R activation of D5R•$GABA_AR$ complex increases D5R-mediated cAMP, and coactivation leads to lesser effect.** • **D5R activation of D5R•$GABA_AR$ complex inhibit $GABA_AR$ -mediated currents.**	(Liu et al, 2000)
D5R•PSD95		• **Interaction demonstrated *in vitro*.** • **No mechanism was proposed.**	(Sun et al, 2009)
NSC-1	**D5R-CT**	• **Interaction demonstrated using yeast two-hybrid system.** • **No mechanism was proposed.**	(Kabbani et al, 2002)
NSF	**D5R-CT**	• **Interaction demonstrated *in vitro*.** • **Possibly modulates D5R recycling.**	(Heydorn et al, 2004)
SNX-1	**D5R**	• **Interaction demonstrated *in vitro*.** • **Possibly modulates D5R lysosomal targeting.**	(Heydorn et al, 2004)
NF-M	**D5R-IL3**	• **Interaction demonstrated using yeast two-hybrid system.** • **NF-M has no effect on D5R binding expression.** • **NF-M has no effect on D5R-mediated cAMP signaling.**	(Kim et al, 2002)

Direct surface interaction between D1R•NMDAR and D5R•$GABA_AR$ dynamically regulate the trafficking distribution at the surface of hippocampal neurons (Ladepeche et al, 2013a, b; Maingret and Groc, 2021). D5R are expressed at excitatory and inhibitory synapses between hippocampal neurons, however, higher density D5R clusters are formed when co-expressed with $GABA_AR$ (Maingret and Groc, 2021). Within the PSD vicinity, D1R surface trafficking is reduced, suggesting the presence of a mechanism that interferes with D1R surface dynamics (Ladepeche et al, 2013a, b). The postsynaptic density protein 95 (PSD95) is a highly scaffolding protein enriched in the PSD (Kim and Sheng, 2004). Interestingly, the diffusion of D1R within PSD95 clusters has been shown to be significantly restricted, further implying the existence of a regulatory mechanism that regulates the synaptic retention for D1R (Ladepeche et al, 2013a). Additionally, *in vivo* binary D1R•PSD95 and ternary D1R•NMDAR•PSD95 complexes regulate the trafficking of NMDAR (Zhang et al, 2007; Zhang et al, 2009). Synaptic D1R surface trafficking regulated by direct interaction with NMDAR is independent from PSD95; this interaction anchors D1R and NMDAR to PSD (Ladepeche et al, 2013a). However, no colocalization has been observed between D1R and AMPAR (Ladepeche et al, 2013b).

PDZ-containing proteins, such as PSD95, physically interact with and regulate the shuttling of NMDAR and AMPAR to synapses (Müller et al, 1996; Sans et al, 2003; Elias et al, 2008; Chen et al, 2012). Whether D1R and D5R preferentially interact with excitatory and inhibitory proteins, respectively, at the synapses remains to be biochemically examined. Hippocampal expression of NMDAR-GluN2B subunit was shown to be significantly reduced in D5R KO-mice, implying an important role for D5R in glutamatergic pathway (Moraga-Amaro et al, 2016). The observed differences in the trafficking behavior of D1-class receptor subtypes modulate synaptic plasticity to regulate dopaminergic•glutamatergic and dopaminergic•GABAergic neurotransmissions.

2.13. Thesis Rationale: Investigating Novel D1-Class-Interacting Proteins

As already described in earlier sections of the introduction, D1-class receptors critically regulate numerous physiological and pathological processes. Nonetheless, one of the most vexing challenges in studying D1-class receptor subtypes remains the inability to pharmacologically discriminate between D1R and D5R, and thus the lack of means to determine potential functional differences between these receptors *in vivo*. Although D1R and D5R share 80% homology in their TM domains, they exhibit notable differences within their IL3 and CT regions that could impart

each receptor with unique signaling and trafficking properties, part of which might conceivably be the result of interacting with distinct protein binding partners within their respective signaling complexes.

In light of all this, and the role of neuronal proteins in modulating DA responsiveness, the Tiberi lab sought to identify novel D1-class interacting proteins. We utilized yeast two-hybrid screens and a human brain cDNA library to address whether IL3- and CT-derived baits of D1R and D5R enable subtype-specific interactions. Screens with bait derived from IL3 of each receptor identified a potential novel binding partner specific to D1R (hD1R-IL3-Bait: Thr213-Val270), called synapse-associated protein 102 (SAP102). Interestingly, parallel studies done by other labs showed that a structural and functional homolog of SAP102—PSD95—also forms a complex with D1R, albeit through its CT (Zhang et al, 2007; Sun et al, 2009). **These findings thus led me to posit an overarching hypothesis that SAP102 and PSD95 act as distinct modulator of D1R signaling complex functional properties. The primary aim of my Ph.D. studies was to develop a mechanistic understanding of how IL3•SAP102 and CT•PSD95 interactions impact D1R signaling properties. Secondly, I also investigated the possible role of PSD95 as a modulator of D5R functional properties. Lastly, in light of a recent study demonstrating that several PDZ-containing proteins including PSD95 interact with βArr2, a canonical modulator of GPCR signaling and trafficking properties, the third and final part of my experimental work focused on uncovering a possible role for SAP102 and PSD95 in D1R recruitment of βArr2.** The following section provides a systematic overview of the properties and functions of SAP102 and PSD95, including their established interactions with the glutamatergic and dopaminergic systems.

3. Membrane-Associated Guanylate Kinases (MAGUKs)

SAP102 and PSD95 (previously known as *SAP90*) are scaffolding proteins belonging to the PSD95 subfamily of the membrane-associated guanylate kinases (PSD-MAGUKs), which also include postsynaptic density protein 93 (PSD93; "*chapsyn-110*") and synapse-associated protein 97 (SAP97; "*hdlg*") (Cho et al, 1992; Kistner et al, 1993; Lue et al, 1994; Müller et al, 1995; Kornau et al, 1995; Niethammer et al, 1996; Müller et al, 1996; Kim et al, 1996). These proteins, which I'll refer to as PSD-MAGUKs, are predominantly located within dendritic spines and highly enriched in PSD; thus, they have a fundamental role in synaptic function (Kim and Sheng, 2004; Xu, 2011; Dunn and Ferguson, 2015; Won et al, 2017). Several different subfamilies of MAGUKs are also found to regulate the dynamics of pre- and post-synaptic signaling, synaptic vesicles, and cell polarity maintenance (Dunn and Ferguson, 2015; Zhu et al, 2016).

Pioneering research from Mary Kennedy, Craig Garner, and Morgan Sheng identified how PSD-MAGUKs regulate synapses through scaffolding the assembly of supercomplexes comprised of neurotransmitter receptors, ion channels, cell-adhesion molecules, and cytoplasmic signaling proteins (Garner et al, 2000; Kim and Sheng, 2004; Kennedy, 2013; Zhu et al, 2016). Cytoplasmic proteins within these complexes influence the activity of the interacting membrane proteins by controlling their surface localization and intrinsic functional properties (Kim and Sheng, 2004; Xu, 2011; Dunn and Ferguson, 2015; Zhu et al, 2016; Won et al, 2017).

3.1. Function of PSD-MAGUKs

PSD-MAGUKs act as scaffolds at the PSD to bind and stabilize protein complexes at synapses and to regulate excitatory postsynaptic receptors and ion channels required for synaptic development and plasticity. While each PSD-MAGUK protein has unique properties, they can functionally compensate for one another. PSD-MAGUKs undergo multimerization to enhance the assembly and synaptic clustering of large multimolecular complexes, which are essential in regulating synaptic transmission (Nakagawa et al, 2004; Kim and Sheng, 2004). Although the PSD-MAGUK proteins have similar structures and overlapping functions, they exhibit differing patterns of developmental expression, subcellular localization, palmitoylation, and protein-protein interactions (Dunn and Ferguson, 2015; Zhu et al, 2016).

3.2. Structure of PSD-MAGUKs

The structure of PSD-MAGUK protein consist of an NT and three highly conserved PDZ-domains followed by a Src-homology-3 (SH3) domain and a catalytically inactive guanylate kinase (GK) domain (Kim and Sheng, 2004; Xu, 2011; Dunn and Ferguson, 2015; Zhu et al, 2016; Won et al, 2017). *Fig. 1.19. illustrate the structural components of PSD-MAGUK proteins.* The NT is the most divergent region among PSD-MAGUK proteins, and is an important contributor to the differential synaptic targeting and trafficking observed between subfamily members (Dunn and Ferguson, 2015; Zhu et al, 2016). PSD95 and PSD93 both contain two cysteine residues within NT, however, synaptic targeting of PSD95, but not PSD93, requires palmitoylation at these sites (El-Husseini et al, 2000a; Firestein et al, 2000). In contrast, the NT of SAP97 and SAP102 are important for synaptic targeting, yet both do not undergo NT palmitoylation (Firestein et al, 2000). Strikingly, imaging studies with chimeric PSD95 constructs showed that the NT of PSD93 and SAP102 can substitute for palmitoylation normally required for the synaptic targeting of PSD95 (Firestein et al, 2000). Unlike PSD95, SAP102 require SH3 and GK domains for synaptic localization (Zheng et al, 2010). Interestingly, SAP97 contains a L27 (Lin-2 and Lin-7) domain in NT capable of multimerization with itself and other L27 domain-containing proteins such as calcium-calmodulin-dependent serine kinase (CASK) (Kim and Sheng, 2004; Dunn and Ferguson, 2015; Zhu et al, 2016). PDZ domains are modular protein interaction domains that are specialized mainly for binding to short motifs (-ESDV or -ESEV) at distal CT of target proteins as well other internal motifs (Kim and Sheng, 2004; Dunn and Ferguson, 2015; Zhu et al, 2016). This imparts PDZ domains with scaffolding properties and gives them a central role in the assembly, trafficking and anchoring of large multiprotein complexes (Zhu et al, 2016). The SH3 and GK domains bind to various cytoskeletal and intracellular signaling proteins, in addition to forming a canonical intramolecular SH3-GK interaction (McGee et al, 1999; Shin et al, 2000; Wu et al, 2000; McGee et al, 2001; Kim and Sheng, 2004; Wei et al, 2015).

3.3. Expression of PSD-MAGUKs

PSD-MAGUK proteins are widely expressed at synapses within different brain regions, e.g., hippocampus, striatum, and cortex, where they contribute to physiological regulation of dynamic synaptic networks (Cho et al, 1992; Kistner et al, 1993; Lue et al, 1994; Müller et al, 1995; Müller et al, 1996; Kim et al, 1996). Indeed, aberrant changes in these networks due to altered

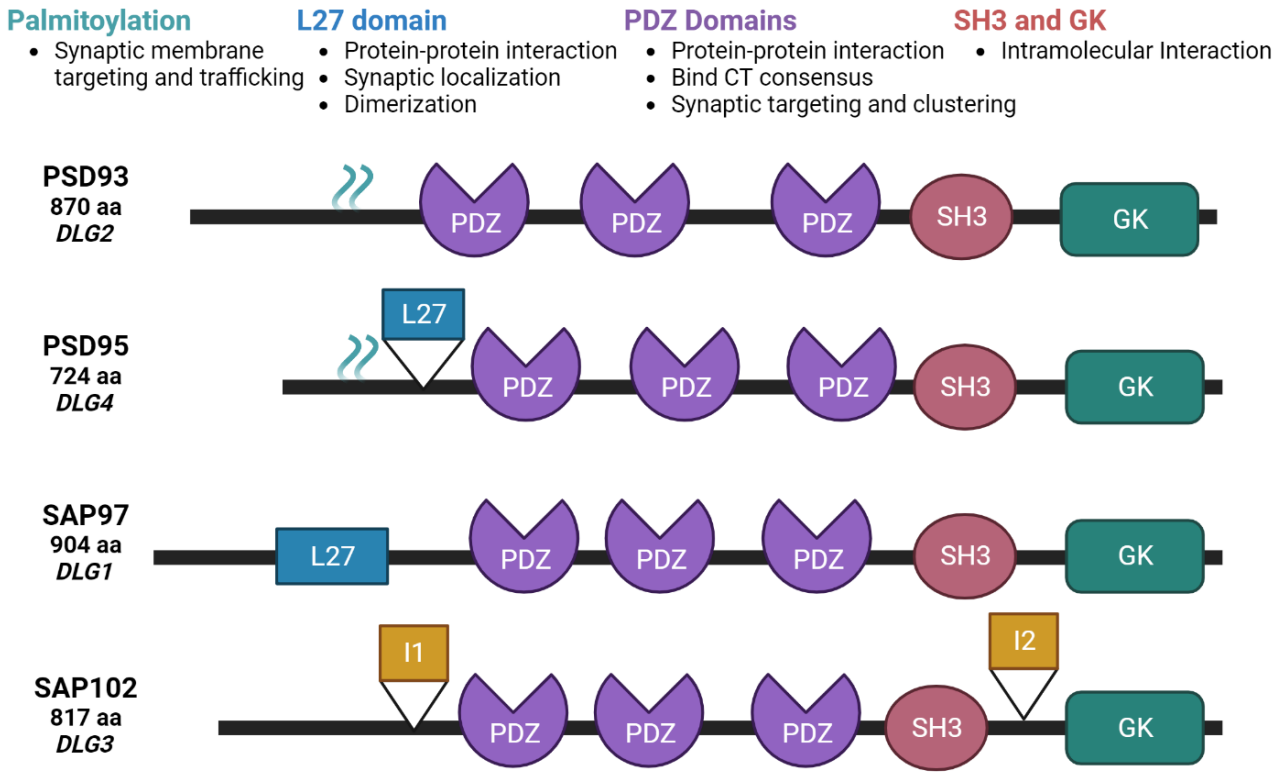

Fig. 1.19. Structure of the PSD-MAGUK Proteins.
PSD-MAGUK proteins contain three PDZ domains, followed by SH3 and a GK domains. PDZ: postsynaptic density protein 95/disc large tumor suppressor/zona occludens domain; SH3: Src homology 3; GK: guanylate kinase domain; L27: Lin-2 and Lin-7 domain; I1: insert 1 of SAP102, I2: insert 2 of SAP102. Created with BioRender.com.

synaptosome architecture is linked to neuropsychiatric disorders (Bayés et al, 2011; Soler et al, 2018).

3.3.1. Subcellular Localization and Mobility of SAP102 and PSD95

SAP102 and PSD95 exhibit differences in their subcellular localization and mobility within spines. While SAP102 and PSD95 colocalize to and are highly enriched within spines, PSD95 is most abundant at the PSD, whereas SAP102 is predominantly localized extrasynaptically (Chen et al, 2008; Zheng et al, 2010; Santuy et al, 2020). Synaptic clustering in the dendritic spines is differentially modulated by PSD95 and SAP102 through PDZ-dependent and -independent mechanisms, respectively (Zheng et al, 2010). For instance, PSD95 mutants decreased the synaptic clustering of pyramidal hippocampal neurons, but enhanced with SAP102 mutants (Nonaka et al, 2006; Minatohara et al, 2013). Moreover, unlike PSD95, SAP102 is not palmitoylated, making it highly mobile in spines and capable of shuttling NMDARs in and out of the synapse (Chen et al, 2012). CK2-mediated phosphorylation of SAP102-Ser632 decreases SAP102 synaptic mobility while simultaneously increasing its synaptic enrichment (Wei et al, 2018). The mobility of spine-localized SAP102 is partly actin-dependent, while the mobility of spine-localized PSD95 is largely actin-independent (Zheng et al, 2010). Overall, these differing properties of SAP102 and PSD95 suggest that they have distinct roles in synapse organization.

3.3.2. Architecture of the Brain Synaptome

Single-synapse-resolution maps in double-homozygous knockin SAP102-mKO2 and PSD95-eGFP mice across the whole brain synaptome revealed differential developmental distribution of SAP102 and PSD95 (Zhu et al, 2018; Cizeron et al, 2020). This work by Seth Grant and colleagues showed that there are unique distributions of SAP102 and PSD95 punctum density (number of puncta per area), intensity (reflecting protein amount), size (reflecting PSD size), and colocalization throughout the brain (Zhu et al, 2018; Cizeron et al, 2020). Indeed, SAP102 and PSD95 have distinct anatomical distributions, within each brain region displaying a distinct signature of synapse subtypes (Broadhead et al, 2016; Roy et al, 2018; Zhu et al, 2018; Cizeron et al, 2020; Curranet al, 2021; Bulovaite et al, 2022). This organized synaptic diversity in SAP102 and PSD95 content throughout the brain suggests an important underlying role for these two PSD-MAGUKs in determining overall brain physiology and behavior. *Fig. 1.20. shows the lifespan expression of SAP102 and PSD95.*

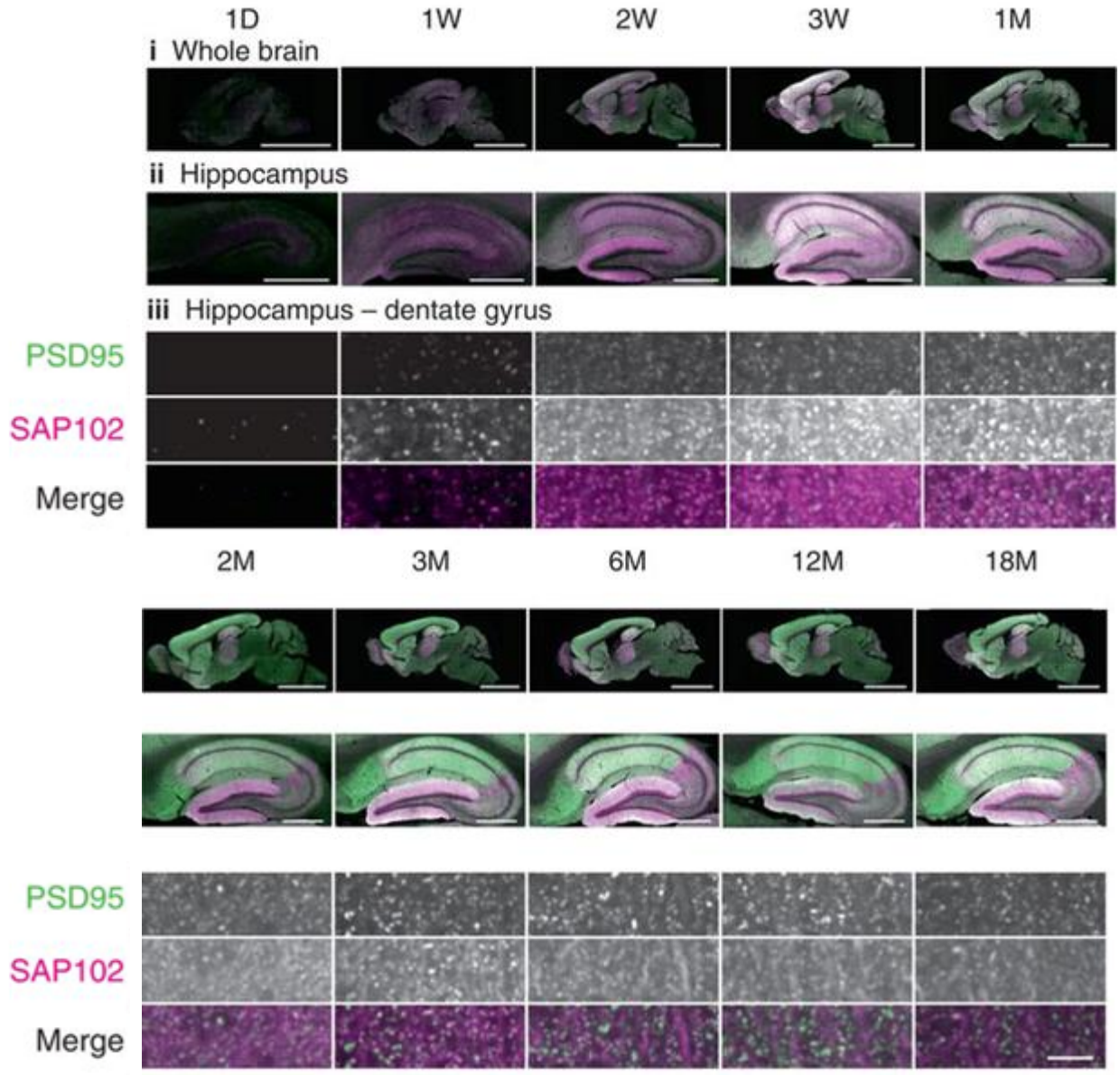

Fig. 1.20. Life-Span Distribution of SAP102 and PSD95.
Distribution of PSD95-eGFP (green) and SAP102-mKO2 (magenta) expression in the whole brain (i), hippocampus (ii), and molecular layer of the dentate gyrus (iii) at 10 ages across the mouse postnatal life span. "From [Cizeron et al. A Brainwide Atlas of Synapses Across the Mouse Life Span. Science. 2020]. Reprinted with permission from AAAS."

3.4. Genes Encoding PSD-MAGUKs

The discs large homologue (*DLG*) genes encode multiple isoforms of PSD-MAGUK proteins through alternate NT promoter usage and alternative splicing within the SH-GK domain linkers (Soler et al, 2018). The *DLG1* gene is located on chromosome 3q29 and encodes SAP97. There are two isoforms of SAP97, α and β, which differ in NT sequence and have opposing effects on synaptic targeting (Lue et al, 1994; Schlüter et al, 2006; Goodman et al, 2017; Soler et al, 2018). The SAP97 β isoform is most abundant and contains a L27 domain, whereas the SAP97 α isoform lacks this domain and instead contains two cysteine residues that can be palmitoylated (Schlüter et al, 2006). The *DLG2* gene is located on chromosome 11q14.1 and encodes PSD93. Six different PSD93 isoforms have been characterized in mouse hippocampus (Krüger et al, 2013; Soler et al, 2018). The *DLG3* gene is located on chromosome Xq13.1 and encodes SAP102. Alternative splicing gives rise to additional two isoforms of rodent SAP102: an 18aa I1 insert within NT, and a 14aa I2 insert within SH-GK linker, whereas the human *Dlg3* gene is lacking the presence of these two functional short inserts (Müller et al, 1996; Soler et al, 2018). The *DLG4* gene encodes PSD95 and is located on chromosome 17p13.1. Like SAP97, PSD95 has two isoforms, α and β, that differ based on the presence or lack of a L27 domain in their NT, and exhibit distinct effects on synaptic targeting. However, in contrast to SAP97, the α isoform of PSD95 predominates over the β isoform (Chetkovich et al, 2002; Schlüter et al, 2006; Soler et al, 2018). Ultimately, the different isoforms of each PSD-MAGUK may have distinct roles in various cellular contexts.

3.5. Regulation of Glutamatergic Signaling by PSD-MAGUKs

PSD-MAGUKs are critical regulators of glutamatergic receptor localization. In the case of NMDARs and kainate receptors, PSD-MAGUKs accomplish this through direct receptor-MAGUK physical interactions. (Müller et al, 1995; Kornau et al, 1995; Niethammer et al, 1996; Müller et al, 1996; Kim et al, 1996; Masuko et al, 1999; Carroll and Zukin, 2002; Kim and Sheng, 2004; Al-Hallaq et al, 2007; Zhu et al, 2016). In contrast, with the exception of SAP97, PSD-MAGUKs do not bind directly to AMPARs (Zhu et al, 2016). Instead, they localize AMPARs at the synapse through interactions with various intermediary proteins including stargazin, transmembrane AMPA regulatory proteins (TARP), and synaptic Ras GTPase activating protein (SynGAP) (Kim and Sheng, 2004; Zhu et al, 2016; Leonard et al, 1998; Kim et al, 1998; Chen et al, 1998; Schnell et al, 2002; Cai et al, 2002; Dakoji et al, 2003; Cia et al, 2006; Zhu et al, 2016).

The CT of AMPAR, however, binds to glutamate-receptor-interacting protein/AMPAR-binding protein (GRIP) and to protein interacting with C kinase 1 (PICK1) (Kim and Sheng, 2004). SAP97 and PSD95 also increase surface expression of GluR1-containing AMPAR, and furthermore, interact with A-kinase-anchoring protein 79/150 (AKAP79/150) to modulate the downstream signaling of synaptic AMPARs (El-Husseini et al, 2000b; Colledge et al, 2000; Regalado et al, 2006; Chen et al, 2015; Zhu et al, 2016; Chen et al, 2021). Interestingly, SAP97 additionally affects presynaptic functions. In particular, overexpression of SAP97 promotes activity of the active zone protein Bassoon and the vesicle proteins synapsin and synaptophysin, thus suggesting that SAP97 may coordinates different transsynaptic protein interactions (Regalado et al, 2006). PSD-MAGUKs also interact with receptor and non-receptor tyrosine kinases, channels, neuronal nitric oxide synthase (nNOS), cell adhesion proteins (e.g. neuroligin), and other scaffolding guanylate kinase domain-associated protein (GKAP), all of which are essential for glutamatergic plasticity (Kim et al, 1995; Brenman et al, 1996; Irie et al, 1997; Komiyama et al, 2002; Kalia LV, Salter, 2003; Seabold et al, 2003; Dosemeci et al, 2007; Murata et al, 2013; Frank et al, 2016).

3.5.1. Developmental Regulation of Synapses: Roles of SAP102 and PSD95

SAP102 and PSD95 have distinct roles during synaptogenesis and synapse maturation. SAP102 is the predominant DLG protein of immature synapses, suggesting its principal function concerns synapse formation (Carroll and Zukin, 2002; van Zundert et al, 2004). Throughout development, PSD95, among other DLG proteins, is increasingly expressed to regulate mature synapses. Expression of the two major GluN2 subunits of NMDAR is also developmentally regulated. GluN2B-containing NMDARs are predominantly expressed during early synaptic development, however, as synapses progress toward maturation, GluN2A-containing NMDARs become favored (Sheng et al, 1994; Carroll and Zukin, 2002; van Zundert et al, 2004). Interestingly, PSD95 and SAP102 are preferentially associated with GluN2A- and GluN2B-containing NMDARs, respectively (Carroll and Zukin, 2002; van Zundert et al, 2004). Indeed, PSD95 and SAP102 are important for enabling the developmental shift in synaptic NMDAR subunit composition; PSD95 associated with GluN2A-containing NMDARs could conceivably displace GluN2B-containing NMDAR•SAP102 complexes to extrasynaptic sites as synapses mature (Sans et al, 2000; Lu et al, 2001; Carroll and Zukin, 2002; Ehlers, 2003; van Zundert et al, 2004; Elias et al, 2008). *Fig. 1.21. depicts the developmental association between NMDAR subunits with SAP102 and PSD95.*

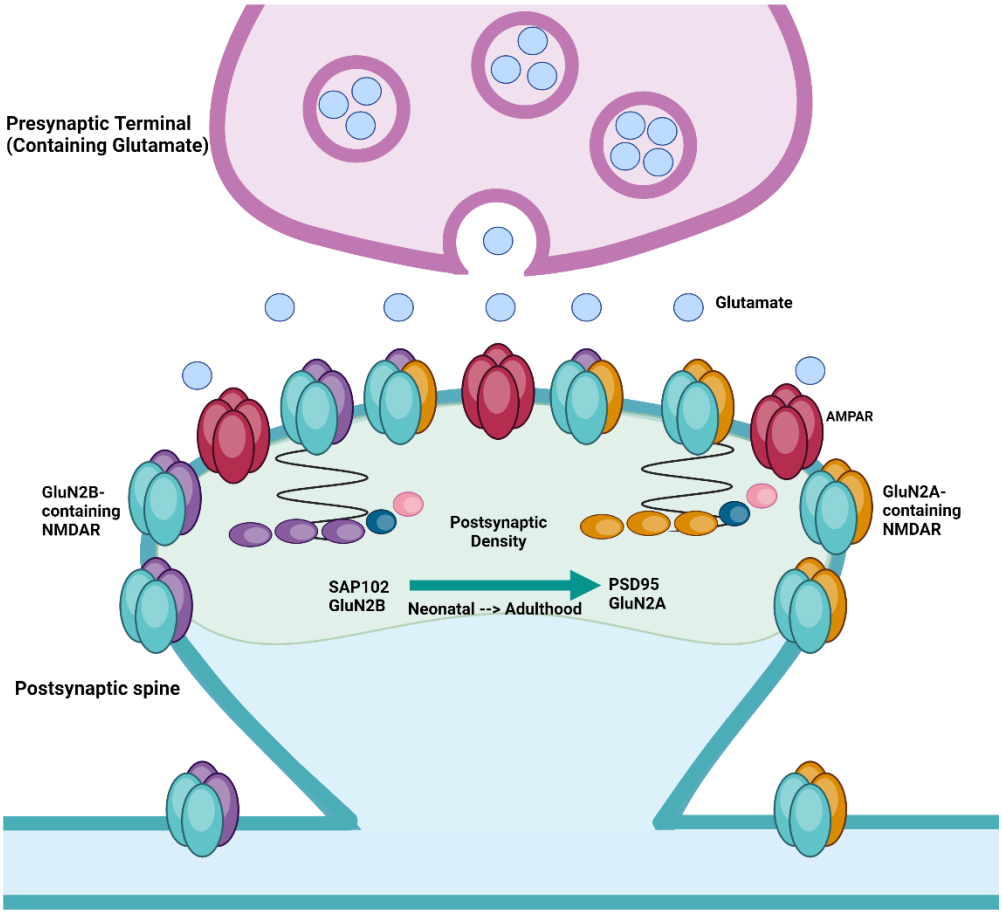

Fig. 1.21. Developmental Association between NMDAR Subunits with SAP102 and PSD95 at Excitatory Synapses.

At the neonatal stage, SAP102 is predominately associated with GluN2B-containing NMDAR. Throughout development, PSD95 is prevalently associated with GluN2A-containing NMDAR. Created with BioRender.com.

3.5.2. Regulation of NMDAR Trafficking by SAP102 and PSD95

PSD-MAGUKs have multifaceted functions in regulating glutamatergic synaptic plasticity. Proper localization of PSD-MAGUKs at the PSD is essential to facilitate transduction of glutamatergic signaling. PDZ-mediated interactions of PSD-MAGUKs with CT of different NMDAR subunits influence their localization, signaling, and trafficking (Kornau et al, 1995; Niethammer et al, 1996; Müller et al, 1996; Lau et al, 1996; Sans et al, 2000; Lim et al, 2002; Al-Hallaq et al, 2007; Cousins et al, 2008). Unlike PSD95, SAP102 mutants of PDZ-domains decreased the synaptic clustering of both GluN2A- and GluN2B-containing NMDAR (Nonaka et al, 2006; Minatohara et al, 2013). Interestingly, alternative splicing of SAP102 is also a critical modulator of NMDAR subunits at the synaptic membrane. The PDZ-independent interaction between the I1 isoform of SAP102 and GluN2B mediates synaptic clearance of GluN2B subunits. In contrast, the I2 isoform negatively modulates surface localization of GluN2A- but not GluN2B-containing NMDARs (Chen et al, 2011; Wei et al, 2015).

SAP102 and PSD95 differentially modulate NMDAR trafficking. Overexpression of PSD95 drives the maturation and formation of glutamatergic synapses by increasing postsynaptic clustering of NMDAR, enhancing development of presynaptic terminals, and increasing the number and size of dendritic spines (El-Husseini et al, 2000b). Surface GluN2B-containing NMDARs are highly mobile and undergo robust endocytosis compared to surface GluN2A-containing receptors (Barria and Malinow, 2002; Lavezzari et al, 2004; Groc et al, 2006). PSD95, but not SAP102, increases GluN2A and GluN2B subunit expression, thereby enhancing surface expression of GluN2A- and GluN2B-containing NMDARs (Cousins et al, 2008). PSD95 stabilizes NMDAR at the plasma membrane, disruption of GluN2B-containing NMDAR•PSD95 complex promotes rapid internalization of NMDAR (Roche et al, 2001; Rácz et al, 2004; Kennedy and Ehlers, 2006). Interestingly, SAP102, but not PSD95, is trafficked together with endocytosed NMDARs (Washbourne et al, 2004). The exocyst complex subunit Sec8 regulates normal delivery of SAP102•GluN2B to the cell surface (Sans et al, 2003). This preferential interaction of SAP102 for GluN2B is also important for synaptic clearance of GluN2B-containing NMDARs out of the synapse (Chen et al, 2012).

Synaptic GluN2B surface expression is also affected following CK2-mediated phosphorylation of GluN2B-Ser1480, which interestingly disrupts SAP102•NMDAR and PSD95•NMDAR

interactions, ultimately reducing GluN2B-containing NMDAR levels at the synapse (Chung et al, 2004). SAP102 and PSD95 also interact with mammalian homologue of *Drosophila melanogaster* partner of inscuteable (mPins) through their SH3 and GK domains, which promotes the formation of a ternary complex with NMDAR (Sans et al, 2005). mPins enhance the trafficking of SAP102 and NMDARs to the synaptic membrane (Sans et al, 2005). Overall, the above findings demonstrate the importance of SAP102 and PSD95 for proper NMDAR localization and synaptic plasticity.

3.5.3. Regulation of Glutamatergic Transmission by SAP102 and PSD95

Extensive studies from Roger Nicoll and Richard Huganir demonstrated how PSD-MAGUKs regulate the synaptic trafficking of glutamatergic receptors to and from synapses to control the strength of excitatory synaptic transmission and orchestrate activity-dependent modulation of synaptic AMPAR and NMDAR functions. Overexpression of PSD-MAGUK enhance AMPAR-EPSCs (excitatory postsynaptic currents), but do not affect NMDAR-EPSCs (El-Husseini et al, 2000b; Béïque and Andrade, 2003; Ehrlich and Malinow, 2004; Nakagawa et al, 2004; Elias et al, 2006; Béïque et al, 2006; Schlüter et al, 2006; Elias et al, 2008; Howard et al, 2010). Overexpression of SAP102, exceptionally, increases the amplitudes of both AMPAR and NMDAR EPSCs during synaptogenesis, but has no effect on glutamate receptor function in mature synapses (Elias et al, 2008). SAP102-knockdown (KD), however, reduced both AMPAR- and NMDAR-EPSC amplitudes during early synapse development, without impacting mature synapses (Elias et al, 2008). In contrast, PSD95 overexpression enhanced AMPAR-EPSCs, but has no effect on NMDAR function, during both synaptogenesis and synapse maturation (Béïque and Andrade, 2003; Béïque et al, 2006; Elias et al, 2008). The AMPAR amplitudes in PSD95-KD was not altered in early development but was reduced during synapse maturation (Elias et al, 2008; Bonnet et al, 2013). Unsurprisingly, triple-KD of SAP102, PSD95, and PSD93 greatly reduce synaptic transmission mediated by both AMPAR and NMDAR, and leads to a significant number of silent synapses (Chen et al, 2015). SAP102 and PSD95 are required during synapse development for normal NMDAR current decay. Indeed, they are conceivably involved in the characteristic switch in NMDAR subunit composition that largely determines NMDAR current kinetics; namely, a shift from primarily GluN2B-containing synaptic NMDAR during early developmental stages to predominantly GluN2A-containing synaptic NMDAR throughout later

stages of development toward synapse maturation (Lu et al, 2001; Béïque et al, 2006; Elias et al, 2008; Crocker-Buque et al, 2016). Overall, in a manner consistent with their differing developmental expression patterns, these findings suggest that during early stages of synaptic differentiation, SAP102 is the primary PSD-MAGUK responsible for modulation of synaptic AMPAR transmission and clustering, while PSD95 and PSD93 appear most important for regulating the targeting and anchoring of AMPAR at mature synapses (Carroll and Zukin, 2002; van Zundert et al, 2004; Elias and Nicoll, 2007).

PSD-MAGUKs also play essential roles in the regulation of silent synapses and LTP (Levy et al, 2015; Chen et al, 2021). Genetic deletion of PSD-MAGUK protein yields a greater proportion of inactive synapses that only contain NMDAR, known as silent synapses (Béïque et al, 2006; Carlisle et al, 2008; Bonnet et al, 2013). In mice selectively lacking PSD95, high and low frequency stimulation leading to hippocampal NMDAR-dependent LTP is increased relative to wild-type littermates (Migaud et al, 1998). In contrast, only low frequency stimulation leading to hippocampal NMDAR-dependent LTP is enhanced within SAP102 KO-mice (Cuthbert et al, 2007). These findings implicate PSD-MAGUKs as important regulators of AMPAR trafficking underlying long-term synaptic plasticity (Elias and Nicoll, 2007).

3.6. SAP102 and PSD95: Physiological and Pathophysiological Roles

PSD-MAGUKs are critical for maintaining normal intracellular signaling pathways. Genetic deletion experiments demonstrate that SAP102 and PSD95 exhibit redundancy of function and the ability to compensate for the loss of each other (Migaud et al, 1998; Cuthbert et al, 2007). Indeed, SAP102 hippocampal expression is elevated in PSD95 KO-mice, while SAP102 KO-mice display a greater number of PSD95•NMDAR complex, relative to their WT counterparts (Migaud et al, 1998; Cuthbert et al, 2007). In contrast, mice with double-KO of SAP102 and PSD95 die prenatally (Cuthbert et al, 2007). Together, these findings highlight that SAP102 and PSD95 have overlapping, essential functions, with the presence of at least one of them necessary for postnatal survival. These results also imply that SAP102 and PSD95 compete for interaction with the same population of NMDAR.

While SAP102 and PSD95 KO-mice have normal dendritic spine volume, they display increased spine length (filopodia-like) (Beique et al, 2006; Vickers et al, 2006; Murata et al, 2013; Chen et al, 2015). Such alteration in spines have impact on synaptic information processing and plasticity,

ultimately affecting memory formation (Bayés et al, 2011). SAP102 KO-mice exhibit elevated basal ERK1/2 activation, which contributes to the enhanced LTP also observed in these mice (Cuthbert et al, 2007). In contrast, NMDAR-mediated ERK1/2 activation is attenuated in SAP102 KO-mice (Cuthbert et al, 2007). The altered signaling and plasticity ultimately impart these mice with impaired cognition, learning, and memory (Migaud et al, 1998; Cuthbert et al, 2007; Nithianantharajah et al, 2013).

Synaptic activation of NMDAR and the resultant downstream signaling effects are modulated by PSD-MAGUKs, and represent important molecular mechanisms underlying learning and memory (Soler et al, 2018). Synaptome mapping shows that SAP102 and PSD95 are crucial for higher cognitive functions, and that disruption of their normal function at glutamatergic synapses throughout different brain regions causes synaptic abnormalities implicated in various psychiatric disorders (Fernández et al, 2009; Bayés et al, 2011; Broadhead et al, 2016; Roy et al, 2018; Zhu et al, 2018; Cizeron et al, 2020; Curran et al, 2021; Bulovaite et al, 2022). For instance, mutation in *DLG3* gene within or just before the third PDZ domain impairs the ability of SAP102 to anchor and modulate synaptic NMDAR signaling, and is associated with non-syndromic mental retardation (Tarpey et al, 2004; Zanni et al, 2010; Kumar et al, 2016; Sandestig et al, 2020). Changes in thalamocortical synaptic function early in development caused by mutations in SAP102 have also been linked to intellectual disability (Crocker-Buque et al, 2016). Similarly, mutations in *DLG4* gene might dysregulate NMDAR activity, and are associated with schizophrenia and autism-spectrum disorders (Feyder et al, 2010). Additionally, postmortem analysis shows altered expression levels of striatal and cortical SAP102 and PSD95 in bipolar disease, schizophrenia, and major depression (Toyooka et al, 2002; Kristiansen and Meador-Woodruff, 2005; Kristiansen et al, 2006; McCullumsmith et al, 2006).

Alterations in SAP102 and PSD95 function may also contribute to the underlying pathophysiology of individuals with drug addiction. Strikingly, a single cocaine injection during adolescence is sufficient to shift cortical dendritic spines toward a filopodia-like morphology, which is associated with a dysfunctional reduction in the synaptic expression level of NMDAR, AMPAR, SAP102, and PSD95, ultimately leading to impaired glutamatergic signaling (Caffino et al, 2018).

3.7. Interplay between GPCR•PSD-MAGUK

In addition to their modulation of glutamatergic function, PSD-MAGUKs also regulate GPCR signaling and trafficking processes that are physiologically important for receptor responsiveness (Dunn and Ferguson, 2015). *Table 1.3. summarizes the proposed functions of GPCRs interacting with PSD-MAGUK proteins.*

β_1 adrenergic receptor (β_1AR) is the first GPCR reported to interact with PSD-MAGUKs (Hu et al, 2000). Among adrenergic receptors, PSD95 selectively interacts with β_1AR, but not with β_2AR (Hu et al, 2000). PSD95 inhibits agonist-mediated endocytosis of β_1AR, while showing no impact on β_1AR-induced cAMP accumulation (Hu et al, 2000; Xu et al, 2001). PSD95 additionally facilitates the formation of a complex between β_1AR and NMDAR (Hu et al, 2000). SAP97 also interacts with β_1AR and enables the formation of β1AR•SAP97•AKAP79•PKA quaternary complex (Gardner et al, 2007). Interestingly, SAP97 and PSD95 exert different effects on β_1AR trafficking; PSD95, but not SAP97, significantly inhibit agonist-mediated internalization and recycling of β_1AR (Hu et al, 2000; Gardner et al, 2007; Nooh et al, 2014).

PSD95 also interacts with 5-HT_{2A} receptor (5-HT_{2A}R) and 5-HT_{2C} receptor (5-HT_{2C}R), with greater binding affinity observed for 5-HT_{2C}R (Bécamel et al, 2002; Xia et al, 2003a, b; Bécamel et al, 2004; Gavarini et al, 2006). PSD95 potentiates $G\alpha_q$-mediated intracellular signaling of both 5-HT_{2A}R and 5-HT_{2C}R, but differentially regulates the trafficking of each receptor (Xia et al, 2003a; Gavarini et al, 2006). PSD95 promotes agonist-independent and dependent internalization for 5-HT_{2C}R, but inhibits 5-HT_{2A}R endocytosis (Xia et al, 2003a; Gavarini et al, 2006). *In vivo* studies suggest that PSD95 is crucial for maintaining 5-HT_{2A}R and 5-HT_{2C}R expression by promoting their targeting to the PSD within apical dendrites and stabilizing their turnover (Xia et al, 2003b; Abbas et al, 2009). PSD95 is also an important contributor to 5-HT_{2A}R-mediated ERK1/2 and GSK3β phosphorylation, along with 5-HT_{2c}R-mediated induction of c-fos, as evidenced by the inhibition of these signaling pathways within PSD95 KO-mice (Abbas et al, 2009). Interestingly, SAP97 also interacts with 5-HT_{2C}R and 5-HT_{2A}R, binding both receptors with equal affinity, while SAP102 interacts selectively with 5-HT_{2C}R (Bécamel et al, 2004; Dunn et al, 2014). SAP97 regulates 5-HT_{2A}R-mediated $G\alpha_{q/11}$ signaling and ERK1/2 phosphorylation, but antagonizes the internalization of 5-HT_{2A}R (Dunn et al, 2014). The signaling mechanisms of SAP97 and SAP102 in regulating 5-HT_{2c}R has yet to be determined.

Interestingly, corticotropin-releasing factor receptor 1 (CRFR1, also known as *CRHR1*) is the only GPCR reported to interact with each member of PSD-MAGUKs, mediated via PDZ-domain mechanism (Dunn et al, 2013; Bender et al, 2015; Dunn et al, 2016). PSD-MAGUKs promotes the synaptic clustering of CRFR1 in transfected hippocampal culture (Bender et al, 2015). While PSD95 and SAP97 have no effect on CRFR1-mediated cAMP production, both suppress CRFR1 endocytosis but SAP97 promotes CRFR1-mediated ERK1/2 signaling (Dunn et al, 2013; Dunn et al, 2016). The role of PSD93 and SAP102 in CRHR1 trafficking remains to be examined.

Finally, SAP102 interacts with $A_{2A}R$ in a manner that modulates $A_{2A}R$-mediated ERK1/2 signaling without affecting cAMP production, and restricts its movement between synaptic compartments (Thurner et al, 2014). Together, these findings demonstrate that PSD-MAGUK proteins play important regulatory roles in GPCR signaling and trafficking.

3.7.1. The Interaction of PDZ-Containing Protein with Gγ Subunit

As discussed in the previous section, PSD-MAGUKs modulate the signaling of GPCR-mediated G-protein subunits. Interestingly, a study reported the complex formation of Gγ13 with PSD95, SAP97, and another PDZ-containing protein, Veli-2, thus could efficiently target heterotrimeric G-proteins to regulate GPCR signaling (Li et al, 2006). Gγ2, Gγ5, Gγ8, and Gγ12, among the Gγ subunits that contain class-I PDZ-binding motif in their CT sequence, yet no report has shown physical interaction with PDZ-containing proteins. Whether Gα and/or Gβ participate in the complex formation with PDZ-containing protein, remain to be examined.

3.7.2. The Role of PSD-MAGUK in GPCR•GRK Phosphorylation

GRKs are important regulators for GPCRs desensitization and phosphorylation, however, their role in the GPCR•MAGUK complex remains to be fully investigated. A study showed that GRK2 and GRK5 associate with β_1AR•PSD95 and enhance the receptor phosphorylation, and this complex is not affected by βArrs (Hu et al, 2002). Expression of GRK5, but not GRK2, decreases PSD95 binding to β_1AR, in a matter dependent on the kinase activity of GRK5 (Hu et al, 2002). Another study showed that GRK5 promotes dissociation of cardiac β_1AR•SAP97 complex and β_1AR•CaMKII signaling in heart failure (Xu et al, 2020). Together, these findings suggest a potential role of GRK•MAGUK in regulating the GPCR function.

Table 1.2. Summary of the complex functions of GPCR interacting with PSD-MAGUK proteins.
Other functions may have been reported by these GPCRs interacting MAGUK proteins that were not discussed in this summary table. GPR30: G-protein coupled estrogen receptor; SSTR: somatostatin receptor.

GPCR•MAGUK	Complex Function	Reference
D1R•PSD95	• **Interaction demonstrated *in vitro* and *in vivo* (brain).** • **PSD95 inhibits (or did not alter) D1R-mediated cAMP production.** • **PSD95 does not alter D1R desensitization, but enhances D1R resensitization.** • **NT-PSD95 facilitates constitutive D1R internalization in dynamin-dependent fashion.** • **PSD95 accelerates membrane D1R recovery via enhancement of receptor recycling.** • **Enhanced behavioral responses to D1R agonists in PSD95-KO mice.**	(Zhang et al, 2007; Zhang et al, 2009; Sun et al, 2009)
D1R•PSD95•NMDAR	• **Interaction demonstrated *in vitro* and *in vivo* (brain).** • **PSD95 and NMDAR-GluN1 subunit bind to an overlapping region on the D1R-CT.** • **PSD95 inhibits D1R•NMDAR-GluN1 interaction.** • **Removal of PSD95 enhances D1R•NMDAR-GluN1 association.** • **PSD95 removes NMDAR inhibition of D1R internalization.** • **PSD95 blocks NMDAR modulation of D1R signaling.**	(Zhang et al, 2009)
β_1AR•PSD95	• **Interaction demonstrated *in vitro* and *in vivo* (brain and heart).** • **PSD95 associates specifically with the β_1AR (but not β_2AR) in vitro and in cells.** • **PSD95 colocalizes with the β_1AR in HEK-293 cells.** • **PSD95 decreases β_1AR internalization and recycling.** • **PSD95 have no effect on β_1AR-induced cAMP or β_1AR desensitization.** • **PSD95 facilitates the formation of a cellular complex between β_1AR and NMDAR.** • **Expression of GRK5 decreases PSD95 binding to β_1AR.** • **GRK2 and GRK5 can associate with β_1AR and enhance its phosphorylation.** • **GRK5 kinase activity is required to regulate the β_1AR association with PSD95.** • **GRK5 regulates β_1AR•PSD95 association by phosphorylation of β_1AR.** • **β_1AR•PSD95 association is not affected by βArrs.**	(Hu et al, 2000; Xu et al, 2001; Hu et al, 2002; Gardner et al, 2007)
β_1AR•SAP97	• **Interaction demonstrated *in vitro* and *in vivo* (brain and heart).** • **SAP97 has no effect agonist-mediated internalization of β_1AR.** • **SAP97 has no effect (or regulate) β_1AR recycling.** • **Enable the formation of β_1AR•SAP97•AKAP79•PKA.**	(Gardner et al, 2007; Nooh et al, 2013; Nooh et al, 2014)
5-HT_{2A}R•PSD95	• **Interaction demonstrated *in vitro* and *in vivo* (brain).** • **PSD95 potentiates Gα_q-mediated IP_3 of 5-HT_{2A}R.** • **PSD95 has no effect on agonist-dependent desensitization of 5-HT_{2A}R.** • **PSD95 inhibits agonist-induced internalization of 5-HT_{2A}R.** • **PSD95 enhances 5-HT_{2A}R-mediated ERK1/2 activation and GSK3β phosphorylation.** • **PSD95 promotes cell surface clustering of 5-HT_{2A}R.** • **PSD95 is essential for maintaining normal 5-HT_{2A}R expression *in vivo*.** • **PSD95 regulates 5-HT_{2A}R turnover.** • **PSD95 is required for the polarized sorting of 5-HT_{2A}R to the apical dendrites of pyramidal neuron.** • **5-HT_{2A}R-mediated head-twitch behavior is attenuated in PSD95 null mice.**	(Bécamel et al, 2004; Xia et al, 2003; Abbas et al, 2009)
5-HT_{2A}R•SAP97	• **Interaction demonstrated *in vitro* and *in vivo* (brain).** • **SAP97 colocalization with 5-HT_{2A}R at the plasma membrane.** • **SAP97 antagonizes the internalization of 5-HT_{2A}R.** • **SAP97 enhances Gα_q-mediated IP_3 of 5-HT_{2A}R.** • **SAP97 regulates 5-HT_{2A}R-mediated ERK1/2 activation.**	(Dunn et al, 2014)
5-HT_{2C}R•PSD95	• **Interaction demonstrated *in vitro* and *in vivo* (brain).** • **PSD95 is essential for maintaining normal 5-HT_{2C}R. expression *in vivo*.** • **PSD95 is required for 5-HT_{2C}R signaling *in vivo* (enhances c-fos).** • **PSD95 potentiates Gα_q-mediated IP_3 of 5-HT_{2C}R.** • **PSD95 facilitates agonist-dependent and independent endocytosis of 5-HT_{2C}R.**	(Bécamel et al, 2002; Bécamel et al, 2004; Gavarini et al, 2006; Abbas et al, 2009)

5-HT$_{2C}$R•SAP97	• **Interaction identified by mass spectrometry.** • **No mechanism was proposed.**	(Bécamel et al, 2004)
5-HT$_{2C}$R•SAP102	• **Interaction identified by mass spectrometry.** • **No mechanism was proposed.**	(Bécamel et al, 2004)
CRFR1•PSD95	• **Interaction demonstrated *in vitro* and *in vivo* (brain).** • **PSD95 increases the synaptic clustering of CRFR1 that is dependent on PDZ-binding motif of CRFR1.** • **PSD95 has no effect on CRFR1-mediated cAMP signaling.** • **Alterations in PSD95 expression did not significantly affect CRFR1-mediated ERK1/2 signaling.** • **PSD95 suppresses CRFR1 endocytosis via the CRFR1 PDZ-binding motif.** • **PSD95 antagonizes agonist-induced βArr2 recruitment to CRFR1.** • **PSD95 is not independently involved in CRFR1-mediated sensitization of 5-HT$_{2A}$R signaling.**	(Bender et al, 2015 Dunn et al, 2016)
CRFR1•SAP97	• **Interaction demonstrated *in vitro* and *in vivo* (brain).** • **SAP97 increases the synaptic clustering of CRFR1 that is dependent on PDZ-binding motif of CRFR1.** • **SAP97 antagonizes CRFR1 endocytosis in a PDZ-binding motif-dependent manner,** • **SAP97 colocalizes with internalized CRFR1.** • **SAP97 has no effect on CRFR1-mediated cAMP signaling.** • **SAP97 enhances CRFR1-mediated ERK1/2 phosphorylation that is dependent on endogenous SAP97 expression.**	(Dunn et al, 2013 Bender et al, 2015)
CRFR1•PSD93	• **Interaction demonstrated *in vitro*.** • **PSD93 increases the synaptic clustering of CRFR1 that is dependent on PDZ-binding motif of CRFR1.**	(Bender et al, 2015)
CRFR1•SAP102	• **Interaction demonstrated *in vitro*.** • **SAP102 increases the synaptic clustering of CRFR1 that is dependent on PDZ-binding motif of CRFR1.**	(Bender et al, 2015)
A$_{2A}$R•SAP102	• **Interaction demonstrated *in vitro*.** • **SAP102 has no effect on agonist-mediated cAMP of A$_{2A}$R.** • **SAP102 enhances agonist-induced ERK1/2 activation of A$_{2A}$R.** • **SAP102 increases the mobility of the agonist-activated A$_{2A}$R but abolishes agonist-induced change in the effective diffusion coefficients.** • **SAP102 precluded access of the A$_{2A}$R to the compartment with restricted mobility.**	(Thurner et al, 2014)
GPR30•PSD95	• **Interaction demonstrated *in vitro* and *in vivo* (brain).** • **PSD95 association increases surface expression of GPR30 at the plasma membrane.** • **GPR30•PSD95•AKAP5 complex is localized in the plasma membrane.**	(Akama et al, 2013; Broselid et al, 2014)
GPR30•SAP97	• **Interaction demonstrated *in vitro*.** • **No mechanism was proposed.**	(Broselid et al, 2014)
SSTR1•SAP97	• **Interaction demonstrated *in vitro* and *in vivo* (brain).** • **Colocalization and possible functional interaction of SAP97 and SSTR1 in growth cones of cultured mouse cortical neurons.**	(Cia et al, 2009)
SSTR1•PSD95	• **Interaction demonstrated *in vitro* and *in vivo* (brain).** • **No mechanism was proposed.**	(Christenn et al, 2007)
SSTR1•PSD93	• **Interaction identified using peptide affinity purification.** • **No mechanism was proposed.**	(Christenn et al, 2007)
SSTR4•PSD95	• **Interaction demonstrated *in vitro* and *in vivo* (brain).** • **Colocalization of SSTR4•PSD95 in somatodendritic hippocampal neurons.** • **PSD95 has no effect on agonist-induced endocytosis of SSTR4.**	(Christenn et al, 2007)
SSTR4•PSD93	• **Interaction identified using peptide affinity purification.** • **No mechanism was proposed.**	(Christenn et al, 2007)

3.7.3. The Role of PDZ Domains in GPCR•β-arrestin2 Signaling

PDZ-containing proteins are important modulators of GPCR•β-arrestin2 signaling complex. A recent study reported that βArr2 interacts with different PDZ-containing proteins, including PSD95 via its PDZ1 domain (Gupta et al, 2019). Indeed, βArr2•PSD95 was detected in hippocampal culture, and the neuronal scaffolding of βArr2•PSD95 complex participates in the downstream activation of JNK3, independently of GPCR activation (Musi et al, 2022). Yet, despite its affinity for βArr2, PSD95 antagonizes agonist-stimulated βArr2 recruitment to CRFR1 (Dunn et al, 2016). Interestingly, this finding contrasts with the effect of another βArr2-interacting PDZ-containing protein called Na^+/H^+ exchange regulatory factor 1 (NHERF1), which promotes βArr2 recruitment to parathyroid hormone receptor 1 (PTHR1) (Klenk et al, 2010). These findings suggest that the scaffolding properties of PDZ-containing proteins modulate receptor-mediated βArr2 recruitment and signaling.

3.8. Regulation of Dopaminergic Signaling: Roles of SAP102 and PSD95

Caron's lab identified PSD95 as an important regulator of DA-mediated behavior and synaptic plasticity. By utilizing mutant mouse models known to elicit heightened sensitivity to psychostimulant; $DAT^{-/-}$, $NET^{-/-}$, and $VMAT2^{+/-}$, and mice chronically treated with cocaine, genomic microarray profiling of striatal transcripts show that PSD95 is significantly reduced in basal ganglia, but unchanged in hippocampus and cortex (Yao et al, 2004). Furthermore, a different study found that repeated amphetamine treatment also reduces striatal PSD95 level (Mao et al, 2009). Interestingly, among PSD-MAGUK proteins, the reduced expression level reported in these studies was specific to PSD95, with normal striatal expression observed for SAP102, SAP97 and PSD93 (Yao et al, 2004; Mao et al, 2009). Yao and colleagues argued that lower PSD95 levels in these experimental models led to overactive D1R, a previously established central tenet of psychostimulant hyperactivity. Subsequent findings demonstrated that PSD95-KO display a reduced locomotor activity and elicit substantial behavioral response to D1-class agonist and the psychostimulants cocaine and amphetamine (Yao et al, 2004; Zhang et al, 2007; Zhang et al, 2014).

Moreover, the medial PFC (mPFC) expression of synaptic and extrasynaptic AMPAR subunits (GluA1, GluA2, and GluA3), and their anchoring proteins (SAP97 and GRIP) were significantly reduced in DAT-deficient rats, and in an opposing fashion, PSD95 expression was enhanced

(Targa et al, 2023). These findings suggest that DA overactivity displayed in DAT-KO alters the homeostatic plasticity of the glutamate synapse in the mPFC and dysregulates AMPAR trafficking.

3.8.1. D1R•PSD95 Complex

In vitro and *in vivo* coimmunoprecipitation and GST-pulldown assays suggest that CT of D1R physically interacts with NT of PSD95. (Zhang et al, 2007; Sun et al, 2009). Importantly, this complex is observed in purified PSD, suggesting that D1R and PSD95 are highly enriched in this region (Zhang et al, 2007). However, whether PSD95 exerts regulatory effects on D1R-mediated trafficking and signaling remains incompletely understood due to several discrepancies between studies. Zhang and colleagues show that PSD95 inhibits D1R-mediated cAMP accumulation, and PSD enhances constitutive, dynamin-dependent endocytosis of D1R (Zhang et al, 2007). Expectedly, truncation of NT-PSD95 abolishes the constitutive D1R endocytosis facilitated by PSD95, while deleting other PSD95 domains has no effect in this regard (Zhang et al, 2007). The selective reduction of D1R surface expression, without a change in total expression, suggests that PSD95 promotes cellular redistribution of D1R toward greater intracellular localization (Zhang et al, 2007). Interestingly, PSD95 also interacts with G-protein γ subunit, which could conceivably affect G-protein coupling to D1R, downstream cAMP production, and/or uncoupling of G protein from activated D1R to initiate receptor desensitization (Li et al, 2006; Zhang et al, 2007). In contrast, Sun and colleagues report no effect of PSD95 on D1R-mediated cAMP production, G-protein activation, or desensitization, but show that PSD95 promotes agonist-induced D1R resensitization. Interestingly PSD95 also accelerates the recycling of internalized D1R, independent of receptor synthesis (Sun et al, 2009). These differing findings between research groups on the particular roles played by PSD95 in D1R signaling and trafficking may in part be accounted for by differences in experimental procedures.

3.8.2. D1R•NMDAR•PSD95 Complex

PSD95 plays an important role in regulating interactions between D1R and NMDAR. Indeed, biochemical and imaging studies reveal tripartite D1R•NMDAR•PSD95 complexes *in vitro* and *in vivo*, mediated via a distinct but overlapping region within the CT of D1R (Zhang et al, 2009). In complexes containing only D1R and NMDAR, D1R is immobilized in the plasma membrane, displays little constitutive endocytosis, and exhibits reduced cAMP production when D1R is activated (Fiorentini et al, 2003). However, when PSD95 is co-expressed with D1R and NMDAR

in heterologous cells, D1R experiences robust constitutive and agonist-induced internalization, and significantly enhanced cAMP production upon D1R activation, presumably due to formation of D1R•NMDAR•PSD95 complexes (Zhang et al, 2009). Additionally, D1R activation within the context of such tripartite complexes—in particular, those with GluN2B-containing-NMDAR—facilitates NMDAR-mediated-Ca^{2+} influx in HEK293 cells (Gu et al, 2007). D1R activation also potentiates cortical NMDAR-mediated EPSCs in PSD95 mutant mice (Zhang et al, 2014). Furthermore, activation of GluN2B-containing NMDAR complexed with D1R alone enhances D1R-mediated cAMP accumulation, while activation of GluN2B-containing NMDAR in the context of D1R•NMDAR•PSD95 complexes has no effect on D1R-mediated cAMP production, highlighting a function for PSD95 in dampening NMDAR-mediated enhancement of canonical D1R signaling (Zhang et al, 2009). Overall, the above findings demonstrate a clear role for PSD95 in modulating the functional interplay between D1R and NMDAR.

3.8.3. L-DOPA-Induced Dyskinesia: Roles of SAP102 and PSD95

SAP102 and PSD95 differentially contribute to the D1R-mediated signaling alterations that underlie LID. Reduced level of striatal PSD95, SAP102, SAP97 and GluN2B-containing NMDARs are exhibited within 6-OHDA-lesioned rats relative to sham-lesioned rats (Picconi et al, 2004; Nash et al, 2005; Gardoni et al, 2006). Chronic L-DOPA treatment rescues the level of PSD95, SAP102, and SAP97, but not GluN2B, within rats experiencing LID compared to sham-lesioned rats (Gardoni et al, 2006). Striatal GluN2A-containing NMDAR expression was not altered in 6-OHDA lesioned-mice, but was enhanced following L-DOPA treatment (Gardoni et al, 2006). While PSD95, SAP102, and SAP97 interactions with GluN2A subunit were unchanged, a profound disruption of the association of PSD95•GluN2B, SAP102•GluN2B, and SAP97•GluN2B complexes were observed in this experimental parkinsonian model (Gardoni et al, 2006). L-DOPA administration, however, rescue the abundance of PSD95•GluN2B and SAP97•GluN2B complexes to control level, but is inefficient to restore the level of SAP102•GluN2B complex (Gardoni et al, 2006). These findings suggest a critical role of SAP102•GluN2B complex formation for the correct delivery of GluN2B-containing NMDARs to the synapse, and in LID development observed in this experimental parkinsonian model (Gardoni et al, 2009).

Moreover, levels of striatal PSD95 and D1R•PSD95 complex are massively increased in dyskinetic MPTP-lesioned macaques (Porras et al, 2012). Interestingly, downregulation of striatal

PSD95 in the MPTP-treated macaque markedly alleviates dyskinesia and alters synaptic D1R surface content and trafficking (Porras et al, 2012). These findings suggest that striatal alterations in the D1R•PSD95 signaling complex are crucial for the development and severity of LID (Porras et al, 2012). PSD95 also modulates D1R-mediated ERK1/2 activation in the context of LID. Elevated D1R-mediated ERK1/2 activation in dyskinetic 6-OHDA-lesioned mice and PSD95 KD reduces the level of ERK1/2 phosphorylation, which suggest that PSD95 is a contributing factor to the pathologically increased D1R-mediated ERK1/2 activation in LID (Porras et al, 2012). It is likely, however, that D1R-mediated LID dysfunction involves altered physical and functional interactions of D1R•PSD95•NMDAR complex. Importantly, no studies have directly assessed a potential role for SAP102 in regulating D1R function in parkinsonian models.

4. Thesis Objectives: Investigating the Role of D1-Class Receptor Interactions with SAP102 and PSD95

GPCRs, including D1-class receptors, serve as hubs that assemble a wide array of non G-protein signaling partners, such as the PSD-MAGUKs: SAP102 and PSD95, which contribute to the regulation of the receptor function. Dysfunction of normal interactions with such signaling partners can lead to altered receptor function and pathophysiological states. Indeed, dysfunctional PSD95 and SAP102 are strongly implicated in diseases with dopaminergic dysfunction—especially those with well-characterized D1-class receptor involvement—including PD and LID. In light of this, a thorough investigation into the mechanistic interplay between PSD95, SAP102 and D1-class receptors is warranted. Although SAP102 and PSD95 have similar structure, they display distinct functionalities in the modulation of glutamatergic transmission. Importantly, the macromolecular organizations that integrate the dopaminergic-glutamatergic transmission in both physiology and disease are highly sophisticated and require further study to fully appreciate the mechanisms governing the formation of DA receptor signaling complexes, especially as it pertains to their linkage with glutamate receptors. While studies reported the expression and regulation of SAP102 in DA system, there is no evidence yet for functional interactions between DA receptors and SAP102. Owing to these facts, it is clearly vital to further our understanding of the potential roles played by SAP102 and PSD95 in these processes that have the potential for novel therapeutic modulation in dopaminergic diseases.

As noted earlier, the Tiberi lab utilized proteomic yeast two-hybrid screens to identify SAP102 as a potential subtype-selective interactor with D1R. In particular, the yeast two-hybrid screens suggest that SAP102 domains located downstream of PDZ2 potentially interact with IL3-D1R. Interestingly, *in vitro* studies from the Tiberi lab found that SAP102 switches the mechanism of D1R-mediated ERK1/2 activation from a PKA-independent to PKA-dependent pathway (Mischuk et al., in preparation). **Taking into account these findings and the established D1R•PSD95 relationship, I hypothesized that SAP102 and PSD95 not only both interact with D1R, but also act to differentially regulate D1R function properties. I aimed to study the role of SAP102 and PSD95 in regulating D1R by i) mapping the binary D1R•SAP102 and D1R•PSD95 interactions *in vivo* and *in vitro*, and ii) assessing the effect of SAP102 and PSD95 on signaling, phosphorylation, and trafficking mechanisms of D1R.**

Furthermore, the role of PSD95 in regulating D5R function has yet to be established. Sun and colleagues showed that, in addition to D1R, PSD95 constitutively interacts with D2R and D5R in heterologous cells, without further elucidating the specific region of D5R participating in the interaction or the significance of these complexes in downstream signaling and trafficking functions (Sun et al, 2009). Another research group reported that distal CT of D5R did not pulldown PSD95 from striatal lysate (Kruusmagi et al, 2009; Blom et al, 2012). Interactions between PSD95 and other regions of D5R, such as IL3 and proximal CT, have yet to be investigated. Interestingly, D5R is implicated as an important player in hippocampal NMDAR signaling as evidenced by the reduced expression of GluN2B-containing NMDAR within hippocampus of D5R-KO mice (Moraga-Amaro et al, 2016). These findings thus suggest that D5R is not only a regulator of inhibitory GABAergic transmission through its interaction with $GABA_AR$, but also an important modulator of excitatory glutamatergic transmission via its apparent effect on NMDAR function. **I argue that these findings support the possibility of D5R linkage to PSD95 in a manner crucial for normal synaptic NMDAR expression and signaling. Thus, I hypothesized that PSD95 interact with D5R and regulate D5R functions. I aimed to investigate this by i) mapping the D5R•PSD95 interaction *in vivo* and *in vitro*, and ii) assessing the effect of PSD95 on D5R signaling and trafficking mechanisms.**

Finally, βArr2 recruitment by D1R is shown to modulate D1R signaling properties and has promising clinical applications. Interestingly, a recent study suggested that βArr2 interacts with PSD95 (Gupta et al, 2019; Musi et al, 2022). These findings, taken together with the known importance of βArr2 in D1R trafficking, open the possibility that βArr2 is an actuator for the interplay between D1R•SAP102 and D1R•PSD95 complexes. Whether βArr1 also associates with PSD-MAGUK has yet to be examined. **I posit that SAP102 and PSD95 modulate D1R•βArr2 trafficking properties. I aimed to study i) the binary interaction between βArr1•SAP102/PSD95 and βArr2•SAP102/PSD95 *in vitro* and *in vivo*, ii) the ternary complex of D1R•SAP102/PSD95•βArr2 and iii) the effect of D1R•SAP102/PSD95•βArr2 complexes on D1R trafficking properties.**

In conclusion, given the importance of SAP102 and PSD95 in regulating NMDAR function, and by deciphering the mechanistic details of SAP102 and PSD95 involvement in D1-class receptor function, critical information will reveal potential intersection between dopaminergic and

glutamatergic mechanisms. Results from these studies may inform rational drug design of new therapeutic approaches for the treatment of dopaminergic disorders.

As my thesis seeks to gain a mechanistic understanding of the scaffolding glutamatergic proteins of SAP102 and PSD95 interacting with D1-class receptors, the results of these hypotheses/objectives addressed above will be presented in the form of three thematically distinct manuscripts in *Chapter Three: Results*, titled as:

I) ***Synapse Associated Protein 102 (SAP102) and Postsynaptic Density 95 (PSD95) Differentially Modulate Dopamine D1 Receptor.***

II) ***Postsynaptic Density 95 (PSD95) Modulates Dopamine D5 Receptor.***

III) ***Synapse-Associated Protein 102 (SAP102) and Postsynaptic Density 95 (PSD95) Facilitate β-arrestin2 (βArr2) Signaling of Dopamine D1 Receptor.***

CHAPTER TWO: MATERIALS AND METHODS

1. Key Reagents or Resources

Table 2.1 summarizes reagents and resources utilized in my thesis studies. Table 2.2. lists the antibodies used in different experimental approached in my thesis.

2. DNA Constructs

The list of different DNA plasmids utilized in transient transfection of mammalian cells are described in Table 2.3. *Fig. 2.1 illustrates the mutant forms of D1R and D5R used in my thesis studies.*

2.1. Construction of Flag-D5R-C375

Untagged-D5R truncated tail at C375 construct was generated using a PCR overlap extension strategy as described by the Tiberi Lab (Plouffle et al, 2010). Flag-D5R-C375 was constructed through digesting untagged D5R-C375-pCMV5 with EcoRI and EagI and subcloning the fragments (~1200 bp) into readily available FLAG-D5R-pCMV5 linearized with the same enzymes. DNA sequences from untagged-D5R-C375 and FLAG-D5R-C375 were confirmed by automated DNA sequencing from Génome Québec (Nanuq) (Montréal, QC, Canada).

Table 2.1. Key Resources and Reagents.

Experimental Model: Organism/Strain	**Supplier**	**Experimental Model: Organism/Strain**	**Supplier**
Sprague-Dawley rats (Kindly provided by Dr. Béïque lab)	(Charles River Laboratories, MA, USA)	CD1 mice (022) (Kindly provided by Dr. Ferguson lab)	Charles River Laboratories
Experimental Model: Cell Lines	**Supplier**	**Experimental Model: Cell Lines**	**Supplier**
HEK293 cells	ATCC (Manassas, VA, USA)	HEK293T-Glo cells	(Kindly provided by Dr. Giguère lab)
HTLA cells	(Kindly provided by Dr. Giguère lab)	HTL cells	(Kindly provided by Dr. Giguère lab)
Culture Reagents	**Supplier**	**Culture Reagents**	**Supplier**
Eagle's Minimal Essential Medium (EMEM)	Wisent Bioproducts (Saint-Jean-Baptiste, QC, Canada).	Dulbecco's Modified Eagle Medium (DMEM)	Corning, Canada
EMEM (without phenol red)	Wisent Bioproducts	DMEM (without phenol red)	Wisent Bioproducts
Fetal Bovin Serum (FBS)	Thermo Fisher Scientific	Bovine Calf Serum (BCS)	Thermo Fisher Scientific
Phosphate-Buffered Saline (PBS)	Wisent Bioproducts	0.25% Trypsin ethylenediaminetetraacetic acid (EDTA)	Thermo Fisher Scientific
Gentamycin	Fisher Scientific	Puromycin	Thermo Fisher Scientific
Hygromycin	Millipore Sigma (Oakville, ON, Canada).	Hanks' Balanced Salt Solution (HPSS)	Thermo Fisher Scientific
Neurobasal media	Thermo Fisher Scientific	B27 Supplement	Thermo Fisher Scientific
N2 Supplement	Thermo Fisher Scientific	GlutaMAX	Thermo Fisher Scientific
Hyclone Penicillin-Streptomycin	Fisher Scientific	Poly-L-Lysine	Millipore Sigma
µ-Slide 4 Well	Ibidi	8 Well Chamber, removable	Ibidi
Ibidi 35 mm #1.5 glass bottom dishes	Ibidi	Millicell Cell Culture Insert	Thermo Fisher Scientific
1.0 µm Gold Microcarriers (1652263)	Bio-Rad laboratories (Mississauga, ON, Canada	100 mm culture dishes	Sarstedt
6-, 12-, and 24-well plates, and 150 mm culture dishes	Fisher Scientific	Nunc 96- and 384-well clear bottom, white plates	Thermo Fisher Scientific
Chemical Reagents	**Supplier**	**Chemical Reagents**	**Supplier**
[^{3}H]-SCH23390	PerkinElmer (Boston, MA, USA).	Sodium L-Ascorbate (Ascorbic acid "AA")	Millipore Sigma
DA hydrochloride	Millipore Sigma	(+)-SCH23390 hydrochloride	Millipore Sigma
Dihydrexidine (DHX)	Bio-Techne (Toronto, ON, Canada)	(+)-SKF81297 hydrobromide	Bio-Techne
Cis-Flupentixol dihydrochloride	Millipore Sigma	Thiothixene	Millipore Sigma
(+)-Butaclamol hydrochloride	Millipore Sigma	Thioridazine hydrochloride	Millipore Sigma
Forskolin (FSK)	Millipore Sigma	Trypsin inhibitor	Millipore Sigma
Aprotinin	Millipore Sigma	Benzamidine	Millipore Sigma
Leupeptin	Millipore Sigma	Pepstatin A	Millipore Sigma
Phenylmethylsulfonyl Fluoride (PMSF)	Millipore Sigma	DNase	Millipore Sigma
DTT (Dithiothreitol)	Millipore Sigma	Ammonium Persulfate (APS)	Bio-Rad laboratories
IPTG (Isopropyl ß-D-1-thiogalactopyranoside)	Wisent Bioproducts	D-Luciferin Sodium Salt	Bio-Techne
Coelenterazine 400a (DeepBlueC)	Nanolight technology	Coelenterazine h	Nanolight technology

Tween-20	Bio-Rad laboratories	Triton X-100	Bio-Rad laboratories
Cytiva HyClone Bovin Serum Albumin (BSA)	Fisher Scientific	HEPES [4-(2hydroxyethyl)-1-piperazineethanesulfonic acid] buffer	Fisher Scientific
Saponin	Fisher Scientific	TEMED (Tetramethyl-ethylenediamine)	Bio-Rad laboratories
Ultrapure Acrylamide	Thermo Fisher Scientific	Ultrapure N,N'-methylenebisacrylamide	Thermo Fisher Scientific
Commercial Assays	**Supplier**	**Commercial Assay**s	**Supplier**
DC Protein Assay Kit	Bio-Rad laboratories	Bradford Protein Assay Dye Reagent Concentrate	Bio-Rad laboratories
O-phenylenediamine dihydrochloride (OPD)	Thermo Fisher Scientific	Pierce stable peroxide substrate buffer	Thermo Fisher Scientific
Prolong Glass Antifade Mountant with NucBlue Stain	Thermo Fisher Scientific	Amersham ECL	GE Healthcare (Mississauga, ON, Canada
Duolink In Situ PLA Probe Anti-Mouse PLUS	Millipore Sigma (DUO92001)	Duolink In Situ PLA Probe Anti-Rabbit MINUS	Millipore Sigma (DUO92005)
Duolink In Situ Detection Reagents FarRed	Millipore Sigma (DUO92013)	Duolink In Situ Mounting Medium with DAPI	Millipore Sigma (DUO82040)
Miscellaneous Materials	**Supplier**	**Miscellaneous Materials**	**Supplier**
pGEX4T1 vector	GE Healthcare	Overexpress C41 (DE3) Chem comp cells	Millipore Sigma
Costume-made primers used to generate the fusion proteins	Thermo Fisher Scientific	Phusion high fidelity DNA polymerase and dNTPs	Thermo Fisher Scientific
Restriction enzymes	Fermentas Life Sciences (Burlingto, ON, Canada)	Restriction enzymes	New England Biolabs (Pickering, ON, Canada)
Polyvinylidene Difluoride (PVDF) membrane	Bio-Rad laboratories	Precision Plus Dual Color Standards	Bio-Rad laboratories
5X Transfer buffer	Bio-Rad laboratories	Paraformaldehyde Aqueous Solution	Electron Microscopy Sciences (Hatfield, PA, USA)
Bio-Safe Degradable Scintillation Cocktail	Research Products International (Mount Prospect, IL, USA)	Glutathione Sepharose 4B	Millipore Sigma
Instruments	**Supplier**	**Instruments**	**Supplier**
Trans-Blot Turbo System	Bio-Rad laboratories	Micro Chemi DNR Bio-Imaging System	Frogga Bio Scientific Solution (Concord, ON, Canada)
Brandel M-48 Semi-Automated Harvesting System	Brandel	Beckman LS 6500 Liquid Scintillation Counter.	Beckman Coulter
Bekman Optima TLX Ultracentrifuge and TLA100.3 Rotor	Beckman Coulter	SpectraMaxM5	Molecular Devices
BioTek Synergy Neo2 Plate Reader	Agilent Technologies	BioTek Synergy H1 Multi-Mode Plate Reader	Agilent Technologies
Bio Mate 3 Spectrophotometer	Thermo Scientific	MX-TS Tissue Slicer	Siskiyou (Grants Pass, OR, USA)
Helios Gene Gun System	Bio-Rad laboratories	MicroBeta Plate Reader	Perkin Elmer
Software	**Supplier**	**Software**	**Supplier**
GraphPad	Prism	Gel Capture Chemi Acquisition Software	Frogga Bio Scientific Solution
Fiji	NIH	ImageJ	NIH
Gen5 software v3.11	BioTek Instruments	IMARIS	Oxford Instruments
Zeiss Zen software: Lite, Blue, Desk	Zeiss	BioRender	BioRender

Table 2.2. List of the Antibodies.

Primary Antibodies	Supplier	Cat#	Epitope	Working Dilution
Rabbit monoclonal **SAP102** (A7R8L) antibody	Cell Signaling Technology (Danvers, MA, USA)	47421	Synthetic peptide corresponding to residues near the CT of human SAP102 protein.	WB (1:1000)
Mouse monoclonal **SAP102** (S19-2) antibody	Invitrogen	MA5-27707	Fusion protein amino acids 1-120 of rat SAP102	IP (1:200) WB (1:1000) PLA (1:100) IF (1:200)
Rabbit monoclonal **PSD95** (D27E11) XP® antibody	Cell Signaling Technology	3450	Synthetic peptide corresponding to residues surrounding Gln53 of human PSD95.	WB (1/1000)
Mouse monoclonal **PSD95** antibody (clone 7E3-1B8)	Millipore Sigma	P246	Recombinant rat PSD95.	IP (1:200) WB (1:1000) PLA (1:100) IF (1/200)
Rat monoclonal **D1R** antibody (clone 1-1-F11 s.E6)	Millipore Sigma	D2944	Recombinant fusion protein containing the CT 97 amino acid of human D1 dopamine receptor.	IP (1:200) IF (1:200) WB (1:500)
Rabbit monoclonal Anti-**Dopamine Receptor D1** antibody (Recombinant)	Abcam (Cambridge, MA, USA)	ab81296	A synthetic peptide within Human Dopamine Receptor D1 aa 400 to CT	PLA (1:100)
Rabbit pT354-D1 (phospho-Dopamine Receptor 1 polyclonal Antibody)	7TM Antibodies	N/A	A synthetic phosphopeptide derived from human D1 around the phosphorylation site of Thr354.	WB (1:1000)
Mouse Anti-Dopamine **D1B (D5R)** Receptor Antibody, clone SG4-D1B	Millipore Sigma	MAB5292	Recombinant rat D1b Receptor, CT	IP (1:200)
Rabbit polyclonal Anti-DRD5 (**D5R**) antibody	Abcam	ab32620	A synthetic peptide within Human DRD5 aa 450 to the CT	PLA (1:100) WB (1:1000)
Rabbit monoclonal **phosphor ERK1/2** (D13.14.4E) XP® antibody [Phospho-p44/42 MAPK (Erk1/2) (Thr202/Tyr204)]	Cell Signaling Technology	4370	Synthetic phosphopeptide corresponding to Thr202/Tyr204 of human p44 MAP kinase.	WB (1:1000)
Rabbit monoclonal **total ERK1/2** (137F5) antibody [p44/42 MAPK (Erk1/2)]	Cell Signaling Technology	4695	Synthetic peptide corresponding to residues near the C-terminus of human p44 MAP kinase.	WB (1:1000)
Rabbit monoclonal **α-Tubulin** (11H10) antibody	Cell Signaling Technology	2125	Synthetic peptide corresponding to the amino terminus of human α-tubulin protein.	WB (1:2000)
Rabbit monoclonal **β-Arrestin 1** (D7Z3W) XP® antibody	Cell Signaling Technology	30036	Synthetic peptide corresponding to residues surrounding Arg363 of human β-arrestin 1 protein.	IP (1:200) WB (1:1000)
Rabbit monoclonal **β-Arrestin 2** (C16D9) antibody	Cell Signaling Technology	3857	Monoclonal antibody is produced by immunizing animals with recombinant human β-arrestin 2.	IP (1:200) WB (1:1000)
Mouse monoclonal **Dynamin-I** (3G4B6) antibody	Cell Signaling Technology	4565	Monoclonal antibody is produced by immunizing animals with a recombinant CT fragment of human dynamin-I.	WB (1:1000)
Rabbit monoclonal NMDA Receptor 1 (**GluN1**) (D65B7)	Cell Signaling Technology	5704	Synthetic peptide corresponding to residues surrounding Pro660 of the human NMDA Receptor 1.	WB (1:1000)
Rabbit NMDA Receptor 2A (**GluN2A**) Antibody	Cell Signaling Technology	4205	Synthetic peptide corresponding to residues surrounding Asn1174 of human NMDAR2A.	WB (1:1000)
Rabbit monoclonal NMDA Receptor 2B (**GluN2B**) (D8E10)	Cell Signaling Technology	14544	Synthetic peptide corresponding to residues surrounding Asp1253 of human NMDA Receptor 2B (GluN2B) protein.	WB (1:1000)
Rabbit monoclonal **Synaptophysin** (D8F6H) XP® antibody	Cell Signaling Technology	25056	Synthetic peptide corresponding to residues surrounding Gly299 of human Synaptophysin protein.	WB (1:1000)
Chicken polyclonal **MAP2** Antibody	Invitrogen	PA1-10005	Mix of recombinant human constructs of projection domain sequences, amino acids 235-1588.	IF (1:400)

Normal **Rabbit IgG** Polyclonal Antibody	Millipore Sigma	12-370		IP (1:200)
Normal **Mouse IgG**	Santa Cruz Biotechnology	SC-2025		IP (1:200)
Normal **rat IgG**	Santa Cruz Biotechnology	SC-2026		IP (1:200)
Mouse anti-FLAG® M2 monoclonal antibody	Millipore Sigma	F3165		IF (1:400)
Rabbit anti-HA polyclonal antibody	Millipore Sigma	H6908		IF (1:400)
Primary Antibodies Conjugated-HRP	**Supplier**	**Cat#**	**Working Dilution**	
Mouse anti-**FLAG**® M2-monoclonal antibody-**HRP**	Millipore Sigma	A8592	WB (1:2000) ELISA (1:20,000)	
Mouse monoclonal Anti-**HA−Peroxidase** antibody	Millipore Sigma	H6533-1VL	WB (1:2000)	
Rabbit **GFP** Polyclonal Antibody, **HRP**	Invitrogen	A10260	WB (1:2000)	
GST Tag Polyclonal Antibody, **HRP**	Thermo Fisher Scientific	A190-122P	WB (1:20,000)	
Primary Antibodies Conjugated-Agarose	**Supplier**	**Cat#**	**Application**	
Anti-FLAG® M2 **Affinity Gel** (mouse monoclonal antibody- agarose)	Millipore Sigma	A2220	IP (50 µl/reaction)	
Pierce™ **Anti-HA Agarose** (Mouse monoclonal antibody)	Thermo Fisher Scientific	26181	IP (50 µl/reaction)	
Protein A/G PLUS-Agarose	Santa Cruz Biotechnology	SC-2003	IP (50 µl/reaction)	
Secondary Antibodies Conjugated-HRP	**Supplier**	**Cat#**	**Working Dilution**	
anti-**Rabbit** IgG, **peroxidase**-linked species-specific whole antibody (from donkey) Secondary Antibody, Cytiva	Fisher Scientific	45000682	WB (1:5000)	
anti-**Mouse** IgG, **peroxidase**-linked species-specific whole antibody (from sheep) Secondary Antibody, Cytiva	Fisher Scientific	45000679	WB (1:5000)	
Amersham ECL **Rat** IgG, **HRP**-linked whole antibody (from goat)	GE Healthcare	NA935	WB (1:5000)	
Secondary Antibodies Conjugated-Alexa Fluor	**Supplier**	**Cat#**	**Working Dilution**	
Chicken anti-**Rabbit** IgG (H+L) Cross-Adsorbed Secondary Antibody, **Alexa Fluor™ 488**	Invitrogen	A-21441	IF (1:800)	

Chicken anti-**Mouse** IgG (H+L) Cross-Adsorbed Secondary Antibody, **Alexa Fluor™ 488**	Invitrogen	A-21200	IF (1:800)	
Goat anti-**Chicken** IgY (H+L) Secondary Antibody, **Alexa Fluor™ 488**	Invitrogen	A-11039	IF (1:800)	
Goat anti-**Mouse** IgG (H+L) Cross-Adsorbed Secondary Antibody, **Alexa Fluor™ 568**	Invitrogen	A-11004	IF (1:800)	
Goat anti-**Rat** IgG (H+L) Cross-Adsorbed Secondary Antibody, **Alexa Fluor™ 568**	Invitrogen	A-11077	IF (1:800)	
Goat anti-**Rabbit** IgG (H+L) Highly Cross-Adsorbed Secondary Antibody, **Alexa Fluor™ 594**	Invitrogen	A-11037	IF (1:800)	
Goat anti-**Mouse** IgG (H+L) Highly Cross-Adsorbed Secondary Antibody, **Alexa Fluor™ 594**	Invitrogen	A-11032	IF (1:800)	
Donkey anti-**Rabbit** IgG (H+L) Highly Cross-Adsorbed Secondary Antibody, **Alexa Fluor™ 647**	Invitrogen	A-31573	IF (1:800)	

Table 2.3. List of the DNA Plasmids.

DNA	Subcloned Vector	Source	DNA	Subcloned Vector	Source
pCMV5	Empty pCMV5 vector	Tiberi's lab	**pCDNA3.1**	Empty pCDNA3.1 vector	Tiberi's lab
D1R	untagged human D1R (hD1R) cloned in pCMV5	Tiberi's lab	**D5R**	untagged human D5R (hD5R) cloned in pCMV5	Tiberi's lab
HA-D1R	HA-tagged hD1R cloned in pCMV5	Tiberi's lab	**HA-D5R**	HA-tagged hD5R cloned in pCMV5	Tiberi's lab
Flag-D1R	Flag-tagged hD1R cloned in pCMV5	Tiberi's lab	**Flag-D5R**	Flag-tagged hD5R cloned in pCMV5	Tiberi's lab
D1R-GFP	hD1R fused with GFP2 cloned in pCMV5	Tiberi's lab	**D5R-GFP**	hD5R fused with GFP2 cloned in pCMV5	Tiberi's lab
D1R-Rluc	hD1R fused with Rluc cloned in pCMV5	Tiberi's lab	**D5R-Rluc**	hD5R fused with Rluc cloned in pCMV5	Tiberi's lab
D1R-Tango	Flag-tagged hD1R cloned in tango vector	Dr. Patrick Giguère	**D5R-Tango**	Flag-tagged hD5R cloned in tango vector	Addgene: 66272 (Dr. Bryan Roth)
Flag-D1R-ΔIL3N	Flag-tagged hD1R mutant (lack the aa Q224-T245) cloned in pCMV5	Tiberi's lab	**Flag-D5R-ΔIL3N**	Flag-tagged hD5R mutant (lack the aa Q255-S275) cloned in pCMV5	Tiberi's lab
Flag-D1R-ΔIL3C	Flag-tagged hD1R mutant (lack the aa G246-K265) cloned in pCMV5	Tiberi's lab	**Flag-D5R-ΔIL3C**	Flag-tagged hD5R mutant (lack the aa A276-K289) cloned in pCMV5	Tiberi's lab
Flag-D1R-ΔCT	Flag-tagged hD1R mutant (lack the aa C347-T446) cloned in pCMV5	Tiberi's lab	**Flag-D5R-ΔCT**	Flag-tagged hD5R mutant (lack the aa C375-H477) cloned in pCMV5	Tiberi's lab
Flag-SAP102	Flag-tagged rat SAP102 (rSAP102) cloned in pCMV5	Tiberi's lab	**Flag-PSD95**	Rat PSD95 (rPSD95)-Flag-tagged cloned in pCDNA5	Addgene: 15463 (Dr. Wei-dong Yao)
HA-SAP102	HA-tagged rSAP102 cloned in pCMV5	Tiberi's lab	**PSD95-RFP**	rPSD95 cloned in pTagRFP vector	Addgene: 52671 (Dr. Johannes Hell)
SAP102-GFP	Human SAP102 cloned in pCMV6-AC-GFP vector	Origene: RG210860	**PSD95-GFP**	rPSD95 in pEGFP-N1 vector	Dr. Richard Bergeron
HA-GbR2-GFP10	$GABA_B$ subtype GbR2-fused GFP subcloned in pcDNA3.1	Dr. Micheal Bouvier	**mCherry**		Dr. Jean-Claude Béïque
βArr1	Untagged βArr1 subcloned in pCMV5	Dr. Robert Lefkowitz	**βArr2**	Untagged βArr2 subcloned in pCMV5	Dr. Robert Lefkowitz
βArr1-YFP	βArr1 fused YFP	Dr. Stéphane Laporte	**βArr2-YFP**	βArr2 fused YFP	Dr. Stéphane Laporte
Flag-βArr2	Flag-tagged βArr2	Dr. Stephen Ferguson	**βArr2-V54D**	Untagged mutant form of βArr2 subcloned in pCMV5	Dr. Marc Caron
βArr1-TEV219	βArr1 fused TEV219 subcloned in pCDNA6	Dr. Patrick Giguère	**βArr2-TEV219**	βArr2 fused TEV219 subcloned in pCDNA6	Dr. Patrick Giguère
HA-dynamin I-K44A	Mutant form of dynamin	Dr. Sandra Schmid			

A-1

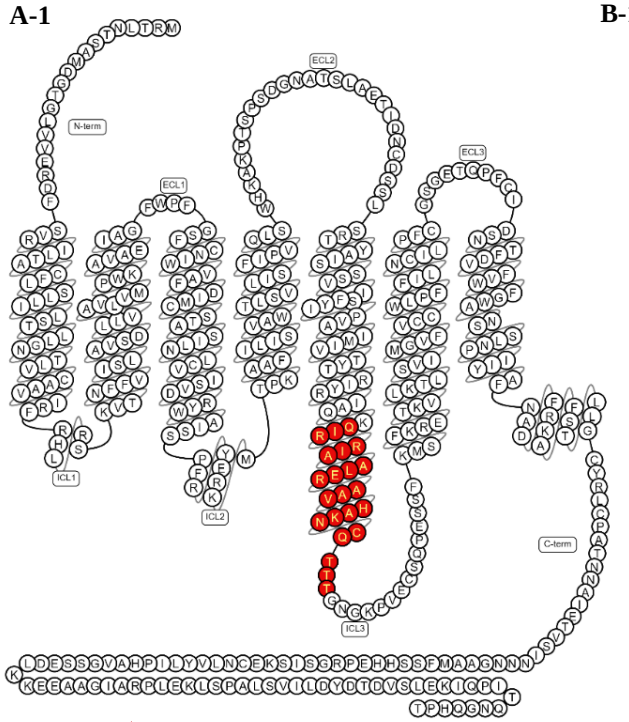

Flag-D1R-ΔIL3N (lack the aa Q224-T245)

B-1

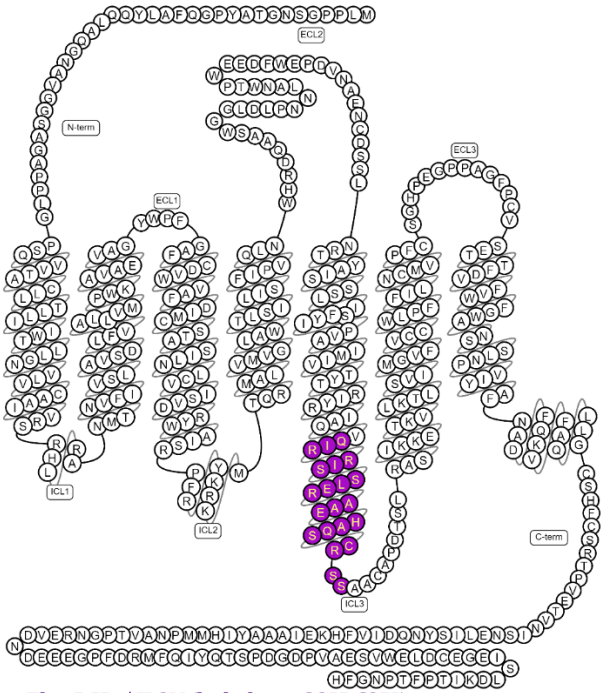

Flag-D5R-ΔIL3N (lack the aa Q255-S275)

A-2

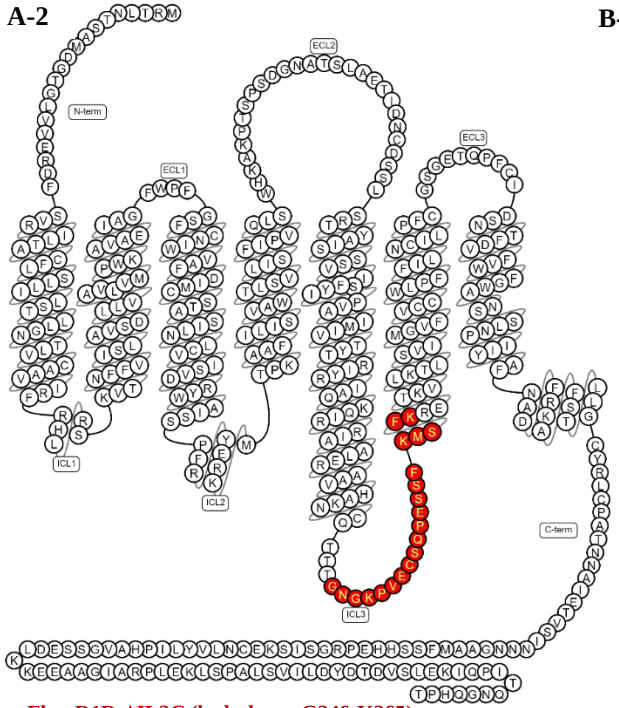

Flag-D1R-ΔIL3C (lack the aa G246-K265)

B-2

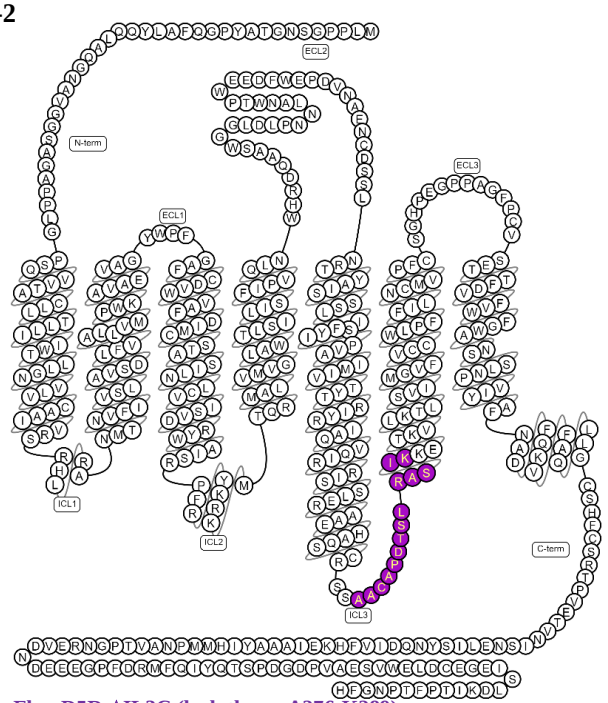

Flag-D5R-ΔIL3C (lack the aa A276-K289)

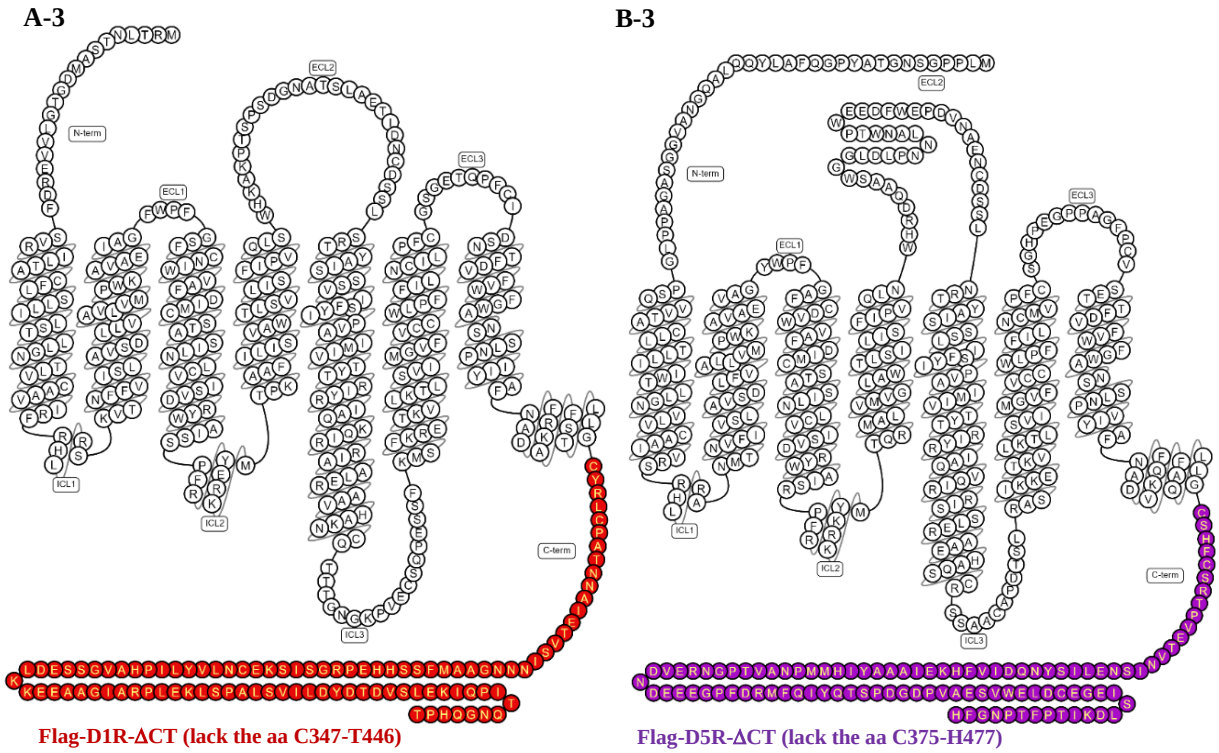

Fig. 2.1. Schematic Representation of Mutant Forms of Flag-D1R and Flag-D5R. Highlighted circles depict the deleted amino acids of Flag-hD1R (A) and Flag-hD5R (B). Created by gpcrdb.org.

3. Construction and Purification of Recombinant GST-Fusion Proteins

3.1. Construction of GST-fusion proteins for D1R and D5R

The IL3 (R219-K272) and CT (R338-T446) fragments of human D1R (UniProt: P21728), and the IL3 (R247-K296) and CT (F361-H477) fragments of human D5R (UniProt: P21918) were amplified by PCR using either hD1R or hD5R in pCMV5 as templates and custom-made primers. The PCR amplicons were digested with BamHI and SalI, except the D1R-CT amplicon, which was digested with BamHI and EcoRI, and ligated into the pGEX4T-1 vector linearized with the corresponding enzymes. DNA sequences from GST-tagged D1R and D5R were confirmed by automated DNA sequencing from Génome Québec (Nanuq). *Fig. 2.2. illustrates the GST-constructs of D1R and D5R utilized in my thesis.* Table 2.4 lists the oligonucleotides used to generate the different GST-D1R and D5R fusion proteins.

3.2. Construction of GST-fusion proteins for SAP102

The NT-PDZ1 (M1-M243), PDZ1 (N139-M243), PDZ2 (P237-A340), PDZ3 (E395-K494), SH3 (E486-H657), and GK (E649-L849) domains of rat SAP102 (UniProt: Q62936) were amplified by PCR using rSAP102 in pCMV5 as a template and custom-made primers. PCR amplicons were digested with EcoRI and SalI, and ligated into the pGEX4T-1 vector linearized with the same enzymes. DNA sequences of GST-tagged SAP102 fusion proteins were confirmed by automated DNA sequencing from Génome Québec (Nanuq). *Fig. 2.3. illustrates the GST-constructs of SAP102 utilized in my thesis.* Table 2.4 lists the oligonucleotides used to generate SAP102 fusion proteins.

3.3. Purification of GST-Fusion Proteins of D1R, D5R, and SAP102

The pGEX-4T1 constructs discussed above were cloned in the OverExpress^{TM} C41(DE3) competent cells and bacterial GST-tagged fusion proteins produced as indicated by the manufacturer. Glutathione-Sepharose 4B was used for protein purification, and the purified recombinant proteins were analyzed by SDS-PAGE followed by Coomassie Brilliant Blue R-250 staining and immunoblotting using an anti-GST antibody.

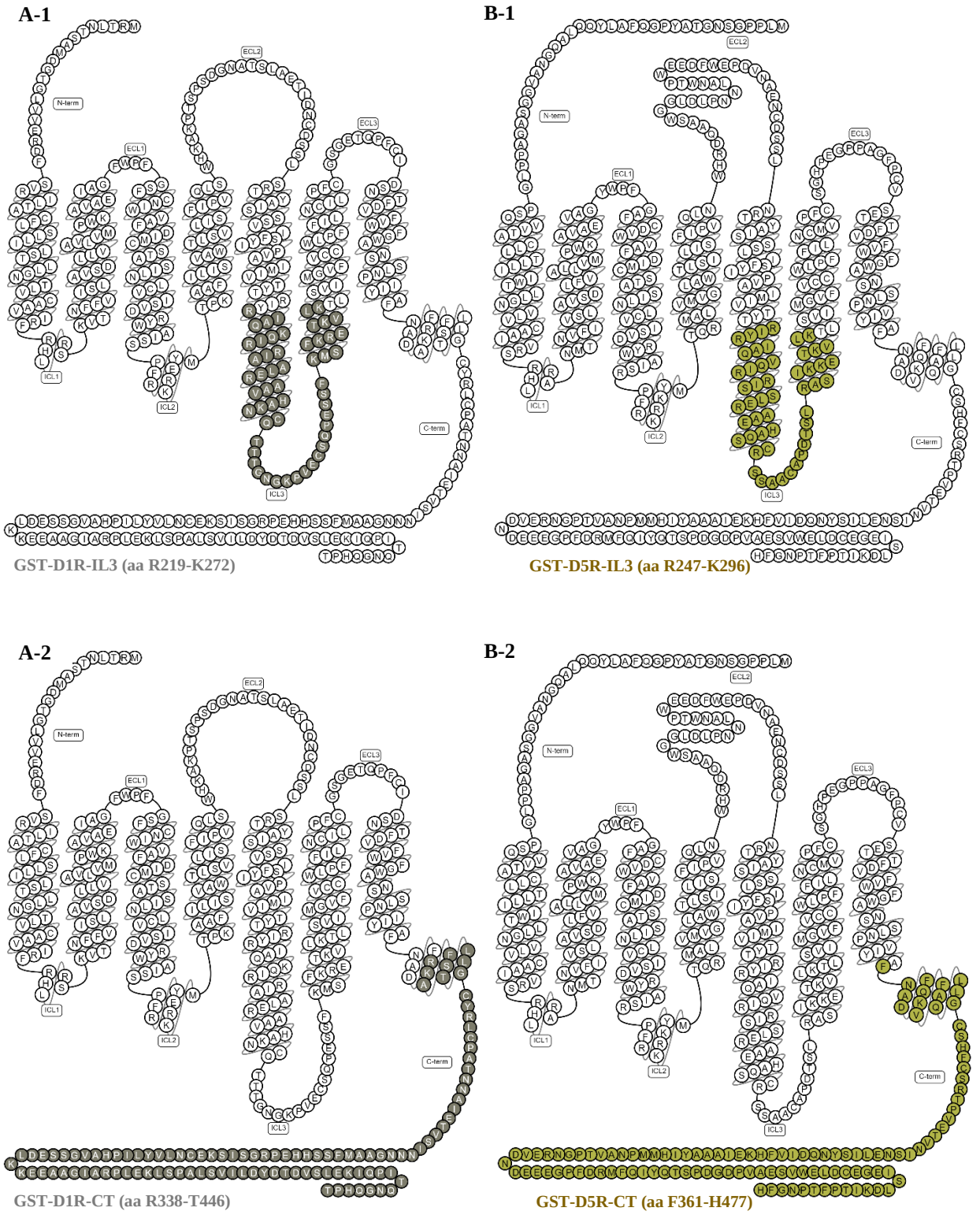

Fig. 2.2. Schematic Representation of the GST-Constructs of Purified Regions for D1R and D5R. Highlighted circles depict the purified regions of hD1R (A) and hD5R (B). Created by gpcrdb.org.

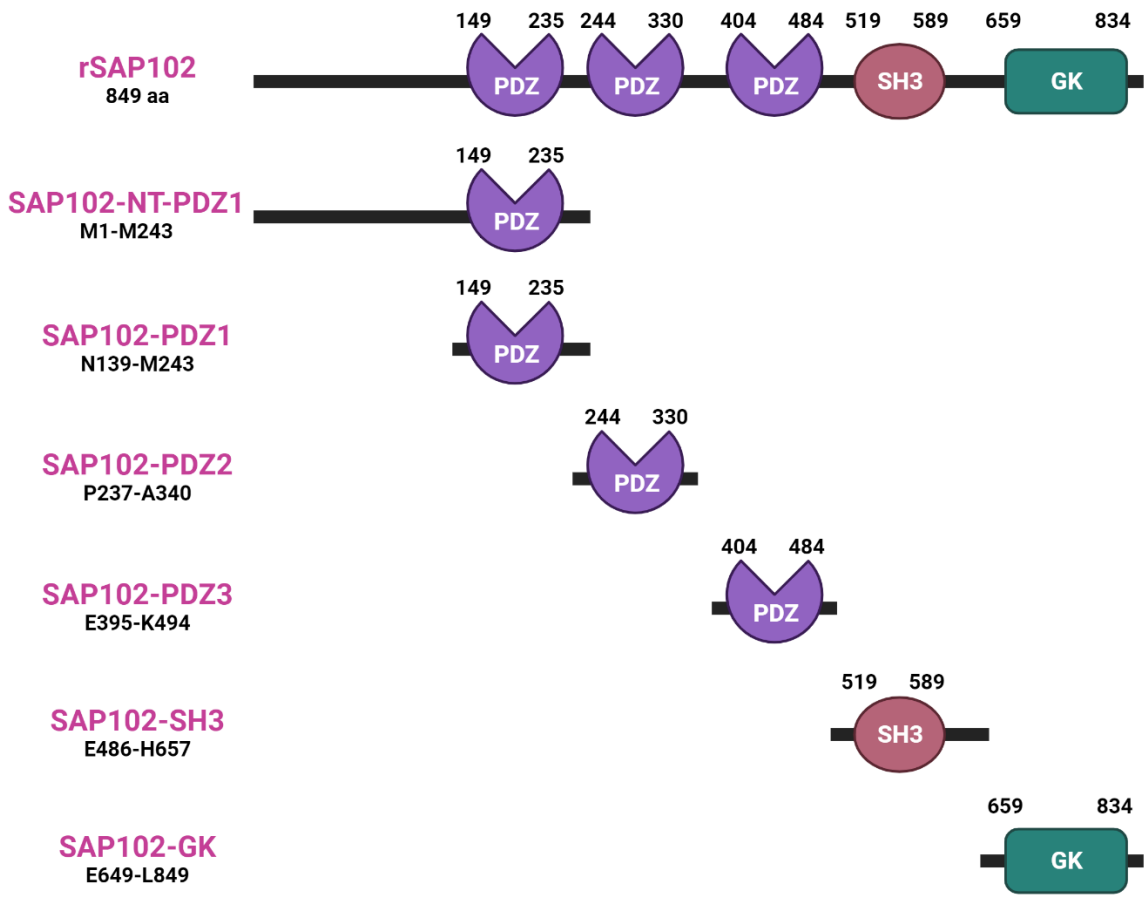

Fig. 2.3. Schematic Representation of the GST-Constructs of Purified Domains for SAP102.
Created with BioRender.com.

Table 2.4. List of the Primers.

Sequences of oligonucleotide primers used for the generation of i) IL3 and CT fusion proteins of D1R and D5R, and ii) NT, PDZ1, PDZ2, PDZ3, SH3, and GK fusion proteins of SAP102. Corresponding amino acid for the each fusion protein, is shown. Restriction enzymes used to subcloned these purified protein in PGEX4.1 are listed in the brackets. Detailed methods are described in material and method, section 3.

Fusion Protein	Oligonuceluotide Primers
D1R-purified proteins	
D1R-IL3 (R219-K272) (BamHI/SalI**)**	Forward: 5'- CTAG **GGATCC** AGG ATT GCT CAG AAA CAA ATA CGG CGC ATT -3' Reverse: 5'- CTAG **GTCGAC ACGCGT TCA** CTT CAG GAC TTT AGT TTC TCT -3'
D1R-CT (R338-T446) (BamHI/EcoRI**)**	Forward: 5'- CTAG **GGATCC** CGG AAG GCA TTT TCA ACC CTC TTA GGA TGC -3' Reverse: 5'- CTAG **GAATTC ACGCGT TCA** GGT TGG GTG CTG ACC GTT TTG -3'
D5R-purified proteins	
D5R-IL3 (R247-K296) (BamHI/SalI**)**	Forward: 5'- CTAG **GGATCC** CGC ATC TAC CGC ATC GCC CAG GTG CAG ATC -3' Reverse: 5'- CTAG **GTCGAC ACGCGT TCA** CTT GAG AAC CTT GGT CTC CTT -3'
D5R-CT (F361-H477) (BamHI/SalI**)**	Forward: 5'- CTAG **GGATCC** TTC AAC GCC GAC AAA CAG AAG GTG TTT GCC -3' Reverse: 5'- CTAG **GTCGAC ACGCGT TCA** ATG GAA TCC ATT CGG GGT GAA -3'
SAP102-purified proteins	
NT-PDZ1 domains (M1-M243), (EcoRI/SalI)	Forward: 5'- CTAG **GAATTC** CAC AAG CAC CAG CAC TGC TGT AAG TGC CCC - 3' Reverse: 5'- CTAG **GTCGAC** TCA CAT GAT AGT CTC AGG TGG GGG CTG TCG - 3'
PDZ1 domain (N139-M243), (EcoRI/SalI)	Forward: 5'- CTAG **GAATTC** GGC AGT GAT GGC ATG TTC AAG TAT GAG GAG - 3' Reverse: 5'- CTAG **GTCGAC** TCA CAT GAT AGT CTC AGG TGG GGG CTG TCG - 3'
PDZ2 domain (P237-A340), (EcoRI/SalI)	Forward: 5'- CTAG **GAATTC** CAG CCC CCA CCT GAG ACT ATC ATG GAG GTC - 3' Reverse: 5'- CTAG **GTCGAC** TCA AGC ATA CAT GTC GTT GAG GTG GAG ACT - 3'
PDZ3 domain (E395-K494), (EcoRI/SalI)	Forward: 5'- CTAG **GAATTC** GAA GAC TTT ACC AGA GAG CCC CGC AAG ATC - 3' Reverse: 5'- CTAG **GTCGAC** TCA CTT GGA TTC AAA GCG ACT GTA CTC TTC - 3'
SH3 domain (E486-H657),(EcoRI/SalI)	Forward: 5'- CTAG **GAATTC** GAA GAG TAC AGT CGC TTT GAA TCC AAG ATC - 3' Reverse: 5'- CTAG **GTCGAC** TCA ATG AAT TTC TTG TCG TGT CAC TGG CTC - 3'
GK domain (E649-L849), (EcoRI/SalI)	Forward: 5'- CTAG **GAATTC** GAG CCA GTG ACA CGA CAA GAA ATT CAT TAT - 3' Reverse: 5'- CTAG **GTCGAC** TCA GAG TTT TTC AGG GGA TGG GAC CCA AAT- 3'

4. Brain Tissue Homogenization

Hippocampal, striatal, and cortical tissues were collected from Sprague-Dawley rats from postnatal day 2 (P2), P8, P21, and from the adult dam (~P60) (kindly provided by Dr. Béïque's lab). In accordance with protocol approved by the University of Ottawa's Animal Care Committee (Protocol: CMM-1711), animals were anesthetized in an isoflurane infused chamber, decapitated, and hippocampi, striatal, and cortical tissues were collected and quickly snap frozen in liquid nitrogen.

4.1. Subcellular Fractionation of Brain Tissues from Adult Rats

The biochemical fractionation of cortical tissues was processed as previously described following sequential centrifugation with minor modification (Carling et al, 1980). All steps were performed on ice setting, ice-cold buffers, and 4°C centrifugation. Cortical tissues of rat (P21, male) were thawed on ice and homogenized using a Dounce tissue homogenizer (10-15 strokes) in a homogenization buffer (20 mM Tris-HCl (pH 7.4); 5 mM EDTA; 1mM EGTA; 1mM $NaHCO_3$; 1mM $MgCl_2$; 0.5mM $CaCl_2$; 10 mM NaF; 2 mM Na_3VO_4) and protease inhibitors (10 µg/ml benzamidine, 10 µg/ml soybean trypsin inhibitor, 20 µg/ml PMSF, 10 µg/ml leupeptin, 2 µg/ml aprotinin, 1 µg/ml pepstatin A) containing 320 mM sucrose. The total homogenates were transferred to microcentrifuge tubes and rotated end-over-end for 30 min, followed by centrifugation at 800 *g* for 10 min, and the resultant supernatants (S1) were subjected to further centrifugation for 15 min at 10,000 *g*. The second pellet (P2) was subjected to hypoosmotic lysis by suspending it in homogenization buffer containing 36 mM sucrose. The P2 suspension was left on ice with occasional mixing and subsequently centrifuged at 25,000 *g* for 30 min. The resultant pellet (crude synaptosomal membrane-P3) was solubilized in ice-cold RIPA buffer (50 mM Tris (pH 8.0); 150 mM NaCl; 0.1% (W/V) SDS; 5 mM of EDTA; 1% (w/v) NP-40; 0.5% (w/v) Na deoxycholate; 10 mM NaF; 10 mM disodium pyrophosphate) with protease inhibitors ($RIPA^+$) at 4°C by rotation for 30 min, then centrifuged for 10 min at 16,000 *g*. The supernatant LP1 were collected, and the P4 pellets were resuspended in the homogenization buffer containing 320 mM sucrose. The suspension was layered on top of a discontinuous sucrose gradient containing 0.8M/1.0M/1.2M sucrose. Ultracentrifugation at 82,500 *g* for 2 h were performed using in a Bekman Optima TLX Ultracentrifuge using a TLA100.3 rotor. The fractions yielded at the 0.8M/1.0M sucrose interface (vesicular fraction, VesF), the 1.0M/1.2M sucrose interface

(synaptosomal membrane fraction, SMF), and the pellet (ER/microsomes/mitochondrial-P5) were collected using a needle syringe. After SMF collection, samples were resuspended in homogenization buffer containing 0.5% Triton X-100 and 160 mM sucrose, and centrifuged for 20 min at 32,000 *g*. The resulting pellets (P6) were resuspended in homogenization buffer without sucrose and was layered on top of a discontinuous sucrose gradient containing 1.0M/1.5M/2.0M sucrose. Ultracentrifugation at 200,000 *g* for 2 h was performed in a Bekman Optima TLX Ultracentrifuge using a TLA100.3 rotor. The fractions yielded at the 1.5M/2.0M sucrose interface (PSD fraction) were collected using a needle syringe, resuspended in homogenization buffer containing 0.5% Triton X-100, recentrifuged again at 200,000 *g* for 20 min, and supernatant of the PSD-enriched fraction was collected. Protein concentration of different fractions was measured using Bio-Rad DC protein assays and BSA as a protein standard. Aliquots were mixed with 50 µl of SDS-loading buffer (25 mM Tris-HCl (pH 6.5); 10% [v/v] glycerol; 8% [w/v] sodium dodecyl sulfate [SDS]; 5% [v/v] β-mercaptoethanol; and 0.004% [w/v] bromophenol blue) and stored at -20°C until further analysis. *Fig. 2.4 summarizes the subcellular fractionation strategy of brain tissue by ultracentrifugation procedure.* Moreover, hippocampal, and cortical LP1 fractions were prepared from P2, P8, P21, and P60. Aliquots of 50 µg proteins were prepared in sample buffer and kept at -20°C until further analysis.

4.2. in vivo Immunoprecipitation

LP1 fractions of hippocampal, striatal, and cortical lysates were collected, solubilized for 60 min, and processed for immunoprecipitation experiments. Protein concentration of lysates was measured using Bio-Rad DC protein assays. Lysates of hippocampus (0.5 mg), striatum (1 mg), and cortex (1.5 mg) were subjected to immunoprecipitation with 5 µg/ml of selected antibodies (indicated in figure legend of corresponding results), and incubated at 4^{o}C by rotation overnight. The following day, 50 µl of protein A/G plus agarose were added to the immunoprecipitated samples and incubated at 4^{o}C by rotation overnight. Beads were then pelleted, washed four times with 1 ml of ice-cold RIPA^{+} buffer with protease inhibitors. The protein complexes were eluted by adding 50 µl of SDS-loading buffer and stored at -20°C until further analysis. In addition, prior to addition of antibodies, inputs of 50 µg of proteins from lysates were prepared in loading buffer and stored at -20°C.

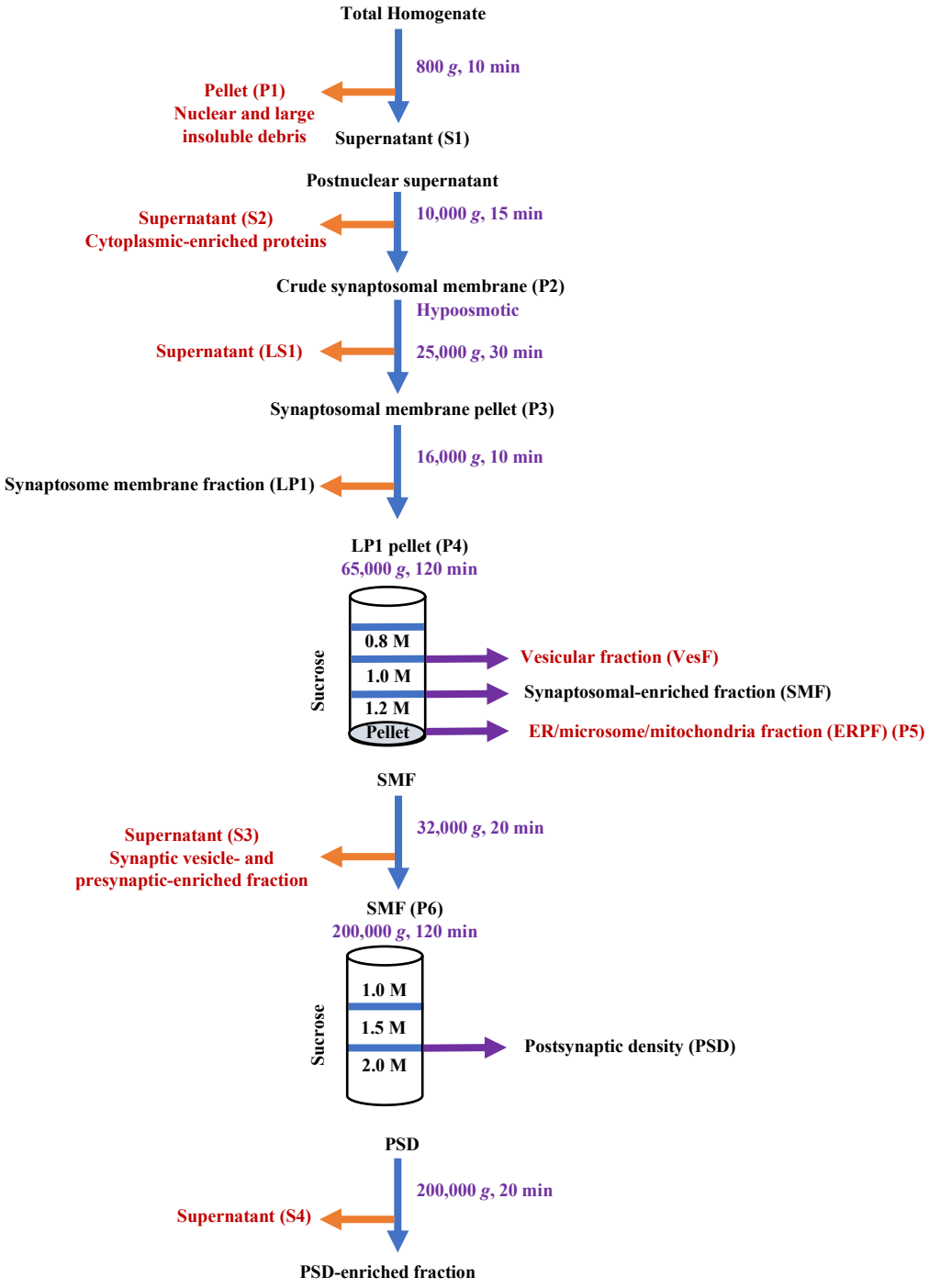

Fig. 2.4. Schematic Summary for the Subcellular Fractionation Procedure by Ultracentrifugation.

4.3. in vivo GST-Pulldown Assay

Cortical lysates (LP1 fraction) were collected and processed for GST-pulldown assay, by incubating 1 mg of lysates with purified GST protein (5 µg of purified protein + 25 µl of glutathione sepharose® 4B resin). Samples were incubated at 4ºC by rotation overnight, then washed four times with 1 ml ice-cold $RIPA^{+}$ buffer. Samples were then eluted and kept at -20°C until further analysis. Inputs of 50 µg of proteins from lysates were prepared in loading buffer.

5. Immunoblotting

Eluted and input samples from coimmunoprecipitation and GST-pulldown experiments were boiled briefly for 5 min prior to loading onto 10% (v/v) acrylamide gels for SDS-PAGE. Bio-Rad Trans-Blot Turbo System and transfer buffer (Bio-Rad) were used to transfer proteins onto PVDF membranes at 25 V for 10 min. Membranes were then incubated in blotto solution (50 mM Tris-HCl (pH 8.0); 80 mM NaCl; 2 mM CaCl2; 5% [w/v] nonfat dry milk; 0.2% [v/v] NP-40; and 0.02% [w/v] NaN3) overnight on a rocking platform shaker at 4°C. The following day, membranes were rinsed three time with Tris-buffered saline containing Tween-20 (TBS-T) (20 mM Tris-HCl (pH 7.4); 137 mM NaCl; and 0.2% [v/v] Tween-20), then incubated with desired antibodies diluted in TBS on a rocking platform shaker at 4°C overnight. Table 2.3. lists the antibodies and dilutions used according to the experimental plan. The following day, membranes were washed three times with TBS-T for 10 min and incubated for 1 hour at room temperature (RT) with appropriate secondary HRP-conjugated antibodies (rabbit, mouse, or rat) diluted in TBS-T (1:5000). Membranes were then washed three times with TBS-T for 30 min and protein bands were visualized using ECL reagents. Images were acquired using MicroChemi DNR Bio-Imaging System and GelCapture Chemi acquisition software. It is worth mentioning that for some experiments membranes were reprobed with different antibodies to measure input levels. To do so, membranes were incubated with stripping buffer (500 mM glacial acetic acid; 100 mM β-mercaptoethanol; and 0.5 % [w/v] SDS) for 20 min to remove bound antibodies. Membranes were then briefly washed with TBS-T and incubated with blotto buffer, and appropriate antibody added to reprobe protein of interest (immunoprecipitated protein, input or loading control). The densitometric analysis of protein bands was performed using ImageJ software, as described in the legend of the corresponding figures.

6. Hippocampal Organotypic Cultures

Organotypic slices (kindly provided by Dr. Béïque's lab) were prepared from both male and female Sprague-Dawley rats (P8) using the interface method (Soares et al, 2014). In accordance with protocol approved by the University of Ottawa's Animal Care Committee (Protocol: CMM-1711), animals were anesthetized in an isoflurane infused chamber, decapitated, and hippocampi were removed in ice cold cutting solution: 119 mM choline chloride, 2.5 mM KCl, 4.3 mM $MgSO_4$, 1 mM $CaCl_2$, 1 mM NaH_2PO_4–H_2O, 1.3 mM Na-ascorbate, 11 mM glucose, 1 mM kynurenic acid, 26.2 mM $NaHCO_3$, saturated with 95% O_2 and 5% CO_2 (pH = 7.3; 295-310 mOsm/L). Transverse slices were cut at 400 μm thickness using a MX-TS tissue slicer and cultured on 0.4 mm millicell culture inserts at a temperature of 34^{o}C. Every third day media was changed.

6.1. Immunostaining of Hippocampal Organotypic Cultures

At day in vitro 28 (DIV28), organotypic cultures were processed for immunostaining as described (Gogolla et al, 2006). Briefly, hippocampal slices were fixed by adding 4% paraformaldehyde dissolved in PBS (4% PFA/PBS) above and beneath the membrane insert for 5 min, followed by the addition of 20% methanol, then slices were permeabilized by adding 0.5% triton X-100 in PBS overnight at 4°C. Blocking solution (20% BSA in PBS), primary antibody, and secondary antibody were added to the slices, and each step was incubated overnight at 4°C. The primary and secondary antibody were diluted in 5% BSA in PBS. After washing step, slices were mounted (ProLong mountant with NucBlue stain) on glass slide and stored at 4°C in dark box. Confocal laser imaging was performed using a Zeiss LSM880 AxioObserver Z1 confocal microscope with AiryScan FAST module, using a 63x/1.4 NA, oil immersion Plan-Apo objective, and Zen Blue 2.3 software. Image z-stack acquisition was performed under the same confocal setting, using laser lines at wavelength: 405nm, 488nm, and 561nm.

6.2. Biolistic DNA Transfection of Hippocampal Organotypic Cultures

Organotypic slices were biolistic transfected using a gene gun method (Soares et al, 2014). Hippocampal slices were transfected at DIV7 using a Helios handheld gene gun (Bio-Rad). Cartridges for the gene gun were prepared in advance by precipitating 50 μg of cDNA plasmid onto 8-10 mg of gold microparticles (1.0 μm diameter; Bio-Rad) at a ratio of 80/20 by weight of D1R-GFP and mCherry plasmids, respectively. The precipitation step was performed in a 0.1 M

KH_2PO_4 buffer solution containing 0.05 mM protamine sulfate. The DNA-gold precipitate was washed and suspended three times in 100% ethanol before loading in the tubing station. Once the cartridges were dried and cut, they were placed in a sealed container with desiccant pellets at 4°C until used. The DNA-coated gold particles were delivered to the slice using ~180 psi of helium air pressure. A modified gene gun barrel was used to protect slices from helium blast. Imaging experiments were performed 3 days after biolistic transfection. Simultaneous two-photon imaging was performed using a Zeiss LSM710 confocal microscope, using two Ti:Sapphire pulsed lasers (MaiTai DeepSee, Spectra Physics) tuned to 810 nm for imaging GFP and mCherry. Image acquisitions were performed by Zen Black 2.3 software using a Plan-Apochromat 20x/1.4 NA, water immersion objective. Image z-stacks were acquired under the same confocal setting along the z-axis.

6.3. Protein Coimmunoprecipitation from Hippocampal Organotypic Cultures

At DIV28, hippocampal slices were collected in glass tube containing $RIPA^+$ buffer, homogenized using Brinkmann Polytron (velocity of 15,000 rpm; 40 sec), solubilized at 4°C by rotation for 1 h, and then centrifuged at 13,000 *g* for 10 min at 4°C. Protein concentration of lysates was measured using Bio-Rad DC protein assays. Hippocampal culture lysates containing 0.5 mg of proteins were subjected to immunoprecipitation using 5 µg/ml of selected antibodies, as described in the legend of corresponding figures. Lysates were mixed with antibodies by rotation overnight at 4°C. The following day, 50 µl of protein A/G plus agarose were added to the immunoprecipitated samples and incubated at 4^oC by rotation overnight. Beads were then pelleted, washed four times with 1 ml of ice-cold $RIPA^+$ buffer with protease inhibitors. The protein complexes were eluted by adding 50 µl of SDS-loading buffer and stored at -20°C until further analysis. In addition, inputs of 50 µg of proteins from lysates were prepared in SDS-loading buffer and stored at -20°C.

7. Embryonic Neuronal Cortical Cultures

Primary embryonic neuronal cultures were prepared from embryos aged E13-14 from CD1 mice as previously described (Kindly provided by Dr. Ferguson's lab) (Khacho et al, 2014). The experimental protocol was approved by the University of Ottawa Animal Care Committee (Protocol: CMMe-3346). In brief, brain cortices were extracted by removing the olfactory bulbs, cerebellum, and meninges. To dissociate into single cells, tissues were chemically digested with

trypsin and mechanically digested using flame-polished pasteur pipettes. Neurons were seeded in 35mm glass bottom culture dish (0.75 x 10^6 cells/mL) or in 6-well plate (1 x 10^6 cells/mL) coated with Poly-L-lysine (PLL) for imaging and immunoblotting studies. Neurons were cultured in a humidified incubator at 37°C with 5% CO_2 in neurobasal media containing B27; N2; 100 Units/mL Penicillin/Streptomycin, and GlutaMAX for 10 days *in vitro*. A half media change was performed every third day.

7.1. Immunostaining of Embryonic Cortical Cultures

At DIV 10, primary neuronal cultures were fixed in 4% PFA/PBS for 15 min at RT, then washed twice with PBS. Cells were then permeabilized in 0.5% Triton X-100 in PBS, and then incubated in blocking solution containing 0.5% Triton X-100 and 5% BSA in PBS for 2 h at RT. The cells were then incubated in primary antibodies diluted in PBS containing 0.3% Triton X-100 and 1% BSA overnight at 4°C, followed by incubation with corresponding species secondary fluorescent antibodies overnight at 4°C. The coverslips with cells were washed and mounted with ProLong mountant with NucBlue stain. Epifluorescence images were acquired using Zeiss AxioObserver Z1 (inverted) microscope with 63x/1.4 NA, oil immersion Plan-Apo objective, AxioCam MRm CCD, X-Cite XYLIS LED, and Zen Blue 2.3 software. Image z-stack acquisition was performed under the same setting, using filters: blue (Ex 395nm, Em 420nm), green (Ex 470/40nm, Em 525/50nm), and red (Ex 545/30nm, Em 620/60nm). Images then were deconvolved using Zen Desk software, and colocalization analysis by ImageJ.

7.2. In situ Proximity Ligation Assay (PLA) on Embryonic Cortical Cultures

At DIV 10, primary neuronal cultures were fixed in 4% PFA/PBS for 15 min at RT. After washes with PBS, cells were permeabilized for in 0.5% Triton X-100/PBS for 15 min. Duolink PLA protocol was then proceeded according to the manufacturer's instructions by adding the blocking buffer for 2 h at RT (Duolink in Situ PLA, Millipore Sigma). This was followed by an overnight incubation of primary antibodies diluted in Duolink antibody diluent (1:100, rabbit-anti D1R; 1:100, rabbit anti-D5R; 1:100, mouse-anti SAP102; 1:100, mouse anti-PSD95) (Table 2.2). Amplification template oligonucleotides were hybridized to pairs of PLA probes (PLUS and MINUS) and circularized by ligation. Consecutive incubation of these neurons with Duolink PLA probes (mouse-conjugated PLUS and rabbit-conjugated MINUS, 1 h), ligation (30 min), and amplification (2 h) were performed in preheated humidity chamber at 37°C. The detection of the

amplicons was carried out using the Duolink *in situ* detection reagent, resulting in far red fluorescence signals (Cy5). After amplification, these cells were incubated with chicken anti-MAP2 antibody (neuronal marker for dendrites) overnight at 4°C, followed by an incubation with secondary anti-chicken-AF488 for 4 h. At the end of incubation period, cells were washed and mounted with Duolink mounting media with DAPI and kept in dark at 4°C. Epifluorescence images were acquired using Zeiss AxioObserver Z1 (inverted) microscope with 63x/1.4 NA, oil immersion Plan-Apo objective, AxioCam MRm CCD, X-Cite XYLIS LED, and Zen Blue 2.3 software. Image z-stack acquisition was performed under the same setting, using filters: blue (Ex 395nm, Em 420nm), green (Ex 470/40nm, Em 525/50nm), and far red (Ex 640/30nm, Em 690/50nm). Images then were deconvolved using Zen Desk software. Neuron labeling was performed using LabKit tool as a function in imageJ, followed by 3D image construction using IMARIS. PLA signals (spots) between 0.8-1.5 μm diameter were quantified, and 3D rendering image were generated.

7.3. Protein Coimmunoprecipitation from Embryonic Cortical Cultures

At DIV10, primary cortical neurons were solubilized with $RIPA^+$ buffer at 4^oC by rotation for 1 h, and then centrifuged at 13,000 *g* for 10 min at 4°C. Protein concentration of lysates was measured using Bio-Rad DC protein assays. 0.5 mg of cortical culture lysates were immunoprecipitated with 5 μg/ml of desired antibodies, as described in the legend of corresponding results, and incubated at 4^oC by rotation overnight. The following day, 50 μl of protein A/G plus agarose were added to the immunoprecipitated samples and incubated at 4^oC by rotation overnight. Beads were then pelleted, washed four times with 1 ml of ice-cold $RIPA^+$ buffer with protease inhibitors. The protein complexes were eluted by adding 50 μl of SDS-loading buffer and stored at -20°C until further analysis. In addition, inputs of 50 μg of proteins from lysates were prepared in loading buffer and stored at -20°C.

8. Studies in HEK293 Cells

Human Embryonic Kidney (HEK293) cells were cultured between passages 40-52 in EMEM supplemented with 10% (v/v) heat-inactivated FBS and 40 μg/ml gentamicin in a humidified atmosphere containing %5 CO_2 incubator at 37°C. HEK293 cells were utilized for radioligand

binding studies, coimmunoprecipitation and GST-pulldown assays, and phosphorylation, western blotting, ELISA, BRET, and immunostaining studies.

8.1. Transfection

Cells were seeded in 100-mm culture dishes (2.5 million cells/dish) and transiently transfected with different DNA plasmids using a modified calcium phosphate precipitation method as described (Plouffe et al, 2010). The amount of D1R and D5R DNA transfected were adjusted to obtain low to moderate receptor expression (1-3 pmol/mg membrane proteins) in line with reported mouse striatal D1R expression. SAP102, PSD95, βArr1, βArr2, and dynamin constructs were transiently transfected with 0.5 μg, unless otherwise stated. Empty pCMV5 vector was used to adjust the total amount up to 5 μg DNA/dish. Cells were incubated with DNA•calcium mixture overnight. The next day, cells were washed with PBS, detached with trypsin, resuspended in appropriate media, and reseeded in culture dishes or plates. Reseeded HEK293 cells were grown for an additional 36-48 h (day of experiment).

8.2. Radioligand Binding Assays

8.2.1. Crude Membrane Preparations

Radioligand binding assays were performed with crude membrane preparations made from transiently transfected HEK293 cells. On the day of the experiment, cells seeded in 100-mm ("mini binding" assays), or 150-mm (saturation and competition binding assays) dishes were put on ice and culture media removed. Cells were then washed with cold PBS, scraped in cold lysis buffer (10 mM Tris-HCl, pH 7.4; 5 mM EDTA, pH 8.0), and centrifuged for 20 min at 40,000 *g* and 4°C. The pellets were washed with lysis buffer and homogenized using a Brinkmann Polytron (velocity of 15,000 rpm for 20 sec), and homogenates centrifuged again for 20 min at 40,000 *g* and 4°C. The final pellets obtained from 100-mm dishes were homogenized in resuspension buffer (62.5 mM Tris-HCl, pH 7.4; and 1.25 mM EDTA, pH 8.0) to perform "mini binding" assays on fresh membrane preparations. Final membrane pellets obtained from 150-mm dishes were homogenized in lysis buffer. An aliquot (0.6 ml) of membranes was added to resuspension buffer (2.4 ml) and used to generate saturation binding curves. The remaining of membrane preparations in lysis buffer were aliquoted in microcentrifuge tubes, snap frozen in liquid nitrogen and stored at -80°C for competition binding studies.

8.2.2. Binding Assays with D1-Class Radioligand [^{3}H]-SCH23390

Radioligand binding assays were carried out for 90-120 min with 100 µl of crude membranes in a final volume of 500 µl of reaction mixture containing binding buffer (50 mM Tris–HCl, pH 7.4; 120 mM NaCl; 5 mM KCl; 4 mM $MgCl_2$; 1.5 mM $CaCl_2$; 1 mM EDTA, pH 8.0), 50 µl of [^{3}H]-SCH23390 with (to determine total binding) or without 50 µl of inverse agonist *cis*-flupentixol (10 µM final, to determine non-specific binding). Membranes were harvested onto Whatman GF-C glass fiber filters using a Brandel M-48 semi-automated harvesting system. Filters were washed three times with cold washing buffer (50 mM Tris-HCl, pH 7.4; and 100 mM NaCl). [^{3}H]-SCH23390-bound filters were placed in Bio-Safe II biodegradable scintillation cocktail and radioactivity measured using a Beckman LS 6500 liquid scintillation counter. The protein concentration of membrane preparations was assessed using the Bio-Rad Bradford assay and BSA as a protein standard.

8.2.3. Saturation and Competition Binding Assays

Saturation binding curves were generated to assess the effect of MAGUKs on the equilibrium dissociation constant (K_d) and the maximal number of binding sites (B_{max}) of the D1-class radioligand [^{3}H]-SCH23390. HEK293 cells were transfected with 4.5 µg of untagged D1R or D5R alone or with 0.5 µg of HA-SAP102 or Flag-PSD95 grown in 150-mm culture dishes to make fresh membrane preparations as described in section 8.2.2. The saturation curves were generated using 100 µL of fresh membrane homogenates and increasing concentrations of [^{3}H]-SCH23390 (0.01-8 nM) to measure total and nonspecific binding levels as described in 8.2.2.

To determine the effect of MAGUKs on the binding of dopaminergic agonists and antagonists, series of competition curve studies to measure inhibitory constant (K_i) values. Frozen aliquots prepared from membrane homogenates used for saturation studies were thawed on ice and mixed in resuspension buffer and homogenized using Brinkmann Polytron (velocity of 15,000 rpm for 20 sec). As for saturation binding curves, 100 µl of membrane preparations were incubated with a fixed concentration of [^{3}H]-SCH23390 corresponding to K_d measured for the experimental condition and increasing concentrations of cold dopaminergic ligands (DA, DHX, SKF81297, thiothixene, SCH23390 and (+)-butaclamol) in a final volume of 500 µl binding reaction mixture as described in 8.2.2. All cold drug dilutions were prepared in milli-Q-water except DA, which was prepared in ascorbic acid (AA, 100 µM final) to prevent its oxidation. Binding parameters

from saturation (K_d, B_{max}) and competition (K_i) curves were best fitted by a nonlinear regression using Prism 10.0.3.

Saturation and competition studies were also performed to assess the effect of fusion proteins (Rluc and GFP) and Tango constructs of D1-class receptors.

8.2.4. "Mini Binding" Assays

To validate the low to moderate receptor expression in studies investigating the MAGUK-induced modulation of D1R and D5R signaling, B_{max} values of [^{3}H]-SCH23390 was determined with a single saturating concentration of the radioligand in the absence (total binding) and presence of cis-flupentixol (nonspecific binding) using fresh membranes prepared from cells seeded in 100-mm dishes as discussed in 8.2.1. The dpm counts obtained for specific binding (total minus nonspecific) and membrane protein concentrations were used to calculate B_{max} in pmol/mg membrane proteins with an equation previously described (Sedaghat et al, 2015).

8.3. GST pulldown, Coimmunoprecipitation, and Phosphorylation Assays

On the day of the experiment, HEK293 cells in 100-mm dishes were washed twice with cold PBS and solubilized in cold RIPA$^+$ buffer with protease inhibitors (~1 ml). Solubilized lysates were collected in microcentrifuge tubes and rotated end-over-end for 1 h at 4°C, and then centrifuged at 13,000 g for 15 min at 4°C to pellet insoluble material and cell debris. Protein concentration of lysates was measured using Bio-Rad DC protein assays and BSA as a protein standard. Prior to perform assays, aliquots of 20 µg proteins used input samples were mixed with loading buffer and stored at -20°C until used.

For GST pulldown assays, microcentrifuge tubes containing 0.5 mg of solubilized lysates, 5 µg of purified GST fusion proteins and 25 µl of glutathione sepharose 4B were incubated at 4^{o}C by rotation overnight. Prior to the solubilization step for immunoprecipitation studies, agonist-induced signaling complex formation and D1R phosphorylation were assessed as follows. Culture media was replaced with incubation buffer (EMEM without phenol red; 20 mM HEPES; and 10 µg/ml gentamicin) containing either AA (100 µM) or DA (10 µM, prepared in AA), and cells incubated for 15 min at 37°C in a humidified atmosphere containing 5% CO_2. Following the solubilisation and input samples steps, 0.5 mg solubilized lysates were incubated with 50 µl of either anti-Flag agarose or anti-HA agarose beads at 4^{o}C by rotation overnight. At the end of

incubation, glutathione sepharose 4B and antibody matrix beads were washed four times with cold $RIPA^+$ buffer, and samples eluted with 50 µl of SDS-loading buffer. Eluted samples from GST-pulldown and coimmunoprecipitation assays, and input samples were boiled briefly for 5 min prior to loading on 10% (v/v) acrylamide gels for SDS-PAGE. D1R and D5R expression were assessed as described in section 8.2.4.

8.4. ERK1/2 Activation Assays

HEK293 cells transfected with Flag-D1R, Flag-D1R+HA-SAP102, Flag-D1R+PSD95-RFP, Flag-D5R, or Flag-D5R+PSD95-RFP, were seeded 6-well plates and grown overnight. The next day, cells were serum starved by replacing complete EMEM with serum-free medium containing 1% (w/v) BSA and 40 µg/ml gentamicin. Cells were grown in serum-free media for an additional 24 hours prior to incubation with AA (100 µM, basal) or DA (10 µM, prepared in AA) for 5 min at 37°C in a humidified atmosphere containing 5% CO_2. Following treatment, cells were washed with cold PBS and then scraped from wells in lysis buffer containing protease inhibitors. Lysates were collected in microcentrifuge tubes and sonicated for 15 sec (20 kHz) (Fisher Brand). Protein concentrations in lysates were then determined using Bradford Bio-Rad protein assays. Western blot samples were prepared with 20 µg of lysate proteins and combined with loading buffer. The D1R and D5R expression was measured as described in section 8.2.4.

8.5. Enzyme-Linked Immunosorbent Assays (ELISA)

HEK293 cells were transfected with Flag-D1R or Flag-D5R alone, co-transfected with HA-SAP102 or PSD95-RFP, or triple-transfected with mutant forms of dynamin (HA-dyn-1-K44A) or βArr2 (βArr2-V54D). For ELISA, cells were transfected with the following amounts of plasmid DNAs: 0.1 µg/dish of receptor, 0.5 µg of HA-SAP102 or PSD95-RFP, and 1 µg of HA-dyn-1-K44A or βArr2-V54D. Empty pCMV5 vector was used to adjust the total amount of transfected DNA to 5 µg/dish. Following transfection, cells were reseeded in 12-well plates (100,000 cells/well) and grown for 36-48 hours.

To measure surface and total expression of receptors, culture media was aspirated, and cells washed with PBS and fixed with 3.7% (v/v) paraformaldehyde in PBS (3.7% PFA) for 10 min at RT. To assay receptor internalization, culture media was replaced with incubation buffer and cells were treated with either AA or DA and SKF81297 (10 µM prepared in AA) for 15min at 37°C in

a humidified atmosphere containing 5% CO_2. For recycling assays, DA containing media were aspirated, and incubation buffer added to allow the receptor recovery for an additional 10-30 min at 37°C in a humidified atmosphere containing 5% CO_2. Afterwards, media was aspirated, and cells washed with PBS and fixed with 3.7% PFA for 10 min at RT.

Following PFA fixation, cells were washed twice with 0.2% (w/v) BSA in PBS (0.2% BSA) for 10 min followed by a 30 min incubation in blocking solution 1% (w/v) BSA in PBS (1% BSA). Then, cells were incubated with anti-Flag-HRP antibody (1:20000) in 1% BSA for 1 h. Cells then were washed twice with 0.2%BSA in PBS for 10 min. To measure total expression (cell surface + internalized receptors), 1% (v/v) Triton-X-100 added in 0.2% or 1% BSA was included in washing and blocking steps. Subsequently, cells were incubated with 400 µl OPD (0.5 mg/ml dissolved in stable peroxide substrate buffer) and incubated in dark for 15 min. The reaction was stopped by adding 100 µl of 3N HCL in each well and 500 µl volume transferred to 96 well-plates. The optical density (OD) at 490 nm was read using a SpectraMaxM5. The background reading obtained from mock-transfected cells was subtracted to obtain corrected OD values. The percentage of receptor internalization was calculated from the difference between corrected OD values of cell surface receptor expression from vehicle and agonist-treated cells [(vehicle-treated−agonist-treated) / (vehicle-treated) × 100]. In addition, radioligand binding assays were performed to determine total D1R and D5R expression as described in section 8.2.4. To validate expression of SAP102, PSD95, βArr2-V54D and HA-dyn-1-K44A, transfected cells were reseeded in 6-well plates, and lysates collected and aliquoted for immunoblotting as described in section 5.

8.6. Immunostaining

HEK293 cells transiently transfected with HA-D1R, HA-D5R, Flag-SAP102, Flag-PSD95, βArr2-YFP, or different combination of these plasmids, as specified in the figure legends, were seeded on 12-mm diameter coverslips in a 24-well plate (50,000 cells/well). 36-48 hr after splitting, cells were fixed with 4% PFA/PBS for 10 min at RT. Coverslips were incubated twice with 0.37% glycine and 0.27% ammonium chloride in PBS for 10min at RT, blocked with 0.2% saponin/1% BSA/PBS for 30 min at RT. Excess blocking solution was decanted and coverslips were incubated overnight with corresponding antibodies: mouse monoclonal Flag-M2 antibody (1:400) and rabbit monoclonal HA antibody (1:400). Cells were then washed twice with 0.2% saponin/1% BSA/PBS followed by 4 h incubation in the dark with secondary antibodies conjugated-fluorophore

corresponding to species of primary antibodies, as described in figure legends. Coverslips were washed twice and treated with Prolong mountant with NucBlue reagent. Epifluorescence images were acquired using Zeiss AxioImager M2 microscope with 63x/1.4 NA, oil immersion Plan-Apo objective, AxioCam MRm CCD, X-Cite XYLIS LED, and Zen Blue 2.3 software. Image z-stack acquisition was performed under the same setting, using filters: blue (Ex 390/22nm, Em 460/50nm), green (Ex 470/20nm, Em 517/25nm), yellow (Ex 500/25nm, Em 535/30nm), red (Ex 560/40nm, Em 630/75nm), and far red (Ex 640/30nm, Em 690/50nm). Images then were deconvolved using Zen Desk software.

8.7. Bioluminescence Resonance Energy Transfer (BRET)

8.7.1. BRET1

BRET1 experiments were performed in HEK293 cells transfected with energy donor D1R-Rluc (0.5 µg), or co-transfected with energy acceptor βArr2-YFP alone (1.5 µg), or in the presence of Flag-SAP102 or Flag-PSD95 (1.5 µg). The following day, cells were reseeded (30,000 cells/well) into poly-L-lysine (PLL; 25 µg/ml)-coated 96-well clear bottom white-plates and cultured for 36-48 h. The day of the experiment, media were removed from the plates, and replaced with 60 µL of HBSS buffer, followed by the addition of 20 µL of DA at a 4X concentration. Plates were incubated at 37 °C for 30 min in a humidified atmosphere containing 5% CO_2 followed by addition of 20 µL of coelenterazine h in each well (5 µM/well). BRET1 signals were collected on a Synergy Neo2 plate reader (BioTek) using 460/40-nm (luciferase) and 540/25-nm (YFP) band pass filters. BRET ratio was determined by calculating the ratio of light that passed by the 540/25 filter to that passed by the 460/40 filter. In addition, radioligand binding assays were used to determine D1R expression as described in section 8.2.4. To validate βArr2, SAP102 or PSD95 expression, transfected cells were reseeded in 6-well plates, and lysates were collected and aliquoted for immunoblotting analysis as described in section 5.

8.7.2. BRET2

BRET2 experiments were performed in HEK293 cells transfected with energy donor D1R-Rluc and D5R-Rluc (0.5 µg) alone and with energy acceptor SAP102-GFP and PSD95-GFP (1.5 µg). As a negative control, $GABA_BR$ type 2 subunit (HA-GbR2-GFP10) was co-transfected with D1R-Rluc and D5R-Rluc. The following day, cells were reseeded (30,000 cells/well) into PLL-coated

96-well clear bottom white-plates and cultured for 36-48 h. On the day of the experiment, media was removed and replaced with 60 µL of HBSS buffer, followed by addition of 20 µL of single or serial dilution of DA at a 4X concentration. Plates were incubated at 37 °C for 30 min in a humidified atmosphere containing 5% CO_2, and 20 µL of coelenterazine 400a (Deep Blue C) was added to each well (5 µM/well). BRET2 signals were collected on a Synergy Neo2 plate reader (BioTek) using 410/80-nm (luciferase) and 515/30-nm (GFP) band pass filters. BRET ratio was determined by calculating the ratio of light that passed by the 515/30 filter to that passed by the 410/80 filter. Mini binding assays were used to determine D1R and D5R levels, as described above.

9. Studies in HEK293T-GloSensor Cells

HEK293T-GloSensor cells stably expressing the luciferase-based cAMP biosensor, GloSensor (kindly provided by Dr. Giguère Lab), were cultured between passages 10-40 in DMEM supplemented with 5% (v/v) heat-inactivated FBS, 5% (v/v) heat-inactivated BCS, 40 µg/ml gentamicin, and 10 µg/ml puromycin at 37°C in a humidified atmosphere containing 5% CO_2.

9.1. cAMP Measurement-GloSensor Assays

HEK293T-GloSensor cells were seeded in 100-mm culture dishes (2.5 million cells/dish) and transiently transfected with untagged-D1R or untagged-D5R (0.05 µg) or co-transfected with HA-SAP102 and flag-PSD95 (0.5 µg). The total amount of transfected DNA was consistently kept as 5 µg/dish by adding empty vector. In the following day, cells were reseeded (30,000 cells/well) into PLL-coated 96-well clear bottom white-plates. After 24 hours, the media was removed and replaced with 0.3 mg/ml luciferin (dissolved in 1X HBSS + 20 mM HEPES; pH 7.4) for 15 min at RT in dark. Cells were either stimulated with increasing concentrations of DA or SKF81297, or single dose of 10 µM of DA for 15 min. The luminescence activity was measured using Synergy H1 Multi-Mode Plate Reader. The relative luminescence units (RLU) for individual dose-response curves of different ligands (DA, SKF81297) were analyzed to obtain the potency of the half maximal effective concentration (EC_{50}) and ligand-induced maximal activation (E_{max}) of AC. The raw RLU for each well was subtracted from basal (non-treated cell) of their respective condition, then normalized as a percent of the E_{max} obtained from the receptor alone (D1R or D5R), and the curve was best-fitted with shared slope parameter using Prism (10.0.3). Normalized values from different experiments were averaged and curves were analyzed again using a simultaneous

nonlinear curve fitting with a shared slope parameter. In addition, mini binding assays were performed to determine D1R and D5R levels. To validate expression of transfected SAP102, PSD95, transfected cells were reseeded in 6-well plates, and lysates were collected and aliquoted for immunoblotting analysis as described in section 5.

10.Studies in HTLA Cells

HEK293T cells stably expressing human βArr2 fused to Tobacco Etch Virus (TEV) protease and a luciferase reported gene for tetracycline-controlled transcriptional activation (tTA)-driven luciferase, known as HTLA cells (kindly provided by Dr. Giguère with permission of Dr. Richard Axel) were maintained in DMEM supplemented with 5% (v/v) heat-inactivated FBS, 5% (v/v) heat-inactivated BCS, 40 μg/ml gentamicin, 2.5 μg/ml of puromycin and 50 μg/ml of hygromycin. HTLA cells were grown between 10-40 passages in 5% CO2 incubator at 37°C to perform Presto-Tango Assays for βArr2 recruitment.

10.1. βArr2 Recruitment-Presto Tango Assays

HTLA cells were seeded in 100-mm culture dishes (2.5 million cells/dish) and transiently transfected with D1R-Tango or D5R-Tango (4 μg) alone or co-transfected with HA-SAP102 or PSD95-RFP (1 μg). Empty vector was used to adjust the total amount of transfected DNA to 5 μg DNA/dish. Following transfection, 45 μl of cells were seeded in PLL-coated 384-well clear bottom white-plates (20,000 cells/well), as described previously (Laroche and Giguère, 2019). After approximately 8 h to allow cell adherence, cells were stimulated overnight with 20 μl/well of increasing concentration of ligands (DA and DHX; prepared at a concentration of 3X) diluted in HBSS (pH 7.4) to induce luciferase expression. In the following day, media was removed by flicking the 384-well plate and taping it gently, and 40 μl of Glo reagent mix added (final concentrations in well: 108 mM Tris–HCl, 42 mM Tris-Base, 75 mM NaCl, 3 mM $MgCl_2$, 5 mM DTT, 0.2 mM coenzyme A, 0.14 mg/ml D-luciferin , 1.1 mM ATP, 0.25% v/v Triton X-100, 2 mM sodium hydrosulfite). After 10 min incubation at RT, luminescence was measured using Synergy H1 Multi-Mode Plate Reader. RLU values for dose-response curves done with different ligands (DA and DHX) were analyzed to obtain the EC_{50} and ligand-induced E_{max} of βArr2. The raw RLU for each well was subtracted from basal (non-treated cell) of their respective condition, then normalized as a percent of the E_{max} obtained from the receptor alone (D1R or D5R), and the

curve was best-fitted with shared slope parameter using Prism (10.0.3). Normalized values from experiments were averaged and curves were analyzed again using a simultaneous nonlinear curve fitting with a shared slope parameter. D1R and D5R levels were assessed using mini binding assays (8.2.4), while SAP102 and PSD95 expression was validated by immunoblotting of lysate aliquots prepared from transfected cells seeded in 6-well plates as described above.

11.Studies in HTL Cells

HEK293T stably expressing a luciferase reporter gene, known as HTL cells (kindly provided by Dr. Giguère with permission of Dr. Richard Axel) were maintained in DMEM supplemented with 5% FBS, 5% BCS, 40 μg/ml gentamicin, 2.5 μg/mL of puromycin and 50 μg/mL of hygromycin. HTL cells were grown between 10-30 passages in a 5% CO_2 incubator at 37°C. These cells were utilized to measure βarr1 and βarr2 recruitment by engineering a modified variant of TEV, S219V-stop (TEV219) carries a stabilizing point mutation and truncation to remove the auto-inhibitory C-terminal region of TEV.

11.1. βArrs Recruitment-Tango Assays

HTL cells were seeded in 100-mm culture dishes (2.5 million cells/dish) and transiently transfected with D1R-Tango or D5R-Tango (4 μg) with HA-βArr1-TEV219 (1 μg) or HA-βArr2-TEV219 (1 μg). Following transfection, 45 μl of cells were seeded in PLL-coated 384-well clear bottom white-plates (20,000 cells/well) and allowed to adhere for ~8 h as described previously (Laroche and Giguère, 2019). Cells were then stimulated overnight with increasing concentration of ligands (20 μl/well: DA and DHX; at a concentration of 3X) diluted in HBSS (pH 7.4) to induce luciferase expression following βArr1 and βArr2 recruitment. The following day, media was removed by flicking the 384-well plate and taping it gently, and 40 μl of Glo reagent mix were added. After 10 min incubation at RT, luminescence was measured using Synergy H1 Multi-Mode Plate Reader. Determination of corrected RLU values, best curve fitting of dose-response curves, and validation of receptor and βArr1/2 expression were done essentially as described for assays in HTLA cells (Section 10.1).

12. Statistical Analysis

Prism (version 10.0.3) was used for statistical analyses and nonlinear curve fitting. All data are expressed as arithmetic mean ± SEM. For coimmunoprecipitation, phosphorylation, and ERK1/2 assays, immunoreactive bands were quantified using imageJ software as described in figure legends. For radioligand binding assays, nonlinear regression curve fitting was used to measure K_d, K_i, and B_{max} of [^{3}H]-SCH23390 and cold dopaminergic ligands. One-sample t test, unpaired-t test and one-way ANOVA were performed as indicated in figure legends using $p \leq 0.05$ as threshold for statistical significance.

CHAPTER THREE: RESULTS

MANUSCRIPT I: Synapse Associated Protein 102 (SAP102) and Postsynaptic Density 95 (PSD95) Differentially Modulate Dopamine D1 Receptor

Synapse Associated Protein 102 (SAP102) and Postsynaptic Density 95 (PSD95) Differentially Modulate Dopamine D1 Receptor

Statement of Author Contribution

I would like to acknowledge the contribution of Kirk Multaz (Béïque Lab) and Jingwei Chen (Ferguson Lab) for the preparation of hippocampal organotypic cultures and embryonic cortical cultures, respectively. I would like also to thank Chantal Binda and Patricia Bilodeau (Tiberi Lab) for making the GST-purified constructs of SAP102 and assisting with phosphorylation assay, respectively. Radioligand binding and cAMP assays for D1R fused with either GFP or Rluc were performed with the assistance of Meriam Zeghal.

Appendix I contains supplementary figures and tables for manuscript I.

Rationale

Postsynaptic D1R localized in dendritic spine of neurons critically modulates numerous physiological behaviors (Beaulieu and Gainetdinov, 2011). The molecular underpinnings that shape the neuronal signaling and trafficking properties of D1R leading to the modulation of brain functions remain unclear. To address this issue, we performed yeast two-hybrid screens using IL3 of D1R and D5R and identified SAP102 as a D1R-specific interacting partner (data not shown). As previous studies showed that PSD95 specifically interacts with the CT of D1R to modulate its functional properties (Zhang et al, 2007; Sun et al, 2009), **I hypothesize that SAP102 and PSD95 differentially regulate D1R signaling and trafficking properties. I aim to study the distinct roles of SAP102 and PSD95 in regulating D1R by i) mapping the D1R•SAP102 and D1R•PSD95 interaction *in vivo* and *in vitro*, and ii) assessing the effect of SAP102 and PSD95 on D1R-mediated signaling, phosphorylation, and trafficking mechanisms.**

Results

1. SAP102 and PSD95 Interact with D1R

1.1. Subcellular Fractionation of D1R and SAP102

To examine the subcellular distribution of D1R that is optimal for coimmunoprecipitation experiments, protein fractionation by sequential density gradient ultracentrifugation was performed from solubilized cortical lysates (Sprague-Dawley rat-P21) (Carlin et al, 1980). 50 µg of fractionation samples were separated on 10% SDS-PAGE for immunoblot analysis. The subcellular fractionation analysis shows that D1R and SAP102 were highly enriched in the crude synaptosome membrane (LP1) fractions (Supplementary Fig. 3.1A). Postsynaptic GluN1-containing NMDAR and SAP102 were also detected at high levels in the PSD fraction with the presence of low levels of presynaptic synaptophysin (Supplementary Fig. 3.1A). In the purified PSD, I also detected D1R, however, due to the low yield of purified PSD, coimmunoprecipitation studies were performed from LP1 preparations (Supplementary Fig. 3.1A).

1.2. In vivo D1R•SAP102 and D1R•PSD95 Complexes

To investigate whether SAP102 associates with D1R *in vivo*, coimmunoprecipitation was performed from male and female brain tissues (Sprague-Dawley rat-P21). As the D1R•PSD95 complex is known to be detected in native tissue, it was included as a positive control (Zhang et al, 2007; Sun et al, 2009). Hippocampal, striatal, and cortical lysates were immunoprecipitated with D1R antibody, followed by immunoblotting with SAP102 and PSD95 antibodies. Results showed that in addition to the input, the endogenous immunoreactivity of SAP102 and PSD95 were detected in D1R immunocomplexes from these different brain tissues (Fig. 3.1A). Conversely, striatal lysates were immunoprecipitated with SAP102 and PSD95 antibodies, followed by immunoblotting with D1R antibody. Results showed that in addition to input, D1R immunoreactivity was observed in SAP102 and PSD95 immunocomplexes (Fig. 3.1B). These findings suggest the existence of the native D1R•SAP102 and D1R•PSD95 complexes.

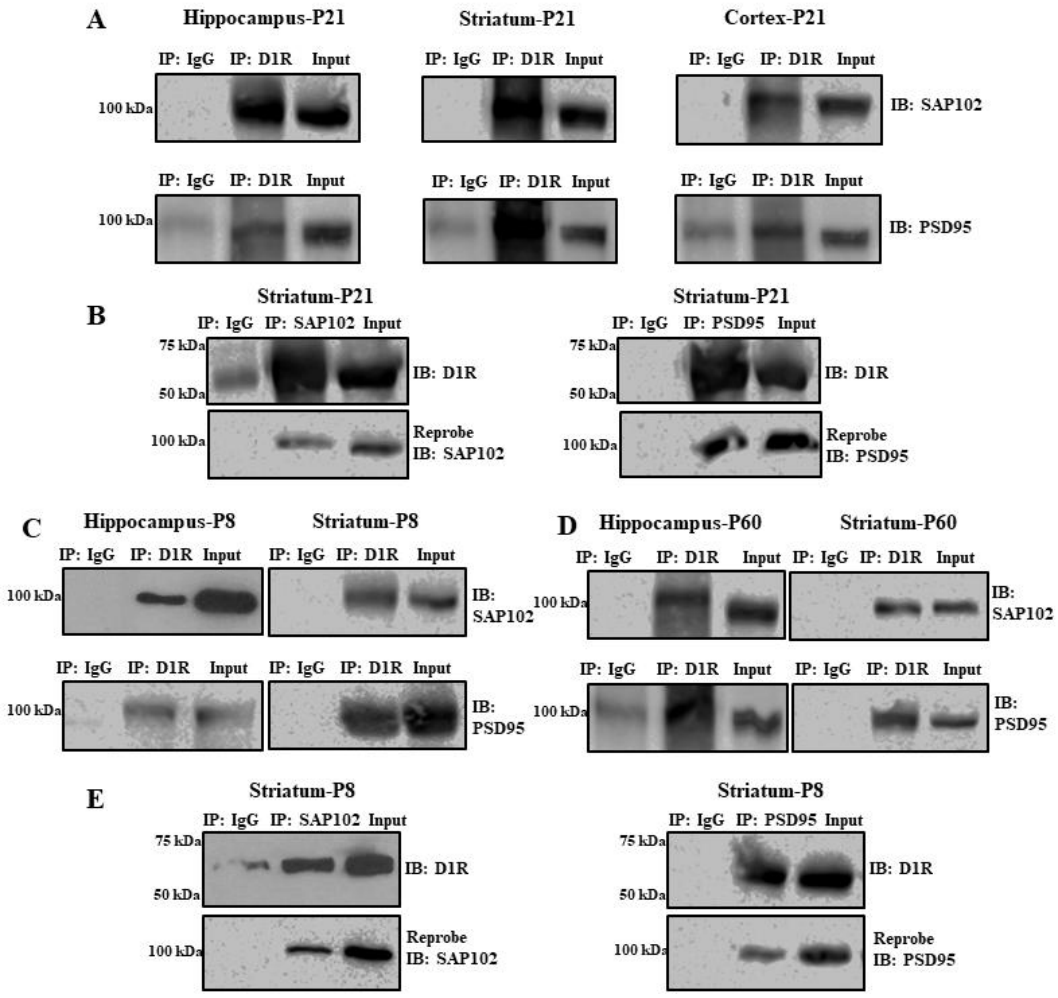

Fig. 3.1. SAP102 and PSD95 Interact with D1R, *in vivo*. (A) Solubilized lysates from hippocampus (0.5 mg), striatum (1 mg), and cortex (1.5 mg) of rat (P21) were subjected to an immunoprecipitation procedure using rat-D1R antibody and resolved immunocomplexes probed with rabbit-SAP102 and rabbit-PSD95 antibodies. Normal rat IgG were used as a negative control. 50 µg of lysate were loaded to the gels as input. Blot is a representative of an experiment repeated three times. (B) Solubilized lysates from striatum (1 mg) of rat (P21) were subjected to an immunoprecipitation procedure using mouse-SAP102 and mouse-PSD95 and resolved immunocomplexes probed with rat-D1R antibody. Normal mouse IgG were used as a negative control. 50 µg of lysate were loaded to the gels as input. Blot is a representative of an experiment repeated three times. (C) Solubilized lysates from hippocampus (0.5 mg) and striatum (1 mg) of rat (P8) were subjected to an immunoprecipitation procedure using rat-D1R antibody and resolved immunocomplexes probed with rabbit-SAP102 and rabbit-PSD95 antibodies. Normal rat IgG were used as a negative control. 50 µg of lysate were loaded to the gels as input. Blot is a representative of an experiment repeated three times. (D) Solubilized lysates from hippocampus (0.5 mg) and striatum (1 mg) of rat (P60) were subjected to an immunoprecipitation procedure using rat-D1R antibody and resolved immunocomplexes probed with rabbit-SAP102 and rabbit-PSD95 antibodies. Normal rat IgG were used as a negative control. 50 µg of lysate were loaded to the gels as input. Blot is a representative of an experiment repeated two times. (E) Solubilized lysates from striatum (1 mg) of rat (P8) were subjected to an immunoprecipitation procedure using mouse-SAP102 and mouse-PSD95 and resolved immunocomplexes probed with rat-D1R antibody. Normal mouse IgG were used as a negative control. 50 µg of lysate were loaded to the gels as input. Blot is a representative of an experiment repeated three times.

1.3. Developmental D1R•SAP102 and D1R•PSD95 Complexes

Unlike SAP102 and PSD95, few studies examined the developmental expression for D1R using radioautography, immunocytochemistry and mRNA *in situ* hybridization (Schambra et al, 1994; Araki et al, 2007; Rothmond et al, 2012). Herein, I assessed the differential protein expression patterns of D1R, SAP102, PSD95, and NMDAR subunits (GluN1, GluN2A, GluN2B) in the hippocampus and cortex from neonatal P3, P8, P21, P60 (Dam) (Sprague-Dawley rat). Immunoblot analysis showed that SAP102, PSD95, and NMDAR subunits are expressed throughout development, but SAP102 and GluN2B predominates earlier in development (Supplementary Fig. 3.1B) (Sans et al, 2000). In a similar manner to PSD95 and GluN2A subunit, the expression of D1R is gradually increasing throughout development (Supplementary Fig. 3.1B) (Sans et al, 2000).

These findings led me to assess whether the native D1R•SAP102 and D1R•PSD95 complexes at earlier stages of brain development are observed. Immunoprecipitation of D1R from hippocampal and striatal lysates (P8), as well preparation from (P60), were performed. Results showed the existence of native endogenous D1R•SAP102 and D1R•PSD95 complexes (Fig. 3.1C, D). Conversely, SAP102 and PSD95 were immunoprecipitated from striatal lysates (P8) and D1R immunoreactivity was observed from SAP102 and PSD95 immunocomplexes (Fig. 3.1E). Collectively, Fig 3.1 shows the importance of these physiological interactions throughout brain development. As SAP102 and PSD95 are important for enabling the developmental shift in synaptic NMDAR subunit composition; herein both are important for regulating D1R interaction, independently (Sans et al, 2000).

1.4. Subcellular Hippocampal Localization of D1R•SAP102 and D1R•PSD95 Complexes

Because SAP102 and PSD95 are major components for PSD, immunostaining experiments were performed in hippocampal organotypic culture (Sprague-Dawley rat, P8-DIV28) to confirm the localization of endogenous D1R, SAP102, and PSD95 (Gogolla et al, 2006; Soares et al, 2014). Confocal airyscan microscopy revealed that subcellular immunolabelling of D1R, SAP102, PSD95 is mostly localized in dendrites and concentrated in dendritic spines (Fig. 3.2A, B). Interestingly, labelled D1R co-localized with discrete immunopositive SAP102 and PSD95 clusters in dendrites and spines of hippocampal neurons (Fig. 3.2A, B).

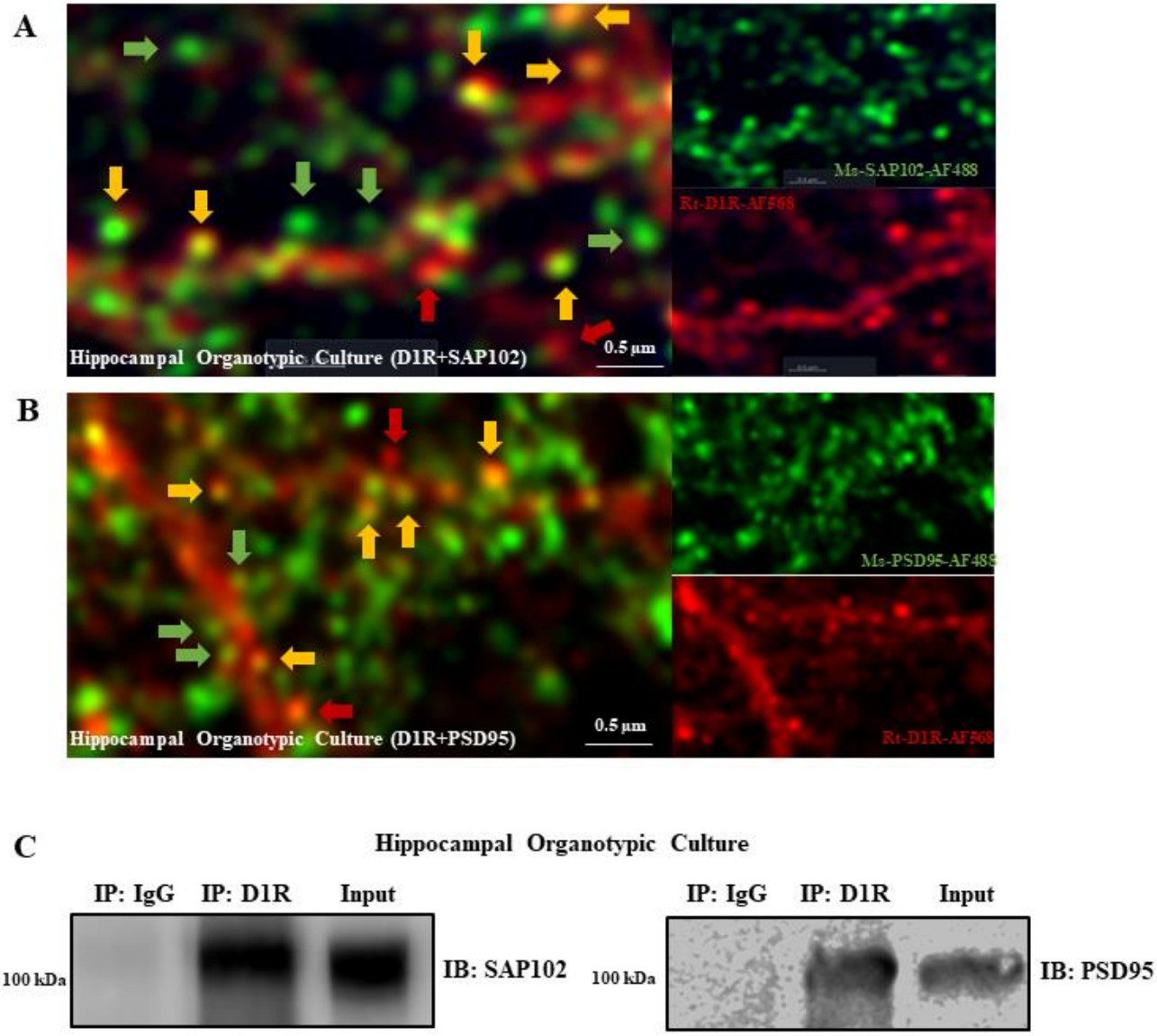

Fig. 3.2. Subcellular localization of D1R•SAP102 and D1R•PSD95 from Hippocampal Organotypic Cultures. (A, B) Representative confocal images of hippocampal organotypic culture (Sprague-Dawley rat, P8, DIV28) immunostained with primary antibodies: rat anti-D1R, mouse anti-SAP102, or mouse anti-PSD95, followed by secondary fluorophore antibodies: anti-rat conjugated Alexa Fluor-568 and anti-mouse conjugated Alexa Fluor-488. Images were acquired using confocal-airy scan microscope with 63x magnification. The image is a representative of an experiment repeated two times. (C) Solubilized lysates from hippocampal organotypic cultures (0.5 mg) were subjected to an immunoprecipitation procedure using rat-D1R antibody and resolved immunocomplexes probed with rabbit-SAP102 and rabbit-PSD-95 antibodies. Normal rat IgG were used as a negative control. 50 µg of lysate were loaded to the gels as input. Blot is a representative of an experiment repeated three times.

Moreover, coimmunoprecipitation studies were performed from these hippocampal organotypic cultures. Results showed that D1R forms a complex with SAP102 and PSD95 (Fig. 3.2C). Together, these results suggest that D1R•SAP102 and D1R•PSD95 colocalized and interact in hippocampal neurons, possibly in PSD.

1.5. Subcellular Cortical Localization and Interaction of D1R•SAP102 and D1R•PSD95

Although the results from hippocampal organotypic culture suggested the formation of D1R•SAP102 and D1R•PSD95 complexes in hippocampal neurons, I sought to further validate these findings by utilizing embryonic neuronal culture (CD1 mice, E13-14) (Khacho et al, 2014). Immunostaining of endogenous D1R, SAP102, and PSD95 at DIV10, revealed subcellular localization of these proteins in dendrites and dendritic spines (Fig. 3.3A, B). Interestingly, clusters of colocalized D1R•SAP102 and D1R•PSD95 were observed in these neurons (Fig. 3.3A, B). Moreover, coimmunoprecipitation were performed from these cortical cultures and results showed the formation of D1R•SAP102 and D1R•PSD95 complexes (Fig. 3.3C).

Further, I assessed whether D1R•SAP102 and D1R•PSD95 complexes can be observed in these neuronal cultures by performing *in situ* proximity ligation assay (PLA). PLA was performed from cortical cultures immunostained with rabbit-anti D1R, mouse-anti SAP102, and mouse-anti PSD95 antibodies, followed by fluorescent-labeled complementary oligonucleotide probes binding to the amplicons (amplified DNA) at the site of protein-protein interactions, producing distinct dots of high fluorescence on the tissue (Fig. 3.4A). Interestingly, *in situ* PLA revealed abundant endogenous interacting signals of D1R•SAP102 and D1R•PSD-95, in dendrites and dendritic spines of cortical cultures (Fig. 3.4C, D). MAP2 antibody was included to visualize neuronal dendrites. Single antibody incubation of D1R in PLA experiment, however, did not exhibit signal generation, attesting the specificity of PLA methodology (Fig. 3.4B). These findings support the notion that D1R interacts with SAP102 and PSD95 in postsynaptic neurons.

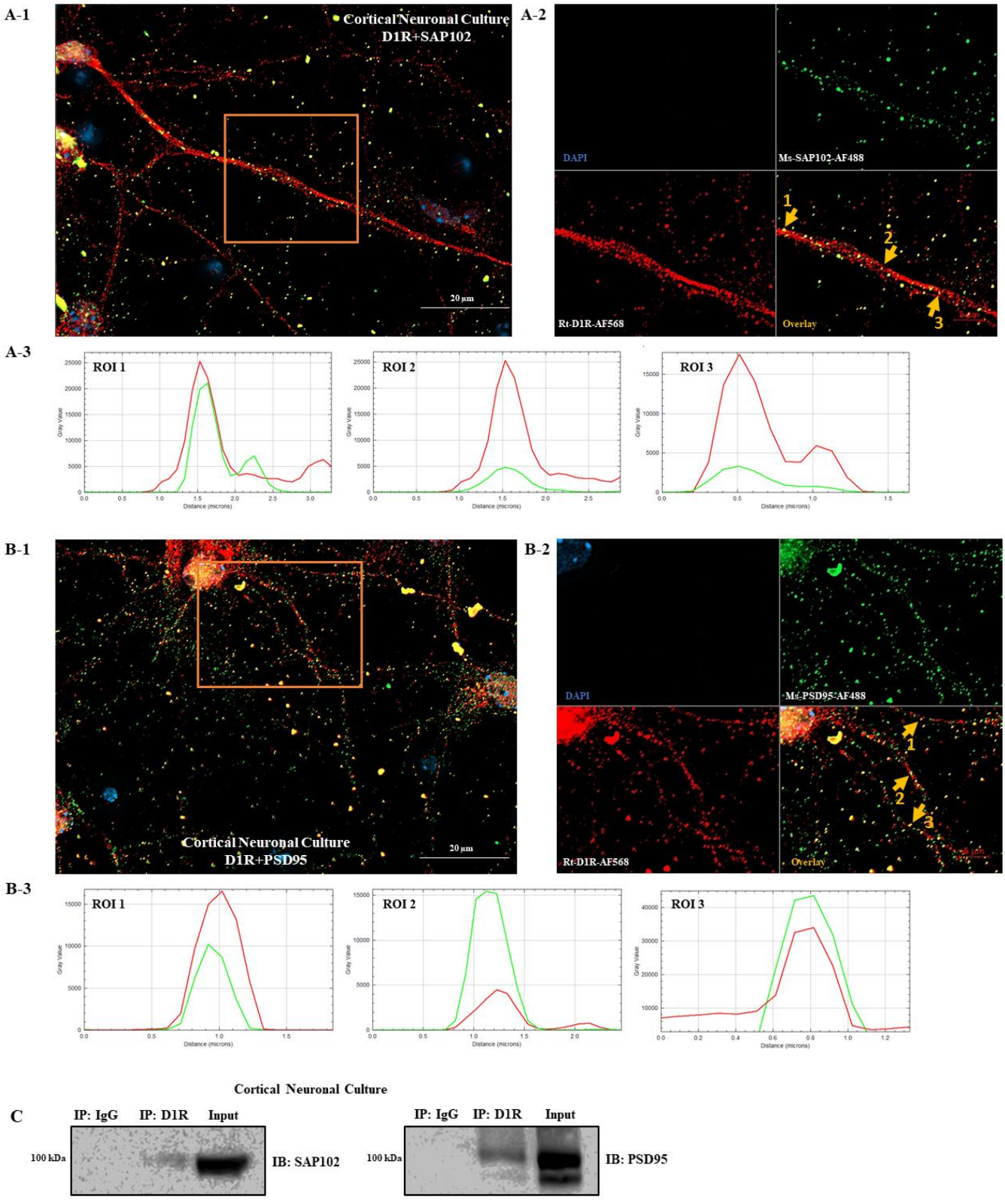

Fig. 3.3. Subcellular localization of D1R•SAP102 and D1R•PSD95 from Embryonic Cortical Cultures.
(A, B) Representative epifluorescence images of embryonic cortical culture (CD1 mice, E13-14, DIV10) immunostained with primary antibodies: rat anti-D1R, mouse anti-SAP102, or mouse anti-PSD95, followed by

secondary fluorophore antibodies: anti-rat conjugated Alexa Fluor-568 and anti-mouse conjugated Alexa Fluor-488. Images were acquired using epifluorescence microscope with 63x magnification. The image is a representative of an experiment performed three times. Region of interests (ROIs) of colocalized D1R•SAP102 (A-3) and D1R•PSD95 (B-3) are shown; SAP102 and PSD95 in green, D1R in red. (C) Solubilized lysates from embryonic cortical cultures (0.5 mg) were subjected to an immunoprecipitation procedure using rat-D1R antibody and resolved immunocomplexes probed with rabbit-SAP102 and rabbit-PSD95 antibodies. Normal rat IgG were used as a negative control. 50 µg of lysate were loaded to the gels as input. Blot is a representative of an experiment repeated two times.

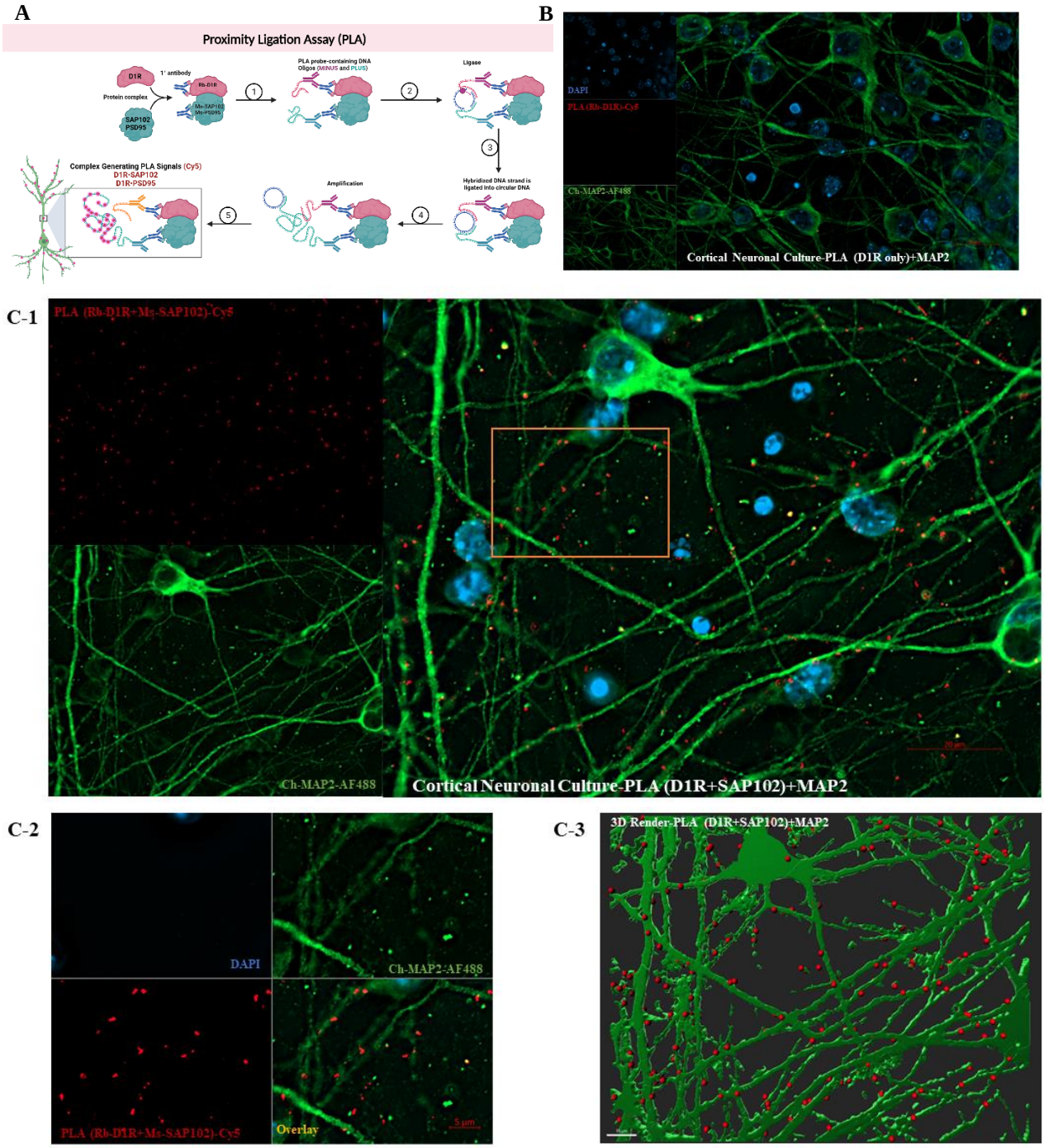
A
Proximity Ligation Assay (PLA)
D1R
Protein complex
SAP102
PSD95
1° antibody
Rb-D1R
Ms-SAP102
Ms-PSD95
PLA probe-containing DNA Oligos (MINUS and PLUS)
Ligase
Hybridized DNA strand is ligated into circular DNA
Amplification
Complex Generating PLA Signals (Cy5)
D1R-SAP102
D1R-PSD95
B
DAPI
PLA (Rb-D1R)-Cy5
Ch-MAP2-AF488
Cortical Neuronal Culture-PLA (D1R only)+MAP2
C-1
PLA (Rb-D1R+Ms-SAP102)-Cy5
Ch-MAP2-AF488
Cortical Neuronal Culture-PLA (D1R+SAP102)+MAP2
C-2
DAPI
Ch-MAP2-AF488
PLA (Rb-D1R+Ms-SAP102)-Cy5
Overlay
5 µm
C-3
3D Render-PLA (D1R+SAP102)+MAP2

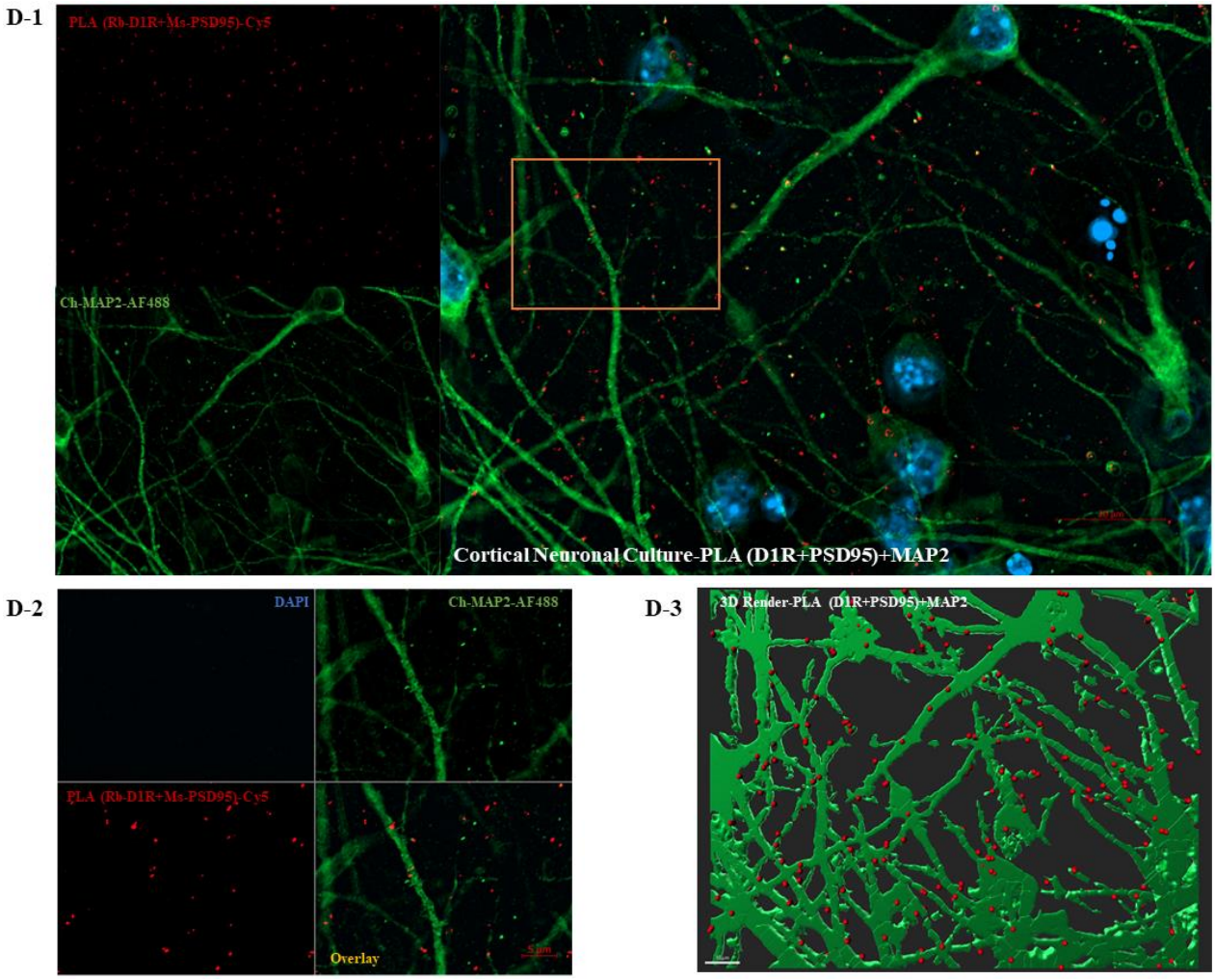

Fig. 3.4. *in situ* PLA Interaction of D1R•SAP102 and D1R•PSD95 from Embryonic Cortical Cultures.
(A) A schematic diagram of the PLA protocol. Created with BioRender.com. (B-D) Representative epifluorescence images of embryonic cortical culture immunostained with primary antibodies: rabbit anti-D1R only (B), co-strained with mouse anti-SAP102 (C) or with mouse anti-PSD95 (D), followed by the addition of PLUS and MINUS PLA probes. Probes were ligated, amplified, and generated PLA signals were visualized using far red (Cy5) filter. Cells were also incubated with chicken anti-MAP2 antibody, followed by the anti-chicken conjugated Alexa Fluor-488. Images were acquired using epifluorescence microscope with 63x magnification. The image is a representative of an experiment performed three times. (C-2, D-2) Subset of higher magnification. (C-3, D-3) IMARIS 3D reconstructed image showing the PLA signals as spots.

2. In vitro D1R•SAP102 and D1R•PSD95 Complexes

To investigate the functionality of SAP102 and PSD95 with D1R *in vitro*, coimmunoprecipitation studies were performed from HEK293 cells transiently transfected with empty vector (mock), HA-D1R alone, or with either Flag-SAP102 or Flag-PSD95. Immunoblot analysis of whole-cell lysates showed that SAP102 and PSD95 coprecipitated with HA-D1R when both proteins are co-expressed (Fig. 3.5A). Conversely, coimmunoprecipitation were also performed in transiently transfected HEK293 cells with mock, D1R-GFP alone, or with either Flag-SAP102 or Flag-PSD95, and results showed that D1R was co-immunoprecipitated with both Flag-SAP102 and Flag-PSD95, suggesting these MAGUKs interacting with D1R in these mammalian cells (Fig. 3.5B). In addition, immunostaining results were performed from transiently transfected HEK293 cells. Results demonstrate that HA-D1R is highly expressed at cell membrane, whereas Flag-SAP102 and Flag-PSD95 are mostly localized in cytosol (Fig. 3.5C). Interestingly, co-expressed D1R•SAP102 and D1R•PSD95 cells showed a localization at the cell surface and in cytosolic compartments (Fig. 3.5D, E). Together, these findings imply a binary interaction of D1R•SAP102 and D1R•PSD95, *in vitro*.

2.1. Orthologs of SAP102 and PSD95 Interact with D1R

Although SAP102 is highly conserved (99.39% identity) between human (hSAP102: 817 aa) and rat (rSAP102: 849 aa) orthologs, I sought to determine if the additional 32 amino acid differences could affect the interaction (Supplementary Fig. 3.2A). Unlike SAP102, there is one amino acid substitution of PSD95 (724 aa) between human (S466) and rat (G466). HEK293 cells were transiently transfected with mock, Flag-D1R, alone, or co-transfected with HA-rSAP102 (HA-SAP102) and hSAP102-GFP (SAP102-GFP). Followed coimmunoprecipitation, immunoblot analysis of whole-cell lysates showed that D1R co-immunoprecipitated with both rat and human orthologs of SAP102, and species differences do not have an impact on the interaction outcome (Supplementary Fig. 3.2B).

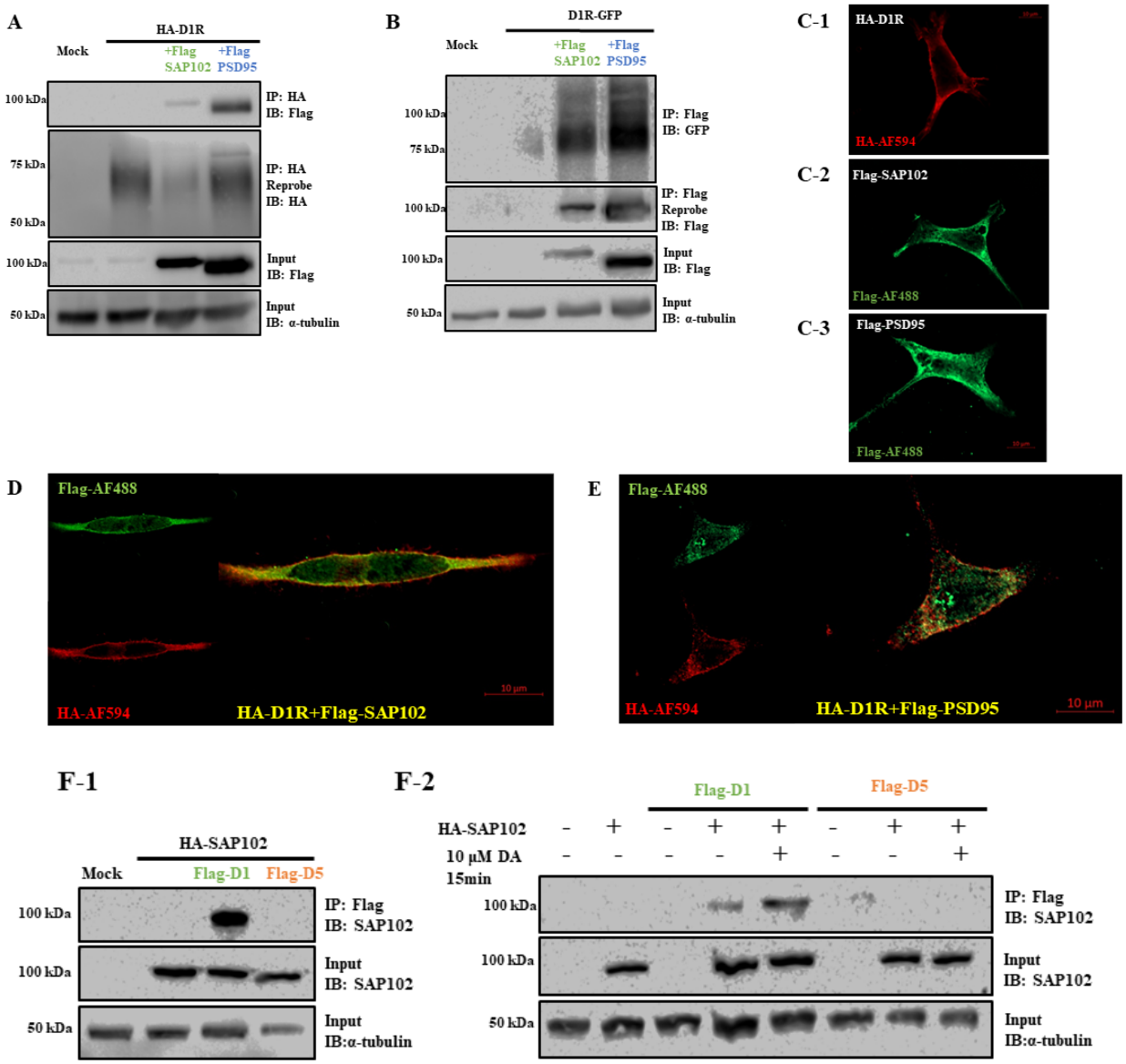

Fig. 3.5. SAP102 and PSD95 Interact with D1R, *in vitro*.

(A) HEK293 cells were transfected with mock, HA-D1R alone, with Flag-SAP102, or with Flag-PSD95. Cells were solubilized and subjected to a sequential immunoprecipitation with anti-HA agarose matrix followed by immunoblotting with anti-Flag antibody. A representative experiment of N=4 is shown. B_{max} values in pmol/mg membrane protein for [^{3}H]-SCH23390 are HA-D1R: 2.03±0.54, HA-D1R+ Flag-SAP102: 2.17±0.18, HA-D1R+Flag-PSD95: 2.33±0.54. (B) HEK293 cells were transfected with mock, D1R-GFP alone, with Flag-SAP102, or with Flag-PSD95. Cells were solubilized and subjected to a sequential immunoprecipitation with anti-Flag agarose matrix followed by immunoblotting with anti-GFP antibody. A representative experiment of N=6 is shown. B_{max} values in pmol/mg membrane protein for [^{3}H]-SCH23390 are D1R-GFP: 8.27±2.32, D1R-GFP+ Flag-SAP102: 9.26±1.95, D1R-GFP+Flag-PSD95: 12.05±3.01. (C-E) Representative images of HEK293 cells transfected with HA-D1R, Flag-SAP102 or Flag-PSD95 (C), co-transfected with HA-D1R+Flag-SAP102 (D), or HA-D1R+Flag-PSD95 (E), followed by immunostaining with primary antibodies: rabbit anti-HA and mouse anti-Flag, and secondary fluorophore antibodies: anti-rabbit conjugated Alexa Fluor-594 and anti-mouse conjugated Alexa Fluor-488. Images were acquired using epifluorescence microscope with 63x magnification. The image is a representative of an experiment performed

four times. B_{max} values in pmol/mg membrane protein for [^{3}H]-SCH23390 are HA-D1R: 2.03±0.54, HA-D1R+ Flag-SAP102: 2.17±0.18, HA-D1R+Flag-PSD95: 2.33±0.54. (F) HEK293 cells were transfected with mock, HA-SAP102, or co-transfected with Flag-D1R+HA-SAP102, Flag-D5R+HA-SAP102 (F-1), or transfected with mock, HA-SAP102, Flag-D1R, Flag-D5R, or co-transfected with Flag-D1R+HA-SAP102, Flag-D5R+HA-SAP102 (F-2). Cells were solubilized and subjected to a sequential immunoprecipitation with anti-Flag agarose matrix followed by immunoblotting with rabbit-SAP102 antibody. A representative experiment of N=3 is shown. B_{max} values in pmol/mg membrane protein for [^{3}H]-SCH23390 for (F-1): Flag-D1R+HA-SAP102: 2.14±1.29. Flag-D5R+HA-SAP102: 2.05±1.11, and for (F-2): Flag-D1R: 2.93±1.95, Flag-D1R+HA-SAP102: 3.10±2.08, Flag-D5R: 2.90±0.82, Flag-D5R+HA-SAP102: 2.21±1.22.

2.2. SAP102 Selectively Interact with D1R, but not D5R

To assess the specificity of SAP102 with respect to D1-class receptor subtypes, *in vitro* coimmunoprecipitation studies were performed from transiently transfected HEK293 cells with Flag-D1R, Flag-D5R, or co-transfected with HA-SAP102. Immunoblots showed that SAP102 could not form a complex with D5R, neither at basal nor stimulated conditions (10 μM DA-15 min) (Fig. 3.5F). However, D1R•SAP102 complex was observed at both conditions (Fig. 3.5F). Together, these results suggest that SAP102 specifically binds to D1R, but not D5R.

2.3. The Functionality of D1R-GFP

Since I utilized D1R-GFP in the previous experiment (Fig 3.5B), functional studies were performed to assess if the fused GFP (~25 kDa) to CT of D1R modulates the receptor function. The results showed that D1R-GFP exerts normal function as assessed by cAMP production and radioligand binding affinity relative to untagged D1R (Supplementary Fig. 3.3A; Supplementary Table 3.1). Confocal live imaging of HEK293 cells transfected with D1R-GFP revealed that D1R is highly localized at plasma membrane (Supplementary Fig. 3.3B). Moreover, two-photon imaging of hippocampal organotypic culture co-transfected with D1R-GFP and mCherry (cellular marker) were also performed. Results showed that D1R is highly expressed in the hippocampal pyramidal neurons, and highly enriched in the dendritic spines (Supplementary Fig. 3.3C). Together, these findings suggest that the insertion of GFP at CT of D1R does not alter the functionality of D1R as obtained by radioligand binding studies and cAMP, and GFP fusion is efficiently localizing the cellular D1R.

3. SAP102-PDZ3 and PSD95 Interact, respectively, with IL3 and CT of D1R

Next, I mapped the intracellular region of D1R that mediates the interaction with SAP102. It was reported that the CT of D1R modulates the interaction with PSD95 (Zhang et al, 2007), and our results from yeast two-hybrid screens suggest that IL3 of D1R is harboring the interaction domain for SAP102. Glutathione S-transferase (GST) fusion proteins encoding D1R-IL3 (R219-K272) and D1R-CT (R338-T446) were constructed and used as baits to precipitate associated interactors (Fig. 3.6A). HEK293 cells expressing Flag-SAP102 or Flag-PSD95 lysates were incubated with GST, GST-D1R-IL3 and GST-D1R-CT. Pull-down assays revealed that GST-D1R-IL3 and GST-D1R-CT interact SAP102 and PSD95, respectively (Fig. 3.6B, C). Cortical lysates (Sprague-

Dawley rat, P21) were also incubated with GST, GST-D1R-IL3 and GST-D1R-CT. Endogenous SAP102 and PSD95 form a protein complex with GST-D1R-IL3 and GST-D1R-CT, respectively (Fig. 3.6D, E). These findings show that SAP102 and PSD95 interact with D1R via different cytosolic domains.

Additionally, our lab generated deletion mutant forms of IL3 and CT of D1R, referred to as Flag-D1R-ΔIL3N (Q224-T245), Flag-D1R-ΔIL3C (G246-K265), and Flag-D1R-ΔCT (C347-T446) (Fig. 3.6F). To further confirm the intracellular region of D1R mediating the interaction with SAP102 and PSD95, Flag-D1R, Flag-D1R-ΔIL3N, Flag-D1R-ΔIL3C, and Flag-D1R-ΔCT were transiently co-transfected in HEK293 cells with either HA-SAP102 or PSD95-RFP. Following coimmunoprecipitation, immunoblot analysis of whole cell lysate suggested that mutant forms of D1R-IL3 cannot form a complex with SAP102, whereas D1R-CT truncation abrogated the interaction with PSD95 (Fig. 3.6G, H). These findings further support that these functional complexes are modulated differentially by D1R via IL3 (SAP102) and CT (PSD95), *in vitro* and *in vivo*.

3.1. SAP102-PDZ3 Interacts with D1R.

Our yeast two-hybrid screens suggested that SAP102 domains located downstream of PDZ2 potentially interact with IL3-D1R (data not shown). GST-fusion proteins encoding different SAP102 domains; NT-PDZ1 (M1-M243), PDZ1 (N139-M243), PDZ2 (P237-A340), PDZ3 (E395-K494), SH3 (E486-H657), and GK (E649-L749) were constructed and used as baits to pinpoint the domain mediating the interaction with D1R (Fig. 3.7A). Lysates of HEK293 cells transfected with D1R-GFP were incubated with these fusion proteins, and immunoblot analysis revealed a co-purification of GST-SAP102-PDZ3 with D1R (Fig. 3.7B). Moreover, cortical lysates (Sprague-Dawley rat, P21) were incubated with these fusion proteins, and the results showed that the endogenous D1R were able to pulldown SAP102-PDZ (Fig. 3.7C). While previous reports have indicated that the NT of PSD95 mediates the interaction with D1R (Zhang et al, 2007), here the PDZ3 domain of SAP102 facilitates the interaction with D1R.

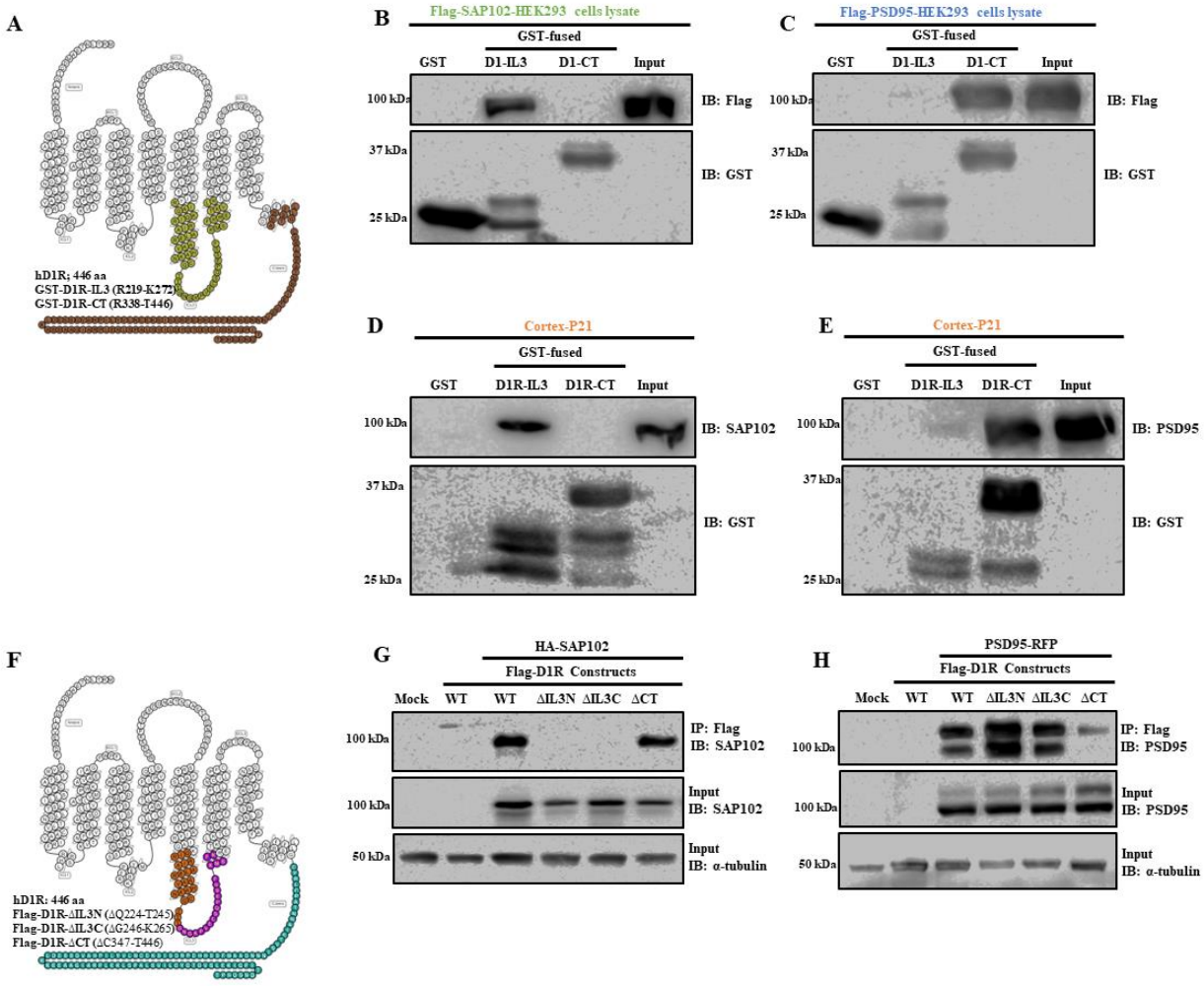

Fig. 3.6. SAP102 and PSD95 Interact with IL3 and CT of D1R.

(A) Schematic diagram of D1R showing the amino acid sequence corresponding fusion protein of GST-constructs: GST-D1R-IL3 and GST-D1R-CT. Created by gpcrdb.org. (B, C) HEK293 cells were transfected with Flag-SAP102 (B) or Flag-PSD95 (C) and lysate (0.5 mg) were incubated with GST, GST-D1R-IL3, and GST-D1R-CT, followed by immunoblotting with anti-Flag antibody. A representative experiment of N=5 is shown. (D, E) Cortical lysates (1 mg) were incubated with GST, GST-D1R-IL3, and GST-D1R-CT, followed by immunoblotting with anti-SAP102 and PSD95 antibodies. A representative experiment of N=5 is shown. (F) Schematic representation of deleted amino acid of D1R mutants: Flag-D1R-ΔIL3N, Flag-D1R-ΔIL3C, Flag-D1R-ΔCT. Created by gpcrdb.org. (G, H) HEK293 cells were co-transfected with Flag-tagged wild-type and mutant forms of D1R and HA-SAP102 (G) or PSD95-RFP (H). Cells were solubilized and subjected to a sequential immunoprecipitation with anti-Flag agarose matrix followed by immunoblotting with rabbit-SAP102 and rabbit-PSD95 antibodies. Blot is a representative of an experiment repeated four times. B_{max} values in pmol/mg membrane protein for [^{3}H]-SCH23390 for (G) are Flag-D1R: 1.81±0.22, Flag-D1R+HA-SAP102: 2.28±0.63, Flag-D1R-ΔIL3N+HA-SAP102: 1.38±0.34, Flag-D1R-ΔIL3C+HA-SAP102: 3.54±1.12. Flag-D1R-ΔCT+HA-SAP102: 3.16±0.68, and for (H) are Flag-D1R: 0.87±0.22, Flag-D1R+PSD95-RFP: 1.27±0.47, Flag-D1R-ΔIL3N+PSD95-RFP: 0.91±0.25, Flag-D1R-ΔIL3C+PSD95-RFP: 3.11±1.17, Flag-D1R-ΔCT+PSD95-RFP: 1.40±0.52.

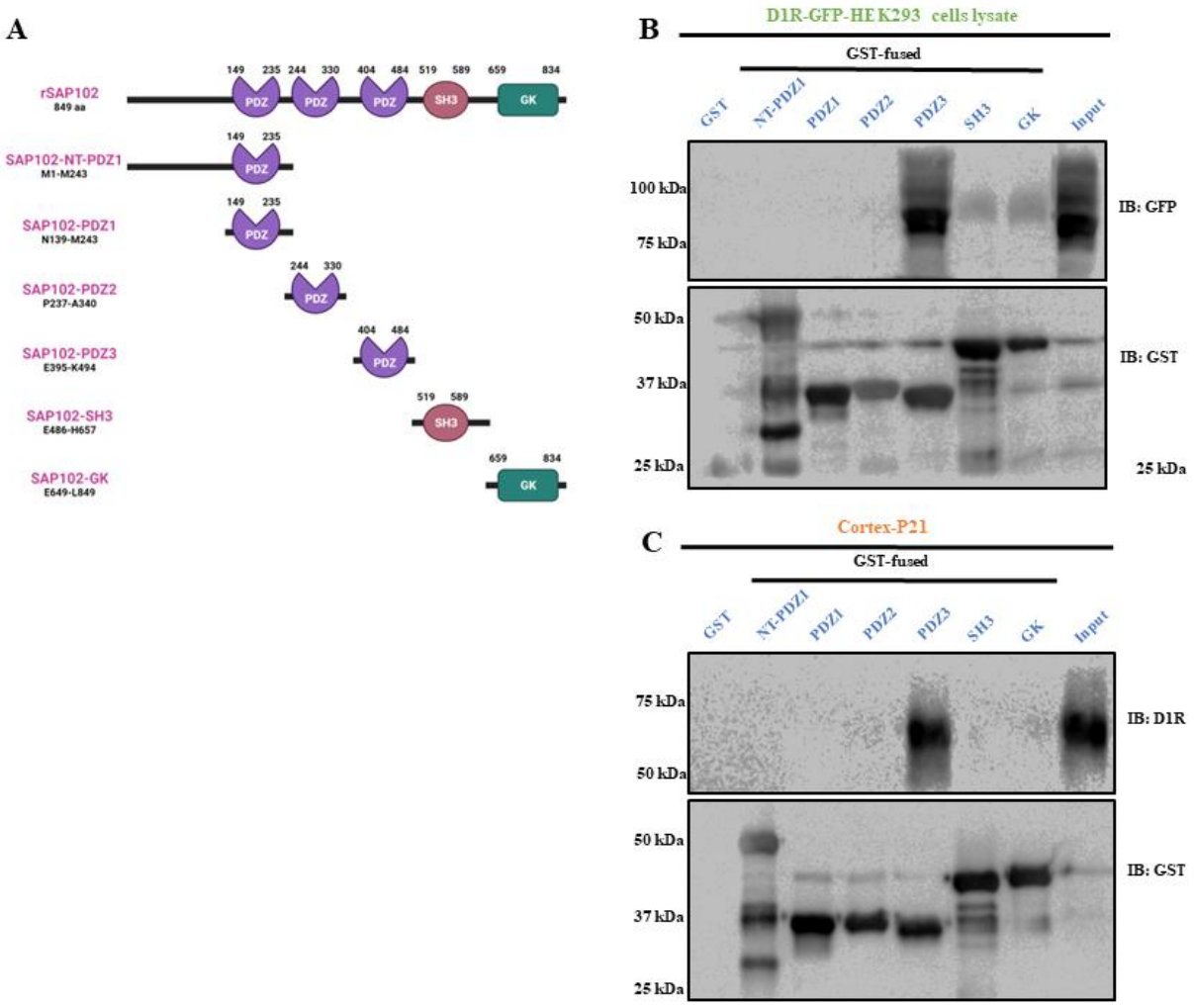

Fig. 3.7. PDZ3 Domain of SAP102 Associates with D1R.

(A) Schematic representation showing SAP102 domains corresponding GST-constructs. Created with BioRender.com. (B) HEK293 cells were transfected with D1R-GFP, and lysate (0.5 mg) were incubated with GST-constructs, followed by immunoblotting with anti-GFP antibody. A representative experiment of N=6 is shown. B_{max} values in pmol/mg membrane protein for [^{3}H]-SCH23390 for D1-GFP: 8.21±2.60. (C) Cortical lysates (1 mg) were incubated with GST-constructs of SAP102, followed by immunoblotting with rat-D1R antibody. A representative experiment of N=3 is shown.

3.2. D1R Binding Affinity is not Impacted by SAP102 or PSD95

Previous work from our lab showed that the IL3 and CT modulate ligands binding affinities of D1R (Charrette, Albaker et al, in preparation; Chaar et al, 2001). As the coimmunoprecipitation studies showed that constitutive association of D1R with SAP102 and PSD95 via the interaction with IL3 and CT of D1R, respectively, I assessed whether D1R•SAP102 and D1R•PSD95 complexes modulate the characteristic ligand binding properties of the D1R by radioligand binding assays. Saturation and competition studies were performed from crude membrane prepared from HEK293 cells transiently transfected with untagged D1R alone, or co-transfected with HA-SAP102 or Flag-PSD95. Using D1R-class radioligand [^{3}H]-SCH23390 with an increasing concentration (0.1-8 nM), SAP102 and PSD95 had no effect on both maximal binding capacity (B_{max}) and dissociation constants of the radioligand (K_d) (Table 3.1). Competition experiments were also performed using D1R full agonists (DA, SKF81297, DHX), inverse agonists (thiothixene, butaclamol), and partial agonist (SCH23390) (Tiberi and Caron, 1994; D'Aoust and Tiberi, 2010). Using a constant concentration of [^{3}H]-SCH23390 tested with increasing concentrations of cold D1R ligands, the inhibitory constant (K_i) of dopaminergic drugs were unaltered by SAP102 and PSD95. Overall, these findings indicate that SAP102 and PSD95 exert no effect on ligand affinity and maximal expression of D1R.

	Saturation Curves [^{3}H]-SCH23390		Competition Curves K_i (nM)					
Receptor	K_d (nM) N=6-8	B_{max} (pmol/mg protein) N=6-8	DA N=6-8	SKF81297 N=6-8	DHX N=3-4	Thiothixene N=6-8	(+) Butaclamol N=4	SCH23390 N=3-4
D1R	**0.76** (0.29-1.28)	**5.0** (2.10-7.69)	**6766** (1948-11320)	**56.3** (39.71-80.87)	**1441** (226-2307)	**84.7** (37.65-161.10)	**1.9** (0.68-2.99)	**0.74** (0.55-1.00)
D1R+SAP102	**0.45** (0.21-0.94)	**3.5** (2.06-5.00)	**5933** (2628-10160)	**37.9** (20.09-62.94)	**375** (179-630)	**72.4** (23.58-120.50)	**1.8** (1.48-2.49)	**0.52** (0.23-0.74)
D1R+PSD95	**0.64** (0.34-1.16)	**4.5** (2.65-10.15)	**8680** (3261-13640)	**49.2** (21.60-62.35)	**714** (216-1363)	**94.6** (50.42-225.50)	**2.0** (1.41-3.56)	**0.77** (0.58-0.96)

Table 3.1. D1R Binding Affinity is not Impacted by SAP102 or PSD95.
Dissociation constants (K_d, K_i) and B_{max} values of radioligand saturation and competition studies of [^{3}H]-SCH23390 performed from HEK293 cells transfected with D1R, co-transfected with HA-SAP102, or co-transfected Flag-PSD95. Values are expressed as arithmetic means, with minimum and maximum value in brackets. No statistical significance was observed using one-way ANOVA, when compared to D1R.

4. Stimulation of D1R Modulates the Interaction between D1R•SAP102 and D1R•PSD95

GPCRs exist in an ensemble of dynamic conformations that can be selectively stabilized by the binding of a ligand (Pierce et al, 2002; Luttrell, 2006; Hilger et al, 2018). To further characterize D1R•SAP102 and D1R•PSD95 interactions, I examined the DA effect on D1R•SAP102 and D1R•PSD95 complex formation in transiently transfected HEK293 cells using coimmunoprecipitation and bioluminescence resonance energy transfer (BRET) studies. Firstly, HEK293 cells were transiently transfected with mock, Flag-D1R alone, or co-transfected with HA-SAP102 or PSD95-RFP. Cells were stimulated with DA (10 μM-15 min), followed by coimmunoprecipitation. Immunoblots results showed that activation of D1R with DA substantially increased the abundance of SAP102 and PSD95 interacting with D1R, implying that the D1R under basal condition couples to SAP102 and PSD95, and the agonist stimulation facilitates the complex formation (Fig. 3.8A, B).

To validate these findings, $BRET^2$ studies were employed using live HEK293 cells transfected with D1R-Rluc (*Renilla luciferase*) alone, or with SAP102-GFP or PSD95-GFP (Fig. 3.8C). Prior to these experiments, functional studies of were performed for D1R-Rluc, and results suggested that the fusion of Rluc protein at the CT of D1R does not change dopaminergic ligand affinity, maximal receptor expression, or cAMP production relative to untagged D1R (Supplementary Fig. 3.3A; Supplementary Table 3.1). To visualize the GFP fusion to SAP102 and PSD95, confocal imaging and immunoblotting were performed. Confocal imaging on live HEK293 cells transfected with SAP102-GFP and PSD95-GFP revealed intracellular localization of these MAGUKs within the cells (Supplementary Fig. 3.4A, B). Immunoblot analysis of transfected SAP102-GFP and PSD95-GFP showed that the fusion of GFP increased the molecular size of MAGUK by ~25 kDa, as recognized by their respective antibody (Supplementary Fig. 3.4D, E).

$BRET^2$ experiments were performed from HEK293 cells transfected with constant amount of D1R-Rluc (0.5 μg) along with increasing ratio of plasmids expressing SAP102-GFP or PSD95-GFP (1:1, 1:3, 1:5, 1:10). The results showed increasing, but saturable BRET signals with D1R•SAP102 and D1R•PSD95, implying the specificity of these BRET signals (Fig. 3.8D).

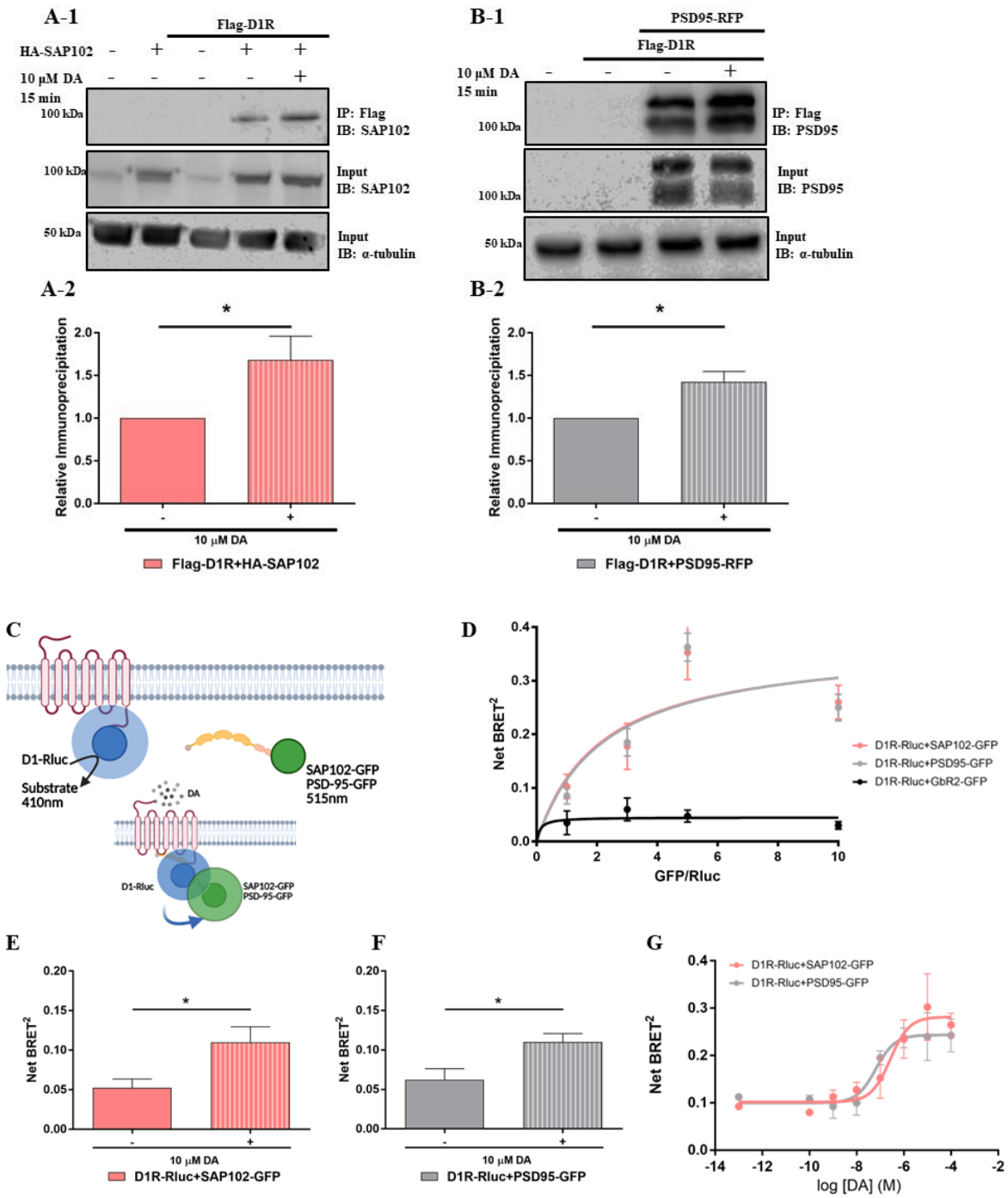

Fig. 3.8. Agonist induced-Stimulation of D1R Regulates the Interaction with SAP102 and PSD95.
(A, B) HEK293 cells were transfected with Flag-D1R, Flag-D1R+HA-SAP102 (A) or Flag-D1R, Flag-D1R+PSD95-RFP (B). Cells were stimulated with DA 15 min, or left untreated (vehicle: AA, denoted as -), then solubilized and subjected to a sequential immunoprecipitation with anti-Flag agarose matrix followed by immunoblotting with rabbit-SAP102 or rabbit-PSD95 antibodies. A representative experiment of N=8 for (A) and N=5 for (B) is shown. (A-2, B-2) shows a relative coimmunoprecipitation quantified in these co-transfected cells for IP-SAP102 over input-SAP102

(A-2) or IP-PSD95 over input-PSD95 (B-2), then stimulated cells were normalized to unstimulated cells (vehicle). *: $p<0.05$, when DA compared with control using one sample t test. B_{max} values in pmol/mg membrane protein for [^{3}H]-SCH23390 for (A) are Flag-D1R: 3.54±0.98, Flag-D1R+HA-SAP102: 2.88±0.762, and for (B) are Flag-D1R: 1.64±0.44, Flag-D1R+PSD95-RFP: 2.86±0.93. (C) Schematic diagram of BRET^2 assay. Created with BioRender.com. (D-G) HEK293 cells were transfected with D1R-Rluc, or co-transfected with SAP102-GFP, PSD95-GFP, GbR2-GFP. Coelenterazine 400a was added, and light emission was measured from the luciferase donor and GFP acceptor at 410 nm and 515 nm wavelength, respectively. Net BRET^2 was quantified as: [(GFP emission at 515 ± 30nm)/(Rluc emission 410 ± 80nm)]−[(emission at 515 ± 30nm)/(emission at 410 ± 80nm)] found with the D1R-Rluc expressed alone in the same experiment. (D) BRET saturation curve was performed by increasing the concentration of SAP102-GFP, PSD95-GFP, and GbR2-GFP over fixed concentration of D1R-Rluc. BRET measurement were quantified from four independent experiments, and B_{max} values in pmol/mg membrane protein for [^{3}H]-SCH23390 for D1R-Rluc: 2.32±1.25, D1R-Rluc+SAP102-GFP (1:1): 3.20±1.66, D1R-Rluc+SAP102-GFP (1:3): 2.37±0.89, D1R-Rluc+SAP102-GFP (1:5): 3.05±0.89, D1R-Rluc+SAP102-GFP (1:10): 3.03±2.01, D1R-Rluc+PSD95-GFP (1:1): 2.37±1.25, D1R-Rluc+PSD95-GFP (1:3): 3.25±2.25, D1R-Rluc+PSD95-GFP (1:5): 3.92±1.19, D1R-Rluc+PSD95-GFP (1:10): 2.87±1.65, D1R-Rluc+GbR2-GFP (1:1): 4.28±1.68, D1R-Rluc+GbR2-GFP (1:3): 3.62±1.21, D1R-Rluc+GbR2-GFP (1:5): 4.12±1.23, D1R-Rluc+GbR2-GFP (1:10): 3.87±1.19. (E-G) Cells were transfected with D1R-Rluc (0.5 μg) alone or co-transfected with SAP102-GFP (1:3), or PSD95-GFP (1:3). Cells treated with AA (vehicle) or 10 μM DA (30 min). BRET measurements for (E, F) were quantified from four independent experiments, and B_{max} values in pmol/mg membrane protein for [^{3}H]-SCH23390 for D1R-Rluc: 2.85±0.81, D1R-Rluc+SAP102-GFP: 4.91±0.57, D1R-Rluc+PSD95-GFP: 3.21±1.37. *: $p<0.05$, when compared using unpaired t test. (G) BRET measurement of cells stimulated with increasing concentration of DA. BRET measurements were quantified from four independent experiments, and B_{max} values in pmol/mg membrane protein for [^{3}H]-SCH23390 for D1R-Rluc: 1.74±1.32, D1R-Rluc+SAP102-GFP: 2.71±1.12, D1R-Rluc+PSD95-GFP: 2.75±1.14.

$GABA_BR$ subunit, GbR2 (GbR2-GFP), a negative control that lacks functional activity in the ER, showed no recruitment to D1R-Rluc (Fig. 3.8D). Moreover, incubation of D1R•SAP102 and D1R•PSD95 with DA (10 μM-30 min) modulated BRET signals, which implies an increased association between D1R and MAGUKs, and/or a dynamic conformational rearrangement for the complex to be more closely associated (stabilized) after receptor activation (Fig. 3.8E, F). Dose-response curves of DA (0.0001 μM-100 μM) showed that D1R exhibits dose-dependent recruitment of SAP102 and PSD95 upon DA treatment (Fig. 3.8G). The results also show no difference in agonist-induced maximal recruitment (E_{max}) and agonist potency (EC_{50}) between D1R•SAP102 and D1R•PSD95 (Fig. 3.8G). These findings suggest intricate dynamics of D1R•MAGUK complexes between a bioluminescent donor moiety and a fluorescent acceptor moiety within 100 Å, which is in the realm of most biological interactions.

5. SAP102 and PSD95 Differentially Modulate D1R-mediated cAMP Signaling

To assess the effect of SAP102 and PSD95 on D1R-mediated stimulation of AC and downstream signaling of D1R, cAMP production was measured using HEK293T cells stably expressing GloSensor, a luciferase-based cAMP biosensor (HEK293T-Glo) (Fig. 3.9A). As our lab employed this cell line for the first time, control experiments were performed in transfected cells with either mock or untagged-D1R. First, to investigate whether this cell line can exhibit pharmacological properties for D1-class receptors in mediating cAMP accumulation, I performed dose-response curves using increasing concentrations of DA. Result shows a dose-dependent increase of D1R-mediated cAMP production, with negligible effect on mock-transfected cells (Supplementary Fig. 3.5A-1). The use of an inverse agonist, cis-flupentixol (FLU-10 μM-15 min), had no effect on mock, but decreased the basal activity of the D1R (Supplementary Fig. 3.5A-2). Additionally, I stimulated these cells with an adenylyl cyclase agonist, forskolin (FSK-10 μM-15 min). The results showed a robust level of cAMP production following FSK stimulation of D1R relative to mock (Supplementary Fig. 3.5A-2). This could be explained by the possibility that under basal condition (no agonist) D1R constitutively couples to $G\alpha_s$, which in turn mediates $G\alpha_s$-primed AC and potentiates cAMP production. Overall, these results imply that this stable cell line is a suitable model to study D1R-mediated cAMP accumulation.

HEK293T-Glo cells were transfected with untagged-D1R alone, with HA-SAP102, with Flag-PSD95 or with both HA-SAP10 and Flag-PSD95. Overexpression of SAP102 did not alter the

basal cAMP levels relative to D1R, and DA activation (10 μM-15min) substantially increased D1R-mediated cAMP production (Fig. 3.9B, C). However, PSD95 overexpression decreased constitutive cAMP levels and D1R-mediated cAMP accumulation by DA relative to D1R alone, in agreement with previous report (Fig. 3.9B, C) (Zhang et al, 2007). A representative RLU values is shown in (Supplementary Fig. 3.5B). Moreover, dose-response curves using increasing concentrations of D1R agonists, DA and SKF81297, were performed to measure the maximum activation (E_{max}) of D1R-mediated cAMP production. SAP102 expression increased maximal activation of D1R-mediated intracellular cAMP accumulation, whereas PSD95 decreased the maximal activation of D1R-mediated cAMP production, without altering the agonist potency (EC_{50}) (Fig. 3.9D, E; Table 3.2). Interestingly, co-expression of D1R together with SAP102 and PSD95 did not lead to changes in basal and DA-induced formation of cAMP (Fig. 3.9B-E; Table 3.2). This suggest that co-expression of SAP102 and PSD95 in the same cellular environment neutralizes the effect on D1R-mediated cAMP production, leading to an intermediate (balanced) level of D1R-mediated cAMP production. Perhaps this phenotype is a result of D1R interaction with both MAGUKs, or potentially with individual MAGUK. Immunoblotting was performed to confirm the overexpression of SAP102 and PSD95 in these cells (Fig. 3.9F). These results suggest differential signaling mechanisms where SAP102 potentiates D1R-mediated cAMP production, and PSD95 inhibit D1R-mediated cAMP production.

6. SAP102 and PSD95 Differentially Modulate D1R-mediated ERK1/2 Activation

Recent studies from our lab showed that D1R-mediated ERK1/2 activation in HEK293 cells occurs in a biphasic pattern with an early G-protein dependent phase of large magnitude (1-10 min), followed by a prolonged phase of lesser magnitude that could potentially be independent of G-protein function (10-60 min) (Mischuk et al, in preparation; Zein et al, in preparation). As SAP102 and PSD95 differentially modulate D1R-mediated cAMP production, here I tested whether these MAGUKs modulate D1R-mediated ERK1/2 activation in a distinct manner. HEK293 cells were transfected with Flag-D1R alone, co-transfected with HA-SAP102, or with co-transfected with PSD95-RFP. Results suggest that following brief exposure to DA (10 μM, 5 min), SAP102 increases D1R-mediated ERK1/2 activation (as evidenced by increased levels on pERK1/2), relative to cells transfected with D1R alone (Fig. 3.9G). In cells expressing PSD95, however, D1R-mediated ERK1/2 activation was insignificant to cells expressing D1R alone (Fig. 3.9G).

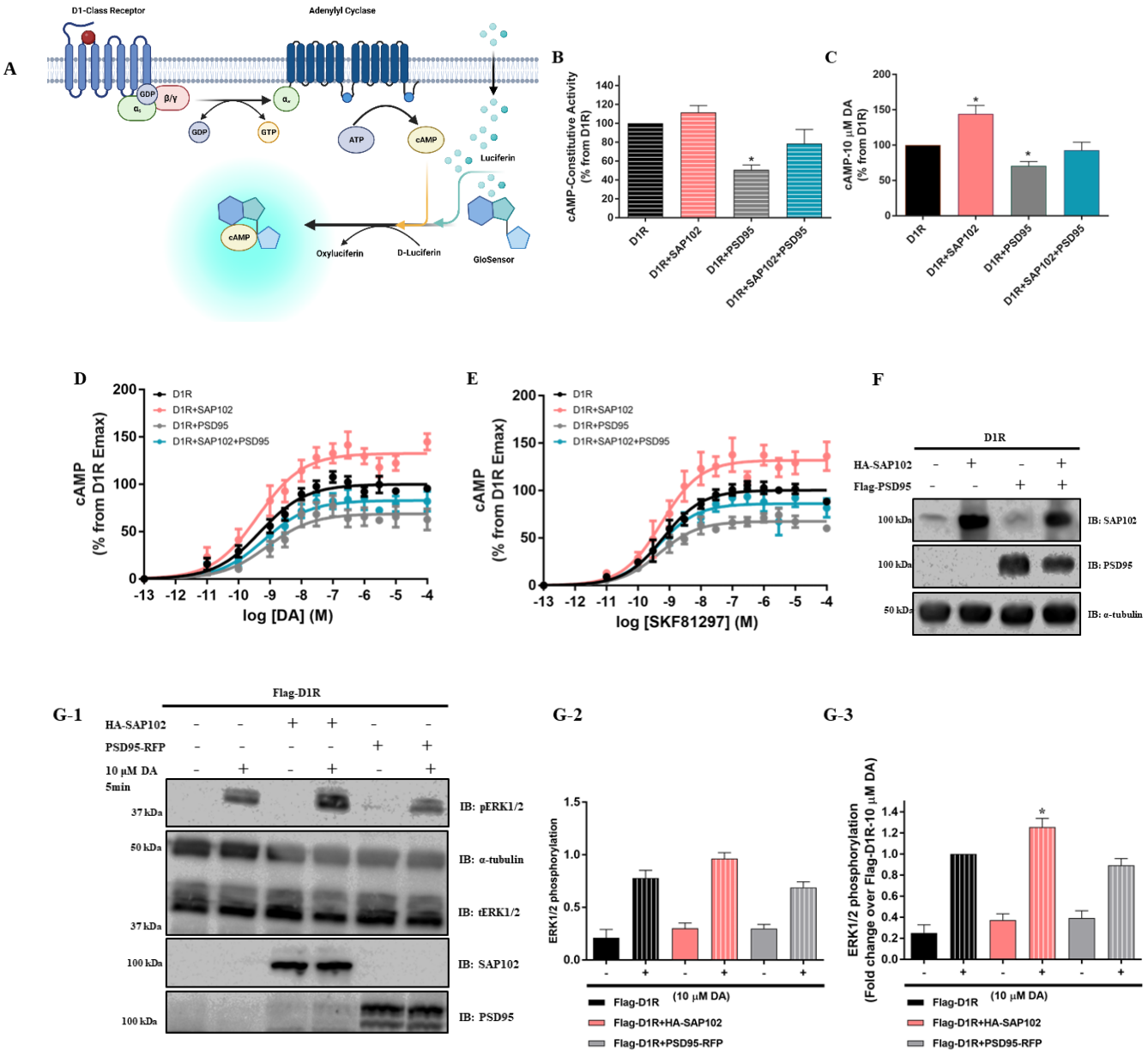

Fig. 3.9. SAP102 and PSD95 Differentially Regulate D1R Signaling.

(A) Schematic representation of the principle of the cAMP-GloSensor assay. Created with BioRender.com. (B-F) HEK293T cells stably expressing GloSensor were transfected with D1R, D1R+HA-SAP102, D1R+Flag-PSD95, and D1R+HA-SAP102+Flag-PSD95. Relative luminance value (RLU) for each experiment done in quadrable determinations for constitutive activity (B) and maximal activation of D1R (10 μM DA) (C). The values then were normalized to D1R alone. Each bar represents the arithmetic mean ± S.E. of normalized values relative to D1R alone from five independent experiments. B_{max} values in pmol/mg membrane protein for [^{3}H]-SCH23390 are: D1R: 2.41±0.73, D1R+HA-SAP102: 1.84±0.38, D1R+Flag-PSD95: 1.85±0.48, and D1R+HA-SAP102+Flag-PSD95: 3.07±1.06. *, $p<0.05$, when compared to D1R alone using one sample t test. (D, E) Dose-response curve in response to increasing concentrations of DA or SKF81297 were done in quadrable determinations. RLU for each condition were subtracted from the basal, then the values were normalized to the maximal activation of D1R alone. The graph

represents the dose response curve for the average doses of 5-10 independent experiments. EC_{50}, E_{max} and B_{max} values are presented in Table 3.2. (F) Representative immunoblotting analysis to validate the overexpression of SAP102 and PSD95. (G) HEK293 cells transfected with Flag-D1R, or co-transected with HA-SAP102, or PSD95-RFP. Cells were stimulated for DA (10 μM) for 5 min or left untreated (AA , denoted as -) to induce ERK1/2 activation. Cell lysates were then prepared and subjected to western blotting with anti-phospho ERK1/2, anti-total ERK1/2, anti α-tubulin (loading control), anti-SAP102, and anti-PSD95 antibodies. Blot shown is a representative of N=4. B_{max} values in pmol/mg membrane protein for [^{3}H]-SCH23390: Flag-D1R: 1.53±0.51, Flag-D1R+HA-SAP102: 2.60±0.70, Flag-D1R+PSD95-RFP: 3.06±0.52. Data are presented as arithmetic mean ± SEM (n=4) of p-ERK1/2 relative to total ERK1/2 (G-2), and then expressed as a fold change over Flag-D1R (10 μM) (G-3). *$p<0.05$ when stimulated condition compared to Flag-D1R (10 μM) using one sample t test.

Receptor	Agonist Efficacy DA (% of D1R-E_{max})	Agonist Potency EC_{50}-DA (nM)	Agonist Efficacy SKF81297 (% of D1R-E_{max})	Agonist Potency EC_{50}-SKF81297 (nM)	B_{max} (pmol/mg protein)
D1R (N=10)	**100**	**1.4** (0.02-6.95)	**100**	**2.4** (0.13-15.20)	**2.9** (0.72-12.11)
D1R+SAP102 (N=10)	**135.6 *** (103.4-189.0)	**1.4** (0.02-4.77)	**133.7 *** (104-231.6)	**1.3** (0.12-5.79)	**2.9** (0.48-8.17)
D1R+PSD95 (N=6)	**70.6 *** (28.6-95.6)	**1.7** (0.06-5.26)	**69.7 *** (52.2-91.0)	**0.8** (0.12-2.71)	**1.7** (0.51-3.16)
D1R+SAP102+PSD95 (N=5)	**82.8** (69.3-102.8)	**1.2** (0.02-2.45)	**89.3** (68-107.1)	**0.7** (0.20-1.01)	**3.1** (1.36-6.70)

Table 3.2. SAP102 and PSD95 Differentially Regulate D1R-mediated cAMP Production.
Best-fitted E_{max} and EC_{50} values of DA and SKF81297 for D1R-mediated cAMP production, in cells expressed with D1R, D1R+HA-SAP102, D1R+Flag-PSD95, and D1R+HA-SAP102+Flag-PSD95 shown in Fig. 3.9 (D, E) are reported, including the B_{max}. Values are expressed as arithmetic means, with minimum and maximum value in brackets. Statistical significance; *: $p<0.05$, using one sample t test, was determined by comparing E_{max} of D1R.

These results suggest a positive modulation of signaling cascades for D1R mediated ERK1/2 activation by SAP102. Together, findings from cAMP production and ERK1/2 activation studies imply that these MAGUKs mediate a differential effect on D1R signaling.

7. SAP102 and PSD95 Differentially Modulate D1R Phosphorylation

Phosphorylation is an important mechanism involved in the regulation of numerous cellular responses that lead to receptor desensitization (Ferguson, 2001). Previous results from our lab and others suggested that IL3 and CT of D1R are important in regulating D1R responsiveness (Jackson et al, 2002; Sedaghat and Tiberi, 2011). As SAP102 and PSD95 interact with different cytosolic regions of D1R, we examined the impact of these MAGUKs on DA-mediated D1R phosphorylation. We employed an antibody-based phosphorylation approach that recognized the phosphorylated residues of CT-D1R: Thr354 (pD1R-T354) and Ser372/Ser373 (pD1R-S372/S373) (Fig. 3.10A). Prior to performing this experiment, we validated these antibodies by utilizing HEK293 cells transfected with mock or Flag-D1R at low and high receptor expression. Following agonist stimulation, D1R was immunoprecipitated and then immunoblotted with pD1R-T354 and pD1R-Ser372/Ser373 antibodies. Results showed that these antibodies recognized phosphorylated D1R (low and high expression) (Supplementary Fig. 3.5C). Moreover, we also transfected HEK293 cells with Flag-D1R, Flag-D1R-ΔCT, or with Flag-D5R. Results indeed showed that pD1R-T354 and pD1R-Ser372/Ser373 antibodies recognized the full-length D1R, but not truncated D1R or D5R, attesting its subtype specificity and selectivity (data not shown). Next, HEK293 cells were transiently transfected with mock, Flag-D1R alone, or co-transfected with MAGUKs. Results showed that SAP102, but not PSD95, promotes agonist-induced phosphorylation of D1R (Fig. 3.10B). This finding implies that interacting SAP102 with D1R-IL3 potentially modulates the extent of DA-induced receptor phosphorylation.

8. SAP102 and PSD95 Differentially Modulate D1R Trafficking

To examine the role of SAP102 and PSD95 on regulating D1R trafficking, ELISA were performed to measure the cell surface expression, total expression (surface D1R+intracellular D1R), internalization, and recycling, in HEK293 cells transiently transfected with mock, Flag-D1R alone, or with HA-SAP102 or with PSD95-RFP.

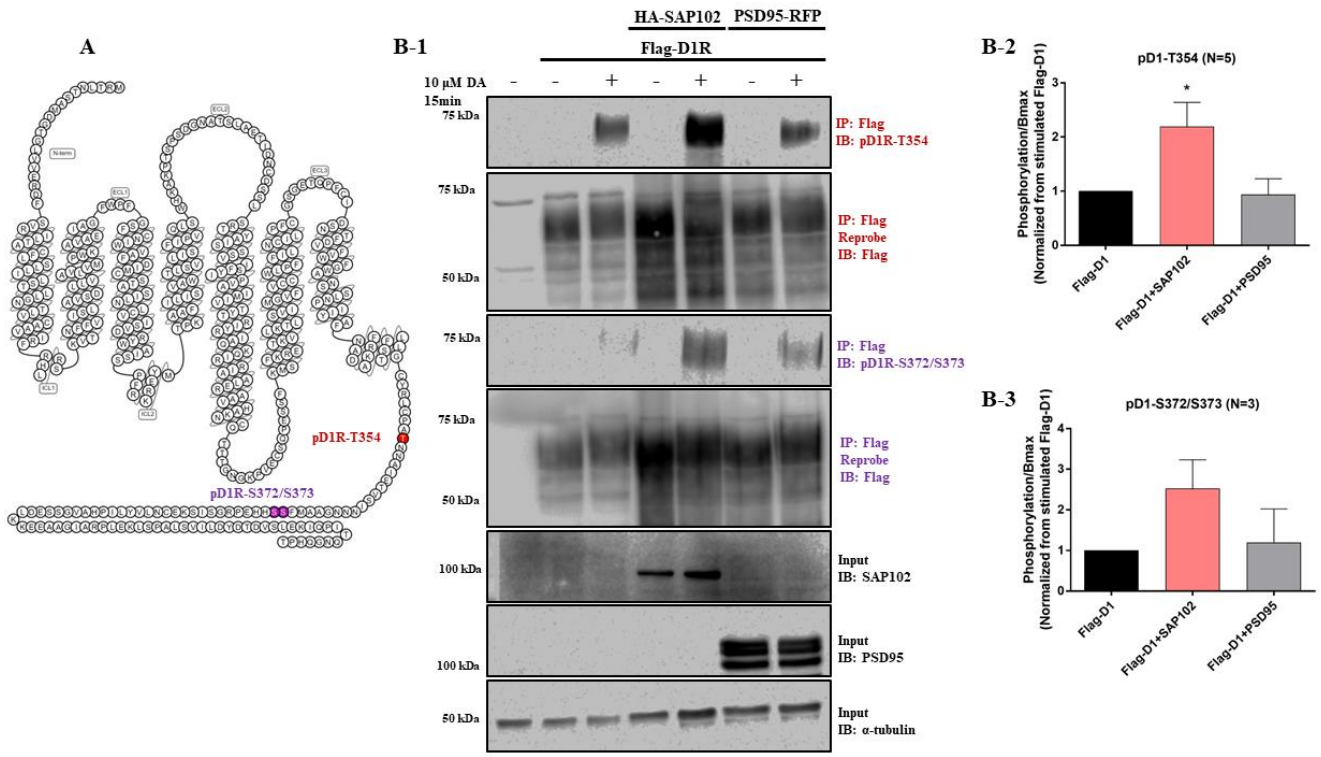

Fig. 3.10. SAP102 promotes D1R-induced phosphorylation.

(A) Schematic diagram of D1R showing the phosphorylation site, Thr354 and Ser372/Ser373. Created by gpcrdb.org. (B, C) HEK293 cells transfected with mock, Flag-D1R, Flag-D1R+HA-SAP102, and Flag-D1R+PSD95-RFP. Cells were treated with vehicle (AA, denoted as -) or stimulated with 10 μM DA for 15 min, then solubilized and subjected to a sequential immunoprecipitation with anti-Flag agarose matrix followed by immunoblotting with rabbit anti-phospho-D1R-Thr354 or rabbit anti-phospho-D1R-Ser372/Ser373. B_{max} values in pmol/mg membrane protein for [^{3}H]-SCH23390 of the representative experiment shown are: Flag-D1R: 1.78, Flag-D1R+HA-SAP102: 5.20, and Flag-D1R+PSD95-RFP: 2.74. B_{max} values in pmol/mg membrane protein for [^{3}H]-SCH23390 for the experments probed with phospho-D1R-Thr354 (N=5) are: Flag-D1R: 4.08±2.24, Flag-D1R+HA-SAP102: 7.12±2.83, and Flag-D1R+PSD95-RFP: 5.13±2.63, whereas B_{max} values for experments probed with phospho-D1R-Ser372/Ser373 (N=3) are: Flag-D1R: 2.50±1.04, Flag-D1R+HA-SAP102: 2.88±1.43, and Flag-D1R+PSD95-RFP: 2.77±1.13. *: $p<0.05$, using one sample t test, when compared to stimulated Flag-D1R.

8.1. PSD95, but not SAP102, Promotes Constitutive Endocytosis of D1R

Interestingly, SAP102 exerted no effect on D1R surface expression (Fig. 3.11A), suggesting that the increased production of cAMP and ERK1/2 observed in D1R•SAP102 transfected cells was not due to a higher cell surface expression of D1R. However, PSD95 constitutively decreased D1R surface expression (Fig.3.11A), which potentially explains the decreased cAMP production in D1R•PSD95 transfected cells, in agreement with previous report (Zhang et al, 2007). Moreover, total expression was measured under permeabilized conditions, and results suggested that neither SAP102 nor PSD95 influences total receptor expression (Fig. 3.11B). PSD95, however, enhances an intracellular pool of D1R (permeabilized condition minus non-permeabilized condition) (Fig. 3.11C). These findings suggest the possibility that PSD95 promotes the constitutive endocytosis of D1R.

8.2. SAP102 and PSD95 Differentially Regulate D1R-induced Endocytosis

To investigate whether SAP102 and PSD95 regulate agonist-mediated D1R endocytosis, transfected cells were stimulated with either DA or SKF81297 (10 μM) for 15 min. In addition to the constitutive internalization of D1R from cell surface by PSD95, DA-induced D1R internalization was substantially increased in cells expressing PSD95 relative to D1R alone, in agreement with previous report (Fig. 3.11D, E) (Zhang et al, 2007). In contrast, SAP102 reduced D1R internalization relative to D1R alone, even though it did not have an impact on D1R subcellular distribution (Fig. 3.11D, E). These findings suggest that SAP102 and PSD95 differentially modulate the internalization of D1R.

8.3. Internalization of D1R is Dynamin and βArr2 Dependent

The striking differences between SAP102 and PSD95 could be explained by distinct mechanisms employed by SAP102 and PSD95 to interact with endocytic machinery proteins, and thus differentially modulate D1R trafficking (e.g., recycling). To assess whether PSD95-mediated constitutive endocytosis of D1R is modulated by dynamin and βArr2, I used dynamin-I and βArr2 mutants that interfere with endocytosis. Results suggested that co-expressing D1R•PSD95 with the negative form of dynamin-I-K44A or βArr2-V54D blocks the constitutive endocytosis, while

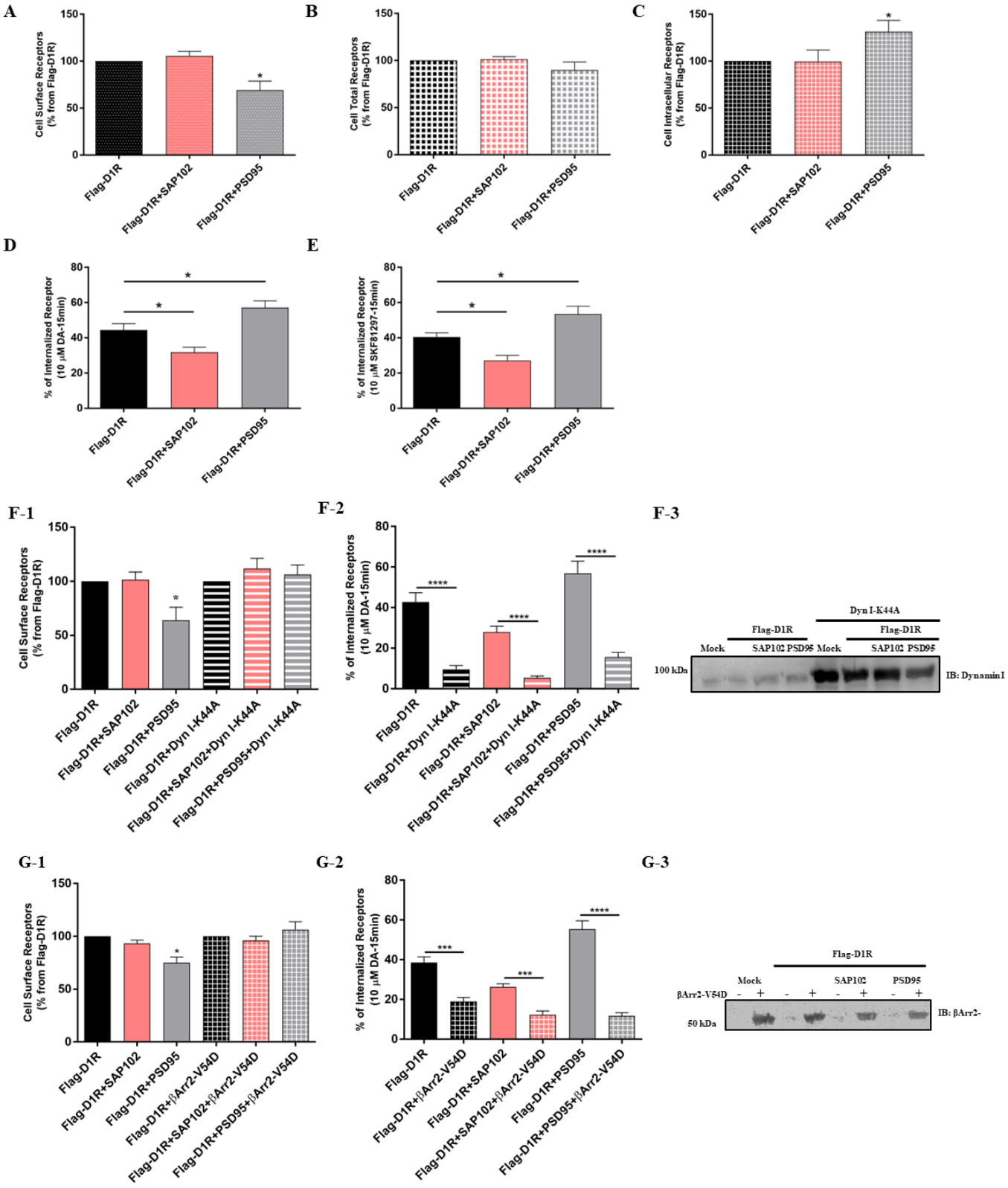
A
Cell Surface Receptors (% from Flag-D1R)
150
100
50
0
*
Flag-D1R
Flag-D1R+SAP102
Flag-D1R+PSD95
B
Cell Total Receptors (% from Flag-D1R)
150
100
50
0
Flag-D1R
Flag-D1R+SAP102
Flag-D1R+PSD95
C
Cell Intracellular Receptors (% from Flag-D1R)
150
100
50
0
*
Flag-D1R
Flag-D1R+SAP102
Flag-D1R+PSD95
D
% of Internalized Receptor (10 μM DA-15min)
80
60
40
20
0
*
*
Flag-D1R
Flag-D1R+SAP102
Flag-D1R+PSD95
E
% of Internalized Receptor (10 μM SKF81297-15min)
80
60
40
20
0
*
*
Flag-D1R
Flag-D1R+SAP102
Flag-D1R+PSD95
F-1
Cell Surface Receptors (% from Flag-D1R)
150
100
50
0
*
Flag-D1R
Flag-D1R+SAP102
Flag-D1R+PSD95
Flag-D1R+Dyn I-K44A
Flag-D1R+SAP102+Dyn I-K44A
Flag-D1R+PSD95+Dyn I-K44A
F-2
% of Internalized Receptors (10 μM DA-15min)
80
60
40
20
0
****
****
****
Flag-D1R
Flag-D1R+Dyn I-K44A
Flag-D1R+SAP102
Flag-D1R+SAP102+Dyn I-K44A
Flag-D1R+PSD95
Flag-D1R+PSD95+Dyn I-K44A
F-3
Dyn I-K44A
Flag-D1R
Flag-D1R
Mock
SAP102
PSD95
Mock
SAP102
PSD95
100 kDa
IB: DynaminI
G-1
Cell Surface Receptors (% from Flag-D1R)
150
100
50
0
*
Flag-D1R
Flag-D1R+SAP102
Flag-D1R+PSD95
Flag-D1R+βArr2-V54D
Flag-D1R+SAP102+βArr2-V54D
Flag-D1R+PSD95+βArr2-V54D
G-2
% of Internalized Receptors (10 μM DA-15min)
80
60
40
20
0
***
***
****
Flag-D1R
Flag-D1R+βArr2-V54D
Flag-D1R+SAP102
Flag-D1R+SAP102+βArr2-V54D
Flag-D1R+PSD95
Flag-D1R+PSD95+βArr2-V54D
G-3
Flag-D1R
Mock
SAP102
PSD95
βArr2-V54D
- + - + - + - +
50 kDa
IB: βArr2-

Fig. 3.11. SAP102 and PSD95 Differentially Regulate D1R Trafficking.

HEK293 cells were transfected with mock, Flag-D1R alone, with HA-SAP102 or with PSD95-RFP. ELISA experiments were performed to assess surface expression (A), total expression (permeabilized cells with Triton-X) (B), and intracellular pool of the D1R (total were subtracted from surface) (C). Each bar represents the arithmetic mean ± S.E. of normalized relative to Flag-D1R alone, from nine independent experiments. *: $p<0.05$, when compared to Flag-D1R using one sample t test, relative to Flag-D1R. (D, E) Agonist induced internalization of D1R was assessed by the % decrease in cell surface expression following 15 mins treatment with 10 μM DA (D) or SKF81297 (E) relative to AA (vehicle). Bar represents the arithmetic mean ± S.E. from nine independent experiments for DA (D) and four independent experiments for SKF81297 (E). *: $p<0.05$, when compared to Flag-D1R using one-way ANOVA, Dunnett's multiple comparison test. B_{max} in pmol/mg membrane proteins for [3H]-SCH23390 in arithmetic means ± S.E. of (A-D): Flag-D1R: 2.86±0.83, Flag-D1R+HA-SAP102: 2.68±0.64, and Flag-D1R+PSD95-RFP: 3.74±0.85, and for (E): Flag-D1R: 2.21±0.87, Flag-D1R+HA-SAP102: 2.37±0.80, and Flag-D1R+PSD95-RFP: 1.35±0.51. (F, G) HEK293 cells were transfected with mock, Flag-D1R alone, with HA-SAP102 or with PSD95-RFP in the presence or absence of dynamin mutant; HA-Dyn I-K44A (F), or βArr2 mutant; βArr2-V54D (G). Surface expression and DA-induced internalization (10 μM-15 min) were assessed by the % decrease in cell surface expression relative to that of AA (vehicle). Each bar represents the arithmetic mean ± S.E. from six independent experiments. (F-3) and (G-3) showed a representation of immunoblotting performed to validate the overexpression of mutant forms of dynamin and βArr2. B_{max} in pmol/mg membrane proteins for [^{3}H]-SCH23390 in arithmetic means ± S.E. for (F): Flag-D1R: 3.18±1.13, Flag-D1R+HA-SAP102: 3.12±0.86, Flag-D1R+PSD95-RFP: 4.78±1.01, Flag-D1R+HA-Dyn I-K44A: 1.80±0.46, Flag-D1R+HA-SAP102+HA-Dyn I-K44A: 2.32±0.54, and Flag-D1R+PSD95-RFP+HA-Dyn I-K44A: 3.81±1.03, and for (G): Flag-D1R: 1.09±0.47, Flag-D1R+HA-SAP102: 1.51±0.60, Flag-D1R+PSD95-RFP: 1.26±0.41, Flag-D1R+βArr2-V54D: 1.29±0.43, Flag-D1R+HA-SAP102+βArr2-V54D: 1.09±0.48, Flag-D1R+PSD95-RFP+βArr2-V54D: 2.33±0.33. *: $p<0.05$, **: $p<0.01$, ***: $p<0.001$, ****: $p<0.0001$ using one sample t test, when compared to Flag-D1R (F-1) and (G-1) or unpaired t test as noted in the graph (F-2) and (G-2).

no effect was observed on either constitutive internalization of D1R or D1R•SAP102 complex (Fig. 3.11F-1, G-1). Since SAP102 and PSD95 differentially modulate D1R-induced internalization, I assessed whether SAP102 and PSD95 alter the dynamin-βArr2 endocytic machinery used by D1R. HEK293 cells, endogenously expressing Dyn-I and βArr2, were transfected with D1R, D1R•SAP102 and D1R•PSD95 in the presence or absence of dynamin mutant; Dyn I-K44A, or βArr2 mutant; βArr2-V54D. Results showed that, regardless of PSD95 and SAP102 expression, cells transfected with these mutants did not display DA-induced D1R internalization (Fig. 3.11F-2, G-2). Immunoblotting was performed to confirm the overexpression of mutant dynamin and βArr2 in these cells (Fig. 3.11F-3, G-3). These results indicate that DA-induced internalization of D1R is dynamin and βArr2 dependent irrespective of PSD95 and SAP102, and PSD95-mediated constitutive endocytosis of D1R is blocked by dominant-negative dynamin and βArr2 mutants.

8.4. SAP102 and PSD95 Differentially Regulate D1R Recycling

To elucidate whether SAP102 and PSD95 modulate the post-endocytic recycling of D1R to plasma membrane, transfected HEK293 cells were stimulated with DA (10 μM) for 15 min to induce internalization, then agonist was removed, and cells were allowed to recover for 10 min and 30 min. Results indicated that in cells lacking SAP102 or PSD95 expression, D1R can recycle back to surface membrane after agonist-induced internalization in a time dependent manner (Fig. 3.12A-1). As PSD95 promotes greater D1R internalization, it also facilitates both the insertion of recycled receptors to plasma membrane, and D1R recovery rate, as measured by half-time, relative to cells expressing D1R alone (8.4 min vs. 11.8 min for D1R) (Fig. 3.12A-3, B, C). This finding in agreement with previous report suggesting that PSD95 promotes D1R resensitization (Sun et al, 2009). While SAP102 inhibits D1R internalization, the smaller internalized D1R pool displays a decreased membrane D1R insertion and recycling, potentially explained by the lower D1R recovery rate in comparison to D1R alone (15.1 min vs. 11.8 min for D1R) (Fig. 3.12A-2, B, C). Overall, these results demonstrate different modalities of SAP102 and PSD95 towards the regulation of D1R trafficking, likely via distinct endosomal compartments.

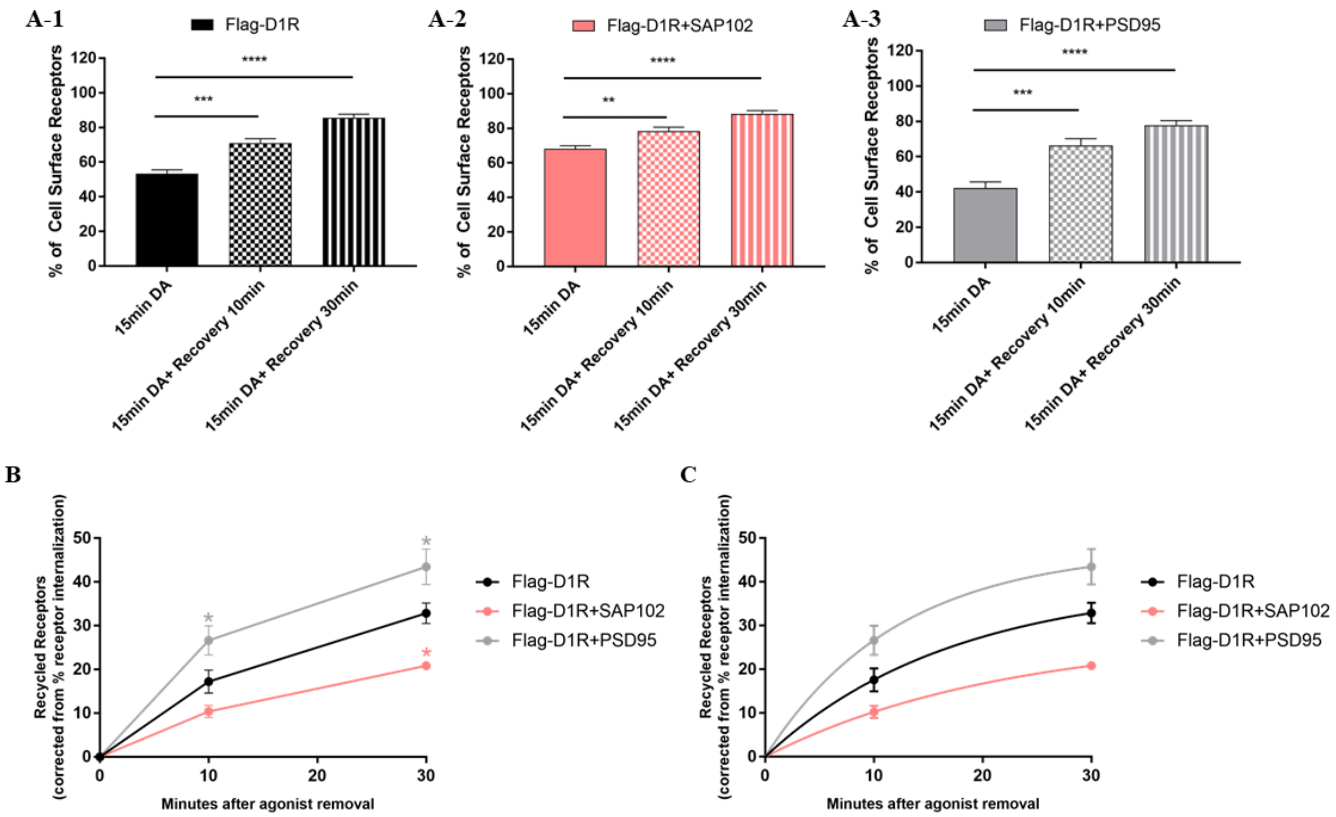

Fig. 3.12. SAP102 and PSD95 Differentially Regulate D1R Recovery to the Plasma Membrane.
ELISA was performed from HEK293 cells transfected with mock, Flag-D1R alone, co-transfected with HA-SAP102 or with PSD95-RFP. Cells were stimulated with 10 μM DA for 15 min, then agonist removed, and cells were allowed recovery for 10 and 30 min. (A) Surface expression was measured to assess the recycling receptor relative to 15 min 10 μM DA. (B) Recycled receptors were subtracted from 15 min 10 μM DA, and the percentage of recycled receptors after 10, 30 min recovery were quantified. (C) Recovery rate was assessed at 10, and 30 min after agonist removal. Each bar represents the arithmetic mean ± S.E. from seven independent experiments, and B_{max} in pmol/mg membrane proteins for [^{3}H]-SCH23390: Flag-D1R: 1.92±0.50, Flag-D1R+SAP102: 2.02±0.46, and Flag-D1R+PSD95: 2.80±0.75. *: p<0.05, **: p<0.01, ***: p<0.001, ****: p<0.0001 when compared as noted in the graph using one-way ANOVA, Dunnett's multiple comparison.

Significance

We identified SAP102 as a novel interactor specifically for D1R, but not D5R, and SAP102-PDZ3 and PSD95 interact with different cytosolic regions of IL3 and CT of D1R, respectively, *in vivo* and *in vitro*. Moreover, pre-associated complexes of D1R•SAP102 and D1R•PSD95 undergo conformational rearrangements leading to an association/stabilisation of the complex following exposure to D1R agonist. Interestingly, we found that SAP102 and PSD95 differentially regulate i) D1R-mediated cAMP production and ERK1/2 activation, ii) D1R-induced phosphorylation, and iii) D1R surface expression, internalization, and recycling, mediated via dynamin-βArr2 dependent pathway. The distinct contrasting effect of these MAGUKs in shaping D1R mechanisms may lead to exploit the pharmacological potential of D1R-IL3•SAP102-PDZ3 and D1R-CT•PSD-95-NT complexes for design of novel therapeutic approaches to mitigate abnormal D1R signaling function observed in various dopaminergic diseases, e.g., PD.

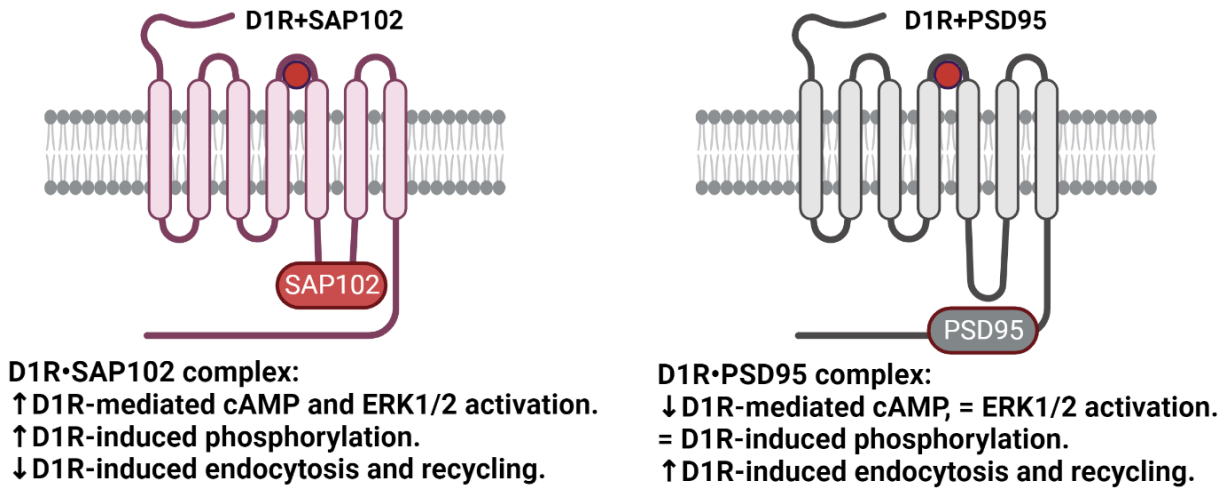

Fig. 3.13. Summary of the Signaling and Trafficking Mechanisms of D1R•SAP102 and D1R•PSD95 complexes.

Appendix I: Supplementary Figures and Tables for Manuscript I

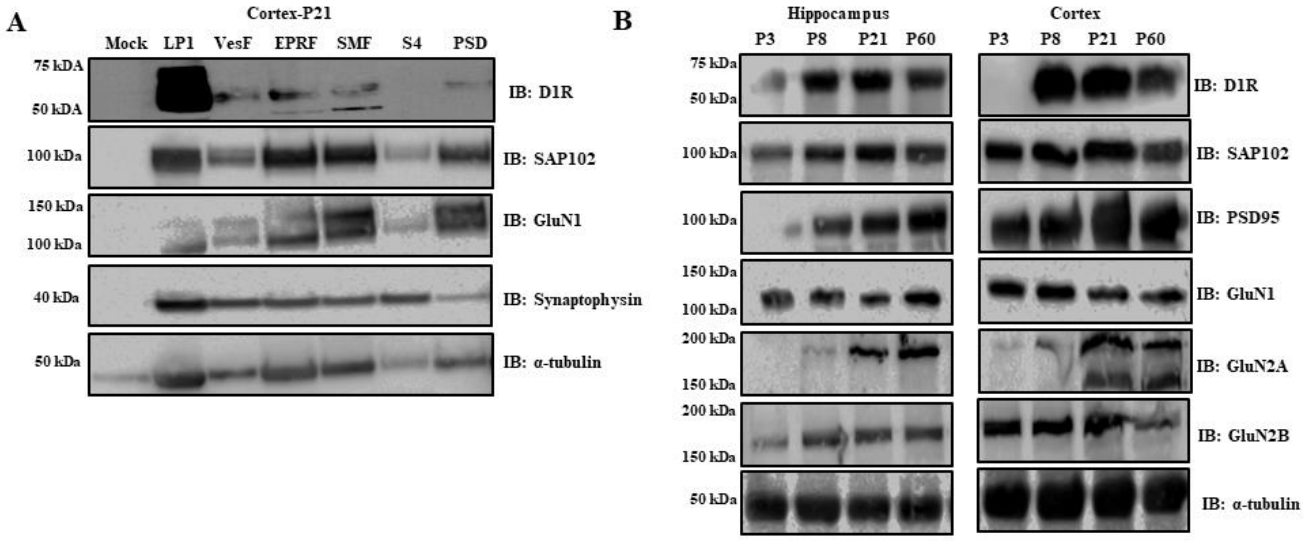

Supplementary Fig. 3.1. Subcellular Fractionation and Developmental Expression of Postsynaptic Proteins.
(A) Cortical tissues were subjected to differential centrifugation to isolate various cellular fractions. 50 μg protein were loaded and blots were probed with primary antibodies: rat-D1R, rabbit-SAP102, rabbit-GluNR1, rabbit-Synaptophysin, rabbit-α-tubulin. LP1: crude synaptosomal membrane fraction, VesF: vesicular fraction, EPRF: ER/microsome/mitochondrial pellet, SMF: synaptosomal membrane fraction, PSD: postsynaptic density. Blot is a representative of an experiment repeated two times. (B) LP1 fractions from hippocampus and cortex (50 μg) were loaded and blots were probed with rat-D1R, rabbit-SAP102, rabbib-PSD95, rabbit-GluNR1, rabbit-GluNR2A, rabbit-GluNR2B, and rabbit-α-tubulin as a loading marker. Blot is a representative of an experiment repeated two times.

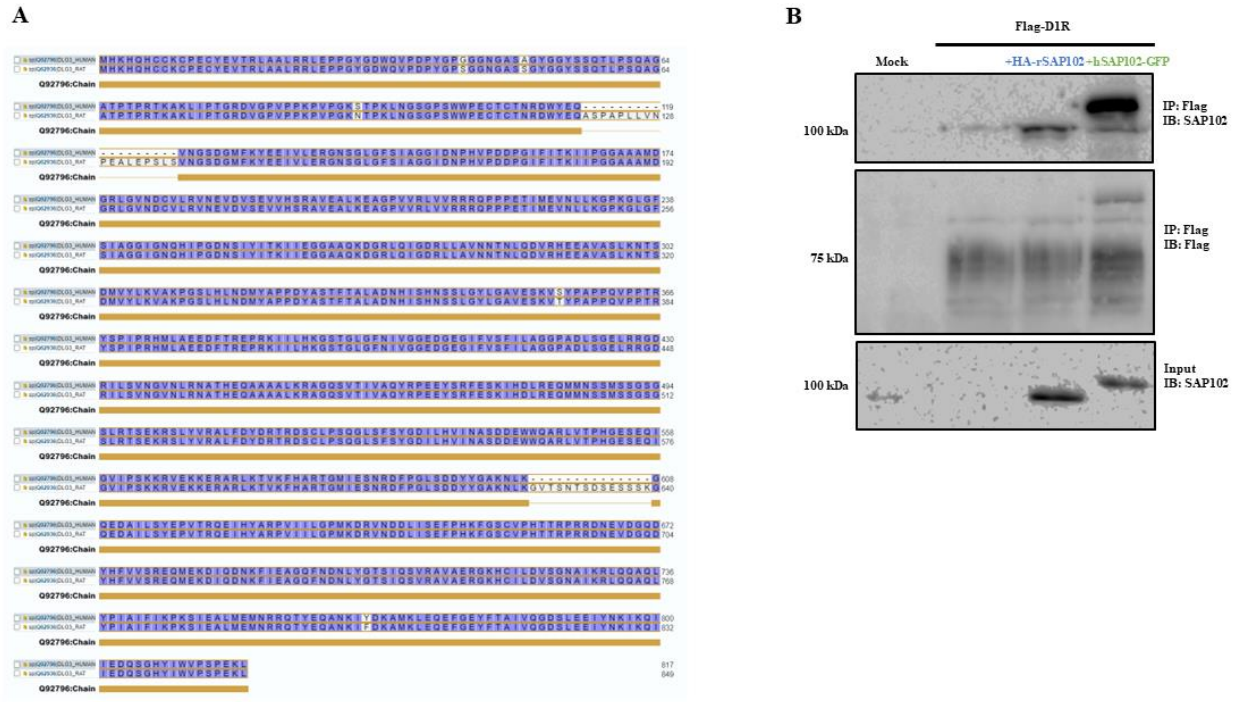

Supplementary Fig. 3.2. hSAP102 and rSAP102 Form an Immunocomplex with D1R.

(A) Alignment of amino acid sequence of human SAP102 (817 aa) and rat SAP102 (849 aa). Highlighted residues show similarities between SAP102 ortholog, with 99.39% identity. Alignment analysis by uniprot.org. (B) HEK293 cells were transfected with mock, Flag-D1R alone, co-transfected with HA-SAP102, or with SAP102-GFP. Cells were solubilized and subjected to a sequential immunoprecipitation with anti-Flag agarose matrix followed by immunoblotting with rabbit-SAP102 antibody. A representative experiment of N=3 is shown. B_{max} values in pmol/mg membrane protein for [^{3}H]-SCH23390 are Flag-D1R: 4.70±1.98, Flag-D1R+HA-SAP102: 3.80±1.59, Flag-D1R+SAP102-GFP: 4.13±1.91.

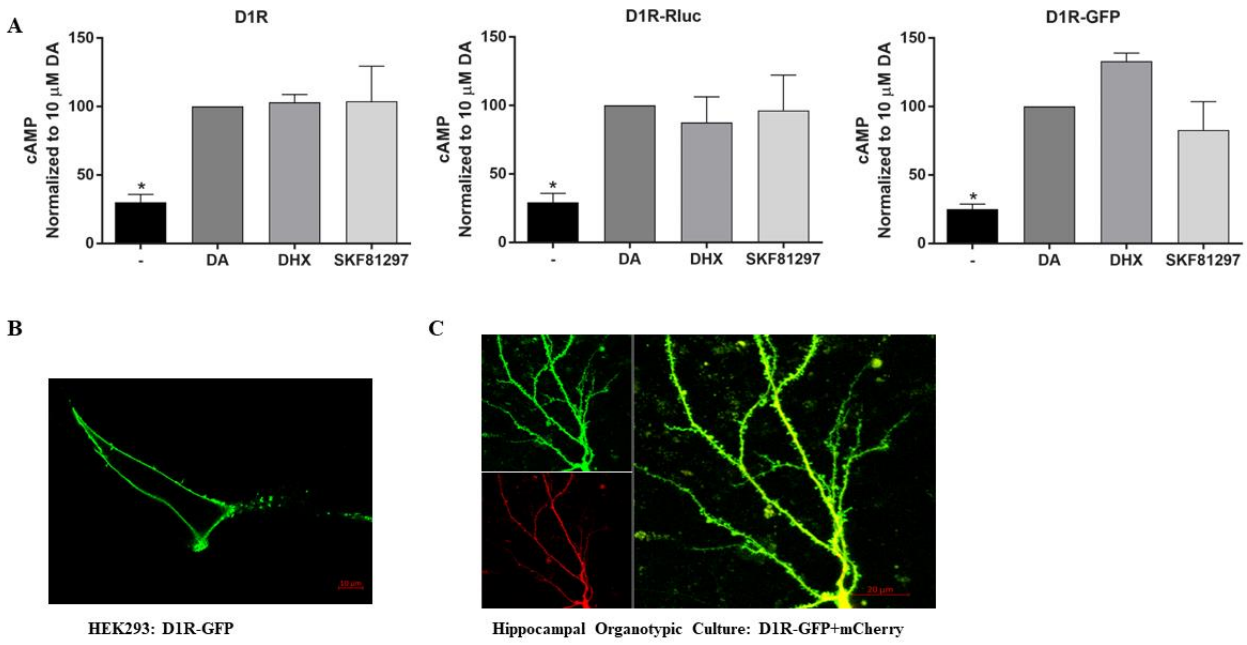

Supplementary Fig. 3.3. Functional Assessment for D1R-Fused with Rluc and GFP.

(A) HEK293T cells stably expressing GloSensor were transfected with D1R, D1R-Rluc, D1R-GFP. Relative luminance value (RLU) for each experiment done in quadrable determinations to measure cAMP level of constitutive activity (AA, denoted as -) or maximal activation (10 μM) of D1R agonists: DA, DHX, SKF81297. Each bar represents the arithmetic mean ± S.E. of normalized values relative to DA from four independent experiments. B_{max} values in pmol/mg membrane protein for [^{3}H]-SCH23390 are D1R: 5.32±3.67, D1R-Rluc: 3.44±2.04, D1R-GFP: 6.16±2.75. *: $p<0.05$, when compared to cells treated with 10 μM DA using one sample t test. (B) Confocal live imaging of HEK293 cells transfected with D1R-GFP using 63x magnification. The image is representative of an experiment repeated two times. B_{max} values for D1R-GFP in pmol/mg membrane protein for [^{3}H]-SCH23390: 4.55±2.49. (C) Two-photon live imaging of hippocampal organotypic slices (Sprague-Dawley rat, P8) were transfected with D1R-GFP and mCherry (40ug+10ug) at DIV7, and imaging were recorded at DIV10. Images were acquired using two-photon microscopy with 20x magnification. The image is representative of an experiment performed five times.

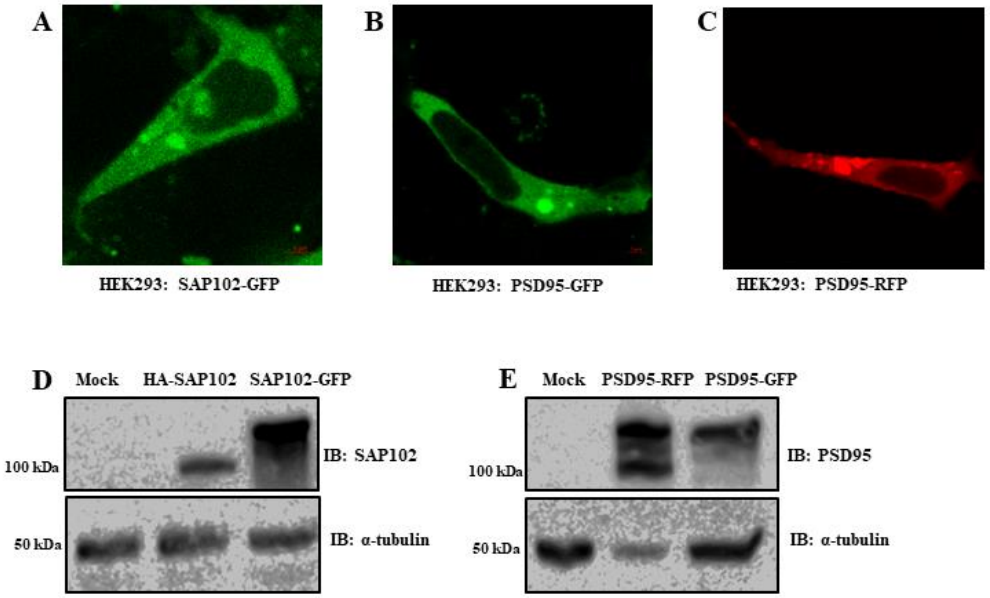

Supplementary Fig. 3.4. Assessment of the Fluorescent Proteins Fused with SAP102 and PSD95.
(A-C) Confocal live imaging of cells transfected with SAP102-GFP, PSD95-GFP, and PSD95-RFP using 63x magnification. Image is a representative of an experiments repeated two times. (D, E) Immunoblot analysis of HEK293 cells transfected with mock, HA-SAP102, and SAP102-GFP (D), or mock, PSD95-RFP, and PSD95-GFP (E). Cells were solubilized, subjected to SDS-Page, and probed with rabbit anti-SAP102, or rabbit-anti-PSD95. Blot is a representative of an experiments repeated two times.

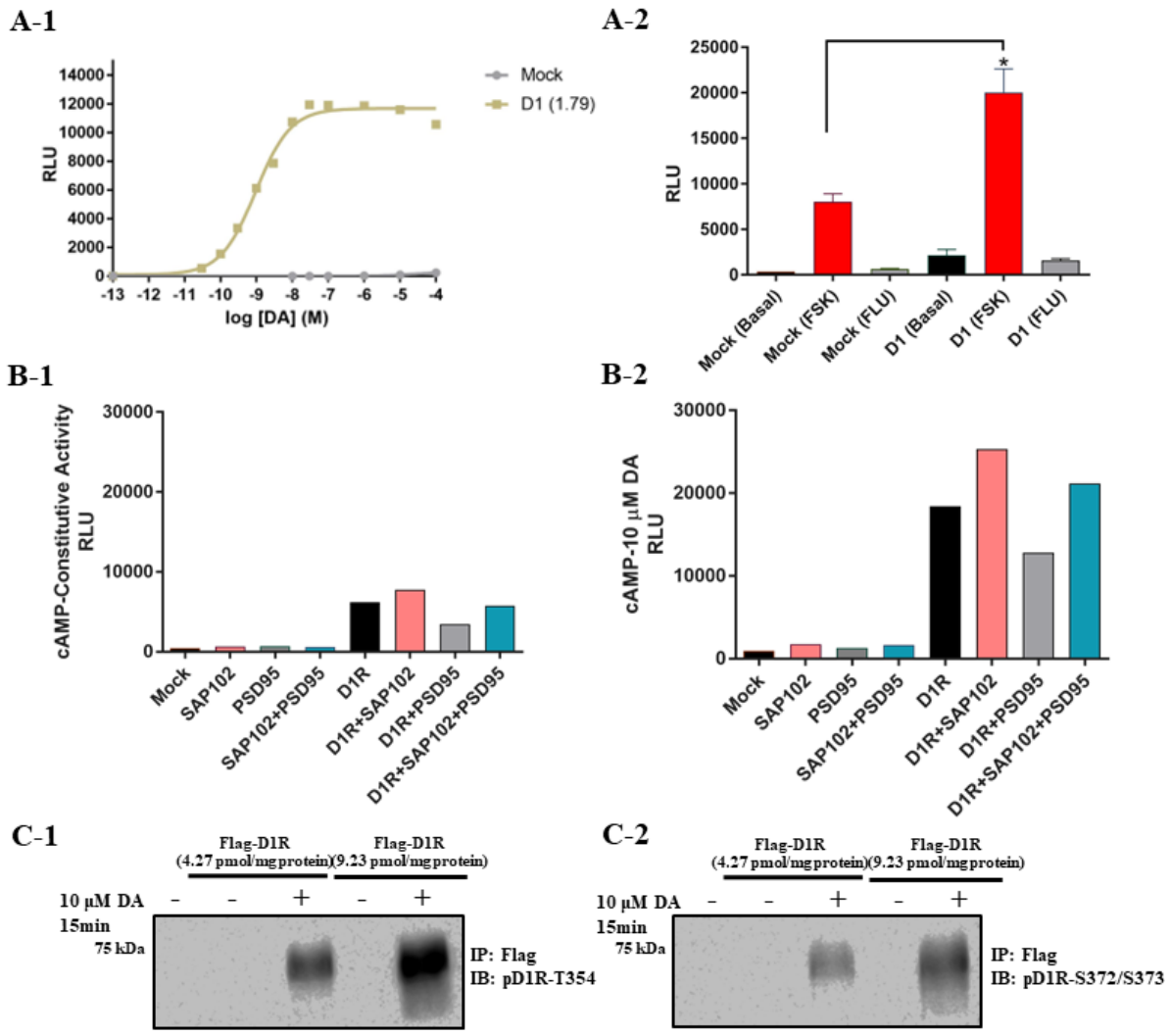

Supplementary Fig. 3.5. Assessment of cAMP Production and Phosphorylation of D1R.

(A) HEK293T-Glo cells transfected with mock or D1R, and cAMP measurement were assessed at basal (constitutive), treated with 10 μM FSK, or 10 μM FLU (A-1), or with increasing concentrations of DA (A-2). A represintative of average RLU calculated in quadrable determinations in response to cAMP production is shown, and B_{max} value for D1R= 1.79 pmol/mg of membrane proteins. (B) HEK293T-Glo cells transfected with mock, HA-SAP102, Flag-PSD95, HA-SAP102+Flag-PSD95, D1R, D1R+HA-SAP102, D1R+Flag-PSD95, and D1R+HA-SAP102+Flag-PSD95. cAMP measurement were assessed at basal (constitutive) (B-1) or 10 μM DA (B-2). A represintative of average RLU calculated in quadrable determinations in response to cAMP production is shown, corresponding to (Fig. 3.9B, C), and B_{max} values in pmol/mg membrane protein for [^{3}H]-SCH23390: D1R: 2.43, D1R+SAP102: 1.82, D1R+PSD95: 1.21, D1R+SAP102+PSD95: 1.36. (C) HEK293 cells transfected with mock, Flag-D1R (0.1 μg), and Flag-D1R (5 μg). Cells were treated with vehicle (AA, denoteed as -) or stimulated with 10 μM DA for 15 min, then solubilized and subjected to a sequential immunoprecipitation with anti-Flag agarose matrix followed by immunoblotting with rabbit anti-phospho-D1R-Thr354 and anti-phospho-D1R-Ser372/Ser373. A representative experiment of N=3 is shown. B_{max} values in pmol/mg membrane protein for [^{3}H]-SCH23390 are: Flag-D1R (0.1 μg): 4.44±1.27, Flag-D1R (5 μg): 13.14±2.69.

	Saturation Curves [^{3}H]-SCH23390		Competition Curves K_i (nM)			
Receptor	**K_d (nM)**	**B_{max} (pmol/mg protein)**	**DA**	**DHX**	**Thioridazine**	**SCH23390**
D1R (N=4)	**0.57** (0.54-0.59)	**6.2** (4.18-7.78)	**3426** (2191-5519)	**745** (582-915)	**44.4** (24.33-57.83)	**0.75** (0.36-1.33)
D1R-Rluc (N=4)	**0.71** (0.31-1.46)	**6.6** (2.15-15.62)	**4522** (1647-8698)	**821** (520-1030)	**40.3** (22.85-55.50)	**0.75** (0.21-1.20)
D1R-GFP (N=4)	**0.68** (0.39-0.99)	**18.4** (3.51-36.92)	**5423** (2593-10740)	**903** (774-1023)	**60.3** (25.64-96.50)	**0.92** (0.49-1.89)

Supplementary Table 3.1. Functional Assessment for D1R-Fused with Rluc and GFP by Radioligand Binding. Dissociation constants (K_d, K_I) and B_{max} values of radioligand saturation and competition studies of [^{3}H]-SCH23390 performed from HEK293 cells transfected with D1R, D1R-Rluc, and D1R-GFP. Values are expressed as arithmetic means, with minimum and maximum value in brackets. No statistical significance was observed using one-way ANOVA, when compared to D1R.

MANUSCRIPT II: Postsynaptic Density 95 (PSD95) Modulates Dopamine D5 Receptor

Postsynaptic Density 95 (PSD95) Modulates Dopamine D5 Receptor

Statement of Author Contribution

I would like to acknowledge the contribution of Kirk Multaz (Béïque Lab) and Jingwei Chen (Ferguson Lab) for the preparation of hippocampal organotypic cultures and embryonic cortical cultures, respectively. Radioligand binding and cAMP assays for D5R fused with either GFP or Rluc, as well D5R-Tango construct were performed with the assistance of Meriam Zeghal.

Appendix II contains supplementary figures and tables for manuscript II.

Rationale

Studies investigating crosstalk between DA, glutamate, and GABA suggest that D1R and D5R modulate excitatory glutamatergic and inhibitory GABAergic ionotropic receptors, respectively (Liu et al, 2000; Scott et al, 2002). As MAGUKs have been specifically associated with glutamatergic neurotransmission, my work described in the previous section and studies from other groups have demonstrated that the CT of D1R partakes in the formation of a complex with PSD95 and modulation of glutamate function (Zhang et al, 2007; Zhang et al 2009; Sun et al, 2009; Ladepeche et al, 2013b). These observations are in line with the view of specific D1R•NMDAR and D5R•$GABA_AR$-linked systems. In support of this, a study has reported that the CT of D5R does not interact with striatal PSD95, implying that neuronal D5R function may not require MAGUKs (Kruusmägi et al, 2009). However, Sun and colleagues showed that both D1R and D5R interact with PSD95 *in vitro*, suggesting that D5R can recruit MAGUK proteins. This study, however, did not investigate further the impact of this complex on signaling and trafficking properties of D5R (Sun et al, 2009). Interestingly, Moraga-Amaro and colleagues (2016) demonstrated that D5R KO-mice exhibit a deficit in long-term potentiation (LTP) and a reduction of hippocampal GluN2B-containing NMDAR expression. These findings demonstrate the importance of D5R in learning and memory and suggest a potential role of D5R in modulating NMDARs. The observed discrepancies between D5R studies may suggest a potential role of D5R not only in inhibitory ionotropic $GABA_AR$ function, but also in the modulation of excitatory NMDAR via glutamatergic scaffolding proteins. One of the mechanisms modulating D5R•GluN2B-containing NMDARs, potentially involves PSD95 interaction. Most importantly, how the interplay between D5R and PSD95 is controlled, and whether PSD95 modulates D5R

function in a similar manner to PSD95-mediated D1R signaling, remain unclear. **Herein, taking into account differences in the cytoplasmic domains of D1R and D5R, I hypothesized that PSD95 interacts with IL3 of D5R and regulates its signaling and trafficking properties in an opposite manner to D1R. I assessed the D5R•PSD95 interaction *in vitro* and *in vivo*, and studied the effect of PSD95 on D5R signaling and trafficking mechanisms.**

Results

1. PSD95 Interacts with D5R

To address whether PSD95 interacts or not with D5R, *in vitro* coimmunoprecipitation were performed from transiently transfected HEK293 cells with empty vector (mock), Flag-D1R, Flag-D1R+PSD95-RFP (included as a positive control; Fig. 3.8B), Flag-D5R, and Flag-D5R+PSD95-RFP. Immunoblots show that PSD95 forms immunocomplexes with both D1R and D5R (Fig. 4.1A). Previously, I showed that SAP102 selectively interacts with D1R, but not with D5R (Fig. 3.5F); thus, I sought to validate the selective formation of D5R complex with PSD95 and not SAP102 in cells co-transfected with HA-D5R alone and Flag-SAP102 or Flag-PSD95. The results indicate that D5R selectively coimmunoprecipitated PSD95 (Fig. 4.1B). Coimmunoprecipitation of Flag-PSD95 and Flag-SAP102 in cells co-expressing D5R-GFP further support that D5R specifically associated with PSD95 but not with SAP102 (Fig. 4.1C). Immunostaining of transfected HEK293 cells showed that HA-D5R is highly localized at cell membrane, whereas Flag-SAP102 and Flag-PSD95 expressed intracellularly within the cells (Fig. 4.1D). Co-transfected HEK293 cells revealed more colocalization of PSD95 with D5R, relative to SAP102, at the cell surface and in cytosolic compartments (Fig. 4.1E, F). These findings suggest that PSD95 interacts with D1-class receptor subtypes, and D5R selectively interacts with PSD95, but not with SAP102 *in vitro*.

To investigate whether PSD95 potentially associates with D5R *in vivo*, hippocampal and cortical lysates (Sprague-Dawley rat, P21, male and female) were immunoprecipitated with D5R antibody, followed by immunoblotting analysis with PSD95 and SAP102 antibodies. In addition to the input, native endogenous D5R•PSD95 complex is detected in hippocampus and cortex, but not observed with SAP102 (Fig. 4.2A, B). Conversely, PSD95 was immunoprecipitated from solubilized cortical lysates, and immunoblot analysis reveals that D5R coimmunoprecipitated with PSD95, but not with SAP102 (Fig. 4.2C).

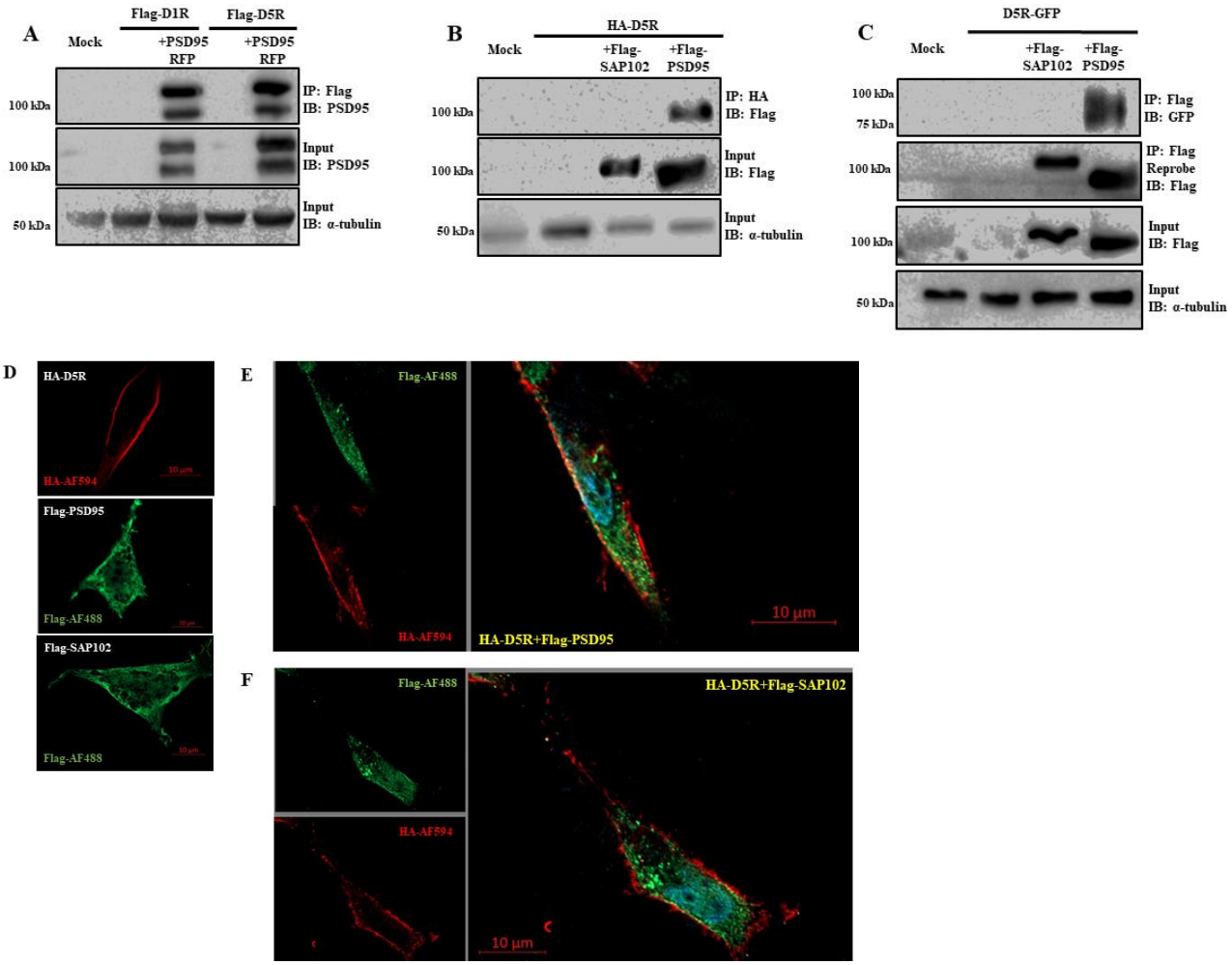

Fig. 4.1. PSD95 Interacts with D5R, *in vitro*.

(A) HEK293 cells transfected with mock, Flag-D1R alone, or with PSD95-RFP, Flag-D5R, or with PSD95-RFP. Cells were solubilized and subjected to a sequential immunoprecipitation with anti-Flag agarose matrix followed by immunoblotting with anti-PSD95 antibody. A representative experiment of N=3 is shown. B_{max} values in pmol/mg membrane protein for [^{3}H]-SCH23390 are Flag-D1R: 2.73±1.06, Flag-D1R+PSD95-RFP: 2.15±0.16, Flag-D5R: 2.14±1.26, Flag-D5R+PSD-95RFP: 1.63±0.92. (B) HEK293 cells transfected with mock, HA-D5 alone, with Flag-SAP102, or with Flag-PSD-95. Cells were solubilized and subjected to a sequential immunoprecipitation with anti-HA agarose matrix followed by immunoblotting with anti-Flag antibodies. A representative experiment of N=4 is shown. B_{max} values in pmol/mg membrane protein for [^{3}H]-SCH23390 are HA-D5R: 1.43±.0.14, HA-D5R+ Flag-SAP102: 1.27±0.37, HA-D5R+Flag-PSD95: 0.87±0.17. (C) HEK293 cells transfected with mock, D5R-GFP alone, with Flag-SAP102, or with Flag-PSD95. Cells were solubilized and subjected to a sequential immunoprecipitation with anti-flag agarose matrix followed by immunoblotting with anti-GFP antibodies. A representative experiment of N=6 is shown. B_{max} values in pmol/mg membrane protein for [^{3}H]-SCH23390 are D5R-GFP: 8.57±3.38, D5R-GFP+ Flag-SAP102: 8.54±2.09, D5R-GFP+Flag-PSD95: 9.72±2.85. (D-F) Representative images for HEK293 cells transfected with HA-D5R, Flag-SAP102 or Flag-PSD95 (D), co-transfected with HA-D5R+Flag-PSD95 (E), or HA-D5R+Flag-SAP102 (F), followed by immunostaining with primary antibodies: rabbit anti-HA and mouse anti-Flag, following by secondary fluorophore antibodies: anti-rabbit conjugated Alexa Fluor-594 and anti-mouse conjugated Alexa Fluor-488. Images were acquired using epifluorescence microscope with 63x magnification. Images are representative of four independent experiments. B_{max} values in pmol/mg membrane protein for [^{3}H]-SCH23390 are HA-D5R: 1.43±.0.14, HA-D5R+ Flag-SAP102: 1.27±0.37, HA-D5R+Flag-PSD95: 0.87±0.17.

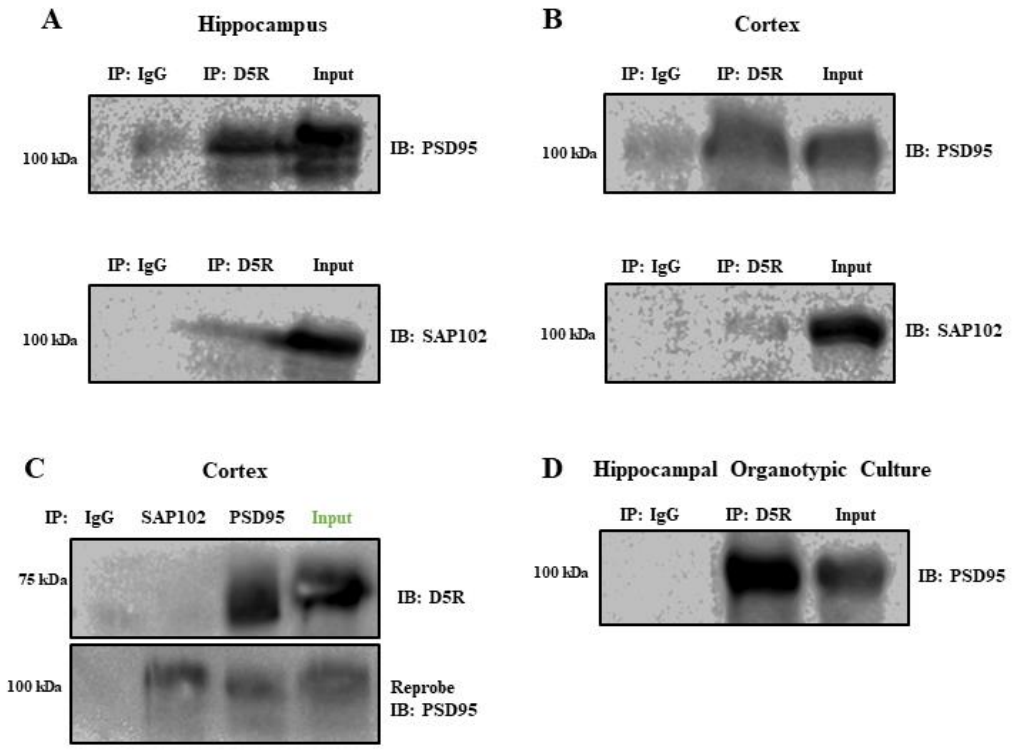

Fig. 4.2. PSD95 Interacts with D5R, *in vivo*.

(A, B) Solubilized lysates from hippocampus (0.5 mg) and cortex (1.5 mg) of rat (P21) were subjected to an immunoprecipitation procedure using mouse-D5R antibody and resolved immunocomplexes probed with rabbit-PSD95 and rabbit-SAP102 antibodies. Normal mouse IgG were used as a negative control. 50ug of lysate were loaded to the gels as input. Blot is a representative for an experiment repeated three times. (C) Solubilized lysates from cortex (1.5 mg) of rat (P21) were subjected to an immunoprecipitation procedure using mouse-SAP102 and mouse-PSD95 and resolved immunocomplexes probed with rabbit-D5R antibody. Normal mouse IgG were used as a negative control. 50ug of lysate were loaded to the gels as input. Blot is a representative of an experiment repeated three times. (D) Solubilized lysates from hippocampal organotypic cultures (0.5 mg) were subjected to an immunoprecipitation procedure using mouse-D5R antibody and resolved immunocomplexes probed with rabbit-PSD95 antibody. Normal mouse IgG were used as a negative control. 50ug of lysate were loaded to the gels as input. Blot is a representative of an experiment repeated two times.

Together, these findings suggest that existence of native endogenous D5R•PSD95 complex.

2. Subcellular Localization of D5R•PSD95 Signaling Complex

I assessed the subcellular endogenous localization of D5R, PSD95, and SAP102 in hippocampal organotypic culture (P8, DIV28). Confocal airyscan microscopy studies reveal that the immunolabelled D5R, SAP102, and PSD95 are localized in dendrites and more concentrated in spines (Supplementary Fig. 4.1A, B). Interestingly, D5R labeling colocalized with discrete immunopositive PSD95 clusters in dendrites and spines of hippocampal neurons (Supplementary Fig. 4.1A). SAP102 is highly enriched in the spines, however, no localization with D5R was observed (Supplementary Fig. 4.1B). Moreover, coimmunoprecipitation studies were performed from these hippocampal organotypic cultures. Results show that PSD95 is detected in D5R immunocomplexes isolated from these organotypic cultures (Fig. 4.2D). These results suggest that PSD95 colocalized and interacts with D5R, perhaps in PSD.

Although the results from hippocampal organotypic culture suggested D5R•PSD95 colocalization in hippocampal neurons, I sought to further validate these findings by utilizing embryonic neuronal culture (CD1 mice, E13-14). Immunostaining of endogenous D5R, SAP102, and PSD95 at DIV10, reveal subcellular localization of these proteins in dendrites and dendritic spines, and more clusters of colocalized D5R with PSD95 than with SAP102 in these neurons (Fig. 4.3A, B).

Further, I assessed whether D5R•PSD95 complexes can be observed in these neuronal cultures by performing *in situ* PLA. Cortical cultures were immunostained with rabbit anti-D5R and mouse anti-PSD95, or mouse anti-SAP102 antibodies, followed by fluorescent-labeled complementary oligonucleotide probes that bind to the amplicons (amplified DNA) at the sites of protein-protein interactions, producing distinct dots of high fluorescence on the tissue (Fig. 4.3C). Interestingly, *in situ* PLA demonstrate abundant endogenous interacting signals of D5R•PSD95, in dendrites and dendritic spines of cortical cultures, whereas negligible, nonspecific signals (smaller than the expected PLA spot size) were detected for D5R•SAP102 (Fig. 4.3E, F). MAP2 antibody was included to visualize neuronal dendrites. Single antibody incubation of D5R in PLA experiments did not exhibit signal generation, attesting the specificity of PLA methodology (Fig. 4.3D). These findings support the notion that D5R interacting with PSD95 in dendrites and spines and the existence of native D5R•PSD95 complex *in vivo*.

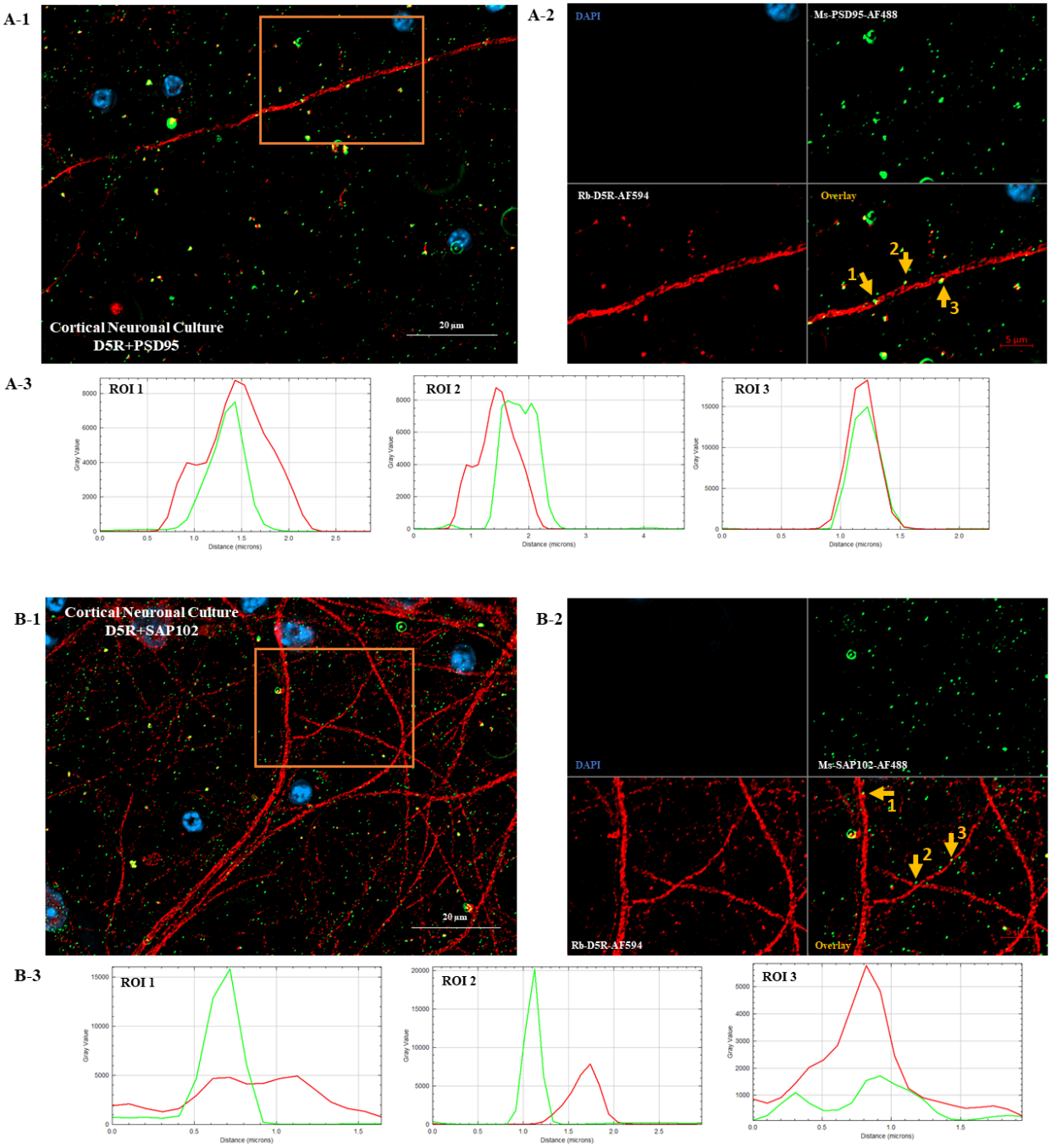
A-1
Cortical Neuronal Culture
D5R+PSD95
20 μm
A-2
DAPI
Ms-PSD95-AF488
Rb-D5R-AF594
Overlay
1
2
3
5 μm
A-3
ROI 1
ROI 2
ROI 3
Gray Value
Distance (microns)
B-1
Cortical Neuronal Culture
D5R+SAP102
20 μm
B-2
DAPI
Ms-SAP102-AF488
Rb-D5R-AF594
Overlay
1
2
3
B-3
ROI 1
ROI 2
ROI 3
Gray Value
Distance (microns)

C

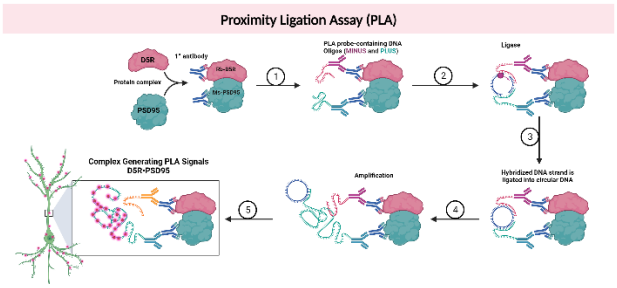
Proximity Ligation Assay (PLA)
D5R
1° antibody
Protein complex
PSD95
Rb-D5R
Ms- PSD95
PLA probe-containing DNA Oligos (MINUS and PLUS)
Ligase
Hybridized DNA strand is ligated into circular DNA
Amplification
Complex Generating PLA Signals D5R-PSD95
1
2
3
4
5

D

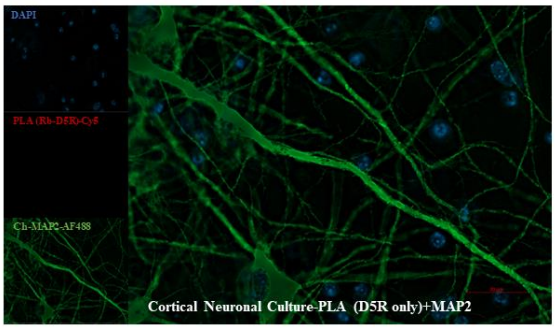
DAPI
PLA (Rb-D5R+Cy5
Ch-MAP2-AF488
Cortical Neuronal Culture-PLA (D5R only)+MAP2

E-1

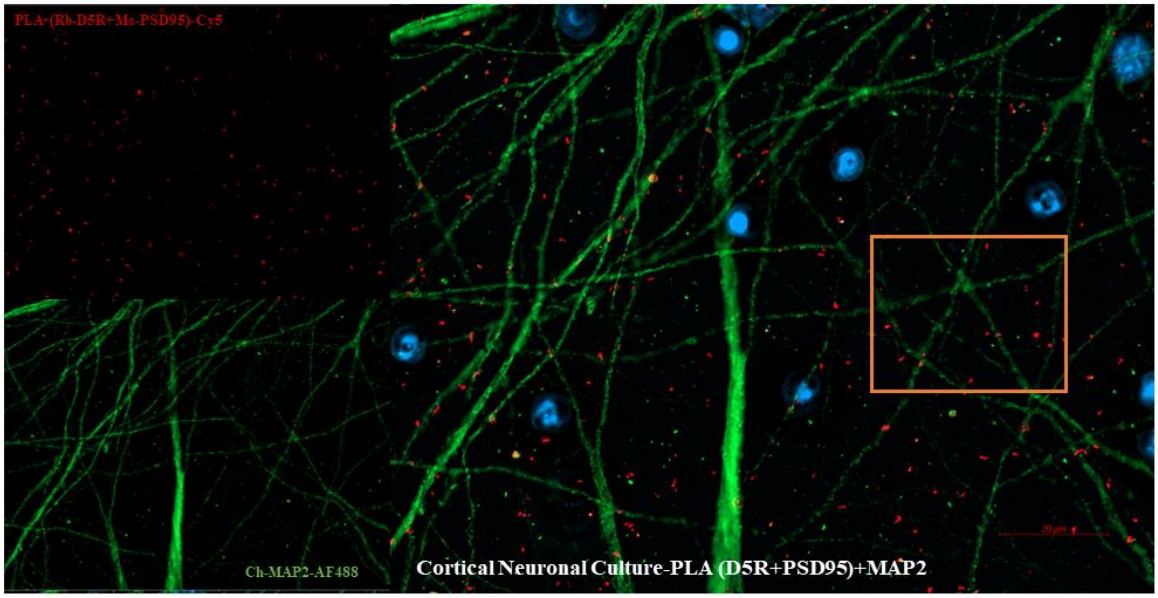
PLA (Rb-D5R+Ms-PSD95)-Cy5
Ch-MAP2-AF488
Cortical Neuronal Culture-PLA (D5R+PSD95)+MAP2

E-2

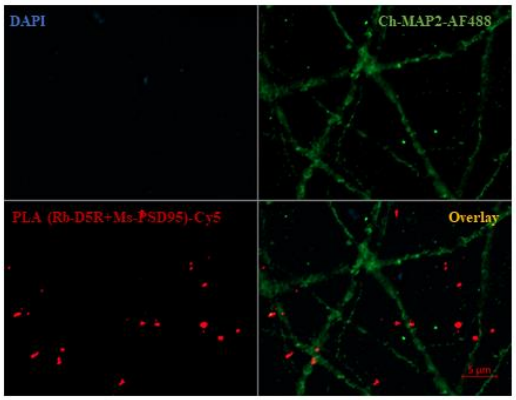
DAPI
Ch-MAP2-AF488
PLA (Rb-D5R+Ms-PSD95)-Cy5
Overlay

E-3

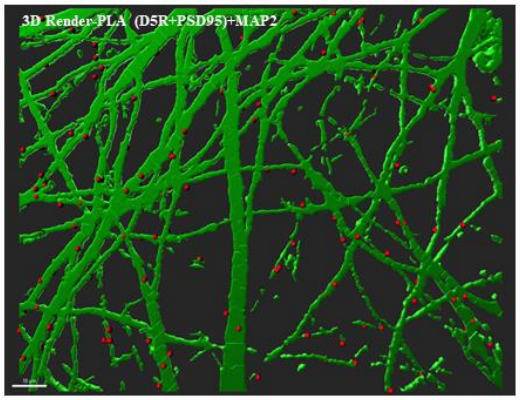
3D Render-PLA (D5R+PSD95)+MAP2

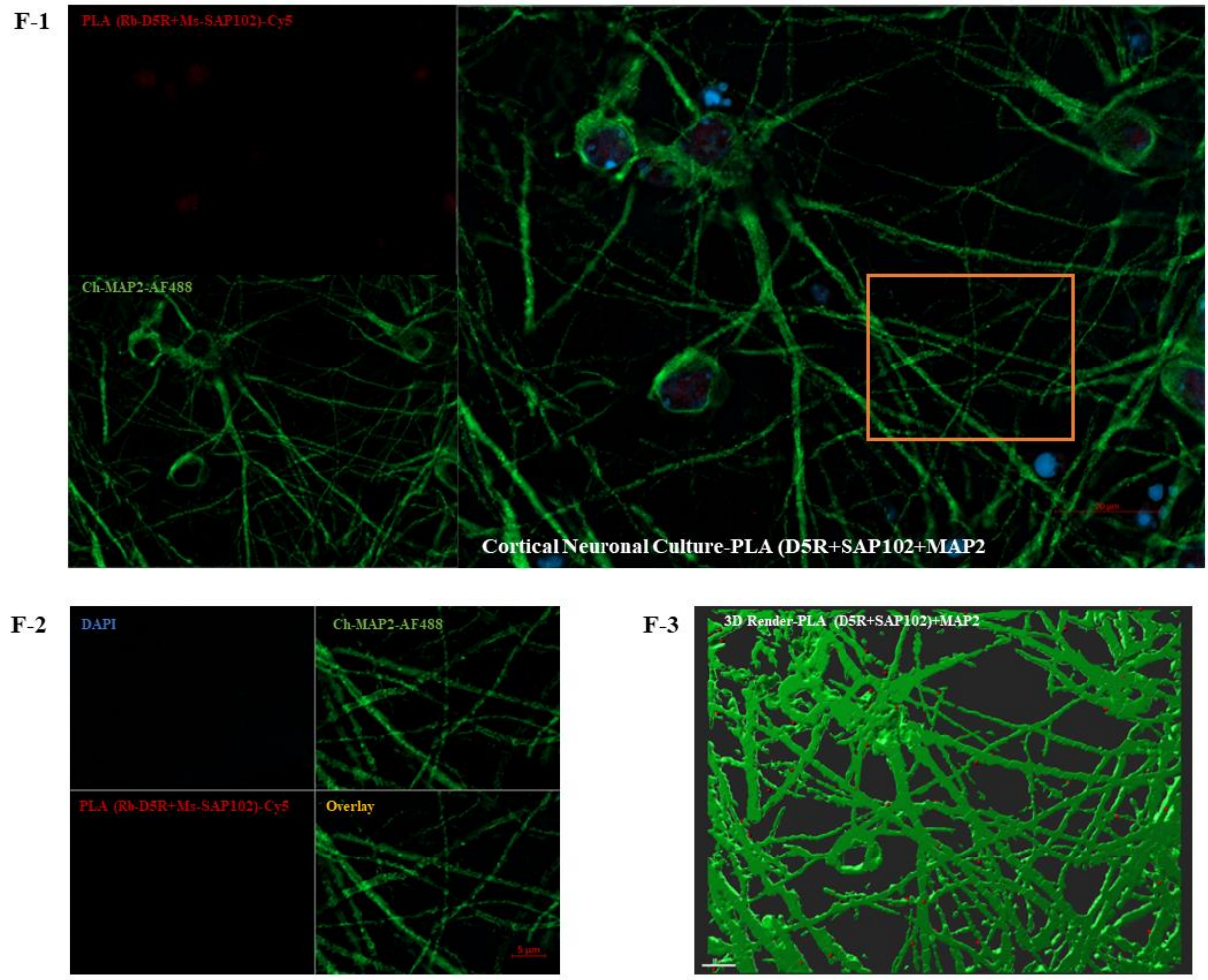

Fig. 4.3. Subcellular localization and PLA Interaction of D5R•PSD95 from Embryonic Cortical Cultures.
(A, B) Representative epiflorescent images of embryonic cortical culture (CD1 mice, E13-14, DIV10) immunostained with primary antibodies: rabbit anti-D5R, mouse anti-PSD95, or mouse anti-SAP102, followed by secondary fluorophore antibodies: anti-rabbit conjugated Alexa Fluor-594 and anti-mouse conjugated Alexa Fluor-488. Images were acquired using epifluorescence microscope with 63x magnification. The image is a representative of an experiment performed three times. Region of interests (ROIs) of colocalized D5R•PSD95 (A-3) and D5R•SAP102 (B-3) are shown; PSD95 and SAP102 in green, D5R in red. (C) A schematic diagram of the PLA protocol. Created with BioRender.com. (D-F) Representative epifluorscent images of embryonic cortical culture immunostained with primary antibodies: rabbit anti-D5R only (D), co-strained with mouse anti-PSD95 (E) or with mouse anti-SAP102 (F), followed by the addition of PLUS and MINUS PLA probes. Probes were ligated, amplified, and generated PLA signals were visualized using far red (Cy5) filter. Cells were also incubated with chicken anti-MAP2 antibody, followed by the anti-chicken conjugated-488. Images were acquired using epifluorescence microscope with 63x magnification. The image is a representative of an experiment performed three times. (E2, F2) Subset of higher magnification. (E-3, F-3) IMARIS 3D reconstructed image showing the PLA signals as spots.

3. PSD95 Interacts with IL3 of D5R

Next, I mapped the intracellular regions of D5R that mediate the interaction with PSD95. GST fusion proteins encoding D5R-IL3 (R247-K296) and D5R-CT (F361-H477) were constructed and used as baits in pull-down assays (Fig. 4.4A). Incubation of GST, GST-D5R-IL3 and GST-D5R-CT with HEK293 cell lysates containing PSD95 or SAP102 revealed that GST-D5R-IL3 copurified selectively with PSD95, whereas SAP102 is not pulled down with GST-D5R-IL3 or GST-D5R-CT (Fig. 4.4B, C). Moreover, cortical lysates were also incubated with GST-purified proteins of D5R, and results show that endogenous PSD95, but not SAP102, copurified specifically with GST-D5R-IL3 (Fig. 4.4D, E).

Additionally, our lab generated deletion mutants of IL3 and CT of D5R referred as: Flag-D5R-ΔIL3N (Q255-S275), Flag-D5R-ΔIL3C (A276-K289), and Flag-D5R-ΔCT (C374-H477) (Fig. 4.4F). To delineate the intracellular region of D5R mediating the interaction with PSD95, coimmunoprecipitation studies with HEK293 cells co-transfected with PSD95-RFP and Flag-D5R, Flag-D5R-ΔIL3N, Flag-D5-ΔIL3C, or Flag-D5-ΔCT were performed. Results show that mutant D5R-ΔIL3N impaired the interaction between D5R and PSD95 (Fig. 4.4G). These findings further support the results from GST-pulldown assays and suggest that formation of a functional complex between D5R and PSD95 is dependent on D5R-IL3. Collectively, these findings suggest that PSD95 interact with different cytosolic regions of D1-class receptors; D1R-CT and D5R-IL3 (Fig. 3.6C, E, H; Fig 4.4C, E, G).

4. D5R Binding Affinity is not Impacted by PSD95

As the coimmunoprecipitation studies showed there is constitutive association of D5R•PSD95 via the interaction with IL3, I assessed whether complex formation of D5R•PSD95 modulates the ligand binding properties of the D5R. PSD95 and SAP102 had no effect on the maximal binding capacity (B_{max}) and dissociation constant of [^{3}H]-SCH23390 (K_d) for D5R (Table 4.1). Likewise, affinity of agonists (K_i) for DA, SKF81297, DHX were not significantly altered (Table 4.1). Overall, these findings indicate that the D5R•PSD95 signaling complex display ligand binding properties similar to PSD95-free D5R.

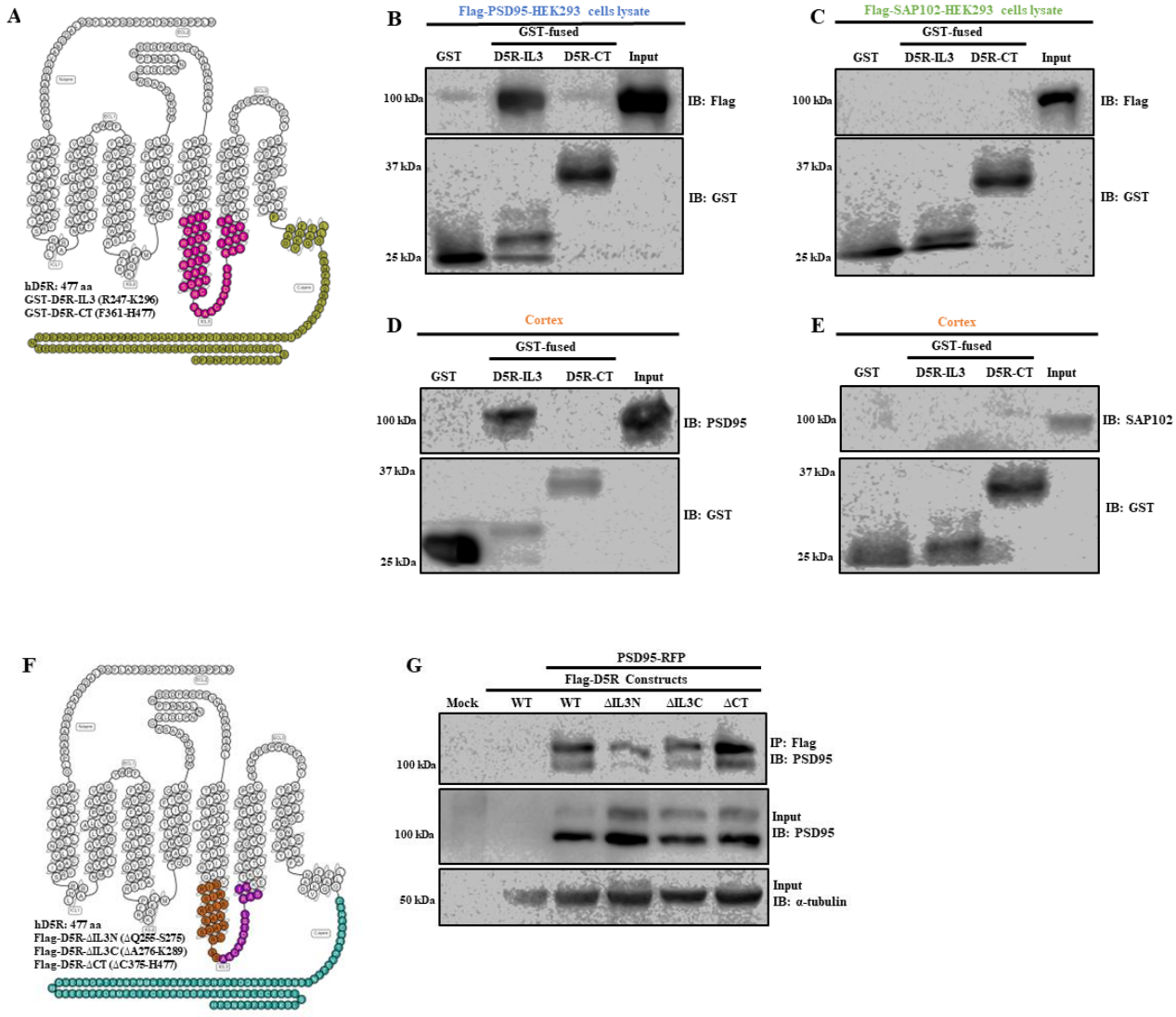

Fig. 4.4. PSD95 Associates with IL3 of D5R.

(A) Schematic diagram of D5R showing the amino acid sequence corresponding fusion protein of GST-constructs: GST-D5R-IL3 and GST-D5R-CT. Created by gpcrdb.org. (B, C) HEK293 cells were transfected with Flag-PSD95 (B) or Flag-SAP102 (C) and lysate (0.5 mg) were incubated with GST, GST-D5R-IL3, and GST-D5R-CT, followed by immunoblotting with anti-Flag antibody. A representative experiment of N=4 is shown. (D, E) Cortical lysates (1 mg) were incubated with GST, GST-D5R-IL3, and GST-D5R-CT, followed by immunoblotting with anti-PSD95 and SAP102 antibodies. A representative experiment of N=4 are shown. (F) Schematic representation of deleted amino acid of D5R mutants: Flag-D5R-ΔIL3N, Flag-D5R-ΔIL3C, Flag-D5R-ΔCT. Created by gpcrdb.org. (G) HEK293 cells were co-transfected with wild-type and mutant forms of D5R and PSD95-RFP. Cells were solubilized and subjected to a sequential immunoprecipitation with anti-Flag agarose matrix followed by immunoblotting with rabbit-PSD95 antibody. Blots shown are representative for an experiment repeated four times. B_{max} values in pmol/mg membrane protein for [^{3}H]-SCH23390: Flag-D5R: 7.32±0.1.83, Flag-D5R+PSD95-RFP: 3.98±1.24, Flag-D5R-ΔIL3N+PSD95-RFP: 4.21±0.94, Flag-D5R-ΔIL3C+PSD95-RFP: 2.11±0.63, Flag-D5R-ΔCT+PSD95-RFP: 2.22±1.04.

	Saturation Curves [^{3}H]-SCH23390		Competition Curves K_i (nM)		
Receptor	**K_d (nM) N=6**	**B_{max} (pmol/mg protein) N=6**	**DA N=5**	**SKF81297 N=6**	**DHX N=3**
D5R	**0.87** (0.39-1.18)	**5.4** (2.28-9.64)	**658** (364-1145)	**16.4** (8.78-24.35)	**42.2** (37.16-50.09)
D5R+SAP102	**0.90** (0.30-1.45)	**5.2** (1.67-9.08)	**453** (211-667)	**13.2** (9.13-19.09)	**37.6** (25.62-56.39)
D5R+PSD95	**0.89** (0.57-1.42)	**5.4** (1.11-10.27)	**533** (397-660)	**14.6** (9.20-21.99)	**52.7** (42.18-58.48)

Table 4.1. D5R Binding Affinity is not Impacted by PSD95.
Affinity dissociation constants (K_d, K_I) and B_{max} values of radioligand saturation and competition studies of [^{3}H]-SCH23390 performed from HEK293 cells transfected with D5R, co-transfected with HA-SAP102, or co-transfected with Flag-PSD95. Values are expressed as arithmetic means, with minimum and maximum value in brackets. No statistical significance was observed using one-way ANOVA, when compared to D5R.

5. The Functionality of the D5R-GFP and D5R-Rluc

Our lab generated D5R-GFP and D5R-Rluc that were subsequently used in various experiments in my thesis (e.g., coimmunoprecipitation, BRET). Functional studies were performed to assess of the fused GFP and Rluc to CT of D5R modulate the receptor function. cAMP assays show that D5R-GFP and D5R-Rluc produce cAMP in response to agonist stimulation similar to untagged D5R (Supplementary Fig. 4.2A). Saturation and competition studies also show unaltered binding function for D5R-Rluc and D5R-GFP relative to untagged D5R (Supplementary Tables 4.1). Confocal live imaging of HEK293 cells transfected with D5R-GFP reveals that D5R is localized at the plasma membrane (Supplementary Fig. 4.2C). Together, these findings suggest that the insertion of GFP or Rluc at CT of D5R does not alter the functionality of D5R and its targeting at plasma membrane.

6. Agonist-induced Stimulation of D5R Regulates the Interaction with PSD95

To determine whether D5R•PSD95 complex can be regulated by D1-class ligands, coimmunoprecipitation and BRET studies were performed. Transfected HEK293 cells were stimulated with DA (10 μM, 15 min) followed by coimmunoprecipitation. Immunoblots results showed that activation of D5R with DA substantially increased the abundance of PSD95 interacting with D5R, implying that the D5R under basal condition couples to PSD95, and the agonist stimulation facilitates the complex formation (Fig. 4.5A).

To validate these findings, $BRET^2$ studies were employed using live HEK293 cells transfected with D5R-Rluc alone, or with PSD95-GFP, or SAP102-GFP (included as a negative control) (Fig. 4.5B). To assess the specificity of these basal BRET signals, HEK293 cells were transfected with a constant amount of D5R-Rluc (0.5 μg) along with an increasing ratio of plasmids expressing SAP102-GFP or PSD95-GFP (1:1, 1:3, 1:5, 1:10). The results showed increasing, but saturable BRET signals with D5R•PSD95, implying the specificity of these BRET signals observed for D5R•PSD95 under basal condition (Fig. 4.5C). SAP102-GFP and GbR2 subunit of $GABA_BR$ (GbR2-GFP), a negative control that lacks functional activity and retains in the ER, showed no recruitments to D5R-Rluc. Moreover, incubation of D5R•PSD95 with DA (10 μM, 30 min) modulated BRET signals, which implies an increased association between D5R and PSD95, and/or a dynamic conformational rearrangement for the complex to be more closely associated (stabilized) after receptor activation (Fig. 4.5D).

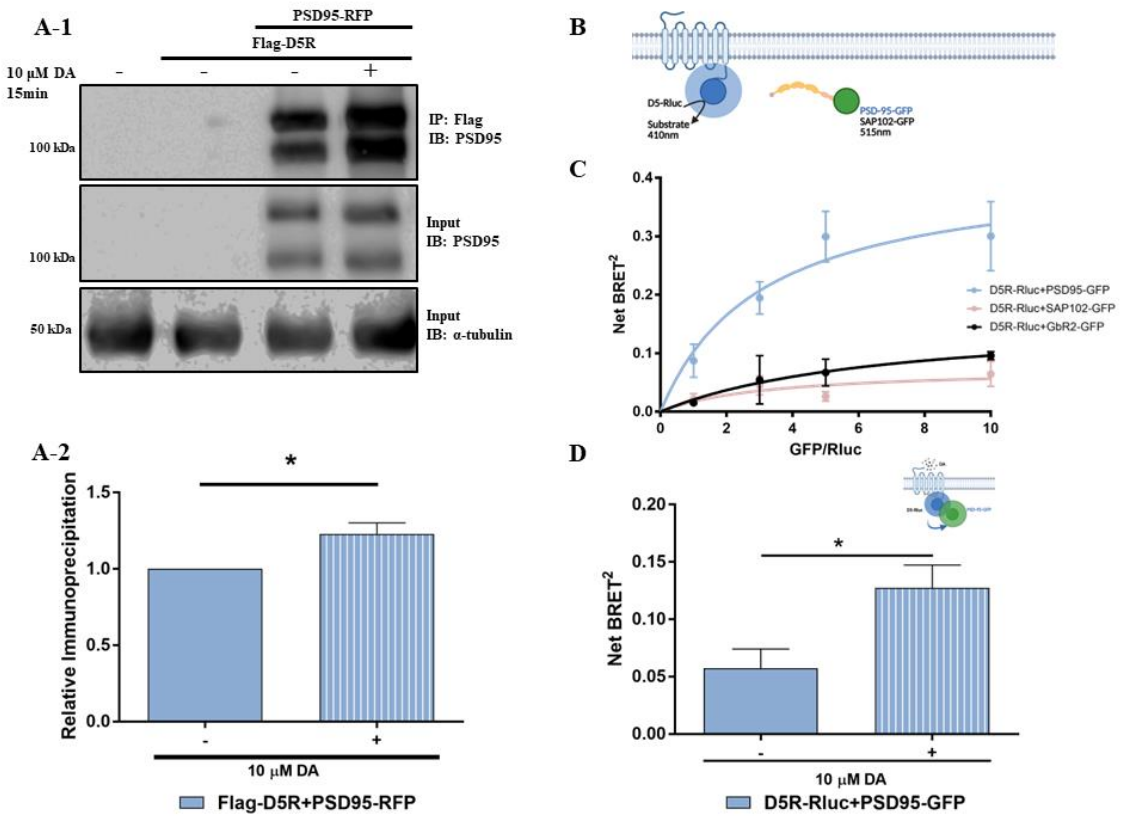

Fig. 4.5. Agonist-induced Stimulation of D5R Regulates the Interaction with PSD95.

(A) HEK293 cells were transfected with mock, Flag-D5R, and Flag-D5R+PSD95-RFP. Cells were stimulated with DA for 15 min, or left untreated (vehicle: AA, denoted as -), then solubilized and subjected to a sequential immunoprecipitation with anti-Flag agarose matrix followed by immunoblotting with rabbit-PSD95 antibody. A representative experiment of N=5 is shown. B_{max} values in pmol/mg membrane protein for [^{3}H]-SCH23390 are Flag-D5R: 4.21±1.57, Flag-D5R+PSD95-RFP: 2.55±0.94. (A-2) showed a relative immunoprecipitation quantified for IP-PSD95 over input-PSD95, then stimulated cells were normalized to unstimulated cells. *: $p<0.05$ when DA compared with control using one sample t test. (B) Schematic diagram of BRET^2 assay. Created with BioRender.com. (C, D) HEK293 cells were transfected with D5R-Rluc, or co-transfected with PSD95-GFP, SAP102-GFP, or GbR2-GFP. Coelenterazine 400a was added, and light emission was measured from the luciferase donor and GFP acceptor at 410 nm and 515 nm wavelength, respectively. Net BRET^2 was quantified as: [(GFP emission at 515 ± 30nm)/(Rluc emission 410 ± 80nm)]−[(emission at 515 ± 30nm)/(emission at 410 ± 80nm)] found with the D5R-Rluc expressed alone in the same experiment. (C) BRET saturation curve was performed by increasing the concentration of PSD95-GFP, SAP102-GFP and GbR2-GFP over fixed concentration of D5R-Rluc. BRET measurement for were quantified from three independent experiments, and B_{max} values in pmol/mg membrane protein for [^{3}H]-SCH23390 for D5R-Rluc: 2.89±1.76, D5R-Rluc+PSD95-GFP (1:1): 4.93±2.82, D5R-Rluc+PSD95-GFP (1:3): 3.77±1.41, D5R-Rluc+PSD95-GFP (1:5): 3.97±1.78, D5R-Rluc+PSD95-GFP (1:10): 1.86±0.72, D5R-Rluc+SAP102-GFP (1:1): 1.19±0.42, D5R-Rluc+SAP102-GFP (1:3): 2.38±1.85, D5R-Rluc+SAP102-GFP (1:5): 2.64±1.20, D5R-Rluc+SAP102-GFP (1:10): 1.99±1.46, D5R-Rluc+GbR2-GFP (1:1): 1.16±0.44, D5R-Rluc+GbR2-GFP (1:3): 1.33±0.44, D5R-Rluc+GbR2-GFP (1:5): 0.91±0.45, D5R-Rluc+GbR2-GFP (1:10): 1.10±0.46. (D) Cells were treated with AA (vehicle, denoted as -) or 10 μM DA (30 min). BRET analyses were quantified from four independent experiments, and B_{max} values in pmol/mg membrane protein for [^{3}H]-SCH23390 for D5R-Rluc: 5.19±1.69, D5R-Rluc+PSD95-GFP: 3.31±2.19. *: $p<0.05$, when compared using unpaired t test.

7. PSD95 Facilitates D5R-mediated cAMP Production and ERK1/2 Activation

As PSD95 interacts with IL3 of D5R, I next tested if this interaction promotes a distinct modulation of D5R signaling properties. I measured cAMP production using HEK293T cells stably expressing GloSensor, a luciferase-based cAMP biosensor (HEK293T-Glo) (Fig. 4.6A). Overexpression of PSD95 exerts no effect on constitutive activity of D5R, however, DA activation (10 μM, 15 min) substantially increased D5R-mediated cAMP production, relative to cells transfected with D5R alone (Fig. 4.6B, C). SAP102 overexpression has no effect on either the constitutive activation or DA-mediated cAMP accumulation in comparison to D5R alone (Fig. 4.6B, C). A representative RLU values is shown in (Supplementary Fig. 4.3A). Moreover, dose-response curves show that PSD95 substantially potentiate D5R-mediated cAMP production (E_{max}) without altering DA potency (EC_{50}) (Fig. 4.6D; Table 4.2). Overall, these findings imply that PSD95 differentially modulates the D1-class receptor signaling mechanisms by inhibiting and stimulating D1R- and D5R-mediated cAMP production, respectively (Fig. 3.9C, D; Fig. 4.6C, D; Table 3.2; Table 4.2)

As PSD95 promotes D5R-mediated cAMP production, here I tested whether PSD95 modulates D5R-mediated ERK1/2 activation. Results suggest that following a brief exposure to DA (10 μM, 5 min), PSD95 increases D5R-mediated ERK1/2 activation relative to D5R alone (Fig. 4.6F). Together, effects of PSD95 on D5R-mediated cAMP production and ERK1/2 activation implies that PSD95 enhances D5R signaling and mediates an opposing effect on D1R and D5R signaling (Fig. 3.9G; Fig. 4.6F).

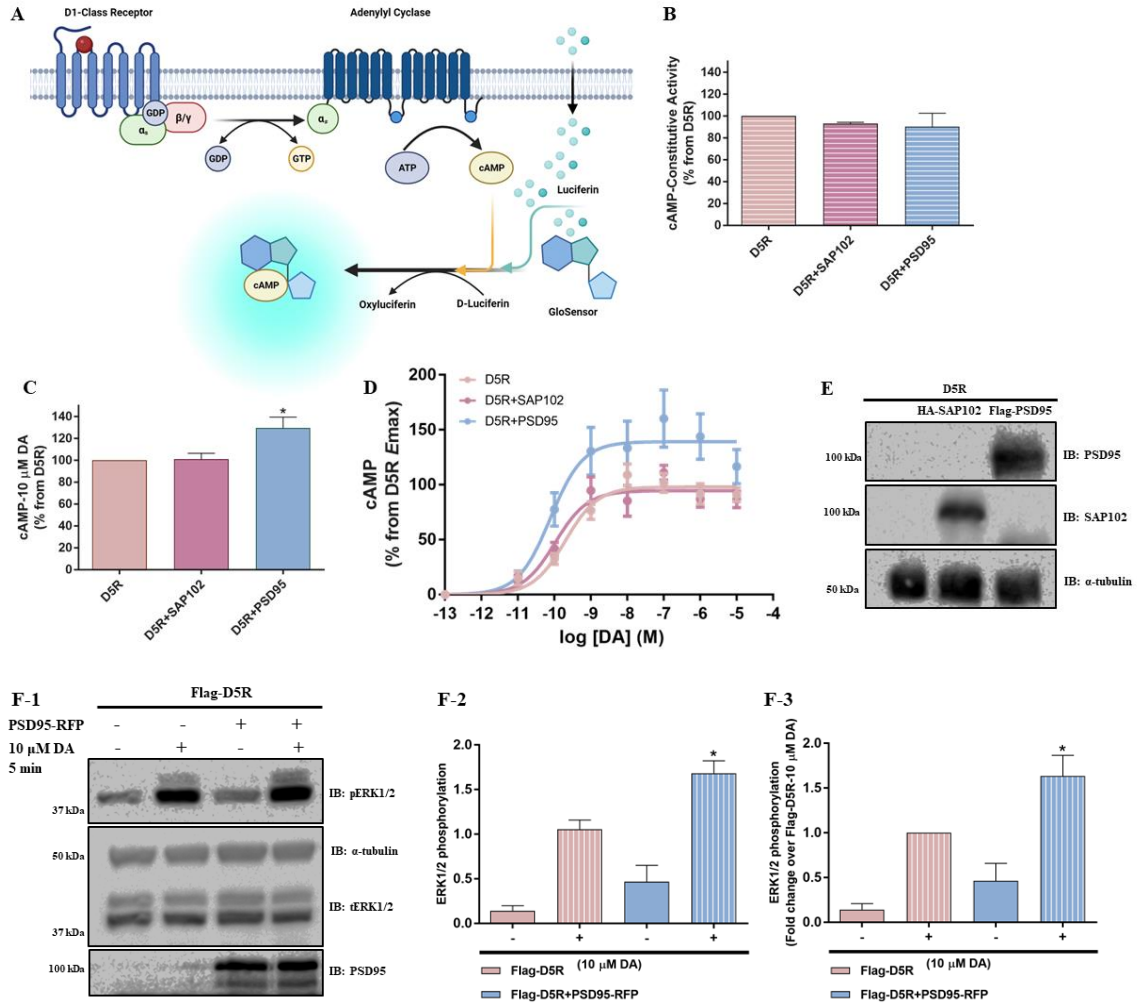

Fig. 4.6. PSD95 Facilitates D5R Signaling.

(A) Schematic representation of the principle of the cAMP-GloSensor assay. Created with BioRender.com. (B-E) HEK293T cells stably expressing GloSensor were transfected with D5R, D5R+HA-SAP102, D5R+Flag-PSD95. RLU for each experiment done in quadrable determinations for (B) constitutive activity and (C) the maximal activation of D5R (10 μM DA). The values then were normalized to D5R alone. Each bar represents the arithmetic mean ± S.E. of normalized values relative to D5R alone from five independent experiments. antibodies. B_{max} values in pmol/mg membrane protein for [^{3}H]-SCH23390 are: D5R: 3.72±1.35, D5R+HA-SAP102: 3.81±1.50, D5R+Flag-PSD95: 3.96±1.53. *, p<0.05, when compared with D5R alone using one sample t test. (D) Dose-response curve in response to increasing concentrations of DA were done in quadrable determinations. RLU for each condition were subtracted from the basal, then the values were normalized to the maximal activation of D5R alone. The graph represents the dose response curve for the average doses of six independent experiments. EC_{50}, E_{max} and B_{max} values are presented in table 4.2. (E) Representative immunoblotting analysis to validate the overexpression of SAP102 and PSD95. (F) HEK293 cells transfected with Flag-D5R, or co-transected with PSD95-RFP. Cells were stimulated for DA (10 μM) for 5 min or left untreated to induce ERK1/2 activation. Cell lysates were then prepared and subjected to western blotting with anti-phospho ERK1/2, anti-total ERK1/2, anti α-tubulin (loading control), and anti-PSD95 antibodies. Blot shown is a representative of N=3. B_{max} values in pmol/mg membrane protein for [^{3}H]-SCH23390: Flag-D5R: 2.15±0.82, Flag-D5R+PSD95-RFP: 2.60±0.74. Data are presented as arithmetic mean ± SEM (n=3) of p-ERK1/2 relative to total ERK1/2 (F-2), and then expressed as a fold change over Flag-D5R (10 μM) (F-3) . *p=0.05 when stimulated condition compared to Flag-D5R (10 μM) using one sample t test.

Receptor	Agonist Efficacy DA (% of D5R-E_{max})	Agonist Potency EC_{50}-DA (nM) (nM)	B_{max} (pmol/mg protein)
D5R (N=6)	**100**	**0.32** (0.11-0.93)	**3.9** (1.13-8.76)
D5R+SAP102 (N=6)	**96.2** (78.2-117.8)	**0.16** (0.04-0.47)	**3.8** (1.47-8.63)
D5R+PSD95 (N=6)	**146.1 *** (94.87-212.1)	**0.65** (0.02-3.35)	**3.9** (0.75-9.25)

Table 4.2. PSD95 Facilitates D5R-mediated cAMP Production.
Best-fitted E_{max} and EC_{50} values of DA for D5R-mediated cAMP production in cells expressed with D5R, D5R+HA-SAP102, D5R+Flag-PSD95, shown in Fig. 4.6 (D) are reported. Values are expressed as arithmetic means, with minimum and maximum value in brackets. Statistical significance; *: $p<0.05$, using one sample t test, was determined by comparing E_{max} of D5R.

8. PSD95 Inhibits DA-induced Endocytosis of D5R

To examine the role of PSD95 on regulating D5R trafficking, ELISA studies were performed to assess the role of PSD95 on the cell surface expression, total expression, and internalization of D5R. Results indicate that neither PSD95 nor SAP102 altered D5R surface expression (Fig. 4.7A). This suggests that the increased production of cAMP production and ERK1/2 activation observed in cells co-transfected with D5R and PSD95 was not due to a higher cell surface expression of D5R. Moreover, total and intracellular expression were measured on permeabilized cells. Results show that neither PSD95 nor SAP102 change the receptor expression i.e. did not promote intracellular retention or constitutive internalization (Fig. 4.7B, C). As discussed previously, PSD95 constitutively internalized D1R from cell surface; while PSD95 had no impact on D5R surface expression, which implies a different modulation of D1-class receptor subtypes by PSD95 in the absence of agonists (Fig. 3.11A; Fig. 4.7A).

To investigate whether PSD95 and/or SAP102 regulates DA-induced D5R endocytosis, transfected HEK293 cells were stimulated with DA (10 μM, 15 min). Results showed that PSD95, but not SAP102, inhibits D5R internalization relative to D5R alone (Fig. 4.7D). Interestingly, PSD95 enhances D1R internalization as shown previously; here PSD95 inhibits D5R internalization, which suggests that PSD95 acts differently on DA-induced internalization of D1R and D5R (Fig. 3.11D; Fig. 4.7D).

To examine whether PSD95-induced modulation of D5R internalization requires dynamin and βArr2, HEK293 cells were co-transfected with dominant-negative mutants Dyn I-K44A or βArr2-V54D. Results showed that overexpression of these mutants, inhibit DA-mediated D5R internalization in cells lacking or expressing PSD95 in comparison to control conditions (Fig. 4.7E, F). These findings suggest that the reduced D5R internalization in cells expressing PSD95 operates through a dynamin- and βArr2-dependent pathway.

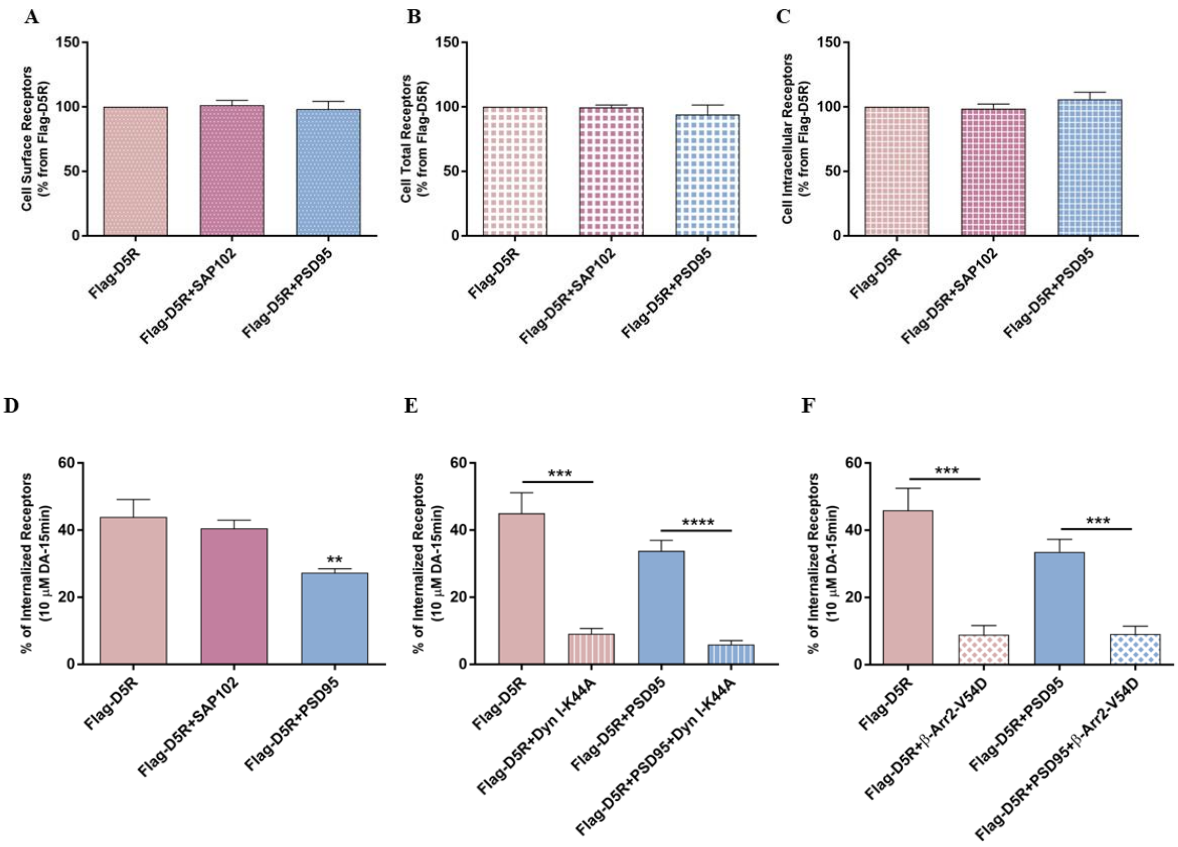

Fig. 4.7. PSD95 Inhibits D5R-induced Endocytosis.

HEK293 cells were transfected with mock, Flag-D5R alone, with HA-SAP102 or with PSD95-RFP. ELISA were performed to assess surface expression (A), total expression (permeabilized cells with Triton-X) (B), and intracellular pool of the D5R (total were subtracted from surface) (C). Agonist induced internalization of D5R was assessed by the % decrease in cell surface expression following 15 mins treatment with 10 μM DA (D) relative to AA (vehicle). Each bar represents the arithmetic mean ± S.E. of normalized relative to Flag-D5R alone, from five independent experiments. B_{max} in pmol/mg membrane proteins for [^{3}H]-SCH23390 in arithmetic means ± S.E. of (A-D): Flag-D5R: 4.93±1.83, Flag-D5R+HA-SAP102: 5.86±1.85, and Flag-D5R+PSD95-RFP: 3.57±1.11. *: $p<0.05$, **: $p<0.01$, when compared to Flag-D5R using one-way ANOVA, Dunnett's multiple comparison test. (E, F) HEK293 cells were transfected with mock, Flag-D5R alone, or with PSD95-RFP in the presence or absence of dynamin mutant HA-Dyn I-K44A (E) or βArr2 mutant-V54D (F). DA-induced internalization (10 μM-15min) was assessed by the % decrease in cell surface expression relative to that of AA (vehicle). Each bar represents the arithmetic mean ± S.E. from six independent experiments for (E) and five independent experiments for (F). B_{max} in pmol/mg membrane proteins for [^{3}H]-SCH23390 in arithmetic means ± S.E. for (E): Flag-D5R: 1.75±0.57, Flag-D5R+PSD95-RFP: 1.94±0.43, Flag-D5R+HA-Dyn I-K44A: 1.29±0.37, and Flag-D5R+PSD95-RFP+HA-Dyn I-K44A: 2.04±0.30, and for (F): Flag-D5R: 1.39±0.26, Flag-D5R+PSD95-RFP: 1.91±0.22, Flag-D5R+βArr2-V54D: 2.08±0.51, Flag-D5R+PSD95-RFP+βArr2-V54D: 2.18±0.60. ***: $p<0.001$, ****: $p<0.0001$ using unpaired t test as noted in the graph (E, F).

9. PSD95 Inhibits D5R-induced Recycling

To elucidate whether PSD95 modulates the post-endocytic recycling of D5R to plasma membrane, cells were stimulated with DA (10 μM) for 15 min to induce internalization. Then, DA was removed, and cells were allowed recovery periods of 10 min and 30 min to assess D5R recycling to plasma membrane. Results indicate that the D5R with or without PSD95 can recycle back to surface membrane after agonist induced internalization (Fig. 4.8A). However, PSD95 significantly decreases D5R insertion and recycling time to plasma membrane by two-fold (16.8 min vs. 8.44 min for D5R alone) (Fig. 4.8B, C). These results suggest an intricate regulation of D5R endosomal and recycling pathways by PSD95. Interestingly, PSD95 differentially regulates recycling of D1R and D5R to the plasma membrane through faster and slower rates, respectively (Fig. 3.12; Fig. 4.8).

10. PSD95 Antagonizes βArr2 Recruitment by D5R

The results described above imply that PSD95 modulates D5R responsiveness. βArr2 is an important integrator for GPCR-mediated trafficking (Ferguson, 2001). A recent finding suggested that PSD95 interacts with βArr2 (Gupta et al, 2019), whether this complex modulates βArr2 recruitment by D5R remains to be examined. The Tango Assay, a luminescence-based approach, was utilized in HEK293 cells stably expressing a TEV fused-βArr2 (HTLA cells) (Fig. 4.9A). Radioligand binding assays showed that the ligand affinity and expression of D5R-Tango were similar to Flag-D5R in HTLA cells (Supplementary Tables 4.2). cAMP assays were also performed, and the results showed that following DA stimulation of cells transfected with Flag-D5R and D5R-Tango, the levels of cAMP were substantially increased relative to untreated cells (Supplementary Fig. 4.2B).

To assess the impact of PSD95 on βArr2 recruitment by D5R, HTLA cells were transiently transfected with D5R-Tango or co-transfected with PSD95-RFP. Dose-response curves using increasing concentrations of DA and DHX were performed, and results showed that PSD95 substantially inhibited βArr2 recruitment by increasing the maximal response (E_{max}) of D5R-mediated βArr2 recruitment relative to D5R alone, without altering the agonist potency (EC_{50}) (Fig. 4.9B-C; Table 4.3). A representative RLU values is shown in (Supplementary Fig. 4.3B). The findings imply a negative modulation of PSD95 on βArr2 recruitment by D5R.

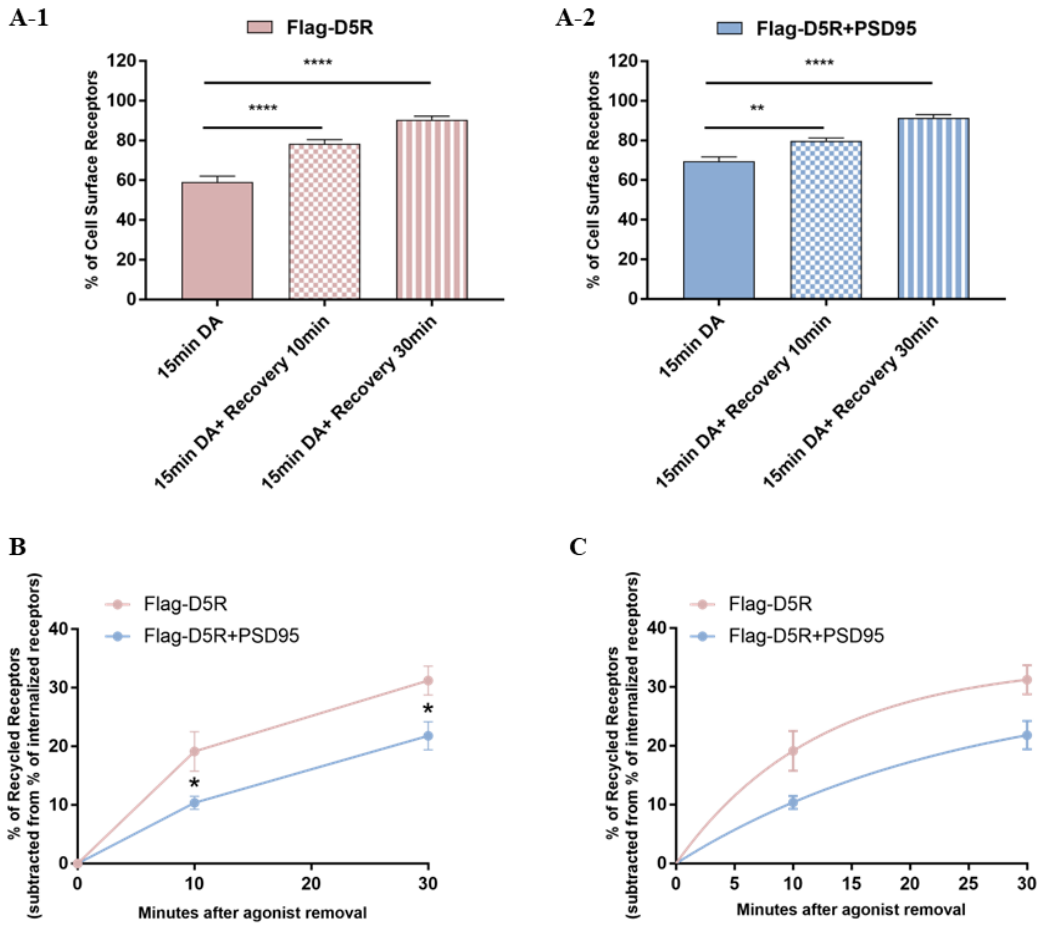

Fig. 4.8. PSD95 Delays D5R Recovery to the Plasma Membrane.

(A-C) ELISA were performed from HEK293 cells were transfected Flag-D5R alone or with PSD95. Cells were stimulated with 10 μM DA for 15 min, then agonist removed, and cells were allowed recovery for 10 and 30 min. (A) Surface expression was measured to assess the recycling receptor relative to 15 min 10 μM DA. *: $p<0.05$, **: $p<0.01$, ***: $p<0.001$, ****: $p<0.0001$ when compared as noted in the graph using one-way ANOVA, Dunnett's multiple comparison. (B) Recycled receptors were subtracted from 15 min 10 μM DA, and the percentage of recycled receptors after 10, 30 min recovery were quantified. *: $p<0.05$, when compared to Flag-D5R as noted in the graph using unpaired t test. (C) Recovery rate was assessed at 10, and 30 min after agonist removal. Each bar represents the arithmetic mean ± S.E. from seven independent experiments. B_{max} in pmol/mg membrane proteins for [^{3}H]-SCH23390: Flag-D5R: 1.78±0.50 and Flag-D5R+PSD95-RFP: 2.34±0.81.

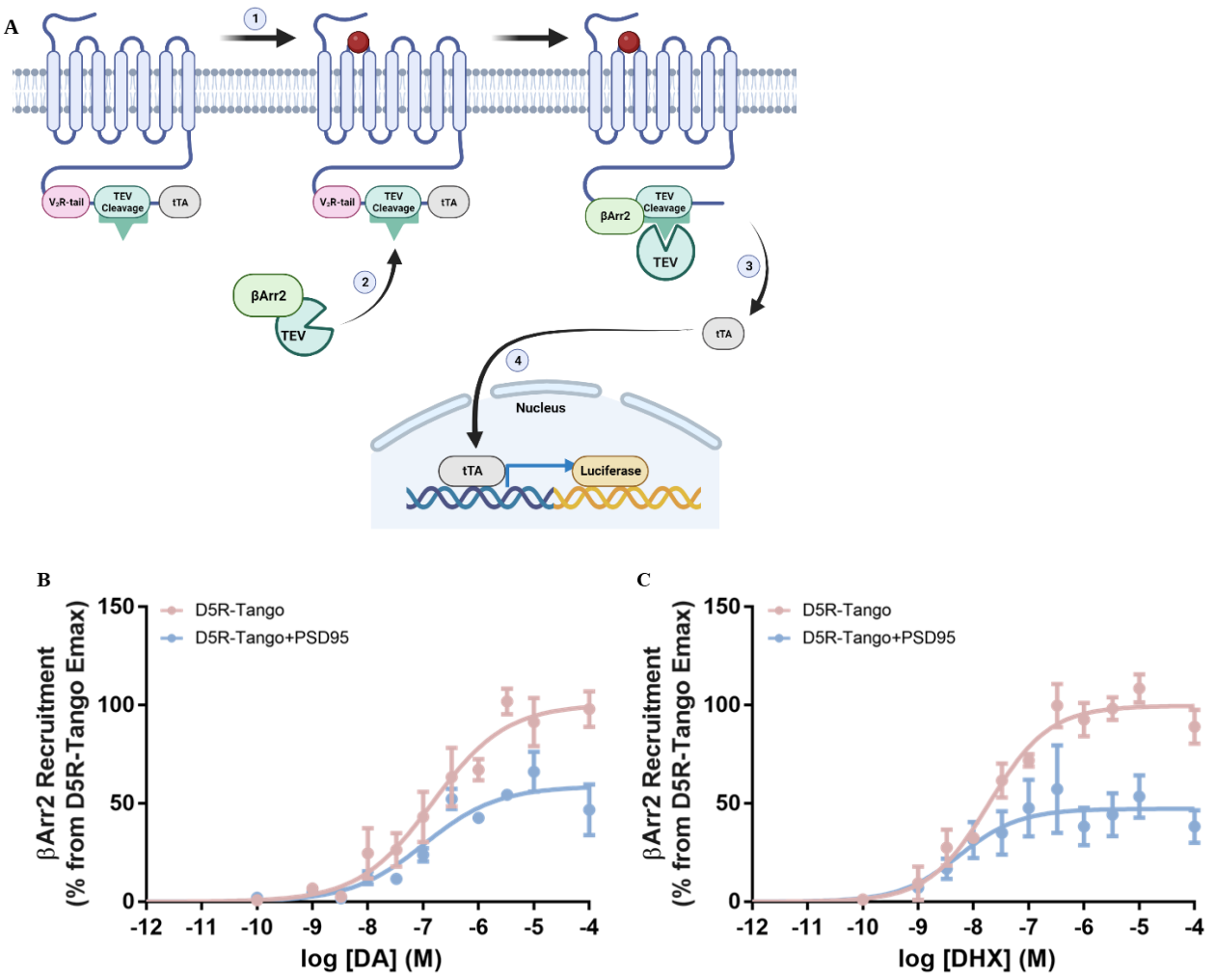

Fig. 4.9. PSD95 Antagonizes D5R-mediated βArr2 Recruitment.

(A) Schematic representation of the principle of the Tango assay. Created with BioRender.com. (B, C) HTLA cells were transfected with D5R-Tango alone, or co-transfected with PSD95-RFP. Dose-response curves in response to increasing concentration of DA and DHX were performed to measure βArr2 recruitment for D5R-Tango. E_{max}, EC_{50}, and B_{max} are shown in arithmetic mean in table 4.3. from four independent experiments.

Receptor	Agonist Efficacy DA (% of D5R-E_{max})	Agonist Potency EC_{50}-DA (nM)	Agonist Efficacy DHX (% of D5R-E_{max})	Agonist Potency EC_{50}-DHX (nM)	B_{max} (pmol/mg protein)
D5R-Tango (N=4)	**100**	**227** (25.55-520)	**100**	**22.1** (7.00-30.24)	**9.2** (3.22-13.19)
D5R-Tango+PSD95 (N=4)	**61.5 *** (45.38-75.33)	**194** (36.32-348)	**47.7 *** (26.98-77.18)	**8.3** (2.02-18.00)	**6.8** (6.22-8.24)

Table 4.3. PSD95 Antagonizes D5R-mediated βArr2 Recruitment.
Best-fitted E_{max} and EC_{50} values of DA and DHX for D5R-mediated βArr2 recruitment in HTLA cells transfected with D5R-Tango and D5R-Tango+PSD95-RFP, shown in Fig. 4.9 (B, C) are reported. Values are expressed as arithmetic means, with minimum and maximum value in brackets. Statistical significance; *: $p<0.05$, using one sample t test, was determined by comparing E_{max} of D5R-Tango.

Significance

We identified PSD95 as a novel interactor for D5R-IL3, *in vitro* and *in vivo*. Preassociated complexes of D5R•PSD95 undergo conformational rearrangements leading to an association/stabilisation of the complex following exposure to agonists. Interestingly, I also found that PSD95 is i) facilitating D5R-mediated cAMP production and ERK1/2 activation, and ii) inhibiting D5R mediated-internalization, recycling, and βArr2 recruitment. Collectively, my studies suggest that PSD95 interacts with both D1-class receptor subtypes, via different cytosolic regions, to shape differentially D1R-CT and D5R-IL3 signaling signatures. As D5R functionally interacts with glutamatergic scaffolding protein PSD95, this novel finding may provide better understanding of the molecular mechanisms underlying D5R signaling and allow exploring the potential of D5R functionality with excitatory ionotropic receptors, especially with GluN2B-containing NMDARs.

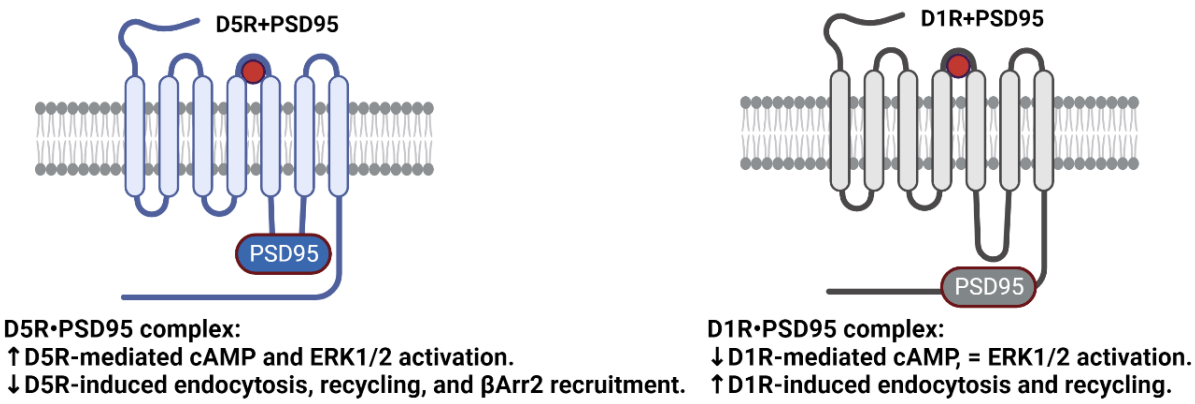

Fig. 4.10. Summary of the Signaling and Trafficking Mechanisms of D5R•PSD95 and D1R•PSD95 complexes.

Appendix II: Supplementary Figures and Tables for Manuscript II

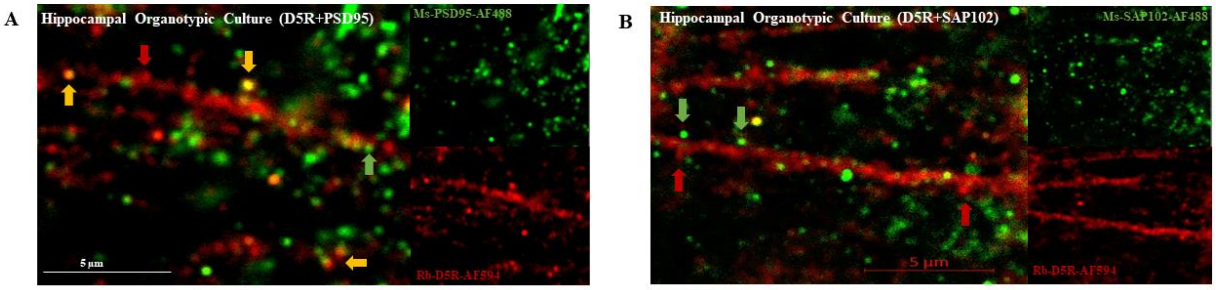

Supplementary Fig. 4.1. Subcellular Localization of D5R•PSD95 from Hippocampal Organotypic Cultures. (A, B) Representative confocal images of hippocampal organotypic culture (Sprague Dawley rat, P8, DIV28) performed once, and immunostained with primary antibodies: rabbit anti-D5R, mouse anti-SAP102, or mouse anti-PSD95, followed by secondary fluorophore antibodies: anti-rabbit conjugated Alexa Fluor-594 and anti-mouse conjugated Alexa Fluor-488. Images were acquired using confocal microscopy with 63x magnification.

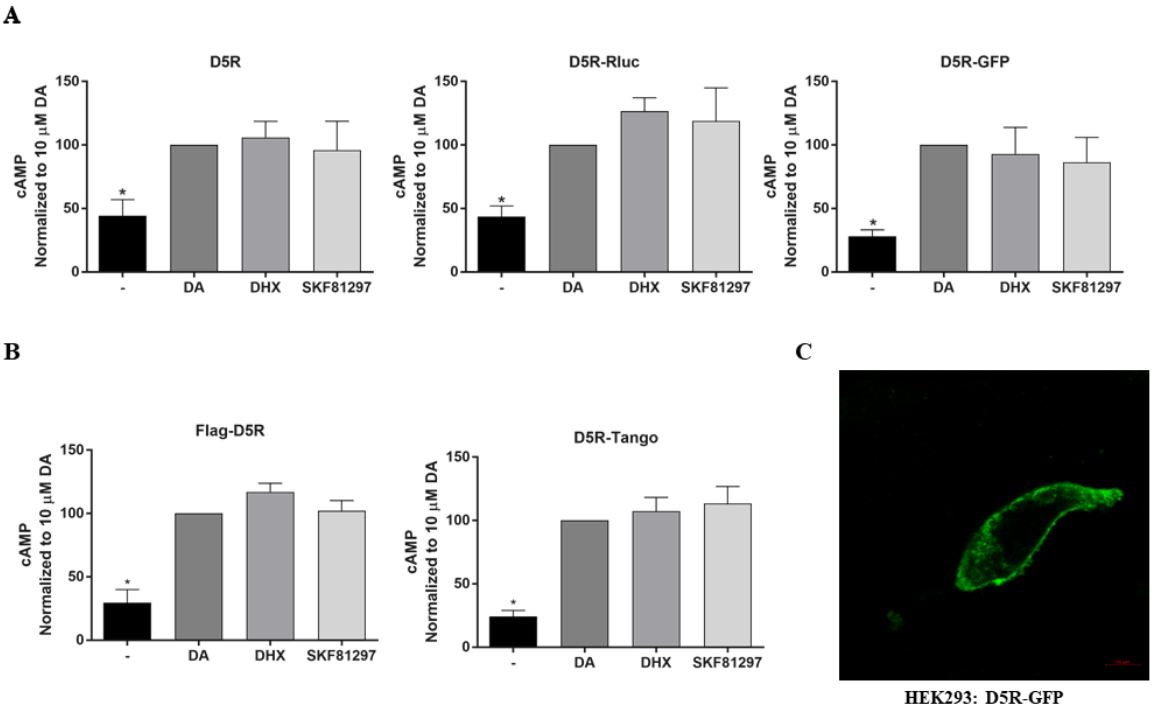

Supplementary Fig. 4.2. Functional Assessment for D5R-Fused with Rluc, GFP, and Tango.
(A, B) HEK293T cells stably expressing GloSensor were transfected with D5R, D5R-Rluc, D5R-GFP (A) or transfected with Flag-D5R and D5R-Tango (B). Relative luminance value (RLU) for each experiment done in quadrable determinations to measure cAMP level of constitutive activity (AA, denoted as -) or maximal activation (10 μM) of D1R agonists: DA, DHX, SKF81297. Each bar represents the arithmetic mean ± S.E. of normalized values relative to DA from four independent experiments. B_{max} values in pmol/mg membrane protein for [^{3}H]-SCH23390 for (A) are D5R: 2.01±1.60, D5R-Rluc: 0.93±0.46, D5R-GFP: 2.94±1.74, and for (B) Flag- D5R: 4.29±2.12, D5R-Tango: 2.60±1.18. *: $p<0.05$, when compared to cells treated with 10 μM DA using one sample t test. (C) Confocal live imaging of HEK293 cells transfected with D5R-GFP. Images were acquired using epifluorescence microscope with 63x magnification. Image is representative of two independent experiments. B_{max} values for D5R-GFP in pmol/mg membrane protein for [^{3}H]-SCH23390: 6.48±3.04.

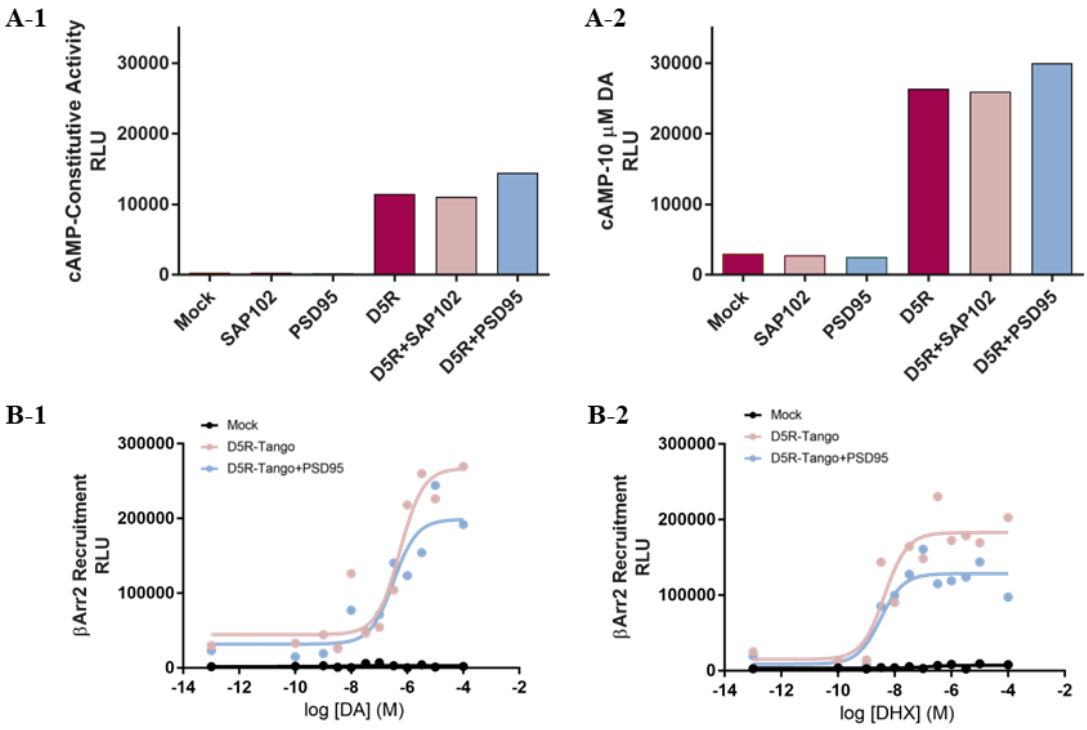

Supplementary Fig. 4.3. PSD95 Modulates D5R-mediated cAMP Production and βArr2 Recruitment.
(A) HEK293T-Glo cells transfected with mock, HA-SAP102, Flag-PSD95, D5R, D5R+HA-SAP102, D5R+Flag-PSD95, and cAMP measurement was assessed at basal (constitutive) (A-1) or and 10 μM DA (A-2). A represintative of average RLU calculated in quadrable determinations in response to cAMP production is shown, corresponding to (Fig. 4.6B, C), and B_{max} values in pmol/mg membrane protein for [^{3}H]-SCH23390: D5R: 2.56, D5R+SAP102: 6.65, D5R+PSD95: 4.14. (B) HTLA cells transfected with mock, D5R-Tango, or co-transfected with PSD95-RFP, and βArr2 recruitment was assessed in reponse to increasing conentration of DA and DHX. A represintative of average RLU calculated in quadrable determinations in response to βArr2 recruitment is shown, corresponding to (Fig. 4.9B, C), and B_{max} values in pmol/mg membrane protein for [^{3}H]-SCH23390: D5R-Tango: 11.22, D5R-Tango+PSD95-RFP: 8.24.

	Saturation Curves [^{3}H]-SCH23390		Competition Curves K_i (nM)			
Receptor	**K_d (nM)**	**B_{max} (pmol/mg protein)**	**DA**	**DHX**	**Thioridazine**	**SCH23390**
D5R (N=3)	**1.06** (0.97-1.12)	**5.2** (2.97-6.95)	**745** (341-1459)	**126** (95.81-166)	**196** (73.31-375)	**1.05** (0.91-1.27)
D5R-Rluc (N=3)	**0.85** (0.51-1.19)	**3.1** (1.55-4.90)	**338** (95.05-584)	**259** (127-373)	**190** (72.59-397)	**0.95** (0.71-1.24)
D5R-GFP (N=3)	**0.98** (0.83-1.13)	**8.2** (4.32-15.36)	**397** (313-534)	**253** (44.52-633)	**239** (92.84-390)	**0.89** (0.72-0.99)

Supplementary Table 4.1. Functional Assessment for D5R-fused with Rluc and GFP by Radioligand Binding.
Dissociation constants (K_d, K_i) and B_{max} values of radioligand saturation and competition studies of [^{3}H]-SCH23390 performed from HEK293 cells transfected with D5R, D5R-Rluc, and D5R-GFP. Values are expressed as arithmetic means, with minimum and maximum value in brackets. No statistical significance was observed using one-way ANOVA, when compared to D5R.

	Saturation Curves [^{3}H]-SCH23390		Competition Curves K_i (nM)			
Receptor	**K_d nM N=5**	**B_{max} (pmol/mg protein) N=5**	**DA N=3**	**SKF81297 N=3**	**DHX N=2**	**SCH23390 N=2**
Flag-D5R	**0.94** (0.62-1.73)	**25.0** (15.20-45.95)	**589** (409-760)	**12.5** (11.01-15.52)	**46.4** (35.66-57.10)	**0.87** (0.61-1.13)
D5R-Tango	**0.81** (0.54-1.39)	**16.7** (3.13-43.84)	**498** (438-540)	**35.1** (9.23-85.84)	**38.8** (29.03-48.66)	**0.39** (0.20-0.59)

Supplementary Table 4.2. Functional Assessment for D5R-Tango by Radioligand Binding.
Dissociation constants (K_d, K_i) and B_{max} values of radioligand saturation and competition studies of [3H]-SCH23390 performed from HTLA cells transfected with Flag-D5R and D5R-Tango. Values are expressed as arithmetic means, with minimum and maximum value in brackets. No statistical significance was observed using unpaired t test, when compared to Flag-D5R.

MANUSCRIPT III: Synapse-Associated Protein 102 (SAP102) and Postsynaptic Density 95 (PSD95) Facilitate β-arrestin2 (βArr2) Signaling of Dopamine D1 Receptor

Synapse-Associated Protein 102 (SAP102) and Postsynaptic Density 95 (PSD95) Facilitate β-arrestin2 (βArr2) Signaling of Dopamine D1 Receptor

Statement of Author Contribution

Functional studies for D1R-Tango (radioligand binding and cAMP assays) as well βArr1 recruitment were performed with the assistance of Meriam Zeghal.

Appendix III contains supplementary figures and tables for manuscript III.

Rationale

βArrs are scaffolding proteins that are ubiquitously expressed in most tissues, including brain, and act as multifunctional adaptors to regulate desensitization, trafficking, and signalling of numerous GPCRs (Wess et al, 2023). While both βArr1 and βArr2 indiscriminately interact with class-B GPCRs (e.g., angiotensin IIA and vasopressin receptors), βArr2 preferentially modulates the trafficking of class-A GPCRs (e.g., adrenergic and dopaminergic receptors) (Pierce and Lefkowitz, 2001; Shenoy and Lefkowitz, 2011). As for other GPCRs, activation of D1R is quickly followed by a GPCR kinase (GRK)-mediated receptor phosphorylation followed by a recruitment of βArr2 to desensitize and internalize D1R and activate cellular signaling, independently of $G\alpha_s$ pathway (Zhang et al, 1999; Oakley et al, 2000; Kim et al, 2004; Beaulieu and Gainetdinov, 2011). βArr2 recruitment by D1R has been shown to modulate its functional selectivity/biased receptor signaling properties, which has promising clinical applications (Gainetdinov et al, 2004; Urs et al, 2011; Beaulieu and Gainetdinov, 2011).

Gupta et al (2019) showed that PDZ-containing proteins such as PSD95, membrane-associated guanylate kinase protein 1 (MAGI), and PDZ domain-containing kidney protein 1 (PDZK1) interact with βArr2 in a PDZ domain-dependent manner. Another recent study also reported of the formation PSD95•βArr2 complex in brain, and this interaction regulates JNK downstream signaling events (Musi et al, 2022). While βArr1 is highly homologous with βArr2 (78%), no study has investigated the connection between βArr1 and MAGUK. **Considering these findings, and collectively, with my results that showed SAP102 and PSD95 (referred to herein as MAGUKs) differentially regulate D1R responsiveness, and the known role of βArr2 mediating D1R trafficking, I sought to determine if a MAGUK•βArr2 complex regulates the**

trafficking of D1R. I aimed i) to assess if a binary interaction between βArr1•MAGUKs and βArr2•MAGUKs can be detected *in vitro* and *in vivo,* and ii) to explore the effect of D1R•MAGUK•βArr2 complexes on D1R trafficking properties.

Results

1. βArr2 Interacts with SAP102 and PSD95

To investigate whether SAP102 interacts with βArr2, coimmunoprecipitation studies were performed. HEK293 cells were transiently transfected with empty vector (mock), Flag-βArr2 alone, or co-transfected with HA-SAP102 or PSD95-RFP. PSD95 was included as a positive interactor with βArr2, as it has been previously reported to bind to βArr2 (Gupta et al, 2019). Results showed that SAP102 and PSD95 coimmunoprecipitated with βArr2 (Fig. 5.1A, B). The converse experiment was also performed in HEK293 cells to detect βArr2-YFP or untagged-βArr2 in Flag-SAP102 or Flag-PSD95 immunocomplexes. Results showed that βArr2 coimmunoprecipitated with SAP102 and PSD95 (Fig. 5.1C; Supplementary Fig. 5.1A). Next, I examined whether the complex interactions of both MAGUK and βArr2 are detected in brain tissue. Cortical lysates (Sprague-Dawley rat, P21, male and female) were used to immunoprecipitate βArr2. Immunoblotting reveals that SAP102 and PSD95 coimmunoprecipitated with βArr2 (Fig. 5.1D, E). Together, these results suggest that PDZ-containing protein SAP102 and PSD95 interact with βArr2 *in vitro* and *in vivo*.

2. βArr1 Interacts with SAP102 and PSD95

As βArr1 is highly conserved with βArr2 and displays similar affinity, I tested whether SAP102 and PSD95 also interact with βArr1. HEK293 cells were transfected with mock, βArr1 (YFP or untagged), co-transfected with Flag-SAP102 or Flag-PSD95. Results showed that βArr1 coimmunoprecipitated with SAP102 and PSD95 (Fig. 5.1F; Supplementary Fig. 5.1B).

To further support these findings, *in vivo* coimmunoprecipitation were performed. Studies using cortical lysates (Sprague-Dawley rat, P21 male and female) show that SAP102 and PSD95 were coimmunoprecipitated with βArr1 and βArr2 (Fig. 5.1G, H). Together, these results suggest that PDZ-containing protein SAP102 and PSD95 interact with both βArr1 and βArr2.

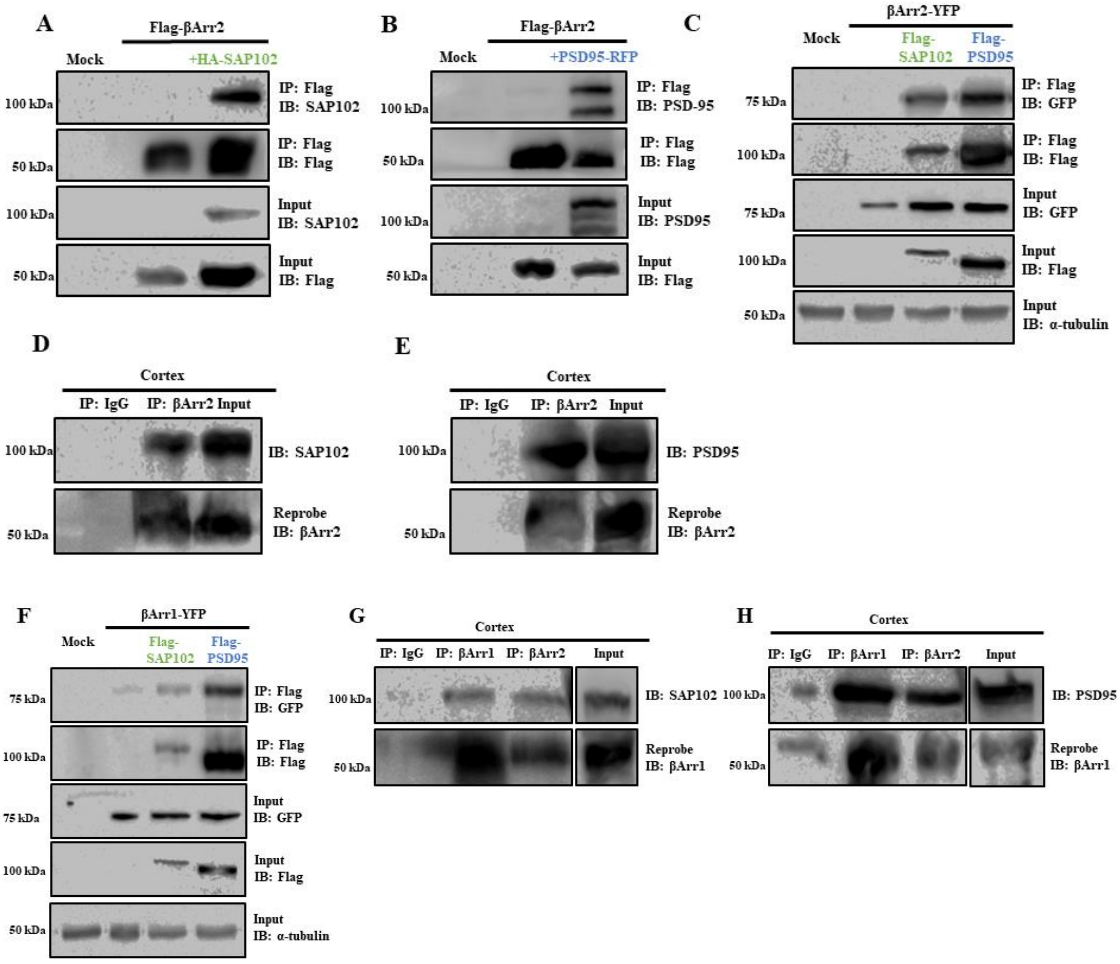

Fig. 5.1. SAP102 and PSD95 form immunocomplexes with βArr1 and βArr2.

(A-C) HEK293 cells were transfected with mock, Flag-βArr2 alone, co-transfected with HA-SAP102 (A), or co-transfected with PSD95-RFP (B), or transfected with mock, βArr2-YFP alone, or co-transfected with Flag-SAP102 or Flag-PSD95 (C). Cells were solubilized and subjected to a sequential immunoprecipitation with anti-Flag-agarose matrix followed by immunoblotting with corresponding antibodies. A representative experiment of N=4 is shown. (D, E) Solubilized cortical lysates (1.5 mg) from rat (P21) were subjected to an immunoprecipitation procedure using rabbit anti-βArr2 antibody and resolved immunocomplexes probed with mouse anti-SAP102 and mouse anti-PSD95 antibodies, respectively. Normal rabbit IgG were used as a negative control. 50ug of lysate were loaded to the gels as input. Blot is a representative for an experiment repeated three times. (F) HEK293 cells were transfected with mock, βArr1-YFP alone, co-transfected with Flag-SAP102, or Flag-PSD95. Cells were solubilized and subjected to a sequential immunoprecipitation with anti-Flag-agarose matrix followed by immunoblotting with GFP antibody. A representative experiment of N=3 is shown. (G, H) Solubilized cortical lysates (1.5 mg) from rat (P21) were subjected to an immunoprecipitation procedure using rabbit anti-βArr1 and rabbit anti- βArr2 antibodies and resolved immunocomplexes probed with mouse anti-SAP102 and mouse anti-PSD95 antibodies. Normal rabbit IgG were used as a negative control. 50ug of lysate were loaded to the gels as input. Blot is a representative for an experiment repeated three times.

3. Agonist-induced Stimulation of D1R Regulates the Interaction with βArr2

As discussed in manuscript I, SAP102 and PSD95 interact with D1R to differentially regulate D1R signaling, phosphorylation, and trafficking, thus βArr2 involvement likely modulates the D1R•MAGUKs. I tested the hypothesis that D1R•SAP102•βArr2, and D1R•PSD95•βArr2 reside in the same protein complex, and whether the pre-formed D1R•MAGUK modulates the DA-induced interaction with βArr2. Coimmunoprecipitation studies show a ~2.5-fold increase in the recruitment of βArr2 upon receptor activation (15 min DA, 10 μM) relative to unstimulated condition without MAGUK expression (Fig. 5.2: A1, A2). In the context of MAGUK expression, DA-induced recruitment of βArr2 was slightly increased (~3-fold) (Fig. 5.2: B1, B2, C1, C2). Reprobing of immunoblots demonstrate that SAP102 and PSD95 are detected in D1R immunocomplexes under basal and stimulated conditions (Fig. 5.2: B3, C3). Previously, I showed that recruitment of SAP102 and PSD95 in the absence of βArr2 is further enhanced in response to DA-induced D1R activation (Fig 3.8A, B; Manuscript I). In contrast, herein, results suggest that MAGUK interaction with D1R is unchanged under stimulatory condition relative to basal in cells expressing βArr2 (Fig. 5.2: B3, C3). These finding implies that βArr2 potentially stabilizes the pre-associated complex of D1R•MAGUK (in the absence of agonists) and restricts further recruitment following DA activation.

To further validate the coimmunoprecipitation findings, BRET[1] assays were assessed on live cells to examine the role of these MAGUKs in regulating βArr2 recruitment by D1R. HEK293 cells were transiently transfected with D1R-Rluc alone, or with βArr2-YFP in the presence or absence of Flag-SAP102 and Flag-PSD95 (Fig. 5.3A). Results show that DA stimulation (10 μM, 30 min) modulates BRET signal for D1R•βArr2, D1R•SAP102•βArr2 and D1R•PSD95•βArr2, which implies an increased in spectral overlap between the donor-D1R and acceptor-βArr2, and thus support the close proximity of D1R and βArr2 (Fig. 5.3B-D). Results also show that MAGUK expression slightly increases net BRET[1] values for D1R•βArr2 (from < 0.3 to >0.3) suggesting that MAGUKs potentially facilitate βArr2 recruitment.

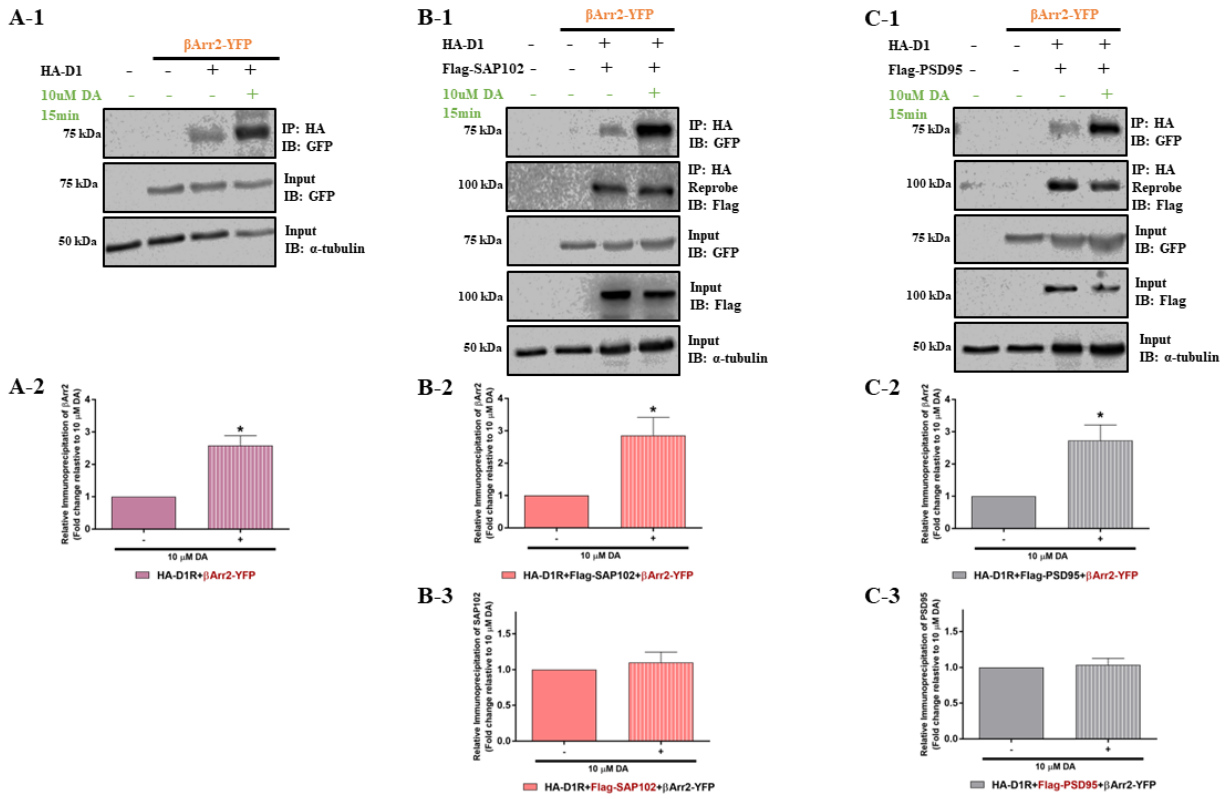

Fig. 5.2. Agonist-induced Stimulation of D1R Regulate the Interaction with βArr2, *in vitro*.

(A-C) HEK293 cells were transfected with mock, βArr2-YFP alone, or with HA-D1 in the presence or absence of Flag-SAP102 and Flag-PSD95. Cells were either stimulated with 10 μM DA for 15 min or left untreated (vehicle: AA, denoted as -), then solubilized and subjected to a sequential immunoprecipitation with anti-HA agarose matrix followed by immunoblotting with anti-GFP and Flag antibodies. A representative experiment of N=4 is shown. Middle panel (A-2, B-2, C-2) showed a relative immunoprecipitation quantified for IP-βArr2 over input-βArr2, then stimulated cells were normalized to unstimulated cells (vehicle). Lower panel (B-3, C-3) showed a relative immunoprecipitation quantified for IP-SAP102 over input-SAP102 (B-3) or relative immunoprecipitation quantified for IP-PSD95 over input-PSD95, stimulated cells were normalized to unstimulated cells (vehicle). *: $p<0.05$ when DA compared with control using one sample t test. B_{max} values in pmol/mg membrane protein for [^{3}H]-SCH23390: HA-D1R+βArr2-YFP: 5.62±2.17, HA-D1R+Flag-SAP102+βArr2-YFP: 6.76±2.05, HA-D1R+Flag-PSD95+βArr2-YFP: 4.86±2.62.

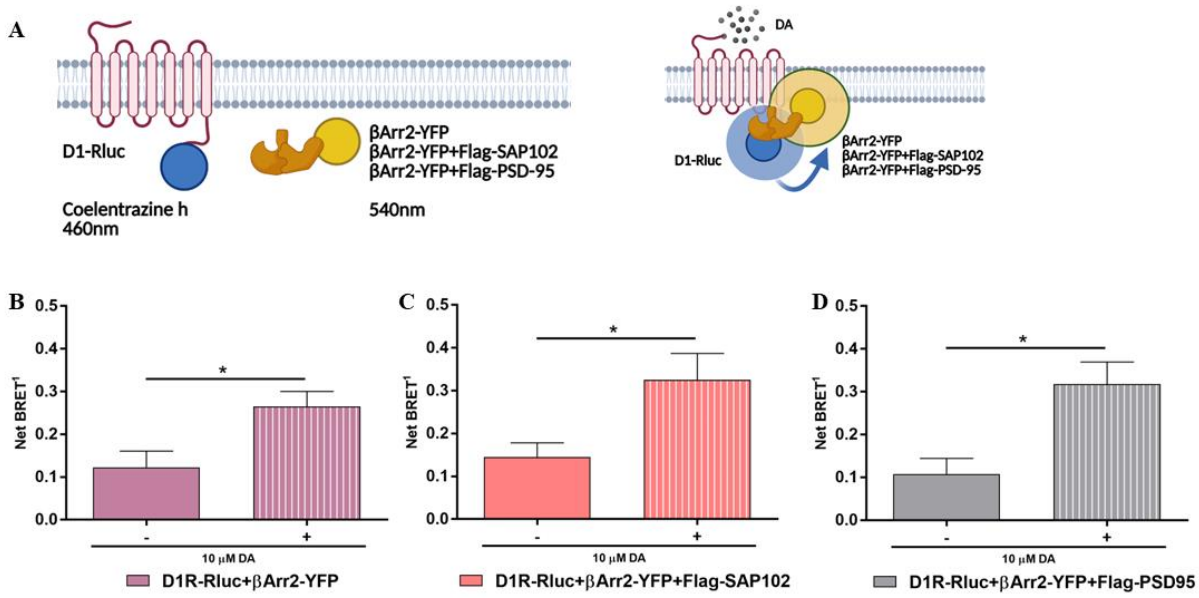

Fig. 5.3. Stimulation of D1R Facilitates βArr2 Recruitment.

(A) Schematic diagram of BRET[1] assay. Created with BioRender.com. (B) HEK293 cells were transfected with D1R-Rluc, or co-transfected with βArr2-YFP alone or with Flag-SAP102 and Flag-PSD95. Coelenterazine h was added, and light emission was measured from the luciferase donor and YFP acceptor at 460 nm and 540 nm wavelength, respectively. Net BRET[1] was quantified as: [(YFP emission at 540 ± 25nm)/(Rluc emission 460 ± 40nm)]−[(emission at 540 ± 25nm)/(emission at 460 ± 40nm)] found with the D1R-Rluc expressed alone in the same experiment. BRET measurements were quantified from four independent experiments, and B_{max} values in pmol/mg membrane protein for [^{3}H]-SCH23390 for D1R-Rluc: 4.41±1.37, D1R-Rluc+βArr2-YFP: 4.75±1.74, D1R-Rluc+βArr2-YFP+Flag-SAP102: 5.71±2.25, D1R-Rluc+βArr2-YFP+Flag-PSD95: 5.87±2.22. *: $p<0.05$, when compared to non-treated (vehicle) using unpaired t test.

4. βArr2 Modulate Cellular Localization of MAGUKs and D1R•MAGUKs

As the results described above support the notion of a MAGUK•βArr2, and D1R•MAGUK• βArr2 complexes, the subcellular localization of these proteins was assessed, in the absence of agonist stimulation. Immunostaining reveal that D1R is localized at the cell membrane, SAP102 and PSD95 are mostly distributed intracellularly, whereas and βArr2 displays a more perinuclear localization (Fig. 5.4A). While βArr2 is not predominantly localized at the plasma membrane, it modulates cellular translocation of SAP102 and PSD95 from intracellular compartments to the cell membrane, with a βArr2•MAGUKs pool localized cytoplasmically (Fig. 5.4B, C). Additionally, co-localization of D1R•βArr2 is detected at the plasma membrane, which is more prominent in the presence of MAGUKs, yet βArr2 is not predominantly compartmentalized at the plasma membrane (Fig. 5.4D-F). Interestingly, βArr2 potentially enhances the translocation of MAGUKs to colocalize with D1R at the plasma membrane (Fig. 5.4). Together, these findings suggest that βArr2 modulates cellular localization of MAGUKs and D1R•MAGUKs.

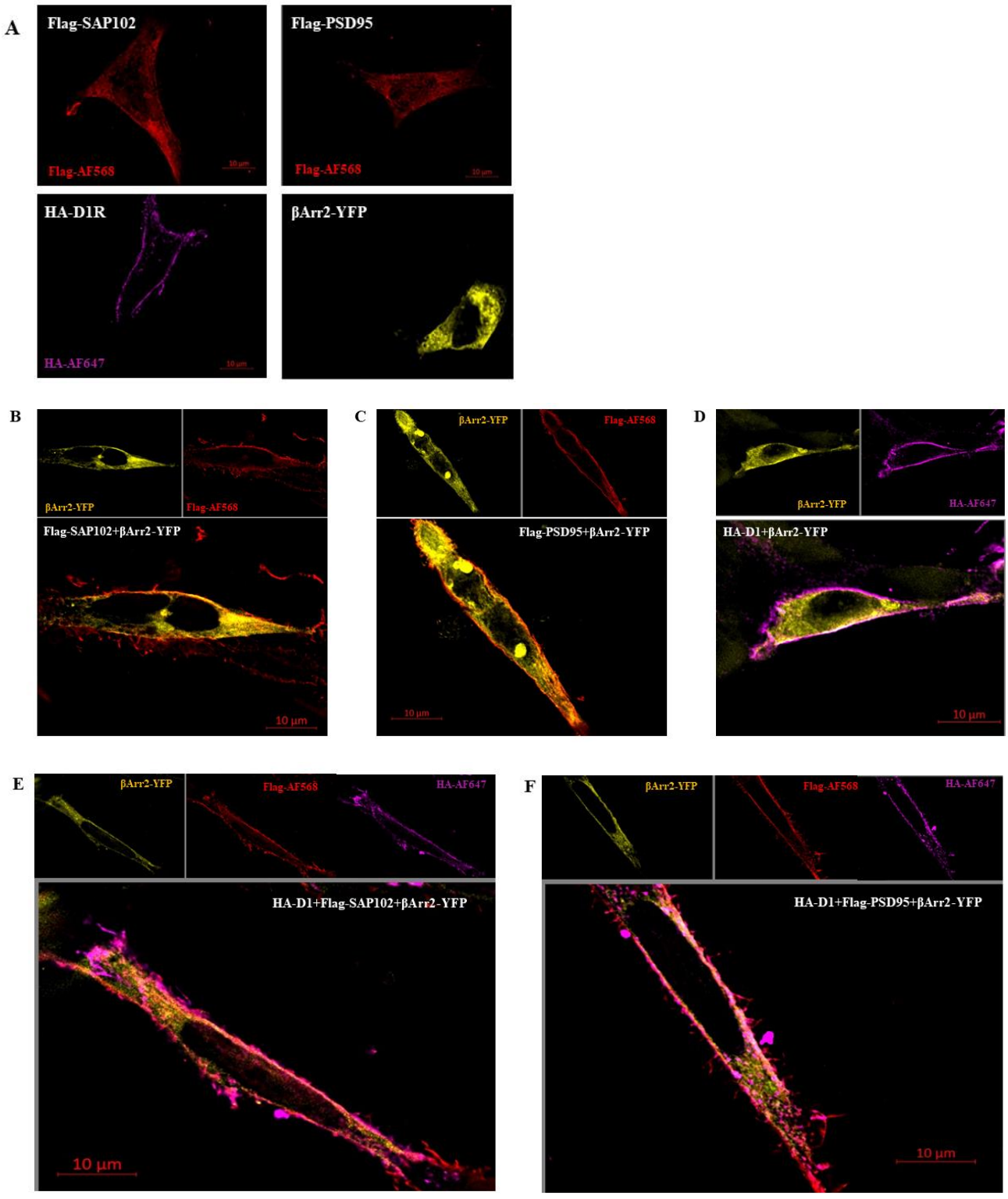

Fig. 5.4. βArr2 Colocalizes with D1R and D1R•MAGUKs, *in vitro.*

(A-F) HEK293 cells transfected with HA-D1, Flag-SAP102 or Flag-PSD95, or βArr2-YFP, or (A), or co-transfected with Flag-SAP102+βArr2-YFP (B), Flag-PSD95+βArr2-YFP (C), HA-D1R+βArr2-YFP (D), HA-D1R+Flag-SAP102+βArr2-YFP (E), HA-D1R+Flag-PSD95+βArr2-YFP (F). Cells were fixed, permeabilized, and followed by

immunostaining with rabbit anti-HA and mouse anti-Flag antibodies, and secondary fluorophore antibodies of anti-rabbit conjugated Alexa Fluor-647 and anti-mouse conjugated Alexa Fluor-568. Images were acquired using epifluorescence microscope with 63x magnification. The image is a representative of experiment repeated three times. B_{max} values in pmol/mg membrane protein for [^{3}H]-SCH23390 B_{max} values in pmol/mg membrane protein for [^{3}H]-SCH23390: HA-D1R: 3.54±1.18, HA-D1R+βArr2-YFP: 3.59±1.09, HA-D1R+Flag-SAP102+βArr2-YFP: 5.08±1.68, HA-D1R+Flag-PSD95+βArr2-YFP: 2.25±0.40.

5. SAP102 and PSD95 Promote βArr2 Recruitment by D1R

As SAP102 and PSD95 interact with D1R via IL3 and CT, respectively, βArr2 also interacts primarily with CT of D1R (Kim et al, 2004; Macey et al, 2005). Here, I examined whether these D1R•MAGUKs modulate βArr2 recruitment by D1R using luminescence-based approach, known as Presto-Tango assay (Tango Assay). This assay utilizes HTLA cells (an HEK293-derived cell line containing stable integrations of a βArr2-TEV fusion gene and a tTA-dependent luciferase reporter), and GPCR-fused at its cytoplasmic tail with a TEV cleavage site upstream of the transcriptional activator, tTA. Upon agonist binding and receptor activation, the TEV-tagged βArr2 is recruited to the GPCR with subsequent cleavage of tTA, which allow the translocation of tTA in the nucleus driving the expression of the luciferase reporter gene (Fig. 5.5A). The CT of GPCR-Tango, including D1R-Tango, is also fused to a small peptide (32 aa) derived from the vasopressin 2 receptor tail (V2R) known to bind to βArr2. Dose-response curves were performed in the presence of DA or V2R agonist, vasopressin (VA), to determine the specificity of D1R-Tango with respect to βArr2 recruitment. As expected, DA, but not VA, elicited βArr2 recruitment to D1R-Tango (Supplementary Fig. 5.2A). Functional studies were also performed to assess the modified D1R-Tango display normal radioligand binding and cAMP measurement. Results shows that the Tango modification does not alter the binding affinity or its response to agonist stimulation of cAMP production relative to Flag-D1R (Supplementary Fig. 5.2B; Supplementary Tables 5.1). Moreover, coimmunoprecipitation studies also suggest that this optimized D1R-Tango interacts with SAP102 and PSD95, and these modification on the CT does not confer the interaction specifically with PSD95 (Supplementary Fig. 5.2C).

To examine if these MAGUKs modulate βArr2 recruitment to D1R, D1R-Tango was transfected alone or with either HA-SAP102 or PSD95-RFP in HTLA cells. Dose-response curves using increasing concentrations of DA and DHX were performed. Results shows that SAP102 and PSD95 substantially promote βArr2 recruitment by increasing the maximal response (E_{max}) of D1R-mediated βArr2 recruitment relative to D1R alone, without altering the agonist potency (EC_{50}) (Fig. 5.5B, C; Table. 5.1). A representative RLU values is shown in (Supplementary Fig. 5.2D). These findings imply a positive modulation of SAP102 and PSD95 on βArr2 recruitment by D1R.

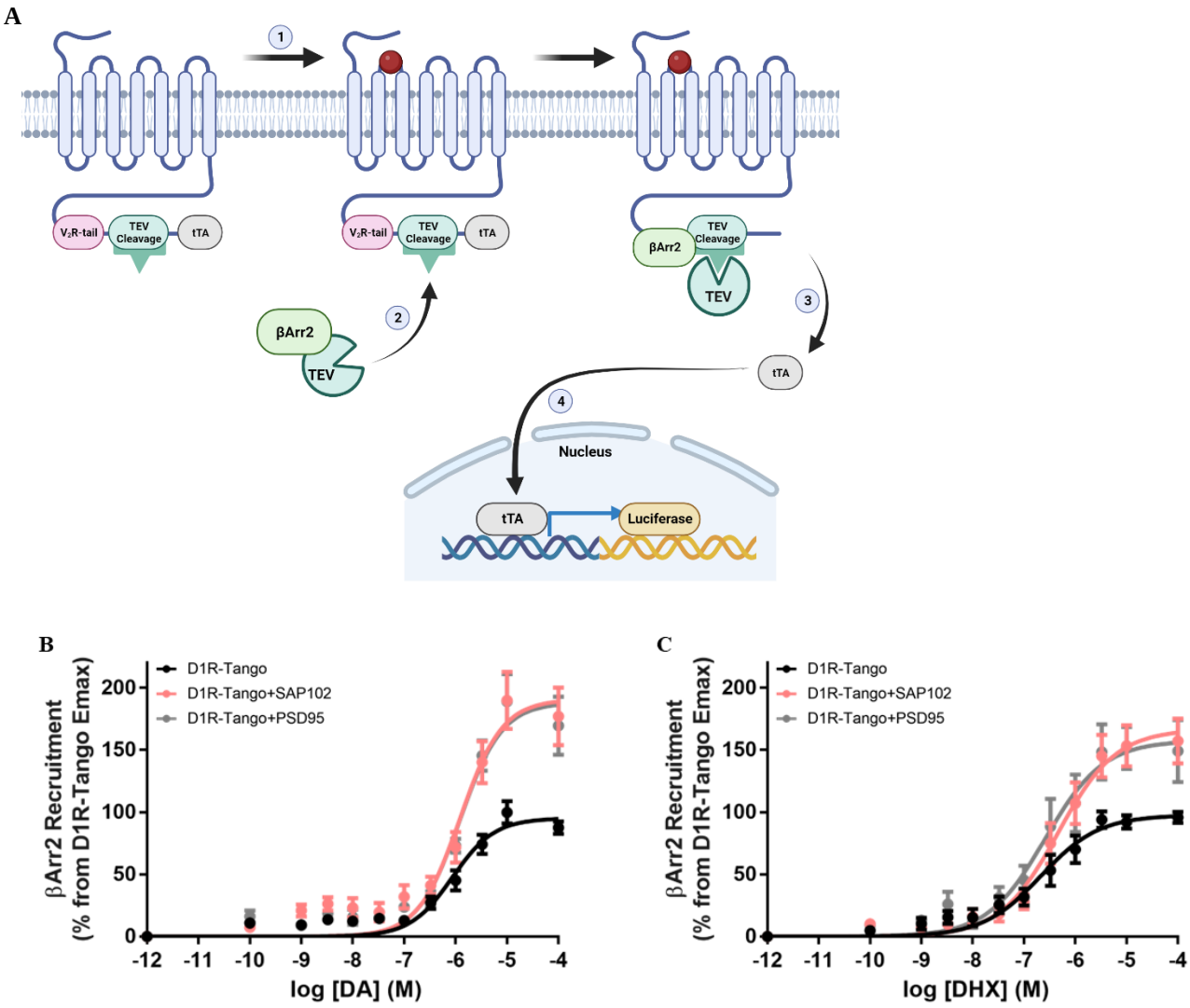

Fig. 5.5. SAP102 and PSD95 Promote D1R-mediated βArr2 Recruitment.

(A) Schematic representation of the principle of the Tango assay. Created with BioRender.com. (B. C) HTLA cells were transfected with D1R-Tango alone, co-transfected with HA-SAP102, or with PSD95-RFP. Dose-response curves in response to increasing concentration of DA and DHX were performed to measure βArr2 recruitment for D1R-Tango. E_{max}, EC_{50}, and B_{max} are shown in arithmetic mean in Table 5.1. from seven independent experiments.

Receptor	Agonist Efficacy DA (% of D1R-E_{max})	Agonist Potency EC_{50}-DA (nM)	Agonist Efficacy DHX (% of D1R-E_{max})	Agonist Potency EC_{50}-DHX (nM)	B_{max} (pmol/mg protein)
D1R-Tango (N=7)	**100**	**1414** (415-3962)	**100**	**570** (23.59-1830)	**3.3** (0.99-6.20)
D1R-Tango+SAP102 (N=7)	**196.7 *** (126.5-297)	**1640** (141-3978)	**167.2 *** (121.4-251.6)	**610** (134.1-1591)	**4.0** (0.41-8.41)
D1R-Tango+PSD95 (N=7)	**190.0 *** (98.6-275.8)	**1232** (335-2462)	**159.6 *** (131.4-280.6)	**595** (92.93-1630)	**4.3** (1.40-7.50)

Table 5.1. SAP102 and PSD95 Promote D1R-mediated βArr2 Recruitment.
Best-fitted E_{max} and EC_{50} values of DA and DHX for D1R-mediated βArr2 recruitment in HTLA cells transfected with D1R-Tango alone, co-transfected with HA-SAP102, or co-transfected with PSD95-RFP, shown in Fig. 5.5 (B, C) are reported. Values are expressed as arithmetic means, with minimum and maximum value in brackets. Statistical significance; *: $p<0.05$, using one sample t test, was determined by comparing E_{max} of D1R-Tango.

6. D1R-mediated βArr1 Recruitment, independent of MAGUKs

βArr2, but not βArr1, preferentially regulates class-A GPCR, such as D1-class receptors. Few studies, however, have demonstrated a βArr1 translocation in response to D1R (Kim et al, 2004; Macey et al, 2005). Since I observed a positive modulation of MAGUK in promoting βArr2 recruitment by D1R, and as I showed MAGUKs interact with βArr1, I tested the hypothesis that perhaps MAGUKs modulate βArr1 recruitment by D1R. Herein, I utilized HEK293-derived cell line containing stable expression of tTA-dependent luciferase reporter (HTL cells) that requires transient expression of either βArr1-TEV219 or βArr2-TEV219, with Tango constructs. In addition to βArr1, I have assessed βArr2 recruitment as a reference to validate this system. HTL cells were transiently transfected with different combination of D1R-Tango, D5R-Tango, βArr1-TEV219, and βArr2-TEV219. Dose-response curve using increasing concentration of DA and DHX were performed. The results showed that βArr2 is more efficiently recruited than βArr1 by D1R and D5R (Fig. 5.6A-B; Table 5.2; Table 5.3). While I observed βArr1 recruitment, yet it was less efficiently recruited by D1R and D5R, which displayed lower agonist potency relative to βArr2 (Fig. 5.6A-B; Table 5.2; Table 5.3). These findings in agreement with the notion that that D1-class receptor preferentially bind βArr2 (Zhang et al, 1999; Oakley et al, 2000; Kim et al, 2004; Macey et al, 2005).

Finally, I examined whether MAGUKs interaction with βArr1 change the modality toward its recruitment by D1R. HTL cells were transiently transfected with D1R-Tango+βArr1-TEV219 alone, with HA-SAP102, or with PSD95-RFP. Dose-response curves using increasing concentrations of DA was performed to measure βArr1 recruitment. Results show that overexpression of SAP102 and PSD95 neither modulate the maximal response (E_{max}) nor altered the agonist potency (EC_{50}) of D1R-mediated βArr1 recruitment (Fig. 5.6C; Table. 5.4). A representative RLU values is shown in (Supplementary Fig. 5.2E). This is in striking contrast to results obtained with βArr2 (Fig. 5.5). These findings suggest that in this system, βArr1 recruitment to D1R is likely independent of MAGUK activity, as no further enhancement or inhibition of βArr1 recruitment is observed. Collectively, MAGUKs preferentially promote D1R-mediated βArr2 recruitment, but not βArr1.

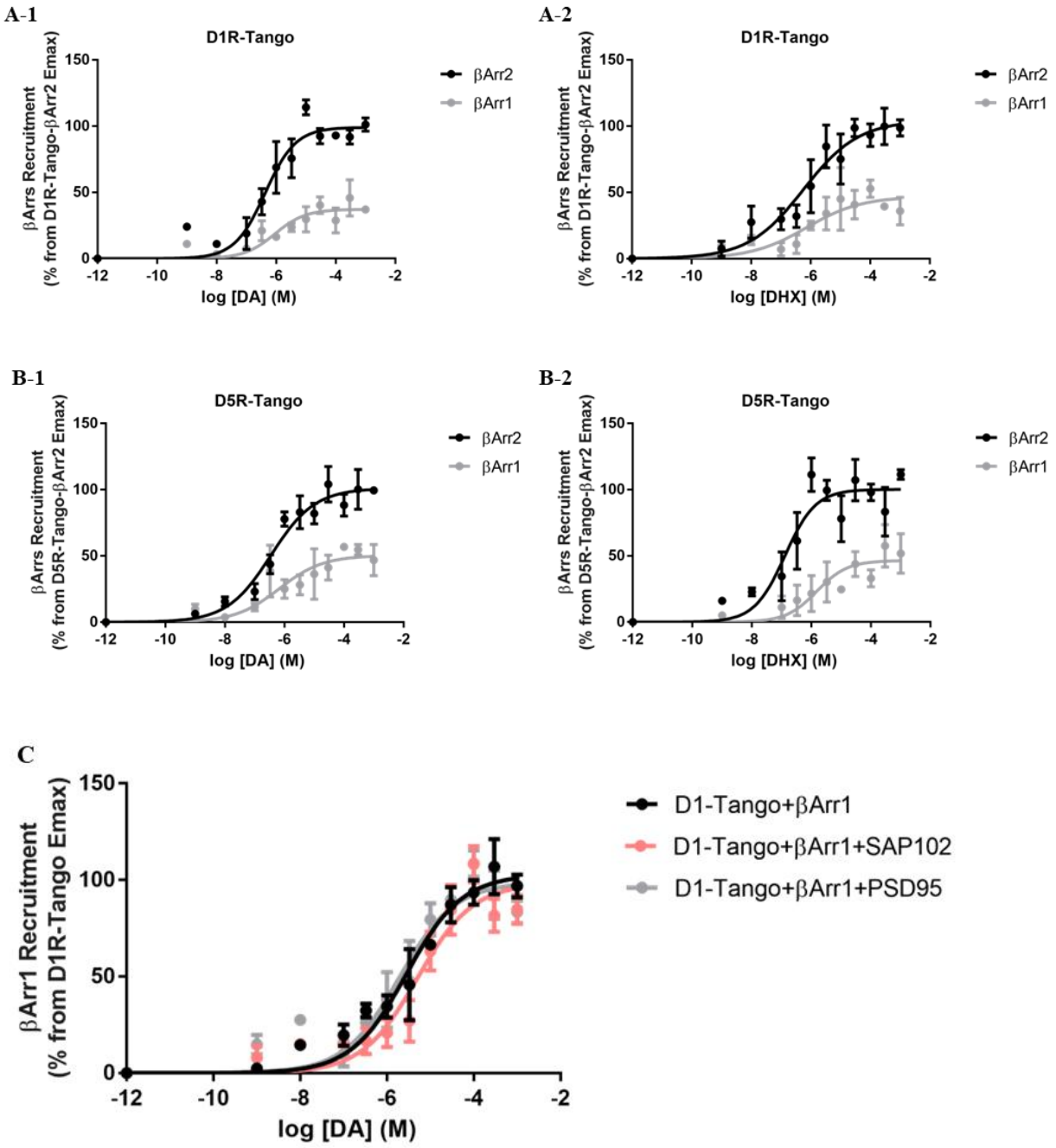

Fig. 5.6. D1R-mediated βArr1 Recruitment, Independent of MAGUKs.

(A-B) HTL cells were transfected with D1R-Tango+βArr1-TEV219, D1R-Tango+βArr2-TEV219 (A), or D5R-Tango+βArr1-TEV219, and D5R-Tango+βArr2-TEV219 (B). Dose-response curves in response to increasing concentration of DA and DHX were performed to measure βArr1 and βArr2 recruitment for D1R-Tango and D5R-Tango. E_{max}, EC_{50}, and B_{max} are shown in arithmetic mean in Table 5.2 for (A), and Table 5.3 for (B), from three independent experiments. (C) HTL cells were transfected with D1R-Tango+βArr1-TEV219, D1R-Tango+βArr1-TEV219+HA-SAP102, or D1R-Tango+βArr1-TEV219+PSD95-RFP. Dose-response curves in response to increasing concentration of DA was performed to measure βArr1 recruitment for D1R-Tango. E_{max}, EC_{50}, and B_{max} are shown in arithmetic mean in Table 5.4. from three independent experiments.

Receptor	Agonist Efficacy DA (% of D1R-Tango+βArr2-E_{max})	Agonist Potency EC_{50}-DA (nM)	Agonist Efficacy DHX (% of D1R-Tango+βArr2-E_{max})	Agonist Potency EC_{50}-DHX (nM)	B_{max} (pmol/mg protein)
D1R-Tango+βArr2 (N=3)	**100**	**693** (145-1190)	**100**	**762** (91.20-1651)	**3.0** (0.72-12.11)
D1R-Tango+βArr1 (N=3)	**51.1 *** (34.07-68.63)	**2815** (1032-5051)	**47.85 *** (34.15-59.36)	**4734 #** (750.2-12000)	**2.9** (0.48-8.17)

Table 5.2. βArr2, but not βArr1, is Preferentially Recruited by D1R.
Best-fitted E_{max} and EC_{50} values of DA for D1R-mediated βArrs recruitment in HTL cells expressed with D1R-Tango+βArr1-TEV219 or D1R-Tango+βArr2-TEV219, shown in Fig. 5.6 (A) are reported. Values are expressed as arithmetic means from three independent experiments, with minimum and maximum value in brackets. Statistical significance; *: $p<0.05$, using one sample t test, was determined by comparing E_{max} of D1R-Tango+βArr2-TEV219, or #: $p<0.05$, using unpaired t test, was determined by comparing EC_{50} of D1R-Tango+βArr2-TEV219.

Receptor	Agonist Efficacy DA (% of D1R-Tango+βArr2-E_{max})	Agonist Potency EC_{50}-DA (nM)	Agonist Efficacy DHX (% of D1R-Tango+βArr2-E_{max})	Agonist Potency EC_{50}-DHX (nM)	B_{max} (pmol/mg protein)
D5R-Tango+βArr2 (N=3)	**100**	**367** (231.8-456.7)	**100**	**221** (28.37-321.6)	**1.74** (0.51-3.16)
D5R-Tango+βArr1 (N=3)	**53.8 *** (47.31-57.59)	**5957 #** (79.65-14450)	**42.6 *** (35.59-55.60)	**2557 #** (88.14-7192)	**3.07** (1.36-6.70)

Table 5.3. βArr2, but not βArr1, is Preferentially Recruited by D5R.
Best-fitted E_{max} and EC_{50} values of DA and DHX for D5R-mediated βArrs recruitment in HTL cells expressed with D5R-Tango+βArr1-TEV219 or D5R-Tango+βArr2-TEV219, shown in Fig. 5.6 (B) are reported. Values are expressed as arithmetic means from three independent experiments, with minimum and maximum value in brackets. Statistical significance; *: $p<0.05$, using one sample t test, was determined by comparing E_{max} of D5R-Tango+βArr2-TEV219, or #: $p<0.05$, using unpaired t test, was determined by comparing EC_{50} of D5R-Tango+βArr2-TEV219.

Receptor	Agonist Efficacy DA (% of D1R-Tango+βArr2-E_{max})	Agonist Potency EC_{50}-DA (nM)	B_{max} (pmol/mg protein)
D1R-Tango+βArr1 (N=3)	**100**	**3352** (1400-6598)	**3.2** (1.30-4.68)
D1R-Tango+βArr1+SAP102 (N=3)	**96.1** (87.9-101)	**5743** (2943-10740)	**3.8** (1.18-5.71)
D1R-Tango+βArr1+PSD95 (N=3)	**98.2** (88.5-107.6)	**2999** (1080-5553)	**3.0** (2.02-3.94)

Table 5.4. D1R-mediated βArr1 Recruitment, Independent of MAGUKs.
Best-fitted E_{max} and EC_{50} values of DA for D1R-mediated βArr1 recruitment in HTL cells transfected with D1R-Tango+βArr1-TEV219, D1R-Tango+βArr1-TEV219+HA-SAP102, or D1R-Tango+βArr1-TEV219+PSD95-RFP, shown in Fig. 5.6 (C) are reported. Values are expressed as arithmetic means, with minimum and maximum value in brackets. No statistical significance was observed using one-sample t test, when compared to E_{max} of D1R-Tango+βArr1-TEV219.

Significance

In this final part of my thesis results, I identified SAP102 and PSD95 interactions with βArr1 and βArr2 *in vivo* and *in vitro*. My results support a potential ternary complex between D1R•MAGUK• βArr2, and that the receptor activation enhances the binding of βArr2 to D1R, but not with MAGUKs. I also showed that βArr2 further modulates the colocalization of D1R•MAGUK at plasma membrane, and MAGUKs positively mediate βArr2 recruitment to D1R, but not with βArr1. These results suggest that MAGUKs not only play a role in the modulation of D1R-mediated $G\alpha_s$ signaling but also D1R-mediated βArr2 signaling. Overall, these findings may help in the development of new pharmacological tool to address the impaired D1R•βArr2 signaling associated with dopaminergic disorders, e.g., PD.

Appendix III: Supplementary Figures and Tables for Manuscript III

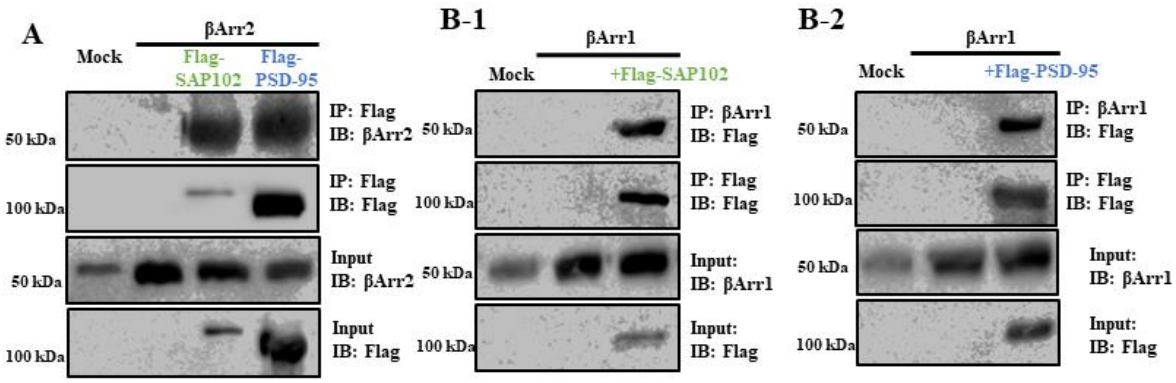

Supplementary Fig. 5.1. SAP102 and PSD95 Interact with βArr1 and βArr2.

(A, B) HEK293 cells were transfected with mock, βArr2 alone, or co-transfected with Flag-SAP102 or Flag-PSD95 (A), or transfected with mock, βArr1 alone, or co-transfected with Flag-SAP102 or Flag-PSD95 (B). Cells were solubilized and subjected to a sequential immunoprecipitation with anti-Flag-agarose matrix followed by immunoblotting with corresponding antibodies. A representative experiment of N=2 is shown.

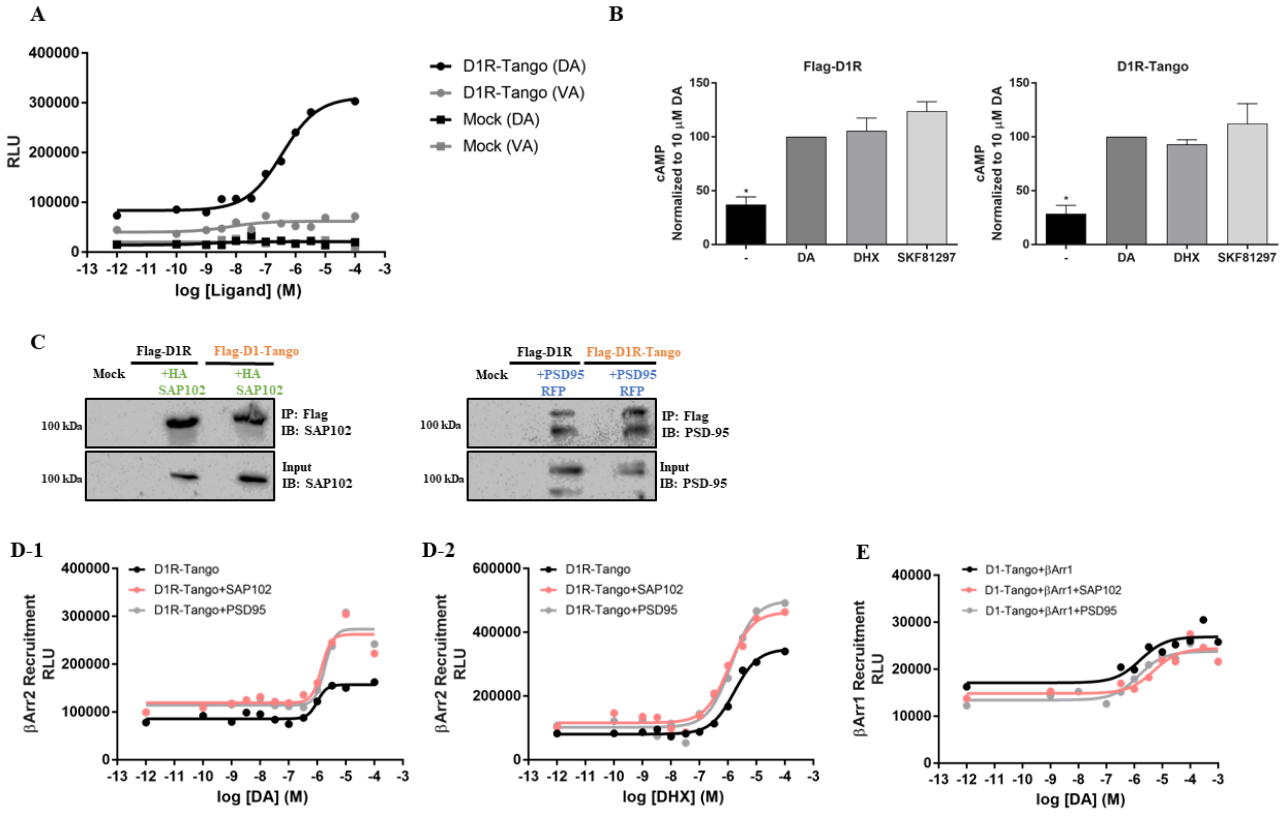

Supplementary Fig. 5.2. SAP102 and PSD95 Promote D1R-mediated βArr2 Recruitment.
(A) HTLA cells transfected with mock, or D1R-Tango, and βArr2 recruitment was assessed in reponse to increasing conentration of DA and vasopressin (VA). A represintative of average RLU calculated in quadrable determinations in response to βArr2 recruitment is shown, and B_{max} for D1R-Tango: 1.54 pmol/mg membrane protein. (B) HEK293T cells stably expressing GloSensor were transfected with Flag-D1R and D1R-Tango. Relative luminance value (RLU) for each experiment done in quadrable determinations to measure cAMP level of constitutive activity (AA) or maximal activation (10 μM) of D1R agonists: DA, DHX, SKF81297. Each bar represents the arithmetic mean ± S.E. of normalized values relative to DA from four independent experiments. B_{max} values in pmol/mg membrane protein for [^{3}H]-SCH23390 for Flag-D1R: 5.33±1.87, D1R-Tango: 3.57±1.22. *: $p<0.05$, when compared to cells treated with 10 μM DA using one sample t test. (C) HEK293 cells transfected with mock, Flag-D1R alone, with HA-SAP102/PSD95-RFP, Flag-D1R-Tango alone or co-transfected with HA-SAP102/PSD95-RFP. Cells were solubilized and subjected to a sequential immunoprecipitation with anti-Flag agarose matrix followed by immunoblotting with anti-SAP102 or anti-PSD95 antibodies, A representative experiment of N=2 is shown. B_{max} values in pmol/mg membrane protein for [^{3}H]-SCH23390 for Flag-D1R: 2.42±1.33, Flag-D1R+HA-SAP102: 3.25±0.83, Flag-D1R+PSD95-RFP: 3.21±0.92, D1R-Tango: 3.81±1.62, D1R-Tango+HA-SAP102: 1.36±0.62, D1R-Tango+PSD95-RFP: 1.44±0.72. (D) HTLA cells transfected with D1R-Tango, co-transfected with HA-SAP102, or with PSD95-RFP, and βArr2 recruitment was assessed in reponse to increasing conentration of DA and DHX. A represintative of average RLU calculated in quadrable determinations in response to βArr2 recruitment is shown, corresponding to (Fig. 5.5B, C), and B_{max} values in pmol/mg membrane protein for [^{3}H]-SCH23390: D1R-Tango: 3.87, D1R-Tango+HA-SAP102: 4.73, D1R-Tango+PSD95-RFP: 3.69. (E) HTL cells transfected with D1R-Tango+βArr1-TEV219, co-transfected with HA-SAP102, or with PSD95-RFP, and βArr2 recruitment was assessed in reponse to increasing conentration of DA. A represintative of average RLU calculated in quadrable determinations in response to βArr1 recruitment is shown, corresponding to (Fig. 5.6C), and B_{max} values in pmol/mg membrane protein for [^{3}H]-SCH23390: D1R-Tango+βArr1-TEV219: 3.56, D1R-Tango+βArr1-TEV219+HA-SAP102: 4.56, D1R-Tango+βArr1-TEV219+PSD95-RFP: 2.62.

	Saturation Curves [^{3}H]-SCH23390		Competition Curves K_i (nM)		
Receptor	**K_d (nM) N=5**	**B_{max} (pmol/mg protein) N=5**	**DA N=3**	**SKF81297 N=2**	**DHX N=2**
Flag-D1R	**0.77** (0.29-1.62)	**16.5** (3.69-41.8)	**5696** (578-9958)	**33.7** (26.42-40.96)	**125** (116-134)
D1R-Tango	**0.65** (0.21-1.83)	**9.8** (2.83-20.5)	**7195** (395-11150)	**33.2** (26.98-39.35)	**552** (504-601)

Supplementary Table 5.1. Functional Assessment for D5R-Tango by Radioligand Binding.
Dissociation constants (K_d, K_i) and B_{max} values of radioligand saturation and competition studies of [^{3}H]-SCH23390 performed from HTLA cells transfected with Flag-D1R and D1R-Tango. Values are expressed as arithmetic means, with minimum and maximum value in brackets. No statistical significance was observed using unpaired t test, when compared to Flag-D1R.

CHAPTER FOUR: DISCUSSION

Discussion

DA receptors are of considerable interest in biomedical research as they are critical for the regulation of a variety of physiological functions. Enormous efforts have been devoted to study the full complement of signaling pathways mediated by individual DA receptors. The two highly homologous D1-class receptors, D1R and D5R, are enriched in several brain regions and modulate many behaviors, which makes them potential targets for therapeutic strategies in a variety of neuropsychiatric conditions (Beaulieu and Gainetdinov, 2011). Studies also demonstrate that DA receptor signaling is regulated by interacting proteins, known as DRIPs, which include various scaffolding and signaling proteins (Yao et al, 2008; Wang et al, 2012). Therefore, it is pivotal to investigate the underlying molecular mechanisms of D1-class receptor function.

The Tiberi lab utilized yeast two-hybrid screens to investigate D1-class receptor interactions with potential binding partners across the entire human brain proteome, and identified SAP102 as a novel subtype-specific interactor for D1R, thus suggesting an even more sophisticated interplay between D1-class receptors and MAGUKs. This discovery was followed by a thorough set of experimental approaches to elucidate the functional importance of D1R•SAP102 complex. The major part of my Ph.D. thesis shed light on the molecular mechanisms governing D1-class receptor functional modulation by SAP102 and one of its structural homologs, PSD95. We identified SAP102 and PSD95 as novel DRIPs for D1R and D5R, respectively. Interestingly, SAP102 and PSD95 differentially regulate D1R signaling, phosphorylation, and trafficking (Fig. 6.1). Furthermore, PSD95 exerts distinct modulatory effects on the signaling and trafficking of D1R relative to that of D5R (Fig. 6.1). Finally, in addition to confirming the previously known complex of βArr2•MAGUK, we uncovered a novel complex of βArr1•MAGUK, and provide evidence that MAGUK and βArr2 modulate D1R•MAGUK•βArr2 complex.

In the following sections, I explore insights gained from my thesis findings, including the potential processes underlying SAP102- and PSD95-mediated regulation of D1-class receptor signaling and trafficking. To conclude this thesis, I discuss the physiological and pathological relevance of my findings, along with potential future studies streaming from the work presented herein.

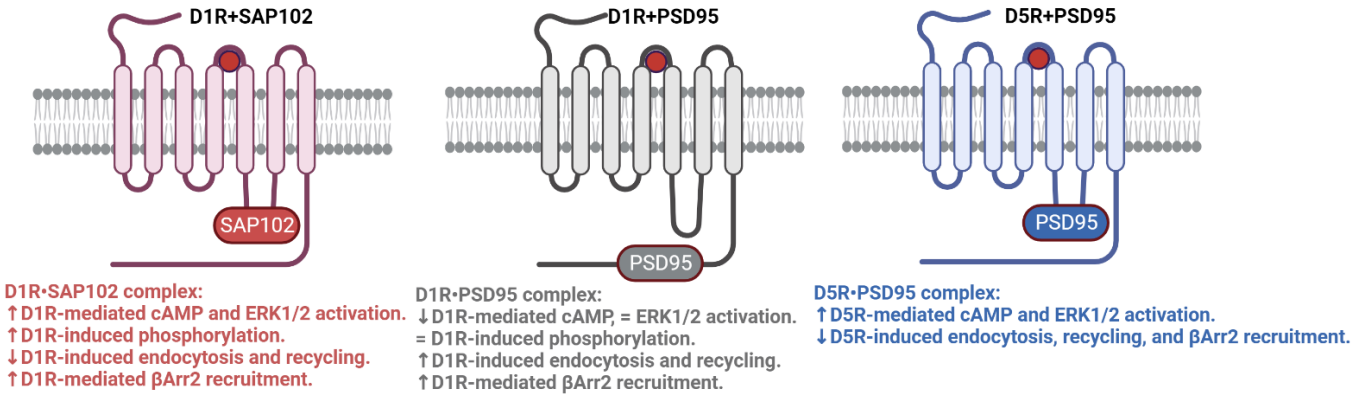

Fig. 6.1. Summary of the Signaling and Trafficking Mechanisms of D1R•SAP102, D1R•PSD95, and D1R•PSD95 complexes.

1. Mechanistic Insights on D1-Class Receptor Complex Formation with SAP102 and PSD95

1.1. Novel D1-Class Receptor Complexes: D1R•SAP102 and D5R•PSD95

In the first results manuscript, we identified SAP102 as a novel interactor with D1R. I sought to include PSD95 as a positive control DRIP in subsequent experimental studies to assess its impact along with SAP102 in D1R functions (Zhang et al, 2007). Coimmunoprecipitation studies using transfected HEK293 cells show that SAP102 and PSD95 interact with D1R (Fig. 3.5). Further coimmunoprecipitation experiments with rat hippocampal, striatal, and cortical lysates (P21 and P60) also identify D1R interactions with SAP102 and PSD95, while D1R•SAP102 and D1R•PSD95 complexes were further detected in neonatal brain preparations (P8) (Fig. 3.1). These findings imply that D1R•SAP102 and D1R•PSD95 complexes have potentially important physiological and developmental functions in different brain regions. In the second results manuscript, we identified PSD95 as a novel regulator of D5R. Coimmunoprecipitation experiments performed with transfected HEK293 cells indicate that PSD95, but not SAP102, interact with D5R (Fig. 4.1). Importantly, further coimmunoprecipitation studies detected endogenous D5R•PSD95 complexes within rat hippocampus and cortex, implying that they are physiologically relevant within these two important brain regions (Fig. 4.2).

I also examined the subcellular localization of D1R, D5R, SAP102 and PSD95 in rat hippocampal organotypic culture (P8, DIV28) and mouse cortical neuronal culture (E13-14, DIV10). Results suggest a high degree of colocalization between SAP102 and D1R, as well as PSD95 and both D1R and D5R, in dendritic shafts and spines (Fig. 3.2, Fig. 3.3; Fig. 4.3). These findings confirm postsynaptic localization of D1R•SAP102, D1R•PSD95, and D5R•PSD95, potentially within PSD. Further supporting these findings, PLA results from cortical culture revealed endogenous, constitutive signals of D1R•SAP102, D1R•PSD95, and D5R•PSD95, along pyramidal cortical dendrites and spines, indicating the possibility that SAP102 and PSD95 may be engaged in sophisticated functional regulation of D1-class receptors, including trafficking of dendritic extrasynaptic receptor complexes to and from postsynaptic structures (Fig. 3.4; Fig. 4.3).

1.2. D1-Class Receptors Interact with SAP102 and PSD95 via IL3 and CT in a Subtype-Specific Manner

GPCRs critically rely on their IL3 and CT regions for multiple aspects of receptor regulation and signaling responses (Gether, 2000; Luttrell, 2006). Modifications or protein interactions within IL3 and CT can profoundly affect GPCR activity and contribute to the specificity and diversity of GPCR-mediated signaling pathways (Gether, 2000; Luttrell, 2006). As MAGUK proteins recognize specific PDZ-binding motifs (x-S/T-x-φ; where x indicates any amino acid and φ indicates any hydrophobic amino acid) interacting with distal CT of GPCRs, yet many reports have also demonstrated internal motifs mediating the formation of a GPCR•MAGUK complex (Table 6.1). Of interest, D1R and D5R do not exhibit PDZ-binding motifs at their extreme CT (Fig. 6.1.). As SAP102 and PSD95 interact in a subtype specific manner with D1-class receptors, we investigated the structural components of D1R and D5R that harbor their MAGUK interactions. *In vivo* and *in vitro* results obtained from GST-pulldown and coimmunoprecipitation experiments indicate that IL3 and CT of D1R respectively facilitate its interaction with SAP102 and PSD95, and that IL3 of D5R is essential for interacting with PSD95 (Fig. 3.6; Fig. 4.4). These findings are in agreement with previous reports emphasizing the importance of D1R-CT for its association with PSD95 (Zhang et al, 2007). Curiously, one previous study concluded that PSD95 does not interact with D5R based on GST-pulldown assays utilizing D5R-CT within striatal culture (Kruusmägi et al, 2009). However, these experiments failed to include pulldowns with D5R-IL3. Herein, our results partially agree with this finding, in that we also demonstrate no interaction between PSD95 and the CT of D5R. Importantly, however, we contradict their conclusion by showing a clear interaction between PSD95 and D5R via its IL3. Overall, these findings demonstrate that D1-class receptor subtypes participate in unique interactions with SAP102 versus PSD95.

1.3. SAP102 and PSD95 Interact with D1R via Respective PDZ Dependent and Independent Interactions

Previous studies suggested that CT of D1R is essential in mediating the interaction with NT of PSD95 (Zhang et al, 2007). Our yeast two-hybrid screen results suggested that a SAP102 domain located downstream of PDZ2 potentially interacts with IL3 of D1R. Interestingly, GST-pulldown assays using purified SAP102 domains from HEK293 cells and cortical lysates point to an interaction between SAP102-PDZ3 domain and D1R (Fig. 3.7). Thus, in contrast to the previously

Table 6.1. PSD-MAGUK Proteins Recognize Class I-PDZ Binding Motif at the End of GPCR-CT and Other Internal Motifs.

GPCR	PSD-MAGUK	Reference
Class I-PDZ Binding Motif (x-S/T-x-φ)		
β_1AR-CT-ESKV	**PSD95 (PDZ3)** **SAP97**	**(Hu et al, 2000; Hu et al, 2002; Nooh et al, 2004; Gardner et al, 2007)**
5-HT$_{2A}$R-CT-VSCV	**PSD95** **SAP97**	**(Xia et al, 2003; Abbas et al, 2009; Betacamel et al, 2004; Dun et al, 2014)**
5-HT$_{2C}$R-CT-ISSV	**PSD95** **SAP97** **SAP102**	**(Bécamel et al, 2002; Gavarini et al, 2006; Abbas et al, 2009)**
CRFR1-CT-STAV	**PSD95 (PDZ1-2, PDZ3)** **PSD93** **SAP97 (PDZ1-2)** **SAP102**	**(Dun et al, 2013; Bender et al, 2015; Dunn et al, 2016)**
SSTR1-CT-ISTL	**PSD95 (PDZ1-2)** **PSD93** **SAP97**	**(Christenn et al, 2007; Cia et al, 2009)**
SSTR4-CT-TTTF	**PSD95 (PDZ1-2)** **PSD93**	**(Christenn et al, 2007)**
GPCR30-CT-SSAV	**PSD95 (PDZ1-2)** **SAP97**	**(Akama et al, 2013; Broselid et al, 2014)**
Internal Binding Motifs		
D1R-CT	**PSD95 (NT)**	**(Zhang et al, 2007)**
D1R-CT	**PSD95•NMDAR**	**(Zhang et al, 2009)**
A$_{2A}$R-CT	**SAP102 (SH3-GK)**	**(Thurner et al, 2014)**

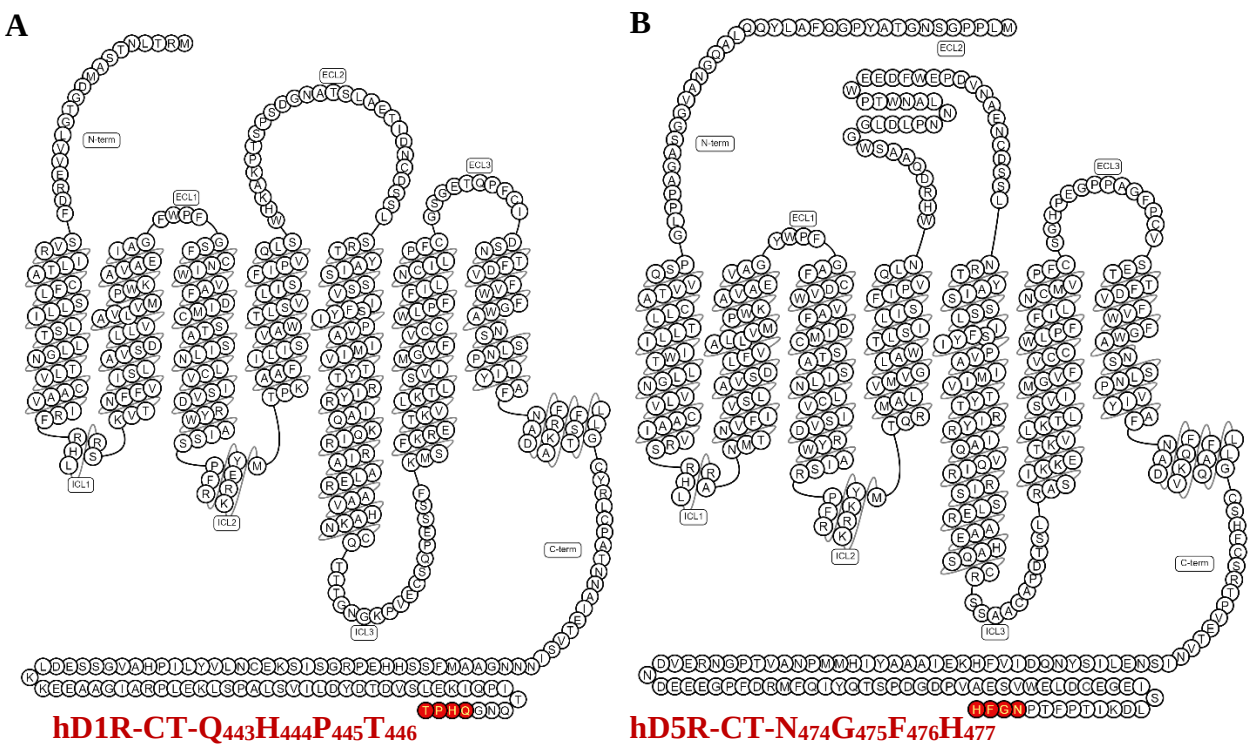

Fig. 6.2. D1-Class Receptor Subtypes do not Exhibit PDZ-Binding Motif.
Secondary structure of human D1R (A) and D5R (B) illustrating the distal amino acids in their CT. Created with gpcrdb.org.

characterized PDZ-independent interaction formed between PSD95 and D1R, herein we have characterized a PDZ-dependent interaction between SAP102 and D1R. It is worth mentioning that my thesis did not pinpoint the PSD95 domains interacting with D1-class receptors. Collectively, SAP102 and PSD95 interact with D1R both *in vitro* and *in vivo* via different cytosolic regions of D1R, in a PDZ-dependent and -independent manner, respectively. One potential factor underlying the contrasting regions of SAP102 and PSD95 that interact with D1R could be the intrinsic structural differences within their NT that leave SAP102 without any NT post-translational modification, but impart PSD95 with NT palmitoylation (Dunn and Ferguson, 2015; Zhu et al, 2016). As the NT of PSD95 is harboring the interaction with D1R, it has yet to be determined if this complex requires PSD95 palmitoylation.

1.4. Activation of D1-Class Receptors Modulate D1R•SAP102, D1R•PSD95, and D5R•PSD95 Complexes

The dynamic activity of a GPCR is regulated by the receptor activation. GPCR activation is best characterized by the ternary complex model which explains the link between the receptor, agonist, and G-protein (Pierce et al, 2002; Hilger et al, 2018). An agonist promotes changes in the inactive receptor conformation that allows G-protein binding and receptor activation by stabilizing the receptor in the active state (R*), which results in a maximal response. When DA binds to its cognate receptors, it promotes conformational plasticity that allows the receptor to interact with numerous signaling partners to produce spatially and temporally textured signals. Therefore, based on this pharmacological model, an agonist such as DA would interact with D1-class receptors, thereby stabilizing it in the R* state, and as a result, could conceivably render it more accessible for SAP102 and PSD95 binding.

Given that I observed constitutive complexes of D1R•SAP102, D1R•PSD95, and D5R•PSD95, I examined whether receptor activation regulates the functionality of these complexes. Importantly, radioligand saturation and competition studies determined that the interactions between SAP102 and PSD95 with D1R and D5R do not impact receptor ligand binding properties (Table 3.1; Table 4.1). This implies that the constitutive interaction does not alter the ligand binding pocket of D1-class receptors. Interestingly, however, while the radioligand binding-determined expression of D1R and D5R were also found to be unaltered in the presence of MAGUKs, coimmunoprecipitation results suggest that D1R activation enhances its avidity for SAP102 and

PSD95 relative to non-stimulated cells, and that similarly, D5R activation enhances its ability to interact with PSD95 relative to cells with silent D5R (Fig. 3.8; Fig. 4.5). These results are in agreement with a previous report showing that D1R activation enhances the association between D1R and PSD95 (Sun et al, 2009). Based on these findings, and results obtain by BRET, it can be hypothesized that under basal state conditions there exist two pools of D1-class receptors: a pool of receptors in complex with MAGUKs, and a distinct pool of receptors trapped in a state that hinders MAGUK binding. Then, upon DA stimulation, the MAGUK-free receptors presumably undergo conformational changes that render them more accessible to interactions with MAGUKs.

In other words, because D1R and D5R are dynamically changing between active and inactive states, they are presumably able to sample multiple conformations that facilitate varying degrees of interaction with MAGUKs. It is possible that DA stimulation simultaneously stabilizes D1-class receptors in an active state and specifically promotes MAGUK recruitment to the receptor complexes. However, in contrast, SAP102 and PSD95 may lose affinity for these D1-class receptors as they return to an inactive state, ultimately leading to destabilization and dissociation of the receptor-MAGUK complexes. Studies using an inverse agonist could be undertaken to investigate this hypothesis. Collectively, these findings suggest that, under basal conditions, only a fraction of the entire population of D1-class receptor is pre-associated with SAP102 and/or PSD95, but that receptor activation induces conformational changes in the residual receptors—previously unbound to MAGUKs—that enhance their avidity for MAGUKs, ultimately leading to the formation of additional receptor•MAGUK complexes.

2. Mechanistic Insights on D1-Class Receptor Functional Modulation by SAP102 and PSD95

2.1. SAP102 and PSD95 Differentially Modulate D1-Class Receptor Signaling

In light of our finding that SAP102 and PSD95 interact with distinct cytosolic regions of D1R, we hypothesized that SAP102 and PSD95 differentially regulate D1R signaling. Indeed, our results show that SAP102 and PSD95 shapeshift D1R signaling in the opposite manner, acting as respective positive and negative allosteric modulators. SAP102 overexpression potentiates D1R-mediated cAMP production and ERK1/2 activation, but PSD95 overexpression inhibits D1R-mediated cAMP accumulation while leaving D1R-mediated ERK1/2 signaling unaffected (Fig.

3.9; Table 3.2). These results are in agreement with a previous report demonstrating that PSD95 antagonizes D1R-mediated cAMP (Zhang et al, 2007).

While the primary mode of ERK1/2 activation downstream of D1R is via a $G\alpha_s$-AC-cAMP-PKA-ERK1/2 pathway, D1R is also capable of activating ERK1/2 via cAMP-mediated EPAC2 or RapGEF2 signaling (Beaulieu and Gainetdinov, 2011). Emerging studies suggest that βArr2 also modulate D1R-mediated ERK1/2 activation (Kaya, et al 2020). Although my thesis studies did not discriminate between these different processes of D1R-mediated ERK1/2 activation, it is interesting to speculate that SAP102 and PSD95 could potentially exert distinct biases toward the particular mechanisms being utilized. Indeed, unpublished results from the Tiberi lab suggest that SAP102 switches D1R-mediated ERK1/2 activation from a PKA-independent to PKA-dependent mechanism (Mischuk et al, manuscript in preparation). Adding further complexity to this matter, SAP102 and PSD95 both interact with βArr2, which could conceivably contribute to the observed effect of SAP102 on D1R-mediated ERK1/2 activation, and/or play a different yet undiscovered role in this signaling pathway. Large-scale analysis using cell lines that lack $G\alpha_s$ or βArr2, perhaps in conjunction with the use of PKA/EPAC2/RapGEF2 inhibitors, is warranted to elucidate the details of D1R-mediated ERK1/2 signaling, including the particular roles played by SAP102 and PSD95 in these processes.

While we demonstrate that PSD95 forms complexes with both D1R and D5R, we hypothesized that PSD95 differentially regulates the function of these receptors by virtue of the differing region of D1R and D5R that it physically interacts with. Indeed, our findings show that PSD95 behaves as a positive allosteric modulator of D5R, but a negative allosteric modulator of D1R. Specifically, overexpression of PSD95 potentiates D5R-mediated cAMP production and ERK1/2 activation, while it inhibits cAMP production downstream of D1R and leaves D1R-mediated ERK1/2 activation unaffected (Fig. 3.9; Fig. 4.6; Table 3.2; Table 4.2). Unlike D1R-mediated ERK1/2 activation, few studies have sought to examine the processes underlying ERK1/2 activation by D5R-mediated ERK1/2 activation, however, whether this signaling is primarily signal through $G\alpha_s$ or βArr2 remained elusive. Further investigation into the particular role played by PSD95 in D1-class receptor signaling pathway is especially warranted.

2.2. SAP102 and PSD95 Differentially Modulate D1R Phosphorylation

The different cytosolic regions of D1R facilitating its complex formation with SAP102 and PSD95 prompted examination into the possibility that said IL3•SAP102 and CT•PSD95 complexes may differentially regulate D1R desensitization. Unlike PSD95, which had no effect, SAP102 enhanced D1R activation-induced phosphorylation (Fig. 3.10). Moritz and colleagues (2023) showed that the phosphorylation sites within the CT of D1R are regulated in hierarchical order, in which the phosphorylation activity in proximal Ser/Thr residues is dependent on the distal residues, leading to βArr2 activation and D1R endocytosis. As PSD95 interacts with CT of D1R (Fig. 3.6), it is possible that PSD95 binds an internal motif containing phosphorylation residues within middle and/or distal portion of the CT (Zhang et al, 2007; Zhang et al, 2009), thereby the phosphorylation barcode of the D1R is competing with PSD95 to bind βArr2.

GRKs specifically recognize the agonist-occupied form of a receptor and terminate G-protein dependent signaling by phosphorylating the active receptor at its CT and/or IL3, thereby allowing βArr2 binding to occur (Gainetdinov et al, 2004; Ribas et al, 2006). βArr2 binds to the phosphorylated, activated receptors with high affinity, which simultaneously inhibits further G-protein coupling, facilitates receptor desensitization, and triggers receptor internalization (Ferguson, 2001). Although no studies have reported interaction between MAGUKs and GRKs, a study showed that GRK2 and GRK5 associate with β_1AR•PSD95 and enhance its phosphorylation (Hu et al, 2002). As GRKs are critical mediators of phosphorylation for all GPCRs, it is possible that the enhanced D1R phosphorylation observed in cells overexpressing SAP102 arises in part from SAP102-mediated facilitation of GRK activity. In other words, SAP102 may create more favourable conditions for GRK-mediated phosphorylation of Ser and Thr residues within cytoplasmic regions of D1R. On the other hand, given the interactions of PSD95 with both D1R-CT and βArr2, the lack of effect on D1R phosphorylation exhibited by PSD95 overexpression could conceivably be explained by the formation of a tripartite megacomplex that hinders GRK from accessing D1R phosphorylation sites. Previous studies in the Tiberi lab demonstrating a critical role for CT in overall D1R phosphorylation status offer support for this idea. Interestingly, these studies also identify D1R phosphorylation as being specifically regulated by GRK2 and GRK3, thus implicating these two particular GRKs as likely contributors to any MAGUK-GRK-related effects on D1R that may exist (Tiberi et al, 1996; Jackson et al, 2002; Sedaghat and Tiberi,

2011). Indeed, preliminary results from our lab showed a native complex of SAP102•GRK2 and PSD95•GRK2 in cortex. Future studies are strongly warranted to confirm the existence of MAGUK•GRK complex and ascertain whether ternary D1R•MAGUK•GRK complexes regulate D1R phosphorylation.

2.3. SAP102 and PSD95 Differentially Modulate D1-Class Receptor Endocytosis

Given the findings described above supporting the notion that overexpression of SAP102 promotes D1R phosphorylation, I examined the role of these MAGUKs in regulating D1R internalization. Results suggest that overexpression of PSD95 promotes constitutive D1R endocytosis that is βArr2- and dynamin-dependent (Fig. 3.11). Our results show that both SAP102 and PSD95 modulate D1R trafficking through respective inhibition and potentiation of D1R internalization in a βArr2- and dynamin-dependent manner (Fig. 3.11). These findings in agreement with a previous report showing that PSD95 promotes constitutive and agonist-induced endocytosis for D1R, that is dynamin-dependent (Zhang et al, 2007). Keeping in mind that both MAGUKs also interact with βArr2, it is possible that D1R-CT•PSD95 interaction makes D1R more accessible for βArr2 binding and subsequent sequestration than PSD95-free D1R, while in contrast that D1R-IL3•SAP102 interaction makes D1R less accessible for βArr2.

I also investigated whether the distinct PSD95 interaction site for D1R versus D5R differentially impacts receptor endocytosis. While PSD95 overexpression promotes constitutive and agonist-induced endocytosis for D1R, PSD95 acts in an opposite fashion by antagonizing the βArr2- and dynamin-dependent sequestration of D5R (Fig. 3.11; Fig. 4.7). Indeed, in cells overexpressing PSD95, the majority of D5R do not undergo endocytosis but instead are restricted from leaving the plasma membrane, much like SAP102-bound D1R. Together, these findings suggest that MAGUK interactions with the IL3 region of D1-class receptors are sufficient to hinder receptor internalization processes. It is tempting to speculate that the MAGUK-IL3 interactions function to block IL3 from binding to trafficking proteins that normally facilitate D1R endocytosis, thereby favouring receptor retention in the plasma membrane. Further studies are warranted to investigate these and other potential mechanisms by which SAP102 and PSD95 are exerting their effects on D1-class receptor endocytosis.

2.4. SAP102 and PSD95 Differentially Modulate D1-Class Receptor Recycling

Internalized receptors can experience several different fates depending on the particular signaling pathways involved and overall cellular context (Seachrist and Ferguson, 2003). Typically, however, internalized receptors are either returned back to the plasma membrane or degraded within lysosomes. Receptors that are recycled back to the cell surface allow the cell to maintain continued receptor responsiveness to the same ligand. In contrast, receptors that are targeted for lysosomal degradation enable the cell to abrogate excessive receptor signaling processes. The majority of internalized D1R and D5R efficiently recycle back to the plasma membrane in a βArr2-independent fashion, via a process that instead requires dephosphorylation of internalized receptor (Vickery and von Zastrow, 1999; Kotowski et al, 2011; Thompson and Whistler, 2011). This process presumably involves members of the Rab family of proteins, which are characterized for their role in modulating the fast-endocytic pathway (Seachrist and Ferguson, 2003). Our results show that overexpression of PSD95 promotes agonist-induced endocytosis and the recycling of D1R back to the plasma membrane, which is in agreement with a previous report (Fig. 3.12) (Zhang et al; Sun et al, 2009). In contrast, SAP102 facilitates the D1R retention at the plasma membrane, and that the D1R that do get internalized within cells co-expressing SAP102 recycle back to the plasma membrane less efficiently relative to cells expressing D1R alone. Interestingly, the effect of PSD95 on D5R recycling mimics that of SAP102 on D1R recycling, with internalized D5R taking significantly longer to return to the plasma membrane in cells expressing versus lacking PSD95 (Fig. 3.12; Fig. 4.8).

It is interesting to hypothesize what role Rab4 or Rab11 may have in the effects of SAP102 and PSD95 on D1-class receptor recycling, given their established importance in these processes for GPCRs as a whole. Yet, the full scale of into these trafficking proteins have not been examined in recycling D1-class receptors. The different patterns of D1R recovery to the plasma membrane in the presence of SAP102 versus PSD95 may involve differential utilization of Rab-orchestrated fast- and/or slow-endocytic machinery. Conceivably, Rab proteins might normally associate with D1-class IL3 and/or CT to facilitate trafficking processes, which would be altered in the presence of D1R-IL3•SAP102, D1R-CT•PSD95, and D5R-IL3•PSD95 interactions. More specifically, it is tempting to speculate that the slowed recycling of D1R and D5R in the presence of a IL3•MAGUK interaction may be the result of hindered IL3•Rab interaction, while on the contrary, the promoted

D1R recycling in the presence of a CT•PSD95 interaction could arise from enhanced IL3•Rab binding. As for D1R-CT•PSD95 complex, it is possible that the dephosphorylated receptor dissociates not only from βArr2, but also from PSD95, and the free PSD95•βArr2 makes these Rab proteins more prevalent to bind D1R and promote recycling to the plasma membrane. Another possibility is that SAP102 and/or PSD95 physically interact with Rab in a manner that alters receptor trafficking. Additional studies are warranted to assess these proposed hypotheses. Collectively, the contrasting effects of SAP102 and PSD95 on D1-class receptor trafficking presumably stem largely from their distinct receptor interaction sites, which impart unique contributions to the regulation of D1-class receptor responsiveness, desensitization and resensitization.

3. Mechanistic Insight of MAGUKs Modulating βArrs Recruitment for D1-Class Receptor

3.1. Novel βArr1•MAGUK Complex

In the third result manuscript, we uncovered the importance of βArrs in modulating SAP102 and PSD95. Intriguingly, although βArr2 is a previously known interactor with PDZ-containing proteins (Gupta et al, 2019), we identified βArr1 as a novel interactor with SAP102 and PSD95. Coimmunoprecipitation performed with transfected HEK293 cells and cortical lysates indicate the existence of both βArr1•MAGUK and βArr2•MAGUK complexes in these preparations (Fig. 5.1). Although my results have not investigated the binding motif(s) mediating the MAGUK•βArrs complexes, Gupta and colleagues suggested that PDZ1 domain of MAGUKs harbor the interaction with βArr2, and that the amino acid residue A175 of βArr2 is essential in enabling βArr2•PSD95 complex formation (Gupta et al, 2019). In agreement with this report, our preliminary result showed that PDZ1 of SAP102 indeed copurified with endogenous cortical βArr2. Further investigation is warranted to more precisely define the interacting regions between βArr1 and MAGUKs. Given the high degree of homology between βArr1 and βArr2, including A175 of βArr2 in comparison with A174 of βArr1, it is safe to speculate that βArr1-A174 may be a critical residue for mediating βArr1-MAGUK complex formation.

3.2. SAP102 and PSD95 Potentiate βArr2 Recruitment for D1R

In light of our findings that D1R desensitization and resensitization is modulated by SAP102 and PSD95, in combination with the well-established role of βArr2 in these processes, and the recently

characterized interaction between βArr2 and MAGUKs, herein I examined how βArr2 might factor into the regulation of D1R by MAGUKs. Coimmunoprecipitation and BRET analysis revealed that a substantial amount of βArr2 is recruited to D1R, D1R•SAP102, and D1R•PSD95 in response to D1R activation (Fig. 5.2; Fig. 5.3). Importantly, overexpression of MAGUK does not interfere the recruitment of βArr2 by D1R, but instead further enhancing this complex (Fig. 5.2; Fig. 5.3). While I observed basal interaction of MAGUKs in this tripartite D1R•MAGUK•βArr2, however, no further recruitment is detected in stimulatory condition (Fig. 5.2). Overexpression of βArr2 potentially stabilizes/maximizes the pre-associated constitutive complex of D1R•MAGUK, thus no further recruitment of MAGUKs in response to receptor activation. Interestingly, in cells not overexpressing βArr2, the recruitment of MAGUKs to D1R is substantially enhanced in response to D1R activation (Fig 3.8), hinting that βArr2 potentially prohibiting MAGUK-free D1R pool under basal state to interact with D1R, and/or perhaps MAGUKs interact with βArr2. Cellular localization in the absence of agonist stimulation shows that βArr2 is predominantly localized intracellularly and subset of colocalized MAGUK•βArr2, D1•βArr2, and D1R•MAGUK•βArr2 on the plasma membrane (Fig. 5.4). Interestingly, βArr2 enhances the translocation of MAGUKs to predominate the plasma membrane, where it colocalized in higher degree with D1R, than in cells not overexpressing βArr2 (Fig. 3.5; Fig. 5.4). While it is already well-established that βArr2 translocate to phosphorylated D1R at the plasma membrane (Zhang et al, 1999; Oakley et al, 2000; Kim et al, 2004; Macey et al, 2005; Thompson and Whistler, 2011), further investigation into the mechanisms underlying MAGUK-modulated D1R-inuced translocation of βArr2 are needed. These mechanistic observations favor a potential ternary complex of D1R•MAGUK•βArr2 than binary complex of D1R•MAGUK and D1R•βArr2 that coexisted in these cells.

Interestingly, however, the dynamic recruitment between D1R and βArr2 observed by Tango assay differed for the D1R alone relative to in the presence of MAGUKs. Specifically, SAP102 and PSD95 were found to enhance βArr2 recruitment with D1R, suggesting that MAGUKs essentially function to bridge the formation of D1R•βArr2 interactions (Fig. 5.5; Table 5.1). The nature of these D1R•MAGUK•βArr2 ternary complexes means that they must form in two distinct steps: D1R•MAGUK interaction and D1R•βArr2 interaction. Three different scenarios can be hypothesized to encompass the required interaction sequence: i) pre-associated D1R•MAGUK complexes promote βArr2 interaction with CT and/or IL3 of D1R, ii) D1R first interacts with

βArr2, which consequently make D1R more accessible for binding MAGUK, iii) D1R interact with pre-associated MAGUK•βArr2 complexes. The first scenario seems most likely, with SAP102 and PSD95 potentially imposing a conformational reorganization of D1R, and/or influencing its phosphorylation barcode in some manner that ultimately facilitates an interaction with βArr2. Regardless, the existence of pre-associated D1R•SAP102 and D1R•PSD95 could conceivably synergize the recruitment of βArr2 to D1R.

Another interesting point to consider is how D1R•MAGUK complexes could possibly alter the balance of D1R•$G\alpha_s$ and D1R•βArr2 signaling processes within certain contexts. The nature of cellular signaling is complex, with coexisting D1R•$G\alpha_s$ and D1R•βArr2 complexes in varying proportions that regulate sophisticated cellular paradigms (Thomsen et al, 2016; Kaya et al, 2020). If MAGUK-bound D1R more effectively recruit and retain βArr2 than MAGUK-free D1R, the relative proportion of $G\alpha_s$- and βArr2-mediated processes downstream of D1R could be significantly impacted by the level of MAGUK expression.

3.3. PSD95 Antagonizes βArr2 Recruitment for D5R

As discussed, PSD95 interacts with distinct cytosolic sites with D1R versus D5R, and differentially impacts receptor trafficking. While PSD95 overexpression potentiates agonist-induced endocytosis, recycling, and βArr2 recruitment for D1R, PSD95 acts in an opposite fashion for D5R by antagonizing each of these processes (Fig. 4.9; Fig. 5.5; Table 4.3; Table 5.1). These contrasting cellular functions demonstrate that PSD95 act as a reciprocal integrator for D1-class receptor subtypes to discriminate numerous cellular responses. Interestingly, PSD95 interact with the CT of CRFR1, and supress agonist-stimulated βArr2 recruitment to CRFR1 (Dunn et al, 2016). These findings further demonstrate the complexity of MAGUKs in regulating GPCR•βArr2 complex.

3.4. D1R-mediated βArr1 Recruitment Independent of MAGUK Activity

Finally, it is worth mentioning that although βArr1•MAGUK complex formation is intriguing, it was unclear how relevant such complexes might be for D1-class receptor signaling, given that Class-A GPCRs, which includes D1-class receptors, are well-known to be preferentially modulated by βArr2. Indeed, few studies have reported βArr1 translocation to the plasma membrane in response to D1R agonist (Kim et al, 2004; Macey et al, 2005). In an attempt to examine the efficacy of D1-class receptors for recruitment of βArr1 relative to βArr2, Tango assay

was performed. Unlike βArr2, which was strongly recruited to D1R and D5R, βArr1 recruitment was significantly reduced and displayed lower agonist potency towards these receptors (Fig. 5.6; Table 5.2, Table 5.3).

As SAP102 and PSD95 interact with βArr1, and positively modulate βArr2 recruitment by D1R, I examined how MAGUKs might impact βArr1 recruitment to D1R. Interestingly, results show that SAP102 and PSD95 exert no modality on D1R-mediated βArr1 recruitment as seen with βArr2 (Fig. 5.5; Fig. 5.6; Table. 5.1; Table 5.4). These results indicate that βArr1•MAGUK complexes might not have much relevance for D1R function, however it is still possible that they contribute to such processes within particular cellular contexts. Regardless, further investigation should be performed to better understand the role of MAGUK complexes with βArr1 and βArr2 in a more broad sense across the entire spectrum of GPCRs.

4. Physiological Relevance and Future Studies

4.1. Modulatory Role of MAGUKs in Dopaminergic-Glutamatergic Transmission

While the findings presented herein characterized the functional D1R•SAP102, D1R•PSD95, and D5R•PSD95 signaling complexes, important future avenues of investigation into different roles of these complexes may play in linking dopaminergic and glutamatergic transmission. As PSD-MAGUKs bind to NMDAR to enact context-dependent interactomes (Carroll and Zukin, 2002), it is vital that future experimental frameworks integrate D1R•SAP102, D1R•PSD95, and D5R•PSD95 into a context with NMDAR to further elucidate these signaling mechanisms.

Reported studies found that simultaneous activation of both D1R and NMDAR within the context of D1R•GluN2B-containing NMDAR complexes enhances D1R-mediated cAMP accumulation, however, activation of both receptors within the context of D1R•NMDAR•PSD95 complexes has no effect on cAMP production by D1R (Pei et al, 2004; Zhang et al, 2009). In a similar experimental approach, preliminary results from the Tiberi lab show that DA and NMDA co-treatment leads to elevated D1R-mediated cAMP production in cells expressing D1R, GluN2B-containing NMDAR, and SAP102, relative to those only expressing D1R and GluN2B-containing NMDAR. Together, these findings suggest the possibility that SAP102 and PSD95 act as respective positive and negative integrators of dopaminergic-glutamatergic neurotransmission through D1R•NMDAR signaling complex.

Previous studies have also shown that activation of D1-class receptors increases NMDAR-mediated currents via mechanisms involving second-messenger dependent pathways and/or direct protein-protein interactions (Lee et al, 2002; Scott and Aperia, 2009). Preliminary electrophysiological studies from the Tiberi lab have confirmed these results; specifically, recordings of NMDAR-mediated currents within acute rat hippocampal slices show an increase in NMDAR activity responses following D1R activation with DHX. Future investigation in the role SAP102 and PSD95 play in this process is warranted.

Of additional interest is the role SAP102 and PSD95 may play in functional interactions between D1R and NMDAR trafficking. SAP102 and PSD95 modulate bidirectional NMDAR trafficking between the PSD/dendritic spines and extrasynaptic dendrites (Carroll and Zukin, 2002; Lua and Zukin, 2007). This modulation is complex and involves physical association with various other proteins in addition to NMDAR. Furthermore, alternative splicing of SAP102 plays a critical role in this process; specifically, PDZ-independent interactions facilitated by I1 and I2 inserts of SAP102 respectively promote synaptic clearance of GluN2B-containing NMDAR and GluN2A-containing NMDAR (Chen et al, 2011; Wei et al, 2015). Interestingly, NMDAR activation selectively recruits D1R to dendritic spines, in a process linked to a diffusion-trap mechanism (Cepeda and Levine, 2006). It is possible that this process occurs in a MAGUK-dependent fashion. Future investigations are needed to shed light on this hypothesized mechanism.

While the crosstalk D5R•$GABA_AR$ is well examined, very little is known about the role of D5R in dopaminergic-glutamatergic functional interactions. Our novel finding of D5R•PSD95 complex strongly suggests that, just like D1R, D5R partakes in tripartite linkage with PSD95 and NMDAR. This idea is further supported by the finding that D5R mutant mice display severely reduced hippocampal GluN2B-containing NMDAR (Moraga-Amaro, 2016). However, the full-scale analysis of these postsynaptic proteins in in mice lacking D1R and D5R, remain incompletely assessed.

It is also interesting to speculate about the physiological significance of distinct D1R•SAP102•NMDAR, D1R•PSD95•NMDAR and D5R•PSD95•NMDAR complexes. Maintaining the proper balance of these complexes could conceivably play an integral part in regulating dopaminergic-glutamatergic interactions under varying cellular conditions. Regulation of D1R•MAGUK•NMDAR complexes might be especially important in the pathology of

neuropsychiatric conditions chiefly characterized by dysfunctional dopaminergic-glutamatergic transmission, like PD. Thus, improving our understanding of the intricacies by which MAGUKs link together D1R and NMDAR functions could have very useful therapeutic applications to treat brain disorders. Additional studies investigating whether MAGUK interactions with D1-class receptors impact dopaminergic functional interactions with other proteins critically involved in glutamatergic transmission will also be required to gain a complete understanding of how MAGUKs integrate dopaminergic and glutamatergic neurotransmission.

4.2. Understanding D1-Class Receptor Structural Components: Insights from MAGUK Interactions

Crystallography has provided valuable information into the molecular dynamics of DA receptors. Yet, despite intensive research on the structural basis of DA receptors and other GPCRs, the underlying functional role of variable IL3 and CT remains incompletely understood, as resolution of GPCR crystal structures necessitates prior modification of IL3 and CT. However, it is interesting to speculate that D1-class receptor IL3- and CT-interacting proteins, such as SAP102 and PSD95, could possibly be useful to improve the crystal structure resolution of these receptor regions. These proteins could hypothetically constrain the receptors in a stable state that is more conducible to crystallization without the need for any IL3 and CT modification.

Within the Tiberi lab, the quest to understand mechanistic details of D1-class receptor cytosolic regions led to previous investigations on the functional importance of IL3 and CT using mutagenesis approaches. Results from these studies have demonstrated a clear importance of these regions for D1-class receptor ligand binding along with both basal and agonist-dependent G-protein coupling; as such, it is reasonable to expect that protein-protein interactions involving IL3 and CT might impact these particular receptor properties. Intriguingly, my results demonstrate that D1-class receptor IL3- and CT-interacting proteins do not necessarily impact receptor ligand affinity. Thus, D1-class receptor ligand binding pockets presumably do not experience any physical disruption by the formation of D1R•MAGUK complexes.

The Tiberi lab has also used 3D homology modeling to explore the inactive states of human D1R and D5R. In the predicted structures, the N and C segments of D1R-IL3 appear closer together relative to those of D5R. Indeed, D5R displays a significantly more “open conformation” of its cytoplasmic surface than D1R, suggesting it is in a more active state, and thus agreeing with the

notion of higher D5R constitutive activity (Tiberi and Caron, 1994). Results obtained herein indicate that MAGUKs interact with D1-class receptor in a subtype specific manner, although it is unclear how the differing basal conformational states of D1R and D5R might influence this phenomenon.

Of additional importance, D1R•SAP102, D1R•PSD95, and D5R•PSD95 complexes each have a unique signalosome, which is primarily dictated by IL3 and CT receptor regions. Thus, modulation of the D1R•SAP102, D1R•PSD95, and D5R•PSD95 signaling complexes likely requires other as-of-yet unknown protein partners. Recently, the Tiberi lab employed an unbiased, BioID-based proteomic analysis that relied on proximity-dependent biotinylation of proteins. We are hopeful that our D1R-TurboID and D5R-TurboID constructs used for this approach will allow us to interrogate the interactome regulating the formation of receptor signaling complexes, and to discover D1-class receptor signaling partners specifically recruited by MAGUKs. This would hopefully shed light on the unique signaling signatures of the three MAGUK-receptor complexes I have characterized. Overall, by bridging D1-class receptor structural and functional information, we can begin to fully appreciate how the sophisticated module of D1-class receptor-interacting proteins, including SAP102 and PSD95, influences receptor function, and uncover important details that may guide in comprehensive applications for drug discovery.

5. Concluding Remarks

Since DA is involved in many physiological functions, it is not surprising that hypo- and hyper-activation of D1-class receptors have been implicated in a plethora of neuropsychiatric disorders. Despite this, the role of D1-class receptor signaling functions in normal and pathological conditions is yet to be fully appreciated. One notable barrier for furthering our understanding on this matter is the lack of subtype selective drugs for distinguishing between D1R and D5R functions *in vivo*. The challenge to develop D1-class receptor subtype-selective drugs stems chiefly from the high level of identity within transmembrane domain of D1R and D5R, which contain many conserved residues involved in ligand binding. One yet untapped, potentially exploitable factor to consider for developing subtype-selective D1-class ligands is the unique complement of protein interactions at intracellular regions involved in receptor activation for D1R versus D5R.

The main goal of this Ph.D. thesis was to develop a comprehensive understanding of the means by which two crucial neuronal scaffolding proteins implicated in dopaminergic diseases, the MAGUK

family members SAP102 and PSD95, interact with D1-class receptors and how these interactions influence receptor functions. In pursuing this goal, my thesis studies have unveiled the structural elements involved in the interplay between D1R•SAP102, D1R•PSD95, and D5R•PSD95, and further shown how these complexes impact D1-class receptor signaling and trafficking processes. SAP102 and PSD95 dictate the signaling for D1-class receptors, not only in $G\alpha_s$-dependent cascade, but also βArr2-dependent pathway.

Future studies should aim to discriminate the importance of these three distinct complexes under both physiological and parkinsonian-like states, via knockdown of SAP102 and/or PSD95, in conjunction with the use of selective interfering peptides. Indeed, *in vivo* infusion of synthetic interfering peptides, capable of selectively disrupting particular receptor•MAGUK complexes, into brain regions critically involved in dopaminergic transmission, should reveal crucial information about the behavioral and pathological signatures of these complexes. Moreover, future studies with interfering peptides would conceivably provide additionally valuable information for the identification of drug-targetable D1-class receptor regions. Conditional knockout of SAP102 and PSD95 in D1R-expressing MSNs will highlight their contribution into the mechanistic locomotor activity of the direct striatal pathway. As PSD95-KO mice exhibit an increased in locomotor activity in response to psychostimulant and D1-class agonist (Yao et al, 2004; Zhang et al, 2007), the motor kinetic behavior of SAP102-KO mice remained to be studied. In addition to the palmitoylation of PSD95 and phosphorylation of SAP102 and PSD95 in regulating D1-class receptor subtypes, it will be with great interest to examine the role of SAP97 and PSD93 in modulating D1-class receptors as well the regulatory of PSD-MAGUKs in regulating D2-class receptors. Collectively, my thesis findings also offer important insights to be relied upon in future studies investigating D1-class receptor-NMDAR functional linkage, and may ultimately, and hopefully, pave the way for improved D1-class receptor drug design to treat pathologies with dopaminergic-glutamatergic dysfunction like PD and schizophrenia.

Finally, my novel demonstration that PSD95 and SAP102 interact with not only βArr2, but also βArr1, has further implications toward understanding how MAGUKs and other PDZ domain-containing proteins might contribute to receptor functional regulation across the entire spectrum of GPCRs, but particularly, class-B GPCRs.

AUTHORIZATION FOR THE USE OF PUBLISHED MATERIALS

Permission to include published figures as part of dissertation/thesis was obtained:
"From [Xu et al. Structural genomics of the human dopamine receptor system. Cell Res. 2023]. Reprinted with permission from Springer Nature", to include figure 1.

SPRINGER NATURE LICENSE

TERMS AND CONDITIONS

Sep 15, 2023

This Agreement between Bassam Albraidy ("You") and Springer Nature ("Springer Nature") consists of your license details and the terms and conditions provided by Springer Nature and Copyright Clearance Center.

License Number	5630501099337
License date	Sep 15, 2023
Licensed Content Publisher	Springer Nature
Licensed Content Publication	Cell Research
Licensed Content Title	Structural genomics of the human dopamine receptor system
Licensed Content Author	Peiyu Xu et al
Licensed Content Date	May 23, 2023
Type of Use	Thesis/Dissertation
Requestor type	academic/university or research institute

Format	print and electronic
Portion	figures/tables/illustrations
Number of figures/tables/illustrations	1
Would you like a high resolution image with your order?	no
Will you be translating?	no
Circulation/distribution	1 - 29
Author of this Springer Nature content	no
Title	SAP102 and PSD-95 Regulate D1-Class Receptors in Subtype-Specific Manner
Institution name	University of Ottawa
Expected presentation date	Dec 2023
Portions	Figure 1
Requestor Location	Bassam Albraidy Ottawa, ON Canada Attn: Bassam Albraidy
Total	0.00 USD
Terms and Conditions	

Permission to include published figures as part of dissertation/thesis was obtained:
"From [Cizeron et al. A brainwide atlas of synapses across the mouse life span. Science. 2020]. Reprinted with permission from AAAS," to include figure 1.

From: Bassam Fahad Albraidy <[redacted]@uottawa.ca>
Sent: Thursday, September 21, 2023 10:49 AM
To: permissions <permissions@aaas.org>
Subject: Permission to reuse a figure in my PhD thesis
Greetings,
Hope this email finds you well.
I'm Bassam Albraidy, a PhD candidate at the University of Ottawa, and I'm requesting the permission to reuse one figure in my thesis. The online system asked me to reach out to the publisher. Below are the information:
Bassam Albraidy, University of Ottawa, PhD candidate, email: [redacted]@uottawa.ca, phone: [redacted]
Mailing Address: [redacted], Ottawa, ON [redacted], Canada
Identify the AAAS material you wish to use:
AAAS publication title (journal title or website name/URL))
https://www.science.org/doi/10.1126/science.aba3163
Article title: A brainwide atlas of synapses across the mouse life span
Authors' names: MÉLISSA CIZERON , ZHEN QIU, BABIS KONIARIS, RAGINI GOKHALE, NOBORU
H. KOMIYAMA, ERIK FRANSÉN, AND SETH G. N. GRANT
Volume number, issue date, page numbers, DOI: SCIENCE, 11 Jun 2020, Vol 369, Issue 6501, pp. 270275, DOI: 10.1126/science.aba3163
Specific figure numbers or portion of text: Figure S2
Next, include the following information about your publication/project:
Type of work in which AAAS material will be used: reuse in a thesis.
Title of that work: Thesis: SAP102 and PSD95 regulate Dopamine D1-Class Receptors in Subtype-Specific Manner
Title of the specific article/chapter in which you are reproducing the AAAS material: Not applicable
Author(s): Bassam Albraidy, Supervisor: Dr. Mario Tiberi
Expected publication date: Thesis to be submitted in December 2023
Publishing company: Not applicable
Retail price (for books only): Not applicable
The formats your work will be distributed in: Printed and Electronic
The rights you are seeking: Not Applicable

From: Dana James
Sent: Tuesday, October 3, 2023 5:15 PM
To: Bassam Fahad Albraidy
Cc: permissions
Subject: RE: THESIS/DISSERTATION USE – SCIENCE FIGURE – CIZERON ET AL 2020 DOI: 10.1126/science.aba3163

AAAS MATERIAL:
Figure S2 from Cizeron et al., SCIENCE, 11 Jun 2020
Vol 369, Issue 6501, pp. 270-275, DOI: 10.1126/science.aba3163
YOUR RE-USE: THESIS/DISSERTATION
Title: SAP102 and PSD95 regulate Dopamine D1-Class Receptors in Subtype-Specific Manner
Publication date: December 2023

Dear Bassam Albraidy:
Thank you very much for your interest in the AAAS material identified in your request.
We are pleased to have you include this material in your thesis or dissertation subject to the following guidelines. These guidelines also appear on our website:
https://www.science.org/content/page/reprints-and-permissions under the heading 'Using AAAS material in a thesis or dissertation'.
If how you wish to use the content falls outside of these guidelines or if you have any questions, please let me know.

Kind regards,

Dana

Dana James (she/her)

Rights and Licensing Coordinator

Science family of journals/AAAS

1200 New York Ave. NW
Washington, DC 20005
_____@aaas.org

RERERENCES

Abbas AI, Yadav PN, Yao WD, Arbuckle MI, Grant SG, Caron MG, Roth BL. PSD-95 is essential for hallucinogen and atypical antipsychotic drug actions at serotonin receptors. J Neurosci. 2009 Jun 3;29(22):7124-36. doi: 10.1523/JNEUROSCI.1090-09.2009. PMID: 19494135; PMCID: PMC2836830.

Abi-Dargham A, Rodenhiser J, Printz D, Zea-Ponce Y, Gil R, Kegeles LS, Weiss R, Cooper TB, Mann JJ, Van Heertum RL, Gorman JM, Laruelle M. Increased baseline occupancy of D2 receptors by dopamine in schizophrenia. Proc Natl Acad Sci U S A. 2000 Jul 5;97(14):8104-9. doi: 10.1073/pnas.97.14.8104. PMID: 10884434; PMCID: PMC16677.

Abi-Dargham A. Do we still believe in the dopamine hypothesis? New data bring new evidence. Int J Neuropsychopharmacol. 2004 Mar;7 Suppl 1: S1-5. doi: 10.1017/S1461145704004110. PMID: 14972078.

Abizaid A. Ghrelin and dopamine: new insights on the peripheral regulation of appetite. J Neuroendocrinol. 2009 Sep;21(9):787-93. doi: 10.1111/j.1365-2826.2009.01896.x. Epub 2009 Jun 12. PMID: 19523165.

Ahmed MR, Berthet A, Bychkov E, Porras G, Li Q, Bioulac BH, Carl YT, Bloch B, Kook S, Aubert I, Dovero S, Doudnikoff E, Gurevich VV, Gurevich EV, Bezard E. Lentiviral overexpression of GRK6 alleviates L-dopa-induced dyskinesia in experimental Parkinson's disease. Sci Transl Med. 2010 Apr 21;2(28):28ra28. doi: 10.1126/scitranslmed.3000664. PMID: 20410529; PMCID: PMC2933751.

Aira Z, Barrenetxea T, Buesa I, Martínez E, Azkue JJ. Spinal D1-like dopamine receptors modulate NMDA receptor-induced hyperexcitability and NR1 subunit phosphorylation at serine 889. Neurosci Lett. 2016 Apr 8;618:152-158. doi: 10.1016/j.neulet.2016.03.006. Epub 2016 Mar 5. PMID: 26957228.

Aizman O, Brismar H, Uhlén P, Zettergren E, Levey AI, Forssberg H, Greengard P, Aperia A. Anatomical and physiological evidence for D1 and D2 dopamine receptor colocalization in neostriatal neurons. Nat Neurosci. 2000 Mar;3(3):226-30. doi: 10.1038/72929. PMID: 10700253.

Albert PR, Neve KA, Bunzow JR, Civelli O. Coupling of a cloned rat dopamine-D2 receptor to inhibition of adenylyl cyclase and prolactin secretion. J Biol Chem. 1990 Feb 5;265(4):2098-104. PMID: 1688845.

Albin RL, Young AB, Penney JB. The functional anatomy of basal ganglia disorders. Trends Neurosci. 1989 Oct;12(10):366-75. doi: 10.1016/0166-2236(89)90074-x. PMID: 2479133.

Al-Fulaij MA, Ren Y, Beinborn M, Kopin AS. Pharmacological analysis of human D1 AND D2 dopamine receptor missense variants. J Mol Neurosci. 2008 Mar;34(3):211-23. doi: 10.1007/s12031-007-9030-x. Epub 2008 Jan 18. PMID: 18210231.

Al-Hallaq RA, Conrads TP, Veenstra TD, Wenthold RJ. NMDA di-heteromeric receptor populations and associated proteins in rat hippocampus. J Neurosci. 2007 Aug 1;27(31):8334-43. doi: 10.1523/JNEUROSCI.2155-07.2007. PMID: 17670980; PMCID: PMC2263005.

Aman TK, Shen RY, Haj-Dahmane S. D2-like dopamine receptors depolarize dorsal raphe serotonin neurons through the activation of nonselective cationic conductance. J Pharmacol Exp Ther. 2007 Jan;320(1):376-85. doi: 10.1124/jpet.106.111690. Epub 2006 Sep 27. PMID: 17005915.

Ambrée O, Richter H, Sachser N, Lewejohann L, Dere E, de Souza Silva MA, Herring A, Keyvani K, Paulus W, Schäbitz WR. Levodopa ameliorates learning and memory deficits in a murine model of Alzheimer's disease. Neurobiol Aging. 2009 Aug;30(8):1192-204. doi: 10.1016/j.neurobiolaging.2007.11.010. Epub 2008 Feb 20. PMID: 18079024.

Amenta F, Chiandussi L, Mancini M, Ricci A, Schena M, Veglio F. Pharmacological characterization and autoradiographic localization of dopamine receptors in the human adrenal cortex. Eur J Endocrinol. 1994 Jul;131(1):91-6. doi: 10.1530/eje.0.1310091. PMID: 8038912.

Amenta F, Collier WL, Ricci A. Autoradiographic localization of vascular dopamine receptors. Am J Hypertens. 1990 Jun;3(6 Pt 2):34S-36S. doi: 10.1093/ajh/3.6.34s. PMID: 2200435.

Amlaiky N, Berger JG, Chang W, McQuade RJ, Caron MG. Identification of the binding subunit of the D1-dopamine receptor by photoaffinity crosslinking. Mol Pharmacol. 1987 Feb;31(2):129-34. PMID: 3807891.

Amlaiky N, Caron MG. Identification of the D2-dopamine receptor binding subunit in several mammalian tissues and species by photoaffinity labeling. J Neurochem. 1986 Jul;47(1):196-204. doi: 10.1111/j.1471-4159.1986.tb02850.x. PMID: 2940337.

ANDEN NE, CARLSSON A, DAHLSTROEM A, FUXE K, HILLARP NA, LARSSON K. DEMONSTRATION AND MAPPING OUT OF NIGRO-NEOSTRIATAL DOPAMINE NEURONS. Life Sci (1962). 1964 Jun;3:523-30. doi: 10.1016/0024-3205(64)90161-4. PMID: 14187491.

Anderson SM, Bari AA, Pierce RC. Administration of the D1-like dopamine receptor antagonist SCH-23390 into the medial nucleus accumbens shell attenuates cocaine priming-induced reinstatement of drug-seeking behavior in rats. Psychopharmacology (Berl). 2003 Jul;168(1-2):132-138. doi: 10.1007/s00213-002-1298-5. Epub 2002 Dec 19. PMID: 12491029.

Anderson SM, Schmidt HD, Pierce RC. Administration of the D2 dopamine receptor antagonist sulpiride into the shell, but not the core, of the nucleus accumbens attenuates cocaine priming-induced reinstatement of drug seeking. Neuropsychopharmacology. 2006 Jul;31(7):1452-61. doi: 10.1038/sj.npp.1300922. Epub 2005 Oct 5. PMID: 16205775.

Antonini A, Leta V, Teo J, Chaudhuri KR. Outcome of Parkinson's Disease Patients Affected by COVID-19. Mov Disord. 2020 Jun;35(6):905-908. doi: 10.1002/mds.28104. Epub 2020 May 28. PMID: 32347572; PMCID: PMC7267273.

Araki KY, Sims JR, Bhide PG. Dopamine receptor mRNA and protein expression in the mouse corpus striatum and cerebral cortex during pre- and postnatal development. Brain Res. 2007 Jul 2;1156:31-45. doi: 10.1016/j.brainres.2007.04.043. Epub 2007 Apr 22. PMID: 17509542; PMCID: PMC1994791.

Arborelius L, Chergui K, Murase S, Nomikos GG, Höök BB, Chouvet G, Hacksell U, Svensson TH. The 5-HT1A receptor selective ligands, (R)-8-OH-DPAT and (S)-UH-301, differentially affect the activity of midbrain dopamine neurons. Naunyn Schmiedebergs Arch Pharmacol. 1993 Apr;347(4):353-62. doi: 10.1007/BF00165384. PMID: 8510763.

Ariano MA, Sortwell CE, Ray M, Altemus KL, Sibley DR, Levine MS. Agonist-induced morphologic decrease in cellular D1A dopamine receptor staining. Synapse. 1997 Dec;27(4):313-21. doi: 10.1002/(SICI)1098-2396(199712)27:4<313::AID-SYN5>3.0.CO;2-F. PMID: 9372554.

Arnsten AF, Pliszka SR. Catecholamine influences on prefrontal cortical function: relevance to treatment of attention deficit/hyperactivity disorder and related disorders. Pharmacol Biochem Behav. 2011 Aug;99(2):211-6. doi: 10.1016/j.pbb.2011.01.020. Epub 2011 Feb 2. PMID: 21295057; PMCID: PMC3129015.

Arnsten AF. Fundamentals of attention-deficit/hyperactivity disorder: circuits and pathways. J Clin Psychiatry. 2006;67 Suppl 8:7-12. PMID: 16961424.

Asano Y, Hiramoto T, Nishino R, Aiba Y, Kimura T, Yoshihara K, Koga Y, Sudo N. Critical role of gut microbiota in the production of biologically active, free catecholamines in the gut lumen of mice. Am J Physiol Gastrointest Liver Physiol. 2012 Dec 1;303(11):G1288-95. doi: 10.1152/ajpgi.00341.2012. Epub 2012 Oct 11. PMID: 23064760.

Ascher P. Inhibitory and excitatory effects of dopamine on Aplysia neurones. J Physiol. 1972 Aug;225(1):173-209. doi: 10.1113/jphysiol.1972.sp009933. PMID: 4679683; PMCID: PMC1331098.

Asghari V, Schoots O, van Kats S, Ohara K, Jovanovic V, Guan HC, Bunzow JR, Petronis A, Van Tol HH. Dopamine D4 receptor repeat: analysis of different native and mutant forms of the human and rat genes. Mol Pharmacol. 1994 Aug;46(2):364-73. PMID: 8078498.

Attademo L, Bernardini F. Are dopamine and serotonin involved in COVID-19 pathophysiology? Eur J Psychiatry. 2021 Jan-Mar;35(1):62-63. doi: 10.1016/j.ejpsy.2020.10.004. Epub 2020 Oct 29. PMID: 33162632; PMCID: PMC7598536.

Aubert I, Guigoni C, Håkansson K, Li Q, Dovero S, Barthe N, Bioulac BH, Gross CE, Fisone G, Bloch B, Bezard E. Increased D1 dopamine receptor signaling in levodopa-induced dyskinesia. Ann Neurol. 2005 Jan;57(1):17-26. doi: 10.1002/ana.20296. PMID: 15514976.

Axelrod J, Weinshilboum R. Catecholamines. N Engl J Med. 1972 Aug 3;287(5):237-42. doi: 10.1056/NEJM197208032870508. PMID: 4402575.

Baik JH, Picetti R, Saiardi A, Thiriet G, Dierich A, Depaulis A, Le Meur M, Borrelli E. Parkinsonian-like locomotor impairment in mice lacking dopamine D2 receptors. Nature. 1995 Oct 5;377(6548):424-8. doi: 10.1038/377424a0. PMID: 7566118.

Balestrino R, Schapira AHV. Parkinson disease. Eur J Neurol. 2020 Jan;27(1):27-42. doi: 10.1111/ene.14108. Epub 2019 Nov 27. PMID: 31631455.

Bamford NS, Zhang H, Schmitz Y, Wu NP, Cepeda C, Levine MS, Schmauss C, Zakharenko SS, Zablow L, Sulzer D. Heterosynaptic dopamine neurotransmission selects sets of corticostriatal terminals. Neuron. 2004 May 27;42(4):653-63. doi: 10.1016/s0896-6273(04)00265-x. PMID: 15157425.

Bannister K, Dickenson AH. What do monoamines do in pain modulation? Curr Opin Support Palliat Care. 2016 Jun;10(2):143-8. doi: 10.1097/SPC.0000000000000207. PMID: 27043287; PMCID: PMC5604728.

Bao YN, Dai WL, Fan JF, Ma B, Li SS, Zhao WL, Yu BY, Liu JH. The dopamine D1-D2DR complex in the rat spinal cord promotes neuropathic pain by increasing neuronal excitability after chronic constriction injury. Exp Mol Med. 2021 Feb;53(2):235-249. doi: 10.1038/s12276-021-00563-5. Epub 2021 Feb 9. PMID: 33558591; PMCID: PMC8080784.

Barak LS, Ferguson SS, Zhang J, Caron MG. A beta-arrestin/green fluorescent protein biosensor for detecting G protein-coupled receptor activation. J Biol Chem. 1997 Oct 31;272(44):27497-500. doi: 10.1074/jbc.272.44.27497. PMID: 9346876.

Barak LS, Tiberi M, Freedman NJ, Kwatra MM, Lefkowitz RJ, Caron MG. A highly conserved tyrosine residue in G protein-coupled receptors is required for agonist-mediated beta 2-adrenergic receptor sequestration. J Biol Chem. 1994 Jan 28;269(4):2790-5. PMID: 7507928.

Barger G, Dale HH. Chemical structure and sympathomimetic action of amines. J Physiol. 1910 Oct 11;41(1-2):19-59. doi: 10.1113/jphysiol.1910.sp001392. PMID: 16993040; PMCID: PMC1513032.

Barger G, Ewins AJ. Some phenolic derivAtives of β-phenylethyIamine. J. Chem. Soc. (London). 1910, 97: 2253-2261.

Barili P, Bronzetti E, Ricci A, Zaccheo D, Amenta F. Microanatomical localization of dopamine receptor protein immunoreactivity in the rat cerebellar cortex. Brain Res. 2000 Jan 31;854(1-2):130-8. doi: 10.1016/s0006-8993(99)02306-9. PMID: 10784114.

Barone P, Poewe W, Albrecht S, Debieuvre C, Massey D, Rascol O, Tolosa E, Weintraub D. Pramipexole for the treatment of depressive symptoms in patients with Parkinson's disease: a randomised, double-blind, placebo-controlled trial. Lancet Neurol. 2010 Jun;9(6):573-80. doi: 10.1016/S1474-4422(10)70106-X. Epub 2010 May 7. PMID: 20452823.

Barral J, Galarraga E, Tapia D, Flores-Barrera E, Reyes A, Bargas J. Dopaminergic modulation of spiny neurons in the turtle striatum. Cell Mol Neurobiol. 2010 Jul;30(5):743-50. doi: 10.1007/s10571-010-9499-7. Epub 2010 Feb 6. PMID: 20140492.

Barria A, Malinow R. Subunit-specific NMDA receptor trafficking to synapses. Neuron. 2002 Jul 18;35(2):345-53. doi: 10.1016/s0896-6273(02)00776-6. PMID: 12160751.

Basu S, Dasgupta PS. Dopamine, a neurotransmitter, influences the immune system. J Neuroimmunol. 2000 Jan 24;102(2):113-24. doi: 10.1016/s0165-5728(99)00176-9. PMID: 10636479.

Basu S, Nagy JA, Pal S, Vasile E, Eckelhoefer IA, Bliss VS, Manseau EJ, Dasgupta PS, Dvorak HF, Mukhopadhyay D. The neurotransmitter dopamine inhibits angiogenesis induced by vascular permeability factor/vascular endothelial growth factor. Nat Med. 2001 May;7(5):569-74. doi: 10.1038/87895. PMID: 11329058.

Bateup HS, Santini E, Shen W, Birnbaum S, Valjent E, Surmeier DJ, Fisone G, Nestler EJ, Greengard P. Distinct subclasses of medium spiny neurons differentially regulate striatal motor behaviors. Proc Natl Acad Sci U S A. 2010 Aug 17;107(33):14845-50. doi: 10.1073/pnas.1009874107. Epub 2010 Aug 3. PMID: 20682746; PMCID: PMC2930415.

Bateup HS, Svenningsson P, Kuroiwa M, Gong S, Nishi A, Heintz N, Greengard P. Cell type-specific regulation of DARPP-32 phosphorylation by psychostimulant and antipsychotic drugs. Nat Neurosci. 2008 Aug;11(8):932-9. doi: 10.1038/nn.2153. Epub 2008 Jul 11. PMID: 18622401; PMCID: PMC2737705.

Battista A, Fuxe K, Goldstein M, Ogawa M. Mapping of central monoamine neurons in the monkey. Experientia. 1972 Jun 15;28(6):688-90. doi: 10.1007/BF01944981. PMID: 4625609.

Baufreton J, Garret M, Rivera A, de la Calle A, Gonon F, Dufy B, Bioulac B, Taupignon A. D5 (not D1) dopamine receptors potentiate burst-firing in neurons of the subthalamic nucleus by modulating an L-type calcium conductance. J Neurosci. 2003 Feb 1;23(3):816-25. doi: 10.1523/JNEUROSCI.23-03-00816.2003. PMID: 12574410; PMCID: PMC6741933.

Bayés A, van de Lagemaat LN, Collins MO, Croning MD, Whittle IR, Choudhary JS, Grant SG. Characterization of the proteome, diseases and evolution of the human postsynaptic density. Nat Neurosci. 2011 Jan;14(1):19-21. doi: 10.1038/nn.2719. Epub 2010 Dec 19. PMID: 21170055; PMCID: PMC3040565.

Beaulieu JM, Espinoza S, Gainetdinov RR. Dopamine receptors - IUPHAR Review 13. Br J Pharmacol. 2015 Jan;172(1):1-23. doi: 10.1111/bph.12906. PMID: 25671228; PMCID: PMC4280963.

Beaulieu JM, Gainetdinov RR. The physiology, signaling, and pharmacology of dopamine receptors. Pharmacol Rev. 2011 Mar;63(1):182-217. doi: 10.1124/pr.110.002642. Epub 2011 Feb 8. PMID: 21303898.

Beaulieu JM, Marion S, Rodriguiz RM, Medvedev IO, Sotnikova TD, Ghisi V, Wetsel WC, Lefkowitz RJ, Gainetdinov RR, Caron MG. A beta-arrestin 2 signaling complex mediates lithium action on behavior. Cell. 2008 Jan 11;132(1):125-36. doi: 10.1016/j.cell.2007.11.041. PMID: 18191226.

Beaulieu JM, Sotnikova TD, Marion S, Lefkowitz RJ, Gainetdinov RR, Caron MG. An Akt/beta-arrestin 2/PP2A signaling complex mediates dopaminergic neurotransmission and behavior. Cell. 2005 Jul 29;122(2):261-73. doi: 10.1016/j.cell.2005.05.012. PMID: 16051150.

Beaulieu JM, Sotnikova TD, Yao WD, Kockeritz L, Woodgett JR, Gainetdinov RR, Caron MG. Lithium antagonizes dopamine-dependent behaviors mediated by an AKT/glycogen synthase kinase 3 signaling cascade. Proc Natl Acad Sci U S A. 2004 Apr 6;101(14):5099-104. doi: 10.1073/pnas.0307921101. Epub 2004 Mar 24. PMID: 15044694; PMCID: PMC387380.

Bécamel C, Alonso G, Galéotti N, Demey E, Jouin P, Ullmer C, Dumuis A, Bockaert J, Marin P. Synaptic multiprotein complexes associated with 5-HT(2C) receptors: a proteomic approach. EMBO J. 2002 May 15;21(10):2332-42. doi: 10.1093/emboj/21.10.2332. PMID: 12006486; PMCID: PMC126011.

Bécamel C, Gavarini S, Chanrion B, Alonso G, Galéotti N, Dumuis A, Bockaert J, Marin P. The serotonin 5-HT2A and 5-HT2C receptors interact with specific sets of PDZ proteins. J Biol Chem. 2004 May 7;279(19):20257-66. doi: 10.1074/jbc.M312106200. Epub 2004 Feb 26. PMID: 14988405.

Becker A, Grecksch G, Kraus J, Peters B, Schroeder H, Schulz S, Höllt V. Loss of locomotor sensitisation in response to morphine in D1 receptor deficient mice. Naunyn Schmiedebergs Arch Pharmacol. 2001 May;363(5):562-8. doi: 10.1007/s002100100404. PMID: 11383718.

Béïque JC, Andrade R. PSD-95 regulates synaptic transmission and plasticity in rat cerebral cortex. J Physiol. 2003 Feb 1;546(Pt 3):859-67. doi: 10.1113/jphysiol.2002.031369. PMID: 12563010; PMCID: PMC2342599.

Béïque JC, Lin DT, Kang MG, Aizawa H, Takamiya K, Huganir RL. Synapse-specific regulation of AMPA receptor function by PSD-95. Proc Natl Acad Sci U S A. 2006 Dec 19;103(51):19535-40. doi: 10.1073/pnas.0608492103. Epub 2006 Dec 5. PMID: 17148601; PMCID: PMC1748260.

Beitz JM. Parkinson's disease: a review. Front Biosci (Schol Ed). 2014 Jan 1;6(1):65-74. doi: 10.2741/s415. PMID: 24389262.

Beckstead MJ, Ford CP, Phillips PE, Williams JT. Presynaptic regulation of dendrodendritic dopamine transmission. Eur J Neurosci. 2007 Sep;26(6):1479-88. doi: 10.1111/j.1460-9568.2007.05775.x. Epub 2007 Sep 6. PMID: 17822435; PMCID: PMC3633601.

Bello EP, Mateo Y, Gelman DM, Noaín D, Shin JH, Low MJ, Alvarez VA, Lovinger DM, Rubinstein M. Cocaine supersensitivity and enhanced motivation for reward in mice lacking dopamine D2 autoreceptors. Nat Neurosci. 2011 Jul 10;14(8):1033-8. doi: 10.1038/nn.2862. PMID: 21743470; PMCID: PMC3175737.

Bender J, Engeholm M, Ederer MS, Breu J, Møller TC, Michalakis S, Rasko T, Wanker EE, Biel M, Martinez KL, Wurst W, Deussing JM. Corticotropin-Releasing Hormone Receptor Type 1 (CRHR1) Clustering with MAGUKs Is Mediated via Its C-Terminal PDZ Binding Motif. PLoS One. 2015 Sep 9;10(9):e0136768. doi: 10.1371/journal.pone.0136768. PMID: 26352593; PMCID: PMC4564177.

Bender M, Drago J, Rivkees SA. D1 receptors mediate dopamine action in the fetal suprachiasmatic nuclei: studies of mice with targeted deletion of the D1 dopamine receptor gene. Brain Res Mol Brain Res. 1997 Oct 3;49(1-2):271-7. doi: 10.1016/s0169-328x(97)00161-7. PMID: 9387887.

Ben-Jonathan N, Hnasko R. Dopamine as a prolactin (PRL) inhibitor. Endocr Rev. 2001 Dec;22(6):724-63. doi: 10.1210/edrv.22.6.0451. PMID: 11739329.

Benoit-Marand M, Jaber M, Gonon F. Release and elimination of dopamine in vivo in mice lacking the dopamine transporter: functional consequences. Eur J Neurosci. 2000 Aug;12(8):2985-92. doi: 10.1046/j.1460-9568.2000.00155.x. PMID: 10971639.

Benovic JL, DeBlasi A, Stone WC, Caron MG, Lefkowitz RJ. Beta-adrenergic receptor kinase: primary structure delineates a multigene family. Science. 1989 Oct 13;246(4927):235-40. doi: 10.1126/science.2552582. PMID: 2552582.

Benovic JL, Mayor F Jr, Somers RL, Caron MG, Lefkowitz RJ. Light-dependent phosphorylation of rhodopsin by beta-adrenergic receptor kinase. Nature. 1986 Jun 26-Jul 2;321(6073):869-72. doi: 10.1038/321869a0. PMID: 3014340. (a)

Benovic JL, Strasser RH, Caron MG, Lefkowitz RJ. Beta-adrenergic receptor kinase: identification of a novel protein kinase that phosphorylates the agonist-occupied form of the receptor. Proc Natl Acad Sci U S A. 1986 May;83(9):2797-801. doi: 10.1073/pnas.83.9.2797. PMID: 2871555; PMCID: PMC323393. (b)

Bergson C, Mrzljak L, Lidow MS, Goldman-Rakic PS, Levenson R. Characterization of subtype-specific antibodies to the human D5 dopamine receptor: studies in primate brain and transfected mammalian cells. Proc Natl Acad Sci U S A. 1995 Apr 11;92(8):3468-72. doi: 10.1073/pnas.92.8.3468. PMID: 7536933; PMCID: PMC42188. (a)

Bergson C, Mrzljak L, Smiley JF, Pappy M, Levenson R, Goldman-Rakic PS. Regional, cellular, and subcellular variations in the distribution of D1 and D5 dopamine receptors in primate brain. J Neurosci. 1995 Dec;15(12):7821-36. doi: 10.1523/JNEUROSCI.15-12-07821.1995. PMID: 8613722; PMCID: PMC6577925. (b)

Berlanga ML, Simpson TK, Alcantara AA. Dopamine D5 receptor localization on cholinergic neurons of the rat forebrain and diencephalon: a potential neuroanatomical substrate involved in mediating dopaminergic influences on acetylcholine release. J Comp Neurol. 2005 Nov 7;492(1):34-49. doi: 10.1002/cne.20684. PMID: 16175554.

Bermak JC, Li M, Bullock C, Weingarten P, Zhou QY. Interaction of gamma-COP with a transport motif in the D1 receptor C-terminus. Eur J Cell Biol. 2002 Feb;81(2):77-85. doi: 10.1078/0171-9335-00222. PMID: 11893085.

Bermak JC, Li M, Bullock C, Zhou QY. Regulation of transport of the dopamine D1 receptor by a new membrane-associated ER protein. Nat Cell Biol. 2001 May;3(5):492-8. doi: 10.1038/35074561. PMID: 11331877.

BERTLER A, ROSENGREN E. Occurrence and distribution of dopamine in brain and other tissues. Experientia. 1959 Jan 15;15(1):10-1. doi: 10.1007/BF02157069. PMID: 13619664.

Bertran-Gonzalez J, Bosch C, Maroteaux M, Matamales M, Hervé D, Valjent E, Girault JA. Opposing patterns of signaling activation in dopamine D1 and D2 receptor-expressing striatal neurons in response to cocaine and haloperidol. J Neurosci. 2008 May 28;28(22):5671-85. doi: 10.1523/JNEUROSCI.1039-08.2008. PMID: 18509028; PMCID: PMC6670792.

Bertran-Gonzalez J, Hervé D, Girault JA, Valjent E. What is the Degree of Segregation between Striatonigral and Striatopallidal Projections? Front Neuroanat. 2010 Oct 7;4:136. doi: 10.3389/fnana.2010.00136. PMID: 20953289; PMCID: PMC2955397.

Besser MJ, Ganor Y, Levite M. Dopamine by itself activates either D2, D3 or D1/D5 dopaminergic receptors in normal human T-cells and triggers the selective secretion of either IL-10, TNFalpha or both. J Neuroimmunol. 2005 Dec;169(1-2):161-71. doi: 10.1016/j.jneuroim.2005.07.013. Epub 2005 Sep 15. PMID: 16150496.

Besson MJ, Cheramy A, Feltz P, Glowinski J. Release of newly synthesized dopamine from dopamine-containing terminals in the striatum of the rat. Proc Natl Acad Sci U S A. 1969 Mar;62(3):741-8. doi: 10.1073/pnas.62.3.741. PMID: 4389748; PMCID: PMC223661.

Bézard E, Ferry S, Mach U, Stark H, Leriche L, Boraud T, Gross C, Sokoloff P. Attenuation of levodopa-induced dyskinesia by normalizing dopamine D3 receptor function. Nat Med. 2003 Jun;9(6):762-7. doi: 10.1038/nm875. Epub 2003 May 12. PMID: 12740572.

Bhattacharya M, Anborgh PH, Babwah AV, Dale LB, Dobransky T, Benovic JL, Feldman RD, Verdi JM, Rylett RJ, Ferguson SS. Beta-arrestins regulate a Ral-GDS Ral effector pathway that mediates cytoskeletal reorganization. Nat Cell Biol. 2002 Aug;4(8):547-55. doi: 10.1038/ncb821. PMID: 12105416.

Bibb JA, Snyder GL, Nishi A, Yan Z, Meijer L, Fienberg AA, Tsai LH, Kwon YT, Girault JA, Czernik AJ, Huganir RL, Hemmings HC Jr, Nairn AC, Greengard P. Phosphorylation of DARPP-32 by Cdk5 modulates dopamine signalling in neurons. Nature. 1999 Dec 9;402(6762):669-71. doi: 10.1038/45251. PMID: 10604473.

BIRKMAYER W, HORNYKIEWICZ O. [The L-3,4-dioxyphenylalanine (DOPA)-effect in Parkinson-akinesia]. Wien Klin Wochenschr. 1961 Nov 10;73:787-8. German. PMID: 13869404.

Björklund A, Dunnett SB. Dopamine neuron systems in the brain: an update. Trends Neurosci. 2007 May;30(5):194-202. doi: 10.1016/j.tins.2007.03.006. Epub 2007 Apr 3. PMID: 17408759. (b)

Björklund A, Dunnett SB. Fifty years of dopamine research. Trends Neurosci. 2007 May;30(5):185-7. doi: 10.1016/j.tins.2007.03.004. Epub 2007 Mar 29. PMID: 17397938. (a)

Björklund A, Lindvall O. Dopamine in dendrites of substantia nigra neurons: suggestions for a role in dendritic terminals. Brain Res. 1975 Jan 17;83(3):531-7. doi: 10.1016/0006-8993(75)90849-5. PMID: 1111820.

BLASCHKO H. Metabolism and storage of biogenic amines. Experientia. 1957 Jan 15;13(1):9-13. doi: 10.1007/BF02156938. PMID: 13404987.

Blesa J, Foffani G, Dehay B, Bezard E, Obeso JA. Motor and non-motor circuit disturbances in early Parkinson disease: which happens first? Nat Rev Neurosci. 2022 Feb;23(2):115-128. doi: 10.1038/s41583-021-00542-9. Epub 2021 Dec 14. PMID: 34907352.

Blom H, Rönnlund D, Scott L, Spicarova Z, Rantanen V, Widengren J, Aperia A, Brismar H. Nearest neighbor analysis of dopamine D1 receptors and Na(+)-K(+)-ATPases in dendritic spines dissected by STED microscopy. Microsc Res Tech. 2012 Feb;75(2):220-8. doi: 10.1002/jemt.21046. Epub 2011 Aug 1. PMID: 21809413.

Boehmler W, Obrecht-Pflumio S, Canfield V, Thisse C, Thisse B, Levenson R. Evolution and expression of D2 and D3 dopamine receptor genes in zebrafish. Dev Dyn. 2004 Jul;230(3):481-93. doi: 10.1002/dvdy.20075. PMID: 15188433.

Bohn LM, Gainetdinov RR, Lin FT, Lefkowitz RJ, Caron MG. Mu-opioid receptor desensitization by beta-arrestin-2 determines morphine tolerance but not dependence. Nature. 2000 Dec 7;408(6813):720-3. doi: 10.1038/35047086. PMID: 11130073.

Bohn LM, Lefkowitz RJ, Gainetdinov RR, Peppel K, Caron MG, Lin FT. Enhanced morphine analgesia in mice lacking beta-arrestin 2. Science. 1999 Dec 24;286(5449):2495-8. doi: 10.1126/science.286.5449.2495. PMID: 10617462.

Bokoch MP, Zou Y, Rasmussen SG, Liu CW, Nygaard R, Rosenbaum DM, Fung JJ, Choi HJ, Thian FS, Kobilka TS, Puglisi JD, Weis WI, Pardo L, Prosser RS, Mueller L, Kobilka BK. Ligand-specific regulation of the extracellular surface of a G-protein-coupled receptor. Nature. 2010 Jan 7;463(7277):108-12. doi: 10.1038/nature08650. PMID: 20054398; PMCID: PMC2805469.

Bonnavion P, Varin C, Fakhfouri G, Olondo PM, De Groote A, Cornil A, Lopez RL, Fernandez EP, Isingrini E, Rainer Q, Xu K, Tzavara E, Vigneault E, Dumas S, de Kerchove d'Exaerde A, Giros B. Unexpected contributions of striatal projection neurons coexpressing dopamine D1 and D2 receptors in balancing motor control. bioRxiv 2022.04.05.487163; doi: https://doi.org/10.1101/2022.04.05.487163

Bonnet SA, Akad DS, Samaddar T, Liu Y, Huang X, Dong Y, Schlüter OM. Synaptic state-dependent functional interplay between postsynaptic density-95 and synapse-associated protein 102. J Neurosci. 2013 Aug 14;33(33):13398-409. doi: 10.1523/JNEUROSCI.6255-11.2013. PMID: 23946397; PMCID: PMC3742927.

Bono F, Tomasoni Z, Mutti V, Sbrini G, Kumar R, Longhena F, Fiorentini C, Missale C. G Protein-Dependent Activation of the PKA-Erk1/2 Pathway by the Striatal Dopamine D1/D3 Receptor Heteromer Involves Beta-Arrestin and the Tyrosine Phosphatase Shp-2. Biomolecules. 2023 Mar 3;13(3):473. doi: 10.3390/biom13030473. PMID: 36979407; PMCID: PMC10046256.

Bono F, Tomasoni Z, Mutti V, Sbrini G, Kumar R, Longhena F, Fiorentini C, Missale C. G Protein-Dependent Activation of the PKA-Erk1/2 Pathway by the Striatal Dopamine D1/D3 Receptor Heteromer Involves Beta-Arrestin and the Tyrosine Phosphatase Shp-2. Biomolecules. 2023 Mar 3;13(3):473. doi: 10.3390/biom13030473. PMID: 36979407; PMCID: PMC10046256.

Borcherding DC, Hugo ER, Idelman G, De Silva A, Richtand NW, Loftus J, Ben-Jonathan N. Dopamine receptors in human adipocytes: expression and functions. PLoS One. 2011;6(9):e25537. doi: 10.1371/journal.pone.0025537. Epub 2011 Sep 26. PMID: 21966540; PMCID: PMC3180449.

Bossé R, Fumagalli F, Jaber M, Giros B, Gainetdinov RR, Wetsel WC, Missale C, Caron MG. Anterior pituitary hypoplasia and dwarfism in mice lacking the dopamine transporter. Neuron. 1997 Jul;19(1):127-38. doi: 10.1016/s0896-6273(00)80353-0. PMID: 9247269.

Bouthenet ML, Souil E, Martres MP, Sokoloff P, Giros B, Schwartz JC. Localization of dopamine D3 receptor mRNA in the rat brain using in situ hybridization histochemistry: comparison with dopamine D2 receptor mRNA. Brain Res. 1991 Nov 15;564(2):203-19. doi: 10.1016/0006-8993(91)91456-b. PMID: 1839781.

Bouvier M, Hausdorff WP, De Blasi A, O'Dowd BF, Kobilka BK, Caron MG, Lefkowitz RJ. Removal of phosphorylation sites from the beta 2-adrenergic receptor delays onset of agonist-promoted desensitization. Nature. 1988 May 26;333(6171):370-3. doi: 10.1038/333370a0. PMID: 2836733.

Bowery NG, Smart TG. GABA and glycine as neurotransmitters: a brief history. Br J Pharmacol. 2006 Jan;147 Suppl 1(Suppl 1):S109-19. doi: 10.1038/sj.bjp.0706443. PMID: 16402094; PMCID: PMC1760744.

Braak H, Del Tredici K, Rüb U, de Vos RA, Jansen Steur EN, Braak E. Staging of brain pathology related to sporadic Parkinson's disease. Neurobiol Aging. 2003 Mar-Apr;24(2):197-211. doi: 10.1016/s0197-4580(02)00065-9. PMID: 12498954.

Branch SY, Goertz RB, Sharpe AL, Pierce J, Roy S, Ko D, Paladini CA, Beckstead MJ. Food restriction increases glutamate receptor-mediated burst firing of dopamine neurons. J Neurosci. 2013 Aug 21;33(34):13861-72. doi: 10.1523/JNEUROSCI.5099-12.2013. PMID: 23966705; PMCID: PMC3755722.

Brenman JE, Chao DS, Gee SH, McGee AW, Craven SE, Santillano DR, Wu Z, Huang F, Xia H, Peters MF, Froehner SC, Bredt DS. Interaction of nitric oxide synthase with the postsynaptic density protein PSD-95 and alpha1-syntrophin mediated by PDZ domains. Cell. 1996 Mar 8;84(5):757-67. doi: 10.1016/s0092-8674(00)81053-3. PMID: 8625413.

Brewer KL, Baran CA, Whitfield BR, Jensen AM, Clemens S. Dopamine D3 receptor dysfunction prevents anti-nociceptive effects of morphine in the spinal cord. Front Neural Circuits. 2014 Jun 11;8:62. doi: 10.3389/fncir.2014.00062. PMID: 24966815; PMCID: PMC4052813.

Brisch R, Saniotis A, Wolf R, Bielau H, Bernstein HG, Steiner J, Bogerts B, Braun K, Jankowski Z, Kumaratilake J, Henneberg M, Gos T. The role of dopamine in schizophrenia from a neurobiological and evolutionary perspective: old fashioned, but still in vogue. Front Psychiatry. 2014 May 19;5:47. doi: 10.3389/fpsyt.2014.00047. PMID: 24904434; PMCID: PMC4032934.

Broadhead MJ, Horrocks MH, Zhu F, Muresan L, Benavides-Piccione R, DeFelipe J, Fricker D, Kopanitsa MV, Duncan RR, Klenerman D, Komiyama NH, Lee SF, Grant SG. PSD95 nanoclusters are postsynaptic building blocks in hippocampus circuits. Sci Rep. 2016 Apr 25;6:24626. doi: 10.1038/srep24626. PMID: 27109929; PMCID: PMC4842999.

BROCK LG, COOMBS JS, ECCLES JC. The recording of potentials from motoneurones with an intracellular electrode. J Physiol. 1952 Aug;117(4):431-60. doi: 10.1113/jphysiol.1952.sp004759. PMID: 12991232; PMCID: PMC1392415.

Brown JH, Makman MH. Stimulation by dopamine of adenylate cyclase in retinal homogenates and of adenosine-3':5'-cyclic monophosphate formation in intact retina. Proc Natl Acad Sci U S A. 1972 Mar;69(3):539-43. doi: 10.1073/pnas.69.3.539. PMID: 4401122; PMCID: PMC426502.

Brown JM, Hanson GR, Fleckenstein AE. Cocaine-induced increases in vesicular dopamine uptake: role of dopamine receptors. J Pharmacol Exp Ther. 2001 Sep;298(3):1150-3. PMID: 11504813.

Brown JM, Riddle EL, Sandoval V, Weston RK, Hanson JE, Crosby MJ, Ugarte YV, Gibb JW, Hanson GR, Fleckenstein AE. A single methamphetamine administration rapidly decreases vesicular dopamine uptake. J Pharmacol Exp Ther. 2002 Aug;302(2):497-501. doi: 10.1124/jpet.302.2.497. PMID: 12130707.

Bulovaite E, Qiu Z, Kratschke M, Zgraj A, Fricker DG, Tuck EJ, Gokhale R, Koniaris B, Jami SA, Merino-Serrais P, Husi E, Mendive-Tapia L, Vendrell M, O'Dell TJ, DeFelipe J, Komiyama NH, Holtmaat A, Fransén E, Grant SGN. A brain atlas of synapse protein lifetime across the mouse lifespan. Neuron. 2022 Dec 21;110(24):4057-4073.e8. doi: 10.1016/j.neuron.2022.09.009. Epub 2022 Oct 5. PMID: 36202095; PMCID: PMC9789179.

Bunney BS, Walters JR, Roth RH, Aghajanian GK. Dopaminergic neurons: effect of antipsychotic drugs and amphetamine on single cell activity. J Pharmacol Exp Ther. 1973 Jun;185(3):560-71. PMID: 4576427.

Bunzow JR, Van Tol HH, Grandy DK, Albert P, Salon J, Christie M, Machida CA, Neve KA, Civelli O. Cloning and expression of a rat D2 dopamine receptor cDNA. Nature. 1988 Dec 22-29;336(6201):783-7. doi: 10.1038/336783a0. PMID: 2974511.

Butcher SP, Fairbrother IS, Kelly JS, Arbuthnott GW. Amphetamine-induced dopamine release in the rat striatum: an in vivo microdialysis study. J Neurochem. 1988 Feb;50(2):346-55. doi: 10.1111/j.1471-4159.1988.tb02919.x. PMID: 2447237.

Cabezas GA, Israili ZH, Velasco M. The actions of dopamine on the airways. Am J Ther. 2003 Nov-Dec;10(6):477-86. doi: 10.1097/00045391-200311000-00019. PMID: 14624291.

Cabezas GA, Lezama Y, Vidal A, Velasco M. Inhaled dopamine induces bronchodilatation in patients with bronchial asthma. Int J Clin Pharmacol Ther. 1999 Oct;37(10):510-3. PMID: 10543319.

Caffino L, Messa G, Fumagalli F. A single cocaine administration alters dendritic spine morphology and impairs glutamate receptor synaptic retention in the medial prefrontal cortex of adolescent rats. Neuropharmacology. 2018 Sep 15;140:209-216. doi: 10.1016/j.neuropharm.2018.08.006. Epub 2018 Aug 7. PMID: 30092246.

Cahill TJ 3rd, Thomsen AR, Tarrasch JT, Plouffe B, Nguyen AH, Yang F, Huang LY, Kahsai AW, Bassoni DL, Gavino BJ, Lamerdin JE, Triest S, Shukla AK, Berger B, Little J 4th, Antar A, Blanc A, Qu CX, Chen X, Kawakami K, Inoue A, Aoki J, Steyaert J, Sun JP, Bouvier M, Skiniotis G, Lefkowitz RJ. Distinct conformations of GPCR-β-arrestin complexes mediate desensitization, signaling, and endocytosis. Proc Natl Acad Sci U S A. 2017 Mar 7;114(10):2562-2567. doi: 10.1073/pnas.1701529114. Epub 2017 Feb 21. PMID: 28223524; PMCID: PMC5347553.

Cai C, Coleman SK, Niemi K, Keinänen K. Selective binding of synapse-associated protein 97 to GluR-A alpha-amino-5-hydroxy-3-methyl-4-isoxazole propionate receptor subunit is determined by a novel sequence motif. J Biol Chem. 2002 Aug 30;277(35):31484-90. doi: 10.1074/jbc.M204354200. Epub 2002 Jun 17. PMID: 12070168.

Cai C, Li H, Kangasniemi A, Pihlajamaa T, Von Ossowski L, Kerkelä K, Schulz S, Rivera C, Keinänen K. Somatostatin receptor subtype 1 is a PDZ ligand for synapse-associated protein 97 and a potential regulator of growth cone dynamics. Neuroscience. 2008 Dec 10;157(4):833-43. doi: 10.1016/j.neuroscience.2008.09.048. Epub 2008 Oct 4. PMID: 18951956.

Cai C, Li H, Rivera C, Keinänen K. Interaction between SAP97 and PSD-95, two Maguk proteins involved in synaptic trafficking of AMPA receptors. J Biol Chem. 2006 Feb 17;281(7):4267-73. doi: 10.1074/jbc.M505886200. Epub 2005 Dec 6. PMID: 16332687.

Cai Y, Ford CP. Dopamine Cells Differentially Regulate Striatal Cholinergic Transmission across Regions through Corelease of Dopamine and Glutamate. Cell Rep. 2018 Dec 11;25(11):3148-3157.e3. doi: 10.1016/j.celrep.2018.11.053. PMID: 30540946; PMCID: PMC6658127.

Calebiro D, Koszegi Z, Lanoiselée Y, Miljus T, O'Brien S. G protein-coupled receptor-G protein interactions: a single-molecule perspective. Physiol Rev. 2021 Jul 1;101(3):857-906. doi: 10.1152/physrev.00021.2020. Epub 2020 Dec 17. PMID: 33331229.

Cao Y, Xie KQ, Zhu XZ. The enhancement of dopamine D1 receptor desensitization by adenosine A1 receptor activation. Eur J Pharmacol. 2007 May 7;562(1-2):34-8. doi: 10.1016/j.ejphar.2007.01.090. Epub 2007 Feb 16. PMID: 17368618.

Carboni E, Spielewoy C, Vacca C, Nosten-Bertrand M, Giros B, Di Chiara G. Cocaine and amphetamine increase extracellular dopamine in the nucleus accumbens of mice lacking the dopamine transporter gene. J Neurosci. 2001 May 1;21(9):RC141: 1-4. doi: 10.1523/JNEUROSCI.21-09-j0001.2001. PMID: 11312315; PMCID: PMC6762548.

Carew TJ, Pinsker HM, Kandel ER. Long-term habituation of a defensive withdrawal reflex in aplysia. Science. 1972 Jan 28;175(4020):451-4. doi: 10.1126/science.175.4020.451. PMID: 17731371.

Carli M, Evenden JL, Robbins TW. Depletion of unilateral striatal dopamine impairs initiation of contralateral actions and not sensory attention. Nature. 1985 Feb 21-27;313(6004):679-82. doi: 10.1038/313679a0. PMID: 3974701.

Carlisle HJ, Fink AE, Grant SG, O'Dell TJ. Opposing effects of PSD-93 and PSD-95 on long-term potentiation and spike timing-dependent plasticity. J Physiol. 2008 Dec 15;586(24):5885-900. doi: 10.1113/jphysiol.2008.163469. Epub 2008 Oct 20. PMID: 18936077; PMCID: PMC2655416.

CARLSSON A, FALCK B, HILLARP NA. Cellular localization of brain monoamines. Acta Physiol Scand Suppl. 1962;56(196):1-28. PMID: 14018711.

CARLSSON A, LINDQVIST M, MAGNUSSON T, WALDECK B. On the presence of 3-hydroxytyramine in brain. Science. 1958 Feb 28;127(3296):471. doi: 10.1126/science.127.3296.471. PMID: 13529006.

CARLSSON A, LINDQVIST M, MAGNUSSON T. 3,4-Dihydroxyphenylalanine and 5-hydroxytryptophan as reserpine antagonists. Nature. 1957 Nov 30;180(4596):1200. doi: 10.1038/1801200a0. PMID: 13483658.

CARLSSON A, LINDQVIST M. EFFECT OF CHLORPROMAZINE OR HALOPERIDOL ON FORMATION OF 3METHOXYTYRAMINE AND NORMETANEPHRINE IN MOUSE BRAIN. Acta Pharmacol Toxicol (Copenh). 1963;20:140-4. doi: 10.1111/j.1600-0773.1963.tb01730.x. PMID: 14060771.

CARLSSON A. The occurrence, distribution and physiological role of catecholamines in the nervous system. Pharmacol Rev. 1959 Jun;11(2, Part 2):490-3. PMID: 13667431.

Carlsson A. Treatment of Parkinson's with L-DOPA. The early discovery phase, and a comment on current problems. J Neural Transm (Vienna). 2002 May;109(5-6):777-87. doi: 10.1007/s007020200064. PMID: 12111467.

Caron MG, Beaulieu M, Raymond V, Gagné B, Drouin J, Lefkowitz RJ, Labrie F. Dopaminergic receptors in the anterior pituitary gland. Correlation of [3H]dihydroergocryptine binding with the dopaminergic control of prolactin release. J Biol Chem. 1978 Apr 10;253(7):2244-53. PMID: 416027.

Carpenter WT Jr, Buchanan RW. Schizophrenia. N Engl J Med. 1994 Mar 10;330(10):681-90. doi: 10.1056/NEJM199403103301006. PMID: 8107719.

Carroll RC, Zukin RS. NMDA-receptor trafficking and targeting: implications for synaptic transmission and plasticity. Trends Neurosci. 2002 Nov;25(11):571-7. doi: 10.1016/s0166-2236(02)02272-5. PMID: 12392932.

Cass WA, Gerhardt GA. Direct in vivo evidence that D2 dopamine receptors can modulate dopamine uptake. Neurosci Lett. 1994 Aug 1;176(2):259-63. doi: 10.1016/0304-3940(94)90096-5. PMID: 7830960.

Cassidy CM, Zucca FA, Girgis RR, Baker SC, Weinstein JJ, Sharp ME, Bellei C, Valmadre A, Vanegas N, Kegeles LS, Brucato G, Kang UJ, Sulzer D, Zecca L, Abi-Dargham A, Horga G. Neuromelanin-sensitive MRI as a noninvasive proxy measure of dopamine function in the human brain. Proc Natl Acad Sci U S A. 2019 Mar 12;116(11):5108-5117. doi: 10.1073/pnas.1807983116. Epub 2019 Feb 22. PMID: 30796187; PMCID: PMC6421437.

Cave JW, Baker H. Dopamine systems in the forebrain. Adv Exp Med Biol. 2009;651:15-35. doi: 10.1007/978-1-4419-0322-8_2. PMID: 19731547; PMCID: PMC2779115.

Ceccarini J, Liu H, Van Laere K, Morris ED, Sander CY. Methods for Quantifying Neurotransmitter Dynamics in the Living Brain With PET Imaging. Front Physiol. 2020 Jul 21;11:792. doi: 10.3389/fphys.2020.00792. PMID: 32792972; PMCID: PMC7385290.

Cenci MA. Dopamine dysregulation of movement control in L-DOPA-induced dyskinesia. Trends Neurosci. 2007 May;30(5):236-43. doi: 10.1016/j.tins.2007.03.005. Epub 2007 Apr 2. PMID: 17400300.

Centonze D, Grande C, Saulle E, Martin AB, Gubellini P, Pavón N, Pisani A, Bernardi G, Moratalla R, Calabresi P. Distinct roles of D1 and D5 dopamine receptors in motor activity and striatal synaptic plasticity. J Neurosci. 2003 Sep 17;23(24):8506-12. doi: 10.1523/JNEUROSCI.23-24-08506.2003. PMID: 13679419; PMCID: PMC6740372.

Centonze D, Usiello A, Gubellini P, Pisani A, Borrelli E, Bernardi G, Calabresi P. Dopamine D2 receptor-mediated inhibition of dopaminergic neurons in mice lacking D2L receptors. Neuropsychopharmacology. 2002 Nov;27(5):723-6. doi: 10.1016/S0893-133X(02)00367-6. PMID: 12431847.

Cepeda C, Levine MS. Where do you think you are going? The NMDA-D1 receptor trap. Sci STKE. 2006 May 2;2006(333):pe20. doi: 10.1126/stke.3332006pe20. PMID: 16670371.

Chaar ZY, Jackson A, Tiberi M. The cytoplasmic tail of the D1A receptor subtype: identification of specific domains controlling dopamine cellular responsiveness. J Neurochem. 2001 Dec;79(5):1047-58. doi: 10.1046/j.1471-4159.2001.00648.x. Erratum in: J Neurochem 2002 Jul;82(1):207. PMID: 11739618.

Channer B, Matt SM, Nickoloff-Bybel EA, Pappa V, Agarwal Y, Wickman J, Gaskill PJ. Dopamine, Immunity, and Disease. Pharmacol Rev. 2023 Jan;75(1):62-158. doi: 10.1124/pharmrev.122.000618. Epub 2022 Dec 8. PMID: 36757901; PMCID: PMC9832385.

Charpentier S, Jarvie KR, Severynse DM, Caron MG, Tiberi M. Silencing of the constitutive activity of the dopamine D1B receptor. Reciprocal mutations between D1 receptor subtypes delineate residues underlying activation properties. J Biol Chem. 1996 Nov 8;271(45):28071-6. doi: 10.1074/jbc.271.45.28071. PMID: 8910419.

Chausmer AL, Elmer GI, Rubinstein M, Low MJ, Grandy DK, Katz JL. Cocaine-induced locomotor activity and cocaine discrimination in dopamine D2 receptor mutant mice. Psychopharmacology (Berl). 2002 Aug;163(1):54-61. doi: 10.1007/s00213-002-1142-y. Epub 2002 Jul 17. PMID: 12185400.

Chen BS, Gray JA, Sanz-Clemente A, Wei Z, Thomas EV, Nicoll RA, Roche KW. SAP102 mediates synaptic clearance of NMDA receptors. Cell Rep. 2012 Nov 29;2(5):1120-8. doi: 10.1016/j.celrep.2012.09.024. Epub 2012 Oct 25. PMID: 23103165; PMCID: PMC3513525.

Chen BS, Thomas EV, Sanz-Clemente A, Roche KW. NMDA receptor-dependent regulation of dendritic spine morphology by SAP102 splice variants. J Neurosci. 2011 Jan 5;31(1):89-96. doi: 10.1523/JNEUROSCI.1034-10.2011. PMID: 21209193; PMCID: PMC3030119.

Chen HJ, Rojas-Soto M, Oguni A, Kennedy MB. A synaptic Ras-GTPase activating protein (p135 SynGAP) inhibited by CaM kinase II. Neuron. 1998 May;20(5):895-904. doi: 10.1016/s0896-6273(00)80471-7. PMID: 9620694.

Chen X, Fukata Y, Fukata M, Nicoll RA. MAGUKs are essential, but redundant, in long-term potentiation. Proc Natl Acad Sci U S A. 2021 Jul 13;118(28):e2107585118. doi: 10.1073/pnas.2107585118. PMID: 34244435; PMCID: PMC8285982.

Chen X, Levy JM, Hou A, Winters C, Azzam R, Sousa AA, Leapman RD, Nicoll RA, Reese TS. PSD-95 family MAGUKs are essential for anchoring AMPA and NMDA receptor complexes at the postsynaptic density. Proc Natl Acad Sci U S A. 2015 Dec 15;112(50):E6983-92. doi: 10.1073/pnas.1517045112. Epub 2015 Nov 24. PMID: 26604311; PMCID: PMC4687590.

Chen X, Winters C, Azzam R, Li X, Galbraith JA, Leapman RD, Reese TS. Organization of the core structure of the postsynaptic density. Proc Natl Acad Sci U S A. 2008 Mar 18;105(11):4453-8. doi: 10.1073/pnas.0800897105. Epub 2008 Mar 7. Erratum in: Proc Natl Acad Sci U S A. 2008 Jun;105(22):7893. PMID: 18326622; PMCID: PMC2393784.

Cheramy A, Leviel V, Glowinski J. Dendritic release of dopamine in the substantia nigra. Nature. 1981 Feb 12;289(5798):537-42. doi: 10.1038/289537a0. PMID: 6258083.

Chéramy A, L'hirondel M, Godeheu G, Artaud F, Glowinski J. Direct and indirect presynaptic control of dopamine release by excitatory amino acids. Amino Acids. 1998;14(1-3):63-8. doi: 10.1007/BF01345244. PMID: 9871443.

Cherezov V, Rosenbaum DM, Hanson MA, Rasmussen SG, Thian FS, Kobilka TS, Choi HJ, Kuhn P, Weis WI, Kobilka BK, Stevens RC. High-resolution crystal structure of an engineered human beta2-adrenergic G protein-coupled receptor. Science. 2007 Nov 23;318(5854):1258-65. doi: 10.1126/science.1150577. Epub 2007 Oct 25. PMID: 17962520; PMCID: PMC2583103.

Cherubini E, Conti F. Generating diversity at GABAergic synapses. Trends Neurosci. 2001 Mar;24(3):155-62. doi: 10.1016/s0166-2236(00)01724-0. PMID: 11182455.

Chetkovich DM, Bunn RC, Kuo SH, Kawasaki Y, Kohwi M, Bredt DS. Postsynaptic targeting of alternative postsynaptic density-95 isoforms by distinct mechanisms. J Neurosci. 2002 Aug 1;22(15):6415-25. doi: 10.1523/JNEUROSCI.22-15-06415.2002. PMID: 12151521; PMCID: PMC6758133.

Chetrit J, Taupignon A, Froux L, Morin S, Bouali-Benazzouz R, Naudet F, Kadiri N, Gross CE, Bioulac B, Benazzouz A. Inhibiting subthalamic D5 receptor constitutive activity alleviates abnormal electrical activity and reverses motor impairment in a rat model of Parkinson's disease. J Neurosci. 2013 Sep 11;33(37):14840-9. doi: 10.1523/JNEUROSCI.0453-13.2013. PMID: 24027284; PMCID: PMC6705171.

Chien EY, Liu W, Zhao Q, Katritch V, Han GW, Hanson MA, Shi L, Newman AH, Javitch JA, Cherezov V, Stevens RC. Structure of the human dopamine D3 receptor in complex with a D2/D3 selective antagonist. Science. 2010 Nov 19;330(6007):1091-5. doi: 10.1126/science.1197410. PMID: 21097933; PMCID: PMC3058422.

Cho KO, Hunt CA, Kennedy MB. The rat brain postsynaptic density fraction contains a homolog of the Drosophila discs-large tumor suppressor protein. Neuron. 1992 Nov;9(5):929-42. doi: 10.1016/0896-6273(92)90245-9. PMID: 1419001.

Christenn M, Kindler S, Schulz S, Buck F, Richter D, Kreienkamp HJ. Interaction of brain somatostatin receptors with the PDZ domains of PSD-95. FEBS Lett. 2007 Nov 13;581(27):5173-7. doi: 10.1016/j.febslet.2007.10.003. Epub 2007 Oct 12. PMID: 17950729.

Christenson JG, Dairman W, Udenfriend S. On the identity of DOPA decarboxylase and 5-hydroxytryptophan decarboxylase (immunological titration-aromatic L-amino acid decarboxylase-serotonin-dopamine-norepinephrine). Proc Natl Acad Sci U S A. 1972 Feb;69(2):343-7. doi: 10.1073/pnas.69.2.343. PMID: 4536745; PMCID: PMC426454.

Chu J, Wilczynski W, Wilcox RE. Pharmacological characterization of the D1- and D2-like dopamine receptors from the brain of the leopard frog, Rana pipiens. Brain Behav Evol. 2001 Jun;57(6):328-42. doi: 10.1159/000047251. PMID: 11713387.

Chuhma N, Zhang H, Masson J, Zhuang X, Sulzer D, Hen R, Rayport S. Dopamine neurons mediate a fast excitatory signal via their glutamatergic synapses. J Neurosci. 2004 Jan 28;24(4):972-81. doi: 10.1523/JNEUROSCI.4317-03.2004. PMID: 14749442; PMCID: PMC6729804.

Chung HJ, Huang YH, Lau LF, Huganir RL. Regulation of the NMDA receptor complex and trafficking by activity-dependent phosphorylation of the NR2B subunit PDZ ligand. J Neurosci. 2004 Nov 10;24(45):10248-59. doi: 10.1523/JNEUROSCI.0546-04.2004. PMID: 15537897; PMCID: PMC6730169.

Ciarka A, Vincent JL, van de Borne P. The effects of dopamine on the respiratory system: friend or foe? Pulm Pharmacol Ther. 2007;20(6):607-15. doi: 10.1016/j.pupt.2006.10.011. Epub 2006 Oct 27. PMID: 17150392.

Ciliax BJ, Nash N, Heilman C, Sunahara R, Hartney A, Tiberi M, Rye DB, Caron MG, Niznik HB, Levey AI. Dopamine D(5) receptor immunolocalization in rat and monkey brain. Synapse. 2000 Aug;37(2):125-45. doi: 10.1002/1098-2396(200008)37:2<125::AID-SYN7>3.0.CO;2-7. PMID: 10881034.

Civelli O, Bunzow JR, Grandy DK. Molecular diversity of the dopamine receptors. Annu Rev Pharmacol Toxicol. 1993;33:281-307. doi: 10.1146/annurev.pa.33.040193.001433. PMID: 8494342.

Cizeron M, Qiu Z, Koniaris B, Gokhale R, Komiyama NH, Fransén E, Grant SGN. A brainwide atlas of synapses across the mouse life span. Science. 2020 Jul 17;369(6501):270-275. doi: 10.1126/science.aba3163. Epub 2020 Jun 11. PMID: 32527927; PMCID: PMC7115813.

Clapham DE, Neer EJ. G protein beta gamma subunits. Annu Rev Pharmacol Toxicol. 1997;37:167-203. doi: 10.1146/annurev.pharmtox.37.1.167. PMID: 9131251.

Claustre J, Serusclat P, Peyrin L. Glucuronide and sulfate catecholamine conjugates in rat and human plasma. J Neural Transm. 1983;56(4):265-78. doi: 10.1007/BF01243495. PMID: 6688268.

Clemens S, Hochman S. Conversion of the modulatory actions of dopamine on spinal reflexes from depression to facilitation in D3 receptor knock-out mice. J Neurosci. 2004 Dec 15;24(50):11337-45. doi: 10.1523/JNEUROSCI.3698-04.2004. PMID: 15601940; PMCID: PMC2731231.

Clemens S. D3 Receptors and Restless Legs Syndrome. Curr Top Behav Neurosci. 2023;60:229-249. doi: 10.1007/7854_2022_351. PMID: 35435646.

Clement-Cormier YC, Kebabian JW, Petzold GL, Greengard P. Dopamine-sensitive adenylate cyclase in mammalian brain: a possible site of action of antipsychotic drugs. Proc Natl Acad Sci U S A. 1974 Apr;71(4):1113-7. doi: 10.1073/pnas.71.4.1113. PMID: 4151517; PMCID: PMC388173.

Clement-Cormier YC, Parrish RG, Petzold GL, Kerabian JW, Greengard P. Characterization of a dopamine-sensitive adenylate cyclase in the rat caudate nucleus. J Neurochem. 1975 Aug;25(2):143-9. doi: 10.1111/j.1471-4159.1975.tb12241.x. PMID: 237983.

Coco ML, Kuhn CM, Ely TD, Kilts CD. Selective activation of mesoamygdaloid dopamine neurons by conditioned stress: attenuation by diazepam. Brain Res. 1992 Sep 11;590(1-2):39-47. doi: 10.1016/0006-8993(92)91079-t. PMID: 1422845.

Cole DG, Kobierski LA, Konradi C, Hyman SE. 6-Hydroxydopamine lesions of rat substantia nigra up-regulate dopamine-induced phosphorylation of the cAMP-response element-binding protein in striatal neurons. Proc Natl Acad Sci U S A. 1994 Sep 27;91(20):9631-5. doi: 10.1073/pnas.91.20.9631. PMID: 7937819; PMCID: PMC44867.

Cole RL, Konradi C, Douglass J, Hyman SE. Neuronal adaptation to amphetamine and dopamine: molecular mechanisms of prodynorphin gene regulation in rat striatum. Neuron. 1995 Apr;14(4):813-23. doi: 10.1016/0896-6273(95)90225-2. PMID: 7718243; PMCID: PMC4207064.

Colledge M, Dean RA, Scott GK, Langeberg LK, Huganir RL, Scott JD. Targeting of PKA to glutamate receptors through a MAGUK-AKAP complex. Neuron. 2000 Jul;27(1):107-19. doi: 10.1016/s0896-6273(00)00013-1. PMID: 10939335.

Conroy JL, Free RB, Sibley DR. Identification of G protein-biased agonists that fail to recruit β-arrestin or promote internalization of the D1 dopamine receptor. ACS Chem Neurosci. 2015 Apr 15;6(4):681-92. doi: 10.1021/acschemneuro.5b00020. Epub 2015 Feb 20. PMID: 25660762; PMCID: PMC5234767.

Contreras F, Fouillioux C, Bolívar A, Simonovis N, Hernández-Hernández R, Armas-Hernandez MJ, Velasco M. Dopamine, hypertension and obesity. J Hum Hypertens. 2002 Mar;16 Suppl 1:S13-7. doi: 10.1038/sj.jhh.1001334. PMID: 11986886.

Cools AR, Van Rossum JM. Excitation-mediating and inhibition-mediating dopamine-receptors: a new concept towards a better understanding of electrophysiological, biochemical, pharmacological, functional and clinical data. Psychopharmacologia. 1976 Feb 2;45(3):243-54. doi: 10.1007/BF00421135. PMID: 175391.

Cools AR, van Rossum JM. Multiple receptors for brain dopamine in behavior regulation: concept of dopamine-E and dopamine-I receptors. Life Sci. 1980 Oct 6;27(14):1237-53. doi: 10.1016/0024-3205(80)90217-9. PMID: 6255271.

Corthell JT, Stathopoulos AM, Watson CC, Bertram R, Trombley PQ. Olfactory bulb monoamine concentrations vary with time of day. Neuroscience. 2013 Sep 5;247:234-41. doi: 10.1016/j.neuroscience.2013.05.040. Epub 2013 May 30. PMID: 23727009; PMCID: PMC3722297.

Cosentino M, Fietta AM, Ferrari M, Rasini E, Bombelli R, Carcano E, Saporiti F, Meloni F, Marino F, Lecchini S. Human CD4+CD25+ regulatory T cells selectively express tyrosine hydroxylase and contain endogenous catecholamines subserving an autocrine/paracrine inhibitory functional loop. Blood. 2007 Jan 15;109(2):632-42. doi: 10.1182/blood-2006-01-028423. Epub 2006 Sep 19. PMID: 16985181.

Cosentino M, Zaffaroni M, Legnaro M, Bombelli R, Schembri L, Baroncini D, Bianchi A, Clerici R, Guidotti M, Banfi P, Bono G, Marino F. Dopaminergic receptors and adrenoceptors in circulating lymphocytes as putative biomarkers for the early onset and progression of multiple sclerosis. J Neuroimmunol. 2016 Sep 15;298:82-9. doi: 10.1016/j.jneuroim.2016.07.008. Epub 2016 Jul 7. PMID: 27609280.

Costa KM, Schoenbaum G. Dopamine. Curr Biol. 2022 Aug 8;32(15):R817-R824. doi: 10.1016/j.cub.2022.06.060. PMID: 35944478.

Cotzias GC. L-Dopa for Parkinsonism. N Engl J Med. 1968 Mar 14;278(11):630. doi: 10.1056/nejm196803142781127. PMID: 5637779.

Cousins SL, Papadakis M, Rutter AR, Stephenson FA. Differential interaction of NMDA receptor subtypes with the post-synaptic density-95 family of membrane associated guanylate kinase proteins. J Neurochem. 2008 Feb;104(4):903-13. doi: 10.1111/j.1471-4159.2007.05067.x. PMID: 18233995.

Cramer SC. Drugs to Enhance Motor Recovery After Stroke. Stroke. 2015 Oct;46(10):2998-3005. doi: 10.1161/STROKEAHA.115.007433. Epub 2015 Aug 11. PMID: 26265126; PMCID: PMC4589468.

Creese I, Burt DR, Snyder SH. Dopamine receptor binding: differentiation of agonist and antagonist states with 3H-dopamine and 3H-haloperidol. Life Sci. 1975 Sep 15;17(6):933-1001. doi: 10.1016/0024-3205(75)90454-3. PMID: 1195989.

Crocker-Buque A, Currie SP, Luz LL, Grant SG, Duffy KR, Kind PC, Daw MI. Altered thalamocortical development in the SAP102 knockout model of intellectual disability. Hum Mol Genet. 2016 Sep 15;25(18):4052-4061. doi: 10.1093/hmg/ddw244. Epub 2016 Jul 27. PMID: 27466188; PMCID: PMC5291236.

Crocq MA, Mant R, Asherson P, Williams J, Hode Y, Mayerova A, Collier D, Lannfelt L, Sokoloff P, Schwartz JC, et al. Association between schizophrenia and homozygosity at the dopamine D3 receptor gene. J Med Genet. 1992 Dec;29(12):858-60. doi: 10.1136/jmg.29.12.858. PMID: 1362221; PMCID: PMC1016201.

Cuevas S, Villar VA, Jose PA, Armando I. Renal dopamine receptors, oxidative stress, and hypertension. Int J Mol Sci. 2013 Aug 27;14(9):17553-72. doi: 10.3390/ijms140917553. PMID: 23985827; PMCID: PMC3794741.

Cull-Candy SG, Leszkiewicz DN. Role of distinct NMDA receptor subtypes at central synapses. Sci STKE. 2004 Oct 19;2004(255):re16. doi: 10.1126/stke.2552004re16. PMID: 15494561.

Curran OE, Qiu Z, Smith C, Grant SGN. A single-synapse resolution survey of PSD95-positive synapses in twenty human brain regions. Eur J Neurosci. 2021 Oct;54(8):6864-6881. doi: 10.1111/ejn.14846. Epub 2020 Jun 25. PMID: 32492218.

Cutando L, Puighermanal E, Castell L, Tarot P, Belle M, Bertaso F, Arango-Lievano M, Ango F, Rubinstein M, Quintana A, Chédotal A, Mameli M, Valjent E. Cerebellar dopamine D2 receptors regulate social behaviors. Nat Neurosci. 2022 Jul;25(7):900-911. doi: 10.1038/s41593-022-01092-8. Epub 2022 Jun 16. PMID: 35710984.

Cuthbert PC, Stanford LE, Coba MP, Ainge JA, Fink AE, Opazo P, Delgado JY, Komiyama NH, O'Dell TJ, Grant SG. Synapse-associated protein 102/dlgh3 couples the NMDA receptor to specific plasticity pathways and learning strategies. J Neurosci. 2007 Mar 7;27(10):2673-82. doi: 10.1523/JNEUROSCI.4457-06.2007. PMID: 17344405; PMCID: PMC2851144.

Daaka Y, Pitcher JA, Richardson M, Stoffel RH, Robishaw JD, Lefkowitz RJ. Receptor and G betagamma isoform-specific interactions with G protein-coupled receptor kinases. Proc Natl Acad Sci U S A. 1997 Mar 18;94(6):2180-5. doi: 10.1073/pnas.94.6.2180. PMID: 9122168; PMCID: PMC20061.

Dahlström A, FUXE K. EVIDENCE FOR THE EXISTENCE OF MONOAMINE-CONTAINING NEURONS IN THE CENTRAL NERVOUS SYSTEM. I. DEMONSTRATION OF MONOAMINES IN THE CELL BODIES OF BRAIN STEM NEURONS. Acta Physiol Scand Suppl. 1964:SUPPL 232:1-55. PMID: 14229500.

Dakoji S, Tomita S, Karimzadegan S, Nicoll RA, Bredt DS. Interaction of transmembrane AMPA receptor regulatory proteins with multiple membrane associated guanylate kinases. Neuropharmacology. 2003 Nov;45(6):849-56. doi: 10.1016/s0028-3908(03)00267-3. PMID: 14529722.

Dal Bo G, St-Gelais F, Danik M, Williams S, Cotton M, Trudeau LE. Dopamine neurons in culture express VGLUT2 explaining their capacity to release glutamate at synapses in addition to dopamine. J Neurochem. 2004 Mar;88(6):1398-405. doi: 10.1046/j.1471-4159.2003.02277.x. PMID: 15009640.

Dale N, Schacher S, Kandel ER. Long-term facilitation in Aplysia involves increase in transmitter release. Science. 1988 Jan 15;239(4837):282-5. doi: 10.1126/science.2892269. PMID: 2892269.

D'Amelio M, Puglisi-Allegra S, Mercuri N. The role of dopaminergic midbrain in Alzheimer's disease: Translating basic science into clinical practice. Pharmacol Res. 2018 Apr;130:414-419. doi: 10.1016/j.phrs.2018.01.016. Epub 2018 Jan 31. PMID: 29391234.

D'Aoust JP, Tiberi M. Role of the extracellular amino terminus and first membrane-spanning helix of dopamine D1 and D5 receptors in shaping ligand selectivity and efficacy. Cell Signal. 2010 Jan;22(1):106-16. doi: 10.1016/j.cellsig.2009.09.020. Epub 2009 Sep 26. PMID: 19786093.

Das S, Grunert M, Williams L, Vincent SR. NMDA and D1 receptors regulate the phosphorylation of CREB and the induction of c-fos in striatal neurons in primary culture. Synapse. 1997 Mar;25(3):227-33. doi: 10.1002/(SICI)1098-2396(199703)25:3<227::AID-SYN1>3.0.CO;2-D. PMID: 9068120.

Dauer W, Przedborski S. Parkinson's disease: mechanisms and models. Neuron. 2003 Sep 11;39(6):889-909. doi: 10.1016/s0896-6273(03)00568-3. PMID: 12971891.

Dawson TM, Arriza JL, Jaworsky DE, Borisy FF, Attramadal H, Lefkowitz RJ, Ronnett GV. Beta-adrenergic receptor kinase-2 and beta-arrestin-2 as mediators of odorant-induced desensitization. Science. 1993 Feb 5;259(5096):825-9. doi: 10.1126/science.8381559. PMID: 8381559.

Day M, Wang Z, Ding J, An X, Ingham CA, Shering AF, Wokosin D, Ilijic E, Sun Z, Sampson AR, Mugnaini E, Deutch AY, Sesack SR, Arbuthnott GW, Surmeier DJ. Selective elimination of glutamatergic synapses on striatopallidal neurons in Parkinson disease models. Nat Neurosci. 2006 Feb;9(2):251-9. doi: 10.1038/nn1632. Epub 2006 Jan 15. PMID: 16415865.

Day M, Wang Z, Ding J, An X, Ingham CA, Shering AF, Wokosin D, Ilijic E, Sun Z, Sampson AR, Mugnaini E, Deutch AY, Sesack SR, Arbuthnott GW, Surmeier DJ. Selective elimination of glutamatergic synapses on striatopallidal neurons in Parkinson disease models. Nat Neurosci. 2006 Feb;9(2):251-9. doi: 10.1038/nn1632. Epub 2006 Jan 15. PMID: 16415865.

De Camilli P, Macconi D, Spada A. Dopamine inhibits adenylate cyclase in human prolactin-secreting pituitary adenomas. Nature. 1979 Mar 15;278(5701):252-4. doi: 10.1038/278252a0. PMID: 423973.

de Castro F. Cajal and the Spanish Neurological School: Neuroscience Would Have Been a Different Story Without Them. Front Cell Neurosci. 2019 May 24;13:187. doi: 10.3389/fncel.2019.00187. PMID: 31178695; PMCID: PMC6542961.

De Lean A, Kilpatrick BF, Caron MG. Dopamine receptor of the porcine anterior pituitary gland. Evidence for two affinity states discriminated by both agonists and antagonists. Mol Pharmacol. 1982 Sep;22(2):290-7. PMID: 7144730.

De Lean A, Stadel JM, Lefkowitz RJ. A ternary complex model explains the agonist-specific binding properties of the adenylate cyclase-coupled beta-adrenergic receptor. J Biol Chem. 1980 Aug 10;255(15):7108-17. PMID: 6248546.

Dearry A, Gingrich JA, Falardeau P, Fremeau RT Jr, Bates MD, Caron MG. Molecular cloning and expression of the gene for a human D1 dopamine receptor. Nature. 1990 Sep 6;347(6288):72-6. doi: 10.1038/347072a0. PMID: 2144334.

DeLange RJ, Kemp RG, Riley WD, Cooper RA, Krebs EG. Activation of skeletal muscle phosphorylase kinase by adenosine triphosphate and adenosine 3',5'-monophosphate. J Biol Chem. 1968 May 10;243(9):2200-8. PMID: 4296832.

Delgado A, Sierra A, Querejeta E, Valdiosera RF, Aceves J. Inhibitory control of the GABAergic transmission in the rat neostriatum by D2 dopamine receptors. Neuroscience. 2000;95(4):1043-8. doi: 10.1016/s0306-4522(99)00495-9. PMID: 10682711.

Desdouits F, Siciliano JC, Greengard P, Girault JA. Dopamine- and cAMP-regulated phosphoprotein DARPP-32: phosphorylation of Ser-137 by casein kinase I inhibits dephosphorylation of Thr-34 by calcineurin. Proc Natl Acad Sci U S A. 1995 Mar 28;92(7):2682-5. doi: 10.1073/pnas.92.7.2682. PMID: 7708705; PMCID: PMC42282.

Devasani K, Yao Y. Expression and functions of adenylyl cyclases in the CNS. Fluids Barriers CNS. 2022 Mar 20;19(1):23. doi: 10.1186/s12987-022-00322-2. PMID: 35307032; PMCID: PMC8935726.

D'haenen HA, Bossuyt A. Dopamine D2 receptors in depression measured with single photon emission computed tomography. Biol Psychiatry. 1994 Jan 15;35(2):128-32. doi: 10.1016/0006-3223(94)91202-5. PMID: 8167208.

Di Chiara G, Bassareo V. Reward system and addiction: what dopamine does and doesn't do. Curr Opin Pharmacol. 2007 Feb;7(1):69-76. doi: 10.1016/j.coph.2006.11.003. Epub 2006 Dec 15. Erratum in: Curr Opin Pharmacol. 2007 Apr;7(2):233. PMID: 17174602.

Di Ciano P, Everitt BJ. Direct interactions between the basolateral amygdala and nucleus accumbens core underlie cocaine-seeking behavior by rats. J Neurosci. 2004 Aug 11;24(32):7167-73. doi: 10.1523/JNEUROSCI.1581-04.2004. PMID: 15306650; PMCID: PMC6729170.

Dickinson SD, Sabeti J, Larson GA, Giardina K, Rubinstein M, Kelly MA, Grandy DK, Low MJ, Gerhardt GA, Zahniser NR. Dopamine D2 receptor-deficient mice exhibit decreased dopamine transporter function but no changes in dopamine release in dorsal striatum. J Neurochem. 1999 Jan;72(1):148-56. doi: 10.1046/j.1471-4159.1999.0720148.x. PMID: 9886065.

DiFeliceantonio AG, Small DM. Dopamine and diet-induced obesity. Nat Neurosci. 2019 Jan;22(1):1-2. doi: 10.1038/s41593-018-0304-0. PMID: 30559474.

Ding L, Perkel DJ. Dopamine modulates excitability of spiny neurons in the avian basal ganglia. J Neurosci. 2002 Jun 15;22(12):5210-8. doi: 10.1523/JNEUROSCI.22-12-05210.2002. Erratum in: J Neurosci 2002 Aug 1;22(15):6835. PMID: 12077216; PMCID: PMC6757730.

Dixon RA, Kobilka BK, Strader DJ, Benovic JL, Dohlman HG, Frielle T, Bolanowski MA, Bennett CD, Rands E, Diehl RE, Mumford RA, Slater EE, Sigal IS, Caron MG, Lefkowitz RJ, Strader CD. Cloning of the gene and cDNA for mammalian beta-adrenergic receptor and homology with rhodopsin. Nature. 1986 May 1-7;321(6065):75-9. doi: 10.1038/321075a0. PMID: 3010132.

Dohlman HG, Thorner J. RGS proteins and signaling by heterotrimeric G proteins. J Biol Chem. 1997 Feb 14;272(7):3871-4. doi: 10.1074/jbc.272.7.3871. PMID: 9064301.

Doi M, Yujnovsky I, Hirayama J, Malerba M, Tirotta E, Sassone-Corsi P, Borrelli E. Impaired light masking in dopamine D2 receptor-null mice. Nat Neurosci. 2006 Jun;9(6):732-4. doi: 10.1038/nn1711. Epub 2006 May 21. PMID: 16715079.

Dosemeci A, Makusky AJ, Jankowska-Stephens E, Yang X, Slotta DJ, Markey SP. Composition of the synaptic PSD-95 complex. Mol Cell Proteomics. 2007 Oct;6(10):1749-60. doi: 10.1074/mcp.M700040-MCP200. Epub 2007 Jul 9. PMID: 17623647; PMCID: PMC2096750.

Dowling JE. Retinal neuromodulation: the role of dopamine. Vis Neurosci. 1991 Jul-Aug;7(1-2):87-97. doi: 10.1017/s0952523800010968. PMID: 1718402.

Downes GB, Gautam N. The G protein subunit gene families. Genomics. 1999 Dec 15;62(3):544-52. doi: 10.1006/geno.1999.5992. PMID: 10644457.

Drago J, Gerfen CR, Lachowicz JE, Steiner H, Hollon TR, Love PE, Ooi GT, Grinberg A, Lee EJ, Huang SP. Altered striatal function in a mutant mouse lacking D1A dopamine receptors. Proc Natl Acad Sci U S A. 1994 Dec 20;91(26):12564-8. doi: 10.1073/pnas.91.26.12564. PMID: 7809078; PMCID: PMC45479.

Dubocovich ML. Presynaptic receptors in the visual system. Ann N Y Acad Sci. 1990;604:82-95. doi: 10.1111/j.1749-6632.1990.tb31984.x. PMID: 2171409.

Dudman JT, Eaton ME, Rajadhyaksha A, Macías W, Taher M, Barczak A, Kameyama K, Huganir R, Konradi C. Dopamine D1 receptors mediate CREB phosphorylation via phosphorylation of the NMDA receptor at Ser897-NR1. J Neurochem. 2003 Nov;87(4):922-34. doi: 10.1046/j.1471-4159.2003.02067.x. PMID: 14622123; PMCID: PMC4203348.

Dumartin B, Caillé I, Gonon F, Bloch B. Internalization of D1 dopamine receptor in striatal neurons in vivo as evidence of activation by dopamine agonists. J Neurosci. 1998 Mar 1;18(5):1650-61. doi: 10.1523/JNEUROSCI.18-05-01650.1998. PMID: 9464990; PMCID: PMC6792610.

Dunn HA, Chahal HS, Caetano FA, Holmes KD, Yuan GY, Parikh R, Heit B, Ferguson SSG. PSD-95 regulates CRFR1 localization, trafficking and β-arrestin2 recruitment. Cell Signal. 2016 May;28(5):531-540. doi: 10.1016/j.cellsig.2016.02.013. Epub 2016 Feb 17. PMID: 26898829.

Dunn HA, Ferguson SS. PDZ Protein Regulation of G Protein-Coupled Receptor Trafficking and Signaling Pathways. Mol Pharmacol. 2015 Oct;88(4):624-39. doi: 10.1124/mol.115.098509. Epub 2015 Mar 25. PMID: 25808930.

Dunn HA, Walther C, Godin CM, Hall RA, Ferguson SS. Role of SAP97 protein in the regulation of corticotropin-releasing factor receptor 1 endocytosis and extracellular signal-regulated kinase 1/2 signaling. J Biol Chem. 2013 May 24;288(21):15023-34. doi: 10.1074/jbc.M113.473660. Epub 2013 Apr 10. PMID: 23576434; PMCID: PMC3663523.

Dunn HA, Walther C, Yuan GY, Caetano FA, Godin CM, Ferguson SS. Role of SAP97 in the regulation of 5-HT2AR endocytosis and signaling. Mol Pharmacol. 2014 Sep;86(3):275-83. doi: 10.1124/mol.114.093476. Epub 2014 Jul 2. PMID: 24989932.

Ehlers MD. Activity level controls postsynaptic composition and signaling via the ubiquitin-proteasome system. Nat Neurosci. 2003 Mar;6(3):231-42. doi: 10.1038/nn1013. PMID: 12577062.

EHRINGER H, HORNYKIEWICZ O. [Distribution of noradrenaline and dopamine (3-hydroxytyramine) in the human brain and their behavior in diseases of the extrapyramidal system]. Klin Wochenschr. 1960 Dec 15;38:1236-9. German. doi: 10.1007/BF01485901. PMID: 13726012.

Ehrlich I, Malinow R. Postsynaptic density 95 controls AMPA receptor incorporation during long-term potentiation and experience-driven synaptic plasticity. J Neurosci. 2004 Jan 28;24(4):916-27. doi: 10.1523/JNEUROSCI.4733-03.2004. PMID: 14749436; PMCID: PMC6729816.

Eichel K, Jullié D, Barsi-Rhyne B, Latorraca NR, Masureel M, Sibarita JB, Dror RO, von Zastrow M. Catalytic activation of β-arrestin by GPCRs. Nature. 2018 May;557(7705):381-386. doi: 10.1038/s41586-018-0079-1. Epub 2018 May 2. PMID: 29720660; PMCID: PMC6058965.

el Mestikawy S, Glowinski J, Hamon M. Presynaptic dopamine autoreceptors control tyrosine hydroxylase activation in depolarized striatal dopaminergic terminals. J Neurochem. 1986 Jan;46(1):12-22. doi: 10.1111/j.1471-4159.1986.tb12919.x. PMID: 2866232.

el Mestikawy S, Hamon M. Is dopamine-induced inhibition of adenylate cyclase involved in the autoreceptor-mediated negative control of tyrosine hydroxylase in striatal dopaminergic terminals? J Neurochem. 1986 Nov;47(5):1425-33. doi: 10.1111/j.1471-4159.1986.tb00775.x. PMID: 2876053.

El-Ghundi M, Fletcher PJ, Drago J, Sibley DR, O'Dowd BF, George SR. Spatial learning deficit in dopamine D(1) receptor knockout mice. Eur J Pharmacol. 1999 Oct 27;383(2):95-106. doi: 10.1016/s0014-2999(99)00573-7. PMID: 10585522.

Elgueta D, Contreras F, Prado C, Montoya A, Ugalde V, Chovar O, Villagra R, Henríquez C, Abellanas MA, Aymerich MS, Franco R, Pacheco R. Dopamine Receptor D3 Expression Is Altered in CD4+ T-Cells From Parkinson's Disease Patients and Its Pharmacologic Inhibition Attenuates the Motor Impairment in a Mouse Model. Front Immunol. 2019 May 1;10:981. doi: 10.3389/fimmu.2019.00981. PMID: 31118938; PMCID: PMC6504698.

El-Husseini AE, Schnell E, Chetkovich DM, Nicoll RA, Bredt DS. PSD-95 involvement in maturation of excitatory synapses. Science. 2000 Nov 17;290(5495):1364-8. PMID: 11082065. (b)

El-Husseini AE, Topinka JR, Lehrer-Graiwer JE, Firestein BL, Craven SE, Aoki C, Bredt DS. Ion channel clustering by membrane-associated guanylate kinases. Differential regulation by N-terminal lipid and metal binding motifs. J Biol Chem. 2000 Aug 4;275(31):23904-10. doi: 10.1074/jbc.M909919199. PMID: 10779526. (a)

Elias GM, Elias LA, Apostolides PF, Kriegstein AR, Nicoll RA. Differential trafficking of AMPA and NMDA receptors by SAP102 and PSD-95 underlies synapse development. Proc Natl Acad Sci U S A. 2008 Dec 30;105(52):20953-8. doi: 10.1073/pnas.0811025106. Epub 2008 Dec 22. PMID: 19104036; PMCID: PMC2634944.

Elias GM, Funke L, Stein V, Grant SG, Bredt DS, Nicoll RA. Synapse-specific and developmentally regulated targeting of AMPA receptors by a family of MAGUK scaffolding proteins. Neuron. 2006 Oct 19;52(2):307-20. doi: 10.1016/j.neuron.2006.09.012. Erratum in: Neuron. 2007 Feb 1;53(3):465. PMID: 17046693.

Elias GM, Nicoll RA. Synaptic trafficking of glutamate receptors by MAGUK scaffolding proteins. Trends Cell Biol. 2007 Jul;17(7):343-52. doi: 10.1016/j.tcb.2007.07.005. Epub 2007 Jul 20. PMID: 17644382.

Elliot EE, Sibley DR, Katz JL. Locomotor and discriminative-stimulus effects of cocaine in dopamine D5 receptor knockout mice. Psychopharmacology (Berl). 2003 Sep;169(2):161-8. doi: 10.1007/s00213-003-1494-y. Epub 2003 May 27. PMID: 12768268.

Elsworth JD, Roth RH. Dopamine synthesis, uptake, metabolism, and receptors: relevance to gene therapy of Parkinson's disease. Exp Neurol. 1997 Mar;144(1):4-9. doi: 10.1006/exnr.1996.6379. PMID: 9126143.

Epstein DH, Shaham Y. Cheesecake-eating rats and the question of food addiction. Nat Neurosci. 2010 May;13(5):529-31. doi: 10.1038/nn0510-529. PMID: 20421898; PMCID: PMC3147141.

Erickson JD, Eiden LE, Hoffman BJ. Expression cloning of a reserpine-sensitive vesicular monoamine transporter. Proc Natl Acad Sci U S A. 1992 Nov 15;89(22):10993-7. doi: 10.1073/pnas.89.22.10993. PMID: 1438304; PMCID: PMC50469.

Ericsson J, Stephenson-Jones M, Pérez-Fernández J, Robertson B, Silberberg G, Grillner S. Dopamine differentially modulates the excitability of striatal neurons of the direct and indirect pathways in lamprey. J Neurosci. 2013 May 1;33(18):8045-54. doi: 10.1523/JNEUROSCI.5881-12.2013. PMID: 23637194; PMCID: PMC6618979.

Ershov PV, Ugrumov MV, Calas A, Krieger M, Thibault J. Degeneration of dopaminergic neurons triggers an expression of individual enzymes of dopamine synthesis in non-dopaminergic neurons of the arcuate nucleus in adult rats. J Chem Neuroanat. 2005 Jul;30(1):27-33. doi: 10.1016/j.jchemneu.2005.04.001. PMID: 15935614.

Ershov PV, Ugrumov MV, Calas A, Krieger M, Thibault J. Differentiation of tyrosine hydroxylase-synthesizing and/or aromatic L-amino acid decarboxylase-synthesizing neurons in the rat mediobasal hypothalamus: quantitative double-immunofluorescence study. J Comp Neurol. 2002 Apr 29;446(2):114-22. doi: 10.1002/cne.10173. PMID: 11932930.

Escande MV, Taravini IR, Zold CL, Belforte JE, Murer MG. Loss of Homeostasis in the Direct Pathway in a Mouse Model of Asymptomatic Parkinson's Disease. J Neurosci. 2016 May 25;36(21):5686-98. doi: 10.1523/JNEUROSCI.0492-15.2016. PMID: 27225760; PMCID: PMC6601837.

Espay AJ, Morgante F, Merola A, Fasano A, Marsili L, Fox SH, Bezard E, Picconi B, Calabresi P, Lang AE. Levodopa-induced dyskinesia in Parkinson disease: Current and evolving concepts. Ann Neurol. 2018 Dec;84(6):797-811. doi: 10.1002/ana.25364. Epub 2018 Nov 30. PMID: 30357892.

Everitt BJ, Robbins TW. Neural systems of reinforcement for drug addiction: from actions to habits to compulsion. Nat Neurosci. 2005 Nov;8(11):1481-9. doi: 10.1038/nn1579. PMID: 16251991.

Ewing AG, Bigelow JC, Wightman RM. Direct in vivo monitoring of dopamine released from two striatal compartments in the rat. Science. 1983 Jul 8;221(4606):169-71. doi: 10.1126/science.6857277. PMID: 6857277.

Fan L, Tan L, Chen Z, Qi J, Nie F, Luo Z, Cheng J, Wang S. Haloperidol bound D2 dopamine receptor structure inspired the discovery of subtype selective ligands. Nat Commun. 2020 Feb 26;11(1):1074. doi: 10.1038/s41467-020-14884-y. PMID: 32103023; PMCID: PMC7044277.

Färber K, Pannasch U, Kettenmann H. Dopamine and noradrenaline control distinct functions in rodent microglial cells. Mol Cell Neurosci. 2005 May;29(1):128-38. doi: 10.1016/j.mcn.2005.01.003. PMID: 15866053.

Farnebo LO, Hamberger B. Drug-induced changes in the release of 3 H-monoamines from field stimulated rat brain slices. Acta Physiol Scand Suppl. 1971;371:35-44. doi: 10.1111/j.1748-1716.1971.tb05213.x. PMID: 4112831.

Feany MB, Bender WW. A Drosophila model of Parkinson's disease. Nature. 2000 Mar 23;404(6776):394-8. doi: 10.1038/35006074. PMID: 10746727.

Felder CC, Blecher M, Jose PA. Dopamine-1-mediated stimulation of phospholipase C activity in rat renal cortical membranes. J Biol Chem. 1989 May 25;264(15):8739-45. PMID: 2566608.

Ferguson SS, Barak LS, Zhang J, Caron MG. G-protein-coupled receptor regulation: role of G-protein-coupled receptor kinases and arrestins. Can J Physiol Pharmacol. 1996 Oct;74(10):1095-110. doi: 10.1139/cjpp-74-10-1095. PMID: 9022829. (a)

Ferguson SS, Downey WE 3rd, Colapietro AM, Barak LS, Ménard L, Caron MG. Role of beta-arrestin in mediating agonist-promoted G protein-coupled receptor internalization. Science. 1996 Jan 19;271(5247):363-6. doi: 10.1126/science.271.5247.363. PMID: 8553074. (b)

Ferguson SS, Ménard L, Barak LS, Koch WJ, Colapietro AM, Caron MG. Role of phosphorylation in agonist-promoted beta 2-adrenergic receptor sequestration. Rescue of a sequestration-defective mutant receptor by beta ARK1. J Biol Chem. 1995 Oct 20;270(42):24782-9. doi: 10.1074/jbc.270.42.24782. PMID: 7559596.

Ferguson SS. Evolving concepts in G protein-coupled receptor endocytosis: the role in receptor desensitization and signaling. Pharmacol Rev. 2001 Mar;53(1):1-24. PMID: 11171937.

Fernández E, Collins MO, Uren RT, Kopanitsa MV, Komiyama NH, Croning MD, Zografos L, Armstrong JD, Choudhary JS, Grant SG. Targeted tandem affinity purification of PSD-95 recovers core postsynaptic complexes and schizophrenia susceptibility proteins. Mol Syst Biol. 2009;5:269. doi: 10.1038/msb.2009.27. Epub 2009 May 19. PMID: 19455133; PMCID: PMC2694677.

Ferrada C, Moreno E, Casadó V, Bongers G, Cortés A, Mallol J, Canela EI, Leurs R, Ferré S, Lluís C, Franco R. Marked changes in signal transduction upon heteromerization of dopamine D1 and histamine H3 receptors. Br J Pharmacol. 2009 May;157(1):64-75. doi: 10.1111/j.1476-5381.2009.00152.x. PMID: 19413572; PMCID: PMC2697789.

Ferré S, Fredholm BB, Morelli M, Popoli P, Fuxe K. Adenosine-dopamine receptor-receptor interactions as an integrative mechanism in the basal ganglia. Trends Neurosci. 1997 Oct;20(10):482-7. doi: 10.1016/s0166-2236(97)01096-5. PMID: 9347617.

Ferré S, Torvinen M, Antoniou K, Irenius E, Civelli O, Arenas E, Fredholm BB, Fuxe K. Adenosine A1 receptor-mediated modulation of dopamine D1 receptors in stably cotransfected fibroblast cells. J Biol Chem. 1998 Feb 20;273(8):4718-24. doi: 10.1074/jbc.273.8.4718. PMID: 9468534.

Feuerstein TJ. Presynaptic receptors for dopamine, histamine, and serotonin. Handb Exp Pharmacol. 2008;(184):289-338. doi: 10.1007/978-3-540-74805-2_10. PMID: 18064418.

Feyder M, Karlsson RM, Mathur P, Lyman M, Bock R, Momenan R, Munasinghe J, Scattoni ML, Ihne J, Camp M, Graybeal C, Strathdee D, Begg A, Alvarez VA, Kirsch P, Rietschel M, Cichon S, Walter H, Meyer-Lindenberg A, Grant SG, Holmes A. Association of mouse Dlg4 (PSD-95) gene deletion and human DLG4 gene variation with phenotypes relevant to autism spectrum disorders and Williams' syndrome. Am J Psychiatry. 2010 Dec;167(12):1508-17. doi: 10.1176/appi.ajp.2010.10040484. Epub 2010 Oct 15. PMID: 20952458; PMCID: PMC3146008.

Fiorentini C, Busi C, Gorruso E, Gotti C, Spano P, Missale C. Reciprocal regulation of dopamine D1 and D3 receptor function and trafficking by heterodimerization. Mol Pharmacol. 2008 Jul;74(1):59-69. doi: 10.1124/mol.107.043885. Epub 2008 Apr 18. PMID: 18424554.

Fiorentini C, Gardoni F, Spano P, Di Luca M, Missale C. Regulation of dopamine D1 receptor trafficking and desensitization by oligomerization with glutamate N-methyl-D-aspartate receptors. J Biol Chem. 2003 May 30;278(22):20196-202. doi: 10.1074/jbc.M213140200. Epub 2003 Mar 19. PMID: 12646556.

Fiorentini C, Gardoni F, Spano P, Di Luca M, Missale C. Regulation of dopamine D1 receptor trafficking and desensitization by oligomerization with glutamate N-methyl-D-aspartate receptors. J Biol Chem. 2003 May 30;278(22):20196-202. doi: 10.1074/jbc.M213140200. Epub 2003 Mar 19. PMID: 12646556.

Fiorillo CD, Tobler PN, Schultz W. Discrete coding of reward probability and uncertainty by dopamine neurons. Science. 2003 Mar 21;299(5614):1898-902. doi: 10.1126/science.1077349. PMID: 12649484.

Firestein BL, Craven SE, Bredt DS. Postsynaptic targeting of MAGUKs mediated by distinct N-terminal domains. Neuroreport. 2000 Nov 9;11(16):3479-84. doi: 10.1097/00001756-200011090-00016. PMID: 11095503.

FISCHER EH, KREBS EG. Conversion of phosphorylase b to phosphorylase a in muscle extracts. J Biol Chem. 1955 Sep;216(1):121-32. PMID: 13252012.

Fitzgerald P, Dinan TG. Prolactin and dopamine: what is the connection? A review article. J Psychopharmacol. 2008 Mar;22(2 Suppl):12-9. doi: 10.1177/0269216307087148. PMID: 18477617.

Flace P, Livrea P, Basile GA, Galletta D, Bizzoca A, Gennarini G, Bertino S, Branca JJV, Gulisano M, Bianconi S, Bramanti A, Anastasi G. The Cerebellar Dopaminergic System. Front Syst Neurosci. 2021 Aug 5;15:650614. doi: 10.3389/fnsys.2021.650614. PMID: 34421548; PMCID: PMC8375553.

Fon EA, Pothos EN, Sun BC, Killeen N, Sulzer D, Edwards RH. Vesicular transport regulates monoamine storage and release but is not essential for amphetamine action. Neuron. 1997 Dec;19(6):1271-83. doi: 10.1016/s0896-6273(00)80418-3. PMID: 9427250.a

Ford CP. The role of D2-autoreceptors in regulating dopamine neuron activity and transmission. Neuroscience. 2014 Dec 12;282:13-22. doi: 10.1016/j.neuroscience.2014.01.025. Epub 2014 Jan 23. PMID: 24463000; PMCID: PMC4108583.

Fortin GM, Bourque MJ, Mendez JA, Leo D, Nordenankar K, Birgner C, Arvidsson E, Rymar VV, Bérubé-Carrière N, Claveau AM, Descarries L, Sadikot AF, Wallén-Mackenzie Å, Trudeau LÉ. Glutamate corelease promotes growth and survival of midbrain dopamine neurons. J Neurosci. 2012 Nov 28;32(48):17477-91. doi: 10.1523/JNEUROSCI.1939-12.2012. PMID: 23197738; PMCID: PMC6621856.

Fox SH, Brotchie JM. The MPTP-lesioned non-human primate models of Parkinson's disease. Past, present, and future. Prog Brain Res. 2010;184:133-57. doi: 10.1016/S0079-6123(10)84007-5. PMID: 20887873.

Frank RA, Komiyama NH, Ryan TJ, Zhu F, O'Dell TJ, Grant SG. NMDA receptors are selectively partitioned into complexes and supercomplexes during synapse maturation. Nat Commun. 2016 Apr 27;7:11264. doi: 10.1038/ncomms11264. PMID: 27117477; PMCID: PMC5227094.

Frederick AL, Yano H, Trifilieff P, Vishwasrao HD, Biezonski D, Mészáros J, Urizar E, Sibley DR, Kellendonk C, Sonntag KC, Graham DL, Colbran RJ, Stanwood GD, Javitch JA. Evidence against dopamine D1/D2 receptor heteromers. Mol Psychiatry. 2015 Nov;20(11):1373-85. doi: 10.1038/mp.2014.166. Epub 2015 Jan 6. PMID: 25560761; PMCID: PMC4492915.

Free RB, Hazelwood LA, Cabrera DM, Spalding HN, Namkung Y, Rankin ML, Sibley DR. D1 and D2 dopamine receptor expression is regulated by direct interaction with the chaperone protein calnexin. J Biol Chem. 2007 Jul 20;282(29):21285-300. doi: 10.1074/jbc.M701555200. Epub 2007 Mar 29. PMID: 17395585.

Freedman NJ, Liggett SB, Drachman DE, Pei G, Caron MG, Lefkowitz RJ. Phosphorylation and desensitization of the human beta 1-adrenergic receptor. Involvement of G protein-coupled receptor kinases and cAMP-dependent protein kinase. J Biol Chem. 1995 Jul 28;270(30):17953-61. doi: 10.1074/jbc.270.30.17953. PMID: 7629102.

Fremeau RT Jr, Duncan GE, Fornaretto MG, Dearry A, Gingrich JA, Breese GR, Caron MG. Localization of D1 dopamine receptor mRNA in brain supports a role in cognitive, affective, and neuroendocrine aspects of dopaminergic neurotransmission. Proc Natl Acad Sci U S A. 1991 May 1;88(9):3772-6. doi: 10.1073/pnas.88.9.3772. PMID: 2023928; PMCID: PMC51535.

Frey U, Huang YY, Kandel ER. Effects of cAMP simulate a late stage of LTP in hippocampal CA1 neurons. Science. 1993 Jun 11;260(5114):1661-4. doi: 10.1126/science.8389057. PMID: 8389057.

Frey U, Schroeder H, Matthies H. Dopaminergic antagonists prevent long-term maintenance of posttetanic LTP in the CA1 region of rat hippocampal slices. Brain Res. 1990 Jul 2;522(1):69-75. doi: 10.1016/0006-8993(90)91578-5. PMID: 1977494.

Frick A, Björkstrand J, Lubberink M, Eriksson A, Fredrikson M, Åhs F. Dopamine and fear memory formation in the human amygdala. Mol Psychiatry. 2022 Mar;27(3):1704-1711. doi: 10.1038/s41380-021-01400-x. Epub 2021 Dec 3. PMID: 34862441; PMCID: PMC9095491.

Friedman E, Jin LQ, Cai GP, Hollon TR, Drago J, Sibley DR, Wang HY. D1-like dopaminergic activation of phosphoinositide hydrolysis is independent of D1A dopamine receptors: evidence from D1A knockout mice. Mol Pharmacol. 1997 Jan;51(1):6-11. doi: 10.1124/mol.51.1.6. PMID: 9016340.

Fuxe K, Manger P, Genedani S, Agnati L. The nigrostriatal DA pathway and Parkinson's disease. J Neural Transm Suppl. 2006;(70):71-83. doi: 10.1007/978-3-211-45295-0_13. PMID: 17017512.

Gagnon D, Petryszyn S, Sanchez MG, Bories C, Beaulieu JM, De Koninck Y, Parent A, Parent M. Striatal Neurons Expressing D1 and D2 Receptors are Morphologically Distinct and Differently Affected by Dopamine Denervation in Mice. Sci Rep. 2017 Jan 27;7:41432. doi: 10.1038/srep41432. PMID: 28128287; PMCID: PMC5269744.

Gainetdinov RR, Mohn AR, Bohn LM, Caron MG. Glutamatergic modulation of hyperactivity in mice lacking the dopamine transporter. Proc Natl Acad Sci U S A. 2001 Sep 25;98(20):11047-54. doi: 10.1073/pnas.191353298. PMID: 11572967; PMCID: PMC58681.

Gainetdinov RR, Premont RT, Bohn LM, Lefkowitz RJ, Caron MG. Desensitization of G protein-coupled receptors and neuronal functions. Annu Rev Neurosci. 2004;27:107-44. doi: 10.1146/annurev.neuro.27.070203.144206. PMID: 15217328.

Gainetdinov RR, Sotnikova TD, Caron MG. Monoamine transporter pharmacology and mutant mice. Trends Pharmacol Sci. 2002 Aug;23(8):367-73. doi: 10.1016/s0165-6147(02)02044-8. Erratum in: Trends Pharmacol Sci 2002 Sep;23(9):443. PMID: 12377578.

Gainetdinov RR, Sotnikova TD, Grekhova TV, Rayevsky KS. In vivo evidence for preferential role of dopamine D3 receptor in the presynaptic regulation of dopamine release but not synthesis. Eur J Pharmacol. 1996 Jul 25;308(3):261-9. doi: 10.1016/0014-2999(96)00300-7. PMID: 8858296.

Galvan A, Devergnas A, Wichmann T. Alterations in neuronal activity in basal ganglia-thalamocortical circuits in the parkinsonian state. Front Neuroanat. 2015 Feb 5;9:5. doi: 10.3389/fnana.2015.00005. PMID: 25698937; PMCID: PMC4318426.

Gangarossa G, Longueville S, De Bundel D, Perroy J, Hervé D, Girault JA, Valjent E. Characterization of dopamine D1 and D2 receptor-expressing neurons in the mouse hippocampus. Hippocampus. 2012 Dec;22(12):2199-207. doi: 10.1002/hipo.22044. Epub 2012 Jul 6. PMID: 22777829.

Gantz SC, Ford CP, Morikawa H, Williams JT. The Evolving Understanding of Dopamine Neurons in the Substantia Nigra and Ventral Tegmental Area. Annu Rev Physiol. 2018 Feb 10;80:219-241. doi: 10.1146/annurev-physiol-021317-121615. Epub 2017 Sep 22. PMID: 28938084.

Garau L, Govoni S, Stefanini E, Trabucchi M, Spano PF. Dopamine receptors: pharmacological and anatomical evidences indicate that two distinct dopamine receptor populations are present in rat striatum. Life Sci. 1978 Oct 30;23(17-18):1745-50. doi: 10.1016/0024-3205(78)90102-9. PMID: 723447.

García-Tornadú I, Ornstein AM, Chamson-Reig A, Wheeler MB, Hill DJ, Arany E, Rubinstein M, Becu-Villalobos D. Disruption of the dopamine d2 receptor impairs insulin secretion and causes glucose intolerance. Endocrinology. 2010 Apr;151(4):1441-50. doi: 10.1210/en.2009-0996. Epub 2010 Feb 10. PMID: 20147524.

Gardner B, Liu ZF, Jiang D, Sibley DR. The role of phosphorylation/dephosphorylation in agonist-induced desensitization of D1 dopamine receptor function: evidence for a novel pathway for receptor dephosphorylation. Mol Pharmacol. 2001 Feb;59(2):310-21. doi: 10.1124/mol.59.2.310. PMID: 11160868.

Gardner LA, Naren AP, Bahouth SW. Assembly of an SAP97-AKAP79-cAMP-dependent protein kinase scaffold at the type 1 PSD-95/DLG/ZO1 motif of the human beta(1)-adrenergic receptor generates a receptosome involved in receptor recycling and networking. J Biol Chem. 2007 Feb 16;282(7):5085-5099. doi: 10.1074/jbc.M608871200. Epub 2006 Dec 14. PMID: 17170109.

Gardoni F, Marcello E, Di Luca M. Postsynaptic density-membrane associated guanylate kinase proteins (PSD-MAGUKs) and their role in CNS disorders. Neuroscience. 2009 Jan 12;158(1):324-33. doi: 10.1016/j.neuroscience.2008.07.068. Epub 2008 Aug 13. PMID: 18773944.

Gardoni F, Picconi B, Ghiglieri V, Polli F, Bagetta V, Bernardi G, Cattabeni F, Di Luca M, Calabresi P. A critical interaction between NR2B and MAGUK in L-DOPA induced dyskinesia. J Neurosci. 2006 Mar 15;26(11):2914-22. doi: 10.1523/JNEUROSCI.5326-05.2006. PMID: 16540568; PMCID: PMC6673976.

Garner CC, Nash J, Huganir RL. PDZ domains in synapse assembly and signalling. Trends Cell Biol. 2000 Jul;10(7):274-80. doi: 10.1016/s0962-8924(00)01783-9. PMID: 10856930.

Geffen LB, Jessell TM, Cuello AC, Iversen LL. Release of dopamine from dendrites in rat substantia nigra. Nature. 1976 Mar 18;260(5548):258-60. doi: 10.1038/260258a0. PMID: 1256567.

Geisler CE, Hayes MR. Metabolic hormone action in the VTA: Reward-directed behavior and mechanistic insights. Physiol Behav. 2023 Sep 1;268:114236. doi: 10.1016/j.physbeh.2023.114236. Epub 2023 May 12. PMID: 37178855.

Gejman PV, Ram A, Gelernter J, Friedman E, Cao Q, Pickar D, Blum K, Noble EP, Kranzler HR, O'Malley S, et al. No structural mutation in the dopamine D2 receptor gene in alcoholism or schizophrenia. Analysis using denaturing gradient gel electrophoresis. JAMA. 1994 Jan 19;271(3):204-8. PMID: 8277546.

Gelernter J, Kennedy JL, van Tol HH, Civelli O, Kidd KK. The D4 dopamine receptor (DRD4) maps to distal 11p close to HRAS. Genomics. 1992 May;13(1):208-10. doi: 10.1016/0888-7543(92)90222-e. PMID: 1349574.

Gerfen CR, Engber TM, Mahan LC, Susel Z, Chase TN, Monsma FJ Jr, Sibley DR. D1 and D2 dopamine receptor-regulated gene expression of striatonigral and striatopallidal neurons. Science. 1990 Dec 7;250(4986):1429-32. doi: 10.1126/science.2147780. PMID: 2147780.

Gerfen CR, Paletzki R, Worley P. Differences between dorsal and ventral striatum in Drd1a dopamine receptor coupling of dopamine- and cAMP-regulated phosphoprotein-32 to activation of extracellular signal-regulated kinase. J Neurosci. 2008 Jul 9;28(28):7113-20. doi: 10.1523/JNEUROSCI.3952-07.2008. PMID: 18614680; PMCID: PMC2585508.

Gerfen CR, Surmeier DJ. Modulation of striatal projection systems by dopamine. Annu Rev Neurosci. 2011;34:441-66. doi: 10.1146/annurev-neuro-061010-113641. PMID: 21469956; PMCID: PMC3487690.

Gerfen CR. Indirect-pathway neurons lose their spines in Parkinson disease. Nat Neurosci. 2006 Feb;9(2):157-8. doi: 10.1038/nn0206-157. PMID: 16439979.

Gerfen CR. Segregation of D1 and D2 dopamine receptors in the striatal direct and indirect pathways: An historical perspective. Front Synaptic Neurosci. 2023 Jan 19;14:1002960. doi: 10.3389/fnsyn.2022.1002960. PMID: 36741471; PMCID: PMC9892636.

Gerfen CR. The neostriatal mosaic: multiple levels of compartmental organization. Trends Neurosci. 1992 Apr;15(4):133-9. doi: 10.1016/0166-2236(92)90355-c. PMID: 1374971.

Gether U. Uncovering molecular mechanisms involved in activation of G protein-coupled receptors. Endocr Rev. 2000 Feb;21(1):90-113. doi: 10.1210/edrv.21.1.0390. PMID: 10696571.

Gilman AG. G proteins and dual control of adenylate cyclase. Cell. 1984 Mar;36(3):577-9. doi: 10.1016/0092-8674(84)90336-2. PMID: 6321035.

Ginés S, Hillion J, Torvinen M, Le Crom S, Casadó V, Canela EI, Rondin S, Lew JY, Watson S, Zoli M, Agnati LF, Verniera P, Lluis C, Ferré S, Fuxe K, Franco R. Dopamine D1 and adenosine A1 receptors form functionally interacting heteromeric complexes. Proc Natl Acad Sci U S A. 2000 Jul 18;97(15):8606-11. doi: 10.1073/pnas.150241097. PMID: 10890919; PMCID: PMC26995.

Giompres P, Delis F. Dopamine transporters in the cerebellum of mutant mice. Cerebellum. 2005;4(2):105-11. doi: 10.1080/14734220510007851. PMID: 16035192.

Giorguieff MF, Kemel ML, Glowinski J. Presynaptic effect of L-glutamic acid on the release of dopamine in rat striatal slices. Neurosci Lett. 1977 Oct;6(1):73-7. doi: 10.1016/0304-3940(77)90068-4. PMID: 19605032.

Giros B, Caron MG. Molecular characterization of the dopamine transporter. Trends Pharmacol Sci. 1993 Feb;14(2):43-9. doi: 10.1016/0165-6147(93)90029-j. PMID: 8480373.

Giros B, el Mestikawy S, Bertrand L, Caron MG. Cloning and functional characterization of a cocaine-sensitive dopamine transporter. FEBS Lett. 1991 Dec 16;295(1-3):149-54. doi: 10.1016/0014-5793(91)81406-x. PMID: 1765147. (a)

Giros B, el Mestikawy S, Godinot N, Zheng K, Han H, Yang-Feng T, Caron MG. Cloning, pharmacological characterization, and chromosome assignment of the human dopamine transporter. Mol Pharmacol. 1992 Sep;42(3):383-90. PMID: 1406597.

Giros B, Jaber M, Jones SR, Wightman RM, Caron MG. Hyperlocomotion and indifference to cocaine and amphetamine in mice lacking the dopamine transporter. Nature. 1996 Feb 15;379(6566):606-12. doi: 10.1038/379606a0. PMID: 8628395.

Giros B, Martres MP, Pilon C, Sokoloff P, Schwartz JC. Shorter variants of the D3 dopamine receptor produced through various patterns of alternative splicing. Biochem Biophys Res Commun. 1991 May 15;176(3):1584-92. doi: 10.1016/0006-291x(91)90469-n. PMID: 2039532. (b)

Giros B, Sokoloff P, Martres MP, Riou JF, Emorine LJ, Schwartz JC. Alternative splicing directs the expression of two D2 dopamine receptor isoforms. Nature. 1989 Dec 21-28;342(6252):923-6. doi: 10.1038/342923a0. PMID: 2531847.

Gloriam DE, Fredriksson R, Schiöth HB. The G protein-coupled receptor subset of the rat genome. BMC Genomics. 2007 Sep 25;8:338. doi: 10.1186/1471-2164-8-338. PMID: 17892602; PMCID: PMC2117022.

Glowinski J, Chéramy A, Romo R, Barbeito L. Presynaptic regulation of dopaminergic transmission in the striatum. Cell Mol Neurobiol. 1988 Mar;8(1):7-17. doi: 10.1007/BF00712906. PMID: 2900072.

Godfrey N, Borgland SL. Diversity in the lateral hypothalamic input to the ventral tegmental area. Neuropharmacology. 2019 Aug;154:4-12. doi: 10.1016/j.neuropharm.2019.05.014. Epub 2019 May 16. PMID: 31103620.

Godfrey N, Borgland SL. Sex differences in the effect of acute fasting on excitatory and inhibitory synapses onto ventral tegmental area dopamine neurons. J Physiol. 2020 Dec;598(23):5523-5539. doi: 10.1113/JP280412. Epub 2020 Sep 18. PMID: 32886798.

Goelet P, Castellucci VF, Schacher S, Kandel ER. The long and the short of long-term memory--a molecular framework. Nature. 1986 Jul 31-Aug 6;322(6078):419-22. doi: 10.1038/322419a0. PMID: 2874497.

Goldberg LI. Cardiovascular and renal actions of dopamine: potential clinical applications. Pharmacol Rev. 1972 Mar;24(1):1-29. PMID: 4554480.

Goldman-Rakic PS. Cellular basis of working memory. Neuron. 1995 Mar;14(3):477-85. doi: 10.1016/0896-6273(95)90304-6. PMID: 7695894.

Goldstein DS, Holmes C. Neuronal source of plasma dopamine. Clin Chem. 2008 Nov;54(11):1864-71. doi: 10.1373/clinchem.2008.107193. Epub 2008 Sep 18. PMID: 18801936; PMCID: PMC2577013.

Goldstein M, Harada K, Meller E, Schalling M, Hokfelt T. Dopamine autoreceptors. Biochemical, pharmacological, and morphological studies. Ann N Y Acad Sci. 1990;604:169-75. doi: 10.1111/j.1749-6632.1990.tb31991.x. PMID: 1977346.

Gonzalez J, Jurado-Coronel JC, Ávila MF, Sabogal A, Capani F, Barreto GE. NMDARs in neurological diseases: a potential therapeutic target. Int J Neurosci. 2015 May;125(5):315-27. doi: 10.3109/00207454.2014.940941. Epub 2014 Jul 30. PMID: 25051426.

GOODALL M. Studies of adrenaline and noradrenaline in mammalian heart and suprarenals. Acta Physiol Scand Suppl. 1951;24(85):7-51. PMID: 14914571.

Goodman L, Baddeley D, Ambroziak W, Waites CL, Garner CC, Soeller C, Montgomery JM. N-terminal SAP97 isoforms differentially regulate synaptic structure and postsynaptic surface pools of AMPA receptors. Hippocampus. 2017 Jun;27(6):668-682. doi: 10.1002/hipo.22723. Epub 2017 Mar 20. PMID: 28244171.

Goodman OB Jr, Krupnick JG, Santini F, Gurevich VV, Penn RB, Gagnon AW, Keen JH, Benovic JL. Beta-arrestin acts as a clathrin adaptor in endocytosis of the beta2-adrenergic receptor. Nature. 1996 Oct 3;383(6599):447-50. doi: 10.1038/383447a0. PMID: 8837779.

Gower A, Tiberi M. The Intersection of Central Dopamine System and Stroke: Potential Avenues Aiming at Enhancement of Motor Recovery. Front Synaptic Neurosci. 2018 Jul 6;10:18. doi: 10.3389/fnsyn.2018.00018. PMID: 30034335; PMCID: PMC6043669.

Grace AA, Bunney BS. Intracellular and extracellular electrophysiology of nigral dopaminergic neurons--1. Identification and characterization. Neuroscience. 1983 Oct;10(2):301-15. doi: 10.1016/0306-4522(83)90135-5. PMID: 6633863.

Grace AA, Bunney BS. Nigral dopamine neurons: intracellular recording and identification with L-dopa injection and histofluorescence. Science. 1980 Nov 7;210(4470):654-6. doi: 10.1126/science.7433992. PMID: 7433992.

Grace AA, Bunney BS. The control of firing pattern in nigral dopamine neurons: single spike firing. J Neurosci. 1984 Nov;4(11):2866-76. doi: 10.1523/JNEUROSCI.04-11-02866.1984. PMID: 6150070; PMCID: PMC6564731. (a)

Grace AA, Bunney BS. The control of firing pattern in nigral dopamine neurons: burst firing. J Neurosci. 1984 Nov;4(11):2877-90. doi: 10.1523/JNEUROSCI.04-11-02877.1984. PMID: 6150071; PMCID: PMC6564720. (b)

Grace AA, Floresco SB, Goto Y, Lodge DJ. Regulation of firing of dopaminergic neurons and control of goal-directed behaviors. Trends Neurosci. 2007 May;30(5):220-7. doi: 10.1016/j.tins.2007.03.003. Epub 2007 Apr 2. PMID: 17400299.

Grace AA. Dysregulation of the dopamine system in the pathophysiology of schizophrenia and depression. Nat Rev Neurosci. 2016 Aug;17(8):524-32. doi: 10.1038/nrn.2016.57. Epub 2016 Jun 3. PMID: 27256556; PMCID: PMC5166560.

Grandy DK, Litt M, Allen L, Bunzow JR, Marchionni M, Makam H, Reed L, Magenis RE, Civelli O. The human dopamine D2 receptor gene is located on chromosome 11 at q22-q23 and identifies a TaqI RFLP. Am J Hum Genet. 1989 Nov;45(5):778-85. PMID: 2573278; PMCID: PMC1683432. (b)

Grandy DK, Marchionni MA, Makam H, Stofko RE, Alfano M, Frothingham L, Fischer JB, Burke-Howie KJ, Bunzow JR, Server AC, et al. Cloning of the cDNA and gene for a human D2 dopamine receptor. Proc Natl Acad Sci U S A. 1989 Dec;86(24):9762-6. doi: 10.1073/pnas.86.24.9762. PMID: 2532362; PMCID: PMC298581. (a)

Grandy DK, Zhang YA, Bouvier C, Zhou QY, Johnson RA, Allen L, Buck K, Bunzow JR, Salon J, Civelli O. Multiple human D5 dopamine receptor genes: a functional receptor and two pseudogenes. Proc Natl Acad Sci U S A. 1991 Oct 15;88(20):9175-9. doi: 10.1073/pnas.88.20.9175. PMID: 1833775; PMCID: PMC52675.

Grandy DK, Zhou QY, Allen L, Litt R, Magenis RE, Civelli O, Litt M. A human D1 dopamine receptor gene is located on chromosome 5 at q35.1 and identifies an EcoRI RFLP. Am J Hum Genet. 1990 Nov;47(5):828-34. PMID: 1977312; PMCID: PMC1683700.

Grattan DR. 60 YEARS OF NEUROENDOCRINOLOGY: The hypothalamo-prolactin axis. J Endocrinol. 2015 Aug;226(2):T101-22. doi: 10.1530/JOE-15-0213. Epub 2015 Jun 22. PMID: 26101377; PMCID: PMC4515538.

Gray DL, Allen JA, Mente S, O'Connor RE, DeMarco GJ, Efremov I, Tierney P, Volfson D, Davoren J, Guilmette E, Salafia M, Kozak R, Ehlers MD. Impaired β-arrestin recruitment and reduced desensitization by non-catechol agonists of the D1 dopamine receptor. Nat Commun. 2018 Feb 14;9(1):674. doi: 10.1038/s41467-017-02776-7. PMID: 29445200; PMCID: PMC5813016.

Graybiel AM. The basal ganglia. Curr Biol. 2000 Jul 13;10(14):R509-11. doi: 10.1016/s0960-9822(00)00593-5. PMID: 10899013.

Greba Q, Gifkins A, Kokkinidis L. Inhibition of amygdaloid dopamine D2 receptors impairs emotional learning measured with fear-potentiated startle. Brain Res. 2001 Apr 27;899(1-2):218-26. doi: 10.1016/s0006-8993(01)02243-0. PMID: 11311883.

GREENFIELD JG, BOSANQUET FD. The brain-stem lesions in Parkinsonism. J Neurol Neurosurg Psychiatry. 1953 Nov;16(4):213-26. doi: 10.1136/jnnp.16.4.213. PMID: 13109537; PMCID: PMC503142.

Greengard P. The neurobiology of dopamine signaling. Biosci Rep. 2001 Jun;21(3):247-69. doi: 10.1023/a:1013205230142. PMID: 11892993. (b)

Greengard P. The neurobiology of slow synaptic transmission. Science. 2001 Nov 2;294(5544):1024-30. doi: 10.1126/science.294.5544.1024. PMID: 11691979. (a)

Grillner S, Robertson B. The Basal Ganglia Over 500 Million Years. Curr Biol. 2016 Oct 24;26(20):R1088-R1100. doi: 10.1016/j.cub.2016.06.041. PMID: 27780050.

Grimes J, Koszegi Z, Lanoiselée Y, Miljus T, O'Brien SL, Stepniewski TM, Medel-Lacruz B, Baidya M, Makarova M, Mistry R, Goulding J, Drube J, Hoffmann C, Owen DM, Shukla AK, Selent J, Hill SJ, Calebiro D. Plasma membrane preassociation drives β-arrestin coupling to receptors and activation. Cell. 2023 May 11;186(10):2238-2255.e20. doi: 10.1016/j.cell.2023.04.018. Epub 2023 May 4. PMID: 37146613; PMCID: PMC7614532.

Groc L, Heine M, Cousins SL, Stephenson FA, Lounis B, Cognet L, Choquet D. NMDA receptor surface mobility depends on NR2A-2B subunits. Proc Natl Acad Sci U S A. 2006 Dec 5;103(49):18769-74. doi: 10.1073/pnas.0605238103. Epub 2006 Nov 21. PMID: 17124177; PMCID: PMC1693737.

Gu WH, Yang S, Shi WX, Jin GZ, Zhen XC. Requirement of PSD-95 for dopamine D1 receptor modulating glutamate NR1a/NR2B receptor function. Acta Pharmacol Sin. 2007 Jun;28(6):756-62. doi: 10.1111/j.1745-7254.2007.00557.x. PMID: 17506933.

Guarraci FA, Frohardt RJ, Falls WA, Kapp BS. The effects of intra-amygdaloid infusions of a D2 dopamine receptor antagonist on Pavlovian fear conditioning. Behav Neurosci. 2000 Jun;114(3):647-51. doi: 10.1037//0735-7044.114.3.647. PMID: 10883814.

Guarraci FA, Frohardt RJ, Kapp BS. Amygdaloid D1 dopamine receptor involvement in Pavlovian fear conditioning. Brain Res. 1999 May 8;827(1-2):28-40. doi: 10.1016/s0006-8993(99)01291-3. PMID: 10320690.

Guiard BP, El Mansari M, Merali Z, Blier P. Functional interactions between dopamine, serotonin and norepinephrine neurons: an in-vivo electrophysiological study in rats with monoaminergic lesions. Int J Neuropsychopharmacol. 2008 Aug;11(5):625-39. doi: 10.1017/S1461145707008383. Epub 2008 Jan 21. PMID: 18205979.

Guitart X, Moreno E, Rea W, Sánchez-Soto M, Cai NS, Quiroz C, Kumar V, Bourque L, Cortés A, Canela EI, Bishop C, Newman AH, Casadó V, Ferré S. Biased G Protein-Independent Signaling of Dopamine D_1-D_3 Receptor Heteromers in the Nucleus Accumbens. Mol Neurobiol. 2019 Oct;56(10):6756-6769. doi: 10.1007/s12035-019-1564-8. Epub 2019 Mar 27. PMID: 30919214; PMCID: PMC6728209.

Guitart X, Navarro G, Moreno E, Yano H, Cai NS, Sánchez-Soto M, Kumar-Barodia S, Naidu YT, Mallol J, Cortés A, Lluís C, Canela EI, Casadó V, McCormick PJ, Ferré S. Functional selectivity of allosteric interactions within G protein-coupled receptor oligomers: the dopamine D1-D3 receptor heterotetramer. Mol Pharmacol. 2014 Oct;86(4):417-29. doi: 10.1124/mol.114.093096. Epub 2014 Aug 5. PMID: 25097189; PMCID: PMC4164978.

Gupta S, Abd-Elrahman KS, Albaker A, Dunn HA, Ferguson SSG. Structural determinants governing β-arrestin2 interaction with PDZ proteins and recruitment to CRFR1. Cell Signal. 2019 Nov;63:109361. doi: 10.1016/j.cellsig.2019.109361. Epub 2019 Jul 22. PMID: 31344440.

Guzmán JN, Hernández A, Galarraga E, Tapia D, Laville A, Vergara R, Aceves J, Bargas J. Dopaminergic modulation of axon collaterals interconnecting spiny neurons of the rat striatum. J Neurosci. 2003 Oct 1;23(26):8931-40. doi: 10.1523/JNEUROSCI.23-26-08931.2003. PMID: 14523095; PMCID: PMC6740391.

Guzmán-Ramos K, Moreno-Castilla P, Castro-Cruz M, McGaugh JL, Martínez-Coria H, LaFerla FM, Bermúdez-Rattoni F. Restoration of dopamine release deficits during object recognition memory acquisition attenuates cognitive impairment in a triple transgenic mice model of Alzheimer's disease. Learn Mem. 2012 Sep 14;19(10):453-60. doi: 10.1101/lm.026070.112. PMID: 22984283.

Halpain S, Girault JA, Greengard P. Activation of NMDA receptors induces dephosphorylation of DARPP-32 in rat striatal slices. Nature. 1990 Jan 25;343(6256):369-72. doi: 10.1038/343369a0. PMID: 2153935.

Hamati R, Ahrens J, Shvetz C, Holahan MR, Tuominen L. 65 years of research on dopamine's role in classical fear conditioning and extinction: A systematic review. Eur J Neurosci. 2023 Oct 17:e16157. doi: 10.1111/ejn.16157. Epub ahead of print. PMID: 37848184.

Hammes GG, Rodbell M. Simple model for hormone-activated adenylate cyclase systems. Proc Natl Acad Sci U S A. 1976 Apr;73(4):1189-92. doi: 10.1073/pnas.73.4.1189. PMID: 4796; PMCID: PMC430226.

Hamon M, Blier P. Monoamine neurocircuitry in depression and strategies for new treatments. Prog Neuropsychopharmacol Biol Psychiatry. 2013 Aug 1;45:54-63. doi: 10.1016/j.pnpbp.2013.04.009. Epub 2013 Apr 19. PMID: 23602950.

Hasbi A, Madras BK, Bergman J, Kohut S, Lin Z, Withey SL, George SR. Δ-Tetrahydrocannabinol Increases Dopamine D1-D2 Receptor Heteromer and Elicits Phenotypic Reprogramming in Adult Primate Striatal Neurons. iScience. 2020 Jan 24;23(1):100794. doi: 10.1016/j.isci.2019.100794. Epub 2019 Dec 24. PMID: 31972514; PMCID: PMC6971351. (b)

Hasbi A, O'Dowd BF, George SR. Heteromerization of dopamine D2 receptors with dopamine D1 or D5 receptors generates intracellular calcium signaling by different mechanisms. Curr Opin Pharmacol. 2010 Feb;10(1):93-9. doi: 10.1016/j.coph.2009.09.011. Epub 2009 Nov 10. PMID: 19897420; PMCID: PMC2818238.

Hasbi A, Perreault ML, Shen MYF, Fan T, Nguyen T, Alijaniaram M, Banasikowski TJ, Grace AA, O'Dowd BF, Fletcher PJ, George SR. Activation of Dopamine D1-D2 Receptor Complex Attenuates Cocaine Reward and Reinstatement of Cocaine-Seeking through Inhibition of DARPP-32, ERK, and ΔFosB. Front Pharmacol. 2018 Jan 4;8:924. doi: 10.3389/fphar.2017.00924. PMID: 29354053; PMCID: PMC5758537.

Hasbi A, Sivasubramanian M, Milenkovic M, Komarek K, Madras BK, George SR. Dopamine D1-D2 receptor heteromer expression in key brain regions of rat and higher species: Upregulation in rat striatum after cocaine administration. Neurobiol Dis. 2020 Sep;143:105017. doi: 10.1016/j.nbd.2020.105017. Epub 2020 Jul 14. PMID: 32679312; PMCID: PMC7450246. (a)

Hassani OK, Cromwell HC, Schultz W. Influence of expectation of different rewards on behavior-related neuronal activity in the striatum. J Neurophysiol. 2001 Jun;85(6):2477-89. doi: 10.1152/jn.2001.85.6.2477. PMID: 11387394.

Hauser AS, Chavali S, Masuho I, Jahn LJ, Martemyanov KA, Gloriam DE, Babu MM. Pharmacogenomics of GPCR Drug Targets. Cell. 2018 Jan 11;172(1-2):41-54.e19. doi: 10.1016/j.cell.2017.11.033. Epub 2017 Dec 14. PMID: 29249361; PMCID: PMC5766829.

Hayashizaki S, Hirai S, Ito Y, Honda Y, Arime Y, Sora I, Okado H, Kodama T, Takada M. Methamphetamine increases locomotion and dopamine transporter activity in dopamine d5 receptor-deficient mice. PLoS One. 2013 Oct 14;8(10):e75975. doi: 10.1371/journal.pone.0075975. PMID: 24155877; PMCID: PMC3796526.

Hemmings HC Jr, Greengard P, Tung HY, Cohen P. DARPP-32, a dopamine-regulated neuronal phosphoprotein, is a potent inhibitor of protein phosphatase-1. Nature. 1984 Aug 9-15;310(5977):503-5. doi: 10.1038/310503a0. PMID: 6087160.

Hermans E. Biochemical and pharmacological control of the multiplicity of coupling at G-protein-coupled receptors. Pharmacol Ther. 2003 Jul;99(1):25-44. doi: 10.1016/s0163-7258(03)00051-2. PMID: 12804697.

Hernández A, Ibáñez-Sandoval O, Sierra A, Valdiosera R, Tapia D, Anaya V, Galarraga E, Bargas J, Aceves J. Control of the subthalamic innervation of the rat globus pallidus by D2/3 and D4 dopamine receptors. J Neurophysiol. 2006 Dec;96(6):2877-88. doi: 10.1152/jn.00664.2006. Epub 2006 Aug 9. PMID: 16899633.

Hernandez-Lopez S, Tkatch T, Perez-Garci E, Galarraga E, Bargas J, Hamm H, Surmeier DJ. D2 dopamine receptors in striatal medium spiny neurons reduce L-type Ca2+ currents and excitability via a novel PLC[beta]1-IP3-calcineurin-signaling cascade. J Neurosci. 2000 Dec 15;20(24):8987-95. doi: 10.1523/JNEUROSCI.20-24-08987.2000. PMID: 11124974; PMCID: PMC6773013.

Hersch SM, Ciliax BJ, Gutekunst CA, Rees HD, Heilman CJ, Yung KK, Bolam JP, Ince E, Yi H, Levey AI. Electron microscopic analysis of D1 and D2 dopamine receptor proteins in the dorsal striatum and their synaptic relationships with motor corticostriatal afferents. J Neurosci. 1995 Jul;15(7 Pt 2):5222-37. doi: 10.1523/JNEUROSCI.15-07-05222.1995. PMID: 7623147; PMCID: PMC6577913.

Hervé D, Lévi-Strauss M, Marey-Semper I, Verney C, Tassin JP, Glowinski J, Girault JA. G(olf) and Gs in rat basal ganglia: possible involvement of G(olf) in the coupling of dopamine D1 receptor with adenylyl cyclase. J Neurosci. 1993 May;13(5):2237-48. doi: 10.1523/JNEUROSCI.13-05-02237.1993. PMID: 8478697; PMCID: PMC6576551.

Heskje J, Heslin K, De Corte BJ, Walsh KP, Kim Y, Han S, Carlson ES, Parker KL. Cerebellar D1DR-expressing neurons modulate the frontal cortex during timing tasks. Neurobiol Learn Mem. 2020 Apr;170:107067. doi: 10.1016/j.nlm.2019.107067. Epub 2019 Aug 9. PMID: 31404656; PMCID: PMC7007827.

HESS SM, CONNAMACHER RH, OZAKI M, UDENFRIEND S. The effects of alpha-methyl-DOPA and alpha-methyl-metatyrosine on the metabolism of norepinephrine and serotonin in vivo. J Pharmacol Exp Ther. 1961 Nov;134:129-38. PMID: 13907002.

Heydorn A, Søndergaard BP, Hadrup N, Holst B, Haft CR, Schwartz TW. Distinct in vitro interaction pattern of dopamine receptor subtypes with adaptor proteins involved in post-endocytotic receptor targeting. FEBS Lett. 2004 Jan 2;556(1-3):276-80. doi: 10.1016/s0014-5793(03)01431-5. PMID: 14706863.

Hilger D, Masureel M, Kobilka BK. Structure and dynamics of GPCR signaling complexes. Nat Struct Mol Biol. 2018 Jan;25(1):4-12. doi: 10.1038/s41594-017-0011-7. Epub 2018 Jan 8. PMID: 29323277; PMCID: PMC6535338.

Hinshaw JE, Schmid SL. Dynamin self-assembles into rings suggesting a mechanism for coated vesicle budding. Nature. 1995 Mar 9;374(6518):190-2. doi: 10.1038/374190a0. PMID: 7877694.

Hnasko TS, Chuhma N, Zhang H, Goh GY, Sulzer D, Palmiter RD, Rayport S, Edwards RH. Vesicular glutamate transport promotes dopamine storage and glutamate corelease in vivo. Neuron. 2010 Mar 11;65(5):643-56. doi: 10.1016/j.neuron.2010.02.012. PMID: 20223200; PMCID: PMC2846457.

Hollerman JR, Schultz W. Dopamine neurons report an error in the temporal prediction of reward during learning. Nat Neurosci. 1998 Aug;1(4):304-9. doi: 10.1038/1124. PMID: 10195164.

Hollerman JR, Tremblay L, Schultz W. Influence of reward expectation on behavior-related neuronal activity in primate striatum. J Neurophysiol. 1998 Aug;80(2):947-63. doi: 10.1152/jn.1998.80.2.947. PMID: 9705481.

Hollon TR, Bek MJ, Lachowicz JE, Ariano MA, Mezey E, Ramachandran R, Wersinger SR, Soares-da-Silva P, Liu ZF, Grinberg A, Drago J, Young WS 3rd, Westphal H, Jose PA, Sibley DR. Mice lacking D5 dopamine receptors have increased sympathetic tone and are hypertensive. J Neurosci. 2002 Dec 15;22(24):10801-10. doi: 10.1523/JNEUROSCI.22-24-10801.2002. PMID: 12486173; PMCID: PMC6758465.

Hollon TR, Bek MJ, Lachowicz JE, Ariano MA, Mezey E, Ramachandran R, Wersinger SR, Soares-da-Silva P, Liu ZF, Grinberg A, Drago J, Young WS 3rd, Westphal H, Jose PA, Sibley DR. Mice lacking D5 dopamine receptors have increased sympathetic tone and are hypertensive. J Neurosci. 2002 Dec 15;22(24):10801-10. doi: 10.1523/JNEUROSCI.22-24-10801.2002. PMID: 12486173; PMCID: PMC6758465.

Holmes A, Hollon TR, Gleason TC, Liu Z, Dreiling J, Sibley DR, Crawley JN. Behavioral characterization of dopamine D5 receptor null mutant mice. Behav Neurosci. 2001 Oct;115(5):1129-44. PMID: 11584926.

Holmes A, Lachowicz JE, Sibley DR. Phenotypic analysis of dopamine receptor knockout mice; recent insights into the functional specificity of dopamine receptor subtypes. Neuropharmacology. 2004 Dec;47(8):1117-34. doi: 10.1016/j.neuropharm.2004.07.034. PMID: 15567422.

Holstege JC, Van Dijken H, Buijs RM, Goedknegt H, Gosens T, Bongers CM. Distribution of dopamine immunoreactivity in the rat, cat and monkey spinal cord. J Comp Neurol. 1996 Dec 23;376(4):631-52. doi: 10.1002/(SICI)1096-9861(19961223)376:4<631::AID-CNE10>3.0.CO;2-P. PMID: 8978475.

Holtz P, Heise R, Lüdtke K. Fermentative degradation of l-dioxyphenylalanine (dopa) by kidney. Naunyn-Schmiedeberg's Archives of Pharmacology. 1938;191:87–118.

Hood S, Cassidy P, Cossette MP, Weigl Y, Verwey M, Robinson B, Stewart J, Amir S. Endogenous dopamine regulates the rhythm of expression of the clock protein PER2 in the rat dorsal striatum via daily activation of D2 dopamine receptors. J Neurosci. 2010 Oct 20;30(42):14046-58. doi: 10.1523/JNEUROSCI.2128-10.2010. PMID: 20962226; PMCID: PMC6634752.

Hornykiewicz O. Dopamine (3-hydroxytyramine) and brain function. Pharmacol Rev. 1966 Jun;18(2):925-64. PMID: 5328389.

Hornykiewicz O. Dopamine miracle: from brain homogenate to dopamine replacement. Mov Disord. 2002 May;17(3):501-8. doi: 10.1002/mds.10115. PMID: 12112197.

HORNYKIEWICZ O. The action of dopamine on the arterial blood pressure of the guinea-pig. Br J Pharmacol Chemother. 1958 Mar;13(1):91-4. doi: 10.1111/j.1476-5381.1958.tb00197.x. PMID: 13523142; PMCID: PMC1481693.

Hornykiewicz O. The mechanisms of action of L-dopa in Parkinson's disease. Life Sci. 1974 Oct 1;15(7):1249-59. doi: 10.1016/0024-3205(74)90306-3. PMID: 4620977.

Howard MA, Elias GM, Elias LA, Swat W, Nicoll RA. The role of SAP97 in synaptic glutamate receptor dynamics. Proc Natl Acad Sci U S A. 2010 Feb 23;107(8):3805-10. doi: 10.1073/pnas.0914422107. Epub 2010 Feb 3. PMID: 20133708; PMCID: PMC2840522.

Hu LA, Chen W, Premont RT, Cong M, Lefkowitz RJ. G protein-coupled receptor kinase 5 regulates beta 1-adrenergic receptor association with PSD-95. J Biol Chem. 2002 Jan 11;277(2):1607-13. doi: 10.1074/jbc.M107297200. Epub 2001 Nov 7. PMID: 11700307.

Hu LA, Tang Y, Miller WE, Cong M, Lau AG, Lefkowitz RJ, Hall RA. beta 1-adrenergic receptor association with PSD-95. Inhibition of receptor internalization and facilitation of beta 1-adrenergic receptor interaction with N-methyl-D-aspartate receptors. J Biol Chem. 2000 Dec 8;275(49):38659-66. doi: 10.1074/jbc.M005938200. PMID: 10995758.

Huang Y, Qiu AW, Peng YP, Liu Y, Huang HW, Qiu YH. Roles of dopamine receptor subtypes in mediating modulation of T lymphocyte function. Neuro Endocrinol Lett. 2010;31(6):782-91. PMID: 21196914.

Huang YY, Kandel ER. D1/D5 receptor agonists induce a protein synthesis-dependent late potentiation in the CA1 region of the hippocampus. Proc Natl Acad Sci U S A. 1995 Mar 28;92(7):2446-50. doi: 10.1073/pnas.92.7.2446. PMID: 7708662; PMCID: PMC42234.

Huang YY, Simpson E, Kellendonk C, Kandel ER. Genetic evidence for the bidirectional modulation of synaptic plasticity in the prefrontal cortex by D1 receptors. Proc Natl Acad Sci U S A. 2004 Mar 2;101(9):3236-41. doi: 10.1073/pnas.0308280101. Epub 2004 Feb 23. PMID: 14981263; PMCID: PMC365773.

Huck JH, Freyer D, Böttcher C, Mladinov M, Muselmann-Genschow C, Thielke M, Gladow N, Bloomquist D, Mergenthaler P, Priller J. De novo expression of dopamine D2 receptors on microglia after stroke. J Cereb Blood Flow Metab. 2015 Nov;35(11):1804-11. doi: 10.1038/jcbfm.2015.128. Epub 2015 Jun 24. PMID: 26104289; PMCID: PMC4635235.

Huntley GW, Morrison JH, Prikhozhan A, Sealfon SC. Localization of multiple dopamine receptor subtype mRNAs in human and monkey motor cortex and striatum. Brain Res Mol Brain Res. 1992 Oct;15(3-4):181-8. doi: 10.1016/0169-328x(92)90107-m. PMID: 1331674.

Ibañez-Sandoval O, Hernández A, Florán B, Galarraga E, Tapia D, Valdiosera R, Erlij D, Aceves J, Bargas J. Control of the subthalamic innervation of substantia nigra pars reticulata by D1 and D2 dopamine receptors. J Neurophysiol. 2006 Mar;95(3):1800-11. doi: 10.1152/jn.01074.2005. Epub 2005 Nov 23. PMID: 16306171.

Ibáñez-Sandoval O, Tecuapetla F, Unal B, Shah F, Koós T, Tepper JM. Electrophysiological and morphological characteristics and synaptic connectivity of tyrosine hydroxylase-expressing neurons in adult mouse striatum. J Neurosci. 2010 May 19;30(20):6999-7016. doi: 10.1523/JNEUROSCI.5996-09.2010. PMID: 20484642; PMCID: PMC4447206.

Ibrahim KS, El Mestikawy S, Abd-Elrahman KS, Ferguson SSG. VGLUT3 Ablation Differentially Modulates Glutamate Receptor Densities in Mouse Brain. eNeuro. 2022 May 9;9(3):ENEURO.0041-22.2022. doi: 10.1523/ENEURO.0041-22.2022. PMID: 35443989; PMCID: PMC9087739.

Ikai Y, Takada M, Shinonaga Y, Mizuno N. Dopaminergic and non-dopaminergic neurons in the ventral tegmental area of the rat project, respectively, to the cerebellar cortex and deep cerebellar nuclei. Neuroscience. 1992 Dec;51(3):719-28. doi: 10.1016/0306-4522(92)90310-x. PMID: 1362601.

Ikemoto K, Kitahama K, Nishimura A, Jouvet A, Nishi K, Arai R, Jouvet M, Nagatsu I. Tyrosine hydroxylase and aromatic L-amino acid decarboxylase do not coexist in neurons in the human anterior cingulate cortex. Neurosci Lett. 1999 Jul 2;269(1):37-40. doi: 10.1016/s0304-3940(99)00409-7. PMID: 10821639.

Imbesi M, Yildiz S, Dirim Arslan A, Sharma R, Manev H, Uz T. Dopamine receptor-mediated regulation of neuronal "clock" gene expression. Neuroscience. 2009 Jan 23;158(2):537-44. doi: 10.1016/j.neuroscience.2008.10.044. Epub 2008 Nov 5. PMID: 19017537; PMCID: PMC3664916.

Inoue A, Raimondi F, Kadji FMN, Singh G, Kishi T, Uwamizu A, Ono Y, Shinjo Y, Ishida S, Arang N, Kawakami K, Gutkind JS, Aoki J, Russell RB. Illuminating G-Protein-Coupling Selectivity of GPCRs. Cell. 2019 Jun 13;177(7):1933-1947.e25. doi: 10.1016/j.cell.2019.04.044. Epub 2019 May 31. PMID: 31160049; PMCID: PMC6773469.

Irie M, Hata Y, Takeuchi M, Ichtchenko K, Toyoda A, Hirao K, Takai Y, Rosahl TW, Südhof TC. Binding of neuroligins to PSD-95. Science. 1997 Sep 5;277(5331):1511-5. doi: 10.1126/science.277.5331.1511. PMID: 9278515.

Ito R, Dalley JW, Howes SR, Robbins TW, Everitt BJ. Dissociation in conditioned dopamine release in the nucleus accumbens core and shell in response to cocaine cues and during cocaine-seeking behavior in rats. J Neurosci. 2000 Oct 1;20(19):7489-95. doi: 10.1523/JNEUROSCI.20-19-07489.2000. PMID: 11007908; PMCID: PMC6772761.

Ito R, Dalley JW, Robbins TW, Everitt BJ. Dopamine release in the dorsal striatum during cocaine-seeking behavior under the control of a drug-associated cue. J Neurosci. 2002 Jul 15;22(14):6247-53. doi: 10.1523/JNEUROSCI.22-14-06247.2002. PMID: 12122083; PMCID: PMC6757945.

Iversen LL. Dopamine receptors in the brain. Science. 1975 Jun 13;188(4193):1084-9. doi: 10.1126/science.2976. PMID: 2976.

Iversen SD, Iversen LL. Dopamine: 50 years in perspective. Trends Neurosci. 2007 May;30(5):188-93. doi: 10.1016/j.tins.2007.03.002. Epub 2007 Mar 26. PMID: 17368565.

Iwasiow RM, Nantel MF, Tiberi M. Delineation of the structural basis for the activation properties of the dopamine D1 receptor subtypes. J Biol Chem. 1999 Nov 5;274(45):31882-90. doi: 10.1074/jbc.274.45.31882. PMID: 10542214.

Jaber M, Koch WJ, Rockman H, Smith B, Bond RA, Sulik KK, Ross J Jr, Lefkowitz RJ, Caron MG, Giros B. Essential role of beta-adrenergic receptor kinase 1 in cardiac development and function. Proc Natl Acad Sci U S A. 1996 Nov 12;93(23):12974-9. doi: 10.1073/pnas.93.23.12974. PMID: 8917529; PMCID: PMC24031. (b)

Jaber M, Robinson SW, Missale C, Caron MG. Dopamine receptors and brain function. Neuropharmacology. 1996;35(11):1503-19. doi: 10.1016/s0028-3908(96)00100-1. PMID: 9025098. (a)

Jackson A, Iwasiow RM, Chaar ZY, Nantel MF, Tiberi M. Homologous regulation of the heptahelical D1A receptor responsiveness: specific cytoplasmic tail regions mediate dopamine-induced phosphorylation, desensitization and endocytosis. J Neurochem. 2002 Aug;82(3):683-97. doi: 10.1046/j.1471-4159.2002.01001.x. PMID: 12153492.

Jackson A, Iwasiow RM, Tiberi M. Distinct function of the cytoplasmic tail in human D1-like receptor ligand binding and coupling. FEBS Lett. 2000 Mar 24;470(2):183-8. doi: 10.1016/s0014-5793(00)01315-6. PMID: 10734231.

Jackson A, Sedaghat K, Minerds K, James C, Tiberi M. Opposing effects of phorbol-12-myristate-13-acetate, an activator of protein kinase C, on the signaling of structurally related human dopamine D1 and D5 receptors. J Neurochem. 2005 Dec;95(5):1387-400. doi: 10.1111/j.1471-4159.2005.03476.x. PMID: 16313517.

Jackson-Lewis V, Blesa J, Przedborski S. Animal models of Parkinson's disease. Parkinsonism Relat Disord. 2012 Jan;18 Suppl 1:S183-5. doi: 10.1016/S1353-8020(11)70057-8. PMID: 22166429.

Javoy F, Glowinski J. Dynamic characteristic of the 'functional compartment' of dopamine in dopaminergic terminals of the rat striatum. J Neurochem. 1971 Jul;18(7):1305-11. doi: 10.1111/j.1471-4159.1971.tb00230.x. PMID: 4399114.

Jin LQ, Goswami S, Cai G, Zhen X, Friedman E. SKF83959 selectively regulates phosphatidylinositol-linked D1 dopamine receptors in rat brain. J Neurochem. 2003 Apr;85(2):378-86. doi: 10.1046/j.1471-4159.2003.01698.x. PMID: 12675914.

Johnson PM, Kenny PJ. Dopamine D2 receptors in addiction-like reward dysfunction and compulsive eating in obese rats. Nat Neurosci. 2010 May;13(5):635-41. doi: 10.1038/nn.2519. Epub 2010 Mar 28. PMID: 20348917; PMCID: PMC2947358.

Jones CA, Watson DJ, Fone KC. Animal models of schizophrenia. Br J Pharmacol. 2011 Oct;164(4):1162-94. doi: 10.1111/j.1476-5381.2011.01386.x. PMID: 21449915; PMCID: PMC3229756.

Jones SR, Gainetdinov RR, Wightman RM, Caron MG. Mechanisms of amphetamine action revealed in mice lacking the dopamine transporter. J Neurosci. 1998 Mar 15;18(6):1979-86. doi: 10.1523/JNEUROSCI.18-06-01979.1998. PMID: 9482784; PMCID: PMC6792915.

Jones-Tabah J, Martin RD, Tanny JC, Clarke PBS, Hébert TE. High-Content Single-Cell Förster Resonance Energy Transfer Imaging of Cultured Striatal Neurons Reveals Novel Cross-Talk in the Regulation of Nuclear Signaling by Protein Kinase A and Extracellular Signal-Regulated Kinase 1/2. Mol Pharmacol. 2021 Dec;100(6):526-539. doi: 10.1124/molpharm.121.000290. Epub 2021 Sep 9. PMID: 34503973.

Jones-Tabah J, Mohammad H, Hadj-Youssef S, Kim LEH, Martin RD, Benaliouad F, Tanny JC, Clarke PBS, Hébert TE. Dopamine D1 receptor signalling in dyskinetic Parkinsonian rats revealed by fiber photometry using FRET-based biosensors. Sci Rep. 2020 Sep 2;10(1):14426. doi: 10.1038/s41598-020-71121-8. PMID: 32879346; PMCID: PMC7468292.

Jones-Tabah J, Mohammad H, Paulus EG, Clarke PBS, Hébert TE. The Signaling and Pharmacology of the Dopamine D1 Receptor. Front Cell Neurosci. 2022 Jan 17;15:806618. doi: 10.3389/fncel.2021.806618. PMID: 35110997; PMCID: PMC8801442.

Jose PA, Eisner GM, Felder RA. Regulation of blood pressure by dopamine receptors. Nephron Physiol. 2003;95(2):p19-27. doi: 10.1159/000073676. PMID: 14610323.

Jose PA, Eisner GM, Felder RA. Renal dopamine and sodium homeostasis. Curr Hypertens Rep. 2000 Apr;2(2):174-83. doi: 10.1007/s11906-000-0079-y. PMID: 10981146.

Jose PA, Eisner GM, Felder RA. Renal dopamine receptors in health and hypertension. Pharmacol Ther. 1998 Nov;80(2):149-82. doi: 10.1016/s0163-7258(98)00027-8. PMID: 9839770.

Jose PA, Raymond JR, Bates MD, Aperia A, Felder RA, Carey RM. The renal dopamine receptors. J Am Soc Nephrol. 1992 Feb;2(8):1265-78. doi: 10.1681/ASN.V281265. PMID: 1627751.

Jose PA, Soares-da-Silva P, Eisner GM, Felder RA. Dopamine and G protein-coupled receptor kinase 4 in the kidney: role in blood pressure regulation. Biochim Biophys Acta. 2010 Dec;1802(12):1259-67. doi: 10.1016/j.bbadis.2010.02.004. Epub 2010 Feb 12. PMID: 20153824; PMCID: PMC2892632.

Joseph JD, Wang YM, Miles PR, Budygin EA, Picetti R, Gainetdinov RR, Caron MG, Wightman RM. Dopamine autoreceptor regulation of release and uptake in mouse brain slices in the absence of D(3) receptors. Neuroscience. 2002;112(1):39-49. doi: 10.1016/s0306-4522(02)00067-2. PMID: 12044470.

Juhasz JR, Hasbi A, Rashid AJ, So CH, George SR, O'Dowd BF. Mu-opioid receptor heterooligomer formation with the dopamine D1 receptor as directly visualized in living cells. Eur J Pharmacol. 2008 Mar 10;581(3):235-43. doi: 10.1016/j.ejphar.2007.11.060. Epub 2007 Dec 14. PMID: 18237729.

Kabbani N, Negyessy L, Lin R, Goldman-Rakic P, Levenson R. Interaction with neuronal calcium sensor NCS-1 mediates desensitization of the D2 dopamine receptor. J Neurosci. 2002 Oct 1;22(19):8476-86. doi: 10.1523/JNEUROSCI.22-19-08476.2002. PMID: 12351722; PMCID: PMC6757796.

Kahsai AW, Pani B, Lefkowitz RJ. GPCR signaling: conformational activation of arrestins. Cell Res. 2018 Aug;28(8):783-784. doi: 10.1038/s41422-018-0067-x. PMID: 30030517; PMCID: PMC6082894.

Kalén P, Skagerberg G, Lindvall O. Projections from the ventral tegmental area and mesencephalic raphe to the dorsal raphe nucleus in the rat. Evidence for a minor dopaminergic component. Exp Brain Res. 1988;73(1):69-77. doi: 10.1007/BF00279662. PMID: 3208862.

Kalia LV, Salter MW. Interactions between Src family protein tyrosine kinases and PSD-95. Neuropharmacology. 2003 Nov;45(6):720-8. doi: 10.1016/s0028-3908(03)00313-7. PMID: 14529711.

Kamberi IA, Mical RS, Porter JC. Prolactin-inhibiting activity in hypophysial stalk blood and elevation by dopamine. Experientia. 1970 Oct 15;26(10):1150-1. doi: 10.1007/BF02112730. PMID: 5483776.

Kandel ER, Schwartz JH. Molecular biology of learning: modulation of transmitter release. Science. 1982 Oct 29;218(4571):433-43. doi: 10.1126/science.6289442. PMID: 6289442.

Kang Y, Zhou XE, Gao X, He Y, Liu W, Ishchenko A, Barty A, White TA, Yefanov O, Han GW, Xu Q, de Waal PW, Ke J, Tan MH, Zhang C, Moeller A, West GM, Pascal BD, Van Eps N, Caro LN, Vishnivetskiy SA, Lee RJ, Suino-Powell KM, Gu X, Pal K, Ma J, Zhi X, Boutet S, Williams GJ, Messerschmidt M, Gati C, Zatsepin NA, Wang D, James D, Basu S, Roy-Chowdhury S, Conrad CE, Coe J, Liu H, Lisova S, Kupitz C, Grotjohann I, Fromme R, Jiang Y, Tan M, Yang H, Li J, Wang M, Zheng Z, Li D, Howe N, Zhao Y, Standfuss J, Diederichs K, Dong Y, Potter CS, Carragher B, Caffrey M, Jiang H, Chapman HN, Spence JC, Fromme P, Weierstall U, Ernst OP, Katritch V, Gurevich VV, Griffin PR, Hubbell WL, Stevens RC, Cherezov V, Melcher K, Xu HE. Crystal structure of rhodopsin bound to arrestin by femtosecond X-ray laser. Nature. 2015 Jul 30;523(7562):561-7. doi: 10.1038/nature14656. Epub 2015 Jul 22. PMID: 26200343; PMCID: PMC4521999.

Karlsson RM, Hefner KR, Sibley DR, Holmes A. Comparison of dopamine D1 and D5 receptor knockout mice for cocaine locomotor sensitization. Psychopharmacology (Berl). 2008 Sep;200(1):117-27. doi: 10.1007/s00213-008-1165-0. Epub 2008 Jul 4. PMID: 18600316; PMCID: PMC2586326.

Katz B, Miledi R. Further study of the role of calcium in synaptic transmission. J Physiol. 1970 May;207(3):789-801. doi: 10.1113/jphysiol.1970.sp009095. PMID: 5499746; PMCID: PMC1348742.

Katz B, Miledi R. Ionic requirements of synaptic transmitter release. Nature. 1967 Aug 5;215(5101):651. doi: 10.1038/215651a0. PMID: 4292912.

Katz JL, Chausmer AL, Elmer GI, Rubinstein M, Low MJ, Grandy DK. Cocaine-induced locomotor activity and cocaine discrimination in dopamine D4 receptor mutant mice. Psychopharmacology (Berl). 2003 Oct;170(1):108-14. doi: 10.1007/s00213-003-1513-z. Epub 2003 May 29. PMID: 12783155.

Kawaguchi Y. Physiological, morphological, and histochemical characterization of three classes of interneurons in rat neostriatum. J Neurosci. 1993 Nov;13(11):4908-23. doi: 10.1523/JNEUROSCI.13-11-04908.1993. PMID: 7693897; PMCID: PMC6576359.

Kaya AI, Perry NA, Gurevich VV, Iverson TM. Phosphorylation barcode-dependent signal bias of the dopamine D1 receptor. Proc Natl Acad Sci U S A. 2020 Jun 23;117(25):14139-14149. doi: 10.1073/pnas.1918736117. Epub 2020 Jun 5. PMID: 32503917; PMCID: PMC7321966.

Kebabian JW, Calne DB. Multiple receptors for dopamine. Nature. 1979 Jan 11;277(5692):93-6. doi: 10.1038/277093a0. PMID: 215920.

Kebabian JW, Greengard P. Dopamine-sensitive adenyl cyclase: possible role in synaptic transmission. Science. 1971 Dec 24;174(4016):1346-9. doi: 10.1126/science.174.4016.1346. PMID: 4332627.

Kebabian JW, Petzold GL, Greengard P. Dopamine-sensitive adenylate cyclase in caudate nucleus of rat brain, and its similarity to the "dopamine receptor". Proc Natl Acad Sci U S A. 1972 Aug;69(8):2145-9. doi: 10.1073/pnas.69.8.2145. PMID: 4403305; PMCID: PMC426888.

Keene AC, Waddell S. Drosophila memory: dopamine signals punishment? Curr Biol. 2005 Nov 22;15(22):R932-4. doi: 10.1016/j.cub.2005.10.058. PMID: 16303554.

Kehr W, Carlsson A, Lindqvist M, Magnusson T, Atack C. Evidence for a receptor-mediated feedback control of striatal tyrosine hydroxylase activity. J Pharm Pharmacol. 1972 Sep;24(9):744-7. doi: 10.1111/j.2042-7158.1972.tb09104.x. PMID: 4404084.

Kelly MA, Rubinstein M, Asa SL, Zhang G, Saez C, Bunzow JR, Allen RG, Hnasko R, Ben-Jonathan N, Grandy DK, Low MJ. Pituitary lactotroph hyperplasia and chronic hyperprolactinemia in dopamine D2 receptor-deficient mice. Neuron. 1997 Jul;19(1):103-13. doi: 10.1016/s0896-6273(00)80351-7. PMID: 9247267.

Kelly RB. Storage and release of neurotransmitters. Cell. 1993 Jan;72 Suppl:43-53. doi: 10.1016/s0092-8674(05)80027-3. PMID: 8094036.

Kempadoo KA, Mosharov EV, Choi SJ, Sulzer D, Kandel ER. Dopamine release from the locus coeruleus to the dorsal hippocampus promotes spatial learning and memory. Proc Natl Acad Sci U S A. 2016 Dec 20;113(51):14835-14840. doi: 10.1073/pnas.1616515114. Epub 2016 Dec 7. PMID: 27930324; PMCID: PMC5187750.

Kennedy MB. Synaptic Signaling in Learning and Memory. Cold Spring Harb Perspect Biol. 2013 Dec 30;8(2):a016824. doi: 10.1101/cshperspect.a016824. PMID: 24379319; PMCID: PMC4743082.

Kennedy MJ, Ehlers MD. Organelles and trafficking machinery for postsynaptic plasticity. Annu Rev Neurosci. 2006;29:325-62. doi: 10.1146/annurev.neuro.29.051605.112808. PMID: 16776589; PMCID: PMC1876664.

Kesby JP, Eyles DW, McGrath JJ, Scott JG. Dopamine, psychosis and schizophrenia: the widening gap between basic and clinical neuroscience. Transl Psychiatry. 2018 Jan 31;8(1):30. doi: 10.1038/s41398-017-0071-9. PMID: 29382821; PMCID: PMC5802623.

Khan ZU, Gutiérrez A, Martín R, Peñafiel A, Rivera A, de la Calle A. Dopamine D5 receptors of rat and human brain. Neuroscience. 2000;100(4):689-99. doi: 10.1016/s0306-4522(00)00274-8. PMID: 11036203.

Khan ZU, Koulen P, Rubinstein M, Grandy DK, Goldman-Rakic PS. An astroglia-linked dopamine D2-receptor action in prefrontal cortex. Proc Natl Acad Sci U S A. 2001 Feb 13;98(4):1964-9. doi: 10.1073/pnas.98.4.1964. PMID: 11172059; PMCID: PMC29365.

Khan ZU, Mrzljak L, Gutierrez A, de la Calle A, Goldman-Rakic PS. Prominence of the dopamine D2 short isoform in dopaminergic pathways. Proc Natl Acad Sci U S A. 1998 Jun 23;95(13):7731-6. doi: 10.1073/pnas.95.13.7731. PMID: 9636219; PMCID: PMC22740.

Kilty JE, Lorang D, Amara SG. Cloning and expression of a cocaine-sensitive rat dopamine transporter. Science. 1991 Oct 25;254(5031):578-9. doi: 10.1126/science.1948035. PMID: 1948035.

Kim E, Cho KO, Rothschild A, Sheng M. Heteromultimerization and NMDA receptor-clustering activity of Chapsyn-110, a member of the PSD-95 family of proteins. Neuron. 1996 Jul;17(1):103-13. doi: 10.1016/s0896-6273(00)80284-6. PMID: 8755482.

Kim E, Niethammer M, Rothschild A, Jan YN, Sheng M. Clustering of Shaker-type K+ channels by interaction with a family of membrane-associated guanylate kinases. Nature. 1995 Nov 2;378(6552):85-8. doi: 10.1038/378085a0. PMID: 7477295.

Kim E, Sheng M. PDZ domain proteins of synapses. Nat Rev Neurosci. 2004 Oct;5(10):771-81. doi: 10.1038/nrn1517. PMID: 15378037.

Kim JH, Liao D, Lau LF, Huganir RL. SynGAP: a synaptic RasGAP that associates with the PSD-95/SAP90 protein family. Neuron. 1998 Apr;20(4):683-91. doi: 10.1016/s0896-6273(00)81008-9. PMID: 9581761.

Kim KM, Valenzano KJ, Robinson SR, Yao WD, Barak LS, Caron MG. Differential regulation of the dopamine D2 and D3 receptors by G protein-coupled receptor kinases and beta-arrestins. J Biol Chem. 2001 Oct 5;276(40):37409-14. doi: 10.1074/jbc.M106728200. Epub 2001 Jul 25. PMID: 11473130.

Kim MO, Koh PO, Kim JH, Kim JS, Kang SS, Cho GJ, Kim K, Choi WS. Localization of dopamine D1 and D2 receptor mRNAs in the rat systemic and pulmonary vasculatures. Mol Cells. 1999 Aug 31;9(4):417-21. PMID: 10515606.

Kim OJ, Ariano MA, Lazzarini RA, Levine MS, Sibley DR. Neurofilament-M interacts with the D1 dopamine receptor to regulate cell surface expression and desensitization. J Neurosci. 2002 Jul 15;22(14):5920-30. doi: 10.1523/JNEUROSCI.22-14-05920.2002. PMID: 12122054; PMCID: PMC6757921.

Kim OJ, Gardner BR, Williams DB, Marinec PS, Cabrera DM, Peters JD, Mak CC, Kim KM, Sibley DR. The role of phosphorylation in D1 dopamine receptor desensitization: evidence for a novel mechanism of arrestin association. J Biol Chem. 2004 Feb 27;279(9):7999-8010. doi: 10.1074/jbc.M308281200. Epub 2003 Dec 4. PMID: 14660631; PMCID: PMC4743542.

Kim YM, Benovic JL. Differential roles of arrestin-2 interaction with clathrin and adaptor protein 2 in G protein-coupled receptor trafficking. J Biol Chem. 2002 Aug 23;277(34):30760-8. doi: 10.1074/jbc.M204528200. Epub 2002 Jun 17. PMID: 12070169.

KIRSHNER N, RORIE M, KAMIN DL. INHIBITION OF DOPAMINE UPTAKE IN VITRO BY RESERPINE ADMINISTERED IN VIVO. J Pharmacol Exp Ther. 1963 Sep;141:285-9. PMID: 14064189.

KIRSHNER N. Uptake of catecholamines by a particulate fraction of the adrenal medulla. Science. 1962 Jan 12;135(3498):107-8. doi: 10.1126/science.135.3498.107. PMID: 14456354.

Kistner U, Wenzel BM, Veh RW, Cases-Langhoff C, Garner AM, Appeltauer U, Voss B, Gundelfinger ED, Garner CC. SAP90, a rat presynaptic protein related to the product of the Drosophila tumor suppressor gene dlg-A. J Biol Chem. 1993 Mar 5;268(7):4580-3. PMID: 7680343.

Klenk C, Vetter T, Zürn A, Vilardaga JP, Friedman PA, Wang B, Lohse MJ. Formation of a ternary complex among NHERF1, beta-arrestin, and parathyroid hormone receptor. J Biol Chem. 2010 Sep 24;285(39):30355-62. doi: 10.1074/jbc.M110.114900. Epub 2010 Jul 23. PMID: 20656684; PMCID: PMC2943313.

Klerman GL. Pharmacotherapy of schizophrenia. Annu Rev Med. 1974;25(0):199-217. doi: 10.1146/annurev.me.25.020174.001215. PMID: 4152997.

Kobilka B, Schertler GF. New G-protein-coupled receptor crystal structures: insights and limitations. Trends Pharmacol Sci. 2008 Feb;29(2):79-83. doi: 10.1016/j.tips.2007.11.009. Epub 2008 Jan 14. PMID: 18194818.

Kobilka BK, Kobilka TS, Daniel K, Regan JW, Caron MG, Lefkowitz RJ. Chimeric alpha 2-,beta 2-adrenergic receptors: delineation of domains involved in effector coupling and ligand binding specificity. Science. 1988 Jun 3;240(4857):1310-6. doi: 10.1126/science.2836950. PMID: 2836950.

Kobilka BK, Matsui H, Kobilka TS, Yang-Feng TL, Francke U, Caron MG, Lefkowitz RJ, Regan JW. Cloning, sequencing, and expression of the gene coding for the human platelet alpha 2-adrenergic receptor. Science. 1987 Oct 30;238(4827):650-6. doi: 10.1126/science.2823383. PMID: 2823383.

Komiyama NH, Watabe AM, Carlisle HJ, Porter K, Charlesworth P, Monti J, Strathdee DJ, O'Carroll CM, Martin SJ, Morris RG, O'Dell TJ, Grant SG. SynGAP regulates ERK/MAPK signaling, synaptic plasticity, and learning in the complex with postsynaptic density 95 and NMDA receptor. J Neurosci. 2002 Nov 15;22(22):9721-32. doi: 10.1523/JNEUROSCI.22-22-09721.2002. PMID: 12427827; PMCID: PMC6757832.

Kong MM, Hasbi A, Mattocks M, Fan T, O'Dowd BF, George SR. Regulation of D1 dopamine receptor trafficking and signaling by caveolin-1. Mol Pharmacol. 2007 Nov;72(5):1157-70. doi: 10.1124/mol.107.034769. Epub 2007 Aug 15. PMID: 17699686.

Konnova EA, Swanberg M. Animal Models of Parkinson's Disease. In: Stoker TB, Greenland JC, editors. Parkinson's Disease: Pathogenesis and Clinical Aspects [Internet]. Brisbane (AU): Codon Publications; 2018 Dec 21. Chapter 5. PMID: 30702844.

Konradi C, Cole RL, Heckers S, Hyman SE. Amphetamine regulates gene expression in rat striatum via transcription factor CREB. J Neurosci. 1994 Sep;14(9):5623-34. doi: 10.1523/JNEUROSCI.14-09-05623.1994. PMID: 8083758; PMCID: PMC6577107.

Kopec AM, Smith CJ, Ayre NR, Sweat SC, Bilbo SD. Microglial dopamine receptor elimination defines sex-specific nucleus accumbens development and social behavior in adolescent rats. Nat Commun. 2018 Sep 25;9(1):3769. doi: 10.1038/s41467-018-06118-z. PMID: 30254300; PMCID: PMC6156594.

Kopin IJ. Biosynthesis and metabolism of catecholamines. Anesthesiology. 1968 Jul-Aug;29(4):654-60. doi: 10.1097/00000542-196807000-00007. PMID: 4385999.

Kornau HC, Schenker LT, Kennedy MB, Seeburg PH. Domain interaction between NMDA receptor subunits and the postsynaptic density protein PSD-95. Science. 1995 Sep 22;269(5231):1737-40. doi: 10.1126/science.7569905. PMID: 7569905.

Korshunov KS, Blakemore LJ, Trombley PQ. Dopamine: A Modulator of Circadian Rhythms in the Central Nervous System. Front Cell Neurosci. 2017 Apr 3;11:91. doi: 10.3389/fncel.2017.00091. PMID: 28420965; PMCID: PMC5376559.

Korshunov KS, Blakemore LJ, Trombley PQ. Illuminating and Sniffing Out the Neuromodulatory Roles of Dopamine in the Retina and Olfactory Bulb. Front Cell Neurosci. 2020 Aug 31;14:275. doi: 10.3389/fncel.2020.00275. PMID: 33110404; PMCID: PMC7488387.

Kosaka T, Pignatelli A, Kosaka K. Heterogeneity of tyrosine hydroxylase expressing neurons in the main olfactory bulb of the mouse. Neurosci Res. 2020 Aug;157:15-33. doi: 10.1016/j.neures.2019.10.004. Epub 2019 Oct 17. PMID: 31629793.

Kotowski SJ, Hopf FW, Seif T, Bonci A, von Zastrow M. Endocytosis promotes rapid dopaminergic signaling. Neuron. 2011 Jul 28;71(2):278-90. doi: 10.1016/j.neuron.2011.05.036. PMID: 21791287; PMCID: PMC3417347.

Kouwenhoven WM, Fortin G, Penttinen AM, Florence C, Delignat-Lavaud B, Bourque MJ, Trimbuch T, Luppi MP, Salvail-Lacoste A, Legault P, Poulin JF, Rosenmund C, Awatramani R, Trudeau LÉ. VGluT2 Expression in Dopamine Neurons Contributes to Postlesional Striatal Reinnervation. J Neurosci. 2020 Oct 21;40(43):8262-8275. doi: 10.1523/JNEUROSCI.0823-20.2020. Epub 2020 Sep 14. PMID: 32928885; PMCID: PMC7577590.

Krashia P, Nobili A, D'Amelio M. Unifying Hypothesis of Dopamine Neuron Loss in Neurodegenerative Diseases: Focusing on Alzheimer's Disease. Front Mol Neurosci. 2019 May 17;12:123. doi: 10.3389/fnmol.2019.00123. PMID: 31156387; PMCID: PMC6534044.

KREBS EG, FISCHER EH. Phosphorylase activity of skeletal muscle extracts. J Biol Chem. 1955 Sep;216(1):113-20. PMID: 13252011.

KREBS EG, GRAVES DJ, FISCHER EH. Factors affecting the activity of muscle phosphorylase b kinase. J Biol Chem. 1959 Nov;234:2867-73. PMID: 14411853.

KREBS EG, KENT AB, FISCHER EH. The muscle phosphorylase b kinase reaction. J Biol Chem. 1958 Mar;231(1):73-83. PMID: 13538949.

Kreiss DS, Bergstrom DA, Gonzalez AM, Huang KX, Sibley DR, Walters JR. Dopamine receptor agonist potencies for inhibition of cell firing correlate with dopamine D3 receptor binding affinities. Eur J Pharmacol. 1995 Apr 24;277(2-3):209-14. doi: 10.1016/0014-2999(95)00069-w. PMID: 7493610.

Kresge N, Simoni RD, Hill RL. Earl W. Sutherland's Discovery of Cyclic Adenine Monophosphate and the Second Messenger System. J Biol Chem. 2005 OCTOBER VOLUME 280, ISSUE 42, E39-E40.

Kresge N, Simoni RD, Hill RL. The process of reversible phosphorylation: the work of Edmond H. Fischer. J Biol Chem. 2011 Jan 21;286(3):e1-2. doi: 10.1074/jbc.o110.000242. PMID: 21294299; PMCID: PMC3023531.

Krimer LS, Muly EC 3rd, Williams GV, Goldman-Rakic PS. Dopaminergic regulation of cerebral cortical microcirculation. Nat Neurosci. 1998 Aug;1(4):286-9. doi: 10.1038/1099. PMID: 10195161.

Kristiansen LV, Beneyto M, Haroutunian V, Meador-Woodruff JH. Changes in NMDA receptor subunits and interacting PSD proteins in dorsolateral prefrontal and anterior cingulate cortex indicate abnormal regional expression in schizophrenia. Mol Psychiatry. 2006 Aug;11(8):737-47, 705. doi: 10.1038/sj.mp.4001844. Epub 2006 May 16. PMID: 16702973.

Kristiansen LV, Meador-Woodruff JH. Abnormal striatal expression of transcripts encoding NMDA interacting PSD proteins in schizophrenia, bipolar disorder and major depression. Schizophr Res. 2005 Oct 1;78(1):87-93. doi: 10.1016/j.schres.2005.06.012. PMID: 16023328.

Krüger JM, Favaro PD, Liu M, Kitlinska A, Huang X, Raabe M, Akad DS, Liu Y, Urlaub H, Dong Y, Xu W, Schlüter OM. Differential roles of postsynaptic density-93 isoforms in regulating synaptic transmission. J Neurosci. 2013 Sep 25;33(39):15504-17. doi: 10.1523/JNEUROSCI.0019-12.2013. PMID: 24068818; PMCID: PMC3782625.

Krupnick JG, Benovic JL. The role of receptor kinases and arrestins in G protein-coupled receptor regulation. Annu Rev Pharmacol Toxicol. 1998;38:289-319. doi: 10.1146/annurev.pharmtox.38.1.289. PMID: 9597157.

Kruusmägi M, Kumar S, Zelenin S, Brismar H, Aperia A, Scott L. Functional differences between D(1) and D(5) revealed by high resolution imaging on live neurons. Neuroscience. 2009 Dec 1;164(2):463-9. doi: 10.1016/j.neuroscience.2009.08.052. Epub 2009 Aug 29. PMID: 19723560.

Kumar R, Ha T, Pham D, Shaw M, Mangelsdorf M, Friend KL, Hobson L, Turner G, Boyle J, Field M, Hackett A, Corbett M, Gecz J. A non-coding variant in the 5' UTR of DLG3 attenuates protein translation to cause non-syndromic intellectual disability. Eur J Hum Genet. 2016 Nov;24(11):1612-1616. doi: 10.1038/ejhg.2016.46. Epub 2016 May 25. PMID: 27222290; PMCID: PMC5110046.

Kupfermann I, Pinsker H, Castellucci V, Kandel ER. Central and peripheral control of gill movements in Aplysia. Science. 1971 Dec 17;174(4015):1252-6. doi: 10.1126/science.174.4015.1252. PMID: 4332285.

Kustrimovic N, Rasini E, Legnaro M, Marino F, Cosentino M. Expression of dopaminergic receptors on human CD4+ T lymphocytes: flow cytometric analysis of naive and memory subsets and relevance for the neuroimmunology of neurodegenerative disease. J Neuroimmune Pharmacol. 2014 Jun;9(3):302-12. doi: 10.1007/s11481-014-9541-5. Epub 2014 Mar 29. PMID: 24682738.

Ladepeche L, Dupuis JP, Bouchet D, Doudnikoff E, Yang L, Campagne Y, Bézard E, Hosy E, Groc L. Single-molecule imaging of the functional crosstalk between surface NMDA and dopamine D1 receptors. Proc Natl Acad Sci U S A. 2013 Oct 29;110(44):18005-10. doi: 10.1073/pnas.1310145110. Epub 2013 Oct 14. PMID: 24127604; PMCID: PMC3816474. (b)

Ladepeche L, Yang L, Bouchet D, Groc L. Regulation of dopamine D1 receptor dynamics within the postsynaptic density of hippocampal glutamate synapses. PLoS One. 2013 Sep 6;8(9):e74512. doi: 10.1371/journal.pone.0074512. PMID: 24040266; PMCID: PMC3765443. (a)

Lamey M, Thompson M, Varghese G, Chi H, Sawzdargo M, George SR, O'Dowd BF. Distinct residues in the carboxyl tail mediate agonist-induced desensitization and internalization of the human dopamine D1 receptor. J Biol Chem. 2002 Mar 15;277(11):9415-21. doi: 10.1074/jbc.M111811200. Epub 2001 Dec 31. PMID: 11773080.

Langer DH, Brown GL, Docherty JP. Dopamine receptor supersensitivity and schizophrenia: a review. Schizophr Bull. 1981;7(2):208-24. doi: 10.1093/schbul/7.2.208. PMID: 7025187.

Langley JN. Observations on the physiological action of extracts of the supra-renal bodies. J Physiol. 1901 Oct 16;27(3):237-56. doi: 10.1113/jphysiol.1901.sp000869. PMID: 16992585; PMCID: PMC1540480.

Langley JN. On the reaction of cells and of nerve-endings to certain poisons, chiefly as regards the reaction of striated muscle to nicotine and to curari. J Physiol. 1905 Dec 30;33(4-5):374-413. doi: 10.1113/jphysiol.1905.sp001128. PMID: 16992819; PMCID: PMC1465797.

Langston JW, Ballard P, Tetrud JW, Irwin I. Chronic Parkinsonism in humans due to a product of meperidine-analog synthesis. Science. 1983 Feb 25;219(4587):979-80. doi: 10.1126/science.6823561. PMID: 6823561.

Laplante F, Sibley DR, Quirion R. Reduction in acetylcholine release in the hippocampus of dopamine D5 receptor-deficient mice. Neuropsychopharmacology. 2004 Sep;29(9):1620-7. doi: 10.1038/sj.npp.1300467. PMID: 15100705.

Laporte SA, Miller WE, Kim KM, Caron MG. beta-Arrestin/AP-2 interaction in G protein-coupled receptor internalization: identification of a beta-arrestin binging site in beta 2-adaptin. J Biol Chem. 2002 Mar 15;277(11):9247-54. doi: 10.1074/jbc.M108490200. Epub 2002 Jan 2. PMID: 11777907.

Laporte SA, Oakley RH, Holt JA, Barak LS, Caron MG. The interaction of beta-arrestin with the AP-2 adaptor is required for the clustering of beta 2-adrenergic receptor into clathrin-coated pits. J Biol Chem. 2000 Jul 28;275(30):23120-6. doi: 10.1074/jbc.M002581200. PMID: 10770944.

Laporte SA, Oakley RH, Zhang J, Holt JA, Ferguson SS, Caron MG, Barak LS. The beta2-adrenergic receptor/betaarrestin complex recruits the clathrin adaptor AP-2 during endocytosis. Proc Natl Acad Sci U S A. 1999 Mar 30;96(7):3712-7. doi: 10.1073/pnas.96.7.3712. PMID: 10097102; PMCID: PMC22359.

Latorraca NR, Wang JK, Bauer B, Townshend RJL, Hollingsworth SA, Olivieri JE, Xu HE, Sommer ME, Dror RO. Molecular mechanism of GPCR-mediated arrestin activation. Nature. 2018 May;557(7705):452-456. doi: 10.1038/s41586-018-0077-3. Epub 2018 May 2. PMID: 29720655; PMCID: PMC6294333.

Lau LF, Mammen A, Ehlers MD, Kindler S, Chung WJ, Garner CC, Huganir RL. Interaction of the N-methyl-D-aspartate receptor complex with a novel synapse-associated protein, SAP102. J Biol Chem. 1996 Aug 30;271(35):21622-8. doi: 10.1074/jbc.271.35.21622. PMID: 8702950.

Lavezzari G, McCallum J, Dewey CM, Roche KW. Subunit-specific regulation of NMDA receptor endocytosis. J Neurosci. 2004 Jul 14;24(28):6383-91. doi: 10.1523/JNEUROSCI.1890-04.2004. PMID: 15254094; PMCID: PMC6729547.

Le Coniat M, Sokoloff P, Hillion J, Martres MP, Giros B, Pilon C, Schwartz JC, Berger R. Chromosomal localization of the human D3 dopamine receptor gene. Hum Genet. 1991 Sep;87(5):618-20. doi: 10.1007/BF00209024. PMID: 1916765.

Le Moine C, Bloch B. D1 and D2 dopamine receptor gene expression in the rat striatum: sensitive cRNA probes demonstrate prominent segregation of D1 and D2 mRNAs in distinct neuronal populations of the dorsal and ventral striatum. J Comp Neurol. 1995 May 8;355(3):418-26. doi: 10.1002/cne.903550308. PMID: 7636023.

Lee FJ, Xue S, Pei L, Vukusic B, Chéry N, Wang Y, Wang YT, Niznik HB, Yu XM, Liu F. Dual regulation of NMDA receptor functions by direct protein-protein interactions with the dopamine D1 receptor. Cell. 2002 Oct 18;111(2):219-30. doi: 10.1016/s0092-8674(02)00962-5. PMID: 12408866.

Lee JH, Lee S, Kim JH. Amygdala Circuits for Fear Memory: A Key Role for Dopamine Regulation. Neuroscientist. 2017 Oct;23(5):542-553. doi: 10.1177/1073858416679936. Epub 2016 Nov 21. PMID: 27872341.

Lee SM, Kant A, Blake D, Murthy V, Boyd K, Wyrick SJ, Mailman RB. SKF-83959 is not a highly-biased functionally selective D1 dopamine receptor ligand with activity at phospholipase C. Neuropharmacology. 2014 Nov;86:145-54. doi: 10.1016/j.neuropharm.2014.05.042. Epub 2014 Jun 12. PMID: 24929112. (b)

Lee SM, Yang Y, Mailman RB. Dopamine D1 receptor signaling: does GαQ-phospholipase C actually play a role? J Pharmacol Exp Ther. 2014 Oct;351(1):9-17. doi: 10.1124/jpet.114.214411. Epub 2014 Jul 22. PMID: 25052835; PMCID: PMC4165024. (a)

Lee SP, So CH, Rashid AJ, Varghese G, Cheng R, Lança AJ, O'Dowd BF, George SR. Dopamine D1 and D2 receptor Co-activation generates a novel phospholipase C-mediated calcium signal. J Biol Chem. 2004 Aug 20;279(34):35671-8. doi: 10.1074/jbc.M401923200. Epub 2004 May 24. PMID: 15159403.

Lefkowitz RJ, Cotecchia S, Samama P, Costa T. Constitutive activity of receptors coupled to guanine nucleotide regulatory proteins. Trends Pharmacol Sci. 1993 Aug;14(8):303-7. doi: 10.1016/0165-6147(93)90048-O. PMID: 8249148.

Lefkowitz RJ, Mullikin D, Caron MG. Regulation of beta-adrenergic receptors by guanyl-5'-yl imidodiphosphate and other purine nucleotides. J Biol Chem. 1976 Aug 10;251(15):4686-92. PMID: 947904.

Lefkowitz RJ, Roth J, Pastan I. Radioreceptor assay of adrenocorticotropic hormone: new approach to assay of polypeptide hormones in plasma. Science. 1970 Nov 6;170(3958):633-5. doi: 10.1126/science.170.3958.633. PMID: 4319388.

Lejeune F, Millan MJ. Activation of dopamine D3 autoreceptors inhibits firing of ventral tegmental dopaminergic neurones in vivo. Eur J Pharmacol. 1995 Mar 14;275(3):R7-9. doi: 10.1016/0014-2999(95)00106-u. PMID: 7768288.

Lejeune F, Millan MJ. Induction of burst firing in ventral tegmental area dopaminergic neurons by activation of serotonin (5-HT)1A receptors: WAY 100,635-reversible actions of the highly selective ligands, flesinoxan and S 15535. Synapse. 1998 Oct;30(2):172-80. doi: 10.1002/(SICI)1098-2396(199810)30:2<172::AID-SYN7>3.0.CO;2-9. PMID: 9723787.

Lejeune F, Newman-Tancredi A, Audinot V, Millan MJ. Interactions of (+)- and (-)-8- and 7-hydroxy-2-(di-n-propylamino)tetralin at human (h)D3, hD2 and h serotonin1A receptors and their modulation of the activity of serotoninergic and dopaminergic neurones in rats. J Pharmacol Exp Ther. 1997 Mar;280(3):1241-9. PMID: 9067310.

Leonard AS, Davare MA, Horne MC, Garner CC, Hell JW. SAP97 is associated with the alpha-amino-3-hydroxy-5-methylisoxazole-4-propionic acid receptor GluR1 subunit. J Biol Chem. 1998 Jul 31;273(31):19518-24. doi: 10.1074/jbc.273.31.19518. PMID: 9677374.

Levey AI, Hersch SM, Rye DB, Sunahara RK, Niznik HB, Kitt CA, Price DL, Maggio R, Brann MR, Ciliax BJ. Localization of D1 and D2 dopamine receptors in brain with subtype-specific antibodies. Proc Natl Acad Sci U S A. 1993 Oct 1;90(19):8861-5. doi: 10.1073/pnas.90.19.8861. PMID: 8415621; PMCID: PMC47460.

Leviel V, Gobert A, Guibert B. Direct observation of dopamine compartmentation in striatal nerve terminal by 'in vivo' measurement of the specific activity of released dopamine. Brain Res. 1989 Oct 16;499(2):205-13. doi: 10.1016/0006-8993(89)90768-3. PMID: 2804675.

LEVIN EY, LEVENBERG B, KAUFMAN S. The enzymatic conversion of 3,4-dihydroxyphenylethylamine to norepinephrine. J Biol Chem. 1960 Jul;235:2080-6. PMID: 14416204.

Levine MS, Altemus KL, Cepeda C, Cromwell HC, Crawford C, Ariano MA, Drago J, Sibley DR, Westphal H. Modulatory actions of dopamine on NMDA receptor-mediated responses are reduced in D1A-deficient mutant mice. J Neurosci. 1996 Sep 15;16(18):5870-82. doi: 10.1523/JNEUROSCI.16-18-05870.1996. PMID: 8795639; PMCID: PMC6578983.

Levy JM, Chen X, Reese TS, Nicoll RA. Synaptic Consolidation Normalizes AMPAR Quantal Size following MAGUK Loss. Neuron. 2015 Aug 5;87(3):534-48. doi: 10.1016/j.neuron.2015.07.015. PMID: 26247861; PMCID: PMC4596923.

L'hirondel M, Chéramy A, Godeheu G, Artaud F, Saiardi A, Borrelli E, Glowinski J. Lack of autoreceptor-mediated inhibitory control of dopamine release in striatal synaptosomes of D2 receptor-deficient mice. Brain Res. 1998 May 11;792(2):253-62. doi: 10.1016/s0006-8993(98)00146-2. PMID: 9593923.

Li P, Shah S, Huang L, Carr AL, Gao Y, Thisse C, Thisse B, Li L. Cloning and spatial and temporal expression of the zebrafish dopamine D1 receptor. Dev Dyn. 2007 May;236(5):1339-46. doi: 10.1002/dvdy.21130. PMID: 17393486.

Li Z, Benard O, Margolskee RF. Ggamma13 interacts with PDZ domain-containing proteins. J Biol Chem. 2006 Apr 21;281(16):11066-73. doi: 10.1074/jbc.M600113200. Epub 2006 Feb 10. PMID: 16473877.

Li Z, Benard O, Margolskee RF. Ggamma13 interacts with PDZ domain-containing proteins. J Biol Chem. 2006 Apr 21;281(16):11066-73. doi: 10.1074/jbc.M600113200. Epub 2006 Feb 10. PMID: 16473877.

Li ZS, Schmauss C, Cuenca A, Ratcliffe E, Gershon MD. Physiological modulation of intestinal motility by enteric dopaminergic neurons and the D2 receptor: analysis of dopamine receptor expression, location, development, and function in wild-type and knock-out mice. J Neurosci. 2006 Mar 8;26(10):2798-807. doi: 10.1523/JNEUROSCI.4720-05.2006. PMID: 16525059; PMCID: PMC6675162.

Lim IA, Hall DD, Hell JW. Selectivity and promiscuity of the first and second PDZ domains of PSD-95 and synapse-associated protein 102. J Biol Chem. 2002 Jun 14;277(24):21697-711. doi: 10.1074/jbc.M112339200. Epub 2002 Apr 5. PMID: 11937501.

Lindgren N, Usiello A, Goiny M, Haycock J, Erbs E, Greengard P, Hokfelt T, Borrelli E, Fisone G. Distinct roles of dopamine D2L and D2S receptor isoforms in the regulation of protein phosphorylation at presynaptic and postsynaptic sites. Proc Natl Acad Sci U S A. 2003 Apr 1;100(7):4305-9. doi: 10.1073/pnas.0730708100. Epub 2003 Mar 21. PMID: 12651945; PMCID: PMC153088.

Lisman JE, Grace AA. The hippocampal-VTA loop: controlling the entry of information into long-term memory. Neuron. 2005 Jun 2;46(5):703-13. doi: 10.1016/j.neuron.2005.05.002. PMID: 15924857.

Liu C, Cai X, Ritzau-Jost A, Kramer PF, Li Y, Khaliq ZM, Hallermann S, Kaeser PS. An action potential initiation mechanism in distal axons for the control of dopamine release. Science. 2022 Mar 25;375(6587):1378-1385. doi: 10.1126/science.abn0532. Epub 2022 Mar 24. PMID: 35324301; PMCID: PMC9081985.

Liu F, Wan Q, Pristupa ZB, Yu XM, Wang YT, Niznik HB. Direct protein-protein coupling enables cross-talk between dopamine D5 and gamma-aminobutyric acid A receptors. Nature. 2000 Jan 20;403(6767):274-80. doi: 10.1038/35002014. PMID: 10659839.

Liu FC, Graybiel AM. Dopamine and calcium signal interactions in the developing striatum: control by kinetics of CREB phosphorylation. Adv Pharmacol. 1998;42:682-6. doi: 10.1016/s1054-3589(08)60840-6. PMID: 9327991.

Liu FC, Graybiel AM. Spatiotemporal dynamics of CREB phosphorylation: transient versus sustained phosphorylation in the developing striatum. Neuron. 1996 Dec;17(6):1133-44. doi: 10.1016/s0896-6273(00)80245-7. PMID: 8982161.

Liu Q, Sobell JL, Heston LL, Sommer SS. Screening the dopamine D1 receptor gene in 131 schizophrenics and eight alcoholics: identification of polymorphisms but lack of functionally significant sequence changes. Am J Med Genet. 1995 Apr 24;60(2):165-71. doi: 10.1002/ajmg.1320600216. PMID: 7485254.

Liu S, Tang Y, Shu H, Tatum D, Bai Q, Crawford J, Xing Y, Lobo MK, Bellinger L, Kramer P, Tao F. Dopamine receptor D2, but not D1, mediates descending dopaminergic pathway-produced analgesic effect in a trigeminal neuropathic pain mouse model. Pain. 2019 Feb;160(2):334-344. doi: 10.1097/j.pain.0000000000001414. PMID: 30325872; PMCID: PMC6344251.

Liu XY, Chu XP, Mao LM, Wang M, Lan HX, Li MH, Zhang GC, Parelkar NK, Fibuch EE, Haines M, Neve KA, Liu F, Xiong ZG, Wang JQ. Modulation of D2R-NR2B interactions in response to cocaine. Neuron. 2006 Dec 7;52(5):897-909. doi: 10.1016/j.neuron.2006.10.011. PMID: 17145509.

Liu YF, Civelli O, Zhou QY, Albert PR. Cholera toxin-sensitive 3',5'-cyclic adenosine monophosphate and calcium signals of the human dopamine-D1 receptor: selective potentiation by protein kinase A. Mol Endocrinol. 1992 Nov;6(11):1815-24. doi: 10.1210/mend.6.11.1282671. PMID: 1282671.

Livingstone MS, Tempel BL. Genetic dissection of monoamine neurotransmitter synthesis in Drosophila. Nature. 1983 May 5-11;303(5912):67-70. doi: 10.1038/303067a0. PMID: 6133219.

Ljungberg T, Apicella P, Schultz W. Responses of monkey dopamine neurons during learning of behavioral reactions. J Neurophysiol. 1992 Jan;67(1):145-63. doi: 10.1152/jn.1992.67.1.145. PMID: 1552316.

Lohse MJ, Benovic JL, Codina J, Caron MG, Lefkowitz RJ. beta-Arrestin: a protein that regulates beta-adrenergic receptor function. Science. 1990 Jun 22;248(4962):1547-50. doi: 10.1126/science.2163110. PMID: 2163110.

Londos C, Salomon Y, Lin MC, Harwood JP, Schramm M, Wolff J, Rodbell M. 5'-Guanylylimidodiphosphate, a potent activator of adenylate cyclase systems in eukaryotic cells. Proc Natl Acad Sci U S A. 1974 Aug;71(8):3087-90. doi: 10.1073/pnas.71.8.3087. PMID: 4607368; PMCID: PMC388626.

LOVENBERG W, WEISSBACH H, UDENFRIEND S. Aromatic L-amino acid decarboxylase. J Biol Chem. 1962 Jan;237:89-93. PMID: 14466899.

Lu HC, Gonzalez E, Crair MC. Barrel cortex critical period plasticity is independent of changes in NMDA receptor subunit composition. Neuron. 2001 Nov 20;32(4):619-34. doi: 10.1016/s0896-6273(01)00501-3. PMID: 11719203.

Lue RA, Marfatia SM, Branton D, Chishti AH. Cloning and characterization of hdlg: the human homologue of the Drosophila discs large tumor suppressor binds to protein 4.1. Proc Natl Acad Sci U S A. 1994 Oct 11;91(21):9818-22. doi: 10.1073/pnas.91.21.9818. PMID: 7937897; PMCID: PMC44908.

Luttrell LM, Ferguson SS, Daaka Y, Miller WE, Maudsley S, Della Rocca GJ, Lin F, Kawakatsu H, Owada K, Luttrell DK, Caron MG, Lefkowitz RJ. Beta-arrestin-dependent formation of beta2 adrenergic receptor-Src protein kinase complexes. Science. 1999 Jan 29;283(5402):655-61. doi: 10.1126/science.283.5402.655. PMID: 9924018.

Luttrell LM, Lefkowitz RJ. The role of beta-arrestins in the termination and transduction of G-protein-coupled receptor signals. J Cell Sci. 2002 Feb 1;115(Pt 3):455-65. doi: 10.1242/jcs.115.3.455. PMID: 11861753.

Luttrell LM, Roudabush FL, Choy EW, Miller WE, Field ME, Pierce KL, Lefkowitz RJ. Activation and targeting of extracellular signal-regulated kinases by beta-arrestin scaffolds. Proc Natl Acad Sci U S A. 2001 Feb 27;98(5):2449-54. doi: 10.1073/pnas.041604898. Epub 2001 Feb 20. PMID: 11226259; PMCID: PMC30158.

Luttrell LM. Transmembrane signaling by G protein-coupled receptors. Methods Mol Biol. 2006;332:3-49. doi: 10.1385/1-59745-048-0:1. PMID: 16878684.

Lynch WJ, Girgenti MJ, Breslin FJ, Newton SS, Taylor JR. Gene profiling the response to repeated cocaine self-administration in dorsal striatum: a focus on circadian genes. Brain Res. 2008 Jun 5;1213:166-77. doi: 10.1016/j.brainres.2008.02.106. Epub 2008 Mar 15. PMID: 18452895; PMCID: PMC2494701.

Macey TA, Liu Y, Gurevich VV, Neve KA. Dopamine D1 receptor interaction with arrestin3 in neostriatal neurons. J Neurochem. 2005 Apr;93(1):128-34. doi: 10.1111/j.1471-4159.2004.02998.x. PMID: 15773912.

MacLeod RM, Fontham EH, Lehmeyer JE. Prolactin and growth hormone production as influenced by catecholamines and agents that affect brain catecholamines. Neuroendocrinology. 1970;6(5):283-94. doi: 10.1159/000121933. PMID: 5482108.

Magro F, Fraga S, Ribeiro T, Soares-da-Silva P. Decreased availability of intestinal dopamine in transmural colitis may relate to inhibitory effects of interferon-gamma upon L-DOPA uptake. Acta Physiol Scand. 2004 Apr;180(4):379-86. doi: 10.1111/j.1365-201X.2004.01260.x. PMID: 15030379.

Maharana J, Sarma P, Yadav MK, Saha S, Singh V, Saha S, Chami M, Banerjee R, Shukla AK. Structural snapshots uncover a key phosphorylation motif in GPCRs driving β-arrestin activation. Mol Cell. 2023 Jun 15;83(12):2091-2107.e7. doi: 10.1016/j.molcel.2023.04.025. Epub 2023 May 19. PMID: 37209686.

Maharana J, Sano FK, Sarma P, Yadav MK, Duan L, Stepniewski TM, Chaturvedi M, Ranjan A, Singh V, Saha S, Mahajan G, Chami M, Shihoya W, Selent J, Chung KY, Banerjee R, Nureki O, Shukla AK. Molecular insights into atypical modes of β-arrestin interaction with seven transmembrane receptors. Science. 2024 Jan 5;383(6678):101-108. doi: 10.1126/science.adj3347. Epub 2024 Jan 4. PMID: 38175886.

Mahoney-Rafferty EC, Tucker HR, Akhtar K, Herlihy R, Audil A, Shah D, Gupta M, Kochman EM, Feustel PJ, Molho ES, Pilitsis JG, Shin DS. Assessing the Location, Relative Expression and Subclass of Dopamine Receptors in the Cerebellum of Hemi-Parkinsonian Rats. Neuroscience. 2023 Jun 15;521:1-19. doi: 10.1016/j.neuroscience.2023.03.020. Epub 2023 Apr 26. PMID: 37116741.

Maingret F, Groc L. Characterization of the Functional Cross-Talk between Surface GABAA and Dopamine D5 Receptors. Int J Mol Sci. 2021 May 4;22(9):4867. doi: 10.3390/ijms22094867. PMID: 34064454; PMCID: PMC8125140.

Mallet N, Ballion B, Le Moine C, Gonon F. Cortical inputs and GABA interneurons imbalance projection neurons in the striatum of parkinsonian rats. J Neurosci. 2006 Apr 5;26(14):3875-84. doi: 10.1523/JNEUROSCI.4439-05.2006. PMID: 16597742; PMCID: PMC6674115.

Mamaligas AA, Ford CP. Spontaneous Synaptic Activation of Muscarinic Receptors by Striatal Cholinergic Neuron Firing. Neuron. 2016 Aug 3;91(3):574-86. doi: 10.1016/j.neuron.2016.06.021. Epub 2016 Jun 30. PMID: 27373830; PMCID: PMC5234077.

Mao LM, Wang W, Chu XP, Zhang GC, Liu XY, Yang YJ, Haines M, Papasian CJ, Fibuch EE, Buch S, Chen JG, Wang JQ. Stability of surface NMDA receptors controls synaptic and behavioral adaptations to amphetamine. Nat Neurosci. 2009 May;12(5):602-10. doi: 10.1038/nn.2300. Epub 2009 Apr 6. PMID: 19349975; PMCID: PMC2749993.

Marcellino D, Ferré S, Casadó V, Cortés A, Le Foll B, Mazzola C, Drago F, Saur O, Stark H, Soriano A, Barnes C, Goldberg SR, Lluis C, Fuxe K, Franco R. Identification of dopamine D1-D3 receptor heteromers. Indications for a role of synergistic D1-D3 receptor interactions in the

striatum. J Biol Chem. 2008 Sep 19;283(38):26016-25. doi: 10.1074/jbc.M710349200. Epub 2008 Jul 21. PMID: 18644790; PMCID: PMC2533781.

Marcott PF, Mamaligas AA, Ford CP. Phasic dopamine release drives rapid activation of striatal D2-receptors. Neuron. 2014 Oct 1;84(1):164-176. doi: 10.1016/j.neuron.2014.08.058. Epub 2014 Sep 18. PMID: 25242218; PMCID: PMC4325987.

Marcott PF, Gong S, Donthamsetti P, Grinnell SG, Nelson MN, Newman AH, Birnbaumer L, Martemyanov KA, Javitch JA, Ford CP. Regional Heterogeneity of D2-Receptor Signaling in the Dorsal Striatum and Nucleus Accumbens. Neuron. 2018 May 2;98(3):575-587.e4. doi: 10.1016/j.neuron.2018.03.038. Epub 2018 Apr 12. PMID: 29656874; PMCID: PMC6048973.

Marder SR, Cannon TD. Schizophrenia. N Engl J Med. 2019 Oct 31;381(18):1753-1761. doi: 10.1056/NEJMra1808803. PMID: 31665579.

Marshall FH. Visualizing GPCR 'Megaplexes' Which Enable Sustained Intracellular Signaling. Trends Biochem Sci. 2016 Dec;41(12):985-986. doi: 10.1016/j.tibs.2016.10.006. Epub 2016 Nov 4. PMID: 27825513.

Martin-Negrier ML, Charron G, Bloch B. Receptor recycling mediates plasma membrane recovery of dopamine D1 receptors in dendrites and axons after agonist-induced endocytosis in primary cultures of striatal neurons. Synapse. 2006 Sep 1;60(3):194-204. doi: 10.1002/syn.20296. PMID: 16739117.

Martinot M, Bragulat V, Artiges E, Dollé F, Hinnen F, Jouvent R, Martinot J. Decreased presynaptic dopamine function in the left caudate of depressed patients with affective flattening and psychomotor retardation. Am J Psychiatry. 2001 Feb;158(2):314-6. doi: 10.1176/appi.ajp.158.2.314. PMID: 11156819.

Martín-Ruiz R, Ugedo L, Honrubia MA, Mengod G, Artigas F. Control of serotonergic neurons in rat brain by dopaminergic receptors outside the dorsal raphe nucleus. J Neurochem. 2001 May;77(3):762-75. doi: 10.1046/j.1471-4159.2001.00275.x. PMID: 11331405.

Martorana A, Koch G. "Is dopamine involved in Alzheimer's disease?". Front Aging Neurosci. 2014 Sep 25;6:252. doi: 10.3389/fnagi.2014.00252. PMID: 25309431; PMCID: PMC4174765.

Mason JN, Kozell LB, Neve KA. Regulation of dopamine D(1) receptor trafficking by protein kinase A-dependent phosphorylation. Mol Pharmacol. 2002 Apr;61(4):806-16. doi: 10.1124/mol.61.4.806. PMID: 11901220.

Masri B, Salahpour A, Didriksen M, Ghisi V, Beaulieu JM, Gainetdinov RR, Caron MG. Antagonism of dopamine D2 receptor/beta-arrestin 2 interaction is a common property of clinically effective antipsychotics. Proc Natl Acad Sci U S A. 2008 Sep 9;105(36):13656-61. doi: 10.1073/pnas.0803522105. Epub 2008 Sep 3. PMID: 18768802; PMCID: PMC2533245.

Masserano JM, Weiner N. Tyrosine hydroxylase regulation in the central nervous system. Mol Cell Biochem. 1983;53-54(1-2):129-52. doi: 10.1007/BF00225250. PMID: 6137760.

Mastroeni D, Grover A, Leonard B, Joyce JN, Coleman PD, Kozik B, Bellinger DL, Rogers J. Microglial responses to dopamine in a cell culture model of Parkinson's disease. Neurobiol Aging. 2009 Nov;30(11):1805-17. doi: 10.1016/j.neurobiolaging.2008.01.001. Epub 2008 Mar 5. PMID: 18325635; PMCID: PMC2762863.

Masuho I, Skamangas NK, Muntean BS, Martemyanov KA. Diversity of the Gβγ complexes defines spatial and temporal bias of GPCR signaling. Cell Syst. 2021 Apr 21;12(4):324-337.e5. doi: 10.1016/j.cels.2021.02.001. Epub 2021 Mar 4. PMID: 33667409; PMCID: PMC8068604.

Masuko N, Makino K, Kuwahara H, Fukunaga K, Sudo T, Araki N, Yamamoto H, Yamada Y, Miyamoto E, Saya H. Interaction of NE-dlg/SAP102, a neuronal and endocrine tissue-specific membrane-associated guanylate kinase protein, with calmodulin and PSD-95/SAP90. A possible regulatory role in molecular clustering at synaptic sites. J Biol Chem. 1999 Feb 26;274(9):5782-90. doi: 10.1074/jbc.274.9.5782. PMID: 10026200.

Matsuyama N, Shibata S, Matoba A, Kudo TA, Danielsson J, Kohjitani A, Masaki E, Emala CW, Mizuta K. The dopamine D1 receptor is expressed and induces CREB phosphorylation and MUC5AC expression in human airway epithelium. Respir Res. 2018 Apr 2;19(1):53. doi: 10.1186/s12931-018-0757-4. PMID: 29606146; PMCID: PMC5879645.

Matt SM, Gaskill PJ. Where Is Dopamine and how do Immune Cells See it?: Dopamine-Mediated Immune Cell Function in Health and Disease. J Neuroimmune Pharmacol. 2020 Mar;15(1):114-164. doi: 10.1007/s11481-019-09851-4. Epub 2019 May 11. PMID: 31077015; PMCID: PMC6842680.

Matthies H, Becker A, Schröeder H, Kraus J, Höllt V, Krug M. Dopamine D1-deficient mutant mice do not express the late phase of hippocampal long-term potentiation. Neuroreport. 1997 Nov 10;8(16):3533-5. doi: 10.1097/00001756-199711100-00023. PMID: 9427321.

McCullumsmith RE, Kristiansen LV, Beneyto M, Scarr E, Dean B, Meador-Woodruff JH. Decreased NR1, NR2A, and SAP102 transcript expression in the hippocampus in bipolar disorder. Brain Res. 2007 Jan 5;1127(1):108-18. doi: 10.1016/j.brainres.2006.09.011. Epub 2006 Nov 17. PMID: 17113057; PMCID: PMC2900828.

McDonald PH, Chow CW, Miller WE, Laporte SA, Field ME, Lin FT, Davis RJ, Lefkowitz RJ. Beta-arrestin 2: a receptor-regulated MAPK scaffold for the activation of JNK3. Science. 2000 Nov 24;290(5496):1574-7. doi: 10.1126/science.290.5496.1574. PMID: 11090355.

McDonald PW, Jessen T, Field JR, Blakely RD. Dopamine signaling architecture in Caenorhabditis elegans. Cell Mol Neurobiol. 2006 Jul-Aug;26(4-6):593-618. doi: 10.1007/s10571-006-9003-6. Epub 2006 May 25. PMID: 16724276.

McGee AW, Bredt DS. Identification of an intramolecular interaction between the SH3 and guanylate kinase domains of PSD-95. J Biol Chem. 1999 Jun 18;274(25):17431-6. doi: 10.1074/jbc.274.25.17431. PMID: 10364172.

McGee AW, Dakoji SR, Olsen O, Bredt DS, Lim WA, Prehoda KE. Structure of the SH3-guanylate kinase module from PSD-95 suggests a mechanism for regulated assembly of MAGUK scaffolding proteins. Mol Cell. 2001 Dec;8(6):1291-301. doi: 10.1016/s1097-2765(01)00411-7. PMID: 11779504.

McKenna F, McLaughlin PJ, Lewis BJ, Sibbring GC, Cummerson JA, Bowen-Jones D, Moots RJ. Dopamine receptor expression on human T- and B-lymphocytes, monocytes, neutrophils, eosinophils and NK cells: a flow cytometric study. J Neuroimmunol. 2002 Nov;132(1-2):34-40. doi: 10.1016/s0165-5728(02)00280-1. PMID: 12417431.

McLennan H. The release of dopamine from the putamen. Experientia. 1965 Dec 15;21(12):725-6. doi: 10.1007/BF02138500. PMID: 5869718.

McMillen BA. CNS stimulants: two distinct mechanisms of action for amphetamine-like drugs. Trends in Pharmacological Sciences. Volume 4, 1983, Pages 429-432, doi.org/10.1016/0165-6147(83)90477-7.

Mehta TR, Monegro A, Nene Y, Fayyaz M, Bollu P. Neurobiology of ADHD: A Review. Curr Dev Disord Rep 6, 235–240 (2019). https://doi.org/10.1007/s40474-019-00182-w

Mela F, Marti M, Dekundy A, Danysz W, Morari M, Cenci MA. Antagonism of metabotropic glutamate receptor type 5 attenuates l-DOPA-induced dyskinesia and its molecular and neurochemical correlates in a rat model of Parkinson's disease. J Neurochem. 2007 Apr;101(2):483-97. doi: 10.1111/j.1471-4159.2007.04456.x. Epub 2007 Jan 15. PMID: 17359492.

Meller E, Bohmaker K, Goldstein M, Basham DA. Evidence that striatal synthesis-inhibiting autoreceptors are dopamine D3 receptors. Eur J Pharmacol. 1993 Nov 2;249(1):R5-6. doi: 10.1016/0014-2999(93)90674-7. PMID: 7904244.

Meltzer HY, Stahl SM. The dopamine hypothesis of schizophrenia: a review. Schizophr Bull. 1976;2(1):19-76. doi: 10.1093/schbul/2.1.19. PMID: 779020.

Mendez JA, Bourque MJ, Dal Bo G, Bourdeau ML, Danik M, Williams S, Lacaille JC, Trudeau LE. Developmental and target-dependent regulation of vesicular glutamate transporter expression by dopamine neurons. J Neurosci. 2008 Jun 18;28(25):6309-18. doi: 10.1523/JNEUROSCI.1331-08.2008. PMID: 18562601; PMCID: PMC6670902.

Mendoza J, Challet E. Circadian insights into dopamine mechanisms. Neuroscience. 2014 Dec 12;282:230-42. doi: 10.1016/j.neuroscience.2014.07.081. Epub 2014 Oct 2. PMID: 25281877.

Meyer JH, Krüger S, Wilson AA, Christensen BK, Goulding VS, Schaffer A, Minifie C, Houle S, Hussey D, Kennedy SH. Lower dopamine transporter binding potential in striatum during depression. Neuroreport. 2001 Dec 21;12(18):4121-5. doi: 10.1097/00001756-200112210-00052. PMID: 11742250.

Mezey E, Eisenhofer G, Harta G, Hansson S, Gould L, Hunyady B, Hoffman BJ. A novel nonneuronal catecholaminergic system: exocrine pancreas synthesizes and releases dopamine. Proc Natl Acad Sci U S A. 1996 Sep 17;93(19):10377-82. doi: 10.1073/pnas.93.19.10377. PMID: 8816808; PMCID: PMC38392.

Migaud M, Charlesworth P, Dempster M, Webster LC, Watabe AM, Makhinson M, He Y, Ramsay MF, Morris RG, Morrison JH, O'Dell TJ, Grant SG. Enhanced long-term potentiation and impaired learning in mice with mutant postsynaptic density-95 protein. Nature. 1998 Dec 3;396(6710):433-9. doi: 10.1038/24790. PMID: 9853749.

Mignini F, Tomassoni D, Traini E, Amenta F. Dopamine, vesicular transporters and dopamine receptor expression and localization in rat thymus and spleen. J Neuroimmunol. 2009 Jan 3;206(1-2):5-13. doi: 10.1016/j.jneuroim.2008.09.018. Epub 2008 Nov 13. PMID: 19012970.

Millan MJ. Descending control of pain. Prog Neurobiol. 2002 Apr;66(6):355-474. doi: 10.1016/s0301-0082(02)00009-6. PMID: 12034378.

Miller GW, Gainetdinov RR, Levey AI, Caron MG. Dopamine transporters and neuronal injury. Trends Pharmacol Sci. 1999 Oct;20(10):424-9. doi: 10.1016/s0165-6147(99)01379-6. PMID: 10498956.

Miller R, Horn A, Iversen L, Pinder R. Effects of dopamine-like drugs on rat striatal adenyl cyclase have implications for CNS dopamine receptor topography. Nature. 1974 Jul 19;250(463):238-41. doi: 10.1038/250238a0. PMID: 4368645.

Minatohara K, Ichikawa SH, Seki T, Fujiyoshi Y, Doi T. Ligand binding of PDZ domains has various roles in the synaptic clustering of SAP102 and PSD-95. Neurosci Lett. 2013 Jan 15;533:44-9. doi: 10.1016/j.neulet.2012.11.019. Epub 2012 Nov 23. PMID: 23178474.

Mirdamadi JL. Cerebellar role in Parkinson's disease. J Neurophysiol. 2016 Sep 1;116(3):917-9. doi: 10.1152/jn.01132.2015. Epub 2016 Jan 20. PMID: 26792889; PMCID: PMC5009206.

Mirenowicz J, Schultz W. Importance of unpredictability for reward responses in primate dopamine neurons. J Neurophysiol. 1994 Aug;72(2):1024-7. doi: 10.1152/jn.1994.72.2.1024. PMID: 7983508.

Mirenowicz J, Schultz W. Preferential activation of midbrain dopamine neurons by appetitive rather than aversive stimuli. Nature. 1996 Feb 1;379(6564):449-51. doi: 10.1038/379449a0. PMID: 8559249.

Misganaw D. Heteromerization of dopaminergic receptors in the brain: Pharmacological implications. Pharmacol Res. 2021 Aug;170:105600. doi: 10.1016/j.phrs.2021.105600. Epub 2021 Apr 6. PMID: 33836279.

Mishra RK, Demirjian C, Katzman R, Makman MH. A dopamine-sensitive adenylate cyclase in anterior limbic cortex and mesolimbic region of primate brain. Brain Res. 1975 Oct 17;96(2):395-9. doi: 10.1016/0006-8993(75)90754-4. PMID: 809114.

Missale C, Lombardi C, De Cotiis R, Memo M, Carruba MO, Spano PF. Dopaminergic receptor mechanisms modulating the renin-angiotensin system and aldosterone secretion: an overview. J Cardiovasc Pharmacol. 1989;14 Suppl 8:S29-39. PMID: 2483440.

Missale C, Memo M, Liberini P, Spano P. Dopamine selectively inhibits angiotensin II-induced aldosterone secretion by interacting with D-2 receptors. J Pharmacol Exp Ther. 1988 Sep;246(3):1137-43. PMID: 2458445.

Missale C, Nash SR, Robinson SW, Jaber M, Caron MG. Dopamine receptors: from structure to function. Physiol Rev. 1998 Jan;78(1):189-225. doi: 10.1152/physrev.1998.78.1.189. PMID: 9457173.

Miyamoto E, Kuo JF, Greengard P. Adenosine 3',5'-monophosphate-dependent protein kinase from brain. Science. 1968 Jul 4;165(3888):63-5. PMID: 4306869.

Mizuta K, Zhang Y, Xu D, Mizuta F, D'Ovidio F, Masaki E, Emala CW. The dopamine D1 receptor is expressed and facilitates relaxation in airway smooth muscle. Respir Res. 2013 Sep 2;14(1):89. doi: 10.1186/1465-9921-14-89. PMID: 24004608; PMCID: PMC3847358.

Momiyama T, Koga E. Dopamine D(2)-like receptors selectively block N-type Ca(2+) channels to reduce GABA release onto rat striatal cholinergic interneurones. J Physiol. 2001 Jun 1;533(Pt 2):479-92. doi: 10.1111/j.1469-7793.2001.0479a.x. PMID: 11389206; PMCID: PMC2278623.

Monsma FJ Jr, Mahan LC, McVittie LD, Gerfen CR, Sibley DR. Molecular cloning and expression of a D1 dopamine receptor linked to adenylyl cyclase activation. Proc Natl Acad Sci U S A. 1990 Sep;87(17):6723-7. doi: 10.1073/pnas.87.17.6723. PMID: 2168556; PMCID: PMC54609.

Monsma FJ Jr, McVittie LD, Gerfen CR, Mahan LC, Sibley DR. Multiple D2 dopamine receptors produced by alternative RNA splicing. Nature. 1989 Dec 21-28;342(6252):926-9. doi: 10.1038/342926a0. PMID: 2480527.

MONTAGU KA. Catechol compounds in rat tissues and in brains of different animals. Nature. 1957 Aug 3;180(4579):244-5. doi: 10.1038/180244a0. PMID: 13451690.

Montague PR. Integrating information at single synaptic connections. Proc Natl Acad Sci U S A. 1995 Mar 28;92(7):2424-5. doi: 10.1073/pnas.92.7.2424. PMID: 7708657; PMCID: PMC42229.

Moore KE, Von Voigtlander PF. The release of H 3 -dopamine from cat brain following electrical stimulation of the substantia nigra and caudate nucleus. Neuropharmacology. 1971 Nov;10(6):733-41. doi: 10.1016/0028-3908(71)90088-8. PMID: 5128028.

Moraga-Amaro R, González H, Ugalde V, Donoso-Ramos JP, Quintana-Donoso D, Lara M, Morales B, Rojas P, Pacheco R, Stehberg J. Dopamine receptor D5 deficiency results in a selective reduction of hippocampal NMDA receptor subunit NR2B expression and impaired memory. Neuropharmacology. 2016 Apr;103:222-35. doi: 10.1016/j.neuropharm.2015.12.018. Epub 2015 Dec 20. PMID: 26714288.

Moreno E, Hoffmann H, Gonzalez-Sepúlveda M, Navarro G, Casadó V, Cortés A, Mallol J, Vignes M, McCormick PJ, Canela EI, Lluís C, Moratalla R, Ferré S, Ortiz J, Franco R. Dopamine D1-histamine H3 receptor heteromers provide a selective link to MAPK signaling in GABAergic neurons of the direct striatal pathway. J Biol Chem. 2011 Feb 18;286(7):5846-54. doi: 10.1074/jbc.M110.161489. Epub 2010 Dec 20. PMID: 21173143; PMCID: PMC3037697.

Moritz AE, Madaras NS, Rankin ML, Inbody LR, Sibley DR. Delineation of G Protein-Coupled Receptor Kinase Phosphorylation Sites within the D1 Dopamine Receptor and Their Roles in Modulating β-Arrestin Binding and Activation. Int J Mol Sci. 2023 Apr 1;24(7):6599. doi: 10.3390/ijms24076599. PMID: 37047571; PMCID: PMC10095280.

Morón JA, Brockington A, Wise RA, Rocha BA, Hope BT. Dopamine uptake through the norepinephrine transporter in brain regions with low levels of the dopamine transporter: evidence from knock-out mouse lines. J Neurosci. 2002 Jan 15;22(2):389-95. doi: 10.1523/JNEUROSCI.22-02-00389.2002. PMID: 11784783.

Mueser KT, McGurk SR. Schizophrenia. Lancet. 2004 Jun 19;363(9426):2063-72. doi: 10.1016/S0140-6736(04)16458-1. PMID: 15207959.

Mukherjee C, Caron MG, Coverstone M, Lefkowitz RJ. Identification of adenylate cyclase-coupled beta-adrenergic receptors in frog erythrocytes with (minus)-[3-H] alprenolol. J Biol Chem. 1975 Jul 10;250(13):4869-76. PMID: 238972.

Müller BM, Kistner U, Kindler S, Chung WJ, Kuhlendahl S, Fenster SD, Lau LF, Veh RW, Huganir RL, Gundelfinger ED, Garner CC. SAP102, a novel postsynaptic protein that interacts with NMDA receptor complexes in vivo. Neuron. 1996 Aug;17(2):255-65. doi: 10.1016/s0896-6273(00)80157-9. PMID: 8780649.

Müller BM, Kistner U, Veh RW, Cases-Langhoff C, Becker B, Gundelfinger ED, Garner CC. Molecular characterization and spatial distribution of SAP97, a novel presynaptic protein homologous to SAP90 and the Drosophila discs-large tumor suppressor protein. J Neurosci. 1995 Mar;15(3 Pt 2):2354-66. doi: 10.1523/JNEUROSCI.15-03-02354.1995. PMID: 7891172; PMCID: PMC6578138.

Munemura M, Eskay RL, Kebabian JW. Release of alpha-melanocyte-stimulating hormone from dispersed cells of the intermediate lobe of the rat pituitary gland: involvement of catecholamines and adenosine 3',5'-monophosphate. Endocrinology. 1980 Jun;106(6):1795-803. doi: 10.1210/endo-106-6-1795. PMID: 6245851.

Murata Y, Constantine-Paton M. Postsynaptic density scaffold SAP102 regulates cortical synapse development through EphB and PAK signaling pathway. J Neurosci. 2013 Mar 13;33(11):5040-52. doi: 10.1523/JNEUROSCI.2896-12.2013. PMID: 23486974; PMCID: PMC3632365.

Musi CA, Marchini G, Giani A, Tomaselli G, Priori EC, Colnaghi L, Borsello T. Colocalization and Interaction Study of Neuronal JNK3, JIP1, and β-Arrestin2 Together with PSD95. Int J Mol Sci. 2022 Apr 8;23(8):4113. doi: 10.3390/ijms23084113. PMID: 35456931; PMCID: PMC9024448.

Nagai T, Yoshimoto J, Kannon T, Kuroda K, Kaibuchi K. Phosphorylation Signals in Striatal Medium Spiny Neurons. Trends Pharmacol Sci. 2016 Oct;37(10):858-871. doi: 10.1016/j.tips.2016.07.003. Epub 2016 Aug 18. PMID: 27546785.

Nagatsu T, Levitt M, Udenfriend S. Conversion of L-tyrosine to 3,4-dihydroxyphenylalanine by cell-free preparations of brain and sympathetically innervated tissues. Biochem Biophys Res Commun. 1964;14:543-9. doi: 10.1016/0006-291x(64)90266-9. PMID: 5836553. (a)

NAGATSU T, LEVITT M, UDENFRIEND S. TYROSINE HYDROXYLASE. THE INITIAL STEP IN NOREPINEPHRINE BIOSYNTHESIS. J Biol Chem. 1964 Sep;239:2910-7. PMID: 14216443. (b)

Nakagawa T, Futai K, Lashuel HA, Lo I, Okamoto K, Walz T, Hayashi Y, Sheng M. Quaternary structure, protein dynamics, and synaptic function of SAP97 controlled by L27 domain interactions. Neuron. 2004 Oct 28;44(3):453-67. doi: 10.1016/j.neuron.2004.10.012. PMID: 15504326.

Nash JE, Johnston TH, Collingridge GL, Garner CC, Brotchie JM. Subcellular redistribution of the synapse-associated proteins PSD-95 and SAP97 in animal models of Parkinson's disease and L-DOPA-induced dyskinesia. FASEB J. 2005 Apr;19(6):583-5. doi: 10.1096/fj.04-1854fje. Epub 2005 Feb 9. PMID: 15703272.

Nataf S. An alteration of the dopamine synthetic pathway is possibly involved in the pathophysiology of COVID-19. J Med Virol. 2020 Oct;92(10):1743-1744. doi: 10.1002/jmv.25826. Epub 2020 Apr 8. PMID: 32246784; PMCID: PMC7228370.

Navarro G, Moreno E, Aymerich M, Marcellino D, McCormick PJ, Mallol J, Cortés A, Casadó V, Canela EI, Ortiz J, Fuxe K, Lluís C, Ferré S, Franco R. Direct involvement of sigma-1 receptors in the dopamine D1 receptor-mediated effects of cocaine. Proc Natl Acad Sci U S A. 2010 Oct 26;107(43):18676-81. doi: 10.1073/pnas.1008911107. Epub 2010 Oct 18. PMID: 20956312; PMCID: PMC2972946.

Neve KA, Seamans JK, Trantham-Davidson H. Dopamine receptor signaling. J Recept Signal Transduct Res. 2004 Aug;24(3):165-205. doi: 10.1081/rrs-200029981. PMID: 15521361.

Nguyen AH, Lefkowitz RJ. Signaling at the endosome: cryo-EM structure of a GPCR-G protein-beta-arrestin megacomplex. FEBS J. 2021 Apr;288(8):2562-2569. doi: 10.1111/febs.15773. Epub 2021 Mar 8. PMID: 33605032; PMCID: PMC8252779.

Nguyen-Legros J, Versaux-Botteri C, Vernier P. Dopamine receptor localization in the mammalian retina. Mol Neurobiol. 1999 Jun;19(3):181-204. doi: 10.1007/BF02821713. PMID: 10495103.

Niciu MJ, Kelmendi B, Sanacora G. Overview of glutamatergic neurotransmission in the nervous system. Pharmacol Biochem Behav. 2012 Feb;100(4):656-64. doi: 10.1016/j.pbb.2011.08.008. Epub 2011 Aug 26. PMID: 21889952.

Niethammer M, Kim E, Sheng M. Interaction between the C terminus of NMDA receptor subunits and multiple members of the PSD-95 family of membrane-associated guanylate kinases. J Neurosci. 1996 Apr 1;16(7):2157-63. doi: 10.1523/JNEUROSCI.16-07-02157.1996. PMID: 8601796; PMCID: PMC6578538.

Nir I, Harrison JM, Haque R, Low MJ, Grandy DK, Rubinstein M, Iuvone PM. Dysfunctional light-evoked regulation of cAMP in photoreceptors and abnormal retinal adaptation in mice lacking dopamine D4 receptors. J Neurosci. 2002 Mar 15;22(6):2063-73. doi: 10.1523/JNEUROSCI.22-06-02063.2002. PMID: 11896146; PMCID: PMC6758276.

Nishi A, Bibb JA, Snyder GL, Higashi H, Nairn AC, Greengard P. Amplification of dopaminergic signaling by a positive feedback loop. Proc Natl Acad Sci U S A. 2000 Nov 7;97(23):12840-5. doi: 10.1073/pnas.220410397. PMID: 11050161; PMCID: PMC18851.

Nithianantharajah J, Komiyama NH, McKechanie A, Johnstone M, Blackwood DH, St Clair D, Emes RD, van de Lagemaat LN, Saksida LM, Bussey TJ, Grant SG. Synaptic scaffold evolution generated components of vertebrate cognitive complexity. Nat Neurosci. 2013 Jan;16(1):16-24. doi: 10.1038/nn.3276. Epub 2012 Dec 2. PMID: 23201973; PMCID: PMC4131247.

Nobili A, Latagliata EC, Viscomi MT, Cavallucci V, Cutuli D, Giacovazzo G, Krashia P, Rizzo FR, Marino R, Federici M, De Bartolo P, Aversa D, Dell'Acqua MC, Cordella A, Sancandi M, Keller F, Petrosini L, Puglisi-Allegra S, Mercuri NB, Coccurello R, Berretta N, D'Amelio M. Dopamine neuronal loss contributes to memory and reward dysfunction in a model of Alzheimer's disease. Nat Commun. 2017 Apr 3;8:14727. doi: 10.1038/ncomms14727. PMID: 28367951; PMCID: PMC5382255.

Nooh MM, Chumpia MM, Hamilton TB, Bahouth SW. Sorting of β1-adrenergic receptors is mediated by pathways that are either dependent on or independent of type I PDZ, protein kinase A (PKA), and SAP97. J Biol Chem. 2014 Jan 24;289(4):2277-94. doi: 10.1074/jbc.M113.513481. Epub 2013 Dec 9. PMID: 24324269; PMCID: PMC3900972.

Nooh MM, Naren AP, Kim SJ, Xiang YK, Bahouth SW. SAP97 controls the trafficking and resensitization of the beta-1-adrenergic receptor through its PDZ2 and I3 domains. PLoS One. 2013 May 16;8(5):e63379. doi: 10.1371/journal.pone.0063379. PMID: 23696820; PMCID: PMC3656048.

Northup JK, Smigel MD, Gilman AG. The guanine nucleotide activating site of the regulatory component of adenylate cyclase. Identification by ligand binding. J Biol Chem. 1982 Oct 10;257(19):11416-23. PMID: 6288684.

Northup JK, Smigel MD, Sternweis PC, Gilman AG. The subunits of the stimulatory regulatory component of adenylate cyclase. Resolution of the activated 45,000-dalton (alpha) subunit. J Biol Chem. 1983 Sep 25;258(18):11369-76. PMID: 6309844. (a)

Northup JK, Sternweis PC, Gilman AG. The subunits of the stimulatory regulatory component of adenylate cyclase. Resolution, activity, and properties of the 35,000-dalton (beta) subunit. J Biol Chem. 1983 Sep 25;258(18):11361-8. PMID: 6309843. (b)

Nowak JZ, Z Urawska E, Zawilska J. Melatonin and its generating system in vertebrate retina: circadian rhythm, effect of environmental lighting and interaction with dopamine. Neurochem Int. 1989;14(4):397-406. doi: 10.1016/0197-0186(89)90027-2. PMID: 20504441.

Oakley RH, Laporte SA, Holt JA, Barak LS, Caron MG. Association of beta-arrestin with G protein-coupled receptors during clathrin-mediated endocytosis dictates the profile of receptor resensitization. J Biol Chem. 1999 Nov 5;274(45):32248-57. doi: 10.1074/jbc.274.45.32248. PMID: 10542263.

Oakley RH, Laporte SA, Holt JA, Caron MG, Barak LS. Differential affinities of visual arrestin, beta arrestin1, and beta arrestin2 for G protein-coupled receptors delineate two major classes of receptors. J Biol Chem. 2000 Jun 2;275(22):17201-10. doi: 10.1074/jbc.M910348199. PMID: 10748214.

Oczkowski W. Pharmacological therapies to enhance motor recovery and walking after stroke: emerging strategies. Expert Rev Neurother. 2013 Aug;13(8):903-9. doi: 10.1586/14737175.2013.814940. PMID: 23965164.

Okamura T, Toda N. Comparison of the effect of dopamine in primate arteries and veins. Hypertens Res. 1995 Jun;18 Suppl 1:S35-7. doi: 10.1291/hypres.18.supplementi_s35. PMID: 8529071.

Okashah N, Wan Q, Ghosh S, Sandhu M, Inoue A, Vaidehi N, Lambert NA. Variable G protein determinants of GPCR coupling selectivity. Proc Natl Acad Sci U S A. 2019 Jun 11;116(24):12054-12059. doi: 10.1073/pnas.1905993116. Epub 2019 May 29. PMID: 31142646; PMCID: PMC6575158.

OLDS J, MILNER P. Positive reinforcement produced by electrical stimulation of septal area and other regions of rat brain. J Comp Physiol Psychol. 1954 Dec;47(6):419-27. doi: 10.1037/h0058775. PMID: 13233369.

Onali P, Olianas MC. Involvement of adenylate cyclase inhibition in dopamine autoreceptor regulation of tyrosine hydroxylase in rat nucleus accumbens. Neurosci Lett. 1989 Jul 17;102(1):91-6. doi: 10.1016/0304-3940(89)90313-3. PMID: 2571111.

Ostrom KF, LaVigne JE, Brust TF, Seifert R, Dessauer CW, Watts VJ, Ostrom RS. Physiological roles of mammalian transmembrane adenylyl cyclase isoforms. Physiol Rev. 2022 Apr 1;102(2):815-857. doi: 10.1152/physrev.00013.2021. Epub 2021 Oct 26. PMID: 34698552; PMCID: PMC8759965.

Otmakhova NA, Lisman JE. D1/D5 dopamine receptors inhibit depotentiation at CA1 synapses via cAMP-dependent mechanism. J Neurosci. 1998 Feb 15;18(4):1270-9. doi: 10.1523/JNEUROSCI.18-04-01270.1998. PMID: 9454837; PMCID: PMC6792711.

Overington JP, Al-Lazikani B, Hopkins AL. How many drug targets are there? Nat Rev Drug Discov. 2006 Dec;5(12):993-6. doi: 10.1038/nrd2199. PMID: 17139284.

Pacheco R, Contreras F, Zouali M. The dopaminergic system in autoimmune diseases. Front Immunol. 2014 Mar 21;5:117. doi: 10.3389/fimmu.2014.00117. PMID: 24711809; PMCID: PMC3968755.

Paladini CA, Robinson S, Morikawa H, Williams JT, Palmiter RD. Dopamine controls the firing pattern of dopamine neurons via a network feedback mechanism. Proc Natl Acad Sci U S A. 2003 Mar 4;100(5):2866-71. doi: 10.1073/pnas.0138018100. Epub 2003 Feb 25. PMID: 12604788; PMCID: PMC151432.

Palczewski K, Kumasaka T, Hori T, Behnke CA, Motoshima H, Fox BA, Le Trong I, Teller DC, Okada T, Stenkamp RE, Yamamoto M, Miyano M. Crystal structure of rhodopsin: A G protein-coupled receptor. Science. 2000 Aug 4;289(5480):739-45. doi: 10.1126/science.289.5480.739. PMID: 10926528.

Palmer AM, DeKosky ST. Monoamine neurons in aging and Alzheimer's disease. J Neural Transm Gen Sect. 1993;91(2-3):135-59. doi: 10.1007/BF01245229. PMID: 8099796.

Palmiter RD. Is dopamine a physiologically relevant mediator of feeding behavior? Trends Neurosci. 2007 Aug;30(8):375-81. doi: 10.1016/j.tins.2007.06.004. Epub 2007 Jun 29. PMID: 17604133.

Parkinson J. An essay on the shaking palsy. 1817. J Neuropsychiatry Clin Neurosci. 2002 Spring;14(2):223-36; discussion 222. doi: 10.1176/jnp.14.2.223. PMID: 11983801.

Patel J, Mooslehner KA, Chan PM, Emson PC, Stamford JA. Presynaptic control of striatal dopamine neurotransmission in adult vesicular monoamine transporter 2 (VMAT2) mutant mice. J Neurochem. 2003 May;85(4):898-910. doi: 10.1046/j.1471-4159.2003.01732.x. PMID: 12716422.

Patriarchi T, Cho JR, Merten K, Marley A, Broussard GJ, Liang R, Williams J, Nimmerjahn A, von Zastrow M, Gradinaru V, Tian L. Imaging neuromodulators with high spatiotemporal resolution using genetically encoded indicators. Nat Protoc. 2019 Dec;14(12):3471-3505. doi: 10.1038/s41596-019-0239-2. Epub 2019 Nov 15. PMID: 31732722.

Pei L, Lee FJ, Moszczynska A, Vukusic B, Liu F. Regulation of dopamine D1 receptor function by physical interaction with the NMDA receptors. J Neurosci. 2004 Feb 4;24(5):1149-58. doi: 10.1523/JNEUROSCI.3922-03.2004. PMID: 14762133; PMCID: PMC6793575.

Pei L, Li S, Wang M, Diwan M, Anisman H, Fletcher PJ, Nobrega JN, Liu F. Uncoupling the dopamine D1-D2 receptor complex exerts antidepressant-like effects. Nat Med. 2010 Dec;16(12):1393-5. doi: 10.1038/nm.2263. Epub 2010 Nov 28. PMID: 21113156.

Pellock SJ, Redinbo MR. Glucuronides in the gut: Sugar-driven symbioses between microbe and host. J Biol Chem. 2017 May 26;292(21):8569-8576. doi: 10.1074/jbc.R116.767434. Epub 2017 Apr 7. PMID: 28389557; PMCID: PMC5448086.

Peppel K, Boekhoff I, McDonald P, Breer H, Caron MG, Lefkowitz RJ. G protein-coupled receptor kinase 3 (GRK3) gene disruption leads to loss of odorant receptor desensitization. J Biol Chem. 1997 Oct 10;272(41):25425-8. doi: 10.1074/jbc.272.41.25425. PMID: 9325250.

Perreault ML, Hasbi A, Alijaniaram M, Fan T, Varghese G, Fletcher PJ, Seeman P, O'Dowd BF, George SR. The dopamine D1-D2 receptor heteromer localizes in dynorphin/enkephalin neurons: increased high affinity state following amphetamine and in schizophrenia. J Biol Chem. 2010 Nov 19;285(47):36625-34. doi: 10.1074/jbc.M110.159954. Epub 2010 Sep 23. PMID: 20864528; PMCID: PMC2978591.

Perreault ML, Hasbi A, Alijaniaram M, O'Dowd BF, George SR. Reduced striatal dopamine D1-D2 receptor heteromer expression and behavioural subsensitivity in juvenile rats. Neuroscience. 2012 Dec 6;225:130-9. doi: 10.1016/j.neuroscience.2012.08.042. Epub 2012 Sep 15. PMID: 22986162; PMCID: PMC3479309.

Perreault ML, Hasbi A, Shen MYF, Fan T, Navarro G, Fletcher PJ, Franco R, Lanciego JL, George SR. Disruption of a dopamine receptor complex amplifies the actions of cocaine. Eur Neuropsychopharmacol. 2016 Sep;26(9):1366-1377. doi: 10.1016/j.euroneuro.2016.07.008. Epub 2016 Jul 30. PMID: 27480020.

Perry SJ, Baillie GS, Kohout TA, McPhee I, Magiera MM, Ang KL, Miller WE, McLean AJ, Conti M, Houslay MD, Lefkowitz RJ. Targeting of cyclic AMP degradation to beta 2-adrenergic receptors by beta-arrestins. Science. 2002 Oct 25;298(5594):834-6. doi: 10.1126/science.1074683. PMID: 12399592.

Peterson SM, Pack TF, Wilkins AD, Urs NM, Urban DJ, Bass CE, Lichtarge O, Caron MG. Elucidation of G-protein and β-arrestin functional selectivity at the dopamine D2 receptor. Proc Natl Acad Sci U S A. 2015 Jun 2;112(22):7097-102. doi: 10.1073/pnas.1502742112. Epub 2015 May 11. PMID: 25964346; PMCID: PMC4460444.

Pezze MA, Feldon J. Mesolimbic dopaminergic pathways in fear conditioning. Prog Neurobiol. 2004 Dec;74(5):301-20. doi: 10.1016/j.pneurobio.2004.09.004. PMID: 15582224.

Phillips PE, Stuber GD, Heien ML, Wightman RM, Carelli RM. Subsecond dopamine release promotes cocaine seeking. Nature. 2003 Apr 10;422(6932):614-8. doi: 10.1038/nature01476. Erratum in: Nature. 2003 May 22;423(6938):461. PMID: 12687000.

Phillipson OT, Horn AS. Substantia nigra of the rat contains a dopamine sensitive adenylate cyclase. Nature. 1976 Jun 3;261(5559):418-20. doi: 10.1038/261418a0. PMID: 934274.

Picconi B, Centonze D, Håkansson K, Bernardi G, Greengard P, Fisone G, Cenci MA, Calabresi P. Loss of bidirectional striatal synaptic plasticity in L-DOPA-induced dyskinesia. Nat Neurosci. 2003 May;6(5):501-6. doi: 10.1038/nn1040. PMID: 12665799.

Picconi B, Gardoni F, Centonze D, Mauceri D, Cenci MA, Bernardi G, Calabresi P, Di Luca M. Abnormal Ca2+-calmodulin-dependent protein kinase II function mediates synaptic and motor deficits in experimental parkinsonism. J Neurosci. 2004 Jun 9;24(23):5283-91. doi: 10.1523/JNEUROSCI.1224-04.2004. PMID: 15190099; PMCID: PMC6729313.

Pickel VM, Garzón M, Mengual E. Electron microscopic immunolabeling of transporters and receptors identifies transmitter-specific functional sites envisioned in Cajal's neuron. Prog Brain Res. 2002;136:145-55. doi: 10.1016/s0079-6123(02)36014-x. PMID: 12143378.

Pierce KL, Lefkowitz RJ. Classical and new roles of beta-arrestins in the regulation of G-protein-coupled receptors. Nat Rev Neurosci. 2001 Oct;2(10):727-33. doi: 10.1038/35094577. PMID: 11584310.

Pierce KL, Premont RT, Lefkowitz RJ. Seven-transmembrane receptors. Nat Rev Mol Cell Biol. 2002 Sep;3(9):639-50. doi: 10.1038/nrm908. PMID: 12209124.

Pinoli M, Marino F, Cosentino M. Dopaminergic Regulation of Innate Immunity: a Review. J Neuroimmune Pharmacol. 2017 Dec;12(4):602-623. doi: 10.1007/s11481-017-9749-2. Epub 2017 Jun 3. PMID: 28578466.

Pinsker HM, Hening WA, Carew TJ, Kandel ER. Long-term sensitization of a defensive withdrawal reflex in Aplysia. Science. 1973 Dec 7;182(4116):1039-42. doi: 10.1126/science.182.4116.1039. PMID: 4748675.

Pippig S, Andexinger S, Daniel K, Puzicha M, Caron MG, Lefkowitz RJ, Lohse MJ. Overexpression of beta-arrestin and beta-adrenergic receptor kinase augment desensitization of beta 2-adrenergic receptors. J Biol Chem. 1993 Feb 15;268(5):3201-8. PMID: 8381421.

Pisani A, Bonsi P, Centonze D, Calabresi P, Bernardi G. Activation of D2-like dopamine receptors reduces synaptic inputs to striatal cholinergic interneurons. J Neurosci. 2000 Apr 1;20(7):RC69. doi: 10.1523/JNEUROSCI.20-07-j0003.2000. PMID: 10729358; PMCID: PMC6772255.

Pitcher JA, Inglese J, Higgins JB, Arriza JL, Casey PJ, Kim C, Benovic JL, Kwatra MM, Caron MG, Lefkowitz RJ. Role of beta gamma subunits of G proteins in targeting the beta-adrenergic receptor kinase to membrane-bound receptors. Science. 1992 Aug 28;257(5074):1264-7. doi: 10.1126/science.1325672. PMID: 1325672.

Pivonello R, Ferone D, de Herder WW, de Krijger RR, Waaijers M, Mooij DM, van Koetsveld PM, Barreca A, De Caro ML, Lombardi G, Colao A, Lamberts SW, Hofland LJ. Dopamine receptor expression and function in human normal adrenal gland and adrenal tumors. J Clin Endocrinol Metab. 2004 Sep;89(9):4493-502. doi: 10.1210/jc.2003-031746. PMID: 15356054.

Plouffe B, D'Aoust JP, Laquerre V, Liang B, Tiberi M. Probing the constitutive activity among dopamine D1 and D5 receptors and their mutants. Methods Enzymol. 2010;484:295-328. doi: 10.1016/B978-0-12-381298-8.00016-2. PMID: 21036239.

Plouffe B, Yang X, Tiberi M. The third intracellular loop of D1 and D5 dopaminergic receptors dictates their subtype-specific PKC-induced sensitization and desensitization in a receptor conformation-dependent manner. Cell Signal. 2012 Jan;24(1):106-18. doi: 10.1016/j.cellsig.2011.08.008. Epub 2011 Aug 26. PMID: 21893192.

Pohl SL, Birnbaumer L, Rodbell M. Glucagon-sensitive adenyl cylase in plasma membrane of hepatic parenchymal cells. Science. 1969 May 2;164(3879):566-7. doi: 10.1126/science.164.3879.566. PMID: 4305077.

Popova E. Role of dopamine in distal retina. J Comp Physiol A Neuroethol Sens Neural Behav Physiol. 2014 May;200(5):333-58. doi: 10.1007/s00359-014-0906-2. Epub 2014 Apr 12. PMID: 24728309.

Porras G, Berthet A, Dehay B, Li Q, Ladepeche L, Normand E, Dovero S, Martinez A, Doudnikoff E, Martin-Négrier ML, Chuan Q, Bloch B, Choquet D, Boué-Grabot E, Groc L, Bezard E. PSD-95 expression controls L-DOPA dyskinesia through dopamine D1 receptor trafficking. J Clin Invest. 2012 Nov;122(11):3977-89. doi: 10.1172/JCI59426. Epub 2012 Oct 8. PMID: 23041629; PMCID: PMC3484432.

Porter-Stransky KA, Petko AK, Karne SL, Liles LC, Urs NM, Caron MG, Paladini CA, Weinshenker D. Loss of β-arrestin2 in D2 cells alters neuronal excitability in the nucleus accumbens and behavioral responses to psychostimulants and opioids. Addict Biol. 2020 Nov;25(6):e12823. doi: 10.1111/adb.12823. Epub 2019 Aug 23. PMID: 31441201; PMCID: PMC7035979.

Pramod AB, Foster J, Carvelli L, Henry LK. SLC6 transporters: structure, function, regulation, disease association and therapeutics. Mol Aspects Med. 2013 Apr-Jun;34(2-3):197-219. doi: 10.1016/j.mam.2012.07.002. PMID: 23506866; PMCID: PMC3602807.

Prange S, Klinger H, Laurencin C, Danaila T, Thobois S. Depression in Patients with Parkinson's Disease: Current Understanding of its Neurobiology and Implications for Treatment. Drugs Aging. 2022 Jun;39(6):417-439. doi: 10.1007/s40266-022-00942-1. Epub 2022 Jun 16. PMID: 35705848; PMCID: PMC9200562.

Premont RT, Inglese J, Lefkowitz RJ. Protein kinases that phosphorylate activated G protein-coupled receptors. FASEB J. 1995 Feb;9(2):175-82. doi: 10.1096/fasebj.9.2.7781920. PMID: 7781920.

Preuschoff K, Bossaerts P, Quartz SR. Neural differentiation of expected reward and risk in human subcortical structures. Neuron. 2006 Aug 3;51(3):381-90. doi: 10.1016/j.neuron.2006.06.024. PMID: 16880132.

Prince J. Catecholamine dysfunction in attention-deficit/hyperactivity disorder: an update. J Clin Psychopharmacol. 2008 Jun;28(3 Suppl 2):S39-45. doi: 10.1097/JCP.0b013e318174f92a. PMID: 18480676.

Pucadyil TJ, Schmid SL. Real-time visualization of dynamin-catalyzed membrane fission and vesicle release. Cell. 2008 Dec 26;135(7):1263-75. doi: 10.1016/j.cell.2008.11.020. Epub 2008 Dec 11. PMID: 19084268; PMCID: PMC2673235.

Puopolo M. The hypothalamic-spinal dopaminergic system: a target for pain modulation. Neural Regen Res. 2019 Jun;14(6):925-930. doi: 10.4103/1673-5374.250567. PMID: 30761995; PMCID: PMC6404492.

Rácz B, Blanpied TA, Ehlers MD, Weinberg RJ. Lateral organization of endocytic machinery in dendritic spines. Nat Neurosci. 2004 Sep;7(9):917-8. doi: 10.1038/nn1303. Epub 2004 Aug 22. PMID: 15322548.

Radl D, Chiacchiaretta M, Lewis RG, Brami-Cherrier K, Arcuri L, Borrelli E. Differential regulation of striatal motor behavior and related cellular responses by dopamine D2L and D2S isoforms. Proc Natl Acad Sci U S A. 2018 Jan 2;115(1):198-203. doi: 10.1073/pnas.1717194115. Epub 2017 Dec 18. PMID: 29255027; PMCID: PMC5776825.

Raiteri M, Cerrito F, Cervoni AM, Levi G. Dopamine can be released by two mechanisms differentially affected by the dopamine transport inhibitor nomifensine. J Pharmacol Exp Ther. 1979 Feb;208(2):195-202. PMID: 216794.

RALL TW, SUTHERLAND EW. Formation of a cyclic adenine ribonucleotide by tissue particles. J Biol Chem. 1958 Jun;232(2):1065-76. PMID: 13549487.

Rangel-Barajas C, Coronel I, Florán B. Dopamine Receptors and Neurodegeneration. Aging Dis. 2015 Oct 1;6(5):349-68. doi: 10.14336/AD.2015.0330. PMID: 26425390; PMCID: PMC4567218.

Rankin ML, Marinec PS, Cabrera DM, Wang Z, Jose PA, Sibley DR. The D1 dopamine receptor is constitutively phosphorylated by G protein-coupled receptor kinase 4. Mol Pharmacol. 2006 Mar;69(3):759-69. doi: 10.1124/mol.105.019901. Epub 2005 Dec 7. PMID: 16338988.

Rankin ML, Sibley DR. Constitutive phosphorylation by protein kinase C regulates D1 dopamine receptor signaling. J Neurochem. 2010 Dec;115(6):1655-67. doi: 10.1111/j.1471-4159.2010.07074.x. Epub 2010 Nov 19. PMID: 20969574; PMCID: PMC2996484.

Rascol O, Brooks DJ, Korczyn AD, De Deyn PP, Clarke CE, Lang AE, Abdalla M; 056 Study Group. Development of dyskinesias in a 5-year trial of ropinirole and L-dopa. Mov Disord. 2006 Nov;21(11):1844-50. doi: 10.1002/mds.20988. PMID: 16958094.

Rashid AJ, So CH, Kong MM, Furtak T, El-Ghundi M, Cheng R, O'Dowd BF, George SR. D1-D2 dopamine receptor heterooligomers with unique pharmacology are coupled to rapid activation of Gq/11 in the striatum. Proc Natl Acad Sci U S A. 2007 Jan 9;104(2):654-9. doi: 10.1073/pnas.0604049104. Epub 2006 Dec 28. PMID: 17194762; PMCID: PMC1766439.

Rasmussen SG, Choi HJ, Rosenbaum DM, Kobilka TS, Thian FS, Edwards PC, Burghammer M, Ratnala VR, Sanishvili R, Fischetti RF, Schertler GF, Weis WI, Kobilka BK. Crystal structure of the human beta2 adrenergic G-protein-coupled receptor. Nature. 2007 Nov 15;450(7168):383-7. doi: 10.1038/nature06325. Epub 2007 Oct 21. PMID: 17952055.

Rasmussen SG, DeVree BT, Zou Y, Kruse AC, Chung KY, Kobilka TS, Thian FS, Chae PS, Pardon E, Calinski D, Mathiesen JM, Shah ST, Lyons JA, Caffrey M, Gellman SH, Steyaert J, Skiniotis G, Weis WI, Sunahara RK, Kobilka BK. Crystal structure of the β2 adrenergic receptor-Gs protein complex. Nature. 2011 Jul 19;477(7366):549-55. doi: 10.1038/nature10361. PMID: 21772288; PMCID: PMC3184188.

Regalado MP, Terry-Lorenzo RT, Waites CL, Garner CC, Malenka RC. Transsynaptic signaling by postsynaptic synapse-associated protein 97. J Neurosci. 2006 Feb 22;26(8):2343-57. doi: 10.1523/JNEUROSCI.5247-05.2006. PMID: 16495462; PMCID: PMC6674804.

Ribas C, Penela P, Murga C, Salcedo A, García-Hoz C, Jurado-Pueyo M, Aymerich I, Mayor F Jr. The G protein-coupled receptor kinase (GRK) interactome: role of GRKs in GPCR regulation and signaling. Biochim Biophys Acta. 2007 Apr;1768(4):913-22. doi: 10.1016/j.bbamem.2006.09.019. Epub 2006 Sep 30. PMID: 17084806.

Richard K, Hume R, Kaptein E, Stanley EL, Visser TJ, Coughtrie MW. Sulfation of thyroid hormone and dopamine during human development: ontogeny of phenol sulfotransferases and arylsulfatase in liver, lung, and brain. J Clin Endocrinol Metab. 2001 Jun;86(6):2734-42. doi: 10.1210/jcem.86.6.7569. PMID: 11397879.

Rico AJ, Dopeso-Reyes IG, Martínez-Pinilla E, Sucunza D, Pignataro D, Roda E, Marín-Ramos D, Labandeira-García JL, George SR, Franco R, Lanciego JL. Neurochemical evidence supporting dopamine D1-D2 receptor heteromers in the striatum of the long-tailed macaque: changes following dopaminergic manipulation. Brain Struct Funct. 2017 May;222(4):1767-1784. doi: 10.1007/s00429-016-1306-x. Epub 2016 Sep 9. PMID: 27612857; PMCID: PMC5406426.

Rietdijk CD, Perez-Pardo P, Garssen J, van Wezel RJ, Kraneveld AD. Exploring Braak's Hypothesis of Parkinson's Disease. Front Neurol. 2017 Feb 13;8:37. doi: 10.3389/fneur.2017.00037. PMID: 28243222; PMCID: PMC5304413.

Rietschel M, Nöthen MM, Lannfelt L, Sokoloff P, Schwartz JC, Lanczik M, Fritze J, Cichon S, Fimmers R, Körner J, et al. A serine to glycine substitution at position 9 in the extracellular N-terminal part of the dopamine D3 receptor protein: no role in the genetic predisposition to bipolar affective disorder. Psychiatry Res. 1993 Mar;46(3):253-9. doi: 10.1016/0165-1781(93)90093-v. PMID: 8493294.

Rivkees SA, Lachowicz JE. Functional D1 and D5 dopamine receptors are expressed in the suprachiasmatic, supraoptic, and paraventricular nuclei of primates. Synapse. 1997 May;26(1):1-10. doi: 10.1002/(SICI)1098-2396(199705)26:1<1::AID-SYN1>3.0.CO;2-D. PMID: 9097400.

Robinson SW, Caron MG. Selective inhibition of adenylyl cyclase type V by the dopamine D3 receptor. Mol Pharmacol. 1997 Sep;52(3):508-14. doi: 10.1124/mol.52.3.508. PMID: 9281614.

Robinson SW, Jarvie KR, Caron MG. High affinity agonist binding to the dopamine D3 receptor: chimeric receptors delineate a role for intracellular domains. Mol Pharmacol. 1994 Aug;46(2):352-6. PMID: 7915820.

Rocha BA, Fumagalli F, Gainetdinov RR, Jones SR, Ator R, Giros B, Miller GW, Caron MG. Cocaine self-administration in dopamine-transporter knockout mice. Nat Neurosci. 1998 Jun;1(2):132-7. doi: 10.1038/381. Erratum in: Nat Neurosci 1998 Aug;1(4):330. PMID: 10195128.

Roche KW, Standley S, McCallum J, Dune Ly C, Ehlers MD, Wenthold RJ. Molecular determinants of NMDA receptor internalization. Nat Neurosci. 2001 Aug;4(8):794-802. doi: 10.1038/90498. PMID: 11477425.

Rodbell M, Birnbaumer L, Pohl SL, Krans HM. The glucagon-sensitive adenyl cyclase system in plasma membranes of rat liver. V. An obligatory role of guanylnucleotides in glucagon action. J Biol Chem. 1971 Mar 25;246(6):1877-82. PMID: 4926550.

Rodbell M. The role of hormone receptors and GTP-regulatory proteins in membrane transduction. Nature. 1980 Mar 6;284(5751):17-22. doi: 10.1038/284017a0. PMID: 6101906.

Rodgers HM, Lim SA, Yow J, Dinkins ML, Patton R, Clemens S, Brewer KL. Dopamine D1 or D3 receptor modulators prevent morphine tolerance and reduce opioid withdrawal symptoms. Pharmacol Biochem Behav. 2020 Jul;194:172935. doi: 10.1016/j.pbb.2020.172935. Epub 2020 Apr 23. PMID: 32335101.

Rodgers HM, Yow J, Evans E, Clemens S, Brewer KL. Dopamine D1 and D3 receptor modulators restore morphine analgesia and prevent opioid preference in a model of neuropathic pain. Neuroscience. 2019 May 15;406:376-388. doi: 10.1016/j.neuroscience.2019.03.034. Epub 2019 Mar 23. PMID: 30910641.

Rodríguez-Ruiz M, Moreno E, Moreno-Delgado D, Navarro G, Mallol J, Cortés A, Lluís C, Canela EI, Casadó V, McCormick PJ, Franco R. Heteroreceptor Complexes Formed by Dopamine D_1, Histamine H_3, and N-Methyl-D-Aspartate Glutamate Receptors as Targets to Prevent Neuronal Death in Alzheimer's Disease. Mol Neurobiol. 2017 Aug;54(6):4537-4550. doi: 10.1007/s12035-016-9995-y. Epub 2016 Jul 1. PMID: 27370794.

Rogan MT, Stäubli UV, LeDoux JE. Fear conditioning induces associative long-term potentiation in the amygdala. Nature. 1997 Dec 11;390(6660):604-7. doi: 10.1038/37601. Erratum in: Nature 1998 Feb 19;391(6669):818. PMID: 9403688.

Romo R, Schultz W. Dopamine neurons of the monkey midbrain: contingencies of responses to active touch during self-initiated arm movements. J Neurophysiol. 1990 Mar;63(3):592-606. doi: 10.1152/jn.1990.63.3.592. PMID: 2329363.

Rosenbaum DM, Cherezov V, Hanson MA, Rasmussen SG, Thian FS, Kobilka TS, Choi HJ, Yao XJ, Weis WI, Stevens RC, Kobilka BK. GPCR engineering yields high-resolution structural insights into beta2-adrenergic receptor function. Science. 2007 Nov 23;318(5854):1266-73. doi: 10.1126/science.1150609. Epub 2007 Oct 25. PMID: 17962519.

Rosenbaum DM, Rasmussen SG, Kobilka BK. The structure and function of G-protein-coupled receptors. Nature. 2009 May 21;459(7245):356-63. doi: 10.1038/nature08144. PMID: 19458711; PMCID: PMC3967846.

Rosenbaum DM, Zhang C, Lyons JA, Holl R, Aragao D, Arlow DH, Rasmussen SG, Choi HJ, Devree BT, Sunahara RK, Chae PS, Gellman SH, Dror RO, Shaw DE, Weis WI, Caffrey M, Gmeiner P, Kobilka BK. Structure and function of an irreversible agonist-β(2) adrenoceptor complex. Nature. 2011 Jan 13;469(7329):236-40. doi: 10.1038/nature09665. PMID: 21228876; PMCID: PMC3074335.

Rosenkranz JA, Grace AA. Dopamine-mediated modulation of odour-evoked amygdala potentials during pavlovian conditioning. Nature. 2002 May 16;417(6886):282-7. doi: 10.1038/417282a. PMID: 12015602.

Rossato JI, Bevilaqua LR, Izquierdo I, Medina JH, Cammarota M. Dopamine controls persistence of long-term memory storage. Science. 2009 Aug 21;325(5943):1017-20. doi: 10.1126/science.1172545. PMID: 19696353.

Roth RH. CNS dopamine autoreceptors: distribution, pharmacology, and function. Ann N Y Acad Sci. 1984;430:27-53. doi: 10.1111/j.1749-6632.1984.tb14497.x. PMID: 6378032.

Rothblat DS, Schneider JS. Regionally specific effects of haloperidol and clozapine on dopamine reuptake in the striatum. Neurosci Lett. 1997 Jun 6;228(2):119-22. doi: 10.1016/s0304-3940(97)00377-7. PMID: 9209113.

Rothmond DA, Weickert CS, Webster MJ. Developmental changes in human dopamine neurotransmission: cortical receptors and terminators. BMC Neurosci. 2012 Feb 15;13:18. doi: 10.1186/1471-2202-13-18. PMID: 22336227; PMCID: PMC3315415.

Roy M, Sorokina O, McLean C, Tapia-González S, DeFelipe J, Armstrong JD, Grant SGN. Regional Diversity in the Postsynaptic Proteome of the Mouse Brain. Proteomes. 2018 Aug 1;6(3):31. doi: 10.3390/proteomes6030031. PMID: 30071621; PMCID: PMC6161190.

Rubí B, Ljubicic S, Pournourmohammadi S, Carobbio S, Armanet M, Bartley C, Maechler P. Dopamine D2-like receptors are expressed in pancreatic beta cells and mediate inhibition of insulin secretion. J Biol Chem. 2005 Nov 4;280(44):36824-32. doi: 10.1074/jbc.M505560200. Epub 2005 Aug 29. PMID: 16129680.

Rubí B, Maechler P. Minireview: new roles for peripheral dopamine on metabolic control and tumor growth: let's seek the balance. Endocrinology. 2010 Dec;151(12):5570-81. doi: 10.1210/en.2010-0745. Epub 2010 Nov 3. PMID: 21047943.

Ryman-Rasmussen JP, Nichols DE, Mailman RB. Differential activation of adenylate cyclase and receptor internalization by novel dopamine D1 receptor agonists. Mol Pharmacol. 2005 Oct;68(4):1039-48. doi: 10.1124/mol.105.012153. Epub 2005 Jun 28. PMID: 15985612.

Sahu A, Tyeryar KR, Vongtau HO, Sibley DR, Undieh AS. D5 dopamine receptors are required for dopaminergic activation of phospholipase C. Mol Pharmacol. 2009 Mar;75(3):447-53. doi: 10.1124/mol.108.053017. Epub 2008 Dec 1. PMID: 19047479; PMCID: PMC2684903.

Saiardi A, Bozzi Y, Baik JH, Borrelli E. Antiproliferative role of dopamine: loss of D2 receptors causes hormonal dysfunction and pituitary hyperplasia. Neuron. 1997 Jul;19(1):115-26. doi: 10.1016/s0896-6273(00)80352-9. PMID: 9247268.

Salahpour A, Ramsey AJ, Medvedev IO, Kile B, Sotnikova TD, Holmstrand E, Ghisi V, Nicholls PJ, Wong L, Murphy K, Sesack SR, Wightman RM, Gainetdinov RR, Caron MG. Increased amphetamine-induced hyperactivity and reward in mice overexpressing the dopamine transporter. Proc Natl Acad Sci U S A. 2008 Mar 18;105(11):4405-10. doi: 10.1073/pnas.0707646105. Epub 2008 Mar 17. PMID: 18347339; PMCID: PMC2393812.

Salinas-Hernández XI, Duvarci S. Dopamine in Fear Extinction. Front Synaptic Neurosci. 2021 Mar 1;13:635879. doi: 10.3389/fnsyn.2021.635879. PMID: 33732133; PMCID: PMC7956961.

Sandestig A, Green A, Aronsson J, Ellnebo K, Stefanova M. A Novel DLG3 Mutation Expanding the Phenotype of X-Linked Intellectual Disability Caused by DLG3 Nonsense Variants. Mol Syndromol. 2020 Jan;10(5):281-285. doi: 10.1159/000502601. Epub 2019 Oct 9. PMID: 32021600; PMCID: PMC6997794.

SANO I, GAMO T, KAKIMOTO Y, TANIGUCHI K, TAKESADA M, NISHINUMA K. Distribution of catechol compounds in human brain. Biochim Biophys Acta. 1959 Apr;32:586-7. doi: 10.1016/0006-3002(59)90652-3. PMID: 14441532.

Sans N, Petralia RS, Wang YX, Blahos J 2nd, Hell JW, Wenthold RJ. A developmental change in NMDA receptor-associated proteins at hippocampal synapses. J Neurosci. 2000 Feb 1;20(3):1260-71. doi: 10.1523/JNEUROSCI.20-03-01260.2000. PMID: 10648730; PMCID: PMC6774158.

Sans N, Prybylowski K, Petralia RS, Chang K, Wang YX, Racca C, Vicini S, Wenthold RJ. NMDA receptor trafficking through an interaction between PDZ proteins and the exocyst complex. Nat Cell Biol. 2003 Jun;5(6):520-30. doi: 10.1038/ncb990. PMID: 12738960.

Sans N, Wang PY, Du Q, Petralia RS, Wang YX, Nakka S, Blumer JB, Macara IG, Wenthold RJ. mPins modulates PSD-95 and SAP102 trafficking and influences NMDA receptor surface expression. Nat Cell Biol. 2005 Dec;7(12):1179-90. doi: 10.1038/ncb1325. Epub 2005 Nov 20. Erratum in: Nat Cell Biol. 2006 Jan;8(1):100. PMID: 16299499.

Santambrogio L, Lipartiti M, Bruni A, Dal Toso R. Dopamine receptors on human T- and B-lymphocytes. J Neuroimmunol. 1993 Jun;45(1-2):113-9. doi: 10.1016/0165-5728(93)90170-4. PMID: 8392516.

Santini E, Alcacer C, Cacciatore S, Heiman M, Hervé D, Greengard P, Girault JA, Valjent E, Fisone G. L-DOPA activates ERK signaling and phosphorylates histone H3 in the striatonigral medium spiny neurons of hemiparkinsonian mice. J Neurochem. 2009 Feb;108(3):621-33. doi: 10.1111/j.1471-4159.2008.05831.x. PMID: 19187092.

Santini E, Feyder M, Gangarossa G, Bateup HS, Greengard P, Fisone G. Dopamine- and cAMP-regulated phosphoprotein of 32-kDa (DARPP-32)-dependent activation of extracellular signal-regulated kinase (ERK) and mammalian target of rapamycin complex 1 (mTORC1) signaling in experimental parkinsonism. J Biol Chem. 2012 Aug 10;287(33):27806-12. doi: 10.1074/jbc.M112.388413. Epub 2012 Jun 29. PMID: 22753408; PMCID: PMC3431653.

Santuy A, Tomás-Roca L, Rodríguez JR, González-Soriano J, Zhu F, Qiu Z, Grant SGN, DeFelipe J, Merchan-Perez A. Estimation of the number of synapses in the hippocampus and brain-wide by volume electron microscopy and genetic labeling. Sci Rep. 2020 Aug 19;10(1):14014. doi: 10.1038/s41598-020-70859-5. PMID: 32814795; PMCID: PMC7438319.

Sariñana J, Tonegawa S. Differentiation of forebrain and hippocampal dopamine 1-class receptors, D1R and D5R, in spatial learning and memory. Hippocampus. 2016 Jan;26(1):76-86. doi: 10.1002/hipo.22492. Epub 2015 Aug 18. PMID: 26174222; PMCID: PMC5583731.

Sarkar C, Basu B, Chakroborty D, Dasgupta PS, Basu S. The immunoregulatory role of dopamine: an update. Brain Behav Immun. 2010 May;24(4):525-8. doi: 10.1016/j.bbi.2009.10.015. Epub 2009 Nov 5. PMID: 19896530; PMCID: PMC2856781.

Sasamori H, Asakura T, Sugiura C, Bouchekioua Y, Nishitani N, Sato M, Yoshida T, Yamasaki M, Terao A, Watanabe M, Ohmura Y, Yoshioka M. Behavioral characteristics of dopamine D5 receptor knockout mice. Sci Rep. 2022 Apr 10;12(1):6014. doi: 10.1038/s41598-022-10013-5. PMID: 35399112; PMCID: PMC8995362.

Saunders BT, Richard JM, Margolis EB, Janak PH. Dopamine neurons create Pavlovian conditioned stimuli with circuit-defined motivational properties. Nat Neurosci. 2018 Aug;21(8):1072-1083. doi: 10.1038/s41593-018-0191-4. Epub 2018 Jul 23. PMID: 30038277; PMCID: PMC6082399.

Schambra UB, Duncan GE, Breese GR, Fornaretto MG, Caron MG, Fremeau RT Jr. Ontogeny of D1A and D2 dopamine receptor subtypes in rat brain using in situ hybridization and receptor binding. Neuroscience. 1994 Sep;62(1):65-85. doi: 10.1016/0306-4522(94)90315-8. PMID: 7816213.

Schiöth HB, Fredriksson R. The GRAFS classification system of G-protein coupled receptors in comparative perspective. Gen Comp Endocrinol. 2005 May 15;142(1-2):94-101. doi: 10.1016/j.ygcen.2004.12.018. Epub 2005 Feb 5. PMID: 15862553.

Schlüter OM, Xu W, Malenka RC. Alternative N-terminal domains of PSD-95 and SAP97 govern activity-dependent regulation of synaptic AMPA receptor function. Neuron. 2006 Jul 6;51(1):99-111. doi: 10.1016/j.neuron.2006.05.016. PMID: 16815335.

Schmidt HD, Anderson SM, Pierce RC. Stimulation of D1-like or D2 dopamine receptors in the shell, but not the core, of the nucleus accumbens reinstates cocaine-seeking behaviour in the rat. Eur J Neurosci. 2006 Jan;23(1):219-28. doi: 10.1111/j.1460-9568.2005.04524.x. PMID: 16420431.

Schmidt HD, Pierce RC. Cooperative activation of D1-like and D2-like dopamine receptors in the nucleus accumbens shell is required for the reinstatement of cocaine-seeking behavior in the rat. Neuroscience. 2006 Oct 13;142(2):451-61. doi: 10.1016/j.neuroscience.2006.06.004. Epub 2006 Jul 14. PMID: 16844308.

Schmitz Y, Benoit-Marand M, Gonon F, Sulzer D. Presynaptic regulation of dopaminergic neurotransmission. J Neurochem. 2003 Oct;87(2):273-89. doi: 10.1046/j.1471-4159.2003.02050.x. PMID: 14511105.

Schmitz Y, Schmauss C, Sulzer D. Altered dopamine release and uptake kinetics in mice lacking D2 receptors. J Neurosci. 2002 Sep 15;22(18):8002-9. doi: 10.1523/JNEUROSCI.22-18-08002.2002. PMID: 12223553; PMCID: PMC6758092.

Schnell E, Sizemore M, Karimzadegan S, Chen L, Bredt DS, Nicoll RA. Direct interactions between PSD-95 and stargazin control synaptic AMPA receptor number. Proc Natl Acad Sci U S A. 2002 Oct 15;99(21):13902-7. doi: 10.1073/pnas.172511199. Epub 2002 Oct 1. PMID: 12359873; PMCID: PMC129795.

Schober A. Classic toxin-induced animal models of Parkinson's disease: 6-OHDA and MPTP. Cell Tissue Res. 2004 Oct;318(1):215-24. doi: 10.1007/s00441-004-0938-y. Epub 2004 Jul 28. PMID: 15503155.

Schöneberg T, Liebscher I. Mutations in G Protein-Coupled Receptors: Mechanisms, Pathophysiology and Potential Therapeutic Approaches. Pharmacol Rev. 2021 Jan;73(1):89-119. doi: 10.1124/pharmrev.120.000011. PMID: 33219147.

Schorderet M, Nowak JZ. Retinal dopamine D1 and D2 receptors: characterization by binding or pharmacological studies and physiological functions. Cell Mol Neurobiol. 1990 Sep;10(3):303-25. doi: 10.1007/BF00711177. PMID: 2174740.

Schultz W, Apicella P, Ljungberg T. Responses of monkey dopamine neurons to reward and conditioned stimuli during successive steps of learning a delayed response task. J Neurosci. 1993 Mar;13(3):900-13. doi: 10.1523/JNEUROSCI.13-03-00900.1993. PMID: 8441015; PMCID: PMC6576600.

Schultz W, Dayan P, Montague PR. A neural substrate of prediction and reward. Science. 1997 Mar 14;275(5306):1593-9. doi: 10.1126/science.275.5306.1593. PMID: 9054347.

Schultz W. Behavioral dopamine signals. Trends Neurosci. 2007 May;30(5):203-10. doi: 10.1016/j.tins.2007.03.007. Epub 2007 Apr 2. PMID: 17400301. (a)

Schultz W. Getting formal with dopamine and reward. Neuron. 2002 Oct 10;36(2):241-63. doi: 10.1016/s0896-6273(02)00967-4. PMID: 12383780.

Schultz W. Multiple dopamine functions at different time courses. Annu Rev Neurosci. 2007;30:259-88. doi: 10.1146/annurev.neuro.28.061604.135722. PMID: 17600522. (b)

Schultz W. Predictive reward signal of dopamine neurons. J Neurophysiol. 1998 Jul;80(1):1-27. doi: 10.1152/jn.1998.80.1.1. PMID: 9658025.

Schultz W. Responses of midbrain dopamine neurons to behavioral trigger stimuli in the monkey. J Neurophysiol. 1986 Nov;56(5):1439-61. doi: 10.1152/jn.1986.56.5.1439. PMID: 3794777.

Schwartz JC, Levesque D, Martres MP, Sokoloff P. Dopamine D3 receptor: basic and clinical aspects. Clin Neuropharmacol. 1993 Aug;16(4):295-314. doi: 10.1097/00002826-199308000-00002. PMID: 8104095.

Schweighofer N, Doya K, Kuroda S. Cerebellar aminergic neuromodulation: towards a functional understanding. Brain Res Brain Res Rev. 2004 Mar;44(2-3):103-16. doi: 10.1016/j.brainresrev.2003.10.004. PMID: 15003388.

Schweitzer J, Driever W. Development of the dopamine systems in zebrafish. Adv Exp Med Biol. 2009;651:1-14. doi: 10.1007/978-1-4419-0322-8_1. PMID: 19731546.

Scott L, Aperia A. Interaction between N-methyl-D-aspartic acid receptors and D1 dopamine receptors: an important mechanism for brain plasticity. Neuroscience. 2009 Jan 12;158(1):62-6. doi: 10.1016/j.neuroscience.2008.10.020. Epub 2008 Oct 18. PMID: 19000746.

Scott L, Kruse MS, Forssberg H, Brismar H, Greengard P, Aperia A. Selective up-regulation of dopamine D1 receptors in dendritic spines by NMDA receptor activation. Proc Natl Acad Sci U S A. 2002 Feb 5;99(3):1661-4. doi: 10.1073/pnas.032654599. Epub 2002 Jan 29. PMID: 11818555; PMCID: PMC122247.

Scott L, Zelenin S, Malmersjö S, Kowalewski JM, Markus EZ, Nairn AC, Greengard P, Brismar H, Aperia A. Allosteric changes of the NMDA receptor trap diffusible dopamine 1 receptors in spines. Proc Natl Acad Sci U S A. 2006 Jan 17;103(3):762-7. doi: 10.1073/pnas.0505557103. Epub 2006 Jan 9. PMID: 16407151; PMCID: PMC1334633.

SCOVILLE WB, MILNER B. Loss of recent memory after bilateral hippocampal lesions. J Neurol Neurosurg Psychiatry. 1957 Feb;20(1):11-21. doi: 10.1136/jnnp.20.1.11. PMID: 13406589; PMCID: PMC497229.

Seabold GK, Burette A, Lim IA, Weinberg RJ, Hell JW. Interaction of the tyrosine kinase Pyk2 with the N-methyl-D-aspartate receptor complex via the Src homology 3 domains of PSD-95 and SAP102. J Biol Chem. 2003 Apr 25;278(17):15040-8. doi: 10.1074/jbc.M212825200. Epub 2003 Feb 7. PMID: 12576483

Seachrist JL, Ferguson SS. Regulation of G protein-coupled receptor endocytosis and trafficking by Rab GTPases. Life Sci. 2003 Dec 5;74(2-3):225-35. doi: 10.1016/j.lfs.2003.09.009. PMID: 14607250.

Sebastianutto I, Cenci MA. mGlu receptors in the treatment of Parkinson's disease and L-DOPA-induced dyskinesia. Curr Opin Pharmacol. 2018 Feb;38:81-89. doi: 10.1016/j.coph.2018.03.003. Epub 2018 Apr 3. PMID: 29625424.

Sebastianutto I, Goyet E, Andreoli L, Font-Ingles J, Moreno-Delgado D, Bouquier N, Jahannault-Talignani C, Moutin E, Di Menna L, Maslava N, Pin JP, Fagni L, Nicoletti F, Ango F, Cenci MA, Perroy J. D1-mGlu5 heteromers mediate noncanonical dopamine signaling in Parkinson's disease. J Clin Invest. 2020 Mar 2;130(3):1168-1184. doi: 10.1172/JCI126361. PMID: 32039920; PMCID: PMC7269571.

Sebastianutto I, Goyet E, Andreoli L, Font-Ingles J, Moreno-Delgado D, Bouquier N, Jahannault-Talignani C, Moutin E, Di Menna L, Maslava N, Pin JP, Fagni L, Nicoletti F, Ango F, Cenci MA, Perroy J. D1-mGlu5 heteromers mediate noncanonical dopamine signaling in Parkinson's disease. J Clin Invest. 2020 Mar 2;130(3):1168-1184. doi: 10.1172/JCI126361. PMID: 32039920; PMCID: PMC7269571.

Sedaghat K, Tiberi M. Cytoplasmic tail of D1 dopaminergic receptor differentially regulates desensitization and phosphorylation by G protein-coupled receptor kinase 2 and 3. Cell Signal. 2011 Jan;23(1):180-92. doi: 10.1016/j.cellsig.2010.09.002. Epub 2010 Sep 17. PMID: 20837135.

Sedaghat K, Zhang B, Yang X, Lefebvre C, Tiberi M. Study of dopamine D1 receptor regulation by G protein-coupled receptor kinases using whole-cell phosphorylation and cross-linking methods. In: Tiberi, M. ed. Dopamine Receptor Technologies Humana Press New York, 101–138 (2015).

Seeman P, Chau-Wong M, Tedesco J, Wong K. Brain receptors for antipsychotic drugs and dopamine: direct binding assays. Proc Natl Acad Sci U S A. 1975 Nov;72(11):4376-80. doi: 10.1073/pnas.72.11.4376. PMID: 1060115; PMCID: PMC388724.

Seeman P, Kapur S. Schizophrenia: more dopamine, more D2 receptors. Proc Natl Acad Sci U S A. 2000 Jul 5;97(14):7673-5. doi: 10.1073/pnas.97.14.7673. PMID: 10884398; PMCID: PMC33999.

Seeman P, Lee T. Antipsychotic drugs: direct correlation between clinical potency and presynaptic action on dopamine neurons. Science. 1975 Jun 20;188(4194):1217-9. doi: 10.1126/science.1145194. PMID: 1145194.

Senogles SE, Amlaiky N, Falardeau P, Caron MG. Purification and characterization of the D2-dopamine receptor from bovine anterior pituitary. J Biol Chem. 1988 Dec 15;263(35):18996-9002. PMID: 3143721.

Shah PJ, Ogilvie AD, Goodwin GM, Ebmeier KP. Clinical and psychometric correlates of dopamine D2 binding in depression. Psychol Med. 1997 Nov;27(6):1247-56. doi: 10.1017/s0033291797005382. PMID: 9403896.

Sharples SA, Burma NE, Borowska-Fielding J, Kwok CHT, Eaton SEA, Baker GB, Jean-Xavier C, Zhang Y, Trang T, Whelan PJ. A dynamic role for dopamine receptors in the control of mammalian spinal networks. Sci Rep. 2020 Oct 2;10(1):16429. doi: 10.1038/s41598-020-73230-w. PMID: 33009442; PMCID: PMC7532218.

Shaywitz AJ, Greenberg ME. CREB: a stimulus-induced transcription factor activated by a diverse array of extracellular signals. Annu Rev Biochem. 1999;68:821-61. doi: 10.1146/annurev.biochem.68.1.821. Erratum in: Annu Rev Biochem. 2003;72:vii. PMID: 10872467.

Sheng M, Cummings J, Roldan LA, Jan YN, Jan LY. Changing subunit composition of heteromeric NMDA receptors during development of rat cortex. Nature. 1994 Mar 10;368(6467):144-7. doi: 10.1038/368144a0. PMID: 8139656.

Shenoy SK, Lefkowitz RJ. β-Arrestin-mediated receptor trafficking and signal transduction. Trends Pharmacol Sci. 2011 Sep;32(9):521-33. doi: 10.1016/j.tips.2011.05.002. Epub 2011 Jun 15. PMID: 21680031; PMCID: PMC3159699.

Shenoy SK, McDonald PH, Kohout TA, Lefkowitz RJ. Regulation of receptor fate by ubiquitination of activated beta 2-adrenergic receptor and beta-arrestin. Science. 2001 Nov 9;294(5545):1307-13. doi: 10.1126/science.1063866. Epub 2001 Oct 4. PMID: 11588219.

Sherrington R, Mankoo B, Attwood J, Kalsi G, Curtis D, Buetow K, Povey S, Gurling H. Cloning of the human dopamine D5 receptor gene and identification of a highly polymorphic microsatellite for the DRD5 locus that shows tight linkage to the chromosome 4p reference marker RAF1P1. Genomics. 1993 Nov;18(2):423-5. doi: 10.1006/geno.1993.1489. PMID: 8288248.

Shimada S, Kitayama S, Lin CL, Patel A, Nanthakumar E, Gregor P, Kuhar M, Uhl G. Cloning and expression of a cocaine-sensitive dopamine transporter complementary DNA. Science. 1991 Oct 25;254(5031):576-8. doi: 10.1126/science.1948034. Erratum in: Science 1992 Mar 6;255(5049):1195. PMID: 1948034.

Shin H, Hsueh YP, Yang FC, Kim E, Sheng M. An intramolecular interaction between Src homology 3 domain and guanylate kinase-like domain required for channel clustering by postsynaptic density-95/SAP90. J Neurosci. 2000 May 15;20(10):3580-7. doi: 10.1523/JNEUROSCI.20-10-03580.2000. PMID: 10804199; PMCID: PMC6772679.

Shohamy D, Adcock RA. Dopamine and adaptive memory. Trends Cogn Sci. 2010 Oct;14(10):464-72. doi: 10.1016/j.tics.2010.08.002. Epub 2010 Sep 9. PMID: 20829095.

Shoichet BK, Kobilka BK. Structure-based drug screening for G-protein-coupled receptors. Trends Pharmacol Sci. 2012 May;33(5):268-72. doi: 10.1016/j.tips.2012.03.007. Epub 2012 Apr 13. PMID: 22503476; PMCID: PMC3523194.

Shuen JA, Chen M, Gloss B, Calakos N. Drd1a-tdTomato BAC transgenic mice for simultaneous visualization of medium spiny neurons in the direct and indirect pathways of the basal ganglia. J Neurosci. 2008 Mar 12;28(11):2681-5. doi: 10.1523/JNEUROSCI.5492-07.2008. PMID: 18337395; PMCID: PMC6670676.

Shukla AK, Westfield GH, Xiao K, Reis RI, Huang LY, Tripathi-Shukla P, Qian J, Li S, Blanc A, Oleskie AN, Dosey AM, Su M, Liang CR, Gu LL, Shan JM, Chen X, Hanna R, Choi M, Yao XJ, Klink BU, Kahsai AW, Sidhu SS, Koide S, Penczek PA, Kossiakoff AA, Woods VL Jr, Kobilka BK, Skiniotis G, Lefkowitz RJ. Visualization of arrestin recruitment by a G-protein-coupled receptor. Nature. 2014 Aug 14;512(7513):218-222. doi: 10.1038/nature13430. Epub 2014 Jun 22. PMID: 25043026; PMCID: PMC4134437.

Shukla AK, Xiao K, Lefkowitz RJ. Emerging paradigms of β-arrestin-dependent seven transmembrane receptor signaling. Trends Biochem Sci. 2011 Sep;36(9):457-69. doi: 10.1016/j.tibs.2011.06.003. Epub 2011 Jul 20. PMID: 21764321; PMCID: PMC3168679.

Shuster MJ, Camardo JS, Siegelbaum SA, Kandel ER. Cyclic AMP-dependent protein kinase closes the serotonin-sensitive K+ channels of Aplysia sensory neurones in cell-free membrane patches. Nature. 1985 Jan 31-Feb 6;313(6001):392-5. doi: 10.1038/313392a0. PMID: 2578623.

Sibley DR, Lefkowitz RJ. Molecular mechanisms of receptor desensitization using the beta-adrenergic receptor-coupled adenylate cyclase system as a model. Nature. 1985 Sep 12-18;317(6033):124-9. doi: 10.1038/317124a0. PMID: 2993919.

Sibley DR, Strasser RH, Benovic JL, Daniel K, Lefkowitz RJ. Phosphorylation/dephosphorylation of the beta-adrenergic receptor regulates its functional coupling to adenylate cyclase and subcellular distribution. Proc Natl Acad Sci U S A. 1986 Dec;83(24):9408-12. doi: 10.1073/pnas.83.24.9408. PMID: 3025843; PMCID: PMC387147.

Simon MI, Strathmann MP, Gautam N. Diversity of G proteins in signal transduction. Science. 1991 May 10;252(5007):802-8. doi: 10.1126/science.1902986. PMID: 1902986.

Sjoerdsma A, Engelman K, Spector S, Udenfriend S. Inhibition of catecholamine synthesis in man with alpha-methyl-tyrosine, an inhibitor of tyrosine hydroxylase. Lancet. 1965 Nov 27;2(7422):1092-4. doi: 10.1016/s0140-6736(65)90062-0. PMID: 4158803.

Slivka A, Brannan TS, Weinberger J, Knott PJ, Cohen G. Increase in extracellular dopamine in the striatum during cerebral ischemia: a study utilizing cerebral microdialysis. J Neurochem. 1988 Jun;50(6):1714-8. doi: 10.1111/j.1471-4159.1988.tb02468.x. PMID: 3373210.

Smiley JF, Levey AI, Ciliax BJ, Goldman-Rakic PS. D1 dopamine receptor immunoreactivity in human and monkey cerebral cortex: predominant and extrasynaptic localization in dendritic spines. Proc Natl Acad Sci U S A. 1994 Jun 7;91(12):5720-4. doi: 10.1073/pnas.91.12.5720. PMID: 7911245; PMCID: PMC44068.

Smith JS, Lefkowitz RJ, Rajagopal S. Biased signalling: from simple switches to allosteric microprocessors. Nat Rev Drug Discov. 2018 Apr;17(4):243-260. doi: 10.1038/nrd.2017.229. Epub 2018 Jan 5. PMID: 29302067; PMCID: PMC5936084.

Smith JS, Pack TF, Inoue A, Lee C, Zheng K, Choi I, Eiger DS, Warman A, Xiong X, Ma Z, Viswanathan G, Levitan IM, Rochelle LK, Staus DP, Snyder JC, Kahsai AW, Caron MG, Rajagopal S. Noncanonical scaffolding of Gαi and β-arrestin by G protein-coupled receptors. Science. 2021 Mar 12;371(6534):eaay1833. doi: 10.1126/science.aay1833. Epub 2021 Jan 21. PMID: 33479120; PMCID: PMC8005335.

So CH, Varghese G, Curley KJ, Kong MM, Alijaniaram M, Ji X, Nguyen T, O'dowd BF, George SR. D1 and D2 dopamine receptors form heterooligomers and cointernalize after selective activation of either receptor. Mol Pharmacol. 2005 Sep;68(3):568-78. doi: 10.1124/mol.105.012229. Epub 2005 May 27. PMID: 15923381.

So CH, Verma V, Alijaniaram M, Cheng R, Rashid AJ, O'Dowd BF, George SR. Calcium signaling by dopamine D5 receptor and D5-D2 receptor hetero-oligomers occurs by a mechanism distinct from that for dopamine D1-D2 receptor hetero-oligomers. Mol Pharmacol. 2009 Apr;75(4):843-54. doi: 10.1124/mol.108.051805. Epub 2009 Jan 26. PMID: 19171671; PMCID: PMC2684927.

So CH, Verma V, O'Dowd BF, George SR. Desensitization of the dopamine D1 and D2 receptor hetero-oligomer mediated calcium signal by agonist occupancy of either receptor. Mol Pharmacol. 2007 Aug;72(2):450-62. doi: 10.1124/mol.107.034884. Epub 2007 May 22. PMID: 17519357.

Sobell JL, Lind TJ, Sigurdson DC, Zald DH, Snitz BE, Grove WM, Heston LL, Sommer SS. The D5 dopamine receptor gene in schizophrenia: identification of a nonsense change and multiple missense changes but lack of association with disease. Hum Mol Genet. 1995 Apr;4(4):507-14. doi: 10.1093/hmg/4.4.507. PMID: 7633397.

Søberg K, Skålhegg BS. The Molecular Basis for Specificity at the Level of the Protein Kinase a Catalytic Subunit. Front Endocrinol (Lausanne). 2018 Sep 12;9:538. doi: 10.3389/fendo.2018.00538. PMID: 30258407; PMCID: PMC6143667.

Sokoloff P, Andrieux M, Besançon R, Pilon C, Martres MP, Giros B, Schwartz JC. Pharmacology of human dopamine D3 receptor expressed in a mammalian cell line: comparison with D2 receptor. Eur J Pharmacol. 1992 Apr 10;225(4):331-7. doi: 10.1016/0922-4106(92)90107-7. PMID: 1354163. (b)

Sokoloff P, Giros B, Martres MP, Bouthenet ML, Schwartz JC. Molecular cloning and characterization of a novel dopamine receptor (D3) as a target for neuroleptics. Nature. 1990 Sep 13;347(6289):146-51. doi: 10.1038/347146a0. PMID: 1975644.

Sokoloff P, Levesque D, Martres MP, Lannfelt L, Diaz G, Pilon C, Schwartz JC. The dopamine D3 receptor as a key target for antipsychotics. Clin Neuropharmacol. 1992;15 Suppl 1 Pt A:456A-457A. doi: 10.1097/00002826-199201001-00238. PMID: 1354048. (a)

Sokoloff P, Schwartz JC. Novel dopamine receptors half a decade later. Trends Pharmacol Sci. 1995 Aug;16(8):270-5. doi: 10.1016/s0165-6147(00)89044-6. PMID: 7482988.

Soler J, Fañanás L, Parellada M, Krebs MO, Rouleau GA, Fatjó-Vilas M. Genetic variability in scaffolding proteins and risk for schizophrenia and autism-spectrum disorders: a systematic review. J Psychiatry Neurosci. 2018 Jul;43(4):223-244. doi: 10.1503/jpn.170066. PMID: 29947605; PMCID: PMC6019351.

Solís O, Garcia-Montes JR, González-Granillo A, Xu M, Moratalla R. Dopamine D3 Receptor Modulates l-DOPA-Induced Dyskinesia by Targeting D1 Receptor-Mediated Striatal Signaling. Cereb Cortex. 2017 Jan 1;27(1):435-446. doi: 10.1093/cercor/bhv231. PMID: 26483399; PMCID: PMC5939228.

Sotnikova TD, Caron MG, Gainetdinov RR. DDD mice, a novel acute mouse model of Parkinson's disease. Neurology. 2006 Oct 10;67(7 Suppl 2):S12-7. doi: 10.1212/wnl.67.7_suppl_2.s12. PMID: 17030735.

Spanagel R, Weiss F. The dopamine hypothesis of reward: past and current status. Trends Neurosci. 1999 Nov;22(11):521-7. doi: 10.1016/s0166-2236(99)01447-2. PMID: 10529820.

Squire LR. The legacy of patient H.M. for neuroscience. Neuron. 2009 Jan 15;61(1):6-9. doi: 10.1016/j.neuron.2008.12.023. PMID: 19146808; PMCID: PMC2649674.

Sriram K, Insel PA. G Protein-Coupled Receptors as Targets for Approved Drugs: How Many Targets and How Many Drugs? Mol Pharmacol. 2018 Apr;93(4):251-258. doi: 10.1124/mol.117.111062. Epub 2018 Jan 3. PMID: 29298813.

Stenkamp RE, Teller DC, Palczewski K. Crystal structure of rhodopsin: a G-protein-coupled receptor. Chembiochem. 2002 Oct 4;3(10):963-7. doi: 10.1002/1439-7633(20021004)3:10<963::AID-CBIC963>3.0.CO;2-9. PMID: 12362360.

Stice E, Spoor S, Bohon C, Small DM. Relation between obesity and blunted striatal response to food is moderated by TaqIA A1 allele. Science. 2008 Oct 17;322(5900):449-52. doi: 10.1126/science.1161550. PMID: 18927395; PMCID: PMC2681095.

Stinear CM. Dopamine for motor recovery after stroke: where to from here? Lancet Neurol. 2019 Jun;18(6):514-515. doi: 10.1016/S1474-4422(19)30162-0. PMID: 31122485.

Stocchi F, Olanow CW. Neuroprotection in Parkinson's disease: clinical trials. Ann Neurol. 2003;53 Suppl 3:S87-97; discussion S97-9. doi: 10.1002/ana.10488. PMID: 12666101.

Stoof JC, Kebabian JW. Opposing roles for D-1 and D-2 dopamine receptors in efflux of cyclic AMP from rat neostriatum. Nature. 1981 Nov 26;294(5839):366-8. doi: 10.1038/294366a0. PMID: 6273735.

Strasser RH, Benovic JL, Caron MG, Lefkowitz RJ. Beta-agonist- and prostaglandin E1-induced translocation of the beta-adrenergic receptor kinase: evidence that the kinase may act on multiple adenylate cyclase-coupled receptors. Proc Natl Acad Sci U S A. 1986 Sep;83(17):6362-6. doi: 10.1073/pnas.83.17.6362. PMID: 3018728; PMCID: PMC386503.

Strobel G, Werle E, Weicker H. Isomer specific kinetics of dopamine beta-hydroxylase and arylsulfatase towards catecholamine sulfates. Biochem Int. 1990;20(2):343-51. PMID: 2317215.

Stuber GD, Wightman RM, Carelli RM. Extinction of cocaine self-administration reveals functionally and temporally distinct dopaminergic signals in the nucleus accumbens. Neuron. 2005 May 19;46(4):661-9. doi: 10.1016/j.neuron.2005.04.036. PMID: 15944133.

Su P, Lai TKY, Lee FHF, Abela AR, Fletcher PJ, Liu F. Disruption of SynGAP-dopamine D1 receptor complexes alters actin and microtubule dynamics and impairs GABAergic interneuron migration. Sci Signal. 2019 Aug 6;12(593):eaau9122. doi: 10.1126/scisignal.aau9122. PMID: 31387938.

Sukhanov I, Dorotenko A, Fesenko Z, Savchenko A, Efimova EV, Mor MS, Belozertseva IV, Sotnikova TD, Gainetdinov RR. Inhibition of PDE10A in a New Rat Model of Severe Dopamine Depletion Suggests New Approach to Non-Dopamine Parkinson's Disease Therapy. Biomolecules. 2022 Dec 21;13(1):9. doi: 10.3390/biom13010009. PMID: 36671394; PMCID: PMC9855999.

Sulston J, Dew M, Brenner S. Dopaminergic neurons in the nematode Caenorhabditis elegans. J Comp Neurol. 1975 Sep 15;163(2):215-26. doi: 10.1002/cne.901630207. PMID: 240872.

Sulzer D, Antonini A, Leta V, Nordvig A, Smeyne RJ, Goldman JE, Al-Dalahmah O, Zecca L, Sette A, Bubacco L, Meucci O, Moro E, Harms AS, Xu Y, Fahn S, Ray Chaudhuri K. COVID-19 and possible links with Parkinson's disease and parkinsonism: from bench to bedside. NPJ Parkinsons Dis. 2020 Aug 20;6:18. doi: 10.1038/s41531-020-00123-0. PMID: 32885037; PMCID: PMC7441399.

Sulzer D, Cassidy C, Horga G, Kang UJ, Fahn S, Casella L, Pezzoli G, Langley J, Hu XP, Zucca FA, Isaias IU, Zecca L. Neuromelanin detection by magnetic resonance imaging (MRI) and its promise as a biomarker for Parkinson's disease. NPJ Parkinsons Dis. 2018 Apr 10;4:11. doi: 10.1038/s41531-018-0047-3. PMID: 29644335; PMCID: PMC5893576.

Sulzer D, Joyce MP, Lin L, Geldwert D, Haber SN, Hattori T, Rayport S. Dopamine neurons make glutamatergic synapses in vitro. J Neurosci. 1998 Jun 15;18(12):4588-602. doi: 10.1523/JNEUROSCI.18-12-04588.1998. PMID: 9614234; PMCID: PMC6792695.

Sulzer D, Maidment NT, Rayport S. Amphetamine and other weak bases act to promote reverse transport of dopamine in ventral midbrain neurons. J Neurochem. 1993 Feb;60(2):527-35. doi: 10.1111/j.1471-4159.1993.tb03181.x. PMID: 8419534.

Sun B, Feng D, Chu ML, Fish I, Lovera S, Sands ZA, Kelm S, Valade A, Wood M, Ceska T, Kobilka TS, Lebon F, Kobilka BK. Crystal structure of dopamine D1 receptor in complex with G protein and a non-catechol agonist. Nat Commun. 2021 Jun 3;12(1):3305. doi: 10.1038/s41467-021-23519-9. PMID: 34083522; PMCID: PMC8175458.

Sun N, Kim KM. Mechanistic diversity involved in the desensitization of G protein-coupled receptors. Arch Pharm Res. 2021 Apr;44(4):342-353. doi: 10.1007/s12272-021-01320-y. Epub 2021 Mar 24. PMID: 33761113.

Sunahara RK, Guan HC, O'Dowd BF, Seeman P, Laurier LG, Ng G, George SR, Torchia J, Van Tol HH, Niznik HB. Cloning of the gene for a human dopamine D5 receptor with higher affinity for dopamine than D1. Nature. 1991 Apr 18;350(6319):614-9. doi: 10.1038/350614a0. PMID: 1826762.

Sunahara RK, Niznik HB, Weiner DM, Stormann TM, Brann MR, Kennedy JL, Gelernter JE, Rozmahel R, Yang YL, Israel Y, et al. Human dopamine D1 receptor encoded by an intronless gene on chromosome 5. Nature. 1990 Sep 6;347(6288):80-3. doi: 10.1038/347080a0. PMID: 1975640.

Suo S, Ishiura S, Van Tol HH. Dopamine receptors in C. elegans. Eur J Pharmacol. 2004 Oct 1;500(1-3):159-66. doi: 10.1016/j.ejphar.2004.07.021. PMID: 15464029.

Surmeier DJ, Bargas J, Hemmings HC Jr, Nairn AC, Greengard P. Modulation of calcium currents by a D1 dopaminergic protein kinase/phosphatase cascade in rat neostriatal neurons. Neuron. 1995 Feb;14(2):385-97. doi: 10.1016/0896-6273(95)90294-5. PMID: 7531987.

Surmeier DJ, Ding J, Day M, Wang Z, Shen W. D1 and D2 dopamine-receptor modulation of striatal glutamatergic signaling in striatal medium spiny neurons. Trends Neurosci. 2007 May;30(5):228-35. doi: 10.1016/j.tins.2007.03.008. Epub 2007 Apr 3. PMID: 17408758.

Surmeier DJ, Eberwine J, Wilson CJ, Cao Y, Stefani A, Kitai ST. Dopamine receptor subtypes colocalize in rat striatonigral neurons. Proc Natl Acad Sci U S A. 1992 Nov 1;89(21):10178-82. doi: 10.1073/pnas.89.21.10178. PMID: 1332033; PMCID: PMC50301.

Surmeier DJ, Reiner A, Levine MS, Ariano MA. Are neostriatal dopamine receptors co-localized? Trends Neurosci. 1993 Aug;16(8):299-305. doi: 10.1016/0166-2236(93)90103-s. PMID: 7691003.

Surmeier DJ, Song WJ, Yan Z. Coordinated expression of dopamine receptors in neostriatal medium spiny neurons. J Neurosci. 1996 Oct 15;16(20):6579-91. doi: 10.1523/JNEUROSCI.16-20-06579.1996. PMID: 8815934; PMCID: PMC6578920.

SUTHERLAND EW, RALL TW, MENON T. Adenyl cylase. I. Distribution, preparation, and properties. J Biol Chem. 1962 Apr;237:1220-7. PMID: 13918525.

SUTHERLAND EW, RALL TW. Fractionation and characterization of a cyclic adenine ribonucleotide formed by tissue particles. J Biol Chem. 1958 Jun;232(2):1077-91. PMID: 13549488.

Sutton LP, Caron MG. Essential role of D1R in the regulation of mTOR complex1 signaling induced by cocaine. Neuropharmacology. 2015 Dec;99:610-9. doi: 10.1016/j.neuropharm.2015.08.024. Epub 2015 Aug 24. PMID: 26314207; PMCID: PMC4703076.

Svenningsson P, Nishi A, Fisone G, Girault JA, Nairn AC, Greengard P. DARPP-32: an integrator of neurotransmission. Annu Rev Pharmacol Toxicol. 2004;44:269-96. doi: 10.1146/annurev.pharmtox.44.101802.121415. PMID: 14744247.

Swanson LW. The projections of the ventral tegmental area and adjacent regions: a combined fluorescent retrograde tracer and immunofluorescence study in the rat. Brain Res Bull. 1982 Jul-Dec;9(1-6):321-53. doi: 10.1016/0361-9230(82)90145-9. PMID: 6816390.

SWEENEY D. Dopamine: its occurrence in molluscan ganglia. Science. 1963 Mar 15;139(3559):1051. doi: 10.1126/science.139.3559.1051. PMID: 13979659.

Szczypka MS, Rainey MA, Kim DS, Alaynick WA, Marck BT, Matsumoto AM, Palmiter RD. Feeding behavior in dopamine-deficient mice. Proc Natl Acad Sci U S A. 1999 Oct 12;96(21):12138-43. doi: 10.1073/pnas.96.21.12138. PMID: 10518589; PMCID: PMC18425.

Takahashi H, Takano H, Kodaka F, Arakawa R, Yamada M, Otsuka T, Hirano Y, Kikyo H, Okubo Y, Kato M, Obata T, Ito H, Suhara T. Contribution of dopamine D1 and D2 receptors to amygdala activity in human. J Neurosci. 2010 Feb 24;30(8):3043-7. doi: 10.1523/JNEUROSCI.5689-09.2010. PMID: 20181600; PMCID: PMC6633940.

Takei K, McPherson PS, Schmid SL, De Camilli P. Tubular membrane invaginations coated by dynamin rings are induced by GTP-gamma S in nerve terminals. Nature. 1995 Mar 9;374(6518):186-90. doi: 10.1038/374186a0. PMID: 7877693.

Tandberg E, Larsen JP, Aarsland D, Cummings JL. The occurrence of depression in Parkinson's disease. A community-based study. Arch Neurol. 1996 Feb;53(2):175-9. doi: 10.1001/archneur.1996.00550020087019. PMID: 8639068.

Tang WJ, Gilman AG. Adenylyl cyclases. Cell. 1992 Sep 18;70(6):869-72. doi: 10.1016/0092-8674(92)90236-6. PMID: 1525824.

Tang XL, Wang Y, Li DL, Luo J, Liu MY. Orphan G protein-coupled receptors (GPCRs): biological functions and potential drug targets. Acta Pharmacol Sin. 2012 Mar;33(3):363-71. doi: 10.1038/aps.2011.210. Epub 2012 Feb 27. PMID: 22367282; PMCID: PMC4077139.

Tao YM, Yu C, Wang WS, Hou YY, Xu XJ, Chi ZQ, Ding YQ, Wang YJ, Liu JG. Heteromers of μ opioid and dopamine D_1 receptors modulate opioid-induced locomotor sensitization in a dopamine-independent manner. Br J Pharmacol. 2017 Sep;174(17):2842-2861. doi: 10.1111/bph.13908. Epub 2017 Jul 18. PMID: 28608532; PMCID: PMC5554314.

Targa G, Mottarlini F, Rizzi B, Leo D, Caffino L, Fumagalli F. Dysregulation of AMPA Receptor Trafficking and Intracellular Vesicular Sorting in the Prefrontal Cortex of Dopamine Transporter Knock-Out Rats. Biomolecules. 2023 Mar 11;13(3):516. doi: 10.3390/biom13030516. PMID: 36979451; PMCID: PMC10046215.

Tarpey P, Parnau J, Blow M, Woffendin H, Bignell G, Cox C, Cox J, Davies H, Edkins S, Holden S, Korny A, Mallya U, Moon J, O'Meara S, Parker A, Stephens P, Stevens C, Teague J, Donnelly A, Mangelsdorf M, Mulley J, Partington M, Turner G, Stevenson R, Schwartz C, Young I, Easton D, Bobrow M, Futreal PA, Stratton MR, Gecz J, Wooster R, Raymond FL. Mutations in the DLG3 gene cause nonsyndromic X-linked mental retardation. Am J Hum Genet. 2004 Aug;75(2):318-24. doi: 10.1086/422703. Epub 2004 Jun 7. PMID: 15185169; PMCID: PMC1216066.

Taussig R, Iñiguez-Lluhi JA, Gilman AG. Inhibition of adenylyl cyclase by Gi alpha. Science. 1993 Jul 9;261(5118):218-21. doi: 10.1126/science.8327893. PMID: 8327893.

Teng X, Chen S, Nie Y, Xiao P, Yu X, Shao Z, Zheng S. Ligand recognition and biased agonism of the D1 dopamine receptor. Nat Commun. 2022 Jun 8;13(1):3186. doi: 10.1038/s41467-022-30929-w. PMID: 35676276; PMCID: PMC9177848.

Tepper JM, Bolam JP. Functional diversity and specificity of neostriatal interneurons. Curr Opin Neurobiol. 2004 Dec;14(6):685-92. doi: 10.1016/j.conb.2004.10.003. PMID: 15582369.

Tepper JM, Sun BC, Martin LP, Creese I. Functional roles of dopamine D2 and D3 autoreceptors on nigrostriatal neurons analyzed by antisense knockdown in vivo. J Neurosci. 1997 Apr 1;17(7):2519-30. doi: 10.1523/JNEUROSCI.17-07-02519.1997. PMID: 9065512; PMCID: PMC6573500.

Thibault D, Giguère N, Loustalot F, Bourque MJ, Ducrot C, El Mestikawy S, Trudeau LÉ. Homeostatic regulation of excitatory synapses on striatal medium spiny neurons expressing the D2 dopamine receptor. Brain Struct Funct. 2016 May;221(4):2093-107. doi: 10.1007/s00429-015-1029-4. Epub 2015 Mar 18. PMID: 25782435.

Thibault D, Loustalot F, Fortin GM, Bourque MJ, Trudeau LÉ. Evaluation of D1 and D2 dopamine receptor segregation in the developing striatum using BAC transgenic mice. PLoS One. 2013 Jul 2;8(7):e67219. doi: 10.1371/journal.pone.0067219. PMID: 23843993; PMCID: PMC3699584.

Thomas Broome S, Louangaphay K, Keay KA, Leggio GM, Musumeci G, Castorina A. Dopamine: an immune transmitter. Neural Regen Res. 2020 Dec;15(12):2173-2185. doi: 10.4103/1673-5374.284976. PMID: 32594028; PMCID: PMC7749467.

Thompson D, Martini L, Whistler JL. Altered ratio of D1 and D2 dopamine receptors in mouse striatum is associated with behavioral sensitization to cocaine. PLoS One. 2010 Jun 9;5(6):e11038. doi: 10.1371/journal.pone.0011038. PMID: 20543951; PMCID: PMC2882949.

Thompson D, Whistler JL. Trafficking properties of the D5 dopamine receptor. Traffic. 2011 May;12(5):644-56. doi: 10.1111/j.1600-0854.2011.01179.x. PMID: 21348911.

Thomsen ARB, Plouffe B, Cahill TJ 3rd, Shukla AK, Tarrasch JT, Dosey AM, Kahsai AW, Strachan RT, Pani B, Mahoney JP, Huang L, Breton B, Heydenreich FM, Sunahara RK, Skiniotis G, Bouvier M, Lefkowitz RJ. GPCR-G Protein-β-Arrestin Super-Complex Mediates Sustained G Protein Signaling. Cell. 2016 Aug 11;166(4):907-919. doi: 10.1016/j.cell.2016.07.004. Epub 2016 Aug 4. PMID: 27499021; PMCID: PMC5418658.

Thurner P, Gsandtner I, Kudlacek O, Choquet D, Nanoff C, Freissmuth M, Zezula J. A two-state model for the diffusion of the A2A adenosine receptor in hippocampal neurons: agonist-induced switch to slow mobility is modified by synapse-associated protein 102 (SAP102). J Biol Chem. 2014 Mar 28;289(13):9263-74. doi: 10.1074/jbc.M113.505685. Epub 2014 Feb 7. PMID: 24509856; PMCID: PMC3979375.

Tiberi M, Caron MG. High agonist-independent activity is a distinguishing feature of the dopamine D1B receptor subtype. J Biol Chem. 1994 Nov 11;269(45):27925-31. PMID: 7525564.

Tiberi M, Jarvie KR, Silvia C, Falardeau P, Gingrich JA, Godinot N, Bertrand L, Yang-Feng TL, Fremeau RT Jr, Caron MG. Cloning, molecular characterization, and chromosomal assignment of a gene encoding a second D1 dopamine receptor subtype: differential expression pattern in rat brain compared with the D1A receptor. Proc Natl Acad Sci U S A. 1991 Sep 1;88(17):7491-5. doi: 10.1073/pnas.88.17.7491. PMID: 1831904; PMCID: PMC52326.

Tiberi M, Nash SR, Bertrand L, Lefkowitz RJ, Caron MG. Differential regulation of dopamine D1A receptor responsiveness by various G protein-coupled receptor kinases. J Biol Chem. 1996 Feb 16;271(7):3771-8. doi: 10.1074/jbc.271.7.3771. PMID: 8631993.

Tillerson JL, Caudle WM, Parent JM, Gong C, Schallert T, Miller GW. Olfactory discrimination deficits in mice lacking the dopamine transporter or the D2 dopamine receptor. Behav Brain Res. 2006 Sep 15;172(1):97-105. doi: 10.1016/j.bbr.2006.04.025. Epub 2006 Jun 9. PMID: 16765459.

Titeler M, Weinreich P, Sinclair D, Seeman P. Multiple receptors for brain dopamine. Proc Natl Acad Sci U S A. 1978 Mar;75(3):1153-6. doi: 10.1073/pnas.75.3.1153. PMID: 418405; PMCID: PMC411427.

Tobler PN, O'Doherty JP, Dolan RJ, Schultz W. Reward value coding distinct from risk attitude-related uncertainty coding in human reward systems. J Neurophysiol. 2007 Feb;97(2):1621-32. doi: 10.1152/jn.00745.2006. Epub 2006 Nov 22. PMID: 17122317; PMCID: PMC2637604.

Todman D. Henry Dale and the discovery of chemical synaptic transmission. Eur Neurol. 2008;60(3):162-4. doi: 10.1159/000145336. Epub 2008 Jul 16. PMID: 18645249. (a)

Todman D. John Eccles (1903-97) and the experiment that proved chemical synaptic transmission in the central nervous system. J Clin Neurosci. 2008 Sep;15(9):972-7. doi: 10.1016/j.jocn.2008.01.001. Epub 2008 Jul 9. PMID: 18617413. (b)

Torvinen M, Ginés S, Hillion J, Latini S, Canals M, Ciruela F, Bordoni F, Staines W, Pedata F, Agnati LF, Lluis C, Franco R, Ferré S, Fuxe K. Interactions among adenosine deaminase, adenosine A(1) receptors and dopamine D(1) receptors in stably cotransfected fibroblast cells and neurons. Neuroscience. 2002;113(3):709-19. doi: 10.1016/s0306-4522(02)00058-1. PMID: 12150791.

Toyooka K, Iritani S, Makifuchi T, Shirakawa O, Kitamura N, Maeda K, Nakamura R, Niizato K, Watanabe M, Kakita A, Takahashi H, Someya T, Nawa H. Selective reduction of a PDZ protein, SAP-97, in the prefrontal cortex of patients with chronic schizophrenia. J Neurochem. 2002 Nov;83(4):797-806. doi: 10.1046/j.1471-4159.2002.01181.x. PMID: 12421351.

Tran J, Anastacio H, Bardy C. Genetic predispositions of Parkinson's disease revealed in patient-derived brain cells. NPJ Parkinsons Dis. 2020 Apr 24;6:8. doi: 10.1038/s41531-020-0110-8. PMID: 32352027; PMCID: PMC7181694.

Tritsch NX, Ding JB, Sabatini BL. Dopaminergic neurons inhibit striatal output through non-canonical release of GABA. Nature. 2012 Oct 11;490(7419):262-6. doi: 10.1038/nature11466. Epub 2012 Oct 3. PMID: 23034651; PMCID: PMC3944587.

Trudeau LE, El Mestikawy S. Glutamate Cotransmission in Cholinergic, GABAergic and Monoamine Systems: Contrasts and Commonalities. Front Neural Circuits. 2018 Dec 18;12:113. doi: 10.3389/fncir.2018.00113. PMID: 30618649; PMCID: PMC6305298.

Trudeau LE, Hnasko TS, Wallén-Mackenzie A, Morales M, Rayport S, Sulzer D. The multilingual nature of dopamine neurons. Prog Brain Res. 2014;211:141-64. doi: 10.1016/B978-0-444-63425-2.00006-4. PMID: 24968779; PMCID: PMC4565795.

Tsuga H, Kameyama K, Haga T, Kurose H, Nagao T. Sequestration of muscarinic acetylcholine receptor m2 subtypes. Facilitation by G protein-coupled receptor kinase (GRK2) and attenuation by a dominant-negative mutant of GRK2. J Biol Chem. 1994 Dec 23;269(51):32522-7. PMID: 7798253.

Tumova K, Iwasiow RM, Tiberi M. Insight into the mechanism of dopamine D1-like receptor activation. Evidence for a molecular interplay between the third extracellular loop and the cytoplasmic tail. J Biol Chem. 2003 Mar 7;278(10):8146-53. doi: 10.1074/jbc.M208059200. Epub 2002 Dec 30. PMID: 12509438.

Tumova K, Zhang D, Tiberi M. Role of the fourth intracellular loop of D1-like dopaminergic receptors in conferring subtype-specific signaling properties. FEBS Lett. 2004 Oct 22;576(3):461-7. doi: 10.1016/j.febslet.2004.09.059. PMID: 15498581.

Tunnicliff G, Rick JT, Connolly K. Locomotor acitvity in Drosophila. V. A comparative biochemical study of selectively bred populations. Comp Biochem Physiol. 1969 Jun;29(3):1239-45. doi: 10.1016/0010-406x(69)91028-7. PMID: 5793768.

Undie AS, Friedman E. Selective dopaminergic mechanism of dopamine and SKF38393 stimulation of inositol phosphate formation in rat brain. Eur J Pharmacol. 1992 Aug 3;226(4):297-302. doi: 10.1016/0922-4106(92)90046-x. PMID: 1327844.

Undie AS, Friedman E. Stimulation of a dopamine D1 receptor enhances inositol phosphates formation in rat brain. J Pharmacol Exp Ther. 1990 Jun;253(3):987-92. PMID: 1972756.

Undie AS, Weinstock J, Sarau HM, Friedman E. Evidence for a distinct D1-like dopamine receptor that couples to activation of phosphoinositide metabolism in brain. J Neurochem. 1994 May;62(5):2045-8. doi: 10.1046/j.1471-4159.1994.62052045.x. PMID: 7908949.

Ungerstedt U. 6-Hydroxy-dopamine induced degeneration of central monoamine neurons. Eur J Pharmacol. 1968 Dec;5(1):107-10. doi: 10.1016/0014-2999(68)90164-7. PMID: 5718510.

Ungerstedt U. 6-hydroxydopamine-induced degeneration of the nigrostriatal dopamine pathway: the turning syndrome. Pharmacol Ther B. 1976;2(1):37-40. doi: 10.1016/0306-039x(76)90016-7. PMID: 772721.

Urs NM, Daigle TL, Caron MG. A dopamine D1 receptor-dependent β-arrestin signaling complex potentially regulates morphine-induced psychomotor activation but not reward in mice. Neuropsychopharmacology. 2011 Feb;36(3):551-8. doi: 10.1038/npp.2010.186. Epub 2010 Oct 27. PMID: 20980993; PMCID: PMC3021093.

Usdin TB, Mezey E, Chen C, Brownstein MJ, Hoffman BJ. Cloning of the cocaine-sensitive bovine dopamine transporter. Proc Natl Acad Sci U S A. 1991 Dec 15;88(24):11168-71. doi: 10.1073/pnas.88.24.11168. PMID: 1722321; PMCID: PMC53095.

Usiello A, Baik JH, Rougé-Pont F, Picetti R, Dierich A, LeMeur M, Piazza PV, Borrelli E. Distinct functions of the two isoforms of dopamine D2 receptors. Nature. 2000 Nov 9;408(6809):199-203. doi: 10.1038/35041572. PMID: 11089973.

Valjent E, Bertran-Gonzalez J, Hervé D, Fisone G, Girault JA. Looking BAC at striatal signaling: cell-specific analysis in new transgenic mice. Trends Neurosci. 2009 Oct;32(10):538-47. doi: 10.1016/j.tins.2009.06.005. Epub 2009 Sep 16. PMID: 19765834.

Valjent E, Pascoli V, Svenningsson P, Paul S, Enslen H, Corvol JC, Stipanovich A, Caboche J, Lombroso PJ, Nairn AC, Greengard P, Hervé D, Girault JA. Regulation of a protein phosphatase cascade allows convergent dopamine and glutamate signals to activate ERK in the striatum. Proc Natl Acad Sci U S A. 2005 Jan 11;102(2):491-6. doi: 10.1073/pnas.0408305102. Epub 2004 Dec 17. PMID: 15608059; PMCID: PMC544317.

van Biesen T, Hawes BE, Luttrell DK, Krueger KM, Touhara K, Porfiri E, Sakaue M, Luttrell LM, Lefkowitz RJ. Receptor-tyrosine-kinase- and G beta gamma-mediated MAP kinase activation by a common signalling pathway. Nature. 1995 Aug 31;376(6543):781-4. doi: 10.1038/376781a0. PMID: 7651538.

van der Bliek AM, Redelmeier TE, Damke H, Tisdale EJ, Meyerowitz EM, Schmid SL. Mutations in human dynamin block an intermediate stage in coated vesicle formation. J Cell Biol. 1993 Aug;122(3):553-63. doi: 10.1083/jcb.122.3.553. PMID: 8101525; PMCID: PMC2119674.

Van Tol HH, Bunzow JR, Guan HC, Sunahara RK, Seeman P, Niznik HB, Civelli O. Cloning of the gene for a human dopamine D4 receptor with high affinity for the antipsychotic clozapine. Nature. 1991 Apr 18;350(6319):610-4. doi: 10.1038/350610a0. PMID: 1840645.

Van Tol HH, Wu CM, Guan HC, Ohara K, Bunzow JR, Civelli O, Kennedy J, Seeman P, Niznik HB, Jovanovic V. Multiple dopamine D4 receptor variants in the human population. Nature. 1992 Jul 9;358(6382):149-52. doi: 10.1038/358149a0. PMID: 1319557.

van Zundert B, Yoshii A, Constantine-Paton M. Receptor compartmentalization and trafficking at glutamate synapses: a developmental proposal. Trends Neurosci. 2004 Jul;27(7):428-37. doi: 10.1016/j.tins.2004.05.010. PMID: 15219743.

Vanderschuren LJ, Di Ciano P, Everitt BJ. Involvement of the dorsal striatum in cue-controlled cocaine seeking. J Neurosci. 2005 Sep 21;25(38):8665-70. doi: 10.1523/JNEUROSCI.0925-05.2005. PMID: 16177034; PMCID: PMC6725521.

Vargas GA, Von Zastrow M. Identification of a novel endocytic recycling signal in the D1 dopamine receptor. J Biol Chem. 2004 Sep 3;279(36):37461-9. doi: 10.1074/jbc.M401034200. Epub 2004 Jun 10. PMID: 15192107.

Verheij MM, Cools AR. Twenty years of dopamine research: individual differences in the response of accumbal dopamine to environmental and pharmacological challenges. Eur J Pharmacol. 2008 May 13;585(2-3):228-44. doi: 10.1016/j.ejphar.2008.02.084. Epub 2008 Mar 15. PMID: 18423601.

Verma V, Hasbi A, O'Dowd BF, George SR. Dopamine D1-D2 receptor Heteromer-mediated calcium release is desensitized by D1 receptor occupancy with or without signal activation: dual functional regulation by G protein-coupled receptor kinase 2. J Biol Chem. 2010 Nov 5;285(45):35092-103. doi: 10.1074/jbc.M109.088625. Epub 2010 Aug 31. PMID: 20807772; PMCID: PMC2966123.

Vicario I, Rigual R, Obeso A, Gonzalez C. Characterization of the synthesis and release of catecholamine in the rat carotid body in vitro. Am J Physiol Cell Physiol. 2000 Mar;278(3):C490-9. doi: 10.1152/ajpcell.2000.278.3.C490. PMID: 10712237.

Vickers CA, Stephens B, Bowen J, Arbuthnott GW, Grant SG, Ingham CA. Neurone specific regulation of dendritic spines in vivo by post synaptic density 95 protein (PSD-95). Brain Res. 2006 May 23;1090(1):89-98. doi: 10.1016/j.brainres.2006.03.075. Epub 2006 May 4. PMID: 16677619.

Vickery RG, von Zastrow M. Distinct dynamin-dependent and -independent mechanisms target structurally homologous dopamine receptors to different endocytic membranes. J Cell Biol. 1999 Jan 11;144(1):31-43. doi: 10.1083/jcb.144.1.31. PMID: 9885242; PMCID: PMC2148123.

Vidal PM, Pacheco R. Targeting the Dopaminergic System in Autoimmunity. J Neuroimmune Pharmacol. 2020 Mar;15(1):57-73. doi: 10.1007/s11481-019-09834-5. Epub 2019 Jan 19. PMID: 30661214.

Vincent SG, Waddell AE, Caron MG, Walker JK, Fisher JT. A murine model of hyperdopaminergic state displays altered respiratory control. FASEB J. 2007 May;21(7):1463-71. doi: 10.1096/fj.06-7248com. Epub 2007 Jan 25. PMID: 17255472.

Violin JD, Lefkowitz RJ. Beta-arrestin-biased ligands at seven-transmembrane receptors. Trends Pharmacol Sci. 2007 Aug;28(8):416-22. doi: 10.1016/j.tips.2007.06.006. Epub 2007 Jul 20. PMID: 17644195.

VON EULER US, HELLNER S. Excretion of noradrenaline, adrenaline, and hydroxytyramine in urine. Acta Physiol Scand. 1951 Apr 25;22(2-3):160-7. doi: 10.1111/j.1748-1716.1951.tb00765.x. PMID: 14933139.

von Zastrow M, Kobilka BK. Ligand-regulated internalization and recycling of human beta 2-adrenergic receptors between the plasma membrane and endosomes containing transferrin receptors. J Biol Chem. 1992 Feb 15;267(5):3530-8. PMID: 1371121.

Waelti P, Dickinson A, Schultz W. Dopamine responses comply with basic assumptions of formal learning theory. Nature. 2001 Jul 5;412(6842):43-8. doi: 10.1038/35083500. PMID: 11452299.

Walaas SI, Aswad DW, Greengard P. A dopamine- and cyclic AMP-regulated phosphoprotein enriched in dopamine-innervated brain regions. Nature. 1983 Jan 6;301(5895):69-71. doi: 10.1038/301069a0. PMID: 6296685.

Walsh DA, Ashby CD, Gonzalez C, Calkins D, Fischer EH. Krebs EG: Purification and characterization of a protein inhibitor of adenosine 3',5'-monophosphate-dependent protein kinases. J Biol Chem. 1971 Apr 10;246(7):1977-85. PMID: 4324557.

Walsh DA, Perkins JP, Krebs EG. An adenosine 3',5'-monophosphate-dependant protein kinase from rabbit skeletal muscle. J Biol Chem. 1968 Jul 10;243(13):3763-5. PMID: 4298072.

Wang GJ, Volkow ND, Logan J, Pappas NR, Wong CT, Zhu W, Netusil N, Fowler JS. Brain dopamine and obesity. Lancet. 2001 Feb 3;357(9253):354-7. doi: 10.1016/s0140-6736(00)03643-6. PMID: 11210998.

Wang JR, Sun PH, Ren ZX, Meltzer HY, Zhen XC. GSK-3β Interacts with Dopamine D1 Receptor to Regulate Receptor Function: Implication for Prefrontal Cortical D1 Receptor Dysfunction in Schizophrenia. CNS Neurosci Ther. 2017 Feb;23(2):174-187. doi: 10.1111/cns.12664. Epub 2016 Dec 20. PMID: 27996211; PMCID: PMC6492711.

Wang M, Wong AH, Liu F. Interactions between NMDA and dopamine receptors: a potential therapeutic target. Brain Res. 2012 Oct 2;1476:154-63. doi: 10.1016/j.brainres.2012.03.029. Epub 2012 Mar 17. PMID: 22472597.

Wang S, Che T, Levit A, Shoichet BK, Wacker D, Roth BL. Structure of the D2 dopamine receptor bound to the atypical antipsychotic drug risperidone. Nature. 2018 Mar 8;555(7695):269-273. doi: 10.1038/nature25758. Epub 2018 Jan 24. PMID: 29466326; PMCID: PMC5843546.

Wang S, Wacker D, Levit A, Che T, Betz RM, McCorvy JD, Venkatakrishnan AJ, Huang XP, Dror RO, Shoichet BK, Roth BL. D4 dopamine receptor high-resolution structures enable the discovery of selective agonists. Science. 2017 Oct 20;358(6361):381-386. doi: 10.1126/science.aan5468. PMID: 29051383; PMCID: PMC5856174.

Wang W, Cohen JA, Wallrapp A, Trieu KG, Barrios J, Shao F, Krishnamoorthy N, Kuchroo VK, Jones MR, Fine A, Bai Y, Ai X. Age-Related Dopaminergic Innervation Augments T Helper 2-Type Allergic Inflammation in the Postnatal Lung. Immunity. 2019 Dec 17;51(6):1102-1118.e7. doi: 10.1016/j.immuni.2019.10.002. Epub 2019 Nov 19. PMID: 31757673; PMCID: PMC6937208.

Wang YM, Gainetdinov RR, Fumagalli F, Xu F, Jones SR, Bock CB, Miller GW, Wightman RM, Caron MG. Knockout of the vesicular monoamine transporter 2 gene results in neonatal death and supersensitivity to cocaine and amphetamine. Neuron. 1997 Dec;19(6):1285-96. doi: 10.1016/s0896-6273(00)80419-5. PMID: 9427251.

Washbourne P, Liu XB, Jones EG, McAllister AK. Cycling of NMDA receptors during trafficking in neurons before synapse formation. J Neurosci. 2004 Sep 22;24(38):8253-64. doi: 10.1523/JNEUROSCI.2555-04.2004. Erratum in: J Neurosci. 2004 Oct 13;24(41):1p following 91266. PMID: 15385609; PMCID: PMC6729693.

Watts VJ, Neve KA. Activation of type II adenylate cyclase by D2 and D4 but not D3 dopamine receptors. Mol Pharmacol. 1997 Aug;52(2):181-6. doi: 10.1124/mol.52.2.181. PMID: 9271339.

Wei Z, Behrman B, Wu WH, Chen BS. Subunit-specific regulation of N-methyl-D-aspartate (NMDA) receptor trafficking by SAP102 protein splice variants. J Biol Chem. 2015 Feb 20;290(8):5105-5116. doi: 10.1074/jbc.M114.599969. Epub 2015 Jan 2. PMID: 25555912; PMCID: PMC4335245.

Wei Z, Wu G, Chen BS. Regulation of SAP102 Synaptic Targeting by Phosphorylation. Mol Neurobiol. 2018 Aug;55(8):6215-6226. doi: 10.1007/s12035-017-0836-4. Epub 2017 Dec 27. PMID: 29282697; PMCID: PMC6599631.

Weihe E, Depboylu C, Schütz B, Schäfer MK, Eiden LE. Three types of tyrosine hydroxylase-positive CNS neurons distinguished by dopa decarboxylase and VMAT2 co-expression. Cell Mol Neurobiol. 2006 Jul-Aug;26(4-6):659-78. doi: 10.1007/s10571-006-9053-9. Epub 2006 May 31. PMID: 16741673; PMCID: PMC4183211.

Wess J, Oteng AB, Rivera-Gonzalez O, Gurevich EV, Gurevich VV. β-Arrestins: Structure, Function, Physiology, and Pharmacological Perspectives. Pharmacol Rev. 2023 Sep;75(5):854-884. doi: 10.1124/pharmrev.121.000302. Epub 2023 Apr 7. PMID: 37028945; PMCID: PMC10441628.

Westin JE, Vercammen L, Strome EM, Konradi C, Cenci MA. Spatiotemporal pattern of striatal ERK1/2 phosphorylation in a rat model of L-DOPA-induced dyskinesia and the role of dopamine D1 receptors. Biol Psychiatry. 2007 Oct 1;62(7):800-10. doi: 10.1016/j.biopsych.2006.11.032. Epub 2007 Jul 26. PMID: 17662258; PMCID: PMC4205578.

Wintle RF, Van Tol HH. Dopamine signaling in Caenorhabditis elegans-potential for parkinsonism research. Parkinsonism Relat Disord. 2001 Jul;7(3):177-183. doi: 10.1016/s1353-8020(00)00055-9. PMID: 11331184.

Wise RA, Rompre PP. Brain dopamine and reward. Annu Rev Psychol. 1989;40:191-225. doi: 10.1146/annurev.ps.40.020189.001203. PMID: 2648975.

Wise RA. Dopamine, learning and motivation. Nat Rev Neurosci. 2004 Jun;5(6):483-94. doi: 10.1038/nrn1406. PMID: 15152198.

Wise RA. Forebrain substrates of reward and motivation. J Comp Neurol. 2005 Dec 5;493(1):115-21. doi: 10.1002/cne.20689. PMID: 16254990; PMCID: PMC2562437.

Witkovsky P. Dopamine and retinal function. Doc Ophthalmol. 2004 Jan;108(1):17-40. doi: 10.1023/b:doop.0000019487.88486.0a. PMID: 15104164.

Wolf ME, Roth RH. Autoreceptor regulation of dopamine synthesis. Ann N Y Acad Sci. 1990;604:323-43. doi: 10.1111/j.1749-6632.1990.tb32003.x. PMID: 2171398.

Won S, Levy JM, Nicoll RA, Roche KW. MAGUKs: multifaceted synaptic organizers. Curr Opin Neurobiol. 2017 Apr;43:94-101. doi: 10.1016/j.conb.2017.01.006. Epub 2017 Feb 23. PMID: 28236779; PMCID: PMC5447471.

Wong AH, Buckle CE, Van Tol HH. Polymorphisms in dopamine receptors: what do they tell us? Eur J Pharmacol. 2000 Dec 27;410(2-3):183-203. doi: 10.1016/s0014-2999(00)00815-3. PMID: 11134669.

Wu H, Reissner C, Kuhlendahl S, Coblentz B, Reuver S, Kindler S, Gundelfinger ED, Garner CC. Intramolecular interactions regulate SAP97 binding to GKAP. EMBO J. 2000 Nov 1;19(21):5740-51. doi: 10.1093/emboj/19.21.5740. PMID: 11060025; PMCID: PMC305801.

Xenias HS, Ibáñez-Sandoval O, Koós T, Tepper JM. Are striatal tyrosine hydroxylase interneurons dopaminergic? J Neurosci. 2015 Apr 22;35(16):6584-99. doi: 10.1523/JNEUROSCI.0195-15.2015. PMID: 25904808; PMCID: PMC4405564.

Xia Z, Gray JA, Compton-Toth BA, Roth BL. A direct interaction of PSD-95 with 5-HT2A serotonin receptors regulates receptor trafficking and signal transduction. J Biol Chem. 2003 Jun 13;278(24):21901-8. doi: 10.1074/jbc.M301905200. Epub 2003 Apr 7. PMID: 12682061. (a)

Xia Z, Hufeisen SJ, Gray JA, Roth BL. The PDZ-binding domain is essential for the dendritic targeting of 5-HT2A serotonin receptors in cortical pyramidal neurons in vitro. Neuroscience. 2003;122(4):907-20. doi: 10.1016/s0306-4522(03)00589-x. PMID: 14643760. (b)

Xiao P, Yan W, Gou L, Zhong YN, Kong L, Wu C, Wen X, Yuan Y, Cao S, Qu C, Yang X, Yang CC, Xia A, Hu Z, Zhang Q, He YH, Zhang DL, Zhang C, Hou GH, Liu H, Zhu L, Fu P, Yang S, Rosenbaum DM, Sun JP, Du Y, Zhang L, Yu X, Shao Z. Ligand recognition and allosteric regulation of DRD1-Gs signaling complexes. Cell. 2021 Feb 18;184(4):943-956.e18. doi: 10.1016/j.cell.2021.01.028. Epub 2021 Feb 10. PMID: 33571432.

Xu B, Li M, Wang Y, Zhao M, Morotti S, Shi Q, Wang Q, Barbagallo F, Teoh JP, Reddy GR, Bayne EF, Liu Y, Shen A, Puglisi JL, Ge Y, Li J, Grandi E, Nieves-Cintron M, Xiang YK. GRK5 Controls SAP97-Dependent Cardiotoxic β1 Adrenergic Receptor-CaMKII Signaling in Heart Failure. Circ Res. 2020 Aug 28;127(6):796-810. doi: 10.1161/CIRCRESAHA.119.316319. Epub 2020 Jun 8. PMID: 32507058; PMCID: PMC7484403.

Xu F, Gainetdinov RR, Wetsel WC, Jones SR, Bohn LM, Miller GW, Wang YM, Caron MG. Mice lacking the norepinephrine transporter are supersensitive to psychostimulants. Nat Neurosci. 2000 May;3(5):465-71. doi: 10.1038/74839. PMID: 10769386.

Xu J, Paquet M, Lau AG, Wood JD, Ross CA, Hall RA. beta 1-adrenergic receptor association with the synaptic scaffolding protein membrane-associated guanylate kinase inverted-2 (MAGI-2). Differential regulation of receptor internalization by MAGI-2 and PSD-95. J Biol Chem. 2001 Nov 2;276(44):41310-7. doi: 10.1074/jbc.M107480200. Epub 2001 Aug 28. PMID: 11526121.

Xu M, Guo Y, Vorhees CV, Zhang J. Behavioral responses to cocaine and amphetamine administration in mice lacking the dopamine D1 receptor. Brain Res. 2000 Jan 3;852(1):198-207. doi: 10.1016/s0006-8993(99)02258-1. PMID: 10661513.

Xu M, Hu XT, Cooper DC, Moratalla R, Graybiel AM, White FJ, Tonegawa S. Elimination of cocaine-induced hyperactivity and dopamine-mediated neurophysiological effects in dopamine D1 receptor mutant mice. Cell. 1994 Dec 16;79(6):945-55. doi: 10.1016/0092-8674(94)90026-4. PMID: 8001143. (b)

Xu M, Moratalla R, Gold LH, Hiroi N, Koob GF, Graybiel AM, Tonegawa S. Dopamine D1 receptor mutant mice are deficient in striatal expression of dynorphin and in dopamine-mediated behavioral responses. Cell. 1994 Nov 18;79(4):729-42. doi: 10.1016/0092-8674(94)90557-6. PMID: 7954836. (a)

Xu P, Huang S, Krumm BE, Zhuang Y, Mao C, Zhang Y, Wang Y, Huang XP, Liu YF, He X, Li H, Yin W, Jiang Y, Zhang Y, Roth BL, Xu HE. Structural genomics of the human dopamine receptor system. Cell Res. 2023 May 23. doi: 10.1038/s41422-023-00808-0. Epub ahead of print. PMID: 37221270.

Xu P, Huang S, Mao C, Krumm BE, Zhou XE, Tan Y, Huang XP, Liu Y, Shen DD, Jiang Y, Yu X, Jiang H, Melcher K, Roth BL, Cheng X, Zhang Y, Xu HE. Structures of the human dopamine D3 receptor-Gi complexes. Mol Cell. 2021 Mar 18;81(6):1147-1159.e4. doi: 10.1016/j.molcel.2021.01.003. Epub 2021 Feb 5. PMID: 33548201.

Xu W. PSD-95-like membrane associated guanylate kinases (PSD-MAGUKs) and synaptic plasticity. Curr Opin Neurobiol. 2011 Apr;21(2):306-12. doi: 10.1016/j.conb.2011.03.001. Epub 2011 Mar 28. PMID: 21450454; PMCID: PMC3138136.

Yang D, Zhou Q, Labroska V, Qin S, Darbalaei S, Wu Y, Yuliantie E, Xie L, Tao H, Cheng J, Liu Q, Zhao S, Shui W, Jiang Y, Wang MW. G protein-coupled receptors: structure- and function-based drug discovery. Signal Transduct Target Ther. 2021 Jan 8;6(1):7. doi: 10.1038/s41392-020-00435-w. PMID: 33414387; PMCID: PMC7790836.

Yang J, Villar VAM, Jose PA, Zeng C. Renal Dopamine Receptors and Oxidative Stress: Role in Hypertension. Antioxid Redox Signal. 2021 Mar 20;34(9):716-735. doi: 10.1089/ars.2020.8106. Epub 2020 May 29. PMID: 32349533; PMCID: PMC7910420.

Yano H, Cai NS, Xu M, Verma RK, Rea W, Hoffman AF, Shi L, Javitch JA, Bonci A, Ferré S. Gs- versus Golf-dependent functional selectivity mediated by the dopamine D1 receptor. Nat Commun. 2018 Feb 5;9(1):486. doi: 10.1038/s41467-017-02606-w. PMID: 29402888; PMCID: PMC5799184.

Yao WD, Gainetdinov RR, Arbuckle MI, Sotnikova TD, Cyr M, Beaulieu JM, Torres GE, Grant SG, Caron MG. Identification of PSD-95 as a regulator of dopamine-mediated synaptic and behavioral plasticity. Neuron. 2004 Feb 19;41(4):625-38. doi: 10.1016/s0896-6273(04)00048-0. PMID: 14980210.

Yao WD, Spealman RD, Zhang J. Dopaminergic signaling in dendritic spines. Biochem Pharmacol. 2008 Jun 1;75(11):2055-69. doi: 10.1016/j.bcp.2008.01.018. Epub 2008 Feb 12. PMID: 18353279; PMCID: PMC2443745.

Yu P, Yang Z, Jones JE, Wang Z, Owens SA, Mueller SC, Felder RA, Jose PA. D1 dopamine receptor signaling involves caveolin-2 in HEK-293 cells. Kidney Int. 2004 Dec;66(6):2167-80. doi: 10.1111/j.1523-1755.2004.66007.x. PMID: 15569306.

Yu Q, Liu YZ, Zhu YB, Wang YY, Li Q, Yin DM. Genetic labeling reveals temporal and spatial expression pattern of D2 dopamine receptor in rat forebrain. Brain Struct Funct. 2019 Apr;224(3):1035-1049. doi: 10.1007/s00429-018-01824-2. Epub 2019 Jan 2. PMID: 30604007; PMCID: PMC6499762.

Yu SS, Lefkowitz RJ, Hausdorff WP. Beta-adrenergic receptor sequestration. A potential mechanism of receptor resensitization. J Biol Chem. 1993 Jan 5;268(1):337-41. PMID: 8380158.

Yuste R. The discovery of dendritic spines by Cajal. Front Neuroanat. 2015 Apr 21;9:18. doi: 10.3389/fnana.2015.00018. PMID: 25954162; PMCID: PMC4404913.

Zaffaroni M, Marino F, Bombelli R, Rasini E, Monti M, Ferrari M, Ghezzi A, Comi G, Lecchini S, Cosentino M. Therapy with interferon-beta modulates endogenous catecholamines in lymphocytes of patients with multiple sclerosis. Exp Neurol. 2008 Dec;214(2):315-21. doi: 10.1016/j.expneurol.2008.08.015. Epub 2008 Sep 12. PMID: 18824168.

Zanassi P, Paolillo M, Montecucco A, Avvedimento EV, Schinelli S. Pharmacological and molecular evidence for dopamine D(1) receptor expression by striatal astrocytes in culture. J Neurosci Res. 1999 Nov 15;58(4):544-52. doi: 10.1002/(sici)1097-4547(19991115)58:4<544::aid-jnr7>3.0.co;2-9. PMID: 10533046.

Zanni G, van Esch H, Bensalem A, Saillour Y, Poirier K, Castelnau L, Ropers HH, de Brouwer AP, Laumonnier F, Fryns JP, Chelly J. A novel mutation in the DLG3 gene encoding the synapse-associated protein 102 (SAP102) causes non-syndromic mental retardation. Neurogenetics. 2010 May;11(2):251-5. doi: 10.1007/s10048-009-0224-y. Epub 2009 Oct 1. PMID: 19795139.

Zawilska JB, Nowak JZ. Dopamine D4-like receptors in vertebrate retina: does the retina offer a model for the D4-receptor analysis? Pol J Pharmacol. 1997 Aug;49(4):201-11. PMID: 9437763.

Zeng C, Armando I, Luo Y, Eisner GM, Felder RA, Jose PA. Dysregulation of dopamine-dependent mechanisms as a determinant of hypertension: studies in dopamine receptor knockout mice. Am J Physiol Heart Circ Physiol. 2008 Feb;294(2):H551-69. doi: 10.1152/ajpheart.01036.2007. Epub 2007 Dec 14. PMID: 18083900; PMCID: PMC4029502.

Zhang B, Albaker A, Plouffe B, Lefebvre C, Tiberi M. Constitutive activities and inverse agonism in dopamine receptors. Adv Pharmacol. 2014;70:175-214. doi: 10.1016/B978-0-12-417197-8.00007-9. PMID: 24931197.

Zhang B, Yang X, Tiberi M. Functional importance of two conserved residues in intracellular loop 1 and transmembrane region 2 of Family A GPCRs: insights from ligand binding and signal transduction responses of D1 and D5 dopaminergic receptor mutants. Cell Signal. 2015 Oct;27(10):2014-25. doi: 10.1016/j.cellsig.2015.07.006. Epub 2015 Jul 15. PMID: 26186971.

Zhang D, Zhao Q, Wu B. Structural Studies of G Protein-Coupled Receptors. Mol Cells. 2015 Oct;38(10):836-42. doi: 10.14348/molcells.2015.0263. Epub 2015 Oct 15. PMID: 26467290; PMCID: PMC4625064.

Zhang H, Sulzer D. Regulation of striatal dopamine release by presynaptic auto- and heteroreceptors. Basal Ganglia. 2012 Mar 1;2(1):5-13. doi: 10.1016/j.baga.2011.11.004. PMID: 22712055; PMCID: PMC3375990.

Zhang J, Barak LS, Anborgh PH, Laporte SA, Caron MG, Ferguson SS. Cellular trafficking of G protein-coupled receptor/beta-arrestin endocytic complexes. J Biol Chem. 1999 Apr 16;274(16):10999-1006. doi: 10.1074/jbc.274.16.10999. PMID: 10196181.

Zhang J, Ferguson SS, Barak LS, Ménard L, Caron MG. Dynamin and beta-arrestin reveal distinct mechanisms for G protein-coupled receptor internalization. J Biol Chem. 1996 Aug 2;271(31):18302-5. doi: 10.1074/jbc.271.31.18302. PMID: 8702465.

Zhang J, Saur T, Duke AN, Grant SG, Platt DM, Rowlett JK, Isacson O, Yao WD. Motor impairments, striatal degeneration, and altered dopamine-glutamate interplay in mice lacking PSD-95. J Neurogenet. 2014 Mar-Jun;28(1-2):98-111. doi: 10.3109/01677063.2014.892486. Epub 2014 Apr 22. PMID: 24702501; PMCID: PMC4406490.

Zhang J, Vinuela A, Neely MH, Hallett PJ, Grant SG, Miller GM, Isacson O, Caron MG, Yao WD. Inhibition of the dopamine D1 receptor signaling by PSD-95. J Biol Chem. 2007 May 25;282(21):15778-89. doi: 10.1074/jbc.M611485200. Epub 2007 Mar 16. PMID: 17369255; PMCID: PMC2649122.

Zhang J, Xu TX, Hallett PJ, Watanabe M, Grant SG, Isacson O, Yao WD. PSD-95 uncouples dopamine-glutamate interaction in the D1/PSD-95/NMDA receptor complex. J Neurosci. 2009 Mar 4;29(9):2948-60. doi: 10.1523/JNEUROSCI.4424-08.2009. PMID: 19261890; PMCID: PMC2693913.

Zheng C, Zhang F. New insights into pathogenesis of l-DOPA-induced dyskinesia. Neurotoxicology. 2021 Sep;86:104-113. doi: 10.1016/j.neuro.2021.07.006. Epub 2021 Jul 28. PMID: 34331976.

Zheng CY, Petralia RS, Wang YX, Kachar B, Wenthold RJ. SAP102 is a highly mobile MAGUK in spines. J Neurosci. 2010 Mar 31;30(13):4757-66. doi: 10.1523/JNEUROSCI.6108-09.2010. PMID: 20357126; PMCID: PMC2874826.

Zhou QY, Grandy DK, Thambi L, Kushner JA, Van Tol HH, Cone R, Pribnow D, Salon J, Bunzow JR, Civelli O. Cloning and expression of human and rat D1 dopamine receptors. Nature. 1990 Sep 6;347(6288):76-80. doi: 10.1038/347076a0. PMID: 2168520.

Zhou QY, Palmiter RD. Dopamine-deficient mice are severely hypoactive, adipsic, and aphagic. Cell. 1995 Dec 29;83(7):1197-209. doi: 10.1016/0092-8674(95)90145-0. PMID: 8548806.

Zhu F, Cizeron M, Qiu Z, Benavides-Piccione R, Kopanitsa MV, Skene NG, Koniaris B, DeFelipe J, Fransén E, Komiyama NH, Grant SGN. Architecture of the Mouse Brain Synaptome. Neuron. 2018 Aug 22;99(4):781-799.e10. doi: 10.1016/j.neuron.2018.07.007. Epub 2018 Aug 2. PMID: 30078578; PMCID: PMC6117470.

Zhu H, Clemens S, Sawchuk M, Hochman S. Expression and distribution of all dopamine receptor subtypes (D(1)-D(5)) in the mouse lumbar spinal cord: a real-time polymerase chain reaction and non-autoradiographic in situ hybridization study. Neuroscience. 2007 Nov 23;149(4):885-97. doi: 10.1016/j.neuroscience.2007.07.052. Epub 2007 Sep 12. PMID: 17936519; PMCID: PMC2185067.

Zhu J, Shang Y, Zhang M. Mechanistic basis of MAGUK-organized complexes in synaptic development and signalling. Nat Rev Neurosci. 2016 Apr;17(4):209-23. doi: 10.1038/nrn.2016.18. PMID: 26988743.

Zhuang Y, Krumm B, Zhang H, Zhou XE, Wang Y, Huang XP, Liu Y, Cheng X, Jiang Y, Jiang H, Zhang C, Yi W, Roth BL, Zhang Y, Xu HE. Mechanism of dopamine binding and allosteric modulation of the human D1 dopamine receptor. Cell Res. 2021 May;31(5):593-596. doi: 10.1038/s41422-021-00482-0. Epub 2021 Mar 9. PMID: 33750903; PMCID: PMC8089099. (b)

Zhuang Y, Xu P, Mao C, Wang L, Krumm B, Zhou XE, Huang S, Liu H, Cheng X, Huang XP, Shen DD, Xu T, Liu YF, Wang Y, Guo J, Jiang Y, Jiang H, Melcher K, Roth BL, Zhang Y, Zhang C, Xu HE. Structural insights into the human D1 and D2 dopamine receptor signaling complexes. Cell. 2021 Feb 18;184(4):931-942.e18. doi: 10.1016/j.cell.2021.01.027. Epub 2021 Feb 10. PMID: 33571431; PMCID: PMC8215686. (a)